

# **& Biotechnology Metals** 2024

Institute of Geotechnics, Slovak Academy of Sciences, Košice  
Faculty of Natural Sciences, University of Ss. Cyril and Methodius in Trnava  
Slovak Mining Society  
ALGAJAS s.r.o.



Editors:

Jana Hroncová, Eva Mačingová, Alena Luptáková, Jana Sedláková-Kaduková

ISBN: 978-80-89883-15-8

October 10-11, 2024, Stará Lesná, High Tatras, Slovakia

# **Biotechnology** **Metals** **2024**

Institute of Geotechnics, Slovak Academy of Sciences, Košice  
Faculty of Natural Sciences, University of Ss. Cyril and Methodius in Trnava  
Slovak Mining Society  
ALGAJAS s.r.o.

## **Proceedings**

**6<sup>th</sup> International Scientific Conference  
on Biotechnology and Metals**



**Editors:**

Jana Hroncová, Eva Mačingová, Alena Luptáková, Jana Sedláková-Kaduková



ISBN: 978-80-89883-15-8

October 10-11, 2024, Stará Lesná, High Tatras, Slovakia

## INTERNATIONAL SCIENTIFIC COMMITTEE

Magdaléna Bálintová	Technical University in Košice, Slovakia
Ljudmilla Bokányi	University of Miskolc, Hungary
Vladimír Čablík	VŠB-TU Ostrava, Czech Republic
Slavomír Hredzák	Slovak Academy of Sciences, Košice, Slovakia
Daniel Kupka	Slovak Academy of Sciences, Košice, Slovakia
Ildikó Matušíková	University of Ss. Cyril and Methodius in Trnava, Slovakia
Anna Kinga Nowak	Cracow University of Technology, Poland
Neil Rowson	University of Birmingham, Great Britain
Mariola Saternus	Silesian University of Technology, Poland
Alexandra Šimonovičová	Comenius University in Bratislava, Slovakia
Stefano Ubaldini	National Research Council, Roma, Italy

## ORGANIZING COMMITTEE

### Chair

Alena Luptáková *Institute of Geotechnics, Slovak Academy of Sciences, Košice*

### Vice-chair

Jana Sedláková-  
Kaduková *Faculty of Natural Sciences, University of Ss. Cyril and Methodius, Trnava;  
ALGAJAS s.r.o., Košice*

### Members

*Institute of Geotechnics SAS, Košice*

*Faculty of Natural Sciences UCM, Trnava*

Zuzana Bártová

Richard Hančinský

Lenka Hagarová

Miroslava Sinčák

Jana Hroncová

Dávid Jáger

Eva Mačingová

Lubica Matisová

ISBN: 978-80-89883-15-8

## Preface

### **Dear colleagues and friends,**

it is honour to welcome you at the 6<sup>th</sup> International Scientific Conference on Biotechnology and Metals.

In the present time, biotechnology contribute to various solution that address many societal and environmental challenges, such as access to and sustainable use of natural resources, restoration of vital nature systems, climate mitigation and adaptation, food supply and security, and human health. They belong to the most promising technologies of this century and have research and technological priorities also within the programs of the European Union.

The rapid development of biotechnological procedures was also noted in the field of environmental biotechnologies, especially regarding the processing of various raw material sources and waste for the purpose of obtaining critical raw materials and protecting the environment.

The goal of the Biotechnology and Metals conference is to support multidisciplinary, to combine the skills of microbiologists, biologists, chemists, physicists, geologists, engineers, economists and other experts, so that they can jointly participate in the development of innovative technologies in order to utilize a vast potential of microorganisms and plants for the restoration and conservation of the environment and for the sustainable utilization of resources.

The conference is organized by four institutions - Institute of Geotechnics, Slovak Academy of Sciences, Košice; Faculty of Natural Sciences, University of Ss. Cyril and Methodius in Trnava; Slovak Mining Society and ALGAJAS s.r.o.

We wish you to enjoy your time at the conference and in Stará Lesná, as well.

We believe that we will meet again also for next, 7<sup>th</sup> year of Biotechnology and Metals conference.

Alena Luptáková and Jana Sedláková-Kaduková



## CONTENT

<b>Mahdi Amiribostanabad</b> RECOVERY OF GOLD AND CRITICAL ELEMENTS FROM E-WASTE USING A BIOTECHNICAL APPROACH.....	8
<b>Peter Andráš, Pavol Midula, Jana Ševčíková, Matej Šuránek, Joao Matos, Jana Janštová, Giuseppe Buccheri, Ján Tomaškin, Marek Drímal</b> BIOAVAILABILITY OF POTENTIALLY TOXIC ELEMENTS IN SELECTED Cu-DEPOSITS OF EUROPE.....	18
<b>Magdalena Balintova, Natalia Junakova, Yelizaveta Chernysh</b> HEAVY METALS AND SULPHATE REMOVAL FROM MODEL SOLUTIONS USING ION EXCHANGE RESINS.....	22
<b>Zuzana Bárťová, Daniel Kupka, Lenka Hagarová, Lucia Ivaničová, Miroslava Václavíková</b> BIOLEACHING OF TETRAHEDRITE - BACTERIAL OXIDATION AND GROWTH YIELD BEHAVIOUR.....	28
<b>Lenka Bobuľská, Lenka Demková, Július Árvay</b> SPATIAL VARIABILITY OF SOIL BIOCHEMICAL PROPERTIES IN THE FORMER MINING AREA.....	32
<b>Jan Cebula, Iwona Wiewiórska, Lesław Świerczek, Adam Cenian</b> DISSOLVING SELECTED SEDIMENTS COLLECTED ON THE SAND FILTER UNDER THE INFLUENCE OF DISINFECTANTS.....	38
<b>Claudia Čičáková, Daniel Kupka, Jana Hroncová, Lenka Hagarová, Tomáš Faragó, Eva Mačingová, Viktória Krajanová, Ľubomír Jurkovič, Miroslava Václavíková</b> ALUMINIUM ELECTROCOAGULATION FOR EFFICIENT TREATMENT OF LANDFILL LEACHATE CONTAMINATED WITH HIGH CONCENTRATION OF FLUORIDES AND CYANIDES.....	48
<b>Katarina Čirković, Aleksandar Ostojić, Ivana Radojević</b> TESTING THE CHARACTERISTICS OF SELECTED MICROORGANISMS FOR POSSIBLE APPLICATION IN WASTEWATER TREATMENT.....	54
<b>Mária Čížková, Milada Vítová, Klára Řeháková, Kateřina Čapková, Marian Rucki</b> MACROALGAE FROM POST-MINING LAKES CAN ACCUMULATE RARE EARTH ELEMENTS.....	62
<b>Vlasta Demeckova, Veronika Demcakova, Jana Sedlakova-Kadukova</b> BIOLOGICALLY SYNTHESIZED SILVER NANOPARTICLES: IMMUNE SYSTEM MODULATION AND BIOMEDICAL POTENTIAL.....	68
<b>Lenka Demková, Lenka Bobuľská, Július Árvay</b> EVALUATION OF BIOCHEMICAL PROPERTIES AND POTENTIALLY TOXIC ELEMENTS IN THE SEDIMENT OF THE SUBTERRANEAN SYSTEM OF THE BRESTOVSKÁ CAVE.....	72
<b>Bence Farkas, Martin Urík</b> EVALUATION OF MANGANESE BIOEXTRACTION POTENTIAL OF MICROSCOPIC FILAMENTOUS FUNGUS.....	80

<b>Rebeka Frueholz, Michael Wasner, Sabine Spiess, Marianne Haberbauer</b> PHOS4PLANT: RECYCLING OF SEWAGE SLUDGE ASH INTO PHOSPHATE-RICH PLANT FERTILIZER.....	84
<b>Zuzana Goneková, Martin Urik, Rebeka Kósaová, Bence Farkas, Marcel B. Migliorini</b> EVALUATION OF FERRIC MINERALS'S STABILITY IN THE PRESENCE OF FILAMENTOUS FUNGI - CHALLENGING THE EXPECTATIONS.....	88
<b>Lenka Hagarová, Daniel Kupka, Zuzana Bártoová</b> MORPHOLOGICAL AND ELEMENTAL EVALUATION OF TETRAHEDRITE GRAINS BEFORE AND AFTER BIOLEACHING.....	92
<b>Richard Hančinský, Laura Žideková, Monika Šutáková, Pavol Hauptvogel, Zuzana Gerši, Ildikó Matušíková</b> RESPONSE OF PATHOGENESIS RELATED PROTEINS TO COMBINED STRESS IN WHEAT.....	96
<b>Pavol Hlubina, Richard Hančinský, Daniel Mihálik, Pavol Hauptvogel, René Hauptvogel, Ildikó Matušíková</b> POTENTIAL OF MYCORRHIZAL FUNGI IN THE EXTRACTION OF METALS FROM SOIL.....	102
<b>Hana Horváthová, Lubomír Jurkovič, Tomáš Faragó, Michaela Marníková</b> BIOLEACHING OF POTENTIALLY TOXIC ELEMENTS FROM CONTAMINATED GEOMATERIALS OF FORMER MINING SITE MEDZIBROD.....	108
<b>Magdalena Jabłońska-Czapla, George Yandem, Joanna Willner</b> CHALLENGES, FUTURE OUTLOOK AND ENVIRONMENTAL RISKS ASSOCIATED WITH THE USE OF PHOTOVOLTAIC TECHNOLOGY AS ALTERNATIVE ENERGY SOURCES IN THE CONTEXT OF SMART CITIES IN POLAND.....	114
<b>Iva Janáková, Vladimír Čablík, Josef Škvarka, Sarah Janštoová</b> BIOLEACHING OF PLATINUM FROM TAILINGS IN THE KRUŠNÉ HORY MOUNTAINS..	118
<b>Eberhard Janneck, Mirko Martin, Christine Stevens, Sabrina Hedrich</b> DEVELOPMENT OF PASSIVE MINE WATER TREATMENT SCHEMES WITH THE APPLICATION OF MICROBIAL SULFATE REDUCTION IN A VERTICAL FLOW BIOREACTOR.....	124
<b>Natália Kabaňová, Zita Tokárová</b> PROPOSAL OF THE LITHIUM-THIONYL CHLORIDE WASTE DETECTION FROM UNCONSUMED LIBS.....	130
<b>Waldemar Kępys, Małgorzata Śliwka, Małgorzata Pawul</b> NATURE-BASED RECOVERY OF METAL-POOR POST-PRODUCTION WASTES.....	136
<b>Anna Khachatryan, Narine Vardanyan, Zaruhi Melkonyan, Ruiyong Zhang, Arevik Vardanyan</b> DEVELOPMENT OF COPPER RECOVERY PROCESS FROM CALCOCITE-DOMINATED FLOTATION CONCENTRATE.....	144
<b>Anna Khachatryan, Narine Vardanyan, Zaruhi Melkonyan, Ruiyong Zhang, Arevik Vardanyan</b> INDIGENOUS ASSOCIATION PERSPECTIVE FOR COPPER BIOLEACHING.....	150
<b>Alexandra Kinder, Pavol Hlubina, René Hauptvogel, Pavol Hauptvogel, Ildikó Matušíková</b> INFLUENCE OF FACTORS ON ZINC INTAKE IN SELECTED VARIETIES OF <i>TRITICUM DURUM</i> FOR IMPROVING NUTRITION IN POPULATIONS.....	156
<b>Daniel Kupka, Lenka Hagarová, Zuzana Bártoová, Lucia Ivaničová</b> GROWTH YIELD OF AUTOTROPHIC Fe-OXIDIZERS ON FERROUS IRON AND TETRAHEDRITE.....	160
<b>Alena Luptáková, Magdaléna Bálintová, Oľga Šestinová, Daniela Guglietta, Stefano Ubaldini, Miloslav Lupták</b> BIOLEACHING OF MINE WASTES FROM THE ABANDONED MINING DEPOSITS IN SLOVAKIA.....	170

<b>Eva Mačingová, Daniel Kupka, Alena Luptáková, Dávid Jáger</b> BIOLEACHING OF TETRAHEDRITE FROM THE STRIEBORNÁ VEIN OF THE ROŽŇAVA ORE FIELD.....	176
<b>Valéria Máдай-Üveges, Lisani Nimira Budagodage, Ljudmilla Bokányi</b> APPLICATION OF HAMILTON INCYTE SENSOR FOR THE MICROBIAL INHIBITION ANALYSIS OF <i>ACIDITHIOBACILLUS FERRIDURANS</i> BACTERIA.....	182
<b>Martin Mandl, Jiří Kučera, Jitka Vechetová</b> SUBSTRATE LIMITATION IN BIOLEACHING CULTURES OF SULFUR-OXIDIZING BACTERIA.....	190
<b>Mária Pavlovičová, Simona Ilavská, Richard Hančinský, Pavol Hauptvogel, Ildikó Matušiková</b> CHITINASES ARE ACTIVE IN FLAX IN PRESENCE OF TOXIC METALS AND MIGHT INDICATE PHYTOREMEDIATION POTENTIAL.....	192
<b>Małgorzata Pawul, Waldemar Kępys, Małgorzata Śliwka</b> BIOLOGICAL METHODS OF METAL RECOVERY FROM MINERAL WASTE AND METAL-POOR ORES.....	198
<b>Mariola Saternus, Magdalena Lisińska</b> POSSIBILITY OF RECOVERING METALS FROM USED ELECTRONIC EQUIPMENT.....	204
<b>Jana Sedlakova-Kadukova, Veronika Demcakova</b> STABILITY OF BIOLOGICALLY PRODUCED SILVER NANOPARTICLES IN VARIOUS ENVIRONMENTS.....	208
<b>Anna Sieber, Nora Schönberger, Franziska Lederer, Doris Ribitsch, Georg M. Guebitz</b> IDENTIFICATION OF HIGHLY SPECIFIC METAL-BINDING PEPTIDES FOR THE SELECTIVE RECOVERY OF METALS FROM WASTE STREAMS.....	212
<b>Miroslava Sincak, Jozef Nosek, Alena Luptakova, Petr Jandacka, Miloslav Luptak, Jana Sedlakova-Kadukova</b> INVESTIGATING MITOCHONDRIAL CONTRIBUTIONS TO MAGNETORECEPTION IN <i>SACCHAROMYCES CEREVISIAE</i> AND THEIR POTENTIAL BIOTECHNOLOGICAL APPLICATIONS UNDER VARIED MAGNETIC FIELDS.....	216
<b>Oľga Šestinová, Lenka Findoráková, Jozef Hančulák</b> INDUSTRIAL EMISSION IMPACT ON METAL ACCUMULATION IN PARK-SOILS USING EKOTOXICITY TESTS ASSOCIATED WITH THE SOIL ORGANIC MATTER ASSESSMENT.....	220
<b>Małgorzata Śliwka, Małgorzata Pawul, Waldemar Kępys</b> RECOVERY OF METALS FROM MINERAL WASTE USING PHYTOREMEDIATION SUPPORTED BY COHERENT LIGHT STIMULATION.....	230
<b>Veronika Špirová, Tomáš Faragó, Peter Hlaváč, Martina Vítková, Szimona Zarzsevszkij, Lubomír Jurkovič</b> GEOCHEMICAL FRACTIONATION OF ARSENIC AND ANTIMONY IN CO-CONTAMINATED SOILS IN A FORMER MINING AREA IN PEZINOK, SLOVAKIA.....	236
<b>Lesław Świerczek, Jan Cebula, Adam Cenian</b> APPLICATION OF GAS NANOBUBBLES IN WASTEWATER TREATMENT AND METHANE DIGESTION: ADVANTAGES AND CHALLENGES.....	244
<b>Marcela Tlčíková, Hana Horváthová, Viktorie Víchová, Lubomír Jurkovič</b> IRON BIONANOPARTICLES (Fe-BNPs) DERIVED FROM GRAPE POMACE.....	252
<b>Arevik Vardanyan, Narine Vardanyan, Anna Khachatryan, Nelli Abrahamyan, Zaruhi Melkonyan</b> TWO-STAGE ECO-FRIENDLY APPROACH FOR RECOVERY OF COPPER FROM PRINTED CIRCUIT BOARDS (PCBs).....	258
<b>Joanna Willner, Agnieszka Fornalczyk, Rafał Zawisz</b> PRELIMINARY STUDY ON COPPER ADSORPTION FROM AQUEOUS SOLUTIONS USING WASTE CORDIERITE.....	264

<b>Slovak Academy of Sciences</b>	
Institute of Geotechnics.....	268
<b>University of Ss. Cyril and Methodius in Trnava</b>	
Faculty of Natural Sciences.....	269
<b>ALGAJAS s.r.o.</b> .....	270
Sponsors.....	271
Photos.....	273

# RECOVERY OF GOLD AND CRITICAL ELEMENTS FROM E-WASTE USING A BIOTECHNICAL APPROACH

**Mahdi Amiribostanabad<sup>a</sup>**

<sup>a</sup> G.E.O.S. Ingenieurgesellschaft mbH, Schwarze Kiefern 2, 09633 Halsbrücke, Germany,  
m.amiribostanabad@geosfreiberg.de

## Abstract

Following the trajectory of an energy transition in the world, the ever-growing demand for key critical elements and considering the modernised economy, the European Union's Parliament has recently adopted the "CRMA" - Critical Raw Material Act, to support strategic autonomy, to diversify the EU's critical raw material supply and to strengthen recycling and circularity. In this context, the INN4MIN project has tested an optimised approach to recover gold, copper, zinc, tin and other metals from PCB (printed circuit boards). To de-solder the respective components of the PCB a combined chemical-biotechnical approach was adopted. Ferric iron solution was used to transform the solder metals, tin and lead into oxide respectively sulphate. In parallel, metals like copper, iron, nickel, cobalt, silver and zinc are dissolved and can be recovered from the solution. Iron-oxidising bacteria in an aerated bioreactor were used to regenerate the ferric iron. The process can take up to 25 days, depending on the concentration of the iron sulphate and can be improved by pre-treatment of conformal coating removal from some components.

Notwithstanding of a relatively long residence time, approximately 99 % of the above-mentioned metals can be recovered in an environmentally friendly manner. The gold, after being separated from the respective components, can be further processed using "greener" leaching reagents like solution of thiourea and ferric sulphate. Depending on the influencing parameters, including the temperature and concentration of the individual components, as well as the pH and Eh conditions, the gold recovery varies between 60 and 70 per cent.

**Keywords:** PCB, Bio-leaching, gold, circular economy, critical raw material

## 1 Introduction

Regular access to raw materials is crucial for industries and the internal market, not only in Europe but also in the world, which requires the countries to secure a sustainable supply of critical raw materials and to try to anticipate and identify the relevant supply risks in order to take appropriate action [1].

Considering the scarcity of many elements in the earth, as well as the environmental impacts resulting from exploration activities, coupled with the rapidly growing battery industry, has highlighted the importance of developing new optimised and environmentally friendly approaches on "Circular Economy" and having a closer look at viable substitutes to provide safe, reliable and resilient critical raw materials.

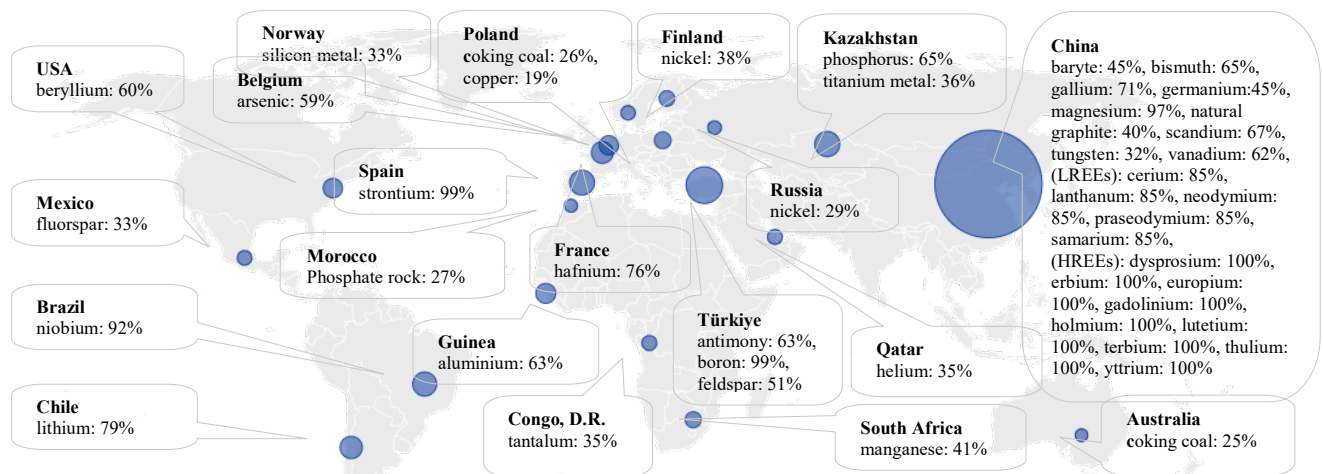


Fig. 1. Major EU suppliers of CRMs (edited) [6]

As the EU is highly dependent on imports of raw materials from third countries, e.g. China as the main supplier of raw materials to EU (Table 1), the European Council after a series of communications from 2008 on “the raw materials initiative” came up with the idea of “substitution, recycling and domestic extraction”, which finally entered into force in May 2024 as “the critical raw materials act” [1-5].

**Table 1. The EU dependency of critical raw materials on China (May 2024), as the main supplier for Europe [1]**

Ba	Bi	Ga	Ge	Mg	C	Sc	W	V	low REE	heavy REE
46 %	65 %	71 %	45 %	97 %	40 %	67 %	32 %	62 %	85 %	100 %

In light of the aforementioned considerations, it is evident that the economic and strategic role of waste cannot be overlooked. The volatility of market prices for raw materials, the depletion of easily accessible deposits and the importance of recycling all contribute to this conclusion. Waste electrical and electronic equipment (WEEE) and discarded printed circuit boards represent a viable source of certain raw materials, including copper, nickel, zinc, tin, gold and silver, among others [7].

In regard to the composition of WEEE, a considerable body of research has been conducted, yielding comparable findings. Figure 2 represents a comparative analysis of four studies examining the composition of WEEE, as referenced in [7-10].

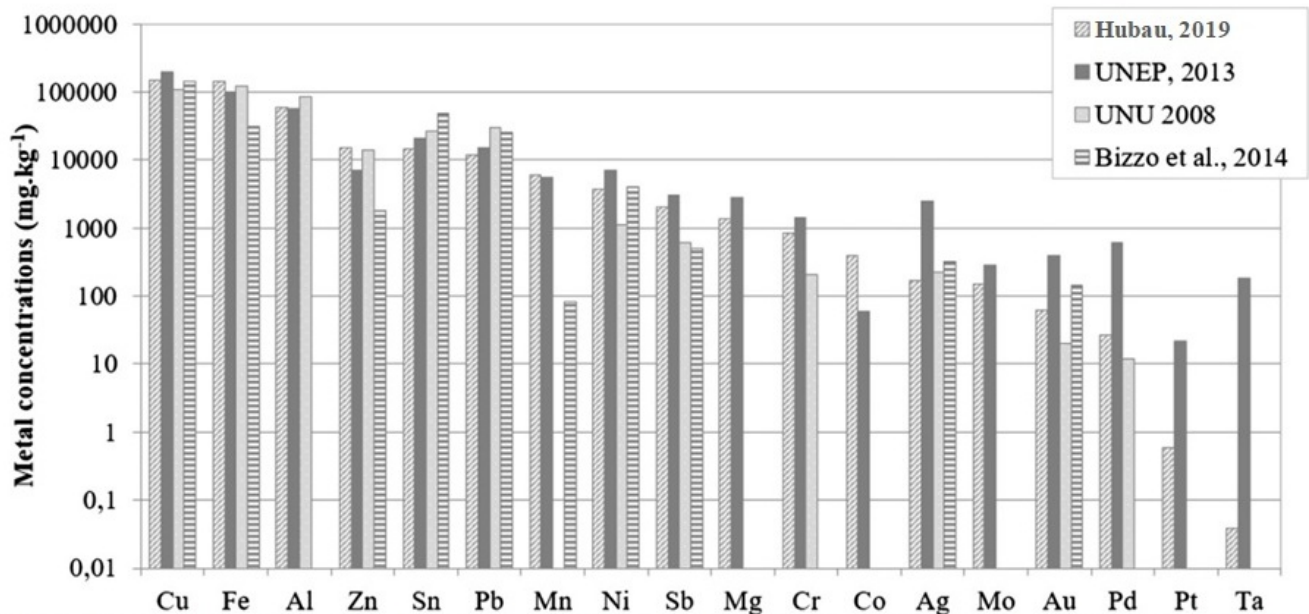


**Fig. 2. Comparison of metal concentrations in waste printed circuit boards from different studies (edited after Hubau, 2019) [7-10]**

It should be noted that the primary objective of the studies conducted as part of the INN4MIN project was identify an environmentally sustainable method for the recovery of gold from PCBs and gold ores. However, the recovery of other metals, such as iron, copper, zinc, tin, and aluminium, is necessary prior to the recovery of gold due to the significant difference in standard potential between gold and these other metals.

In order to gain access to the entirety of PCBs, it is first necessary to undertake a disassembly process or mechanical pre-treatment. This may entail crushing, grinding, magnetic separation, electrostatic separation or gravimetric separation [12]. Nevertheless, the utilisation of ferric sulphate as an oxidising reagent obviates the necessity for this step, as ferric sulphate would oxidise the tin/lead solder and dismantle the components from the PCB. However, in order to oxidise the copper traces in PCBs, the conformal coating (lacquer) must first be removed.

Pyrometallurgy, as a general approach to the recovery of metals from PCB, has both advantages and disadvantages. As [11] provided an exhaustive review of this method, the recovery of copper as the primary metal will result in a significant loss of other metals in the slag. Additionally, the process requires a considerable amount of energy [13], and the use of molten salts to dissolve and destroy plastics without oxidising the metals eliminates the necessity for mechanical treatment [12].

The current study is about finding an environmentally friendly and economic plausible approach to be replaced with using cyanide containing solutions to dissolve and recovery of the gold from primary resources as gold containing minerals and secondary resources as being called urban mining to recover gold from PCBs.

Ferric sulphate has been proposed by [14] in a patented approach being used to oxidize and remove the solders, by which the components would be off from the PCB. In this method the ferric from of iron was used as a strong reagent to oxidize the metals in solder, then ferric iron would have been reduced to ferrous, which will be oxidized again by means of iron oxidizing bacteria, i.e. *Leptospirillum ferriphilum* or *Acidithiobacillus ferrooxidans*, as well as providing an optimum environment based on [15], e.g. the proper temperature, necessity of agitation and the relevant medium for specific type of bacteria, then forming a cyclic process and bringing the oxidizing reagent back to the process [14].

Nevertheless, in this study the described methodology from [14] has been further developed in a way that all metals will be dissolved, except for silver and gold, which need one more step to complete the cycle of recycling precious metals from PCBs.

Replacement of the cyanide-based solutions by the thiourea-based lixivants has been researched and developed in a number of research projects to bring the gold from PCBs in the solution and recover it.

By application of a mix solution containing thiourea, thiocyanate and ferric sulphate was the gold leaching in many different conditions analysed, e.g. different pH values and temperatures as well as different concentration of lixivants components, in which a very promising result has been reached [16].

In another literature, instead of thiocyanate it was sulphuric acid has been used to adjust the pH. Either by this method different affecting parameters have been studied and an optimum concentration as well as optimum environment have been determined. By using this mix solution, formamidine disulphide as the side product plays an important role in terms of gold leaching [17].

After all, in this study it was attempted to find an optimized approach to work on and recovery of all corresponding metals from the PCBs, in which an about 97 % efficiency on gold recovery has been reached.

## 2 Material and methods

### 2.1 Sample preparation

E-waste samples as being tens of out-dated printed circuit boards were collected from TDE-recycling GmbH and ARG - Recuperação de Metais and some of traditional and innovative novel approaches have been employed to prepare samples for running the characterisation analyses and recovery tests.

The comminution stage is generally the first step being used as a common industrial procedure to reduce the size and study mass ration, in order to begin with the process and making it possible to have access to all parts of the sample, known as the Umicore Procedure [7, 18]. However, in this study a hot air device has been employed to have the solder molten and set the component free from the board. Which made it easier to categorize the parts of PCB in different groups, namely 1) pins and CPU, 2) electrolytic capacitors, 3) adaptors and ports and 4) plastic components.

Next, as it is explained in literature, those different groups were digested first with hydrochloric acid and nitric acid, followed by digestion with the aqua regia dissolving the gold content and other value metals that were not dissolved [7]. Also, the parts made out of plastic were just weighted to be added later on to have a total mass of a processed PCB.

### 2.2 Pyrolyzing

As mentioned above, by means of hot air the pins, CPU and other components were de-soldered and prepared for the acidic digestion step. Although, using the hot air was practically helpful, but due to the conformal coating covering the board, having access to the copper content was not possible, by which it was required another step to be added. There are possible alternatives, to shred the board, or to scratch the surface and remove the coating material, which would not help in the case confronting multi-layered motherboard.

Therefore, to analyse the board, one possible way is to pyrolyze. Thus, one sample board has been heated up by 800 °C for 2 hours, then milled with mortar and pestle to homogenize the particles and then dissolved in nitric acid and send for analyses (ICP-MS or ICP-AES).

### 2.3 Leaching solutions

In terms of providing a reference characteristic of PCBs and their general composition, it was necessary to begin with the common industrial method, by which the efficiency was already approved. The

highly concentrated acids as being hydrochloric acid and nitric acid and aqua regia were used to dissolve all anticipated valuable metals.

Nevertheless, the method of leaching in this study was completely different than usual methods. It means, an already available leaching solution containing ca. 43 g/L ferric iron was used to test the accountability of the hypothesis suggested by Monneron et al. 2020 [14]. First the goal was to de-solder the components on PCB, as it was described in the literature [14].

After getting promising results from using the mentioned leaching solution, the experiment was further developed targeting all of possibly solvable valuable metals out of PCBs, i.e. Fe, Cu, Sb, Al, Ni, Pb, Sn, Zn, Ag, Au and Pd among others. Doing so, at a certain amount of time, depending on different influencing parameters such as temperature, pH-level and concentration of leaching solution, all of considered metals were dissolved, except for Pd, Ag and Au.

The advantage of using ferric sulphate as a strong oxidizing reagent was its bio-recoverability, i.e. the reduced iron in the leaching lixiviant was again oxidized by certain microorganisms and bacteria.

Afterward, to process the rest metals, that were not reacted with the leaching solution, two different leaching solutions have been used [16, 17], each containing thiourea as the main component. By which approx. 97 % gold recovery was obtained.

#### **2.4 Tin oxide dissolution in hydrochloric acid**

After processing the PCB in the leaching solution, after all possible metals being dissolved, there are yellow-light brownish solids remaining at the bottom. These sedimented solids contain mostly Sn, Fe and Cu, but also small amount of Au, Ag, Ni and Zn.

They will be processed with a solution containing thiourea to dissolve the gold.

#### **2.5 Copper extraction**

In this study, it was supposed to prepare a certain amount of ferric sulphate at the beginning, and put it in a cyclic reaction with iron oxidizing bacteria and then again being used as an active oxidizing reagent back in to the process.

However, the copper content in the solution could play as a toxic element to the iron oxidizing bacteria (IOB). Therefore, after the iron content was almost reduced forming ferrous sulphate, the copper content should have been precipitated via electrolysis, then being transferred to the next container and let react with microorganisms.

#### **2.6 Gold containing tin oxide**

As it was briefly mentioned, the tin oxide deposits should be prepared to have been processed in a thiourea containing solution, in order to separate and dissolve the gold content.

To do so, two different thiourea containing solutions were prepared and used in analyses. Since the thiourea plays the main role as an oxidizing agent to process gold, both solutions were resulted in a very promising result.

It should be noted though, the other metals were dissolved in the solution as well, except for silver, which should be processed in a selective mode of using the same lixiviant. The metals should be selectively let react with this mentioned lixiviant according to their different electrochemical potentials [16, 17].

### **3 Results and discussion**

#### **3.1 General characterization of PCBs**

The samples were first analyzed by considering the mass balance in general. Three different PCBs were selected, i.e. the producing company and the color was the basis to differentiate them, following by disassembly by means of hot air to de-solder components from the mainboard.

Using hot air actually works in practice very well, but the problem was the respective energy consumption by doing so and working in a larger scale. However, to have a preliminary data, it was of the most necessities to use hot air, otherwise by the approach as “comminution or size reduction”, it was not possible to get the information about the value parts and the plastic containing components.

Nevertheless, after getting the first results regarding the mass balance (Table 2), each PCB was categorized into 5 different sections, as:

- a) mainboard (which contains mostly of Cu-traces and plastic),
- b) pins and CPU (the highest gold content plus other metals, Au, Cu, Pb, Ni, Zn and Sn),



- c) electrolytic capacitors (mostly out of Al and Ta),
- d) adapters and ports (mostly plastic, and pins),
- e) plastic (not considering the plastic content in mainboard).

**Table 2. The general characterization of three randomly selected PCBs**

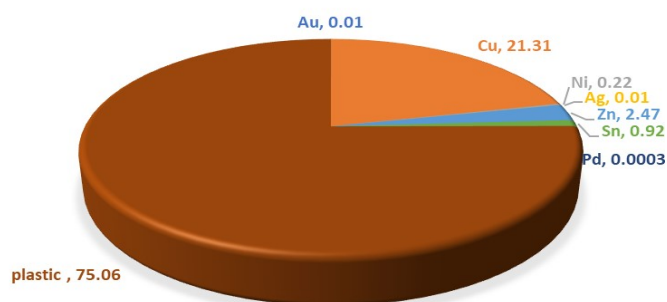
	Mainboard	Pins + CPU	Electrolytic capacitors	Adapters & ports	Plastic	Total mass
	[g]	[g]	[g]	[g]	[g]	[g]
LP1	264.2	66.3	43.7	129.9	125	629.1
LP2	264.7	78.4	46.4	139.4	142	670.9
LP3	280.7	69.4	52.2	132.7	117.8	652.8
[g]	269.9	71.4	47.4	134.0	128.3	650.9
[%]	<b>41.5</b>	<b>11.0</b>	<b>7.3</b>	<b>20.6</b>	<b>19.7</b>	<b>100.0</b>

The mainboard contains the copper traces, obviously. But there are two problems about it on the recycling process. To increase the heat stability of mainboard, they were conditioned in epoxy resin, which inhibits its reactivity with leaching solutions, later on. Hence, the mainboard was cut in small pieces with a metal scissor.

Apart from the plastic part, the electrolytic capacitors were digested in hydrochloric acid and other three groups, namely pins and CPU, adapters and ports and mainboard pieces were digested in nitric acid. There were some parts that were not reacted with acids completely, thus the aqua regia was in the last stage used to digest all metals possibly.

Initially was it important how the metals are distributed in different components of the randomly selected PCBs. After having the samples analyzed, the composition of a random PCB determined as follows:

According to the results, a random PCB is made out of plastic (fiber glass, epoxy resin) (75.06 %), Cu (21.3 %), Zn (2.5 %), Ni (0.22 %), Sn (0.92 %), Pd (0.0003 %), Au (0.0077 %) and Ag (0.0073 %) (Figure 3).

**Fig. 3. Calculated share of each analysed element in a random PCB (in W%)**

## 3.2 Bio-Leaching

### 3.2.1 De-Soldering by means of ferric iron and bacteria

Ferric sulphate is known as an active oxidizing agent. As it is already discussed, Monneron-Enaud 2020 [14] has articulated processing the solder with ferric sulphate, followed by using iron oxidizing bacteria to put iron back in the cycle, after it being reduced.

According to the results in this study, ferric sulphate can act as a strong oxidant and oxidize Sn and probable Pb and Zn contents in the solder and dismantle the components. However, depending on the provided condition, including the iron concentration, pH and the temperature, the kinetics could be influenced enormously.

This study has begun by using a small piece of a PCB (ca. 6 g) putting in a ferric sulphate solution (55 ml), containing ca. 43 g/L iron (Figure 4).

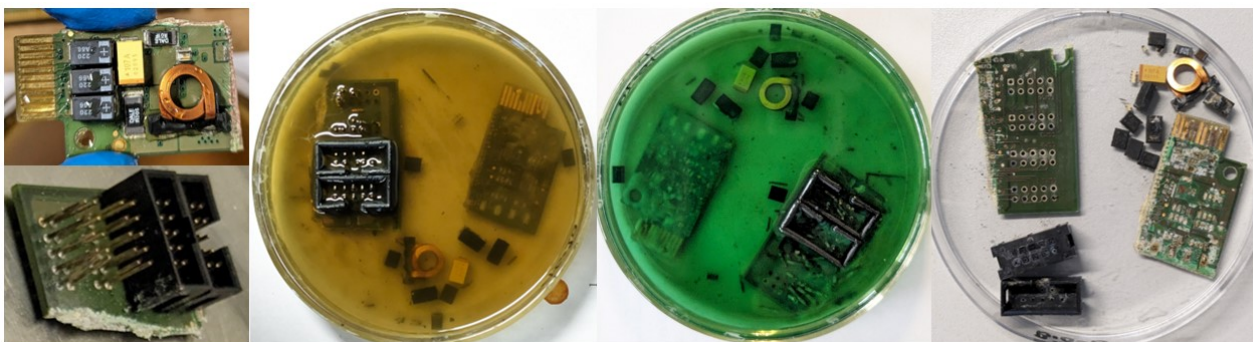


**Fig. 4. Running preliminary experiment using ferric sulphate as an active reagent**

As it is recognizable, after iron was completely reduced, the solder was digested in ferric sulphate, including other metals, there was some small metal parts, could be processed by ferric sulphate, the solution and ferric iron content should had been refreshed though, but so far that was not the point to consider.

It is obvious on the picture, the gold plated connector has not reacted with ferric sulphate, either has the copper content of toroidal inductor not reacted. In the latter case, the toroidal inductor was coated with somehow similar to epoxy resin coating material, which inhibited the access of the solution to the material.

At this stage, as you can determine from the picture, the both two different types of solder have been tested. So, both types have reacted with lixiviant and digested, but surface bridge solder reacts much faster.

### 3.2.2 Bioleaching of the PCB

After that the effectivity was approved, another parameter was considered, which was the time. The aim was to know, how long it would take to process a PCB and oxidize the reduced iron, simultaneously. Four different PCBs have cut in half and the 8 pieces of PCBs put in a ferric sulphate solution as a lixiviant. This time, a mix culture of two different iron oxidizing bacteria, i.e. *Acidithiobacillus ferrooxidans* and *Leptospirillum ferriphilum*, has been adapted and added to the lixiviant. To feed bacteria a list of different salts has been used, which was according to the reference from so called “HBS medium”. An air compressor was also used to provide the oxygen needed by microorganisms.

Five PCBs with the total mass of 2637.9 g were positioned in 6657.5 l of the leaching solution. The parameters pH, redox potential and electric conductivity, ferric/ferrous ratio, and the number of cells of bacteria in the leaching solution were monitored for a month.

Depending on the activities of the bacteria ferrous concentration was fluctuating between 15 - 25 g/L, and the cells number was also between 6.0E+08 to 1.5E+09 cells/l. The pH value was kept between 1.5 - 2.0 with sulphuric acid (this was the optimum pH range to have a better performance from the bacteria.). The temperature was around 35 °C and redox potential was 705 mV at the beginning, which during the experiment was fluctuating between 700 to 600 mV, at the lowest point. Electric conductivity was 44 mS/cm, which was almost unchanged at the end.

The copper could be toxic for the activity of microorganisms; thus, the copper was deposited off from the solution by using electrolyse cells. This was an effective approach regarding the fact that by employing electrolyse cells and applying such a low voltage (1.5 V, 0.5 A) would not disturb bacteria.

After only one day, the colour of the solution was changed to bright green, showing the iron reduction. The analyses on the solution after 24 h have indicated ca. 2.1 g/L Zn and 144 mg/L dissolution, which was logically acceptable, since at the beginning the solder should had been digested and dissolved in the solution (Table 3). However, the tin was precipitating, by which the gold pieces after being released from other elements, which were dissolved in the solution, was co-precipitating with tin oxide, which was approved at the end of the experiment by collecting and analysing the brownish sediments.

The electrolyse cells were providing a perfect effectivity on the copper deposition, however, at the end and after having the last sample analysed, there were still 6.6 g/L copper in the solution. Also, some of iron content was co-precipitated with tin oxide (Table 3).

**Table 3. The analyses on the last sample after one month bioleahcing of PCBs**

	Fe	Cu	Ni	Zn	Sn	Pb
mg/L	30500	6650	635	8350	325	12.75

By making a comparison between the metal concentrations in the leaching solution and the source values in a random PCB (i.e. data from Figure 3), it shows that only 8 percent copper after using electrolyse cells was still left in the solution. The preliminary results showed so far that 72 % Ni, 84 % Zn and 91.3 % Sn (as precipitant) were recovered.

This test has given a very promising performance of using ferric sulphate and microorganisms parallel with copper electrolyses. Afterwards, the sedimented tin oxide with impurities of gold, silver, iron and zinc were air dried and prepared for gold recovery.

**Table 4. The metal recovery performance at the end of the test, compared with the data from Figure 3**

Composition	Au	Cu	Ni	Ag	Zn	Sn	Pd	Plastic
[%]	0.0077	21.3	0.22	0.0073	2.5	0.92	0.0003	75.1
[g] in 6657 mL		44.3	4.2		55.6	2.2		
[%] recovered in the solution		1.7	0.16		2.1	0.08		

### 3.3 Gold recovery

According to the observations of the rest of leached solid materials (the leached PCBs and the sedimented tin oxide), the copper traces were partly reacted with the lixiviant, which was due to coating material covering them, and all other metal containing parts were completely reacted and dissolved in the lixiviant, i.e. the gold was just detached from the components and settled with tin oxide sediments in the bottom of the glass. Nevertheless, the main objective in this study was the gold recovery.

To process the gold, as it was mentioned before, there were two alternatives. Both of them included the ferric sulphate and thiourea (Tu) (in different concentrations), but in one of them was the sulfuric acid used to adjust the pH and in other one thiocyanate was used for its complexation features and synergistic effects with thiourea.

The main oxidant reagent in both approaches was ferric sulphate, by which the main role was to oxidizing thiourea, which after that was forming a complex with gold and bringing it in the solution. The composition of the lixiviants was as follows:

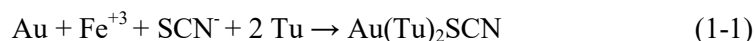
Lixiviant 01 [16]:

- SCN<sup>-</sup> 0.005 M
- Tu 10 mM
- Ferric sulphate 0.055 M
- pH 1.5
- Temp. 35 °C

Lixiviant 02 [17]:

- Tu 42 g/L
- Ferric sulphate 9 g/L
- Sulfuric acid 0.1 M
- Temp. 20 °C

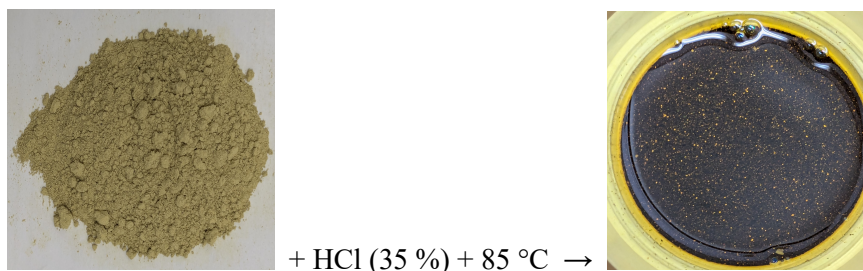
By using the first solution (lixiviant 01) the probable reaction would be [16]:



To describe the chemical equation 1-1 regarding the lixiviant 01, ferric sulphate provides the oxidation features, thiocyanate leads the complexation features, which in parallel with thiourea generates synergistic effect, also thiourea itself can improve the half reaction in gold oxidation procedure [16].

On the other side, in lixiviant 02, ferric iron would oxidize thiourea, by which a temporary side product called formamidine disulphide would be generated, which acts as a gold oxidant, which is not stable and the sulfur would precipitate and cover the sample surface which could partly hinder the reaction progression [17].

There were multiple experiments have been conducted to mobilize the tin content, due to its hinderance properties while it was attempted to process the gold with acids. Using concentrated hydrochloric acid by high temperature (85 °C) helped though to have a better (still mixed) product containing gold, but regarding the energy consumption, it was not plausible.

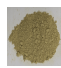


**Fig.5. Using heated hydrochloric acid to remove the impurities (tin oxide) out of the sedimented material**

To process the deposited material with proposed solutions, and to leach the gold content, both lixiviant have been prepared. A piece of pure gold strip has been taken as a blind sample and next sample was the gold containing light brown powder (Au-powder) (Figure 5 left hand side).

The composition of the Au-powder was determined before running the test (Table 5), by dissolving it in aqua regia solution. By doing so, it was possible to compare the kinetics of gold leaching by taking the piece of gold, as well as monitoring its behavior next to tin oxide.

**Table 5. Chemical composition of Au-powder (i.e. gold containing sedimented tin oxide)**

	Fe	Au	Cu	Ni	Ag	Zn	Sn
[mg/kg]	151000	469	8420	1300	81	1200	101000

In order to get a better understanding about influence of surface area on material digestion performance, the test was conducted using either a solid piece of gold as well as gold powder, which was produced by rubbing the gold piece on a sand paper.

By using the lixiviant 01 and after one week from the beginning of the test, about 78 % of the gold in the sample tin oxide powder were dissolved, which was a very promising result. However, the test duration was longer than the expected timeline. Nevertheless, the test has been kept running for a month, by which the result was shockingly disappointing, the ration was returned back to 2 %. It could mean that after that all oxidant material was completely used, the gold should have been precipitated again somehow. By this experiment, it was afterwards recognised, that the iron concentration was somehow very low, which lead to the decision to run next test with lixiviant 02.

Actually, after getting incredibly better performance by using lixiviant 02, it was not again attempted to find out about the probable problem regarding the test with lixiviant 01. Thus, it is highly recommended to employ both lixiviants.

Again, it was a piece of gold strip and an aliquot of deposited tin oxide powder were used putting in the solution 02. According to the observations, only after one hour, the gold content in tin powder was dissolved.

In this case, and after about 72 hours, a gold strip piece of 28 mg was dissolved in the lixiviant 02. As it was mentioned before, the gold content in second sample (tin oxide powder) has taken only an hour to be dissolved in the solution.

#### 4 Conclusions

In this study it was at the utmost importance to use a most possible environmentally friendly approach in order to process and dissolve the gold content from primary (gold minerals) and secondary (recycling e-waste) resources.

The main material being used as an oxidant in this experiment was ferric sulphate, which can be completely regenerated after that the ferric iron being reduced to the ferrous iron by means of iron oxidizing bacteria, which is not a complicated process and works perfectly.

By using ferric sulphate, it would be possible to mobilize all value metals (except for gold and silver) from e-waste (here the PCB) into the solution and then recover them.

According to the observations during this study and the respective lab results of the chemical composition of multiple samples from the leaching solutions containing thiourea, it was determined that the thiourea being used next to the ferric sulphate, as well as manipulating the concentration rations of both chemicals, could be also used in a selective based recovery process of metals from PCB and e-waste.

The very low iron content, which was mixed with the powder during the test, as well as other valuable elements, which were the main goal of this study, such as Ni, Ag and Au were dissolved in the leaching solution, especially with a very high efficiency (96 %) of gold recovery.

However, still there are multiple questions and ambiguities, that needs to run more experiments to find out the right answer and to optimize the procedure.

## Acknowledgements

The work was supported and funded from the European Union's Horizon 2020, respectively Horizon Europe Research and Innovation programmes.

## References

- [1] European Commission Report from the commission to the European Parliament, the Council, the European Economic and Social Committee and the Committee of the Regions on the implementation of the Raw Materials Initiative, 24 (6) 2013, 19 p.
- [2] European Commission Report from the commission to the European Parliament, the Council, the European Economic and Social Committee and the Committee of the Regions on making the recovery circular and green\_ST-13852-2020-INIT\_en, 2020, 32 p.
- [3] European Commission Report from the commission to the European Parliament, the Council, the European Economic and Social Committee and the Committee of the Regions on a green deal industrial plan for the net zero age\_CELEX\_52023DC0062\_EN, 2023, 21 p.
- [4] European Commission Proposal for REGULATION OF THE EUROPEAN PARLIAMENT AND OF THE COUNCIL on establishing a framework of measures for strengthening Europe's net-zero technology products manufacturing ecosystem (Net Zero Industry Act), 2023, 87 p.
- [5] European Parliament and Council REGULATION (EU) 2024/1252 OF THE EUROPEAN PARLIAMENT AND OF THE COUNCIL establishing a framework for ensuring a secure and sustainable supply of critical raw materials and amending Regulations (EU) No 168/2013, (EU) 2018/858, (EU) 2018/1724 and (EU) 2019/1020, 2024, 67 p.
- [6] European Commission [online]. c2024 [ct. 09.08.2024]. WWW: <https://www.consilium.europa.eu/>
- [7] Hubau, A., Chagnes, A., Minier, M., Touze, S., Chapron, S., Guezennec, A.G. Recycling-oriented methodology to sample and characterize the metal composition of waste Printed Circuit Boards. *Waste Management*, 91, 2019, p. 62-71.
- [8] Reuter, M.A., Hudson, C., van Schaik, A., Heiskanen, K., Meskers, C., Hagelüken, C. Metal Recycling: Opportunities, Limits, Infrastructure. A Report of the Working Group on the Global Metal Flows to the International Resource Panel, UNEP, 2013.
- [9] United Nations University Final Report on the Review of Directive 2002/96 on Waste Electrical and Electronic Equipment (WEEE), 2008, Study No. 07010401/2006/442493/ETU/G4.
- [10] Bizzo, W.A., Figueiredo, R.A., de Andrade, V.F. Characterization of printed circuit boards for metal and energy recovery after milling and mechanical separation. *Materials*, 7, 2014, p. 4555-4566.
- [11] Cui, J., Zhang, L. Metallurgical recovery of metals from electronic waste: a review, *Journal of Hazardous Materials*, 158, 2008, p. 228-256.
- [12] Ghosh, S.K., Lee, J., Godwin, A.C., Oke, A., Al-Rawi, R., El-Hoz, M. Waste Management in USA through case studies: E-waste recycling and waste to energy plant. *Journal of Solid Waste Technology & Management*, 42 (1), 2016.
- [13] Flandinet, L., Tedjar, F., Ghattac, V., Fouletier, J. Metals recovering from waste printed circuit boards (WPCBs) using molten salts. *Journal of Hazardous Materials*, 213-214, 2012, p. 485-490.
- [14] Monneron-Enaud, B., Wiche, O., Schlömann, M. Biodismantling, a Novel Application of Bioleaching in Recycling of Electronic Wastes. *Recycling*, 5 (22), 2020, p. 1-14.
- [15] Hedrich, S., Schippers, A. Distribution of Acidophilic Microorganisms in Natural and Man-Made Acidic Environments. *Current issues in molecular biology*, 40, 2020, p. 25-48.
- [16] Yang, X., Moats, M. S., Miller, J. D., Wang, X., Shi, X., Xu, H. Thiourea–thiocyanate leaching system for gold. *Hydrometallurgy*, 106, 2011, p. 58-63.
- [17] Li, J., Miller, J.D. A review of gold leaching in acid thiourea solutions. *Mineral Processing and Extractive Metallurgy Review*, 27 (3), 2006, p. 177-214.

- [18] Hagelueken, C. Recycling of Electronic Scrap at Umicore's Integrated Metals Smelter and Refinery. *World of Metallurgy - ERZMETALL*, 59 (3), 2006, p. 152-161.



## BIOAVAILABILITY OF POTENTIALLY TOXIC ELEMENTS IN SELECTED Cu-DEPOSITS OF EUROPE

**Peter András<sup>a</sup>, Pavol Midula<sup>b</sup>, Jana Ševčíková<sup>a</sup>, Matej Šuránek<sup>a</sup>, Joao Matos<sup>c</sup>, Jana Janštová<sup>d</sup>,  
Giuseppe Buccheri<sup>e</sup>, Ján Tomaškin<sup>a</sup>, Marek Drimal<sup>a</sup>**

<sup>a</sup>Matej Bel University, Faculty of Natural Sciences, Tajovského 40, 974 01 Banská Bystrica, Slovakia,  
peter.andras@umb.sk, jana.sevcikova@umb.sk, matej.suraneck@umb.sk, jan.tomaskin@umb.sk, marel.drimal@umb.sk

<sup>b</sup>Zittau/Görlitz University of Applied Sciences, Küllzuffer 2, 02763 Zittau, Germany,  
pavol.midula@gmail.com

<sup>c</sup>Laboratório Nacional de Energia e Geologia (Portuguese Geological Survey), Portugal,  
joao.matos@Ineg.pt

<sup>d</sup>The Slovak Environment Agency, Tajovského 28, 974 01 Banská Bystrica, Slovakia,  
jana.janstvova@sazp.sk

<sup>e</sup>INAIL - Italian Workers Compensation Authority, UOT Napoli, Via Nuova Poggioreale - 80143 Napoli, Italy,  
giubuc@gmail.com

### Abstract

Bioavailability of potentially toxic elements from four dump-field material at several abandoned European Cu-deposits: Špania Dolina (Slovakia), Caporciano and Libiola (Italy) and São Domingos (Portugal) was studied. The three steps sequential analyse study show some relation among geological setting and mineralogical composition of ores vs. bioavailability of metals. The best bioavailable metals at first three mentioned deposits are Cu and Cd (in one case, at São Domingos As and Co). The results confirmed that the geological setting substantially influence the order of the bioavailability.

**Keywords:** Cu-deposits, abandoned dump-fields, potentially toxic elements, bioavailability

### 1 Introduction

The aim of the study is to compare the bioavailability of potentially toxic elements (PTEs) at dump-fields of several European abandoned Cu-deposits. Three copper deposits situated in different geological settings were studied. Špania Dolina belongs to the important Cu-deposits of Slovakia. The investigation was realized at Richrárová dump-field. The second studied deposit was the dump-field Caporciano in Val di Cecina and Libiola (Italy). For comparison was selected the area of extensive mining field in São Domingos (Portugal; Fig. 1).

The volcano-sedimentary Cu-mineralization at Špania Dolina is situated in crystalline complex of Permian age. The main exploited economically important minerals were chalcopyrite and tetrahedrite [1, 2]. The chalcopyrite, bornite and chalcocite ore body at great Caporciano mine is associated with ophiolites, formed by diabase, gabbros and serpentinites [3]. The Libiola mine is situated in the ophiolite complex. There are two types of mineralization: the first one is connected to and the second one is serpentinite hosted. The ore mineralization is represented mainly by pyrite and chalcopyrite (less also by sphalerite and pyrrhotite) [4]. São Domingos belongs to the very important world deposits. The mineralization is situated in the Iberian Pyrite Belt black shales and basic volcanics of the volcano sedimentary complex near Spanish border. The exploited ore predominantly consists of following sulphides: chalcopyrite, pyrite sphalerite, tetrahedrite and arsenopyrite. [5, 6]. The average pH at Špania Dolina is 5.29, at Caporciano 6.56, at Libiola 4.03 and in São Domingos is more acid pH = 4.29 [7].

### 2 Material and methods

At each studied locality 25 - 30 technosol samples were taken from the dump-field polygon in such a way to characterize the average dump-material. The samples were dried and mixed to get average sample. Subsequently these samples were homogenized and pulverized (80 mesh).



Fig. 1. Localization of the studied Cu-deposits (A - Špania Dolina, B - Caporciano, Libiola)

The identification of the bioavailability of selected PTEs was studied by sequential extraction procedure [8]. At first the analyzed sample was dried at 60 °C for 24 hours. 1 g of sample in 50 ml falcon tube was extracted using 5 extraction solutions: The ICP-MS analyses were realized in laboratories of TU-Bergakademie Freiberg. The analyses took the place in the laboratories of Biowissenschaften at TU-Bergakademie Freiberg (Germany). The total concentration of PTEs was measured using 100 mg of sample dissolved in aqua regia. For the sequential extraction analysis was used 1 g of technosol sample. Four steps of sequential extraction was executed: I. distilled resp. deionized water; II. 1M solution of  $\text{NH}_4\text{CH}_3\text{CO}_2$  (ammonium acetate) at pH 7; III. 0.01M  $\text{C}_6\text{H}_8\text{O}_7$  (citric acid) solution. First 2 fractions can be considered as exchangeable [9].

### 3 Results and discussion

There are interesting similarities between Špania Dolina and Caporciano. At the dump-fields of both deposits are the most bioavailable PTEs Cu and Cd, only the order of these elements at individual localities is different: at Špania Dolina is the most bioavailable metal Cu and in Caporciano and in Libiola Cd (Fig. 2). The less bioavailable PTEs in Špania Dolina are As and Co, whereas in Caporciano Co and As (Fig. 2). At Libiola decrease the bioavailability in rate:  $\text{Cu} > \text{Zn} > \text{Cd} > \text{Co} > \text{As}$ .

The results from São Domingos show the best bioavailability surprisingly for As and Co. The bioavailability decreases in rate  $\text{As} > \text{Co} > \text{Cu} > \text{Cd} > \text{Zn}$  (Fig. 2). The degree of bioavailability corresponds for example with results published by Kim [10] and Lalhruaitluanga [11].

The results show that the bioavailability is substantially influenced by geological setting, geochemical conditions (different characteristics of the rocks/technosol), pH and mineralogical forms of the present PTEs.



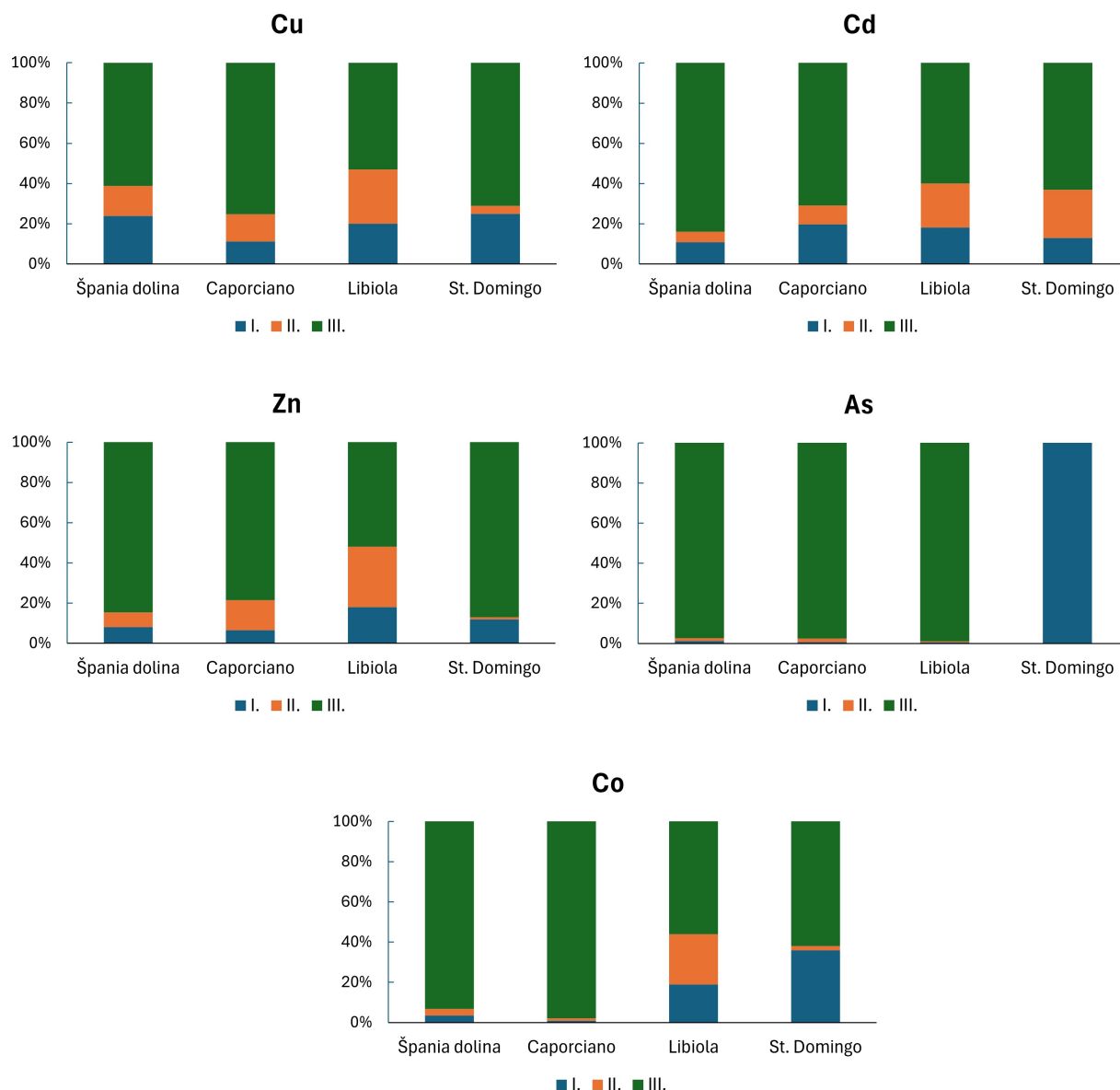


**Fig. 2. Bioavailability of PTEs at the studied deposits**  
(First 2 fractions can be consider as bioavailable)

#### 4 Conclusions

The substantial part of the bioavailable PTEs was generally released from the technosol in the deionized water and less also in 1 M solution of ammonium acetate. At first three deposits (Špania Dolina, Caporciano in Val di Cecina and Libiola) is possible distinguish generally two bioavailable PTEs: Cu and Cd. Less bioavailable are Co and Zn. Except the dump-field São Domingos the less immobile metals are As and Co. In São Domingos are the most bioavailable metals As and Co. The relationship between the bioavailable PTEs and pH was not proved.

#### Acknowledgements

The article was supported by of grant agency VEGA 1/0220/23.

#### References

- [1] Jeleň, S., Galvánek, J., Andráš, P., Križáni, I. História baníctva Španej Doliny. *Minerál*, 20 (4), 2012, p. 291-308.
- [2] Andráš, P., Jeleň, S., Ferenc, Š. Geologicko-ložisková charakteristika Cu-ložísk Špania Dolina, Staré Hory, Ľubietová a Poniky. In Andráš, P., Dirner, V., Turisová, I., Vojtková, H. *Staré báňské zátěže*

- opuštěných Cu-ložisek*. Remnants of old activity at abandoned Cu-deposits. Mendelej, Ostrava, 2013, p.123-141. ISBN 978-80-86832-75-3.
- [3] Dolfini, A., Angelini, I., Artioli, G. Copper to Tuscany - Coals to Newcastle? The dynamics of metalwork exchange in early Italy. *PLoS ONE*, 15 (1), 2020, p. 1-35.
- [4] Buccheri, G., Andráš, P., Astolfi, M.L., Canepari, S., Ciucci, M., Marino, A. Heavy metal contamination in water at Libiola abandoned copper mine, Italy. *Romanian Journal of Mineral*, 87 (1), 2014, p. 65-70.
- [5] Matos, J.X., Oliveira, D.P.S., Batista, M.J., Pereira, Z., Albardeiro, L., Morais, I., Mendes, M., Marques, F., Solá, R., Salgueiro, R., Carvalho, J., Gonçalves, P., Oliveira, J.T. Iberian Pyrite Belt Exploration. *Comunicações Geológicas*, 107, 2020, p.150.
- [6] Vieira, A., Matos, J.X., Lopes, L., Martins, R. Evaluation of the mining potential of the São Domingos mine waste, Iberian Pyrite Belt, Portugal. *Comunicações Geológicas*, 107, 2020, p. 91-100.
- [7] Andráš, P., Midula, P., Matos, J.X., Buccheri, G., Drímal, M., Dirner, V., Melichová, Z., Turisová, I. Comparison of soil contamination at the selected European copper mines. *Carpathian Journal of Earth and Environmental Sciences*, 16 (1), 2021, p. 163-174. ISSN-1842-4090.
- [8] Midula, P., Wiche, O., Wiese, P., Andráš, P. Concentration and bioavailability of toxic trace elements, germanium, and rare earth elements in contaminated areas of the Davidschacht dump-field in Freiberg (Saxony). *Freiberg ecology online*, 2, 2017, p. 101-112.
- [9] Midula, P., Wiche, O., Wiese, P., Andráš, P. Concentration and bioavailability of toxic trace elements, germanium, and rare earth elements in contaminated areas of the Davidschacht dump-field in Freiberg (Saxony). *Freiberg ecology online*, 2, 2017, p. 101-112.
- [10] Kim, R.Y., Yoon, J.K., Kim, T.S., Yang, J.E., Owens, G., Kim, K.R. Bioavailability of heavy metals in soils: definitions and practical implementation - a critical review. *Environmental Geochemistry and Health*, 37, 2015, p. 1041-1061.
- [11] Lalhruaitluanga, H., Prasad M.N.V., Radha, K. Potential of chemically activated and raw charcoals of *Melocanna baccifera* for removal of Ni(II) and Zn(II) from aqueous solutions. *Desalination*, 271 (1-3), 2011, p. 301-308.

## HEAVY METALS AND SULPHATE REMOVAL FROM MODEL SOLUTIONS USING ION EXCHANGE RESINS

**Magdalena Balintova<sup>a</sup>, Natalia Junakova<sup>a</sup>, Yelizaveta Chernysh<sup>b,c,d</sup>**

<sup>a</sup> *Institute for Sustainable and Circular Construction, Faculty of Civil Engineering, Technical University of Kosice, Vysokoskolska 4, 042 00 Kosice, Slovakia, magdalena.balintova@tuke.sk, natalia.junakova@tuke.sk*

<sup>b</sup> *2International Innovation and Applied Center "Aquatic Artery", Sumy State University, 2, Kharkivska st. 116, 40007 Sumy, Ukraine, e.chernish@ssu.edu.ua*

<sup>c</sup> *Faculty of Tropical Agrisciences, Czech University of Life Sciences Prague, Kamycka 129, Prague, 16500, State, Czech Republic*

<sup>d</sup> *Department of Water Supply and Wastewater Treatment, T. G. Masaryk Water Research Institute, Podbabska 2582/30, Prague, 16000, Czech Republic*

### Abstract

Currently, a large number of commercial resins are available for various applications, whether in the food or industrial sector. On the other hand, there is little information available in the literature to scientifically explain the effectiveness and behaviour of new commercial resins under different application conditions.

The paper deals with the study of the use of Purolite MB400 ion exchange resin for the simultaneous removal of metal cations (Cu, Zn, Fe) and sulphates from model solutions. The resin efficiency was highest for the CuSO<sub>4</sub> model solution (10 mg/L), where the Cu<sup>2+</sup> removal efficiency was 97.8 % and SO<sub>4</sub><sup>2-</sup> was 95.1 %. With increasing concentration of metals and sulphates in solutions the efficiency decreased.

**Keywords:** heavy metals, sulphate, ion exchange, Purolite MB400

### 1 Introduction

Surface waters, including rivers, lakes, and streams, are vital resources for ecosystems and human activities. However, these water bodies are increasingly subjected to contamination by various pollutants, among which heavy metals and sulphates are of significant concern [1]. While some heavy metals are essential in trace amounts for biological processes their elevated concentrations in surface waters pose serious environmental and health risks [2]. Heavy metals are not biodegradable; therefore, they tend to bioaccumulate in living organisms. They are also persistent and can directly or indirectly affect various organisms due to biomagnification. Many heavy metal ions are toxic or carcinogenic [3, 4].

Mining is one of the key sectors to be considered, particularly because it plays a central role in the economies of developed and developing countries. This activity generates a large presence of heavy metals, released due to the extraction of minerals, and transported through rivers and streams, in which they can be dissolved in water or as part of sediments. These metal species tend to seep into groundwater, and can also cause water scarcity, prevent the growth of crops due to soil erosion, and bring serious health problems on animals and local human communities [5].

Sulphates, on the other hand are naturally present in the environment, often as a result of mineral weathering. Sulphur is a vital nutrient element form for living stocks, thus sulphate is a common nutrient and naturally occurs in water and wastewaters [6]. Its concentration varies depending on the location for example, in rivers from 0 to 630 mg/L, lakes 2-250 mg/L, ground water 0-230 mg/L, sea water up to 2700 mg/L and in rain water 1-6 mg/L [7]. However, anthropogenic activities such as industrial discharges, mining, and agricultural runoff significantly increase sulphate concentrations in surface waters. Elevated sulphate levels can lead to the acidification of water bodies, which can harm aquatic life, disrupt water chemistry, and enhance the solubility of toxic metals [8].

To mitigate the environmental and health risks associated with heavy metals and sulphates in surface waters, various treatment technologies have been developed, among which ion exchange resins are particularly effective. Compared with other usual methods ion exchange provides advantages. Using ion exchange, all ions can be removed from a solution or substances [9]. Ion exchange resins are synthetic polymers capable of exchanging specific ions within a solution with ions attached to the resin. These resins can selectively remove heavy metals and sulphates from contaminated water by exchanging them with less harmful ions, such as sodium or chloride, present on the resin [10, 11]. Therefore, we can divide ion exchange resins designed for selective ions removal of contamination and complete deionization of

wastewaters. The choice of between both, depends mainly on the composition of the solution and on the extent of decontamination required. Selectivity is achieved by selected types of ion exchangers with specific affinity to definite metal ions or groups of metals. In the most cases ion exchange is replacing the undesirable ion by another one which is neutral within aquatic environment [12]. This process is highly efficient, offering the advantages of high removal capacity, reusability of the resin, and the ability to target specific contaminants. Ion exchange resins are widely used in water treatment plants and in industrial applications to purify surface waters and ensure they meet environmental standards [13, 14].

Understanding the sources, pathways, and effects of heavy metals and sulphates in surface waters, along with effective removal methods such as ion exchange resins, is crucial for developing comprehensive strategies to protect aquatic ecosystems and ensure water quality for human use.

The aim of this paper is a study of the efficiency of removing  $\text{SO}_4^{2-}$  and heavy metal ions from model solutions using Purolite MB400 ion exchange resin.

## 2 Material and methods

### 2.1 Ion exchange resin characterization

The ion exchange resin, Purolite MB400, was obtained from a commercial resin supplier in Slovakia and was used for static adsorption experiments. Purolite MB400 is a mixture of high-quality ion exchange resin used for water purification. It is suitable for usage in both regenerable and non-regenerable cartridges and large ion exchange units. The mixture is composed from an ion-balanced mixed resin in a ratio of 40 % catex to 60 % anex. This resin was developed for preparation of high purity water where 97 % of the ionex resin has a grain smaller than 0.3 mm. It is also most commonly used for the preparation of demineralized water free of silica and carbon dioxide.

### 2.2 Synthetic solutions

Copper, zinc and iron stock solutions (1,000 mg/L) were prepared by dissolving a given amount of sulphate salts (Merck, Darmstadt, Germany) in distilled water. Lower concentrations (10, 50, 100, 200, and 300 mg/L) of metals and appropriate amount of sulphates were prepared by diluting the stock solutions with distilled water.

Model solutions of  $\text{CuSO}_4$  with different initial concentrations ( $c_0$ ) of sulfate anions in the range from 100 to 2900 mg/L (10 different concentrations) were used to obtain data for mathematical modeling of adsorption isotherms. All solutions were adjusted to the desired initial  $\text{pH} \approx 4$  value with 0.001M  $\text{H}_2\text{SO}_4$ .

### 2.3 Sorption experiments

1 g of resin was mixed with 100 mL of each model solution (laboratory temperature  $t = 20 \pm 1$  °C). The reaction was carried out under static conditions in a batch adsorption system with an interaction time of 24 h. After absorption, resins were filtrated. Colorimetric method (Colorimeter DR 890, HACH Company, Loveland, USA) was applied for the determination of residual sulphate and metal concentration. The pH values of solutions were also measured with a pH meter inoLab pH 730 (WTW, Weilheim, Germany). In addition, the efficiency of ion removal was calculated using the following equation (Eq. 1),

$$\eta = \frac{(c_0 - c_e)}{c_0} \cdot 100 \quad (1)$$

where:  $\eta$  - sorption efficiency [%],  $c_0$  - the initial concentration of appropriate ions [ $\text{mg} \cdot \text{L}^{-1}$ ],  $c_e$  - equilibrium concentration of ions [ $\text{mg} \cdot \text{L}^{-1}$ ].

All adsorption experiments were performed in triplicate under batch conditions, and the results are expressed as arithmetic mean values with standard deviations.

## 3 Results and discussion

Purolite MB400 ion exchange resin was used in this experiment to determine the efficiency of removing  $\text{SO}_4^{2-}$  and heavy metal ions from model solutions using ion exchange materials. The influence of PUROLITE MB400 for removing Cu, Zn, Fe and sulphates from model solutions is shown in Table 1-3.

**Table 1. Initial concentration of Zn<sup>2+</sup> and SO<sub>4</sub><sup>2-</sup> and concentration after 24 hours of contact time with PUROLITE MB400 resin; ZnSO<sub>4</sub> solution; dosage 1 g / 100 mL**

Sample		(mg/L)				
Initial concentration	Zn <sup>2+</sup>	10	50	100	200	300
	SO <sub>4</sub> <sup>2-</sup>	14.69	73.4	146.9	293.8	440
Concentration after 24 hours	Zn <sup>2+</sup>	0.25	1.85	2.2	14	35.2
	SO <sub>4</sub> <sup>2-</sup>	0.8	3,6	4.6	16	31

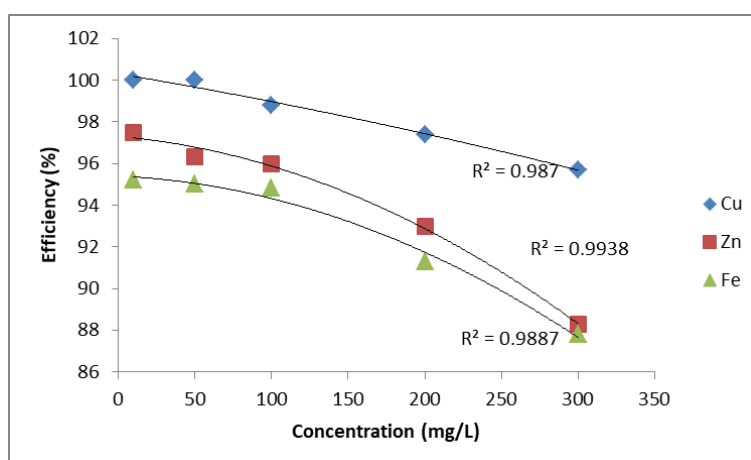
**Table 2. Initial concentration of Cu<sup>2+</sup> and SO<sub>4</sub><sup>2-</sup> and concentration after 24 hours of contact time with PUROLITE MB400 resin; CuSO<sub>4</sub> solution; dosage 1 g / 100 mL**

Sample		(mg/L)				
Initial concentration	Cu <sup>2+</sup>	10	50	100	200	300
	SO <sub>4</sub> <sup>2-</sup>	15.12	75.6	151.24	302.4	453.7
Concentration after 24 hours	Cu <sup>2+</sup>	<0.05	<0.05	1.2	5.2	13
	SO <sub>4</sub> <sup>2-</sup>	0.2	0.4	0.9	7.4	48

**Table 3. Initial concentration of Fe<sup>2+</sup> and SO<sub>4</sub><sup>2-</sup> and concentration after 24 hours of contact time with PUROLITE MB400 resin; FeSO<sub>4</sub> solution; dosage 1 g / 100 mL**

Sample		(mg/L)				
Initial concentration	Fe <sup>2+</sup>	10	50	100	200	300
	SO <sub>4</sub> <sup>2-</sup>	17.2	86.04	172.1	344.2	516.2
Concentration after 24 hours	Fe <sup>2+</sup>	0.48	2.3	3.2	17.4	36.6
	SO <sub>4</sub> <sup>2-</sup>	1.4	4.1	9	46.6	111.6

This experiments showed the possibility of removing Cu<sup>2+</sup>, Zn<sup>2+</sup>, Fe<sup>2+</sup> and SO<sub>4</sub><sup>2-</sup> ions from the model solutions using PUROLITE MB400 synthetic ion exchange resin. A comparison of removal efficiency is shown in the Fig. 1 and 2. As can be seen from Fig. 1 and Fig. 2 the resin efficiency was highest for the CuSO<sub>4</sub> model solution (10 mg/L), where the Cu<sup>2+</sup> removal efficiency was 97.8 % and SO<sub>4</sub><sup>2-</sup> was 95.1 % With increasing concentration of metals and sulphates in solutions the efficiency decreases.

**Fig. 1. Removal efficiency Zn<sup>2+</sup>, Cu<sup>2+</sup> a Fe<sup>2+</sup> using PUROLITE MB400**

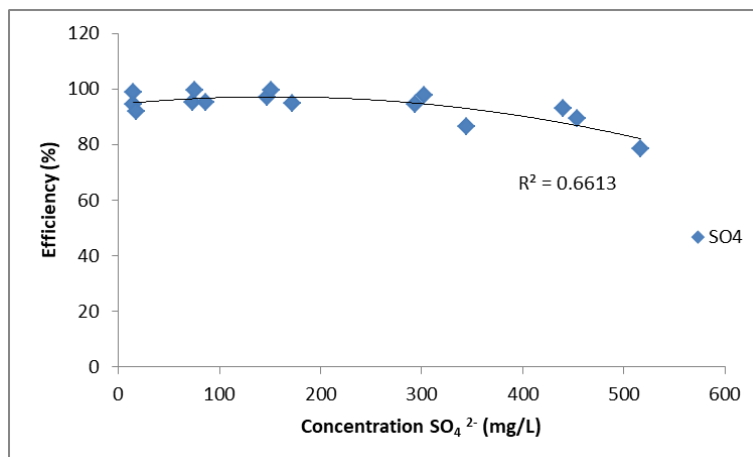


Fig. 2. Sulphate removal efficiency with PUROLITE MB400 resin; solutions  $\text{ZnSO}_4$ ,  $\text{CuSO}_4$ ,  $\text{FeSO}_4$

The pH is one of the important parameters controlling the absorption of sulphates and heavy metals from aqueous solutions. In all solutions, the initial pH of the solutions was not adjusted, but in all experiments, the pH of the solutions increased after ion exchange process. Fig. 3 shows the effect of ion exchange on the pH of  $\text{CuSO}_4$  solution for different concentrations.

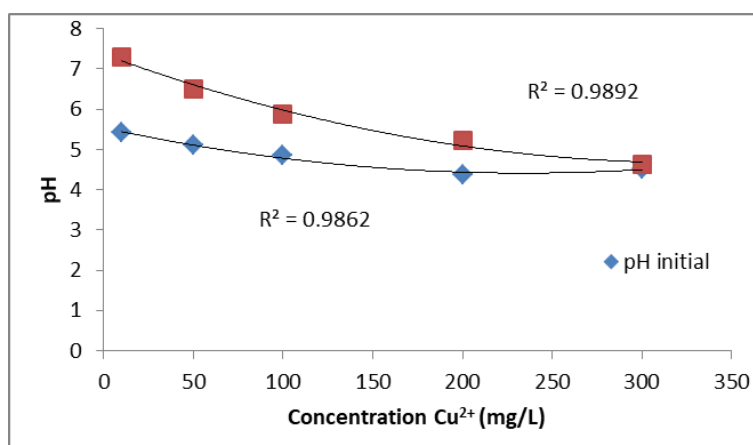


Fig. 3. Influence of ion exchange on the pH of  $\text{CuSO}_4$

#### 4 Conclusions

Ion exchange is widely used for pollutant removal from wastewater due to their many advantages, such as high treatment capacity, high removal efficiency and fast kinetics. As the experiment shows, the using Purolite MB400 ion exchange resin for sulphates and the selected cations of Zn, Cu and Fe removal from model solutions is applicable. The resin efficiency was highest for the  $\text{CuSO}_4$  model solution (10 mg/L), where the  $\text{Cu}^{2+}$  removal efficiency was 97.8 % and  $\text{SO}_4^{2-}$  was 95.1 %. With increasing concentration of metals and sulphates in solutions the efficiency decreases.

Ion exchange may be suitable for small volumes of water contaminated with sulphates and heavy metals due to its simplicity, efficiency, selectivity and relatively low operating costs.

#### Acknowledgements

The work was supported by the Slovak Research and Development Agency under the contract APVV-20-0140 and by the Slovak Scientific Grant Agency under the contracts 2/0108/23.

#### References

- [1] Carolin, C.F., Kumar, P.S., Saravanan, A., Joshiba, G.J., Naushad, M. Efficient techniques for the removal of toxic heavy metals from aquatic environment: A review. *Journal of Environmental Chemical Engineering*, 5, 2017, p. 2782-2799.

- [2] Zamora-Ledezma, C., Negrete-Bolagay, D., Figueroa, F., Zamora-Ledezma, E., Ni, M., Alexis, F., Guerrero, V.H. Heavy metal water pollution: A fresh look about hazards, novel and conventional remediation methods. *Environmental Technology & Innovation*, 22, 2021, p. 101504.
- [3] Kumar, A., Cabral-Pinto, M., Kumar, A., Kumar, M., Dinis, P.A. Estimation of risk to the eco-environment and human health of using heavy metals in the Uttarakhand Himalaya, India. *Applied Sciences*, 10, 2020, p.1-18.
- [4] Fu, F., Wang, Q. Removal of heavy metal ions from wastewaters: A review. *Journal of Environmental Management*, 92, 2011, p. 407-418.
- [5] Birn, A.E.A., Shipton, L., Schrecker, T., Shipton, L. Canadian mining and ill health in Latin America: a call to action. *Canadian Journal of Public Health*, 109, 2018, p. 18-22.
- [6] Zak, D., Hupfer, M., Cabezas, A., Jurasinski, G., Audet, J., Kleeberg, A., McInnes, R., Kristiansen, S.M., Petersen, R.J., Liu, H., Goldhammer, T. Sulphate in freshwater ecosystems: a review of sources, biogeochemical cycles, ecotoxicological effects and bioremediation. *Earth-Science Reviews*, 212, 2021, p. 103446.
- [7] Runtti, H., Tolonen, E.T., Tuomikoski, S., Luukkonen, T., Lassi, U. How to tackle the stringent sulfate removal requirements in mine water treatment—a review of potential methods, *Environmental Research*, 167, 2018, p. 207-222.
- [8] Chatla, A., Almanassra, I.W., Abushawish, A., Laoui, T., Alawadhi, H., Atieh, M.A., Ghaffour, N. Sulphate removal from aqueous solutions: State-of-the-art technologies and future research trends. *Desalination*, 558, 2023, p. 116515.
- [9] Dabrowski, A., Hubicki, Z., Podkościelny, P., Robens, E. Selective removal of the heavy metal ions from waters and industrial wastewaters by ion-exchange method. *Chemosphere*, 56, 2004, p. 91-106.
- [10] Ozturk, Y., Ekmeci, Z. Removal of sulfate ions from process water by ion exchange resins. *Minerals Engineering*, 159, 2020, p. 106613.
- [11] Benalla, S., Addar, F.Z., Tahaikt, M., Elmidaoui, A., Taky, M. Heavy metals removal by ion-exchange resin: experimentation and optimization by custom designs. *Desalination and Water Treatment*, 262, 2022, p. 347-358.
- [12] Fu, F., Wang, Q. Removal of heavy metal ions from wastewaters: a review. *Journal of Environmental Management*, 92 (3), 2011, p.407-418,
- [13] Priyabrata, P., Banat, F. Comparison of heavy metal ions removal from industrial lean amine solvent using ion exchange resins and sand coated with chitosan. *Journal of Natural Gas Science and Engineering*, 18, 2014, p. 227-236.
- [14] Demcak, S., Balintova, M., Holub, M. The removal of sulphate ions from model solutions and their influence on ion exchange resins. *Economics and Environment*, 73 (2), 2020, p. 59-70.





## BIOLEACHING OF TETRAHEDRITE - BACTERIAL OXIDATION AND GROWTH YIELD BEHAVIOUR

**Zuzana Bártová<sup>a</sup>, Daniel Kupka<sup>a</sup>, Lenka Hagarová<sup>a</sup>, Lucia Ivaničová<sup>a</sup>, Miroslava Václavíková<sup>a</sup>**

*Institute of Geotechnics of the Slovak Academy of Sciences,  
Watsonova 45, 040 01 Kosice, Slovakia, bartova@saske.sk*

### Abstract

This study describes the bioleaching of tetrahedrite concentrate by acidophilic chemolithotrophic iron- and sulfur-oxidizing bacteria under aerobic conditions. On-line gas analyses showed, that the efficiency of bacterial CO<sub>2</sub> fixation, i.e. the molar ratio of CO<sub>2</sub> fixed to O<sub>2</sub> consumed, changed during the course of tetrahedrite bioleaching. In the initial stage, the exponentially grown culture oxidized abundant dissolved ferrous iron that served as an electron donor. The rates of CO<sub>2</sub> and O<sub>2</sub> consumption increased exponentially, (time period 4 - 7.5 days in the graphs) and growth yield coefficient (Y<sub>ox</sub>) approached 0.06 (C-mole/O-mole), which is typical value for cultures grown on ferrous sulfate. Iron acts as an important intermediary electron carrier in the tetrahedrite oxidation reactions. Bacterial Fe<sup>2+</sup> oxidation rate highly outcompeted the concurrent Fe<sup>3+</sup> reduction rate at the tetrahedrite surface, which caused limitation of bacterial growth and oxidation rates by the availability of Fe<sup>2+</sup>. In the next stage of bioleaching, (time period from 7.5 days onwards in the graphs) the ratio of CO<sub>2</sub> fixed to O<sub>2</sub> consumed has increased, approaching almost twice the yield value that would be predicted from exclusive growth on ferrous iron, most likely due to co-utilization of sulfur intermediates. Our observations are consistent with previously published findings that the efficiency of CO<sub>2</sub> fixation is much greater when sulfur rather than ferrous ion is being oxidized, showing that the transport of electrons derived from RISC yielded more energy than the transport of electrons from Fe<sup>2+</sup>.

**Keywords:** bacterial growth, tetrahedrite, iron- and sulfur-oxidizing bacteria, bioleaching

### 1 Introduction

Tetrahedrite is a copper antimony sulfosalt that can be described by the simplified chemical formula Cu<sub>10</sub>(Fe,Zn)<sub>2</sub>Sb<sub>4</sub>S<sub>13</sub>. In nature, the minerals of the tetrahedrite group constitute a complex isotypic series with multiple iso- and heterovalent substitutions [1-4].

Tetrahedrite is generally known as a refractory mineral characterized by its recalcitrance to chemical oxidative dissolution [5-7].

Tetrahedrite and tennantite are significant copper and precious metal resources, however, their treatment entails severe toxicological and environmental risks due to high content of toxic components [8].

Nowadays, the exploitation of tetrahedrite-tennantite deposits is being revisited, justified mostly by the high precious-metals content. Furthermore, given the continued strategic importance of raw materials for the EU manufacturing industry, antimony, amongst another 30 mineral raw materials, was added to the list of Critical Raw Materials for Europe published by the European Commission.

In the current investigation, we studied bioleaching of tetrahedrite sample originated from the Silver vein of the Rožňava mine, eastern Slovakia [9-11]. The main minerals of economic interest are silver-bearing tetrahedrite and siderite. The high Cu content (40 - 46 wt%) and relatively high content of Ag (up to 1 %) make tetrahedrite mining at this mineral deposit economically attractive.

### 2 Material and methods

#### 2.1 Tetrahedrite sample

The sample of natural tetrahedrite originated from the Strieborná žila (Silver vein) of the Rožňava mine (eastern Slovakia). The geological background and mineralogy of the ore deposit are described in details elsewhere [9-11] and references therein. The main minerals of economic interest are silver-bearing tetrahedrite and siderite.

The mined ore was dry crushed and milled to a grain size < 100 μm. The ground ore was upgraded by froth flotation. The flotation concentrate was further conditioned for 24 hours with diluted sulfuric acid (pH 1) at 90 °C under N<sub>2</sub> atmosphere to remove the residual siderite. The final siderite-free tetrahedrite concentrate was separated from the slurry by filtration, washing and drying.

The tetrahedrite (bio)leaching was carried out in magnetically stirred baffled reaction flasks with the working volume 0.5 L at temperature 25 °C. The leaching medium contained: 1.6 mM MgSO<sub>4</sub>·7H<sub>2</sub>O, 6.1 mM NH<sub>4</sub>H<sub>2</sub>PO<sub>4</sub>, 0.23 mM K<sub>2</sub>HPO<sub>4</sub> and 120 mM FeSO<sub>4</sub>·7 H<sub>2</sub>O in 4 mM H<sub>2</sub>SO<sub>4</sub> (pH 1.63).

The medium was inoculated with Fe-oxidizing bacteria *A. ferrooxidans*, *A. ferrivorans* and *L. ferriphilum*. The grown bacterial cultures were transferred to reaction flasks with tetrahedrite. The pulp density was 20 g/L. Abiotic control series were performed with sterile liquids of the same chemical composition, containing iron in either divalent or trivalent form. Experiments were performed in replicates and showed a good reproducibility.

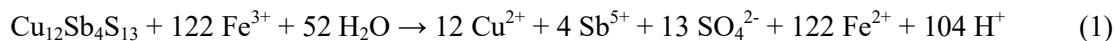
The oxidation reaction of the tetrahedrite was monitored by continuous measurements of ORP and pH of the leaching liquors, and by chemical analyses of the slurry samples. Bacterial O<sub>2</sub> and CO<sub>2</sub> consumption rates were monitored by on-line analyses of the reactor headspace gas.

## 2.2 Chemical analyses

The samples of leaching slurry were taken at regular intervals and filtered through 0.2 µm syringe filters. Elemental analysis of the filtrate was performed using AAS (Varian AA240Z, AA240FS) and ICP-MS 7700 Agilent. Ferric iron was determined by a UV-spectrophotometric method at 300 nm [12]. Ferrous iron concentrations were determined by modified o-phenantroline spectrophotometric method, insensitive to Fe<sup>3+</sup> interference [13].

## 3 Results and discussion

The oxidation of 1 mole of tetrahedrite (nominally Cu<sub>10</sub><sup>+</sup>Cu<sub>2</sub><sup>2+</sup>Sb<sub>4</sub><sup>3+</sup>S<sub>13</sub><sup>2-</sup>) to produce sulfate involves the transfer of 122 moles of electrons. The stoichiometry of the reaction was confirmed by gas analyses and the concentration profiles of the oxidation products and can be described by the equation 1.



The role of acidophilic prokaryotes in this process is to oxidize ferrous iron to ferric iron (eq. 2) which helps to maintain high redox potential, defined by the Fe<sup>3+</sup>/Fe<sup>2+</sup> ratio.



The acidity generated by tetrahedrite oxidation is attenuated by concurrent bacterial ferrous iron oxidation reaction that competes for protons. Further acidification is produced by the hydrolytic reaction of ferric iron.

Autotrophic bacteria use carbon dioxide as a sole carbon source to produce organic matter. In this work, the concentration of bacterial biomass is expressed in moles of organic carbon per liter [C-mole L<sup>-1</sup>]. The production rate of bacteria equals the consumption rate of carbon dioxide (Fig. 1b).

$$dX/dt = r_X = -r_{\text{CO}_2} \quad (3)$$

The yield coefficient, commonly referred to as the substrate-to-biomass yield, is used to convert between cell growth rate ( $r_X$ ) and substrate (e.g. oxygen) utilization rate ( $-r_{\text{O}_2}$ ) (Fig. 1d).

$$-r_{\text{CO}_2} = Y_{\text{OX}} \cdot (-r_{\text{O}_2}) \quad (4)$$

In the initial stage of bioleaching, the exponentially grown culture oxidized abundant dissolved ferrous iron that served as an electron donor. The rates of CO<sub>2</sub> and O<sub>2</sub> consumption increased exponentially (Fig. 1, time period 4 - 7.5 days) and growth yield coefficient (Y<sub>OX</sub>) approached 0.06 (C-mole/O-mole), which is typical value for cultures grown on ferrous sulfate. Iron acts as an important intermediary electron carrier in the tetrahedrite oxidation reactions. Bacterial Fe<sup>2+</sup> oxidation rate highly outcompeted the concurrent Fe<sup>3+</sup> reduction rate at the tetrahedrite surface, which caused limitation of bacterial growth and oxidation rates by the availability of Fe<sup>2+</sup>. In the next stage of bioleaching, (time period from 7.5 days onwards in Fig. 1) the yield coefficient (Y<sub>OX</sub>) has increased, approaching almost twice the value that would be predicted from exclusive growth on ferrous iron, most likely due to bacterial co-utilization of intermediate products of tetrahedrite oxidation.

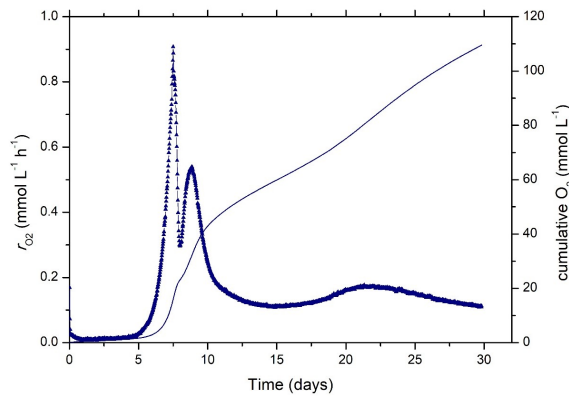


Fig. 1a. Oxygen consumption during bioleaching of tetrahedrite by *L. ferriphilum*

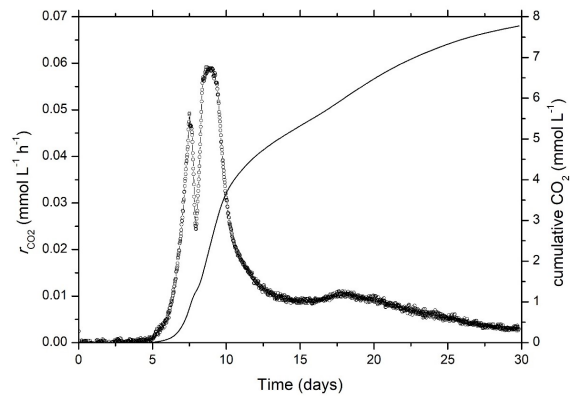


Fig. 1b. Carbon dioxide fixation during bioleaching of tetrahedrite by *L. ferriphilum*

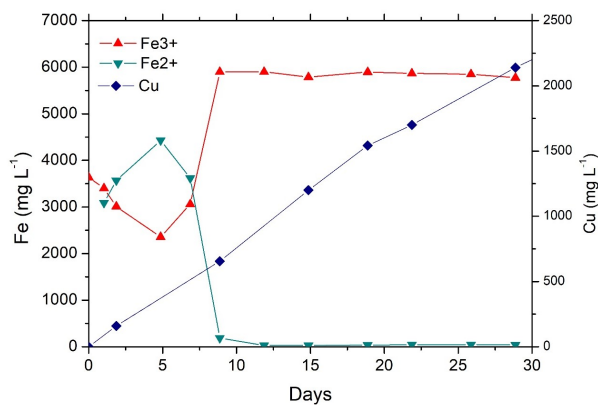


Fig. 1c. Iron speciation and copper extraction during bioleaching of tetrahedrite by *L. ferriphilum*

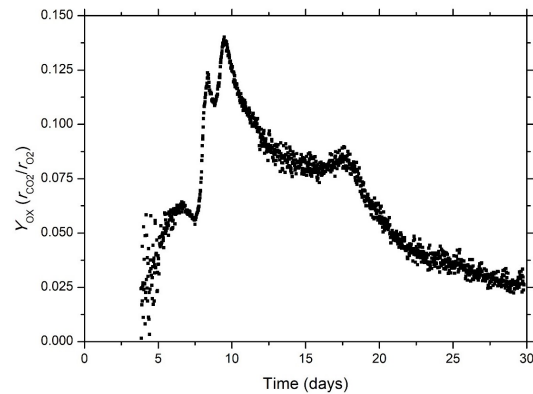
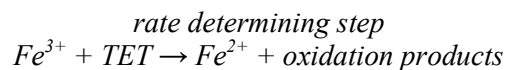


Fig. 1d. Changes of the yield coefficient  $Y_{OX}$  in the course of tetrahedrite oxidation by *L. ferriphilum*

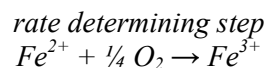
#### 4 Conclusions

In the current investigation, we studied bioleaching of tetrahedrite sample originated from the Silver vein of the Rožňava mine, eastern Slovakia. Iron acts as an important intermediary electron carrier in the tetrahedrite oxidation reactions.

Bacterial  $Fe^{2+}$  oxidation rate highly outcompeted the concurrent  $Fe^{3+}$  reduction rate at the tetrahedrite surface, as indicated the high  $Fe^{3+}$  to  $Fe^{2+}$  ratio in the leaching liquors.



Abiotic leaching of tetrahedrite by acidic  $Fe^{3+}/Fe^{2+}$  solutions approached an equilibrium between the rate of ferrous iron oxidation by molecular oxygen and the rate of ferric iron reduction on the mineral surface.



#### Acknowledgements

Funded by the EU NextGenerationEU through the Recovery and Resilience Plan for Slovakia under the project No. 09I03-03-V04-00271. It was supported by the Slovak Grant Agency (VEGA), Grant No. 2/0108/23 and Slovak Research and Development Agency under the contract No. APVV-20-0140.

## References

- [1] King, R.J. The tetrahedrite group. *Geology Today*, 17 (2), 2001, p. 77-80.
- [2] Moëlo, Y., Makovicky, E., Mozgova, N.N., Jambor, J.L., Cook, N., Pring, A., Paar, W., Nickel, E.H., Graeser, S., Karup-Møller, S., Balic-Žunic, T., Mumme, W.G., Vurro, F., Topa, D., Bindi, L., Bente, K., Shimizu, M. Sulfosalt systematics: a review. Report of the sulfosalt sub-committee of the IMA Commission on Ore Mineralogy. *European Journal of Mineralogy*, 20 (1), 2008, p. 7-46.
- [3] Patrick, R.A.D., Hall, A.J. Silver substitution into synthetic zinc, cadmium, and iron tetrahedrites. *Mineralogical Magazine*, 47 (345), 1983, p. 441-45.
- [4] Repstock, A., Voudouris, P., Zeug, M., Melfos, V., Zhai, M., Li, H., Kartal, T., Matuszczak, J. Chemical composition and varieties of fahlore-group minerals from Oligocene mineralization in the Rhodope area, Southern Bulgaria and Northern Greece. *Mineralogy and Petrology*, 110 (1), 2016, p. 103-123.
- [5] Correia, M., Carvalho, J., Monhemius, J. The leaching of tetrahedrite in ferric chloride solutions. *Hydrometallurgy*, 57, 2000, p. 167-179.
- [6] Dutrizac, J.E., Morrison, R.M. The Leaching of Some Arsenide and Antimonide Minerals in Ferric Chloride Media. In R.G. Bautista (Ed.), *Hydrometallurgical Process Fundamentals*. Springer US, Boston, MA, 1984, p. 77-112.
- [7] Riveros, P.A., Dutrizac, J.E. The leaching of tennantite, tetrahedrite and enargite in acidic sulphate and chloride media. *Canadian Metallurgical Quarterly*, 47 (3), 2008, p. 235-244.
- [8] Filippou, D., St-Germain, P., Grammatikopoulos, T. Recovery of metal values from copper-arsenic minerals and other related resources. *Mineral Processing and Extractive Metallurgy Review*, 28 (4), 2007, p. 247-298.
- [9] Jacko, S., Farkašovský, R., Kondela, J., Mikuš, T., Ščerbáková, B., Dirnerová, D. Boudinage arrangement tracking of hydrothermal veins in the shear zone: example from the argentiferous Strieborna vein (Western Carpathians). *Journal of Geosciences*, 64 (3), 2019, p. 179-195.
- [10] Mikuš, T., Kondela, J., Jacko, S., Milovská, S. Garavellite and associated sulphosalts from the Strieborná vein in the Rožňava ore field (Western Carpathians). *Geologica Carpathica*, 69, 2018, p. 221-236.
- [11] Sasvári, T., Maťo, E. The characteristics of the Rožňava ore district, in relation to the structural-tectonic analysis and mineralization exemplified by the deposition conditions of the Strieborná vein, Mária mine, Rožňava. *Acta Montanistica Slovaca*, 3 (1), 1998, p. 33-117.
- [12] Basaran, A., Tuovinen, O. An ultraviolet spectrophotometric method for the determination of pyrite and ferrous ion oxidation by *Thiobacillus ferrooxidans*. *Applied Microbiology and Biotechnology*, 24, 1986, p. 338-341.
- [13] Herrera, L., Ruiz, P., Aguillon, J.C., Fehrmann, A. A new spectrophotometric method for the determination of ferrous iron in the presence of ferric iron. *Journal of Chemical Technology & Biotechnology*, 44 (3), 1989, p. 171-181.

## SPATIAL VARIABILITY OF SOIL BIOCHEMICAL PROPERTIES IN THE FORMER MINING AREA

**Lenka Bobuľská<sup>a</sup>, Lenka Demková<sup>a</sup>, Július Árvay<sup>b</sup>**

<sup>a</sup> Department of Ecology, Faculty of Humanities and Natural Sciences, University of Prešov,  
17.november 1, 080 01 Prešov, Slovakia, lenka.bobulska@unipo.sk

<sup>b</sup> Institute of Food Sciences, Faculty of Biotechnology and Food Sciences, Slovak University of Agriculture in Nitra,  
Tr. A. Hlinku 2, Nitra, 949 76, Slovakia

### Abstract

Soil, the main factor affecting the course and nature of the landscape, is constantly influenced by various waste substances that threaten the integrity and circulation of the food chain. Contamination of soils by heavy metals in mining areas leads to deterioration of soil quality and other environmental components. During anthropogenic activities, a large number of chemical substances enter the environment, which can be considered toxic. Among the most contaminated areas, we include locations and regions in which enterprises that directly handle or even produce such substances are located. Soil microorganisms, which form different communities with different diversities, play a major role in the quality and usability of soil. Changes in their quantity and activity are important indicators of soil quality, and are reflected in the size and thickness of the biomass created. The aim of this study was to determine the level of heavy metal soil pollution in the surroundings of processing plant, depending on the different distances of sampling points from the source of pollution, and to determine the effect of risk elements on enzyme activity and selected chemical soil parameters. The total content of risk elements (Cu, As, Cd, Pb, and Zn), activity of soil urease, acid phosphatase, alkaline phosphatase, catalase, soil reaction, organic carbon, and nutrients were determined. Risk elements exhibit toxic effects on enzyme activity, resulting in increased soil enzyme activity with decreasing risk elements content. Significant positive correlations were observed between risk elements and some enzymes. We found no direct influence of risk elements to the organic carbon, soil reaction and nutrients.

**Keywords:** mining activities, soil enzymes, risk elements

### 1 Introduction

Pollution of the environment by toxic substances has industrial origins and agricultural activities. There are huge areas in Slovakia that are polluted by high heavy metal content as a result of long-term mining and processing activities [1, 2]. Heavy metals enter the soil environment as wastewater or dust particles, which seriously disturb the environment and ultimately threaten human health [3]. Enzymatic activity has been used as a relatively stable and highly sensitive biochemical indicator of soil pollution [4, 5]. The reaction of soil enzymes to the presence of toxic substances is much faster compared to the chemical reactions and physical soil parameters [6, 7]. The importance of enzymes that represents urease, acid and alkaline phosphatases, consists in the transformation of plant nutrients. Urease catalyses the hydrolysis of urea into carbon dioxide and ammonia, depending on soil reaction and organic carbon [8]. Phosphatases are important for the transformation of organic phosphorus into inorganic forms that are accessible to growth lines. Catalase is an oxidoreductase that protects organisms from hydrogen peroxide toxicity [9]. Contamination of the soil environment owing to the high content of heavy metals is a serious problem that negatively affects soil parameters and consequently limits the productivity and environmental function of the soil. Numerous studies [10-12] have recorded that such polluted soils are no longer suitable for agricultural production because they have reduced nutrient content and limited microbial diversity.

The aim of the work was to determine the influence of risk elements on selected chemical and biological soil parameters in the cadastral territory of the municipality of Krompachy [48°55'24, 1"N;20°53'59,2"E] and Slovinky [48°55'48.9"N; 20°53'51.0"E]. These localities are typical example of the municipalities of the middle Spiš that are characterized by long-term mining and processing ore material focused primarily on copper production.

### 2 Material and methods

Soil samples were collected during the summer season, where a total of the 15 soil samples on 5 permanent grasslands (3 samples on each grassland) were collected (Figure 1). The sampling sites were located 0.3, 1.0, 1.5, 2.5, and 5.0 km from the industrial enterprise Kovohuty Krompachy. At each sampling

site, 500 g of the soil was sampled, stored in the plastic bag, transported to the laboratory, where part of the samples were air-dried at the room temperatures for 1-2 weeks. Fresh soil samples were directly stored in the fridge for the determination of soil enzyme activity. Before all analysis, the samples were homogenized and sieved (<0.2 mm).

The total content of risk elements (Cu, As, Cd, Pb, Zn) was determined in the laboratory using the AAS (atomic absorption spectrometry) method and RFS method (X-ray fluorescence spectrometry). Soil reaction (pH) was determined as follows: 10 g of the soil sample was mixed in a 25 ml 0.01M CaCl<sub>2</sub> solution using the inoLab pH 720-WTW device. The nutrient content (P, K, Mg) was determined in the laboratory according to Mehlich III and the content of organic carbon (C<sub>ox</sub>) according to Tiurin's method [13]. The activity of soil urease (URE) and catalase (CAT) was determined according to Khaziev [14]. More specifically, activity of urease was colorimetrically determined as an ammonia release after the incubation (for 24 h at 37 °C) of soil samples with urea solution. Ammonium determination was measured by spectrometer at 410 nm. Activity of acid (ACP) and alkaline phosphatase (ALP) was colorimetrically determined as a phenol release after the incubation (for 3 h at 37 °C) of soil samples with phenyl phosphate solution and acetate buffer (for acid phosphatase) and acetate buffer (for alkaline phosphatase) according to Grejtovský [15]. Phenol release was measured by the spectrometer at 510 nm.

Statistical software Statistica 10 was used to calculate statistical analyses. Correlation dependencies between soil characteristics were calculated according to Spearman correlation coefficient.

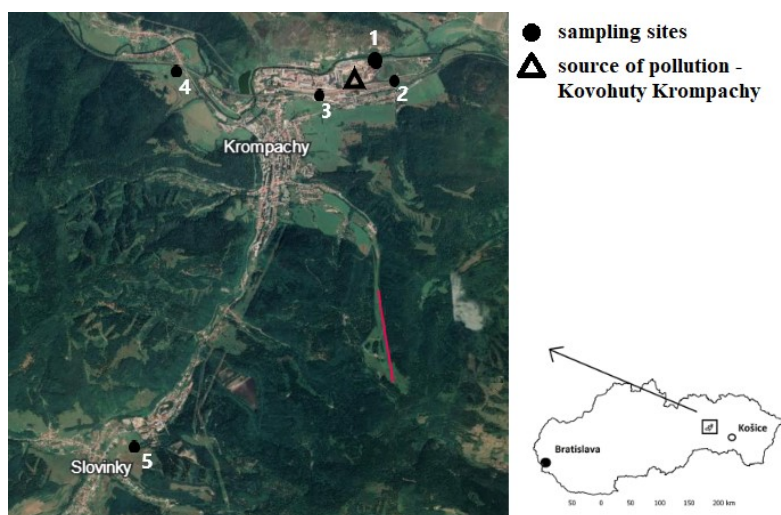


Fig. 1. Soil sampling sites

### 3 Results and discussion

#### 3.1 Risk elements content

Determined values of risk elements at five sampling points located at different distances from the source of pollution are listed in Table 1. Serious copper contamination was detected at sampling point 1 where the limit value of copper was exceeded 1.5 times and at site 4, where up to 21 times the limit value of this element was exceeded. Arsenic and cadmium showed the highest values at location 1, which represented a pile of mining material mixed with the debris from the mine. It has been proven several times that landfills of mining contain sludge from the production of copper and zinc [16] and solid waste, which is used to build piles of mining material, contains residues of lead, arsenic and cadmium [17], the presence of which was confirmed by our study. Extremely high and above limit values of copper, lead and zinc were measured at site 4, which is located to the west of the industrial company and therefore in the direction of the prevailing winds. The lowest values of risk elements were measured at site 5, which is located at the greatest distance from the source of pollution and at the same time away from the prevailing wind direction. Values (median  $\pm$  standard deviation) of the total content of copper (718 $\pm$ 451.3) and arsenic (168 $\pm$ 53.83) were above the permitted limit value in all evaluated places. The same situation, with the exception of site 5, was detected for cadmium (2.9 $\pm$ 1.7), lead (218 $\pm$ 136.9) and zinc (857 $\pm$ 423.1). In accordance with our findings, the study of Hronec et al. [18] recorded above-limit values in Krompachy locality of cadmium, copper, zinc and arsenic. There was the significant correlation ( $P < 0.05$ ) among all evaluated risk elements (with the exception between Zn and Pb).

**Table 1. The values of risk elements determined at sampling sites and their limit values**

Risk elements	Cu	As	Cd	Pb	Zn
	(mg/kg)				
<b>min</b>	89	39	0.5	25	126
<b>max</b>	1271	181	5.7	380	1333
<b>average</b>	745	135	3.1	229	760
<b>standard deviation</b>	505	60	1.9	153	473
<b>limit value*</b>	<b>60</b>	<b>25</b>	<b>0.7</b>	<b>70</b>	<b>150</b>

Limit values for Slovak soils according to Act no.188/2003 Coll. of laws [19]

### 3.2 Soil chemical characteristics

The chemical properties determined for the individual sampling sites are shown in Table 2. The values of the soil reaction (pH) ranged from weakly alkaline (7.5; site 1) to acidic (4.6; site 4) (Table 2). The value of organic carbon ( $C_{ox}$ ) ranged from medium to very high values, but statistical testing did not confirm any direct dependence of this parameter with respect to the distance of the sampling point from the pollution source. According to the agrochemical standards valid for medium-heavy soils of Slovakia, the optimal values for individual nutrients are as follows: phosphorus (66-100 mg/kg), potassium (151-210 mg/kg), and magnesium (131-175 mg/kg). In places where high magnesium values were determined, potassium and phosphorus values were below optimal values, while the lowest phosphorus and potassium values were determined in the least polluted locations. Compared to uncontaminated soils, polluted soils have few nutrients, which negatively affects plant production [20].

**Table 2. Average values of soil properties at individual sampling points**

Sampling points	pH	$C_{ox}$ (%)	P (mg/kg)	K (mg/kg)	Mg (mg/kg)
<b>1</b>	7.5	1.64	15	101	280
<b>2</b>	6.0	3.68	69	50	235
<b>2</b>	4.9	2.71	40	45	266
<b>4</b>	4.6	5.49	179	216	101
<b>5</b>	4.9	2.05	99	374	102

### 3.3 Soil biological characteristics

Monitoring methods aimed at evaluating microbiological and biological soil parameters are successfully used to determine the degree of soil pollution. The activity of soil urease ( $0.2 \pm 0.108$ ) varied depending on the distance of the sampling site from the pollution source. Urease activity was higher at the least polluted site by more than 180 % compared to the most polluted site. The activity of acid ( $183 \pm 59.14$ ) and alkaline phosphatase ( $122.3 \pm 36.7$ ) varied depending on the content of risk elements in the soil. The highest value of acid and alkaline phosphatase was detected at site 5, which was the least polluted site. Compared to the site 1, that represents the most polluted site, phosphatases activity increased by 178 % in the case of acid and 89 % in the case of alkaline phosphatase. Some studies report [6, 21] that phosphatases do not change significantly due to the medium-high content of heavy metals in the soil environment, but the high content of these toxic elements has an inhibitory effect on their activity. The activity of soil catalase ( $0.41 \pm 0.06$ ) changed insignificantly compared to other enzymes. Wang et al. [22] reported that some contaminants have the ability to increase catalase activity under specific conditions. The results of our research confirmed that soil pollution by risk elements was associated with a decrease in the activity of soil enzymes. Due to the fact that microbes consume a lot of energy to adapt to a polluted environment, their activity decreases [23]. In soil ecosystems, the increased content of heavy metals has a negative effect on the number and activity of microorganisms. The authors [6, 24, 25] explained the effect of heavy metals on enzyme activity as follows: i) metals react with sulfhydryl groups of enzymes, which cause inhibition or deactivation of enzymatic activity. ii) metals indirectly affect the activity of enzymes by changing the microbial community that synthesizes these enzymes; iii) a combination of these factors.

### 3.4 Correlation dependences among evaluated soil parameters

The results of statistical testing confirmed a significant positive relationship ( $P < 0.05$ ) between urease and acid phosphatase, which is consistent with the findings of Khan et al. [26]. A significant positive dependence was also shown between acid and alkaline phosphatase. Risk elements have a complex effect on enzymatic activity, with different enzymes reacting to heavy metals in different ways (Table 3). In the case

of urease, we noted a significant negative correlation with total arsenic content ( $P < 0.05$ ). The changes in soil urease activity due to the content of risk elements were reported by Zhang et al. [20], that was also confirmed by our study. At the same time, a significant negative correlation was found between acid phosphatase and the total content of arsenic and cadmium ( $P < 0.05$ ), which coincides with the findings of Wieczorek et al. [27], who detected the negative effect of cadmium on acid phosphatase. Alkaline phosphatase was negatively significantly dependent ( $P < 0.05$ ) with all monitored risk elements (with the exception of cadmium). In the study of Gülser and Erdoğan [28], the authors focused on the effect of heavy metals on alkaline phosphatase, and their findings, as in our case, confirmed the dependence of alkaline phosphatase with all evaluated risk elements, except cadmium. In agreement with the works of some authors [9, 29, 30] that carried out research on localities affected by mining activity, have shown a serious impact of heavy metals on the activity of soil enzymes. In the case of catalase, any significant correlation was shown with the evaluated risk elements. Soil catalase activity is more likely more tolerant to high heavy metal content compared to other enzymes.

**Table 3. Correlation among the activity of soil enzymes and the total content of risk elements**

	<b>Cu</b>	<b>As</b>	<b>Cd</b>	<b>Pb</b>	<b>Zn</b>
<b>URE</b>	ns	<b>-0.939*</b>	ns	ns	ns
<b>ACP</b>	ns	<b>-0.922*</b>	<b>-90.932*</b>	ns	ns
<b>ALP</b>	<b>-0.924*</b>	<b>-0.941*</b>	ns	<b>-0.924*</b>	<b>-0.912*</b>
<b>CAT</b>	ns	ns	ns	ns	ns
<b>pH</b>	ns	ns	ns	ns	ns
<b>C<sub>ox</sub></b>	ns	ns	ns	ns	ns
<b>P</b>	ns	ns	ns	ns	ns
<b>K</b>	ns	ns	ns	ns	ns
<b>Mg</b>	ns	ns	ns	ns	ns
<b>Cu</b>		<b>0.895*</b>	<b>0.914*</b>	<b>0.999**</b>	<b>0.971**</b>
<b>As</b>			<b>0.891*</b>	<b>0.903*</b>	<b>0.902*</b>
<b>Cd</b>				<b>0.932*</b>	ns
<b>Pb</b>					<b>0.962**</b>

URE - urease, ACP - acid phosphatase, ALP - alkaline phosphatase, CAT - catalase, C<sub>ox</sub> - organic carbon  
 \* $P < 0.05$ , \*\* $P < 0.001$ , significant relationship are shown in bold, ns - no significance

In the case of the soil reaction, we found a positive (not significant) dependence with all risk elements and a negative correlation with soil enzymes, organic carbon and nutrients. Salazar et al. [31] showed the similar results and noted a negative correlation between soil reaction and soil enzyme activity. A negative correlation dependence was found between magnesium and other nutrients, but it was significant only in the case of phosphorus ( $P < 0.05$ ). At the same time, we noted a significant positive correlation between potassium and soil urease activity (Table 4). A number of authors dealt with the relationship between enzyme activity and soil parameters, e.g. organic carbon. Badiane et al. [32] found no direct relationship between these two soil characteristics, which agrees with our results. A positive, although not significant, relationship was found between organic carbon and all evaluated risk elements, which agrees with the findings of some authors [33, 34]. At the same time, we did not notice any statistically significant dependence between the evaluated soil parameters with the respect to the distance of the sampling point from the pollution source.

**Table 4. Correlation among soil characteristics**

	<b>ACP</b>	<b>ALP</b>	<b>CAT</b>	<b>pH</b>	<b>Cox</b>	<b>P</b>	<b>K</b>	<b>Mg</b>
<b>URE</b>	<b>0.943*</b>	n	ns	ns	ns	ns	<b>0.881*</b>	ns
<b>ACP</b>		<b>0.945*</b>	ns	ns	ns	ns	ns	ns
<b>ALP</b>			ns	ns	ns	ns	ns	ns
<b>CAT</b>				ns	ns	ns	ns	ns
<b>pH</b>					ns	ns	ns	ns
<b>C<sub>ox</sub></b>						ns	ns	ns
<b>P</b>							ns	<b>-0.884*</b>
<b>K</b>								ns

URE - urease, ACP - acid phosphatase, ALP - alkaline phosphatase, CAT - catalase, C<sub>ox</sub> - organic carbon  
 \* $P < 0.05$ , significant relationship are shown in bold, ns - no significance



#### 4 Conclusions

The determined values of risk elements at all evaluated localities exceeded the limit values determined for the soils of Slovakia. As the content of risk elements increased, the activity of soil enzymes decreased. Contamination of the environment with risk elements in the vicinity of mining areas negatively affects the activity of urease, acid and alkaline phosphatase. We noted a positive significant relationship between urease and acid phosphatase, as well as alkaline phosphatase. None of the evaluated soil characteristics had an impact on the nutrient content. We did not notice a relationship between organic carbon and soil enzyme activity, but a positive relationship was found between organic carbon and total risk elements content. It was statistically confirmed that the evaluated soil characteristics were not affected by the distance of the sampling point from the pollution source.

#### Acknowledgements

The work was supported by Slovak Scientific Agency VEGA No. 1/0213/22 and Slovak Research and Development Agency APVV-20-0140.

#### References

- [1] Bálintová, M., Luptáková, A. *Úprava kyslých banských vôd* (in Slovak). Košice: Technická univerzita v Košiciach, Stavebná fakulta, Ústav geotechniky SAV, Košice, 2012, 131 p. ISBN 978-80-553-0868-5.
- [2] Demková, L., Árvay, J., Bobuľská, L., Hauptvogel, M., Hrstková, M. Open mining pits and heaps of waste material as the source of undesirable substances: biomonitoring of air and soil pollution in former mining area (Dubník, Slovakia). *Environmental Science and Pollution Research*, 26, 2019, p. 35227-35239.
- [3] Liu, H.Y., Probst, A., Liao, B.H. Metal contamination of soils and crops affected by the Chenzhou lead/zinc mine spill (Hunan, China). *Science of the Total Environment*, 339 (1-3), 2005, p. 153-166.
- [4] Bobuľská, L., Fazekašová, D., Angelovičová, L., Kotorová, D. Impact of ecological and conventional farming systems on chemical and biological soil quality indices in a cold mountain climate in Slovakia. *Biological Agriculture & Horticulture*, 31 (3), 2015, p. 205-218.
- [5] Bhaduri, D., Sihi, D., Bhowmik, A., Verma, B.C., Munda, S., Dari, B. A review on effective soil health bio-indicators for ecosystem restoration and sustainability. *Frontiers in Microbiology*, 13, 2022, 938481.
- [6] Aponte, H., Meli, P., Butler, B., Paolini, J., Matus, F., Merino, C., Cornejo, P., Kuzyakov, Y. Meta-analysis of heavy metals effects on soil enzyme activities. *Science of the Total Environment*, 737, 2020, 139744.
- [7] Hinojosa, M.B., Carreira, J.A., Garcia-Ruiz, R., Dick, R.P. Soil moisture pre-treatment effect on enzyme activities as indicators of heavy metal-contaminated and reclaimed soils. *Soil Biology and Biochemistry*, 36 (10), 2004, p. 1559-1568.
- [8] Gao, Y., Zhou, P., Mao, L., Zhi, Y., Shi, W. Assessment of effect of heavy metals combined pollution on soil enzyme activities and microbial community structure modified ecological dose-response model and PCR-RAPD. *Environmental Earth Science*, 60 (3), 2010, p. 603-612.
- [9] Cang, L., Zhou, D.M., Wang, Q.Y., Wu, D.W. Effect of electrokinetic treatment of heavy metal contaminated soil on soil enzyme activities. *Journal of Hazardous Materials*, 172, 2008, p. 1602-1607.
- [10] Rashid, A., Schutte, B.J., Ulery, A., Deyholos, M.K., Sanogo, S., Lehnhoff, E.A., Beck, L. Heavy metal contamination in agricultural soils: Environmental pollutants affecting crop health. *Agronomy*, 13 (6), 2023, 1521.
- [11] Xiang, M., Li, Y., Yang, J., Li, Y., Li, F., Hu, B., Cao, Y. Assessment of heavy metal pollution in soil and classification of pollution risk management and control zones in the industrial developed city. *Environmental Management*, 66, 2020, p. 1105-1119.
- [12] Zhang, Q., Zou, D., Zeng, X., Li, L., Wang, A., Liu, F., Wang, H., Zeng, Q., Xiao, Z. Effect of the direct use of biomass in agricultural soil on heavy metals - activation or immobilization? *Environmental Pollution*, 272, 2021, 115989.

- [13] Fiala, K., Barančíková, G., Búrik, V., Houšková, B., Chomaničová, A., Kobza, J. et al. *Partial monitoring system – soil. Binding methods* (in Slovak). Bratislava: VÚPOP, 1999, 139 p. ISBN 80-85361-55-8.
- [14] Khaziev, F.K. *Soil enzyme activity* (in Russian). Moskwa: Nauka, 1976, p. 152-180.
- [15] Grejtovský, A. Effects of improvements practices on enzymatic activities of heavy-textured alluvial soil. *Rostlinná Výroba*, 1, 1991, p. 299-307.
- [16] Somani, M., Datta, M., Ramana, G.V., Sreekrishnan, T.R. Contaminants on soil-like material recovered by landfill mining from five old dumps in India. *Process Safety and Environmental Protection*, 137, 2020, p. 82-92.
- [17] Akhavan, A., Golchin, A. Estimation of arsenic leaching from Zn-Pb mine tailings under environmental conditions. *Journal of Cleaner Production*, 295, 2021, 126477.
- [18] Hronec, O., Vilček, J., Tóth, T., Andrejovský, P., Adamišin, P., Andrejovská, A., Daňová, M., Huttmanová, E., Vilimová, M., Škultéty, P., Juhásová, M. Heavy metals in soils and lants contaminated area “Rudňany-Gelnica”. *Acta Regionalia et Environmentalica*, 5 (1), 2008, p. 24-28.
- [19] Act No 188/2003 Coll. On application of sewage sludge and bottom sediment into the soil and amending and supplementing Act No 223/2001 Coll.
- [20] Zhang, X., Yang, L., Li, Y., Li, H., Wang, W., Ye, B. Impacts of lead/zinc and smelting on the environment and human health in China. *Environmental Monitoring and Assessment*, 184, 2012, p. 2261-2273.
- [21] Yang, J.S., Yang, F.L., Yang, Y., Xing, G.L., Deng, C.P., Shen, Y.T., Luo, L.Q., Li, B.Z., Yuan, H.L. A proposal of “core enzyme” bioindicator in long-term Pb-Zn ore pollution areas based on topsoils property analysis. *Environmental Pollution*, 213, 2016, p. 760-769.
- [22] Wang, Y.P., Shi, J.Y., Lin, Q., Chen, Y.X. Heavy metals availability and impaction on activity of soil microorganisms along a Cu/Zn zone contamination gradient. *Journal of Environmental Science*, 19 (3), 2007, p. 848-853.
- [23] Renella, G., Mench, M., Landi, L., Nannipieri, P. Microbial diversity and hydrolase synthesis in long-term Cd-contaminated soils. *Soil Biology and Biochemistry*, 37 (1), 2005, p. 133-139.
- [24] Madejón, E., Burgos, P., López, R., Cabrera, F. Soil enzymatic response to addition of heavy metals with organic residues. *Biology and Fertility of Soils*, 34, 2001, p. 144-150.
- [25] Yeboah, J., Shi, G., Shi, W. Effect of heavy metal contamination on soil enzymes activities. *Journal of Geoscience and Environmental Protection*, 9, 2021, p. 135-154.
- [26] Khan, S., Hesham, E.L., Qiao, M., Rehman, S., He, J.Z. Effects of Cd and Pb on soil microbial community structure an activities. *Environmental Science and Pollution Research*, 17 (2), 2010, p. 288-296.
- [27] Wiczorek, K., Wyszowska, J., Kucharski, J. Influence of zinc, copper, nickel, cadmium and lead in soils on acid phosphatase activity. *Fresenius Environmental Bulletin*, 23 (1), 2014, p. 274-284.
- [28] Gülser, F., Erdoğan, E. The effect of heavy metals pollution on enzyme activities and basal soil respiration of roadside soils. *Environmental Monitoring and Assessment*, 145 (1-3), 2008, p. 127-133.
- [29] Karaca, A., Naseby, D.C., Lynch, J.M. Effect of cadmium contamination with sewage sludge and phosphate fertiliser amendments on soil enzyme activities, microbial structure and available cadmium. *Biology and Fertility of Soils*, 35, 2002, p. 428-434.
- [30] Kizilkaya, R., Aşkın, T., Bayraklı, B., Sağlam, M. Microbiological characteristics of soils contaminated with heavy metals. *European Journal of Soil Biology*, 40 (2), 2004, p. 95-102.
- [31] Salazar, S., Sánchez, L.E., Alvarez, J., Valverde, A., Galindo, P., Igual, J.M., Peix, A., Santa-Regina, I. Correlation among soil enzyme activities under different forest system management practices. *Ecological Engineering*, 37 (8), 2011, p. 1123-1131.
- [32] Badiane, N.N.Y., Chotte, J.L., Pate, E., Masse, D., Rouland, C. Use of soil enzyme activities to monitor soil quality in natural and improved fallows in semi-arid tropical regions. *Applied Soil Ecology*, 18 (3), 2001, p. 229-238.
- [33] Khaledian, Y., Pereira, P., Brevik, E.C., Pundyte, N., Paliulis, D. The influence of organic carbon and pH on heavy metals, potassium, and magnesium levels in Lithuanian Podzols. *Land Degradation & Development*, 28 (1), 2017, p. 345-354.
- [34] Wang, X.S. Correlations between heavy metals and organic carbon extracted by dry oxidation procedure in urban roadside soils. *Environmental Geology*, 54, 2008, p. 269-273.

## DISSOLVING SELECTED SEDIMENTS COLLECTED ON THE SAND FILTER UNDER THE INFLUENCE OF DISINFECTANTS

**Jan Cebula<sup>a</sup>, Iwona Wiewiórska<sup>b</sup>, Lesław Świerczek<sup>a</sup>, Adam Cenian<sup>a</sup>**

<sup>a</sup> *The Szewalski Institute of Fluid - Flow Machinery Polish Academy of Science, Fiszerza st.14, 80-231 Gdańsk*

<sup>b</sup> *Sądeckie Wodociągi Spółka z o. o., Wincentego Pola 22, 33-300 Nowy Sącz*

### Abstract

The composition of groundwater, surface water, and mining water, as well as the methods by which they are treated in water treatment plants, determine the properties of the sludge produced as a result of technological processes.

In the article, the authors present an innovative approach to evaluating the contamination of sludge from sand filter beds by selected metals. They outline the principles and assess the effectiveness of dissolving the sludge accumulated on sand bed filters under the influence of disinfectants commonly used in water treatment plants. They conducted an assessment of the mobility of metals using the Rudd speciation method, which involves sequential chemical extraction by treating the sludge with solutions of increasing leaching strength.

In the sludge retained on the sand filter from a zinc and lead ore mine, zinc was found in sulfide form (44.08 %) and carbonate-bound form (41.33 %). Other forms, such as zinc bound to organic matter, exchangeable zinc, and adsorbed zinc, were present in negligible amounts. In the sludge from the zinc and lead ore mine, lead was found mostly in the carbonate form (43.03 %) and sulfide form (29.93 %). The other forms constituted a small percentage. The sludge from the surface of the filter mainly contained zinc and lead sulfides, which, under the influence of oxidizing agents, dissolved into the solution as sulfates.

The article summarizes the current state of knowledge regarding the dissolution of metal compounds under the influence of disinfectants before conducting research on the introduction of nanoxidation technology.

**Keywords:** dissolving sediments, sediments from sand deposits, metal contamination, water treatment

### 1 Introduction

The new European Parliament and Council Directive on the quality of water intended for human consumption (2020/2184) [1] imposes priority actions on Member States to minimize the risk of metal contamination in water environments. This opens opportunities for studying water quality not only at its extraction points but also during water intake and treatment processes. The practical implementation of Directive 2020/2184 [1] necessitates a review of operational practices to ensure that water suppliers have reliable knowledge of the forms in which metals occur in the aquatic environment.

The presence of metals in drinking water is caused by several factors, including the geological structure of the area where the water is sourced, the presence of compounds in the raw water (often due to sewage discharge upstream from the water intake), reduction of these substances through water treatment processes, such as metal precipitation, and the increase in metal and metalloid concentrations during the treatment process.

The authors of the research study examined the effect of oxidizers (disinfectants) on the dissolution of selected sludge retained on sand filters and sludge from zinc and lead ore mines. Heavy metals are commonly found in the mine drainage water of ore mines, primarily due to the oxidation of sulfide ores and the breakdown of carbonate ores [2]. The oxidation of sulfides lowers the pH of the water, leading to the dissolution of heavy metal hydroxides and hydrated oxides.

Mine drainage water from mine dewatering often poses a serious problem for surface water bodies due to its low pH and high levels of salts and heavy metals [3, 4]. Biological treatment of mine drainage water involves using algae to adjust pH and adsorb heavy metals. In a 14-day treatment process, depending on light intensity, 80-95 % of zinc, lead, and copper can be removed. Closing a lead mine does not immediately reduce heavy metal levels in the river where the sludge was deposited [2]. Waste rocks and flotation tailings also affect the heavy metal content of the surrounding plants. Due to the high levels of lead and zinc in the soil, the lead content in plant roots is also high, ranging from 800 to 1050 ppm [5]. Lead demonstrates a lower migration potential in soil profiles compared to other elements [6, 7].

The zinc and lead content in sludge is primarily due to the insoluble forms of these elements and the strong sorption properties of clay minerals, iron, and manganese hydroxides. Metal compounds that precipitate under specific conditions can be reoxidized and dissolved. As a result, sludge acts as a reservoir of metals. Changes in pH, oxygen concentration, carbon dioxide levels, and redox potential contribute to shifts in the forms of heavy metal ions present in the water [8-12].

Metals in sludge can exist in various forms: exchangeable, carbonate-bound, organic, sulfide-bound, and residual. The exchangeable form includes trace metals that are exchangeable bound to solid particles, influenced by sorption and desorption phenomena. The carbonate form comprises trace metals associated with carbonates, and its size changes with pH. Organic forms are linked to different types of organic matter, which can be released under oxidizing conditions. The sulfide form includes metals bound to sulfides, which depend on oxidizing-reducing conditions. The residual form includes metals strongly bound within the crystal lattice, released only by strong mineral acids.

The mobility of trace metals can be assessed using sequential chemical extraction, where sludge is treated with solutions of increasing leaching strength. This allows for the identification of specific metal forms, representing only a portion of the total content. For fractionation, the Rudd speciation method can be used. In a given sample, the following metal forms can be identified:

- Exchangeable metals;
- Adsorbed metals;
- Metals bound to organic matter;
- Metals bound to carbonates;
- Metals in sulfide form.

According to the Rudd method, exchangeable, adsorbed, organic-bound, carbonate-bound, and sulfide-bound metals are sequentially extracted using solutions of 1M KNO<sub>3</sub>, 0.5M KF, 0.1M Na<sub>4</sub>P<sub>2</sub>O<sub>7</sub>, 0.1M EDTA, and 6M HNO<sub>3</sub>, respectively [13-16].

The metal content in the tested samples after sequential chemical extraction or total mineralization can be measured using atomic absorption spectrometry. This method is based on the absorption of light at a wavelength specific to the element being analyzed by unexcited atoms of that element, using an atomic absorption spectrophotometer [17-18].

## 2 Material and methods

### 2.1 Research setup

The sludge used for the study was sourced from a Water Treatment Plant located in Chrzanów County, within the Małopolska Voivodeship. The water treated in this system was mine water from a zinc and lead mine, which is why the authors also analysed sludge originating from the mine. Sodium hypochlorite (NaOCl) was dosed into the water before it passed through the sand filters.

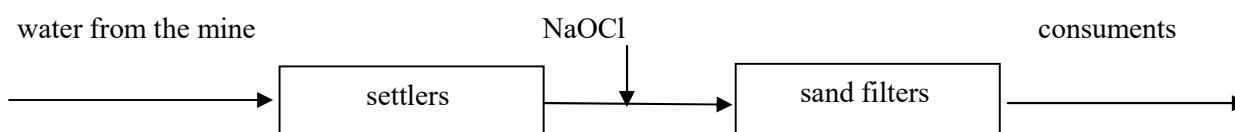


**Fig. 1. Block diagram of water treatment processes**

Before the tests, the sludge was dried and ground by crushing it in a porcelain mortar. The diagram of the research setup is shown in Figure 2.

The appropriate reagent (NaOCl + LB-151.2 quartz lamp by Bak Med Łódź, KMnO<sub>4</sub>, H<sub>2</sub>O<sub>2</sub> + LB-151.2 quartz lamp, CO<sub>2</sub>, O<sub>3</sub>) from the tank (1) was pumped into the reaction vessel (3) using a peristaltic pump (2) PP 1B - 05. The reaction vessel contained a previously prepared mixture of 1000 ml of water and the appropriate amount of sludge. These reagents were dosed continuously or once directly into the reaction vessel. During the experiment, with continuous stirring, samples were taken, and measurements of pH (pH meter CP - 315 by Elmetron), potential (CPC - 551 by Elmetron), and conductivity (CC - 311 by Elmetron) were conducted.

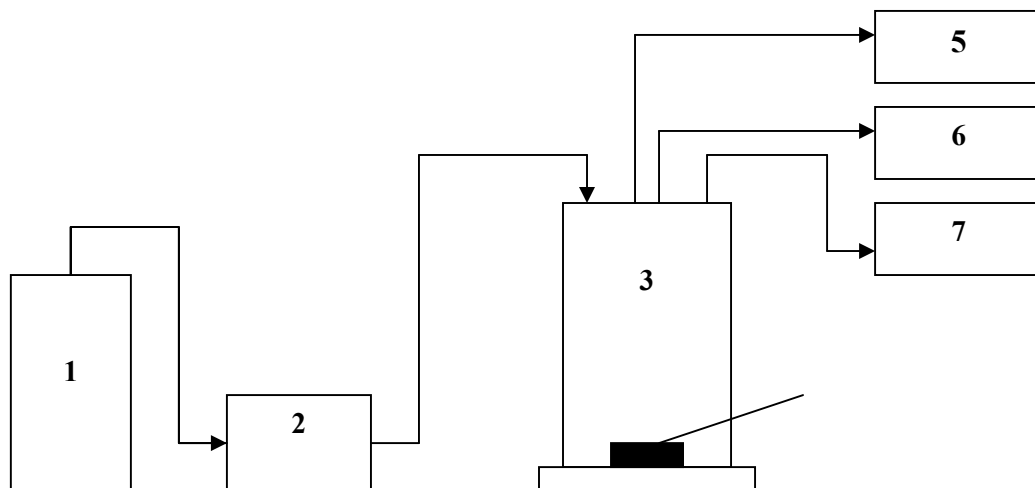


**Fig. 2. Research stand**

Legend: 1-tank with reagent; 2-pump; 3-reaction tank; 4-stirrer; 5-pH-meter; 6-potentiometer; 7-conductivity meter

## 2.2 Research methodology

### 2.2.1 Investigation of zinc and lead forms in sludge (speciation) retained on sand filters

To determine the total amount of metals (Zn, Pb, and Mn), a sludge sample weighing approximately 1 g was subjected to mineralization. To identify the specific compounds in which these metals occur, a speciation analysis was conducted. For this purpose, a 1 g sludge sample was sequentially treated with the following reagents at specific concentrations: 1M KNO<sub>3</sub>, 0.5M KF, 0.1M Na<sub>4</sub>P<sub>2</sub>O<sub>7</sub>, 0.1M EDTA, and 6M HNO<sub>3</sub>, in 25 cm<sup>3</sup> volumes.

After adding the first reagent to the sludge, the mixture was shaken for 60 minutes and then left to stand for 24 hours. After this period, the mixture was shaken again for 10 minutes and centrifuged for 15 minutes, and the supernatant liquid was separated from the sludge. The sludge was then washed with distilled water, shaken for 15 minutes, and centrifuged again, after which the supernatant was separated. These steps were repeated for the remaining reagents. The zinc and lead content was determined in each sample.

### 2.2.2 Study of the effect of sodium hypochlorite on the leaching of zinc and lead from sludge

To determine the effect of NaOCl on the leaching of zinc and lead from sludge, an experiment was conducted using different sludge amounts: 2 g, 4 g, and 6 g. The experiment was carried out in two ways:

Method 1: In a beaker containing 1000 cm<sup>3</sup> of water with a given amount of sludge, 20 cm<sup>3</sup> of NaOCl was added. The NaOCl solution contained 2240 mg Cl<sub>2</sub>/L. While continuously stirring, measurements and samples were taken at specific time intervals. In these samples, the content of zinc and lead, as well as manganese, was determined. The experiment lasted 180 minutes.

Method 2: In a beaker containing 1000 cm<sup>3</sup> of water with a given amount of sludge, NaOCl was continuously supplied for the first 90 minutes at a flow rate of 50 cm<sup>3</sup>/h. The entire experiment lasted 300 minutes. Samples were taken at specific time intervals, and the content of zinc, lead, and manganese was determined.

### 2.2.3 Study of the effect of hydrogen peroxide on the leaching of zinc and lead from sludge

To investigate the effect of H<sub>2</sub>O<sub>2</sub> on the leaching of zinc and lead from the sludge, an experiment was conducted with 2 g and 4 g of sludge. In each trial, 1000 cm<sup>3</sup> of water was used, and 30 % hydrogen peroxide was continuously supplied for 90 minutes at a flow rate of 50 cm<sup>3</sup>/h. Measurements and sampling were carried out over 210 minutes. A similar experiment was conducted with simultaneous UV radiation exposure. The collected samples were analysed for zinc, lead, and manganese content.

### 2.2.4 Study of the effect of potassium permanganate on the leaching of zinc and lead from sludge

To examine the effect of KMnO<sub>4</sub> on zinc and lead leaching from the sludge, 2 g of sludge was added to a beaker containing 1000 cm<sup>3</sup> of water. Potassium permanganate was continuously supplied at a constant

flow rate of 50 cm<sup>3</sup>/h, with continuous stirring for 90 minutes. Measurements and sample collection were carried out over 300 minutes, and the samples were analysed for zinc, lead, and manganese content.

### 2.2.5 Study of the effect of UV radiation on the leaching of zinc and lead from sludge

The effect of UV radiation on the release of zinc and lead from sludge was examined in conjunction with other compounds, such as NaOCl and H<sub>2</sub>O<sub>2</sub>. The experiment was conducted over 300 minutes, with NaOCl or H<sub>2</sub>O<sub>2</sub> supplied to the reaction vessel during the first 90 minutes at a flow rate of 50 cm<sup>3</sup>/h. Measurements and sample collection were performed at specific time intervals to determine zinc, lead, and manganese content.

### 2.2.6 Study of the effect of carbon dioxide on the leaching of zinc and lead from sludge

The effect of CO<sub>2</sub> on the release of zinc and lead from the sludge was experimentally determined. For this experiment, 500 cm<sup>3</sup> of water and 1 g of sludge were used. CO<sub>2</sub> was supplied to the reaction vessel for 60 minutes, and during this time, measurements and sample collection were carried out at specific intervals to analyze the zinc, lead, and manganese content.

### 2.2.7 Study of the effect of ozone on the leaching of zinc and lead from sludge

To determine the effect of ozone on the release of zinc and lead from the sludge, an experiment was conducted by passing ozone through the tested water. The experiment lasted for 15 minutes with a flow rate of 0.1 m<sup>3</sup>/h. During the experiment, 25 g of O<sub>3</sub> per cubic meter of water was used.

## 3 Results and discussion

### 3.1 Forms of lead and zinc in the sludge

According to the speciation analysis (Table 1), the highest amounts of zinc in the sludge are found in the sulfide form. Among the samples analysed, this form ranges from 44.08 % to 67.30 % of the total zinc content. Zinc associated with carbonates constitutes 24.19 % to 41.33 % of the total. Zinc bound to organic matter accounts for 6.08 % to 11.65 % of the total zinc content, while exchangeable zinc is only 0.02 % to 0.03 %, and adsorbed zinc makes up 0.02 % to 0.09 % of the sludge.

Table 1. Zinc content in the sediment

Sample	Percentage of zinc forms [%]						Total Zn after mineralization [mg/g]
	KNO <sub>3</sub>	KF	Na <sub>4</sub> P <sub>2</sub> O <sub>7</sub>	EDTA	HNO <sub>3</sub>	Remaining specification	
1	0.03	0.04	6.08	24.19	67.30	2.35	14.631
2	0.02	0.04	7.01	32.62	57.75	2.56	25.331
3	0.02	0.07	6.70	28.25	62.71	2.25	23.235
4	0.03	0.03	6.69	27.05	64.10	2.09	25.903
5	0.02	0.03	7.00	27.09	63.29	2.56	23.706
6	0.03	0.09	7.32	26.26	64.09	2.21	24.298
7	0.02	0.04	7.05	26.14	65.24	1.52	29.408
8	0.02	0.03	6.80	26.66	65.90	0.59	24.008
Sediment from the filter surface	0.02	0.02	11.65	41.33	44.08	2.91	32.905

Compared to zinc, lead occurs in somewhat different quantities. The largest proportion of lead is found in the carbonate form, ranging from 33.63 % to 43.03 %. In most of the samples analysed, lead compounds associated with organic matter constitute 15.01 % to 26.11 %, while lead in the sulphide form ranges from 10.83 % to 19.22 %. In each of these samples, the amount of lead associated with organic matter was greater than that in the sulphide form. An exception was the sample taken from the surface of the filter, where the amount of lead in the sulphide form was 29.93 %, while that associated with organic matter was 2.19 %. This sample contained the highest proportion of lead associated with carbonates, at 43.03 %. The remaining forms of lead were present in minor quantities, with adsorbed lead ranging from 0.03 % to 0.20 % and exchangeable lead from 0.02 % to 0.08 % (Table 2).

Table 2. Lead content in the sediment

Sample	Percentage of lead forms [%]						Total Pb after mineralization [mg/g]
	KNO <sub>3</sub>	KF	Na <sub>4</sub> P <sub>2</sub> O <sub>7</sub>	EDTA	HNO <sub>3</sub>	Remaining specification	
1	0.08	0.18	22.45	34.77	19.22	23.31	15.518
2	0.04	0.04	17.34	36.70	12.41	33.47	10.690
3	0.04	0.03	17.77	35.22	13.43	33.52	9.643
4	0.06	0.04	20.80	41.17	14.03	23.90	11.049
5	0.04	0.05	16.39	35.15	13.69	34.68	10.939
6	0.03	0.03	15.01	37.72	13.31	33.91	12.015
7	0.04	0.20	26.11	33.63	13.86	26.17	15.062
8	0.04	0.16	22.34	37.87	13.69	25.90	12.069
Sediment from the filter surface	0.02	0.06	2.19	43.03	29.93	24.77	10.205

### 3.2 Effect of Sodium Hypochlorite (NaOCl) on Zinc and Lead Leaching

The amount of zinc, lead, and manganese released under the influence of NaOCl varied depending on the method of the process. In the experiment where 20 cm<sup>3</sup> of NaOCl was introduced all at once into the reaction vessel, the maximum amount of zinc leached from 2 g, 4 g, and 6 g of sludge, with initial metal concentrations in water of 1.886 mg/L, 1.632 mg/L, and 1.409 mg/L respectively, was 19.873 mg/L, 19.737 mg/L, and 18.789 mg/L. Zinc leaching occurred within the first five minutes, after which the amount of Zn began to decrease (Figure 3).

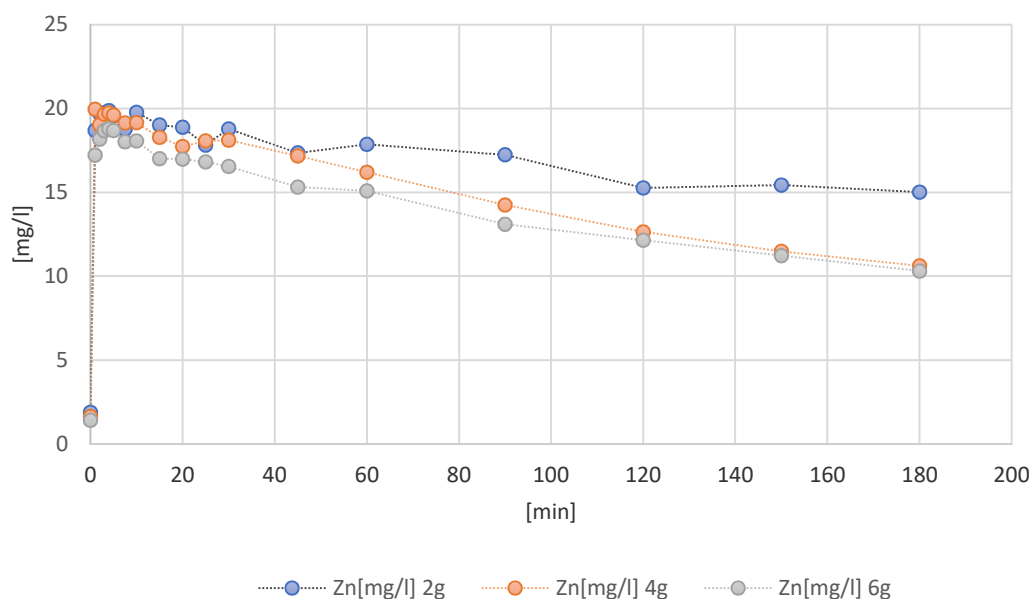
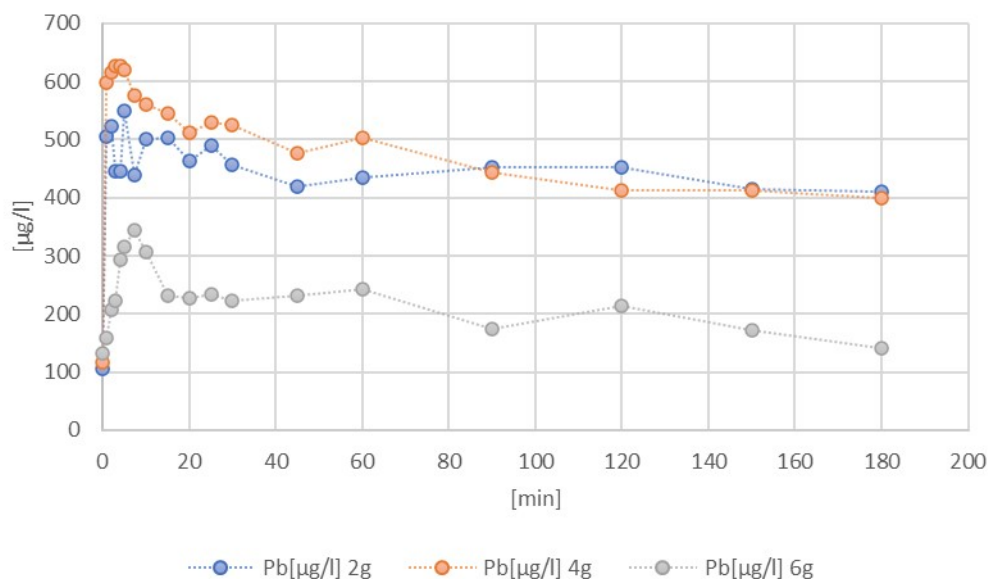


Fig. 3. The effect of NaOCl on the leaching of zinc from the sediment retained on the filters

For lead, the initial concentrations were 106.22 µg/L for 2 g of sludge, 116.17 µg/L for 4 g of sludge, and 132.85 µg/L for 6 g of sludge. The maximum amount of lead released under the influence of NaOCl was 549.46 µg/L, 626.41 µg/L, and 345.29 µg/L, respectively. Similar to zinc, lead leaching occurred within the first 5-7 minutes, after which the amount of lead began to decrease, as shown in Figure 4.

Mangan behaves differently depending on its quantity when exposed to NaOCl added all at once to a mixture of water and sediment. For 4 g and 6 g of sediment, the amount of manganese in the water increased to a maximum value of 619.97 µg/L and 791.03 µg/L, respectively. In the case of 2 g of sediment, the amount of manganese in the solution decreased. Its minimum concentration in the water was 164.73 µg/L, but later it increased.



**Fig. 4. The effect of NaOCl on the leaching of lead from the sediment retained on the filters**

During the experiment with 2 g of sediment, the pH decreased from 7.64 to 7.05 during the first 10 minutes, then increased again to 7.62. The potential, after the addition of NaOCl to the water, increased from 310 mV to 704 mV and then began to decrease, ending at 308 mV. In the experiment with 4 g of sediment, the pH decreased from 7.71 to 7.14 and then increased to 7.62. The potential increased from 318 mV to 582 mV and then decreased to 272 mV over the course of the experiment. For 6 g of sediment, the pH decreased from 7.71 to 7.14 and then increased to 7.64. The potential increased from 299 mV to 422 mV and then decreased to 271 mV during the process.

In the experiment where chlorine was continuously supplied to the reaction vessel, the initial zinc content was 1.082 mg/L for 2 g of sediment, 0.939 mg/L for 4 g, and 0.628 mg/L for 6 g. The maximum amount of zinc released from 2 g of sediment was 14.219 mg/L, from 4 g of sediment was 12.707 mg/L, and from 6 g was 11.847 mg/L. After stopping the NaOCl supply, the zinc amount started to decrease. For lead, the situation was similar except that the amount of lead in the water initially increased for 4 g and 6 g of sediment, then decreased and began to increase again. The lead release process from 2 g of sediment showed a continuous increase in lead in the water throughout the experiment. The manganese release process under continuous NaOCl supply was similar to the zinc release process, i.e. for 2 g, 4 g, and 6 g, the amount of manganese in the water increased while NaOCl was supplied and then began to decrease. The maximum amount of manganese in the water was 496.75 µg/L for 6 g.

In the experiment where NaOCl was continuously supplied, pH decreased and the potential increased until the NaOCl supply was stopped, after which the pH began to rise and the potential decreased. For 2 g, 4 g, and 6 g of sediment, the initial pH values were 8.01, 8.03, and 7.99, respectively, which decreased to 7.54, 7.62, and 7.59 and then increased to 7.74, 7.82, and 7.84. The potential values initially were 244 mV for 2 g, 246 mV for 4 g, and 216 mV for 6 g. These values increased to 608 mV, 369 mV, and 329 mV, respectively. At the end of the process, the potential values were 302 mV for 2 g, 248 mV for 4 g, and 234 V for 6 g.

In the experiment where NaOCl was applied with UV radiation, the zinc release process from the sediment proceeded until NaOCl supply was stopped, after which the zinc amount in the solution began to decrease. The maximum zinc amounts released were 12.428 mg/L for 2 g of sediment, 15.143 mg/L for 4 g, and 10.798 mg/L for 6 g.

The lead release process from sediment showed variability. Similar to other reagents, the amount of lead in the water increased in the first minutes, then decreased and increased again. The maximum lead released from 2 g of sediment was 244.70 µg/L (initially 31.60 µg/L), from 4 g was 236.73 µg/L (initially 37.50 µg/L), and from 6 g was 173.70 µg/L (initially 50.83 µg/L). The manganese amount under NaOCl and UV exposure increased in the water while NaOCl was supplied and then began to decrease. The maximum manganese concentrations were: 226.11 µg/L for 2 g, 375.53 µg/L for 4 g, and 499.36 µg/L for 6 g.



In the experiment with continuous NaOCl supply supported by UV radiation, pH decreased and the potential increased until NaOCl supply was stopped. After that, pH began to rise and the potential decreased. For 2 g, 4 g, and 6 g of sediment, the initial pH values were 7.96, 8.01, and 8.00, which decreased to 7.48, 7.61, and 7.58 and then increased to 7.75, 7.79, and 7.85. The potential values initially were 245 mV for 2 g, 244 mV for 4 g, and 228 mV for 6 g, rising to 458 mV, 366 mV, and 346 mV, respectively. At the end of the process, the potential values were 243 mV for 2 g, 238 mV for 4 g, and 244 mV for 6 g.

### 3.3 Effect of hydrogen peroxide on the leaching of zinc and lead

The process of leaching zinc, lead, and manganese from sediment under the influence of H<sub>2</sub>O<sub>2</sub> for 4 g of sediment is presented in Table 3.

**Table 3. Zinc, lead and manganese isolated from 4 g of sediment under the influence of H<sub>2</sub>O<sub>2</sub> and UV**

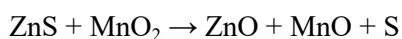
t [min]	pH	mV	uS	Zn [mg/L]	Mn [µg/L]	Pb [µg/L]
0	7.98	247	1361	0.527	194.43	42.03
1	8.01	247	1352	0.417	218.13	83.91
2	8.01	248	1354	0.418	226.98	121.18
5	7.99	249	1357	0.444	228.57	172.63
7,5	7.98	250	1356	0.506	234.57	192.00
10	7.96	251	1358	0.553	265.55	202.57
15	7.93	254	1362	0.777	287.91	201.43
20	7.92	259	1365	1.172	346.93	203.72
25	7.88	261	1360	1.699	407.65	199.39
30	7.86	264	1345	2.952	440.22	246.30
45	7.86	269	1349	5.389	489.63	276.42
60	7.85	271	1345	8.390	431.98	256.78
90	7.83	270	1283	14.358	377.00	279.64
120	7.73	267	1416	19.575	327.65	265.57
150	7.76	263	1323	23.312	293.79	236.22
180	7.88	261	1336	22.489	298.95	260.18
210	7.92	259	1140	20.623	297.47	238.05

The process of zinc leaching occurred slowly. The increase in zinc concentration in the solution happened while H<sub>2</sub>O<sub>2</sub> was being added. After stopping the supply, the amount of zinc leached began to decrease. For lead, its concentration in the water increased to 419.41 µg/L for 4 g of sediment during the experiment. After discontinuing the H<sub>2</sub>O<sub>2</sub> supply, the amount of lead leached from the sediment began to decrease. Under the influence of H<sub>2</sub>O<sub>2</sub>, manganese transitioned into the solution, with a maximum concentration of 293.63 µg/L for 4 g of sediment.

In the experiment with hydrogen peroxide combined with UV irradiation, the zinc leaching process from the sediment was similar to the experiment with H<sub>2</sub>O<sub>2</sub> alone. The initial zinc concentrations were 1.307 mg/L and 0.527 mg/L. Similarly, after stopping the hydrogen peroxide supply and continuing UV irradiation, the amount of zinc began to decrease. The lead leaching process under the influence of H<sub>2</sub>O<sub>2</sub> and UV irradiation also showed a similar trend, but with slightly lower concentrations. The maximum amount of lead leached from 2 g of sediment was 346.60 µg/L, while from 4 g it was 279.64 µg/L. Manganese behaved similarly to zinc and lead under H<sub>2</sub>O<sub>2</sub> and UV radiation, increasing in concentration during the H<sub>2</sub>O<sub>2</sub> supply and decreasing after the supply was stopped.

### 3.4 Discussion of the effect of potassium permanganate (VII) on the leaching of zinc and lead

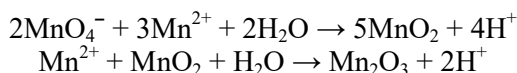
The effect of potassium permanganate (VII) on zinc contained in sediment retained on sand filters, under laboratory conditions, was different from the effects of other reagents. During the process, no increase in the amount of zinc in the water was observed; rather, the opposite phenomenon was noted according to the reaction. The reaction likely occurring was:



The concentration of zinc in the solution decreased over time. Its initial concentration was 1.420 mg/L, and at the end of the process, it was 0.703 mg/L. The change in zinc concentration over time is graphically represented in Figure 21.

The impact of KMnO<sub>4</sub> on the leaching of lead from the sediment differed from that on zinc. After an initial increase in lead concentration in the water during the first 10 minutes, the amount decreased to 93.40 µg/L and then showed a general increasing trend for the remainder of the process.

The manganese concentration in the water under the influence of KMnO<sub>4</sub> decreased to 8.88 µg/L within the first few minutes, then began to increase until the KMnO<sub>4</sub> supply was stopped, reaching a value of 201.79 µg/L. Subsequently, the manganese concentration in the water started to decrease. This is likely due to the transition of manganese to less soluble forms, such as:



The manganese leaching process is shown in Table 4.

**Table 4. Zinc, lead and manganese separated from 2 g of sediment under the influence of KMnO<sub>4</sub>**

t [min]	pH	mV	uS	Zn [mg/L]	Mn [µg/L]	Pb [µg/L]
0	7.93	252	1415	1.420	141.80	57.69
1	7.92	470	1410	1.334	52.87	123.17
2	7.92	512	1405	1.378	19.34	129.51
3	7.93	523	1400	1.320	15.21	128.71
4	7.94	530	1407	1.323	8.88	136.91
5	7.93	532	1406	1.295	14.32	145.90
7,5	7.94	539	1404	1.233	11.98	148.98
10	7.93	539	1404	1.233	5.07	151.22
15	7.96	542	1390	1.196	5.36	118.32
20	7.97	545	1394	1.173	14.18	104.90
25	7.99	546	1389	1.137	14.53	93.45
30	7.99	546	1384	1.133	41.61	94.36
45	7.99	548	1371	1.049	81.25	108.35
60	8.01	550	1357	0.931	164.67	107.49
90	8.02	560	1340	0.912	201.79	117.27
120	8.03	569	1312	0.927	151.22	126.69
150	8.05	564	1313	0.904	99.35	129.74
180	8.08	552	1313	0.868	11.73	130.12
210	8.12	535	1316	0.878	0	152.89
240	8.14	491	1324	0.716	0	156.87
270	8.16	460	1327	0.703	0	169.70
300	8.19	438	1327	0.732	0	177.78

### 3.5 The influence of carbon dioxide (IV) on the leaching of zinc and lead

Under the influence of CO<sub>2</sub>, the concentration of zinc in the solution increased during the first 2 minutes. The maximum amount of zinc released during this time was 16.476 mg/L, with an initial concentration of 3.544 mg/L in the solution. After this period, the amount of zinc released remained nearly constant, fluctuating between 15 and 17 mg/L until the end of the process.

The maximum amount of lead released from 2 g of sediment under the influence of CO<sub>2</sub>, with an initial concentration of 45.67 µg/L in the water, was 262.47 µg/L. The zinc and lead concentrations under CO<sub>2</sub> influence are graphically represented in Figures 39 and 40.

Under CO<sub>2</sub> influence, the manganese concentration in the water increased, reaching a maximum of 1009.01 µg/L. After 10 minutes of the process, the manganese concentration stabilized at a nearly constant level.

The pH decreased from 7.79 to 5.75 during the first 10 minutes, then increased slightly to 5.93. The potential initially increased from 301 mV to 545 mV, and then decreased to 494 mV.

### 3.6 The influence of ozone on the leaching of zinc and lead

The maximum amount of zinc released from the sediment under the influence of ozone after 15 minutes was 38.709 mg/L. The maximum amounts of lead and manganese released from the sediment were 442.00 µg/L and 16.61 µg/L, respectively, with initial concentrations of these metals being 2.47 µg/L for lead and 347.23 µg/L for manganese. The pH, conductivity, and potential values changed as follows: pH decreased from 8.09 to 7.62; conductivity decreased from 1421 µS to 1340 µS; and potential increased from 225 mV to 862 mV.

## 4 Conclusions

In the sediment collected from a sand filter at a zinc and lead ore mine, zinc was predominantly present in the form of sulfides (44.08 %) and associated with carbonates (41.33 %). The remaining forms, such as organic-bound zinc, exchangeable zinc, and adsorbed zinc, constituted minor amounts. In the sediment from the same mine, lead was mostly found in carbonate form (43.03 %) and sulfide form (29.93 %), with the remaining forms being in minor proportions. The sediment from the surface of the filter primarily contained zinc and lead sulfides, which, under the influence of oxidizers, were converted into sulfates and released into the solution.

The largest amounts of zinc and lead were released under the influence of H<sub>2</sub>O<sub>2</sub>. Ultraviolet rays had an inhibitory effect on the release of zinc and lead into the water. Potassium permanganate did not cause the release of zinc from the sediment but did lead to the release of lead into the water. In contrast, carbon dioxide caused the immediate release of zinc and lead from the sediment. The process of zinc and lead release from the sediment was associated with the release of manganese. This process had a greater impact on lead release than on zinc release.

The problem of excessive zinc and lead in the treated water at the Water Treatment Plant is most likely due to the use of an inappropriate disinfectant. To select the appropriate disinfectant, further studies are needed.

## References

- [1] Directive (EU) 2020/2184 of the European Parliament and of the council of 16 December 2020 on the quality of water intended for human consumption. <https://eur-lex.europa.eu/legal-content/EN/TXT/PDF/?uri=CELEX:32020L2184> [day access: 28.05.2023].
- [2] Boshoff, G.A., Rose P.D., Duncan J.R. A Continuous Process for the Biological Treatment of Heavy Metal Contaminated Acid Mine Water, R.P. Van Hille, Rhodes University, Grahamstown, South Africa, Resour Conserv Recycl, Jul 99, v27, n1-2, p157(11) (from Int Soc for Environ Biotechnol Fourth Int Symp, Belfast, Northern Ireland (Jun 20-25, 98)).
- [3] Marino, N., Vaquero, M.C., Ansorena, J., Egorburu, I. Metal Pollution by Old Lead-Zinc Mines in Urumea River Valley (Basque Country, Spain). Soil, Biota and Sediment, J. Sanchez, University Pais Vasco, San Sebastian, Spain, Water Air Soil Pollut, Oct 98, v107, n1-4, p303(17).
- [4] Beckstead, G., Long, D. Integrated Mine Water Management Planning for Environmental Protection and Mine Profitability, Leslie F. Sawatsky, AGRA Earth and Environment, Calgary, Canada, Int J Surface Mining Reclamation Environ, 1998, v12, n1, p37(3).
- [5] Baranowski, R., Kot, B. Leaching of Metal Ions in Mine Water from Solid Mine Wastes, Silesian Technical University, Gliwice, Poland; Polish J Environ Stud, 1996, v5, n3, p11(4).
- [6] Wojcik, M. Soil Contamination Caused by Discharge of a Mine Water, University of Mining and Metallurgy, Krakow, Poland; Am Soc Agric Eng/et al Environ Sound Agric Proc of the Second Conf, Orlando, FL, Apr 20-22, 94, p523(10).
- [7] Gonzalez, M.J. Influence of Acid Mine Water in the Distribution of Heavy Metal in Soils of Donana National Park. Application of Multivariate Analysis, Inst de Quimica Organica General, Madrid, Spain, M. Fernandez and L. M. Hernandez; Environ Technol, Nov 90, v11, n11, p 1027(12).
- [8] Christensen, B.J., Botma, J.J., Christensen, T.H. Complexation of Cu and Pb by doc in polluted groundwater: a comparison of experimental data. Water Research, v33, n15, 1999.
- [9] Kabat-Pendias, A., Pendias, H. Biogeochemia pierwiastków śladowych. Warszawa, Wydawnictwo Naukowe PWN, 1999.
- [10] Wang, F., Chen, J. Relation of sediment characteristics to trace metal concentrations: A statistical study. Water Research, v34, n2, 2000.

- [11] White, W.M. Reactions at the earth's surface: Weathering, soils, and stream chemistry. *Geochemistry*-January 25, 1998.
- [12] Kuang-Chung, Y., Li-Jyur, T. Correlation analyses on binding behavior of heavy metals with sediment matrices. *Water Research*, v.35, n10, 2001.
- [13] Kabata-Pendias, A., Szeke, B. *Problemy jakości analizy śladowej w badaniach środowiska przyrodniczego*. Warszawa, Wydawnictwo Edukacyjne Zofii Dobkowskiej, 1998.
- [14] Kocjan, R. *Chemia analityczna*. Warszawa, Wydawnictwo Lekarskie PZWL, 2000.
- [15] Polański, A. *Podstawy geochemii*. Warszawa, Wydawnictwa Geologiczne, 1988.
- [16] Rudd, T., Lake, T., Mehrotra, I., Sterritt, R.M., Kirk P.W.P., Campbell, J.A. Characterisation of metal forms in sewage sludge by chemical extraction and progresive acidification the science of the total. *Environment*, 74, 1988.
- [17] Ciba, J. *Poradnik chemika-analityka. Analiza instrumentalna*. Warszawa, Wydawnictwo Naukowo-Techniczne, 1991.
- [18] Siepak, J. *Problemy analityczne badań osadów dennych*. Poznań, Zakład Analizy Wody i Gruntów, 2001.

# ALUMINIUM ELECTROCOAGULATION FOR EFFICIENT TREATMENT OF LANDFILL LEACHATE CONTAMINATED WITH HIGH CONCENTRATION OF FLUORIDES AND CYANIDES

**Claudia Čičáková<sup>a</sup>, Daniel Kupka<sup>b</sup>, Jana Hroncová<sup>b</sup>, Lenka Hagarová<sup>b</sup>, Tomáš Faragó<sup>a</sup>,  
Eva Mačingová<sup>b</sup>, Viktória Krajanová<sup>c</sup>, Ľubomír Jurkovič<sup>a</sup>, Miroslava Václavíková<sup>b</sup>**

<sup>a</sup> Comenius University, Faculty of Natural Sciences, Department of Geochemistry,  
Ilkovičova 6, 842 15, Bratislava 4, cicakova13@uniba.sk

<sup>b</sup> Slovak Academy of Sciences, Institute of Geotechnics, Watsonova 45, 040 01, Košice, dankup@saske.sk

<sup>c</sup> SNM-Natural History Museum, Vajanského nábr. 2, 810 06, Bratislava, v.krajanova@gmail.com

## Abstract

Landfill leachate with a high concentration of fluorides (1470 mg.L<sup>-1</sup>) and cyanides (75 mg.L<sup>-1</sup>) poses a significant risk of environmental contamination. To effectively remove fluorides and cyanides, an electrocoagulation approach was tested. Electrocoagulation is a process of passing a steady direct electric current through a liquid using aluminium or iron electrodes (so-called sacrificial electrodes) to remove impurities from water. The most effective removal of fluorides was observed with Al-electrodes. Various current densities of 8 mA.cm<sup>-2</sup> and 24 mA.cm<sup>-2</sup> were tested. Another important parameter in Al-electrocoagulation is pH, which must be maintained in the range of pH 6 - 8 during the process. Using Al-electrodes, fluoride removal ranged from about 33 % at a current density of 8 mA.cm<sup>-2</sup> (without continuous pH adjustment) to 95 % at 24 mA.cm<sup>-2</sup> (with continuous pH adjustment). Cyanide removal reached a maximum efficiency of 15 %. Therefore, the next step - BDD electrooxidation was examined. During BDD electrooxidation, chlorates and perchlorates are produced as intermediate products, which can be reduced to chlorides through bacterial reduction. However, these steps are still under investigation and will not be part of this report.

**Keywords:** aluminium electrocoagulation, landfill leachate, cyanides, fluorides

## 1 Introduction

Fluorine is a vital element for the human body [1]. However, excessive amounts of fluoride ions in drinking water pose a significant public health concern due to their beneficial and detrimental effects. While an optimal fluoride concentration of 1 mg.L<sup>-1</sup> helps prevent dental caries, prolonged exposure to drinking water with high fluoride levels (1.5 mg.L<sup>-1</sup>) can cause dental and skeletal fluorosis [2]. Electrocoagulation (EC) is a water treatment method that removes impurities by passing a direct electric current through the water using sacrificial electrodes, such as aluminium or iron [2, 3]. In this process, Al<sup>3+</sup> ions dissolve at the Al-anode while hydrogen gas is produced at the cathode. The resulting coagulating agent binds with pollutants to form larger flocs. These flocs then attach to rising gas bubbles, allowing the pollutants to float to the water's surface - in electroflocculation process [3].

EC and electrocoagulation/flotation (ECF) processes can be effectively utilized in a wide range of water and wastewater treatment systems, particularly for removing inorganic contaminants (cyanides) and pathogens [3]. These methods have demonstrated high efficiency in treatment of water, offering advantages such as minimal sludge production, no need for chemical additives, and simple operation [3, 4].

The contaminated landfill leachate comes from a partially recultivated landfill near Žiar nad Hronom. Waste from aluminium production at ZSNP was disposed of at an industrial waste landfill. The landfill was created in the 1963. During the operation of the landfill, municipal waste was also deposited in the landfill. The operation of the landfill was terminated in 1998. The leachate is characterized by a high fluoride concentration of up to 1400 mg.L<sup>-1</sup> and cyanide concentration 75 mg.L<sup>-1</sup>, and high base pH ~ 10 pose a risk to the surrounding environment [5].

## 2 Material and methods

### 2.1 Characteristics of metal binding experiment

EC of the solution was performed under galvanostatic conditions in a single-compartment (undivided) electrochemical cell using a batch system. The electrochemical reactor consisted of a 1 L glass beaker, a magnetic stirrer, and commercially available aluminium electrodes (dimensions 250 x 50 x 1.5 mm). The gap between two neighbouring electrode plates was kept constant at 5 mm for all experiments. The initial pH of the landfill leachate was between 10.17 and 10.4. The pH was adjusted with 5M H<sub>2</sub>SO<sub>4</sub> before and during the

Al-electrocoagulation process (according on tests in Table 2). Besides test (ZnH-07) where pH was adjusted with and 4M HNO<sub>3</sub>. The water quality of contaminated landfill leachate is described in Table 1.

**Table 1. The analysis of water**

Item	Concentration mg.L <sup>-1</sup>	Item	Concentration mg.L <sup>-1</sup>
Na <sup>+</sup>	7977.6	F <sup>-</sup>	1426
K <sup>+</sup>	25.52	Cl <sup>-</sup>	195.31
Li <sup>+</sup>	0.723	SO <sub>4</sub> <sup>2-</sup>	105.07
NH <sub>4</sub> <sup>+</sup>	239.5	NO <sub>3</sub> <sup>-</sup>	0.12
Mg <sup>2+</sup>	0.1	COD	817
Ca <sup>2+</sup>	0.91	CN <sup>-</sup> (toxic)	0.187
Al	<0.4 (u DL)	CN <sup>-</sup> (total)	75.0

Note: uDL - under detection limit

Electrochemical tests were conducted under two various current densities 8 mA.cm<sup>-2</sup> and 24 mA.cm<sup>-2</sup> and under different pH condition. The description of single tests is shown in Table 2.

**Table 2. The description of tests**

Test	Adjusted pH before Al-EC/acid	Adjusted pH/acid continuously during Al-EC	Current density	Specifics
ZnH-01	no	no	8 mA.cm <sup>-2</sup>	-
ZnH-02	Yes/ 5M H <sub>2</sub> SO <sub>4</sub> , pH 7.4	no	8 mA.cm <sup>-2</sup>	-
ZnH-03	Yes/ 5M H <sub>2</sub> SO <sub>4</sub> , pH 6.5	no	24 mA.cm <sup>-2</sup>	-
ZnH-06 <sup>+</sup>	Yes/ 5M H <sub>2</sub> SO <sub>4</sub> , pH 6.5	yes	24 mA.cm <sup>-2</sup>	-
ZnH-07 <sup>+</sup>	Yes/ 4M HNO <sub>3</sub> , pH 6.5	yes	24 mA.cm <sup>-2</sup>	-
ZnH-08	Yes/ 5M H <sub>2</sub> SO <sub>4</sub> , pH 6.5	yes	24 mA.cm <sup>-2</sup>	Filtration of Al-sludge after 50 min
ZnH-09	Yes/ 5M H <sub>2</sub> SO <sub>4</sub> , pH 6.5	yes	24 mA.cm <sup>-2</sup>	Polarity reversal (10min interval)

The high initial pH 10.17 - 10.4 was adjusted at pH 7.4 (ZnH-02) and pH 6.5 (in all other tests) before Al-electrocoagulation. The exception was the first test (ZnH-01) where pH stayed unchanged during the whole electrolysis process.

Sampling and pH measurements were carried out at 10-minute intervals after the interruption of direct current (DC). The pH was adjusted, and acid was added after each sampling (every 10 minutes) during Al-electrocoagulation. Fluoride concentrations and other anionic and cationic species (Table 1) were analysed using ion chromatography. Samples were filtered through a 0.22 µm filter before analysis. Aluminium concentrations were measured by flame atomic absorption spectrometry. After the electrocoagulation, the solution was filtrated through 0.22 µm filter, and the filtrate of the sludge was analysed by Raman microspectroscopy and by scanning electron microscope.

Raman microspectroscopy of the produced sludge was performed using a DXR3xi Raman Imaging Microscope (NICOLET) in the laboratories of the Slovak National Museum - Natural History Museum in Bratislava. A laser with a wavelength of 532 nm was used.

Subsequently, the surface morphology of the sludge was examined using a MIRA 3 FE-SEM (TESCAN) scanning electron microscope fitted with an Elemental distribution was assessed by EDX mapping using energy-dispersive X-ray (EDX) detector from Oxford Instruments.

### 3 Results and discussion

#### 3.1 Impact of adjustment of pH on fluoride removal and polarity reversal

During the Al-electrocoagulation test (ZnH-01), where the pH of wastewater was left unchanged (pH 10.3), the concentration of fluoride decreased by only about 5 % in 60 minutes. Therefore, the pH of the solution had to be adjusted to the range of 6-8, as recommended by other studies [3, 6, 7]. In the subsequent test (test ZnH-02), the pH was modified to 7.4 before EC but was not controlled during the EC process. Under these conditions, moderate decrease in fluoride concentration, about 33.68 %, was observed, from value 1414.04 mg.L<sup>-1</sup> to 937.72 mg.L<sup>-1</sup> (Fig. 1). In the following tests, the pH was controlled throughout the EC processes.

In the test ZnH-06, where pH was controlled throughout the entire experiment, a high fluoride removal efficiency of 95.7 % was achieved (Fig. 1). The highest removal of fluoride 98.6 % was observed during the test ZnH-08 where after 50 min of Al-electrocoagulation the precipitates were separated by filtration through 0.22 µm filter and subsequently the process of EC of the filtrate continued for 120 minutes.

Polarity reversal (PR) of electrodes (test ZnH-09) demonstrated similar fluoride removal efficiencies, with 96.2 % in the PR test compared to 95.7 % in the non-reversed test (ZnH-06). The reversal of polarity can result in higher coagulant production efficiency, improved sludge properties, reduced energy consumption, and diminished electrode fouling [8-10]. The optimal frequency for PR should be determined based on the solution chemistry. For low concentrations of contaminants and buffering agents, shorter PR intervals are suitable, as they facilitate effective alterations of interfacial pH and manipulation of sludge properties. In contrast, higher concentrations of buffering agents require longer PR intervals to fully leverage the benefits of pH alteration and sludge property manipulation [10].

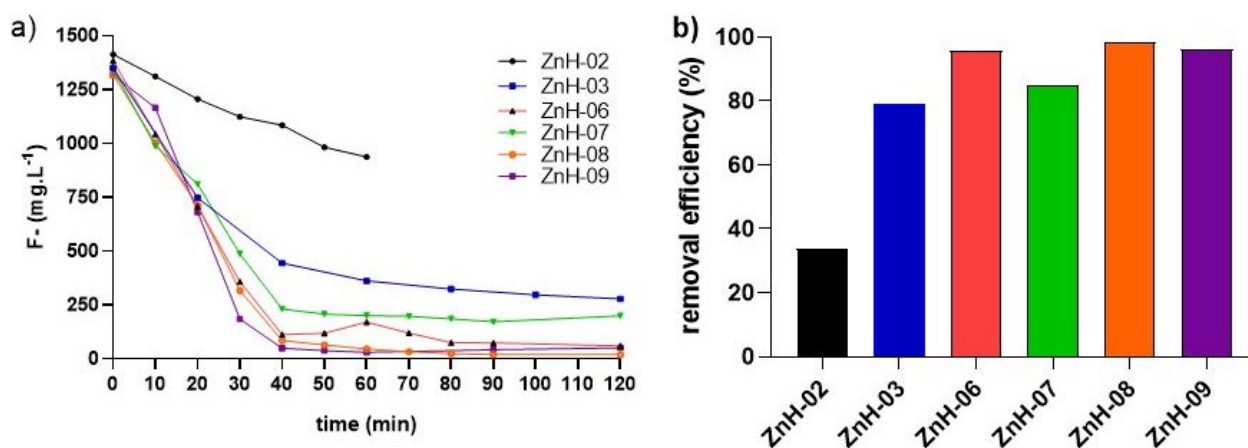


Fig. 1. Decrease of a) concentration of fluoride during Al-electrocoagulation and b) efficiency of fluoride removal

#### 3.2 The effect of acids

The effect of different acids on the fluoride removal was also investigated in this research. Test (ZnH-07) using HNO<sub>3</sub> demonstrated that NO<sub>3</sub><sup>-</sup> anions do not have a more significant effect on fluoride removal compared to SO<sub>4</sub><sup>2-</sup> ions. Efficiency of fluoride removal obtained 85.6 % with HNO<sub>3</sub> (in test ZnH-07) in comparison to test ZnH-06 with removal efficiency of fluorides 95.7 % with H<sub>2</sub>SO<sub>4</sub>. This result is consistent with findings by [11], where the effect of co-existing anions showed the sequence SO<sub>4</sub><sup>2-</sup> > NO<sub>3</sub><sup>-</sup> > Cl<sup>-</sup> for fluoride removal. The lowest fluoride removal efficiency was observed in tests with the presence of Cl<sup>-</sup>, while the highest efficiency was observed in the presence of SO<sub>4</sub><sup>2-</sup>.

The fluoride elimination was proportional to the amount of electrogenerated Al<sup>3+</sup> during 40 minutes of electrocoagulation. Beyond this point, the curve is no longer linear, suggesting that the actual current density was no longer effective. The molar ratio of removed fluoride to electrogenerated Al<sup>3+</sup> ions is shown in Fig. 2. The slope indicates that approx. 5.7 mM of fluoride reacted with 1 mM of Al<sup>3+</sup>. Based on these results, it was calculated that the removal of 1 mM F<sup>-</sup> required 0.175 mM of Al<sup>3+</sup> in the solution. The Al<sup>3+</sup>/F<sup>-</sup> molar ratio changed over the course of Al-electrocoagulation. In the studies performed at low F<sup>-</sup> concentrations [3], the Al<sup>3+</sup>/F<sup>-</sup> ratio was found to be between 10 and 15 to achieve satisfactory results. Accordingly, 10 to 15 mM of Al<sup>3+</sup> is consumed to reduce 1 mM of F<sup>-</sup>.

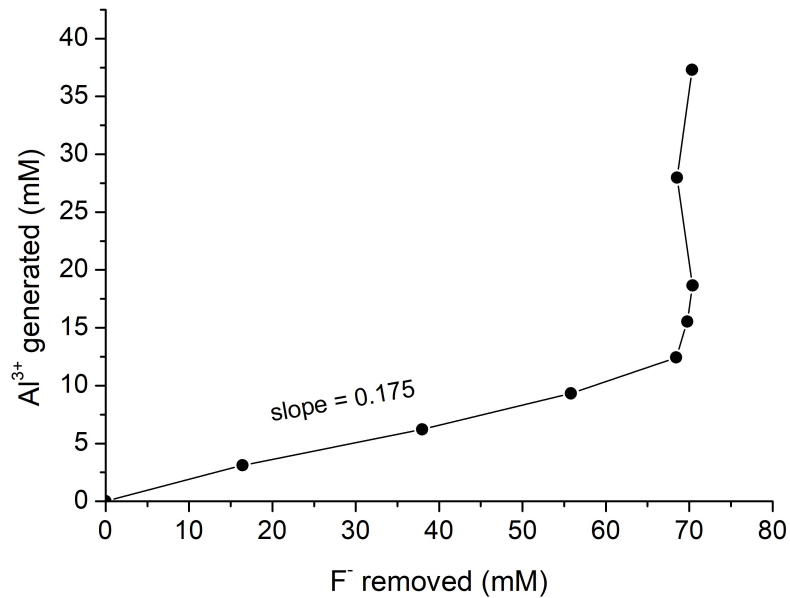


Fig. 2. Molar ratio of removed fluorides to added aluminium (mM)

### 3.3 Characterisation of the sludge

During Al-electrocoagulation, aluminium flocs were formed and subsequently separated after treatment using a 0.22 µm filter. Raman microspectrometry analysis of the filtrate revealed the presence of the mineral cryolite. This is in accordance with the study [3], which mentions that fluoride ions migrate toward the anode. The following reaction may occur through the combination of F<sup>-</sup> with Al<sup>3+</sup>, Na<sup>+</sup>, and the subsequent precipitation of cryolite (Na<sub>3</sub>AlF<sub>6</sub>) [3]. SEM-EDX images were used to investigate the morphology of the sludge (Fig. 3). Based on the SEM-EDX analysis the sludge in test ZnH-06 consists of Al 34 wt%, O 33.6 wt%, F 16.1 wt%, Na 12.3 wt%, S 5.6 wt%; and the sludge from the test ZnH-07 consists of Al 33.4 wt%, O 28.5 wt%, F 20.4 wt%, Na 15.8 wt%.

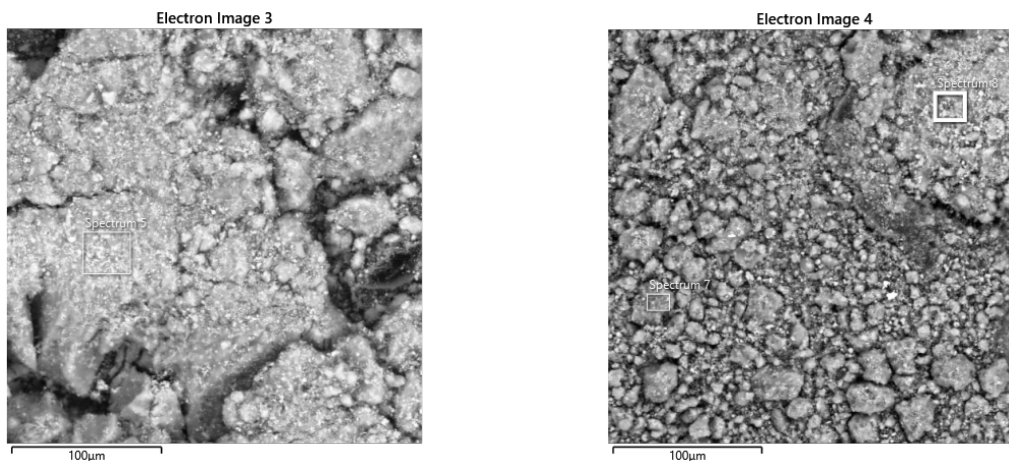


Fig. 3. SEM images of the Al-sludge filtrate from a) test ZnH-06 with H<sub>2</sub>SO<sub>4</sub> and b) test ZnH-07 with HNO<sub>3</sub>

### 3.4 Impact of electrocoagulation on cyanides removal

Degradation of cyanides was not proved to be effective during Al-electrocoagulation. The maximum removal efficiency 15 % was obtained. Therefore, the next step advanced electrooxidation process (AEOP) with BDD electrodes was examined. During BDD electrooxidation, oxo-chlorine species are produced as by-products, which can be reduced back to chlorides through bacterial reduction. However, the tests of electrooxidation with BDD and bacterial reduction are still under investigation, so they are not part of this text.



As a result of continuous pH adjustment using 5M H<sub>2</sub>SO<sub>4</sub>, the final treated water had an increased SO<sub>4</sub><sup>2-</sup> concentration up to 14,000 mg.L<sup>-1</sup>. The next step, aimed at reducing these high SO<sub>4</sub><sup>2-</sup> concentrations through the addition of Ca(OH)<sub>2</sub> to precipitate CaSO<sub>4</sub> in the solid phase, is also currently under investigation.

#### 4 Conclusions

This study successfully demonstrated the efficiency of Al-electrocoagulation for the treatment of landfill leachate contaminated with high concentrations of fluorides and cyanides. By generating Al<sup>3+</sup> ions in situ through the anodic dissolution of aluminum electrodes, the process achieved a fluoride removal efficiency of approximately 95 %, reducing the concentration from ~1400 mg.L<sup>-1</sup> to ~20 mg.L<sup>-1</sup>. Maintaining a pH range of 6 - 8 was crucial for efficient fluoride precipitation. The use of HNO<sub>3</sub> acid did not prove more effective in defluorination than H<sub>2</sub>SO<sub>4</sub>.

The molar ratio of electrogenerated Al<sup>3+</sup> ions to F<sup>-</sup> removed was ~ 0.175 during 40 minutes. The production of Al<sup>3+</sup> ions can be regulated by the amount of applied electrical current. PR showed similar defluorination efficiency, achieving 96.2 %. PR in Al-electrocoagulation can reduce costs by minimizing electrode fouling and improving energy efficiency [10].

Cyanide removal, however, was limited to a maximum of 15 %, indicating the need for additional treatment methods, such as BDD electrooxidation with subsequent bacterial reduction of electrooxidation by-products, which is still under investigation. Careful management of cyanide emissions during water acidification with H<sub>2</sub>SO<sub>4</sub> is necessary to ensure safety in field applications. While pH management was essential for optimal fluoride removal, the issue of the SO<sub>4</sub><sup>2-</sup> increase from acidification must also be addressed. The on-going evaluation of SO<sub>4</sub><sup>2-</sup> reduction through Ca(OH)<sub>2</sub> precipitation holds promise for mitigating potential secondary pollution issues.

#### Acknowledgements

The work was funded by the Grant UK/3136/2024 EU NextGenerationEU through the Recovery and Resilience Plan for Slovakia under the projects No. 09I03-03-V05-00012, and by the Slovak Research and Development Agency under contract No. APVV-21-0212. The work was funded by EU NextGenerationEU through the Recovery and Resilience Plan for Slovakia under the project No. 09I03-03-V03-00083.



Funded by the  
European Union  
NextGenerationEU

[RECOVERY  
AND RESILIENCE]  
PLAN

#### References

- [1] Zhao, H.Z., Yang, W., Zhu, J., Ni, R.N. Defluorination of drinking water by combined electrocoagulation: Effects of the molar ratio of alkalinity and fluoride to Al(III). *Chemosphere*, 74, 2009, p. 1391-1395.
- [2] Emmamjomeh, M.M. *Electrocoagulation technology as a process for a defluorination in water treatment*. Doctor of Philosophy thesis, School of Civil, Mining and Environmental Engineering, University of Wollongong, 2006, 184 p.
- [3] Emmamjomeh, M.M., Sivakumar, M. Review of pollutants removed by electrocoagulation and electrocoagulation/flotation processes. *Journal of Environmental Management*, 90, 2009, p. 1663-1679.
- [4] Rajeshwar, K., Ibanez, J. *Environmental electrochemistry: fundamentals and applications in pollution abatement*. In Tarr, Matthew A. (Ed.), *Chemical Degradation Methods for Wastes and Pollutants*. Academic USA Press, 1997, 720 p.
- [5] Tupý, P., Macek, J., Drábik, A. et al. Čiastková záverečná správa s predsanačnou analýzou rizika znečisteného územia. Sanácia environmentálnej záťaže ZH (015) / Žiar and Hronom - Stará skládka po ZSNP (SK/EZ/ZH/1101). Bratislava: SGÚDŠ, Archív GEOFOND, MŽP SR, 2023, 8 p. (in Slovak)
- [6] Sivakumar, M., Emmamjomeh, M.M. Speciation and mechanisms of defluorination by an electrochemical method. In The Second International Association of Science and Technology for Development (IASTED) Conference on Advanced Technology in the Environmental Field (ATEF), February 6-8, 2006. Lanzarote, Canary Islands, Spain.

- [7] Sivakumar, M., Emamjomeh, M.M. Defluoridation using a continuous electrocoagulation (EC) reactor, In 47th Annual New Zealand Water and Wastewater Association (NZWWA) Conference and Expo (EnviroNZ05-Water matters), 28<sup>th</sup>-30th September, 2005. Aotea Centre, Auckland, New Zealand.
- [8] Das, D., Nandi, B.K. Removal of co-existing Fe(II), As(V) and fluoride ions from groundwater by electrocoagulation. *Groundwater for Sustainable Development*, 17, 2022, p. 100752.
- [9] Chow H., Pham, A.L-T. Mitigating Electrode Fouling in Electrocoagulation by Means of Polarity Reversal: The Effects of Electrode Type, Current Density, and Polarity Reversal Frequency. *Water Research*, 197, 2021, p. 117074.
- [10] Fuladpanjeh-Hojaghan, B., Shah, R.S., Roberts, E.P.L., Trifkovic, M. Effect of polarity reversal on floc formation and rheological properties of a sludge formed by the electrocoagulation process. *Water Research*, 242, 2023, p. 120201.
- [11] Govindan, K., Raja, M., Maheshwari, S.U., Noel, M., Oren, Y. Comparison and understanding of fluoride removal mechanism in Ca<sup>2+</sup>, Mg<sup>2+</sup> and Al<sup>3+</sup> ion assisted electrocoagulation process using Fe and Al electrodes. *Journal of Environmental Chemical Engineering*, 3, 2015, p. 1784-1793.

## TESTING THE CHARACTERISTICS OF SELECTED MICROORGANISMS FOR POSSIBLE APPLICATION IN WASTEWATER TREATMENT

**Katarina Ćirković<sup>a</sup>, Aleksandar Ostojić<sup>a</sup>, Ivana Radojević<sup>a</sup>**

<sup>a</sup> University of Kragujevac, Faculty of Science, Department of Biology and Ecology,  
Radoja Domanovića 12, 34000 Kragujevac, Republic of Serbia,  
katarina.cirkovic@pmf.kg.ac.rs, aleksandar.ostojic@pmf.kg.ac.rs, ivana.radojevic@pmf.kg.ac.rs

### Abstract

Indigenous microorganisms isolated from wastewater can play a vital role in sustainable wastewater treatment by helping the existing community of microorganisms to effectively transform pollutants like heavy metals into less toxic forms. Isolated microorganisms must be resistant to heavy metals and withstand diverse environmental conditions that change during wastewater treatment. Thus, the current study aimed to test the resistance of selected microorganisms isolated from a wastewater treatment plant to different environmental conditions such as temperature, pH and salts, as well as to selected heavy metals and antibiotics. Using morphological and biochemical tests, as well as MALDI-TOF, selected isolates were identified as *Pseudomonas aeruginosa*, *Aeromonas veronii*, and *Enterococcus hirae*. Growth capabilities under different temperature, pH and NaCl concentrations, were analyzed using a spectrophotometer. Resistance to tested substances was evaluated by determining the minimal inhibitory concentration (MIC) and minimal microbicidal concentration (MMC). Except for *E. hirae*, results showed that the other two isolates prefer neutral and alkaline pH, while their growth was inhibited in acidic environments and in environments with high salt concentrations. All tested isolates demonstrated notable resistance to heavy metals, particularly Pb<sup>2+</sup>, Zn<sup>2+</sup>, and Cu<sup>2+</sup>, while displaying sensitivity to most antibiotics. This is considered an ideal feature because there is concern that heavy metals can function as a selective agents in the proliferation of antibiotic resistance, posing a potential threat to human health.

**Keywords:** wastewater, indigenous bacteria, ecological factors, heavy metals, antibiotics

### 1 Introduction

Heavy metals primarily originate from human activities such as mining, metal-based industrial discharges, and domestic use [1]. Due to their persistent and non-biodegradable nature, they accumulate in the environment, including wastewater, causing significant ecological and health issues even at low concentrations. Besides traditional techniques that have been used to treat wastewater before discharge into natural ecosystems, new and cost-effective methods have been developed to help in this process. One such method focuses on using indigenous microorganisms isolated from wastewater to accelerate and enhance the transformation of heavy metals into less toxic and more mobile forms [2, 3]. These microorganisms must be resistant to heavy metals and capable of surviving the various abiotic changes during wastewater treatment.

Abiotic factors can greatly impact the effectiveness of microorganisms in wastewater treatment, influencing both their activity and the state and bioavailability of heavy metals [4]. Temperature is particularly important for heavy metal adsorption; as it increases, the solubility of heavy metals and the enzymatic activity of microorganisms rise, thereby accelerating the bioremediation process [5]. Another key factor is pH, which affects not only the heavy metals, but also the functional groups on the bacterial cell wall [6]. Soluble metals can readily penetrate cell membranes and can cause oxidative stress and damage cell components like proteins, lipids, and nucleic acids [7]. To counteract this, microorganisms evolved specific mechanisms to utilize heavy metals and survive in their presence. Some of these mechanisms include precipitation, intracellular accumulation, and extracellular sequestration in exopolysaccharides (EPSs). For instance, extracellular barriers, including cell walls, plasma membranes, and surface structures like EPS, are key to heavy metal resistance by preventing heavy metals from entering the cell. Efflux pumps are also another mechanism commonly employed by microorganisms to manage heavy metals, enabling them to regulate their internal environment by expelling toxic compounds [8, 9].

While they become resistant to heavy metals, there is concern that metals may also act as selective agents, promoting the spread of antibiotic resistance which poses a potential threat to human health. Genes conferring resistance to heavy metals and antibiotics are typically located on mobile genetic elements, such as plasmids, transposons, and integrons, and can be transferred between different microorganisms. This transfer can cause even sensitive strains to become resistant [10]. Numerous studies have shown that microorganisms often use the same resistance mechanisms against various antimicrobial agents, including

heavy metals and antibiotics, which act similarly in killing microbial cells [11]. Therefore, the desired properties of indigenous microorganisms are resistance to heavy metals and sensitivity to antibiotics. As a result, the current study's goal is to investigate properties in selected microorganisms isolated from wastewater to assess their potential in practical applications.

## 2 Material and methods

### 2.1 Isolation and identification of microorganisms

Wastewater samples were taken at the beginning of May 2023 from the municipal wastewater treatment plant "Cvetojevac" (Kragujevac, Serbia). For further analysis, we singled out the colonies of those species that were most prevalent in the tested samples and that grew on selective and differential medium. Pure cultures of bacteria were obtained by the depletion method, and identification was performed by examining their morphological and biochemical characteristics [12], as well as with the assistance of MALDI-TOF mass spectrometry.

### 2.2 Influence of different temperatures, pH, and salt concentrations on planktonic growth

The effect of temperature (25 and 37 °C) on the growth of tested isolates was examined using Tryptic soy broth (TSB) (Torlak, Serbia), either in its standard form or with a modified composition according to Mladenović et al. [13]. To study the effect of pH, media with different pH levels (4.0, 7.0, and 8.5) were prepared. The pH was adjusted to 4.0 and 7.0 using HCl and to 8.5 using NaOH. Additionally, TSB was modified by adding NaCl (5.0 %, 6.5 %, and 8.0 %) to investigate the effects of various salt concentrations. Ten µl of the initial bacterial suspension ( $1.5 \times 10^8$  CFU/ml) was added to 3 ml of each type of medium. Samples were incubated for 24 h. Pure TSB was used as a sterility control, and an unmodified inoculated medium served as a control to determine if the modified medium with different pH or salt concentrations affected the growth of the isolates. Growth absorbance was calculated by measuring the OD<sub>600</sub> of the bacterial cultures using a spectrophotometer (Iskra, Slovenia). OD values were obtained for each culture, and the mean value of three individual repetitions was recorded as the growth absorbance.

### 2.3 Preparation of the solutions of metals and antibiotics

The susceptibility of planktonic cells was tested in the presence of heavy metals (Pb<sup>2+</sup>, Zn<sup>2+</sup>, Cu<sup>2+</sup>, Mn<sup>2+</sup>, Cd<sup>2+</sup>, Hg<sup>2+</sup> and Cr<sup>6+</sup>) originating from the Pb(NO<sub>3</sub>)<sub>2</sub>, ZnSO<sub>4</sub>, CuSO<sub>4</sub>, MnCl<sub>2</sub>, CdSO<sub>4</sub>, HgCl<sub>2</sub>, and K<sub>2</sub>Cr<sub>2</sub>O<sub>7</sub> salts (Sigma-Aldrich, USA) and antibiotics (ampicillin (Am) (ATB Pharma, Serbia), azithromycin (He) (Hemofarm, Serbia), cefepime (C) (Hemofarm, Serbia), ceftriaxone (Az) (Hemofarm, Serbia), ertapenem (E) (Merck Sharp & Dohme d.o.o., Serbia), tetracycline (T) (Pfizer Inc., USA), levofloxacin (Le) (Zentiva Pharma d.o.o., Serbia)). All tested substances were dissolved in sterile distilled water.

### 2.4 Microdilution method

The influence of selected heavy metals and antibiotics on the planktonic growth of isolated bacteria was determined using the microdilution method [14]. Twofold serial dilutions of metals and antibiotics were prepared in sterile 96-well microtiter plates containing 100 µl of TSB (Torlak, Serbia) per well. Concentration range for Pb<sup>2+</sup>, Cu<sup>2+</sup> and Mn<sup>2+</sup> was from 4 to 0.031 mg/ml, for Zn<sup>2+</sup> and Cd<sup>2+</sup> from 20 to 0.156 mg/ml, for Hg<sup>2+</sup> and Cr<sup>6+</sup> from 0.5 to 0.003 mg/ml, while the obtained concentration range for all antibiotics was from 0.5 to 0.003 mg/ml. In the plates where heavy metals were dispensed, 2.5 µl of glutathione (TvinLab) was added, and served for neutralization of heavy metals, while the growth of the bacteria was monitored by adding 10 µl of resazurin (Alfa Aesar GmbH & Co., Germany) to all wells of the plate. Bacterial suspensions were obtained from cultures incubated for 24 h at 25 °C and were adjusted around 10<sup>6</sup> CFU/ml by dilution. Ten µl of suspension of each tested microorganism was added to the plates. The inoculated plates were incubated for 24 h at 25 °C and after that, MIC values were determined, while MMC values were determined after 48 h. The MIC was defined as the lowest concentration of the tested substance that inhibited microorganism growth and prevented the resazurin color change from blue to pink. Each test included growth control and sterility control.

## 3 Results and discussion

### 3.1 Isolation and identification of microorganisms

Bacterial strains were identified as *Pseudomonas aeruginosa*, *Aeromonas veronii*, and *Enterococcus hirae*. The obtained results showed that the analyzed strains matched with high score values with each

corresponding strain type already present in the Bruker MALDI Biotyper database. Score values were between 2.06 and 2.30.

### 3.2 Influence of different temperatures, pH, and salt concentrations on planktonic growth

Except for *E. hirae*, results showed that the other two isolates prefer neutral and alkaline pH, while their growth was inhibited in acidic environments and in environments with high salt concentrations (Figure 1 and 2).

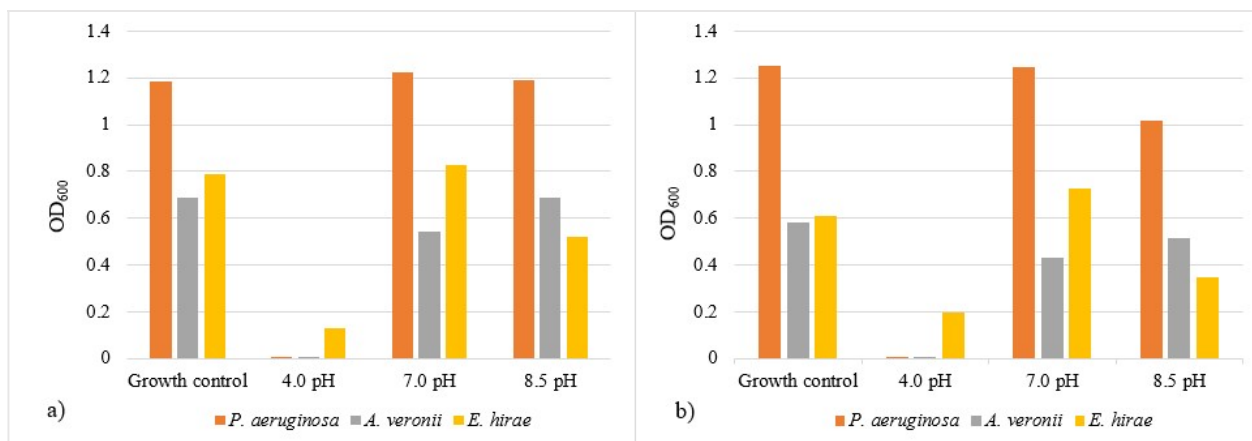


Fig. 1. Influence of different pH on bacterial growth at a) 25 °C and b) 37 °C

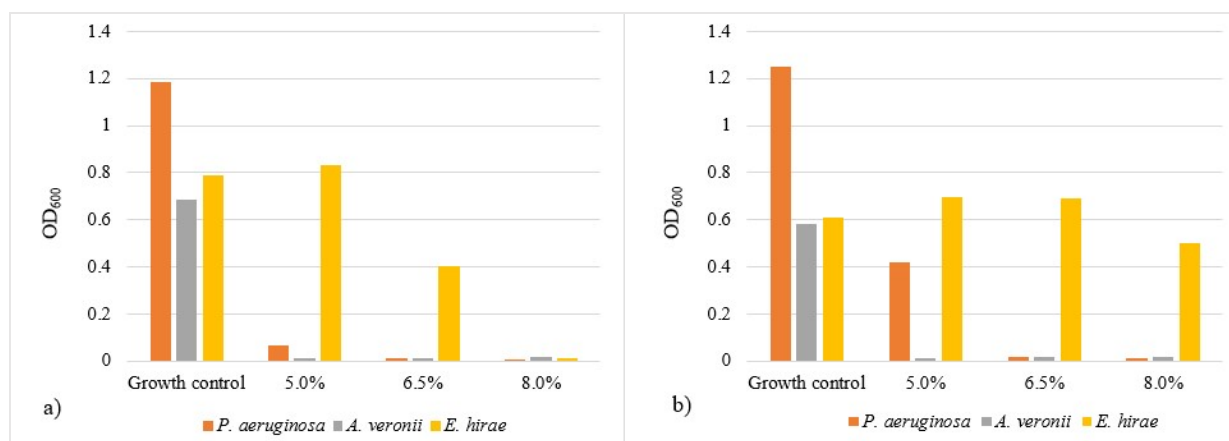


Fig. 2. Influence of different salt concentrations on bacterial growth at a) 25 °C and b) 37 °C

Obtained results for *P. aeruginosa* and *A. veronii* are in accordance with the findings of studies conducted by Rael and Frankenberger [15], Vivekanandhan et al. [16], Wang and Gu [17], and Abel and Evvie [18]. Our isolates grew well at both tested temperatures. The nature of enterococci and their high tolerance to heat, salt and acidity can guarantee the presence of this group in different habitats. In the study by Morandi et al. [19] tested species, *Enterococcus faecium* and *Enterococcus faecalis*, were able to adapt to adverse cultural conditions (low values of pH and temperature). This is also in accordance with our results for *E. hirae*, which showed better growth in tested conditions than the other two isolates.

### 3.3 Resistance of planktonic cells to heavy metals and antibiotics

By determining the minimum inhibitory concentration (MIC) and minimum microbicidal concentration (MMC), the resistance of planktonic microorganisms was tested in the presence of heavy metals and antibiotics (Table 1 and 2). All tested isolates showed resistance to Pb<sup>2+</sup> (MIC between 2 and >4 mg/ml), Zn<sup>2+</sup> (MIC between 5 and >20 mg/ml), and Cu<sup>2+</sup> (MIC between 0.83 and 2 mg/ml). *A. veronii* and *E. hirae* also showed good resistance in the presence of Hg<sup>2+</sup> (MIC between 0.104 and 0.125 mg/ml), and Cr<sup>6+</sup> (MIC 0.25 mg/ml), while *P. aeruginosa* showed resistance in the presence of Cd<sup>2+</sup> (MIC 5 mg/ml).

Various studies have shown that *P. aeruginosa* can quickly adapt to contaminated environments, making it a suitable biosorbent for removing heavy metals, either in the form of planktonic cells or

biofilms [20]. This strain demonstrates significant resistance to Cd<sup>2+</sup>, which is consistent with our results. For instance, *P. aeruginosa* PU21 was effective in removing and recovering Cd<sup>2+</sup>, Cu<sup>2+</sup>, and Pb<sup>2+</sup> from polluted water [21], while in the study by Alfarras and Hamid [22], two *Pseudomonas* spp. isolates from sludge and sewage in Iraq were resistant to various heavy metals, including Cd<sup>2+</sup>, Hg<sup>2+</sup>, Cu<sup>2+</sup>, and Ni<sup>2+</sup>. In our research, the *P. aeruginosa* strain showed significant resistance to Pb<sup>2+</sup> and Cu<sup>2+</sup>, but not to Hg<sup>2+</sup>. The *P. aeruginosa* RW9 strain studied by Mat Arisah et al. [23] is promising candidate for Cr<sup>6+</sup> bioremediation, tolerating up to 60 mg/l of Cr<sup>6+</sup> through mechanisms like intracellular and extracellular sequestration by membrane-bound metabolites such as reductase and biosurfactant. However, the *P. aeruginosa* strain used in our study was sensitive to Cr<sup>6+</sup>.

**Table 1. Resistance of planktonic cells to the presence of heavy metals**

Isolates	Metals													
	Pb		Zn		Cu		Mn		Cd		Hg		Cr	
	MIC	MMC	MIC	MMC	MIC	MMC	MIC	MMC	MIC	MMC	MIC	MMC	MIC	MMC
<i>P. aeruginosa</i>	4	>4	5	10	2	2	<0.031	<0.031	5	10	<0.003	<0.003	<0.003	<0.003
<i>A. veronii</i>	2	2	1.66	5	1	1	4	4	<0.156	0.312	0.104	0.104	0.25	0.25
<i>E. hirae</i>	>4	>4	0.52	>20	0.83	0.83	0.83	>4	<0.156	<0.156	0.125	0.125	0.25	0.33

MIC values (mg/ml) - means inhibitory activity; MMC values (mg/ml) - means microbicidal activity

**Table 2. Resistance of planktonic cells to the presence of antibiotics**

Isolates	Antibiotics													
	Am		Az		C		E		He		T		Le	
	MIC	MMC	MIC	MMC	MIC	MMC	MIC	MMC	MIC	MMC	MIC	MMC	MIC	MMC
<i>P. aeruginosa</i>	0.5	>0.5	0.007	0.009	<0.003	<0.003	0.007	0.007	0.041	0.104	0.005	0.020	<0.003	<0.003
<i>A. veronii</i>	0.208	0.208	0.020	0.025	0.005	0.051	<0.003	<0.003	0.041	0.083	<0.003	<0.003	<0.003	<0.003
<i>E. hirae</i>	<0.003	<0.003	0.007	0.041	0.031	0.083	<0.003	0.007	<0.003	<0.003	0.041	0.062	<0.003	<0.003

ampicillin (Am), ceftriaxone (Az), cefepime (C), ertapenem (E), azithromycin (He), tetracycline (T), levofloxacin (Le)

*A. veronii* used in our study showed very good resistance in the presence of all tested metals, except for Cd<sup>2+</sup>. Previous studies proved that *Aeromonas* spp. can be found in wide range of habitats and potentially can resist different concentrations of metals such as Zn<sup>2+</sup>, Pb<sup>2+</sup>, Cd<sup>2+</sup>, and Ni<sup>2+</sup>. In the study conducted by Qurbani et al. [24] *Aeromonas sobria* reduced 54.89 % of the Cu<sup>2+</sup>, 62.33 % of the Ni<sup>2+</sup>, and 36.41 % of the Zn<sup>2+</sup> after 72 h. Using Transmission electron microscopy (TEM) their findings suggested that this isolate accumulated both Cu<sup>2+</sup> and Ni<sup>2+</sup>, whereas Zn<sup>2+</sup> was reduced by biosorption. *Aeromonas* spp. employ various strategies to mitigate heavy metal toxicity, one of which involves trapping metals using negatively charged groups like phosphoryl, hydroxyl, and carboxyl present on the *Aeromonas* spp. cell wall [24]. It is likely that *A. veronii* used in the current study also employed similar strategies to demonstrate resistance in the presence of the tested metals, such as Cu<sup>2+</sup> and Zn<sup>2+</sup>. Good resistance to Cd<sup>2+</sup>, Cu<sup>2+</sup>, Zn<sup>2+</sup>, and Pb<sup>2+</sup>, also showed *Aeromonas hydrophila* tested in the study by Matyar [25]. This isolate was especially resistant in the presence of Mn<sup>2+</sup> (MIC > 3.2 mg/ml), which is also in accordance with our results for *A. veronii*.

Results for *E. hirae* tested in current study showed strong resistance to Cu<sup>2+</sup>. The copYZAB operon from *E. hirae* was the first described copper homeostasis system [26]. The cop operon includes two structural genes encoding P-type ATPases: CopA, which facilitates copper uptake and nutrition, and CopB, which is 35 % identical to CopA, responsible for copper efflux and detoxification [27, 28]. It is likely that the *E. hirae* used in our study showed strong resistance to Cu<sup>2+</sup> due to this copper homeostasis system. This strain also demonstrated good resistance to Pb<sup>2+</sup>, Zn<sup>2+</sup>, Mn<sup>2+</sup>, Hg<sup>2+</sup>, and Cr<sup>6+</sup>. Vignaroli et al. [29] isolated enterococci from coastal marine sediment and evaluated their ability to grow in agar plates supplemented with Cu<sup>2+</sup>, Cd<sup>2+</sup>, and Hg<sup>2+</sup>. The strains exhibited a high frequency (68 %) of resistance to Cd<sup>2+</sup> and/or Cu<sup>2+</sup> and consistent susceptibility to Hg<sup>2+</sup>. In the study by Niederhäusern et al. [30] all tested enterococci strains were resistant to Cu<sup>2+</sup>, Ni<sup>2+</sup>, Pb<sup>2+</sup>, and Zn<sup>2+</sup>, but susceptible to Ag<sup>2+</sup> and Hg<sup>2+</sup>. They concluded there is no correlation between current pollution levels and the observed heavy metal resistance in isolates, as heavy metal concentrations in Monte Cotugno Lake water samples were below Italian legal limits. Mondragón et al. [31] reported a 100 % of Hg<sup>2+</sup> resistance in enterococci strains isolated from Molola river, while 86.8 % were resistant to Cr<sup>6+</sup> and 42.1 % resistant to Cd<sup>2+</sup>. Our findings for *E. hirae* align with previously mentioned studies.

Numerous studies have indicated that even low levels of heavy metals in various environments can create selection pressure, leading to antibiotic resistance in bacteria [22, 25]. Alfarras et al. [22] found that

*P. aeruginosa* isolates from sewage resistant to heavy metals were also resistant to ampicillin, but susceptible to chloramphenicol and erythromycin, with one isolate additionally resistant to nalidixic acid. Similarly, Raja et al. [32] reported that *P. aeruginosa* with multiple metal tolerances also showed resistance to antibiotics such as ampicillin, tetracycline, chloramphenicol, erythromycin, kanamycin, and streptomycin. This extensive resistance suggests that *Pseudomonas* species may carry plasmids with genes for both antibiotic and metal resistance [22]. Matyar [25] studied the resistance patterns of *A. hydrophila* and *P. aeruginosa* from hospital effluent water, finding that metal-resistant *A. hydrophila* isolates were highly resistant to cefazolin, cefaclor, and cefprozil, while *P. aeruginosa* isolates were highly resistant to seven different antibiotics, including: cefazolin, cefuroxime, ceftazidime, cefepime, cefaclor, cefprozil, cefixime, and ceftizoxime. The frequent co-occurrence of heavy metal and antibiotic resistance, often within the same genetic elements like transposons or plasmids, suggests that industrial pollution may promote antibiotic resistance and vice versa [33, 25]. In our study *P. aeruginosa* and *A. veronii* showed resistance to ampicillin and azithromycin which is in accordance with previously mentioned studies. Both isolates are generally known to exhibit intrinsic resistance to ampicillin, due to the presence of beta-lactamase enzymes [34, 35]. They can also be resistant to cephalosporins like ceftriaxone and cefepime [25]. Vignaroli et al. [29] discovered a significant correlation between Cd and erythromycin resistance in enterococci, and between Cd or Cu, and quinupristin/dalfopristin (Q/D). However, Niederhäusern et al. [30] found no correlation between antibiotic and heavy metal resistance or environmental pollution in enterococci isolated from Monte Cotugno Lake. *E. hirae* used in our study showed resistance to cefepime and tetracycline. It is well known that enterococci are intrinsic resistant to cephalosporins, and can show resistance to tetracycline [36, 37]. While significant progress has been made in studying the connection between antibiotic and heavy metal resistance, ongoing research is necessary to fully understand and address this complex issue.

#### 4 Conclusions

The results suggest that the tested isolates can grow at both of the examined temperatures and are better adapted to neutral and alkaline conditions. Except for *E. hirae*, the isolates showed limited growth in environments with high salt concentrations and low pH. In terms of heavy metal resistance, all isolates demonstrated the highest resistance to Pb<sup>2+</sup>, Zn<sup>2+</sup>, and Cu<sup>2+</sup>. *A. veronii* and *E. hirae* also exhibited strong resistance to Hg<sup>2+</sup> and Cr<sup>6+</sup>, while *P. aeruginosa* showed resistance to Cd<sup>2+</sup>. The isolates were mostly sensitive to the tested antibiotics, though some showed greater resistance to specific antibiotics, likely due to their ineffectiveness against these isolates. Given their resistance to certain heavy metals, these isolates could be further investigated for potential use in bioremediation. Additionally, studying the effects of these heavy metals on individual and mixed biofilms formed by the tested species could help assess their effectiveness in heavy metal removal.

#### Acknowledgments

This work was supported by the Serbian Ministry of Science, Technological Development and Innovation (Agreement No. 451-03-65/2024-03/ 200122 and 451-03-66/2024-03/ 200122).

#### References

- [1] Cheng, S. Heavy metals in plants and phytoremediation. *Environmental Science and Pollution Research International*, 10, 2003, p. 335-340.
- [2] Malik, A. Metal bioremediation through growing cells. *Environment International*, 30, 2004, p. 261-278.
- [3] Rehman, A., Farooq, H., Hasnain, S. Biosorption of copper by yeast, *Loddermyces elongisporus*, isolated from industrial effluents: Its potential use in wastewater treatment. *Journal of Basic Microbiology*, 48, 2008, p. 195-201.
- [4] Shukla, K.P., Sharma, S., Singh, N.K., Singh, V., Bisht, S., Kumar, V. Rhizoremediation: a promising rhizosphere technology. *Applied Bioremediation Active and Passive Approaches*, 2, 2013, p. 333-352.
- [5] Bandowe, B.A.M., Bigalke, M., Boamah, L., Nyarko, E., Saalia, F.K., Wilcke, W. Polycyclic aromatic compounds (PAHs and oxygenated PAHs) and trace metals in fish species from Ghana (West Africa): bioaccumulation and health risk assessment. *Environment international*, 65, 2014, p. 135-146.
- [6] Esposito, A., Pagnanelli, F., Vegliò, F. pH-related equilibria models for biosorption in single metal systems. *Chemical Engineering Science*, 57 (3), 2002, p. 307-313.

- [7] Wang, S., Shi, X. Molecular mechanisms of metal toxicity and carcinogenesis. *Molecular and Cellular Biochemistry*, 222 (1-2), 2001, p. 3-9.
- [8] Ramírez-Díaz, M.I., Díaz-Pérez, C., Vargas, E., Riveros-Rosas, H., Campos-García, J., Cervantes, C. Mechanisms of bacterial resistance to chromium compounds. *Biometals*, 21 (3), 2008, p. 321-332.
- [9] Ianeva, O.D. Mechanisms of bacteria resistance to heavy metals. *Microbiological Journal*, 71 (6), 2009, p. 54-65.
- [10] Narasimhulu, K., Sreenivasa Rao, P.S., Vinod, A.V. Isolation and identification of bacterial strains and study of their resistance to heavy metals and antibiotics. *Journal of Microbial and Biochemical Technology*, 2, 2010, p. 74-76.
- [11] Vats, P., Kaur, U.J., Rishi, P. Heavy metal-induced selection and proliferation of antibiotic resistance: A review. *Journal of Applied Microbiology*, 132 (6), 2022, p. 4058-4076.
- [12] Reddy, C.A., Beveridge, T.J., Breznak, J.A., Marzluf, G.A., Schmidt, T.M., Snyder, L.R. *Methods for general and molecular microbiology*. Wiley Online Library, 3rd Edition, 2007, 1069 p.
- [13] Mladenović, K.G., Muruzović, M.Ž., Žugić-Petrović, T.D., Čomić, L.R. The influence of environmental factors on the planktonic growth and biofilm formation of *Escherichia coli*. *Kragujevac Journal of Science*, 40, 2018, p. 205-216.
- [14] Sarker, S.D., Nahar, L., Kumarasamy, Y. Microtitre plate-based antibacterial assay incorporating resazurin as an indicator of cell growth, and its application in the in vitro antibacterial screening of phytochemicals. *Methods*, 42 (4), 2007, p. 321-324.
- [15] Rael, R.M., Frankenberger Jr, W.T. Influence of pH, salinity, and selenium on the growth of *Aeromonas veronii* in evaporation agricultural drainage water. *Water Research*, 30 (2), 1996, p. 422-430.
- [16] Vivekanandhan, G., Savithamani, K., Lakshmanaperumalsamy, P. Influence of pH, salt concentration and temperature on the growth of *Aeromonas hydrophila*. *Journal of Environmental Biology*, 24 (4), 2003, p. 373-379.
- [17] Wang, Y., Gu, J. Influence of temperature, salinity and pH on the growth of environmental *Aeromonas* and *Vibrio* species isolated from Mai Po and the Inner Deep Bay Nature Reserve Ramsar Site of Hong Kong. *Journal of Basic Microbiology: An International Journal on Biochemistry, Physiology, Genetics, Morphology, and Ecology of Microorganisms*, 45 (1), 2005, p. 83-93.
- [18] Abel, E.S., Evvie, S.E. Effect of varying environmental conditions on the growth and viability of selected microorganisms using conventional cultures. *Journal of Applied Sciences and Environmental Management*, 26 (3), 2022, p. 393-397.
- [19] Morandi, S., Brasca, M., Alfieri, P., Lodi, R., Tamburini, A. Influence of pH and temperature on the growth of *Enterococcus faecium* and *Enterococcus faecalis*. *Le Lait*, 85 (3), 2005, p. 181-192.
- [20] Teitzel, G.M., Parsek, M.R. Heavy metal resistance of biofilm and planktonic *Pseudomonas aeruginosa*. *Applied and environmental microbiology*, 69 (4), 2003, p. 2313-2320.
- [21] Chang, J.S., Law, R., Chang, C.C. Biosorption of lead, copper and cadmium by biomass of *Pseudomonas aeruginosa* PU21. *Water research*, 31 (7), 1997, p. 1651-1658.
- [22] Alfarras, F., Hamid, A.F.M. Heavy Metal Resistance Ability of *Pseudomonas* Species Isolated from Sludge and Sewage in Iraq. *Archives of Razi Institute*, 77 (3), 2022, p. 1041.
- [23] Mat Arisah, F., Amir, A. F., Ramli, N., Ariffin, H., Maeda, T., Hassan, M.A., Mohd Yusoff, M.Z. Bacterial resistance against heavy metals in *Pseudomonas aeruginosa* RW9 involving hexavalent chromium removal. *Sustainability*, 13 (17), 2021, p. 9797.
- [24] Qurbani, K., Khdir, K., Sidiq, A., Hamzah, H., Hussein, S., Hamad, Z., Abdulla, R., Abdulla, B., Azizi, Z. *Aeromonas sobria* as a potential candidate for bioremediation of heavy metal from contaminated environments. *Scientific Reports*, 12 (1), 2022, 21235.
- [25] Matyar, F. Investigation of Cephalosporin and Heavy Metal Resistance of *Aeromonas hydrophila* and *Pseudomonas aeruginosa* Strains Isolated from Hospital Sewage in Türkiye. *Acta Aquatica Turcica*, 19 (4), 2023, p. 312-322.
- [26] Garrido, A.M., Gálvez, A., Pulido, R.P. Antimicrobial resistance in enterococci. *Journal of Infectious Diseases and Therapy*, 2 (4), 2014, p. 1-7.
- [27] Odermatt, A., Krapf, R., Solioz, M. Induction of the putative copper ATPases, CopA and CopB, of *Enterococcus hirae* by Ag<sup>+</sup> and Cu<sup>2+</sup>, and Ag<sup>+</sup> extrusion by CopB. *Biochemical and Biophysical Research Communications*, 202 (1), 1994, p. 44-48.



- [28] Shoeb, E., Ahmed, N. Genetic basis of heavy metal tolerance in bacteria: A review. *International Journal of Biology and Biotechnology (Pakistan)*, 9 (1-2), 2012, p. 115-121.
- [29] Vignaroli, C., Pasquaroli, S., Citterio, B., Di Cesare, A., Mangiaterra, G., Fattorini, D., Biavasco, F. Antibiotic and heavy metal resistance in enterococci from coastal marine sediment. *Environmental pollution*, 237, 2018, p. 406-413.
- [30] De Niederhäusern, S., Bondi, M., Anacarso, I., Iseppi, R., Sabia, C., Bitonte, F., Messi, P. Antibiotics and heavy metals resistance and other biological characters in enterococci isolated from surface water of Monte Cotugno Lake (Italy). *Journal of Environmental Science and Health, Part A*, 48 (8), 2013, p. 939-946.
- [31] Mondragón, V.A., Llamas-Pérez, D.F., González-Guzmán, G.E., Márquez-González, A.R., Padilla-Noriega, R., Durán-Avelar, M.D.J., Franco, B. Identification of *Enterococcus faecalis* bacteria resistant to heavy metals and antibiotics in surface waters of the Mololoa River in Tepic, Nayarit, Mexico. *Environmental monitoring and assessment*, 183, 2011, p. 329-340.
- [32] Raja, C.E., Anbazhagan, K., Selvam, G.S. Isolation and characterization of a metal-resistant *Pseudomonas aeruginosa* strain. *World Journal of Microbiology and Biotechnology*, 22, 2006, p. 577-585.
- [33] Baker-Austin, C., Wright, M.S., Stepanauskas, R., McArthur, J.V. Co-selection of antibiotic metal resistance. *Trends in Microbiology*, 14 (4), 2006, p. 176-182.
- [34] Ghenghesh, K.S., El-Mohammady, H., Levin, S.Y., Zorgani, A., Tawil, K. Antimicrobial resistance profile of *Aeromonas* species isolated from Libya. *Libyan Journal of Medicine*, 8 (1), 2013, 21320.
- [35] Pachori, P., Gothalwal, R., Gandhi, P. Emergence of antibiotic resistance *Pseudomonas aeruginosa* in intensive care unit; a critical review. *Genes & diseases*, 6 (2), 2019, p. 109-119.
- [36] Miller, W.R., Munita, J.M., Arias, C.A. Mechanisms of antibiotic resistance in enterococci. *Expert review of anti-infective therapy*, 12 (10), 2014, p. 1221-1236.
- [37] Ibekwe, A.M., Obayiuwana, A.C., Murinda, S.E. *Enterococcus* Species and Their Antimicrobial Resistance in an Urban Watershed Affected by Different Anthropogenic Sources. *Water*, 16 (1), 2023, p. 116.



## MACROALGAE FROM POST-MINING LAKES CAN ACCUMULATE RARE EARTH ELEMENTS

Mária Čížková<sup>a</sup>, Milada Vítová<sup>a</sup>, Klára Řeháková<sup>a,b</sup>, Kateřina Čapková<sup>a,b</sup>, Marian Rucki<sup>c</sup>

<sup>a</sup> Department of Phycology, Institute of Botany, Czech Academy of Sciences, Třeboň, Czech Republic, maria.cizkova@ibot.cas.cz

<sup>b</sup> Biology Centre, Institute of Hydrobiology, Czech Academy of Sciences, České Budějovice, Czech Republic

<sup>c</sup> Laboratory of Predictive Toxicology, National Institute of Public Health, Prague, Czech Republic

### Abstract

Post-mining lakes of northern Czechia represent an exceptional aquatic ecosystem. They are yearlong habitats of underwater macroalgal meadows. To evaluate their bioremediation potential, two genera of macroalgae *Vaucheria* sp. (Xanthophyceae) and *Chara* spp. (Charophyceae) were collected by scuba diving technique from these meadows. Sampling was conducted in the post-mining lakes Most, Medard, and Milada in different seasons to follow concurrently seasonality of the species. The individual algae samples were incubated under controlled laboratory conditions in photobioreactors in the lake water of their origin, at natural temperature (ranging 4 °C – 23 °C), and natural light intensity (ranging 5 - 180  $\mu\text{mol}\cdot\text{m}^{-2}\cdot\text{s}^{-1}$ ) for 96 h. To determine their capacity for metal accumulation a mixture of rare earth elements (REEs) was added to the cultures in final concentration 40  $\mu\text{M}$  ( $\text{LaCl}_3$ ,  $\text{CeCl}_3$ ,  $\text{NdCl}_3$ ,  $\text{GdCl}_3$ ). The algae biomass was harvested after 4 days of treatment, washed thoroughly with distilled water, frozen at -60 °C, and freeze-dried. Quantitative analysis of REEs in the algae biomass was done by inductively coupled plasma-mass spectrometry (ICP-MS). Both macroalgae accumulated REEs from aquatic environment, *Vaucheria* sp. being a more efficient accumulator than *Chara* spp. Variability in the REE content in algae biomass was found, depending on location and season.

**Keywords:** post-mining lakes, *Chara*, *Vaucheria*, algal mats, rare earth elements, bioaccumulation

### 1 Introduction

Post-mining lakes, artificial water bodies created because of the cessation of mining and hydric reclamation, are increasing globally. These lakes are ecologically and socio-economically important as freshwater resources, natural habitats, and places for recreation [1]. Periphyton, primarily composed of algae and cyanobacteria, often plays a crucial role in newly formed aquatic ecosystems. The study of periphyton communities and their responses to abiotic factors in the littoral zones of three post-mining lakes located in northern Bohemia revealed a huge diversity of phototrophs [2]. Algal mats and meadows, naturally occurring in the post-mining lakes Most, Medard, and Milada, are important primary producers [1] and could play a critical role in accumulating excess nutrients and metals, including rare earth elements (REEs). This study focuses on the potential of two species of algae, *Vaucheria* sp. (Xanthophyceae) and *Chara* spp. (Charophyceae), for the bioremediation of REEs. In general, Xanthophyte algae are not the preferred autotrophic organisms for phycoremediation experiments [3-5]. Although some of them have been laboratory tested for potential use in the bioremediation process. The biosorption effect of *Vaucheria* itself was tested on multiple sources of pollution [6, 7].

Both *Vaucheria* and *Chara* are known for their ability to bioaccumulate contaminants, making them excellent candidates for remediating polluted waters [8-10]. Specifically, this research investigates the capacity of these macroalgal species to accumulate rare earth elements (REEs) such as lanthanum (La), cerium (Ce), neodymium (Nd), and gadolinium (Gd). These elements, while valuable for various technological applications, pose a risk to aquatic ecosystems when present in elevated concentrations [11]. By testing the ability of *Vaucheria* and *Chara* to bioaccumulate REE mixtures, this study aims to assess their effectiveness in remediating not only common pollutants like nitrogen and phosphorus but also trace elements that are of emerging environmental concern.

The goal of this research is to develop ecologically sustainable and economically viable strategies for water quality management in post-mining lakes. By utilizing locally occurring algal species, the study seeks to provide a natural solution for the long-term ecological, socioeconomic, and recreational management of these unique aquatic ecosystems. The findings from this study could serve as a valuable basis for the planning and management of current and future mining lakes.

## 2 Material and methods

### 2.1 Algal biomass and growth conditions

Macroalgae *Vaucheria* sp. (Xanthophyceae) and *Chara* spp. (Charophyceae) were collected by scuba diving technique from the vegetation in the post-mining lakes Most (Mo), Medard (Me) and Milada (Mi). Sampling was conducted in different seasons of the year (February, July, October). The individual algae samples were incubated under controlled laboratory conditions, in the lake water of their origin, at natural temperature (ranging 4 °C – 23 °C), and natural light intensity (ranging 5 - 180  $\mu\text{mol.m}^{-2}.\text{s}^{-1}$ ) for 96 h. Algal suspensions were bubbled with air. Laboratory incubation and accumulation experiments took place in glass culture bottles (Tamy bottles) with a volume of 500 mL in a cultivation unit with adjustable temperature and light intensity (Fig. 1).

### 2.2 Accumulation experiment

The algae (CH; *Chara*, V; *Vaucherie*) were tested for the ability to grow in the presence of rare earth elements, and for their capacity for metal accumulation. A mixture of rare earth elements (REEs) was added to the cultures in final concentration 40  $\mu\text{M}$  ( $\text{LaCl}_3$ ,  $\text{CeCl}_3$ ,  $\text{NdCl}_3$ ,  $\text{GdCl}_3$ ). The algae biomass was harvested after 4 days of treatment, washed thoroughly with lake water, and freeze-dried. Quantitative analysis of REEs in the algae biomass was done by inductively coupled plasma-mass spectrometry (ICP-MS).

### 2.3 Inductively coupled plasma-mass spectrometry

Freeze dried samples of algal biomass with or without treatment were digested with 30 %  $\text{H}_2\text{O}_2$  and 67 %  $\text{HNO}_3$  (Merck, Suprapure) in a PTFE microwave oven (MLS1200 MEGA, Gemini bv, Apeldoorn, The Netherlands) at 250–600W for 20 min. Quantitative analysis of REEs was performed using an Elan DRC-e (Perkin Elmer, Concord, ON, Canada) which is equipped with a concentric PTFE nebulizer and cyclonic spray chamber. Algal samples were passed through a 0.45 $\mu\text{m}$  nylon syringe filter (Millipore, Molsheim, France) and diluted 1:10 with distilled water. Values were expressed as micrograms per gram dry weight ( $\mu\text{g.g}^{-1}\text{DM}$ ).

## 3 Results and discussion

Figure 1 shows the biomass of *Chara* spp. (a) and *Vaucheria* sp. (b) in photobioreactors using lake water, under controlled laboratory conditions that mimic natural temperature (ranging from 4 °C to 23 °C) and light intensity (5 - 180  $\mu\text{mol.m}^{-2}.\text{s}^{-1}$ ). The biomass, later treated with REEs (La, Ce, Nd, Gd), was collected under natural conditions, with water temperature and irradiance varying according to season and depth. The algal biomass successfully acclimated to laboratory conditions and was subjected to the bioaccumulation experiment.

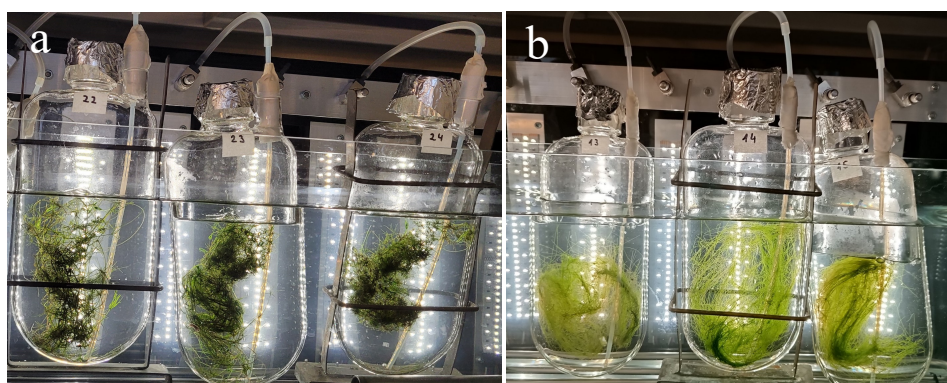
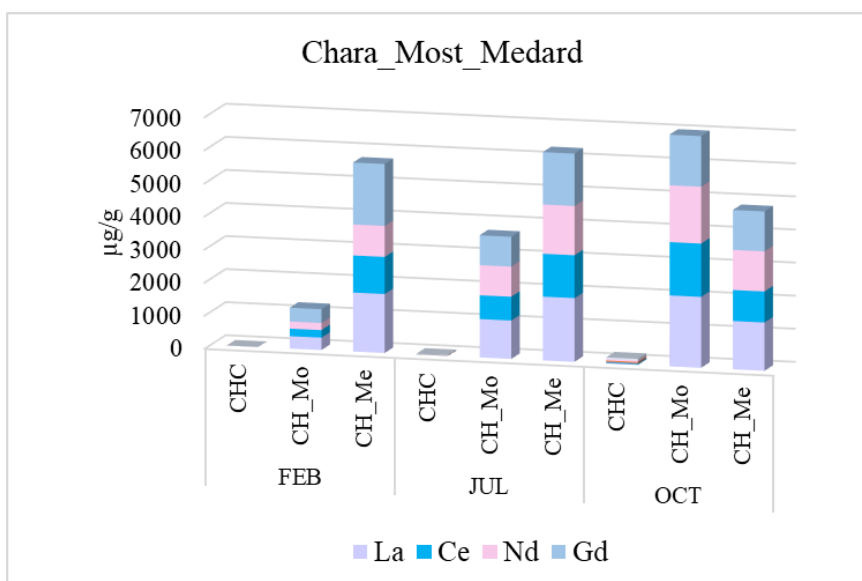


Fig. 1. Photobioreactor with biomass of *Chara* (a) and *Vaucheria* (b)

The accumulation of lanthanides in *Chara* and *Vaucheria* species varied by lake, season, and element, with distinct patterns for each genus.

In *Chara* spp., the highest accumulation in Lake Medard occurred in July, where lanthanum (La) reached 1927  $\mu\text{g/g}$  of biomass, followed by gadolinium (Gd) at 1873  $\mu\text{g/g}$  in February. Neodymium (Nd) and cerium (Ce) were also most concentrated in July at 1489  $\mu\text{g/g}$  and 1295  $\mu\text{g/g}$ , respectively. In contrast, in

Lake Most, the order of lanthanide accumulation was consistent with Lake Medard but occurred at higher concentrations, particularly in October. *Chara* accumulated La at 2143  $\mu\text{g/g}$ , Gd at 1919  $\mu\text{g/g}$ , Nd at 1716  $\mu\text{g/g}$ , and Ce at 1610  $\mu\text{g/g}$  (Fig. 2).



**Fig. 2. Bioaccumulation of REEs (La, Ce, Nd, Gd) by *Chara* collected from lakes Most and Medard in different seasons**

CHC = *Chara*, control without treatment, CH\_Mo = *Chara* from lake Most, CH\_Me = *Chara* from lake Medard

*Vaucheria* sp. exhibited higher bioaccumulation capacities across all elements. In Lake Most, the highest accumulation was observed in October, with La reaching 4196  $\mu\text{g/g}$ , Nd at 3772  $\mu\text{g/g}$ , Gd at 3606  $\mu\text{g/g}$ , and Ce at 2653  $\mu\text{g/g}$ . Meanwhile, in Lake Milada, the peak accumulation occurred in July, with Gd at 4046  $\mu\text{g/g}$ , La at 3747  $\mu\text{g/g}$ , Nd at 3513  $\mu\text{g/g}$ , and Ce at 2726  $\mu\text{g/g}$  (Fig. 3).

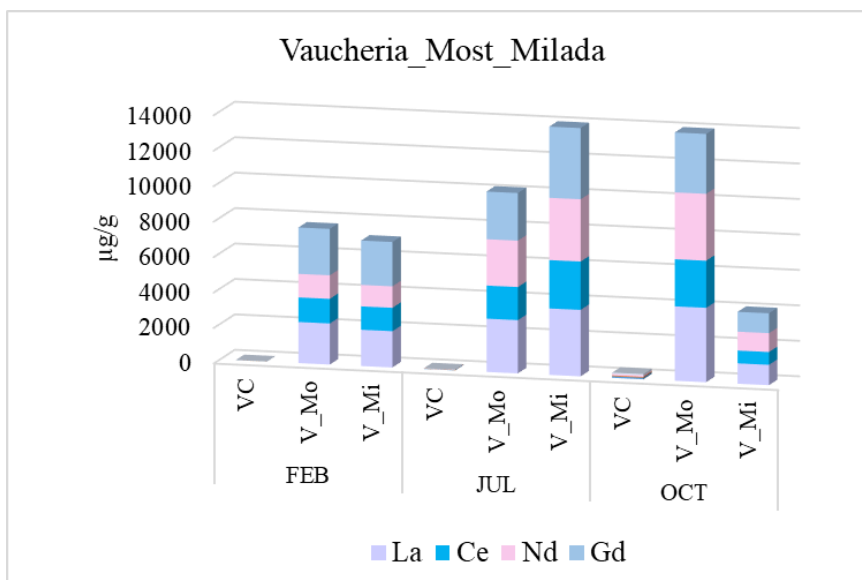


**Fig. 3. Bioaccumulation of REEs (La, Ce, Nd, Gd) by *Vaucheria* collected from lakes Most and Milada in different seasons**

VC = *Vaucheria*, control without treatment, V\_Mo = *Vaucheria*, lake Most, V\_Mi = *Vaucheria*, lake Milada

The results of the bioaccumulation experiment reveal significant differences in lanthanide uptake between *Chara* spp. and *Vaucheria* sp., as well as across different lakes and seasons. *Vaucheria* sp. consistently accumulated higher concentrations of REEs compared to *Chara* spp., particularly in Lake Most,

where lanthanum (La) reached 4196 µg/g. This difference may be attributed to the filamentous structure of *Vaucheria*, which provides a larger surface area for adsorption, as well as potential differences in cell wall composition and cation exchange capacity between the two genera. Previous studies have also shown that filamentous algae tend to be more efficient at metal and REE uptake due to their greater surface area for metal ion binding [12, 13].

Seasonal variation played a key role in bioaccumulation patterns. In *Chara* spp., the highest REE concentrations were observed in July and October, while in *Vaucheria* sp., accumulation peaked in October for Lake Most and July for Lake Milada. These differences may be influenced by temperature-related metabolic activity, which could enhance the uptake of metals during warmer months. Additionally, environmental factors such as pH and REE availability in each lake likely contributed to the observed variations in bioaccumulation. For instance, the higher La and Gd concentrations in Lake Most could reflect greater bioavailability of these elements in that lake's specific water chemistry.

From an ecological perspective, these findings highlight the potential of *Vaucheria* sp. for use in bioremediation, especially for REE-contaminated water bodies. Its superior bioaccumulation capacity suggests that it could be an effective tool for reducing REE concentrations in aquatic environments. Further research should focus on the underlying mechanisms of REE uptake in *Vaucheria*, as well as its potential for long-term application in bioremediation projects.

#### 4 Conclusions

Both macroalgae accumulated REEs from aquatic environment, *Vaucheria* sp. being a more efficient accumulator than *Chara* spp. Variability in the REE content in algae biomass was found, depending on location and season.

#### Acknowledgements

This work was done in the frame of the COST Action 19116 Trace metal metabolism in plants - PLANTMETALS, this project is co-financed from the state budget by the Technology agency of the Czech Republic under the Programme Environment For Life (SS07020018), and by the Czech Academy of Sciences within the program of Strategy AV 21, Land save and recovery.

#### References

- [1] Řeháková, K., Čapková, K., Konopáčová, E., Nedoma, J., Mareš, J., Bešta, T., Štenclová, L., Kust, A. Unveiling the ecological significance of algal mats and meadows: Insights into phosphorus cycling and primary production of benthic algae in post-mining lakes. ARPHA Conference Abstracts 6, 2023, e107027.
- [2] Bešta, T., Mareš, J., Čapková, K., Janeček, E., Štenclová, L., Kust, A., Říha, M., Konopáčová, E., Řeháková, K. Littoral periphyton dynamics in newly established post-mining lakes. *Aquatic Sciences*, 85 (21), 2023, <https://doi.org/10.1007/s00027-022-00914-y>.
- [3] Silva, A., Delerue-Matos, C., Figueiredo, S., Freitas, O. The Use of Algae and Fungi for Removal of Pharmaceuticals by Bioremediation and Biosorption Processes: A Review. *Water*, 11, 2019, 1555, <https://doi.org/10.3390/w11081555>.
- [4] Kandasamy, S., Narayanan, M., He, Z., Liu, G., Ramakrishnan, M., Thangavel, P., Pugazhendhi, A., Raja, R., Carvalho, I.S. Current strategies and prospects in algae for remediation and biofuels: An overview. *Biocatalysis and Agricultural Biotechnology*, 35, 2021, 102045, <https://doi.org/10.1016/j.bcab.2021.102045>.
- [5] Ankit, Bauddh K., Korstad, J. Phycoremediation: Use of Algae to Sequester Heavy Metals. *Hydrobiology*, 1, 2022, p. 288-303, <https://doi.org/10.3390/hydrobiology1030021>.
- [6] Khataee, A.R., Zarei, M., Dehghan, G., Ebadi, E., Pourhassan, M. Biotreatment of a triphenylmethane dye solution using a Xanthophyta alga: Modeling of key factors by neural network. *Journal of the Taiwan Institute of Chemical Engineers*, 42 (3), 2011, p. 380-386, <https://doi.org/10.1016/j.jtice.2010.08.006>.

- [7] Ayele, A., Getachew, D., Kamaraj, M., Suresh, A. Phycoremediation of Synthetic Dyes: An Effective and Eco-Friendly Algal Technology for the Dye Abatement. *Journal of Chemistry*, 2021, p. 1-14, <https://doi.org/10.1155/2021/9923643>.
- [8] Peña-Vázquez, E., Carballera, R., Bermejo-Barrera, P., Bermejo-Barrera, A. Use of macroalgae in environmental pollution control. *Marine Pollution Bulletin*, 58 (4), 2009, p. 658-662.
- [9] Gaur, J.P., Rai, L.C. Heavy metal tolerance in algae. In *Algal Adaptation to Environmental Stresses*. Springer, 2001.
- [10] Kufel, L., Kufel, I. Chara beds acting as nutrient sinks in shallow lakes - a review. *Aquatic Botany*, 72 (3-4), 2002, p. 249-260.
- [11] Vítová, M., Mezricky, D. Microbial recovery of rare earth elements from various waste sources: a mini review with emphasis on microalgae. *World Journal of Microbiology and Biotechnology*, 40, 2024, 189, <https://doi.org/10.1007/s11274-024-03974-4>.
- [12] Raji, Z., Karim, A., Karam, A., Khalloufi, S. Adsorption of Heavy Metals: Mechanisms, Kinetics, and Applications of Various Adsorbents in Wastewater Remediation - A Review. *Waste*, 1, 2023, p. 775-805, <https://doi.org/10.3390/waste1030046>.
- [13] Sarma, U., Hoque, M.E., Thekkangil, A., Venkatarayappa, N., Rajagopal, S. Microalgae in removing heavy metals from wastewater - An advanced green technology for urban wastewater treatment. *Journal of Hazardous Materials Advances*, 15, 2024, 100444, <https://doi.org/10.1016/j.hazadv.2024.100444>.





## BIOLOGICALLY SYNTHESIZED SILVER NANOPARTICLES: IMMUNE SYSTEM MODULATION AND BIOMEDICAL POTENTIAL

**Vlasta Demeckova<sup>a</sup>, Veronika Demcakova<sup>a</sup>, Jana Sedlakova-Kadukova<sup>b,c</sup>**

<sup>a</sup> Faculty of Natural Science, Pavol Jozef Safarik University in Kosice,  
Srobarova 2, 041 54, Kosice, Slovakia,

*vlasta.demeckova@upjs.sk; veronika.demcakova1@student.upjs.sk*

<sup>b</sup> Institute of Chemistry and Environmental Sciences, Faculty of Natural Sciences,  
Ss. Cyril and Methodius University in Trnava, Nám. J. Herdu 2, Trnava, 917 01, Slovakia,  
*jana.sedlakova.fpv@ucm.sk*

<sup>c</sup> ALGAJAS s.r.o., Pražská 16, 040 11 Košice, *jana.sedlakova@algajas.com*

### Abstract

Silver nanoparticles (AgNPs) are widely used for antimicrobial purposes, but concerns regarding toxicity persist. This study compares the effects of biologically synthesized AgNPs (BAGNPs) and chemically synthesized AgNPs (CAGNPs) on blood components and immune response. BAGNPs, synthesized using *Parachlorella kessleri*, demonstrated more pronounced effects on immune cells and cytokine levels. In healthy samples, BAGNPs increased echinocytes and reduced neutrophil viability, whereas in rheumatoid arthritis patients, pro-inflammatory cytokines decreased. These findings suggest BAGNPs could be advantageous in biomedical applications, though cytotoxicity warrants further research.

**Keywords:** silver nanoparticles, blood cells, nanoparticle toxicity

## 1 Introduction

Silver nanoparticles (AgNPs) are widely used due to their strong antimicrobial properties [1]. However, as their use increases in various industries, concerns about environmental and health risks have grown. While the toxicological effects of chemically synthesized AgNPs (CAGNPs) are well-documented [2], there is limited information on biologically synthesized AgNPs (BAGNPs), which are produced using environmentally friendly methods involving organisms like bacteria and algae.

This study focuses on the comparison between BAGNPs and CAGNPs in their interactions with blood components and immune responses, providing insights into the potential biomedical applications of AgNPs, particularly in immune modulation and inflammatory conditions like rheumatoid arthritis.

## 2 Material and methods

### 2.1 Preparation of AgNPs

CAGNPs were produced using the citrate reduction method. BAGNPs were prepared using the alga *Parachlorella kessleri*. Both types of nanoparticles were characterized by their size and shape, with BAGNPs showing enhanced colloidal stability compared to CAGNPs [3]. Following a modified procedure, an extract was prepared from the algae, after which an AgNO<sub>3</sub> solution was added to the extract to achieve a final silver concentration of 100 mg/L [4].

### 2.2 Preparation and incubation of blood samples

Blood samples were collected from both healthy individuals and patients with rheumatoid arthritis. These samples were incubated with BAGNPs and CAGNPs, and the impact on red blood cells, leukocytes, and cytokine production was evaluated using standard assays microtube. The blood samples, including the control, were incubated for 3 hours at 37 °C.

### 2.3 Analysis of viability and apoptosis of blood leukocytes

Dead cells were analyzed using the Muse™ Count and Viability kit (Muse™Cell Analyzer; Millipore, USA) according to the manufacturer's instructions. The percentage of apoptotic cells in the blood was determined using the Muse Annexin-V & Dead Cell Assay kit™ (Muse™Cell Analyzer; Millipore, USA).

## 2.4 Preparation of M1 and M2 macrophages

Monocytes (THP-1) were sourced from the European Collection of Authenticated Cell Cultures. To differentiate and polarize the THP-1 monocytes into M1 (classically activated) and M2 (alternatively activated) macrophages, we followed the protocol established by Foey et al. [5].

## 2.5 Real-time analysis of cell proliferation

To continuously monitor the effect of nanoparticles on the proliferation of differentiated macrophages, we employed the xCELLigence system following the methodology described in the study by Amrichová et al. [6].

## 2.6 Statistical analysis

Statistical analyses of the results were conducted using Minitab version 16 (Minitab Inc., 2013, State College, PA, USA).

# 3 Results and Discussion

## 3.1 Nanoparticle characterization

Both types of AgNPs were spherical, but BAgNPs exhibited a stable biomolecular corona derived from the algae, whereas CAgNPs had a citrate anion surface. This difference in surface coating significantly affected their biological activity.

## 3.2 Impact on red and white blood cells

BAgNPs induced significant erythrocyte aggregation and echinocyte formation, which was not observed with CAgNPs. This suggests that the biological effects of BAgNPs are strongly influenced by the algae-derived surface, contributing to the differences in cellular interactions. Based on changes in the percentage representation of leukocytes, we can infer which subgroups of white blood cells were more affected and killed by the presence of BAgNP, CAgNP, or Ag<sup>+</sup> ions (Table 1). Some studies suggest that Ag<sup>+</sup> ion release from AgNP surfaces is the primary driver of their toxicity, contributing to increased ROS production, pro-inflammatory cytokines, and apoptosis [7, 8]. However, other studies argue that AgNPs themselves, rather than the ions, cause distinct biological effects [9, 10]. Pratsinis et al. [11] explain this discrepancy by nanoparticle size-smaller AgNPs (<10 nm) release more ions due to a higher surface-to-volume ratio, making toxicity ion-dependent, whereas larger AgNPs induce cytotoxicity mainly through particle-cell interactions. Silver ions are recognized for their strong cytotoxic and genotoxic properties, as they readily bind to sulfur- and phosphorus-containing groups in DNA and proteins [7, 11]. Although Ag<sup>+</sup> ions are expected to be toxic to all leukocytes, lymphocytes exhibit a heightened sensitivity, potentially due to specific cellular vulnerabilities. BAgNPs reduced neutrophil viability more significantly than CAgNPs in both healthy and diseased blood samples. The percentage of viable leukocytes decreased in the presence of BAgNPs, while CAgNPs had a lesser effect. This suggests that BAgNPs may induce a stronger immune response, possibly through increased cellular uptake or interaction with phagocytic cells.

**Table 1. The effect of different treatments on the differential leukocyte counts**

WBC (%)	BAgNPs <i>n</i> =5	CAgNPs <i>n</i> =5	Ag <sup>+</sup> ions <i>n</i> =5	Control <i>n</i> =5
Neutrophils	59.0 ± 2.50*	63.83 ± 1.26	66.00 ± 4.09	63.17 ± 1.26
Eosinophils	1.33 ± 0.58	1.50 ± 0.50	2.00 ± 1.00	0.67 ± 0.29
Basophils	0.83 ± 0.29	1.33 ± 0.58	2.33 ± 0.29	1.33 ± 0.58
Lymphocytes	35.5 ± 2.78*	27.83 ± 2.75	22.17 ± 4.07	28.67 ± 1.53
Monocytes	3.33 ± 0.29	5.50 ± 0.87	7.50 ± 0.87	6.17 ± 0.76

Data are expressed as mean ± SD. CAgNPs - chemically synthesized silver nanoparticles; BAgNPs - biologically synthesized silver nanoparticles; \* P<0.05 different from Ag<sup>+</sup>ions treatment

## 3.3 Comparative analysis of BAgNP and CAgNP impact on blood components in healthy individuals and rheumatoid arthritis patients

Rheumatoid arthritis is an autoimmune disorder characterized by chronic inflammation, elevated cytokine production, and joint destruction [12]. Nanomedicine offers a promising approach for delivering targeted therapies to treat inflammatory diseases and other related conditions [13]. While previous studies

suggested that BAgNPs could reduce inflammation, especially in arthritis models [12, 13], our results indicate differences in their effects on immune cells. BAgNPs, unlike CAgNPs, induced significant erythrocyte coagulation and morphological changes (e.g. echinocyte formation) in both healthy and RA patients. This phenomenon has also been confirmed by previous studies showing that AgNPs can cause morphological changes in erythrocytes [14]. The question remains why BAgNPs caused greater procoagulant activity and morphological alterations in red blood cells, while CAgNPs did not. One possible explanation is the lower colloidal stability of CAgNPs, which may lead to aggregation and the formation of larger silver particles. This could explain the significantly fewer echinocytes observed with CAgNPs compared to BAgNPs. Notable differences were observed in leukocyte counts, particularly in neutrophils and monocytes, which likely recognize and engulf AgNPs. Once inside the phagolysosome, AgNPs release silver, potentially causing cytotoxicity and cell death [15]. In both patient groups, BAgNP exposure led to a marked reduction in neutrophils by 12 % in healthy patients and 8.5 % in arthritis patients. In contrast, CAgNPs showed no significant effect, likely due to their larger size and lower stability, resulting in reduced cytotoxicity. In rheumatoid arthritis patients, neutrophil counts decreased even during incubation alone, observed in both AgNP-treated and control samples. This is likely due to the heightened sensitivity of neutrophils, driven by chronic inflammation. This heightened activation makes them more vulnerable to various stimuli, leading to functional changes, altered immune responses, and a higher risk of cell death. These factors suggest that blood components in patients with chronic inflammatory diseases are more sensitive to environmental influences, which should be considered in therapy planning.

### 3.4 Differential effects of BAgNP and CAgNP on macrophage proliferation

Macrophages are key immune cells, with M1 macrophages driving inflammation and M2 macrophages involved in tissue repair. Both nanoparticles were evaluated using the xCELLigence system, with BAgNPs showing a more pronounced inhibitory effect on cell proliferation compared to CAgNPs. The doubling time of M1 macrophages exposed to BAgNPs was nearly 12 times longer than those exposed to CAgNPs, suggesting that BAgNPs exert a stronger inhibitory effect, likely due to their smaller size and enhanced stability. A similar trend was observed with M2 macrophages, where BAgNPs significantly delayed cell division compared to CAgNPs.

These findings suggest that BAgNPs, due to their smaller size and higher stability, may possess greater cytotoxicity and potential therapeutic effects, particularly in modulating macrophage activity. Furthermore, their ability to inhibit the proliferation of tumor cell line (THP-1) suggests potential anticancer applications, warranting further investigation.

## 4 Conclusion

The distinct biological effects observed between BAgNPs and CAgNPs can be attributed to differences in colloidal stability and surface properties. The smaller size and higher stability of BAgNPs likely enhance their interaction with blood components, leading to increased immune activation in healthy individuals but a suppressive effect on inflammation in rheumatoid arthritis patients.

These findings highlight the potential for biologically synthesized AgNPs in therapeutic applications, particularly in immune modulation and inflammation management. However, the observed cytotoxicity, particularly toward neutrophils, suggests that careful consideration must be given to dosage and delivery methods to avoid unintended side effects. BAgNPs exhibit unique interactions with blood components and immune cells that differ from chemically synthesized AgNPs. Their potential to modulate immune responses, particularly in inflammatory diseases, warrants further investigation. Future studies should focus on optimizing the size, stability, and surface properties of BAgNPs to maximize their therapeutic potential while minimizing cytotoxic risks.

## Acknowledgements

The work was supported by project VEGA 1/0018/22.

## References

- [1] Rai, M.K., Deshmukh, S.D., Ingle, A.P., Gade, A.K. Silver nanoparticles: the powerful nanoweapon against multidrug-resistant bacteria. *Journal of Applied Microbiology*, 112, 2012, p. 841-852.

- [2] Zhang, X.F., Liu, Z.G., Shen, W., Gurunathan, S. Silver Nanoparticles: Synthesis, Characterization, Properties, Applications, and Therapeutic Approaches. *International Journal of Molecular Sciences*, 17, 2016, 1534.
- [3] Mikac, L., Ivanda, M., Gotić, M., Mihelj, T., Horvat, L. Synthesis and characterization of silver colloidal nanoparticles with different coatings for SERS application. *Journal of Nanoparticle Research*, 16, 2014, 2748.
- [4] Kadukova, J. Surface sorption and nanoparticle production as a silver detoxification mechanism of the freshwater alga *Parachlorella kessleri*. *Bioresource Technology*, 216, 2016, p. 406-413.
- [5] Foey, A.D., Crean, S. Macrophage subset sensitivity to endotoxin tolerisation by *Porphyromonas gingivalis*. *PLoS One*, 8, 2013, p. e67955.
- [6] Amrichová, J., Špaková, T., Rosocha, J., Harvanová, D., Bačenkova, D., Lacko, M., Horňák, S. Effect of PRP and PPP on proliferation and migration of human chondrocytes and synoviocytes in vitro. *Central European Journal of Biology*, 9, 2014, p. 139-148.
- [7] Greulich, C., Diendorf, J., Gessmann, J., Simon, T., Habijan, T., Eggeler, G., Schildhauer, T.A., Epple, M., Koller, M. Cell type-specific responses of peripheral blood mononuclear cells to silver nanoparticles. *Acta Biomaterialia*, 7, 2011, p. 3505-3514.
- [8] Pareek, V., Gupta, R., Panwar, J. Do physico-chemical properties of silver nanoparticles decide their interaction with biological media and bactericidal action? A review. *Materials Science and Engineering: C, Materials for Biological Applications*, 90, 2018, p. 739-749.
- [9] Li, Y., Qin, T., Ingle, T., Yan, J., He, W., Yin, J.J., Chen, T. Differential genotoxicity mechanisms of silver nanoparticles and silver ions. *Archives of Toxicology*, 91, 2017, p. 509-519.
- [10] Bélteky, P., Rónavári, A., Zakupszky, D., Boka, E., Igaz, N., Szerencsés, B., Pfeiffer, I., Vágvölgyi, C., Kiricsi, M., Kónya, Z. Are Smaller Nanoparticles Always Better? Understanding the Biological Effect of Size-Dependent Silver Nanoparticle Aggregation Under Biorelevant Conditions. *International Journal of Nanomedicine*, 16, 2021, p. 3021-3040.
- [11] Pratsinis, A., Hervella, P., Leroux, J.C., Pratsinis, S.E., Sotiriou, G.A. Toxicity of silver nanoparticles in macrophages. *Small*, 9, 2013, p. 2576-2584.
- [12] Janakiraman, K., Krishnaswami, V., Rajendran, V., Natesan, S., Kandasamy, R. Novel nano therapeutic materials for the effective treatment of rheumatoid arthritis-recent insights. *Materials Today Communications*, 17, 2018, p. 200-213.
- [13] Mani, A., Vasanthi, C., Gopal, V., Chellathai, D. Role of phyto-stabilised silver nanoparticles in suppressing adjuvant induced arthritis in rats. *International Immunopharmacology*, 41, 2016, p. 17-23.
- [14] Al-Baker, A.A., Al-Kshab, A.A., Ismail, H.K. Effect of silver nanoparticles on some blood parameters in rats. *Iraqi Journal of Veterinary Sciences*, 34, 2020, p. 389-395.
- [15] Wang, F., Yu, L., Monopoli, M.P., Sandin, P., Mahon, E., Salvati, A., Dawson, K.A. The biomolecular corona is retained during nanoparticle uptake and protects the cells from the damage induced by cationic nanoparticles until degraded in the lysosomes. *Nanomedicine*, 9, 2013, p. 1159-1168.

## EVALUATION OF BIOCHEMICAL PROPERTIES AND POTENTIALLY TOXIC ELEMENTS IN THE SEDIMENT OF THE SUBTERRANEAN SYSTEM OF THE BRESTOVSKÁ CAVE

**Lenka Demková<sup>a</sup>, Lenka Bobuľská<sup>a</sup>, Július Árvay<sup>b</sup>**

<sup>a</sup> *Department of Ecology, Faculty of Humanities and Natural Sciences, University of Prešov, 17. Novembra 1, 080 01, Prešov, Slovakia, lenka.demkova@unipo.sk, lenka.bobulska@unipo.sk*

<sup>b</sup> *Institute of Food Sciences, Faculty of Biotechnology and Food Sciences, Slovak University of Agriculture in Nitra, Tr. A. Hlinku 2, 949 76 Nitra, Slovakia, julius.arvay@uniag.sk*

### **Abstract**

Caves, which are hydrologically connected to the earth's surface, represent vulnerable underground habitats that are highly influenced, or threatened by the conditions of the external environment. Human-caused disturbances of underground ecosystems in the form of released substances, chemicals, and various non-native sediments have an extremely adverse impact on the entire karst environment. The aim of the study was to determine the content of risk elements (As, Cd, Co, Cu, Fe, Hg, Mn, Ni, Pb, Zn) in sediments of inside and outside Brestovská cave environment and the influence of pollution on nutrients (Ca, Na, K, Mg) and activity of soil enzymes (urease, acid phosphatase, alkaline phosphatase,  $\beta$ -glucosidase, FDA). Content of elements was analysed using ICP-OES. The results showed serious pollution of evaluated area predominantly by arsenic and cobalt, both inside and outside cave environment. The presence of heavy metals in sediments significantly negatively influenced the activity of soil enzymes and soil nutrients, predominantly Ca and Mg. The source of pollution is numerous sinkholes in the vicinity of the cave, which are directly connected to the cave system.

**Keywords:** enzymatic activity, karst landscape, cave ecosystems, psychrophilic microorganisms, risk elements, anthropogenic impact

### **1 Introduction**

Caves, which are hydrologically more closely connected to the earth's surface, represent vulnerable underground habitats that are highly influenced or threatened by external environmental conditions. Underground streams and lakes, whose primary source is water from the epikarst zone, are much more stable in terms of flow, temperature, and chemical properties than water streams that are directly connected to the surface through large open inlets or dives.

The geological structure of the aquifer and climate in which the ecosystem is located also significantly affect the stability of the cave environment [1]. Humans can significantly change the availability of energy by increasing the supply of organic matter and nutrients to the caves. Microorganisms use organic matter that is anthropically introduced into the underground system and thus can indirectly change the environmental conditions (e.g. by reducing the availability of oxygen). Conversely, in some cases, humans can reduce the energy input to caves by severing connections to the surface or altering the surface vegetation, soil, and hydrologic regime in ways that eliminate the entry of organic matter into subterranean ecosystems. As a result of these disturbances, there have been changes in the abundance and diversity of cave animals. Human-caused disturbances of underground ecosystems in the form of released foreign substances, chemicals, and various non-native sediments have an extremely adverse impact on the entire karst environment [2]. Soil and soil sediment are critically endangered environments because of their ability to accumulate potentially risky elements as products of anthropic activity. Many of these elements (e.g. Co, Cu, Mn, Fe, and Zn) are essential micronutrients for soil organisms in small concentrations, but in increased amounts, they have harmful effects on organisms, and some others (e.g. As, Cd, Hg, Pb) are toxic. In caves and karst systems, these elements can occur in parent rocks and are part of the speleothems, coatings, fillings, and other cave sediments. Underground water flows can contain these elements in the form of dissolved ions in the complex of organic matter, which are in colloidal form, or together with separated sediments. The degree to which the risk element is reduced in caves is mediated and catalyzed by microorganisms as part of their metabolic processes [3]. The aim of this study was to determine the level of occurrence of risk elements in the soil, or sediment and enzyme activities of soil microorganisms, as biological indicators that will allow us to identify the extent of the impact of human activity on the

subterranean ecosystem of Brestovská cave. Changes in the biological properties of soil and soil sediment as a result of environmental disturbances indicate a change in the activity of the microbial community, level of biological balance, and quality of the investigated ecosystems. The study of microbial and chemical indicators also contributes to a better understanding of ecological processes and the relationships between individual components in surface and underground ecosystems. Understanding these ecological links can help us in the future to improve the condition and protection of threatened areas in which important cave systems are located.

## 2 Material and methods

The longest known cave of the geomorphological subdivision of the Western Tatras - Rohace is the Brestovská cave (49°15'32.3"N; 19°39'38.2"E) with a total focused length of underground spaces of 2026 m [4]. It is localised in the forested part of the Madajka massif near the village of Zuberec (Tvrdošín district). Its entrance is at an altitude of 867 m [5].

Soil and sediment samples were collected in 2019. Five sampling points were determined in the interior of the Brestovská cave (Figure 1). Other sampling points are: Dip - a large occasional dip of the surface waters of the Studený Potok, approx. 500 m southeast of the entrance to the Brestovská Cave; Water spout (WS) - Brestovská cave water spout with the spring of an underground stream from the Brestovská cave approx. 200 m southwest of its entrance. The last sample was taken from the forest terrain in the immediate vicinity above the entrance of the Brestovská cave (control sample). Each sampling point was represented by three random samples, and the individual data represented the average value of the indicator. The samples were transferred to the laboratory in plastic bags, where they were temporarily stored at 6 °C. Before analysis, parts of the soil and soil substrate samples were dried at room temperature, and all samples were sieved through a sieve with a mesh size of 2 mm.

The soil reaction (pH) was determined in a mixture of soil and CaCl<sub>2</sub> solution (c = 0.01 mol/L) at a ratio of 1:3 using a digital pH meter. The activities of the soil enzymes β-glucosidase [6], FDA hydrolase [7], acid and alkaline phosphatase [8], and urease [9] were also determined. For each soil enzyme activity, a corresponding control was performed using the same analytical method but without the addition of the substrate at the time of initiation of the enzymatic reaction. Soil respiration was determined by capturing the released CO<sub>2</sub> from fresh soil samples that were incubated at 25 °C for 24 h in hermetically sealed bottles. Carbon dioxide was captured by a NaOH solution (c = 0.05 mol/L), which was subsequently titrated with HCl (c = 0.05 mol/L) after the addition of BaCl<sub>2</sub> (c = 0.5 mol/L) [10]. The content of organic carbon (C<sub>ox</sub>) and total nitrogen (N<sub>tot</sub>) in the soil samples was determined using the ISO10694 method. The content of the monitored elements As, Cd, Co, Cu, Fe, Mn, Ni, Pb and Zn was determined by the OES-ICP method (Agilent 720, Agilent Technologies, USA) and Hg by the CV-AAS method (AMA-254, AlTec, Prague, CR), using methodological procedures published in the works of Árvay et al. [11] and Demková et al. [12]. Statistical operations were performed using the STATISTICA 12, where all data were log+1 transformed before analysis.

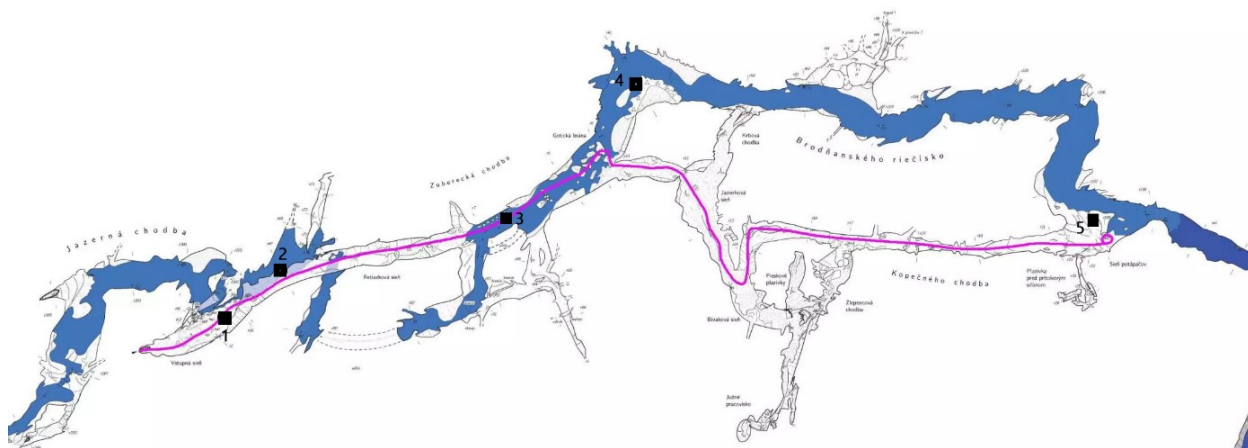


Fig. 1. Location of sampling points in the Brestovská Cave

### 3 Results and discussion

Monitoring the condition of the individual components of the underground system of Brestovská cave is a prerequisite for the proper management of the cave's operation after its opening to the public. The exchange soil reaction (pH/CaCl<sub>2</sub>) at the Brestovská cave, including its dip and water spout part, ranged from 7.0 to 7.6 (Table 1), indicating a neutral to slightly alkaline subterranean environment. The pH values showed a positive relationship with all the risk elements. This dependence was statistically significant at ( $p < 0.05$ ) only in the case of Zn (Figure 4). Soil reactions fundamentally affect the availability of hazardous substances in soil. As the pH increases, the precipitation of metal elements into insoluble hydroxides, carbonates, and organic complexes increases, and the adsorption of hazardous substances onto clay minerals and organic substances also increases. However, the availability of these trace elements for plant uptake is generally greater at lower pH values than at higher pH values [2]. Table 2 lists the average values of the chemical properties of the soil sediment and soil samples at the monitored locations. The highest values of organic carbon content ( $C_{ox}$ ) were measured at the control point in the forest (12.40 %) and in Brestovská WS (11.20 %).

**Table 1. Average values of chemical properties of soil/sediment samples on research localities**

Sampling sites	pH/CaCl <sub>2</sub>	C <sub>ox</sub> (%)	N <sub>tot</sub> (%)
Cave 1	7.4	2.81	0.17
Cave 2	7.6	7.40	0.03
Cave 3	7.4	1.16	0.03
Cave 4	7.5	1.64	0.04
Cave 5	7.3	0.81	0.05
Dip	7.6	0.75	0.06
WS	7.0	11.2	0.68
Forest - control sample	7.0	12.4	0.57

The total nitrogen content ( $N_{tot}$ ) reached the highest value at the Brestovská WS site (0.68 %), followed by that of the control sample in the forest (0.57 %). In contrast, the lowest values of the organic carbon content were recorded at the Dip sampling site (0.75 %), and in the case of the nitrogen content, it was the sediment above and next to the underground flow (0.03 %) in the inner spaces of the Brestovská cave (sampling sites 2 and 3). Using Spearman's correlation coefficient, a significant positive relationship ( $p < 0.01$ ) was found between  $C_{ox}$  and  $N_{tot}$ , and between soil respiration and soil reaction (Figure 2). Most of the assessed risk substances had an inhibitory effect on the content of organic carbon and total nitrogen in sediment samples from Brestovská cave and its surroundings. A significant negative correlation was confirmed in the case of Cu -  $C_{ox}$  ( $p < 0.01$ ), Cu -  $N_{tot}$  ( $p < 0.01$ ) and Fe -  $N_{tot}$  ( $p < 0.01$ ). In contrast, Pb and Zn were significantly positively correlated with organic carbon and total nitrogen content (Figure 4).

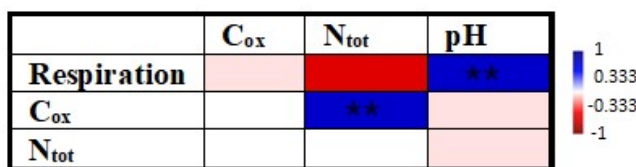


**Fig. 2. Correlation relationships among soil respiration, organic matter content ( $C_{ox}$ ) and total nitrogen content ( $N_{tot}$ )**

Notes: \* ( $p < 0.05$ ), \*\* ( $p < 0.01$ )

The properties of soils and soil substrates are closely related to the activity of microbial enzymes, which can serve as a sensitive indicator of soil quality and can also reflect its load and utilization rate [13]. This is due to unique microbial properties, such as large biomass, diversity, and activity [14]. Determining the activities of various microbial enzymes and the factors that influence them can help us understand the current state of underground ecosystems (Table 3). In the interior of the Brestovská cave, we recorded the

highest  $\beta$ -glucosidase activity with a value of 17.2  $\mu\text{g pNP/g.1h}$ . In the case of the enzymes FDA hydrolase (32.2  $\mu\text{g FS/g.1h}$ ) and urease (8.44  $\mu\text{g NH}_4\text{/g.1h}$ ), the highest values of their activity were recorded at the control point in the forest. At the same time, this sampling site had the highest value of soil respiration (133  $\mu\text{g C/g}$ ), which is twice as much compared to most other sampling sites. The maximum enzymatic activity of acid phosphatase was observed in WS sampling site (146  $\text{mg P/g.3h}$ ) and at the control point in the forest (145  $\text{mg P/g.3h}$ ).

**Table 2. Values of microbial properties of soil/sediment samples collected in Brestovská Cave and its vicinity**

Sampling sites	BG	FDA	ACP	ALP	URE	SR
Cave 1	6.72	9.10	48.1	114	4.18	58.6
Cave 2	6.45	0.00	74.2	18.7	0.39	43.9
Cave 3	2.92	0.88	39.5	103	1.36	59.0
Cave 4	14.5	0.88	0.00	101	4.56	59.4
Cave 5	17.2	0.26	47.1	72.6	7.92	43.9
Dip	4.55	0.10	72.2	51.1	2.52	44.1
WS	9.53	25.3	146	104	7.50	73.2
Forest - control sample	14.3	32.2	145	110	8.44	133

Notes: BG ( $\beta$ -glucosidase [ $\mu\text{g pNP/g soil.1h}$ ]), FDA (fluorescein diacetate hydrolysis hydrolase, [ $\mu\text{g FS/g soil.1h}$ ]), KF (acid phosphatase [ $\text{mg P/g soil.3h}$ ]), ZF (alkaline phosphatase [ $\text{mg P/g soil.3h}$ ]), URE (urease [ $\mu\text{g NH}_4\text{/g soil.1h}$ ]), SR (soil respiration, [ $\mu\text{g C/g soil dry}$ ])

Overall, the highest values of alkaline phosphatase (114  $\text{mg P/g.3h}$ ) of all sampling sites were recorded in the entrance part of the Brestovská cave and in the forest above its entrance; however, high activity was also demonstrated in other internal cave spaces. The high values of alkaline phosphatase are related to the fact that this enzyme increases its activity with increasing pH, which was found in this karst area. In contrast, zero values were recorded in some internal parts of the cave for FDA hydrolase and acid phosphatase (Table 2). The activity of soil enzymes was negatively correlated with the content of organic carbon and total nitrogen, and a significant negative correlation was also found between alkaline phosphatase and  $C_{ox}$  (Figure 3).



**Fig. 3. Correlation relationships of evaluated parameters of soil/sediment with soil enzymes from Brestovská Cave**

Notes: \* ( $p < 0.05$ ), \*\* ( $p < 0.01$ )

On the other hand, all evaluated enzymes showed a positive correlation with soil respiration, and in the case of pH, a significant negative correlation was found with the activity of all monitored enzymes. The activity of soil enzymes usually decreases due to the influence of risk substances, which was also confirmed in this subterranean site, as a negative correlation was demonstrated in all cases (Figure 4). In the case of FDA hydrolase, a significant negative correlation ( $p < 0.05$ ) was observed with Cd, Co, Mn, and Zn. In addition, this relationship was observed between alkaline phosphatase activity and Co ( $p < 0.01$ ), Cd ( $p < 0.05$ ), and Mn ( $p < 0.01$ ), and between urease activity and Mn ( $p < 0.05$ ). A negative relationship was noted between the risk elements and soil respiration in all cases, even for Pb and Zn ( $p < 0.05$ ).



**Table 3. Risk elements content [mg/kg] at the individual sampling points**

Sampling site	Mn	Fe	Ni	Co	Cu	Zn	As	Cd	Hg	Pb
Cave 1	50	4923	6.10	7.49	11.1	30.9	3.60	0.86	0.03	8.74
Cave 2	<b>722</b>	13177	18.9	16.2	14.8	40.8	13.4	<b>1.65</b>	0.10	10.5
Cave 3	87	14495	9.8	12.2	14.1	37.4	15.6	<b>1.49</b>	0.01	10.7
Cave 4	78	12167	7.3	10.2	12.4	36.3	19.4	<b>1.20</b>	0.03	10.9
Cave 5	14	14119	9.9	13.5	15.8	47.7	19.8	<b>1.50</b>	0.04	11.9
Dip	225	11182	25.8	10.7	14.3	33.7	13.5	<b>1.20</b>	0.07	8.73
WS	300	5978	8.5	11.9	10.3	37.2	7.80	<b>1.43</b>	0.22	20.2
Forest - control sample	323	8670	34.5	15.9	14.2	95.4	8.10	<b>1.54</b>	0.17	21.6
<b>Limit value</b>	<b>550</b>	-	<b>60</b>	<b>20</b>	<b>70</b>	<b>200</b>	<b>30</b>	<b>1</b>	<b>0.75</b>	<b>115</b>

Limit values for the content of hazardous substances in the soil, which are a criterion for assessing their contamination, were established based on Act no. 220/2004 Coll. [15]. According to the aforementioned legal regulations and on the basis of the limit values for Fe and Mn according to [16], these limits were exceeded in the investigated location of Brestovská cave's surroundings by two risk elements (Table 3). Exceeding the limit value of Cd (>1 mg/kg) was detected in almost every sample except for one sampling point, the entrance of Brestovská cave ("Cave 1"). In the case of Mn, an above-limit value (>550 mg/kg) was found only in the Zuberecka corridor near the cave entrance ("Cave 2"). Exceeding the limit values of As (30 mg/kg), Cd (20 mg/kg), Cu (70 mg/kg), Hg (0.75 mg/kg), Ni (60 mg/kg), Pb (115 mg/kg) and Zn (200 mg/kg) was not recorded in any soil substrate sample. Most metals occur naturally in the soil, but human activity disturbs their natural balance in the environment [17].

Soil pollution, or sediments with hazardous substances, subsequently leads to groundwater contamination and the release of hazardous elements into the air at concentrations that are harmful to the environment [18]. The state of the environment with a higher degree of pollution has a negative impact on the quality of the ecosystem, the extent of which depends on the size of the affected area, the depth of the soil into which pollutants penetrate, and the chemical composition of these substances [19].

The results of the Mann-Whitney test confirmed statistically significant differences ( $p < 0.01$  in all cases) in the values of pH, FDA hydrolase, acid phosphatase, urease, and soil respiration between the inner cave spaces and the control surface sample in the forest. In the case of the soil reaction, higher values were measured inside the Brestovská cave. In contrast, for FDA hydrolase, acid phosphatase, urease, and soil respiration, the values in the cave were significantly lower than those in the external control sample. When comparing the values of the content of risk elements, no statistically significant difference between the deeper inner and entrance parts of Brestovská cave was found. However, in this cave, as well as in Brestovská WS and the surface environment, a higher content of some elements (Cd) than the permitted limits was found. A higher level of contamination with these risk elements may result in the reduced activity of microbial enzymes or disturb other biological properties of the soil, which are important for the stability of underground ecosystems. Based on these results, we can evaluate the differences between the biotic and abiotic conditions of cave spaces and the outer parts of the karst landscape. Higher pH values, lower values of total nitrogen and organic carbon content, and enzymatic activity of the soil, which reflect the activity of microorganisms, together with soil respiration, confirm the specific and even extreme conditions that persist in the cave environment.

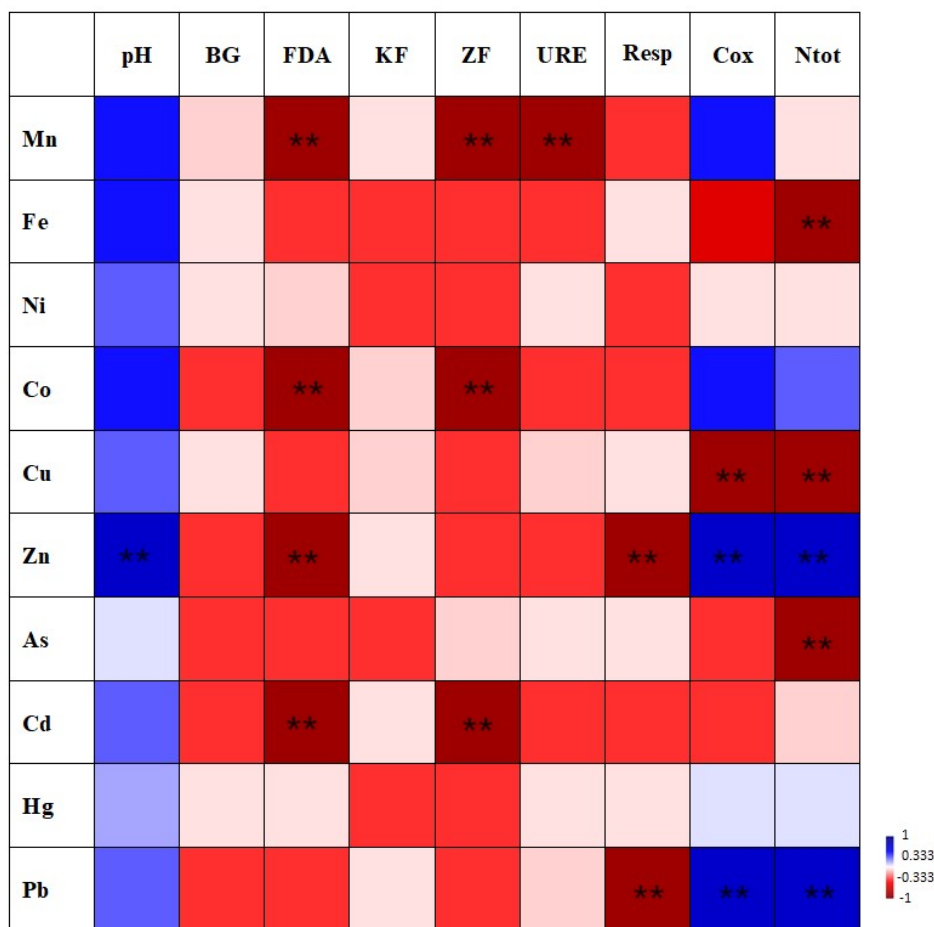


**Fig. 4. Correlation relationships of evaluated parameters of soil/sediment with risk elements from Brestovská Cave**

Notes: BG ( $\beta$ -glucosidase), FDA (fluorescein diacetate hydrolysis), KF (acid phosphatase), ZF (alkaline phosphatase), URE (urease), \*  $p < 0.05$ , \*\*  $p < 0.01$

No or only slight exceeding of the limit values of the other investigated risk elements in the soil samples from the Brestovská cave and its surroundings at the time of our research did not indicate more serious interventions in the karst landscape by humans. Potentially risky, however, remains the vicinity of dives, through which contamination of the cave system can occur from any part of the surface area in its catchment area through the waters of the Studený potok and its tributaries or precipitation seepage waters, with which the underground system is demonstrably hydrologically connected [20, 21].

#### 4 Conclusions

The biological properties of the soil are suitable indicators of its health and quality, because they react very quickly to the disturbance of the natural environment. This helps us in early detection of degradation of surface and underground ecosystems. The analysis of the biochemical properties and content of risk elements in the soil and soil sediment in the Brestovská cave and its immediate surroundings, which was carried out in September 2019, revealed above-limit values of some risk elements (Cd, Mn). They point out that the monitored location is partially exposed to environmental stress, which mainly results in a reduced activity of microbial enzymes and a change in other biological properties of this labile ecosystem. Therefore, increased interest in the protection of both types of environment - underground and surface - is necessary, not only in the karst area in question with the cave system, but also in the adjacent part of the non-karst area, which is part of the water catchment area subsidizing the underground hydrological system of Brestovská cave with water. In this area, it is important to eliminate deforestation of the territory and sources of environmental pollution with foreign, risky substances that most threaten the entire cave ecosystem through organically or

chemically contaminated waters flowing underground through sinkholes and hidden transitions from surface flows or seeping through karst overburden or sinkholes.

### Acknowledgements

This research was funded by the Grant Agency of the The Ministry of Education, Research, Development and Youth of the Slovak Republic VEGA No. 1/0213/22 and Slovak Research and Development Agency APVV-20-0140.

### References

- [1] Candiroglu, B., Dogruoz Gungor, N. Cave Ecosystems: Microbiological View. *European Journal of Biology*, 76 (1), 2017, p. 36-42.
- [2] Simon, K.S. Cave ecosystems. In White, W., Culver, D., Pipan, T. (Eds.): *Encyclopedia of Caves*, Cambridge, Massachusetts: Academic Press, 3, 2019, p. 223-226.
- [3] Vesper, D.J. Contamination of cave waters by heavy metals. In White, W., Culver, D., Pipan, T. (Eds.): *Encyclopedia of Caves*, Cambridge, Massachusetts: Academic Press, 3, 2019, p. 320-325.
- [4] Bella, P., Hlaváčová, I., Holúbek, P. *Zoznam jaskýň Slovenskej republiky* (stav k 31.12.2017). Slovenské múzeum ochrany prírody a jaskyniarstva, Liptovský Mikuláš, 2018, 528 p.
- [5] Bella, P., Haviarová, D., Višňovská, Z., Kunáková, L., Zelinka, J., Kudla, M., Labaška, P. Brestovská jaskyňa - ďalšia prístupná jaskyňa na Slovensku. *Aragonit*, 21 (1-2), 2016, p. 3-10.
- [6] Eivazi, F., Tabatabai, M.A. Glucosidases and galactosidases in soils. *Soil Biology and Biochemistry*, 20, 1988, p. 601-606.
- [7] Green, V.S., Stott, D.E., Diack, M. Assay for fluorescein diacetate hydrolytic activity: optimization for soil samples. *Soil Biology and Biochemistry*, 38, 2006, p. 693-701.
- [8] Grejtovský A. Vplyv zúrodňovacích opatrení na enzymatickú aktivitu ťažkej nivnej pôdy. *Rostlinná výroba*, 37, 1991, p. 289-295.
- [9] Khaziev, F. *Fermentativnaja aktivnost' počv*. Moskva: Nauka, 1976, p. 142-150.
- [10] Alef, K., Nannipieri, P. *Methods in applied soil microbiology and biochemistry*. London: Academic Press, 1995, 608 p.
- [11] Árvay, J., Demková, L., Hauptvogel, M., Michalko, M., Bajčan, D., Stanovič, R., Tomáš, J., Hrstková, M., Trebichalský, P. Assessment of environmental and health risks in former polymetallic ore mining and smelting area, Slovakia: Spatial distribution and accumulation of mercury in four different ecosystems. *Ecotoxicology and Environmental Safety*, 144, 2017, p. 236-244.
- [12] Demková, L., Árvay, J., Bobuľská, L., Hauptvogel, M., Hrstková, M. Open mining pits and heaps of waste material as the source of undesirable substances: biomonitoring of air and soil pollution in former mining area (Dubník, Slovakia). *Environmental Science and Pollution Research*, 26, 2019, p. 35227-35239.
- [13] Kubát, J., Nováková, J., Cerhanová, D. Výskyt a aktivita pôdných mikroorganizmů ve dlouhodobých polních pokusech na orné půdě. *Biologické indikátory kvality půd*, Brno: MZLU, 2002, p. 18-25.
- [14] Šarapatka, B. Možnosti využití aktivity enzymů jako indikátorů produktivity a kvality systémů. *Biologické indikátory kvality půd*, Brno: MZLU, 2002, p. 26-31.
- [15] Act no. 220/2004 Coll. Of Laws. on the Protection and use of agricultural land and on Act no. 245/2003 Coll. modification on Integrated prevention and control of environment pollution and on amendment of certain laws.
- [16] Kabata-Pendias, A. *Trace elements in soils and plants*. New York: CRC Press Taylor & Francis Group, 2011, 548 p.
- [17] Lyubenova, L., Schröder, P. Uptake and effect of heavy metals on the plant detoxification cascade in the presence and absence of organic pollutants. *Soil Heavy Metals*, 19, 2010, p. 65-85.
- [18] Angelovičová, L., Bobuľská, L., Fazekašová, D. Toxicity of heavy metals to soil biological and chemical properties in conditions of environmentally polluted area Middle Spiš (Slovakia). *Carpathian Journal of Earth and Environmental Sciences*, 10 (1), 2015, p. 193-201.
- [19] Bálintová, M., Luptáková, A. *Treatment of acid mine waters*. Košice: Technical University in Košice, 2012, 131 p.
- [20] Haviarová, D. Základné hydrogeochemické pomery a charakteristika režimu vôd Brestovskej jaskyne. *Slovenský kras*, 46 (1), 2010, p. 67-80.

- [21] Haviarová, D., Pristaš, P. Riešenie otázky komunikácie povrchových vôd Studeného potoka s podzemným tokom v Brestovskej jaskyni. *Aragonit*, 18 (1), 2013, p. 17-21.

## EVALUATION OF MANGANESE BIOEXTRACTION POTENTIAL OF MICROSCOPIC FILAMENTOUS FUNGUS

**Bence Farkas<sup>a</sup>, Martin Urik<sup>a</sup>**

<sup>a</sup> Institute of Laboratory Research on Geomaterials, Faculty of Natural Sciences, Comenius University in Bratislava, Mlynská Dolina, Ilkovičova 6, 842 15 Bratislava, Slovakia, [bence.farkas@uniba.sk](mailto:bence.farkas@uniba.sk)

### **Abstract**

The aim of this work was to examine the bioleaching of manganese oxides at various oxidation states (MnO, Mn<sub>3</sub>O<sub>4</sub>, Mn<sub>2</sub>O<sub>3</sub> and MnO<sub>2</sub>) by a strain of the filamentous fungus *Aspergillus niger*, a frequent soil representative. Our results showed that the fungus effectively disintegrated the crystal structure of selected mineral manganese phases. Thereby, during a 31-day static incubation of oxides in the presence of fungus, manganese was bioextracted into the culture medium. The Mn(II,III)-oxide was the most susceptible to fungal biodeterioration, and up to 26 % of the manganese content in oxide was extracted by the fungus into the medium. Our results highlight the significance of fungal activity in manganese mobilization. The soil fungi should be considered an important geoactive agent that affects the stability of natural geochemical barriers.

**Keywords:** bioextraction, bioleaching, filamentous fungi, manganese oxide

### **1 Introduction**

Manganese is a transition metal that is the 10th most abundant chemical element on Earth and makes up to 0.1 % of the Earth's crust. It is a structural component of more than 250 minerals and, in the case of several other minerals, is a substituent of Fe<sup>2+</sup> and Mg<sup>2+</sup> cations [1]. Manganese occurs in various oxidation states of which the +II, +III and +IV are predominant under natural conditions [2]. In the soil environment, it occurs in dissolved form, and it is partially adsorbed onto the surface of non-manganese mineral phases or organic compounds, or it is immobilized in organisms. Most of the manganese in the soil is found as a component of primary mineral phases or is bound to secondary minerals [3]. Manganese oxides and (oxo)hydroxides are among the most common secondary minerals of manganese in the soil. These are reactive phases that play an important role in the geochemical cycling of various elements. They generally participate in redox transformations of organic and inorganic compounds, since they represent the strongest oxidizing agents found in the environment [4].

Our research is therefore based on the assumption that the MnO, Mn<sub>3</sub>O<sub>4</sub>, Mn<sub>2</sub>O<sub>3</sub> and MnO<sub>2</sub>, which are constituents of naturally occurring geochemical barriers, should react differently with the metabolites of *Aspergillus niger*, a common soil filamentous fungus. We evaluated the contribution of the fungus to the chemical biodeterioration of manganese oxides using advanced analytical and mineralogical techniques. They allowed us to observe the kinetics of this fundamental process and led us to a better understanding of mechanisms that microorganisms employ to affect the manganese geochemistry in the environment.

### **2 Material and methods**

#### **2.1 Fungal strain**

The fungus *Aspergillus niger* strain CBS 140837 was obtained from the fungal collection of the Department of Mycology and Physiology at the Institute of Botany, Slovak Academy of Sciences. The fungal strain was maintained on the Sabouraud agar plates at 25 °C.

#### **2.2 Bioextraction of manganese**

The 31-day long manganese extraction experiments using the *A. niger* strain were performed in 100 ml sterile Erlenmeyer flasks with the mixture of 50 ml Sabouraud Dextrose Broth culture medium (HiMedia, Mumbai, India) and 0.635 g of MnO, 0.600 g of Mn<sub>3</sub>O<sub>4</sub>, 0.826 g of Mn<sub>2</sub>O<sub>3</sub>, or 0.844 g of MnO<sub>2</sub>.

#### **2.3 Analytical procedures**

The culture media filtrates were analyzed for the total manganese content by flame atomic absorption spectroscopy (F AAS) at line Mn 279.5 nm using an AAS spectrometer Perkin-Elmer Model 1100 (Perkin-Elmer, Überlingen, Germany).

The low-molecular-weight organic acids in the culture medium were analyzed by capillary isotachopheresis. Analysis of anions in 10 ml filtrate (0.45  $\mu\text{m}$ ) from the culture medium collected in the desired time intervals was performed by a ZKI 01 isotachophoretic analyzer (Villa Labeco, Spišská Nová Ves, Slovakia) using the itp-itp mode.

### 3 Results and discussion

The sensitivity of the *A. niger* strain to oxides and bioextracted manganese can be evaluated using the recorded changes of dry weights of fungal biomasses (Figure 1). The biomass harvested from the Mn(II)-oxide (MnO) treatment almost achieved the weight of the manganese-free control at the end of cultivation. It was followed by the biomass cultivated in the presence of the Mn(IV)-oxide (MnO<sub>2</sub>) and Mn(III)-oxide (Mn<sub>2</sub>O<sub>3</sub>). The least amounts of biomasses were recorded in the presence of Mn(II,III)-oxide (MnO.Mn<sub>2</sub>O<sub>3</sub>). The length of lag phase of each treatment, which was calculated along the maximum growth rate using the modified Gompertz's equation [5], indicated when a considerable cell division and, thus, the exponential growth phase occurred. It was the longest for the fungus cultivated in the presence of Mn(II)-oxide (2.3 days), followed by the Mn(IV)-oxide treatment (2.0 days). In the presence of Mn(II,III)-oxide and Mn(III)-oxide (Mn<sub>2</sub>O<sub>3</sub>), the exponential growth phase was achieved by the fungus significantly faster, after a day. The maximum growth rate was reduced only in the presence of Mn(II)-oxide (0.03 day<sup>-1</sup>). The rates estimated in the presence of all other oxides approximated the growth rate of fungus cultivated on manganese-free media (0.05 day<sup>-1</sup>).

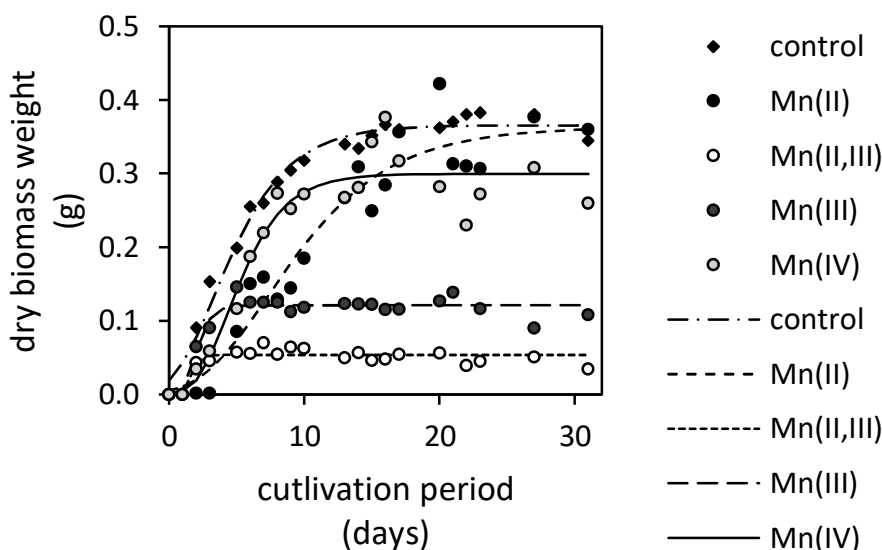


**Fig. 1. Changes in biomass weight of *Aspergillus niger* cultivated for 31 days in the culture medium supplemented with various manganese oxides (control is a manganese-free treatment)**  
Experimental data were fitted using modified Gompertz's equation [5]

Figure 2 depicts that the filamentous fungus *A. niger* was capable of mobilizing manganese from all oxides. Since the extraction efficiencies in non-inoculated control during a 31-day experiment were negligible, it was concluded that the manganese oxides' deterioration and subsequent stabilization of extracted manganese in solution resulted solely from fungal activity. The extraction kinetics revealed various distinctive phases that are similar to the characteristics of microbial growth. The slow initial phase is followed by the steep increase in manganese extraction that is subsequently diminished after the 10th cultivation day (Figure 2). These are the general features of Mn(II,III), Mn(III) and Mn(IV)-oxides' biodeterioration. There, the Mn(II,III)-oxide was the most susceptible to fungal activity, reaching the 26 % extraction efficiency (2340 mg.L<sup>-1</sup>). It was followed by Mn(II), Mn(III) and Mn(IV)-oxides, which did not display a statistically significant difference in maximum amounts of extracted manganese due to high variabilities in observed values. However, the average maximums of manganese in culture medium were 1210, 1140 and 700 mg.L<sup>-1</sup> for Mn(II), Mn(III) and Mn(IV)-oxides, respectively.

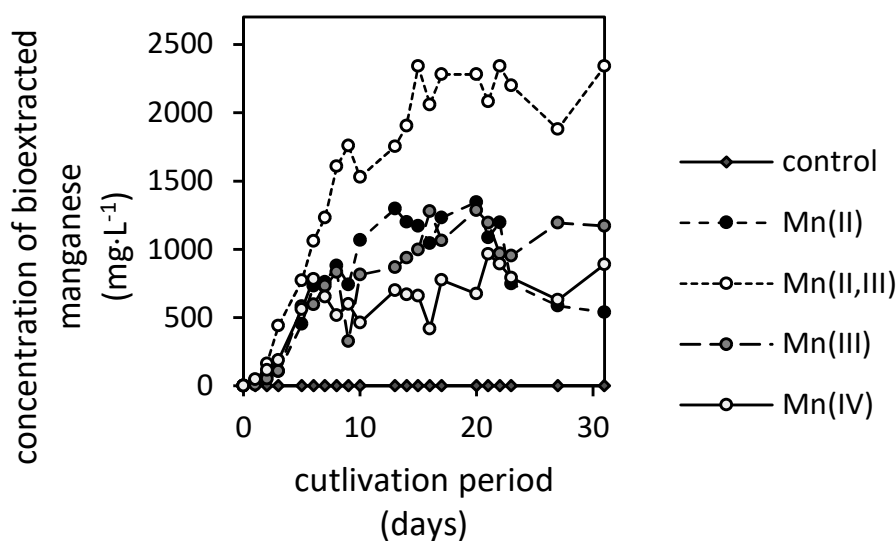


Fig. 2. Concentrations of bioextracted manganese from its oxides ( $\text{MnO}$ ,  $\text{Mn}_3\text{O}_4$ ,  $\text{Mn}_2\text{O}_3$  and  $\text{MnO}_2$ ) at different oxidation states during the static cultivation of microscopic filamentous fungus *Aspergillus niger*

#### 4 Conclusions

Our experimental observations confirmed that filamentous fungus *A. niger* was capable of dissolving all naturally occurring manganese oxides ( $\text{MnO}$ ,  $\text{Mn}_3\text{O}_4$ ,  $\text{Mn}_2\text{O}_3$ ,  $\text{MnO}_2$ ) and that it can act as a geoactive agent regarding manganese mobilization in the environment. We have successfully simulated the process of fungal deterioration of Mn(II), Mn(II,III), Mn(III) and Mn(IV)-oxide minerals via mechanisms of acidolysis, complexolysis and reductive dissolution.

Thus, our results highlight the importance of fungi in biogeochemical cycling and the environmental behavior of manganese, and provide insight into the actual process of manganese oxides' biodeterioration.

#### Acknowledgements

The work was Funded by the EU NextGenerationEU through the Recovery and Resilience Plan for Slovakia under the project No. 09I03-03-V04-00170.

#### References

- [1] Gilkes, R.J., McKenzie, R.M. Geochemistry and Mineralogy of Manganese in Soils. In Manganese in Soils and Plants, Proceedings of the International Symposium on 'Manganese in Soils and Plants', Adelaide, Australia, 22-26 August 1988; Graham, R.D., Hannam, R.J., Uren, N.C., Eds., Springer: Dordrecht, The Netherlands, 1988, p. 23-35. ISBN 978-94-010-7768-2.
- [2] Tebo, B.M., Bargar, J.R., Clement, B.G., Dick, G.J., Murray, K.J., Parker, D., Verity, R., Webb, S.M. Biogenic manganese oxides: Properties and mechanisms of formation. *Annual Review of Earth and Planetary Sciences*, 32, 2004, p. 287-328.
- [3] Robson, A.D. Manganese in Soils and Plants - An Overview. In Manganese in Soils and Plants, Proceedings of the International Symposium on 'Manganese in Soils and Plants', Adelaide, Australia, 22-26 August 1988, Graham, R.D., Hannam, R.J., Uren, N.C., Eds., Springer: Dordrecht, The Netherlands, 1988, p. 329-333. ISBN 978-94-010-7768-2.
- [4] Remucal, C.K., Ginder-Vogel, M. A critical review of the reactivity of manganese oxides with organic contaminants. *Environmental Science: Processes and Impacts*, 16, 2014, p. 1247-1266.
- [5] Zwietering, M.H., Jongenburger, I., Rombouts, F.M., van't Riet, K. Modeling of the bacterial growth curve. *Applied and Environmental Microbiology*, 56, 1990, p. 1875-1881.





## PHOS4PLANT: RECYCLING OF SEWAGE SLUDGE ASH INTO PHOSPHATE-RICH PLANT FERTILIZER

**Rebeka Frueholz<sup>a</sup>, Michael Wasner<sup>a</sup>, Sabine Spiess<sup>a</sup>, Marianne Haberbauer<sup>a</sup>**

<sup>a</sup> K1-MET GmbH, Stahlstrasse 14, 4020 Linz, rebeka.frueholz@k1-met.com

### Abstract

Phosphorus, currently derived from phosphate rock, is an essential resource for the production of phosphate fertilizers, thus playing a vital role in the food industry. Both phosphate and phosphate rock are listed in the EU's list of critical raw materials, where present acquisition is highly dependent on imports from non-EU regions.

The here described Interreg ATCZ project PHOS4PLANT aims to dissolve phosphorus from sewage sludge ash by biological leaching with an efficiency >85 % and to obtain a bioavailable phosphate fertilizer. A pretreatment of the sewage sludge ash is planned to accommodate bacterial adaptation to the ash matrix. The resulting phosphate fertilizer will subsequently be tested on model crops, and parameters of the plant root system and plant growth characteristics will be analyzed. At the same time, the levels of toxic metals in the soil and plants will be analyzed and the microbial diversity in the soil will be identified. Lastly, a comprehensive ecological and economical analysis of the entire process will be conducted, to highlight advantages and limitations of the results drawn from this project. The novelty of linking bioleaching processes to the generation of phosphate fertilizer with subsequent testing of the produced fertilizer proposes an innovative solution. The project consortium consists of four partners from Austria and the Czech Republic: K1-MET GmbH, Masaryk University, Brno University of Technology and BOKU University.

**Keywords:** phosphorus, bioleaching, sewage sludge ash, phosphate fertilizer, circular economy

## 1 Introduction

Phosphorus (P), utilized in the production of phosphate fertilizers, is an undisputedly essential resource in the food industry. The regional concentration of rock phosphate, along with problematic mining practices call for alternatives to the currently conventional rock phosphate sourcing. As of May 2014, P has been listed on the EU's list of critical raw material, along with rock phosphate since 2017.

In Austria around 7,000 tons of P is yearly lost through the disposal of sewage sludge, raising the question of effective recycling strategies. Moreover, changes in legislation have been issued regarding the incineration of sewage sludge call for a P recovery of  $\geq 80$  % by January 2030, further prioritizing the issue of P extraction and a closed P cycle.

With this, PHOS4PLANT aims to solubilize P from sewage sludge ash with a leaching efficiency of >85 % by applying concepts of bioleaching to obtain a bioavailable phosphate fertilizer. The fertilizer product will then consequentially be tested on model crops, using parameters of the plant root system and plant growth characteristics to evaluate the efficacy of the fertiliser. Lastly, a life-cycle assessment is planned to evaluate the different process chains and to identify the most applicable method.

## 2 Material and methods

### 2.1 Description of Work Packages

This project is divided into four individual work packages (WP) each focusing on a different aspect of the described project:

WP1: Preparation of sewage sludge ashes suitable for bioleaching

The thermal treatment process of the sewage sludge incineration is evaluated and optimized to produce suitable ash for the P leaching. Further, the carbonation rates of the ashes are to be determined.

WP2: Optimization of biological phosphorus leaching from sewage sludge ash

Microorganisms are to be enriched from the sewage sludge and their bioleaching activity will be evaluated. The cultivation medium of the bacteria is to be optimized in order to reduce or eliminate the addition of phosphates. Direct and indirect bioleaching processes will be tested out to assess the effectiveness of each method. Lastly, microbial proteins involved will be analysed using biochemical methods.

**WP3: Production of a phosphate fertilizer**

Phosphorus in the form of struvite will be recovered using bioelectrochemical method. Further, the struvite precipitation from the bioleachate produced in WP2 is to be optimized, as this reaction depends on a variety of parameters. A life cycle assessment along with an environmental life cycle cost calculation should then quantitatively assess each process.

**WP4: Optimising the application of phosphate fertilizer to crops**

Here the optimization of cultivation and phenotypic analysis of selected crops is performed along with the assessment of the effects of recycled phosphate fertilizer on crop growth and soil microbiome structure and recycled phosphate fertilizer on compost properties.

**2.2 WP2: Evaluating the effect of reduced phosphate in cultivation media**

Three different media with different phosphate concentrations were used for the cultivation of *Acidithiobacillus thiooxidans*, where the optical density (OD) at 600 nm in addition to the pH were monitored regularly. As a measurement of bacterial turbidity, the OD600 is an indirect indicator for bacterial growth. Table 1 describes the composition of a basal salt medium (Medium 1) modified from Nancucheo et al. [1]. A phosphate-reduced DSMZ Medium 882 (Medium 2) is described in Table 2 [2] meanwhile Table 3 lists a further phosphate-reduced medium (Medium 3) modified from Falagán et al. [3], 2024). Medium 2 was slightly amended in order to use the same trace element solution for all three media. As the bacterial culture *A. thiooxidans* does not require an iron source, iron was not added to any of the media. All cultures were grown at 30 °C and stirred at 120 rpm. Further, the bacteria were supplemented with 10 g/l of elemental sulfur. Solely Medium 1 was additionally supplemented with 0.2 g/l yeast extract. After 7 days, a 10 ml inoculum was withdrawn from the grown cultures and transferred into fresh medium.

**Table 1. Medium 1; pH adjusted to 3.5**

Basal Salt Solution		Trace Element Solution			
Compounds	mg.L <sup>-1</sup>	Compounds	mg.L <sup>-1</sup>	Compounds	mg.L <sup>-1</sup>
Na <sub>2</sub> SO <sub>4</sub> ·10H <sub>2</sub> O	150	ZnSO <sub>4</sub> ·7H <sub>2</sub> O	10	Na <sub>2</sub> MoO <sub>4</sub> ·2H <sub>2</sub> O	0.5
(NH <sub>4</sub> ) <sub>2</sub> SO <sub>4</sub>	450	CuSO <sub>4</sub> ·5H <sub>2</sub> O	1	NiSO <sub>4</sub> ·6H <sub>2</sub> O	1
KCl	50	MnSO <sub>4</sub> ·4H <sub>2</sub> O	1	Na <sub>2</sub> SeO <sub>4</sub> ·10H <sub>2</sub> O	1
MgSO <sub>4</sub> ·7H <sub>2</sub> O	500	CoSO <sub>4</sub> ·7H <sub>2</sub> O	1	Na <sub>2</sub> WO <sub>4</sub> ·2H <sub>2</sub> O	0.1
KH <sub>2</sub> PO <sub>4</sub>	50	Cr <sub>2</sub> (SO <sub>4</sub> ) <sub>3</sub> ·15H <sub>2</sub> O	0.5	NaVO <sub>3</sub>	0.1
Ca(NO <sub>3</sub> ) <sub>2</sub> ·4H <sub>2</sub> O	14	H <sub>3</sub> BO <sub>3</sub>	0.6		

**Table 2. Medium 2; pH adjusted to 2.0**

Basal Salt Solution		Trace Element Solution			
Compounds	mg.L <sup>-1</sup>	Compounds	mg.L <sup>-1</sup>	Compounds	mg.L <sup>-1</sup>
(NH <sub>4</sub> ) <sub>2</sub> SO <sub>4</sub>	132	ZnSO <sub>4</sub> ·7H <sub>2</sub> O	10	Na <sub>2</sub> MoO <sub>4</sub> ·2H <sub>2</sub> O	0.5
CaCl <sub>2</sub> ·2H <sub>2</sub> O	147	CuSO <sub>4</sub> ·5H <sub>2</sub> O	1	NiSO <sub>4</sub> ·6H <sub>2</sub> O	1
MgCl <sub>2</sub> ·6H <sub>2</sub> O	53	MnSO <sub>4</sub> ·4H <sub>2</sub> O	1	Na <sub>2</sub> SeO <sub>4</sub> ·10H <sub>2</sub> O	1
KH <sub>2</sub> PO <sub>4</sub>	27	CoSO <sub>4</sub> ·7H <sub>2</sub> O	1	Na <sub>2</sub> WO <sub>4</sub> ·2H <sub>2</sub> O	0.1
		Cr <sub>2</sub> (SO <sub>4</sub> ) <sub>3</sub> ·15H <sub>2</sub> O	0.5	NaVO <sub>3</sub>	0.1
		H <sub>3</sub> BO <sub>3</sub>	0.6		

**Table 3. Medium 3; pH adjusted to 1.8**

Basal Salt Solution		Trace Element Solution			
Compounds	mg.L <sup>-1</sup>	Compounds	mg.L <sup>-1</sup>	Compounds	mg.L <sup>-1</sup>
Na <sub>2</sub> SO <sub>4</sub> ·10H <sub>2</sub> O	9	ZnSO <sub>4</sub> ·7H <sub>2</sub> O	10	Na <sub>2</sub> MoO <sub>4</sub> ·2H <sub>2</sub> O	0.5
(NH <sub>4</sub> ) <sub>2</sub> SO <sub>4</sub>	9	CuSO <sub>4</sub> ·5H <sub>2</sub> O	1	NiSO <sub>4</sub> ·6H <sub>2</sub> O	1
KCl	1	MnSO <sub>4</sub> ·4H <sub>2</sub> O	1	Na <sub>2</sub> SeO <sub>4</sub> ·10H <sub>2</sub> O	1
MgSO <sub>4</sub> ·7H <sub>2</sub> O	10	CoSO <sub>4</sub> ·7H <sub>2</sub> O	1	Na <sub>2</sub> WO <sub>4</sub> ·2H <sub>2</sub> O	0.1
KH <sub>2</sub> PO <sub>4</sub>	1	Cr <sub>2</sub> (SO <sub>4</sub> ) <sub>3</sub> ·15H <sub>2</sub> O	0.5	NaVO <sub>3</sub>	0.1
Ca(NO <sub>3</sub> ) <sub>2</sub> ·4H <sub>2</sub> O	0.28	H <sub>3</sub> BO <sub>3</sub>	0.6		

### 3 Results and discussion

The results of the pH and the OD600 of multiple bacterial growth cycles in the different media are presented in Figure 1. Overall, all cultures except for one, were able to lower the pH to around 0.65, regardless of the cultivation medium. The same trend holds true for the OD600 measurements, indicating bacterial growth throughout the course of the 7-day cultivation period. These results indicate that for the actual leaching experiments, the bacteria are supplied with sufficient nutrients when cultivated in Medium 3, which contains solely traces of phosphate.

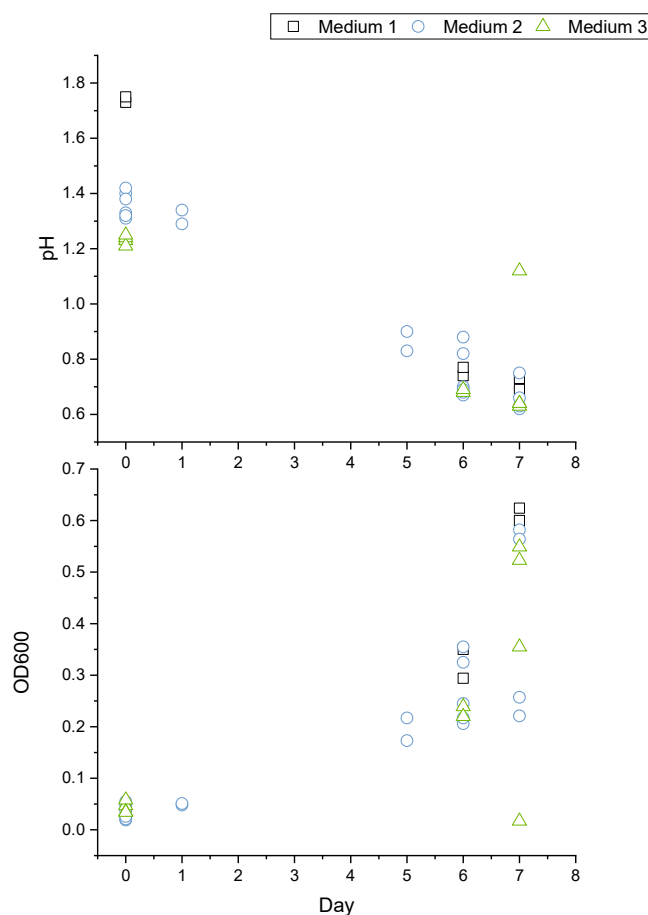


Fig. 1. pH and OD600 measurements of bacterial cultures in different media

### 4 Conclusions

The here described project aims to contribute research towards the recycling of the critical element P from waste products such as sewage sludge ash. Generally, the cultivation of bacterial cultures such as *A. thiooxidans* call for phosphate-rich media, however as phosphate is aimed to be recovered by bioleaching of sewage sludge ash, the supplementation of phosphate in the medium should be reduced to the minimal amount possible. With this, the parameters pH and OD600 of the bacterial cultures grown in three distinct media were evaluated, concluding that a concentration of 0.7 mg/l of  $\text{PO}_4^{3-}$  seems to indicate sufficient bacterial activity. Taking these results into consideration, further investigations are planned using Medium 3.

### Acknowledgements

The project is co-funded by the European Regional Development Fund (programme Interreg Austria-Czechia 2021-2027), project ATCZ00043, PHOS4PLANT (From Waste to Resource - Recycling Sewage Sludge Ash into Phosphate-rich Plant Fertilizer). Furthermore, the authors gratefully acknowledge the funding support of K1-MET GmbH, metallurgical competence center. The research programme of the K1-MET competence center is supported by COMET (Competence Center for Excellent Technologies), the Austrian programme for competence centers. COMET is funded by the Federal Ministry for Climate Action,

Environment, Energy, Mobility, Innovation and Technology, the Federal Ministry for Digital and Economic Affairs, the Federal States of Upper Austria, Tyrol and Styria as well as the Styrian Business Promotion Agency (SFG) and the Standortagentur Tyrol. Furthermore, we thank Upper Austrian Research GmbH for the continuous support.

## References

- [1] Nancucheo, I., Rowe, O.F., Hedrich, S., Johnson, D.B. Solid and liquid media for isolating and cultivating acidophilic and acid-tolerant sulfate-reducing bacteria. *FEMS Microbiology Letters*, 363(10), 2016, <https://doi.org/10.1093/femsle/fnw083>.
- [2] Atlas, R. M. *Handbook of microbiological media* (4th ed.). CRC Press, 2010.
- [3] Falagán, C., Sbaffi, T., Williams, G.B., Bargiela, R., Dew, D.W., Hudson-Edwards, K.A. Nutrient optimization in bioleaching: are we overdosing? *Frontiers in Microbiology*, 15, 2024, <https://doi.org/10.3389/fmicb.2024.1359991>.

## EVALUATION OF FERRIC MINERALS'S STABILITY IN THE PRESENCE OF FILAMENTOUS FUNGI - CHALLENGING THE EXPECTATIONS

Zuzana Goneková<sup>a</sup>, Martin Urik<sup>a</sup>, Rebeka Kósaová<sup>a</sup>, Bence Farkas<sup>a</sup>, Marcel B. Miglierini<sup>a,b</sup>

<sup>a</sup> Institute of Laboratory Research on Geomaterials, Faculty of Natural Sciences, Comenius University in Bratislava, Mlynská dolina, Ilkovičova 6, 84215 Bratislava, Slovakia, martin.urik@uniba.sk

<sup>b</sup> Slovak Technical University in Bratislava, Institute of Nuclear and Physical Engineering, Ilkovičova 3, Bratislava, 84104, Slovakia

### Abstract

This study examines the impact of fungal activity on iron-bearing ochreous sediments from abandoned mining site. Using a bioleaching experiment, fungal-treated sediments were analysed with X-ray diffraction (XRD) and Mössbauer spectroscopy. While XRD results showed no new crystalline phases or structural changes, Mössbauer spectroscopy revealed a redistribution of ferric iron. Specifically, the disappearance of a sextet component and an increase in poorly ordered ferric sites, likely ferrihydrite, were observed. These subtle fungal-induced modifications can influence the mobility and bioavailability of toxic elements in contaminated environments.

**Keywords:** *Aspergillus*, arsenic, bioleaching, ferric ochres, sediments

### 1 Introduction

Filamentous fungi naturally possess a high capacity to alter the physicochemical composition of minerals. This is typically initiated and facilitated by the acidolysis, a process involving the secretion of acidic metabolites that promote mineral dissolution, extracting metallic ions into the extracellular environment [1]. This process involves a combination of chemical and physical interactions between fungal hyphae and solid mineral surfaces in their natural habitat, leading to the partial or total dissolution of chemical components exposed in minerals. This also naturally affects the structural and mineralogical properties of the iron oxides, occurring in the vicinity of growing microorganisms to various extent [2].

Since these changes can be subtle, their successful characterization relies on the implementation of a highly sensitive method to determine the iron structure in the samples. Thus, in our study, we have addressed the critical issue of fungal impact on the structural and chemical stability of iron-bearing sediments using Mössbauer spectroscopy and other techniques suitable for solid phase and elemental analysis.

### 2 Material and methods

#### 2.1 Microorganisms and iron-bearing phases

In this study, we have utilized wild strain of microscopic filamentous fungus *Aspergillus niger*, for the modification of iron bearing ochreous material collected from the stream sediment at the adit of abandoned mine Buducnost (Pezinok, Slovakia).

#### 2.2 Bioleaching experiment

An autoclaved set of 150 mL Czapek-Dox Broth culture media in 250 mL glass bottles was supplemented with ochreous sediment to prepare suspensions for the fungal treatment. A volume of 10 µL of fungal spore suspension was introduced into the culture media with supplemented ochreous sediment. The mixture underwent a static 15-day incubation at 25 °C in the dark. The fungal biomass that developed on the surface of the culture medium or in form of a submerged culture was collected, rinsed with distilled water, and dried at 80 °C. The spent culture medium was vacuum filtered through a 0.45 µm mixed cellulose ester membrane filter. The solid residues were subjected to analytical measurements.

#### 2.3 Analytical measurements

The XRD analyses were performed with the X-ray diffractometer Bruker D8 DISCOVER equipped with an X-ray tube with a rotating Cu anode operating at 12 kW (40 kV/300 mA). Also, the <sup>57</sup>Fe Mössbauer spectroscopy was used to identify any structural changes of iron in the residual solids in comparison to control. <sup>57</sup>Fe Mössbauer spectroscopy was applied in the transmission geometry. The <sup>57</sup>Co(Rh) source of γ

radiation was kept at room temperature; and conventional spectrometer (WissEl, GmbH, Germany) working in constant acceleration mode was used.

### 3 Results and discussion

Despite the major structural components of the ochreous sediment being subjected to the intense bioleaching effects of the fungus, the XRD analysis did not reveal any microbially induced changes in mineralogical parameters (Figure 1b and Figure 1d). Furthermore, the XRD patterns showed no presence of well-crystallized, matured, or newly formed structures.

The Mössbauer spectra recorded at room temperature revealed the extinction of the sextet distribution, associated with the disappearance of the asymmetry in the fit of the fungus-treated ochreous sediment (Figure 1c), which had been previously detected in the untreated (Figure 1a). This sextet-disappearance-related redistribution of ferric iron resulted in an increase of the relative doublet  $D_{low}$  area to 42 %, while doublet  $D_{high}$  changed negligibly within the margin of error (Table 1).

We proposed that, in addition to ferrihydrite, which comprises the less ordered ( $D_{high}$ ) and well ordered ( $D_{low}$ ) iron site, there is a magnetic component in the untreated material likely representing more thermodynamically stable crystallites, such as disordered nanosized goethite.

**Table 1. The relative distribution of each structural component of ochreous sediments**

	Component	Relative area (%)
<b>untreated</b>	distributed sextet	15
	doublet $D_{low}$	57
	doublet $D_{high}$	28
<b>fungus-treated</b>	distributed sextet	0
	doublet $D_{low}$	58
	doublet $D_{high}$	42

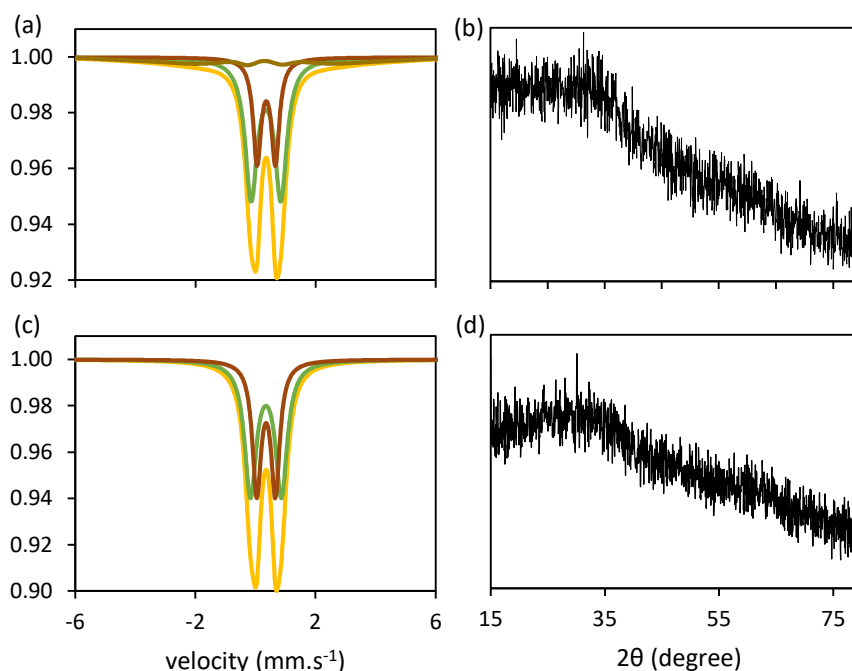


**Fig. 1. The recorded XRD patterns and Mössbauer spectra of untreated (a,b) or fungus-treated (b,c) ochreous sediments**

### 4 Conclusions

Our bioleaching experiments demonstrated that filamentous fungi can significantly alter the structural properties of ochreous sediments. Structural analysis using Mössbauer spectroscopy revealed distinct changes in the iron mineralogy of the sediments after exposure to fungi. Specifically, evidence showed

dissolution of goethite-like phases and less ordered ferric iron sites within ferrihydrite. These findings provide insights into the biogeochemical processes affecting iron oxides in mining-impacted areas.

### **Acknowledgements**

This work was supported by the Scientific Grant Agency of the Slovak Republic Ministry of Education and the Slovak Academy of Sciences under VEGA contract No. 1/0175/22.

### **References**

- [1] Urík, M., Polák, F., Bujdoš, M., Miglierini, B.M., Milová-Žiaková, B., Farkas, B., Goneková, Z., Vojtková, H., Matúš, P. Antimony leaching from antimony-bearing ferric oxyhydroxides by filamentous fungi and biotransformation of ferric substrate. *Science of The Total Environment*, 664, 2019, p. 683-689.
- [2] Vyhnálek, S., Miglierini, M.B., Dekan, J., Bujdoš, M., Dobročka, E., Farkas, B., Matúš, P., Urík, M. Encapsulating magnetite nanopowder with fungal biomass: Investigating effects on chemical and mineralogical stability. *Separation and Purification Technology*, 333, 2024, p. 125899.





# MORPHOLOGICAL AND ELEMENTAL EVALUATION OF TETRAHEDRITE GRAINS BEFORE AND AFTER BIOLEACHING

**Lenka Hagarová<sup>a</sup>, Daniel Kupka<sup>a</sup>, Zuzana Bártová<sup>a</sup>**

<sup>a</sup> Institute of Geotechnics of the Slovak Academy of Sciences, Watsonova 45, 040 01 Kosice, Slovakia,  
hagarova@saske.sk

## Abstract

The bioleaching of Ag-bearing tetrahedrite mineral from the Strieborná vein of the Rožňava mine in Slovakia was investigated. Tetrahedrite from this region is characterized by high copper and silver content, with additional potential for antimony recovery. Morphological and elemental changes in tetrahedrite grains were monitored using scanning electron microscopy (SEM) and energy-dispersive X-ray spectroscopy (EDX) and analyzed before and after bioleaching using the iron-oxidizing acidophilic species *Leptospirillum ferriphilum*. This study provides insights into the morphological and chemical evolution of tetrahedrite during bioleaching, demonstrating the role of bioleaching in enhancing the extraction of valuable elements from complex sulfide minerals.

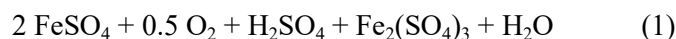
**Keywords:** tetrahedrite, bioleaching, morphology, elemental analysis, *Leptospirillum ferriphilum*

## 1 Introduction

Tetrahedrite, belonging to the sulfosalt mineral group, is a complex copper antimony sulfosalt with the chemical formula  $\text{Cu}_{10}(\text{Fe,Zn})_2\text{Sb}_4\text{S}_{13}$ . This mineral is of considerable interest due to its ability to host economically significant quantities of metals such as copper, silver, and antimony. Tetrahedrite's complex chemistry is further characterized by various isomorphous substitutions, including elements like arsenic, mercury, and cadmium, which can lead to the formation of different mineral species within the tetrahedrite group [1].

The extraction and processing of tetrahedrite pose both economic opportunities and environmental challenges. The presence of valuable metals like Cu and Ag in tetrahedrite makes it a target for metallurgical processing. However, traditional pyrometallurgical and hydrometallurgical methods often face limitations due to the mineral's complex structure and the potential release of toxic elements such as arsenic and antimony during processing and contributing this way to the potential environmental challenges associated with their waste products [2, 3].

Acidophilic iron-oxidizing bacteria, particularly members of the genera *Acidithiobacillus* and *Leptospirillum* (*L.*), have shown high efficiency in oxidizing iron, thereby enhancing the dissolution of minerals like tetrahedrite. The efficiency of these bacteria in various temperature ranges has been studied, demonstrating that their growth and iron oxidation kinetics can vary significantly with temperature changes. In particular, the study by Kupka et al. (2023) offers insights into bacterial kinetics over a wide range of temperatures (5-45 °C), highlighting the adaptability of these microorganisms to diverse environmental conditions. Ferric iron serves as a critical oxidant for the dissolution of sulfide minerals, and the role of iron-oxidizing bacteria, such as *L. ferriphilum*, is to oxidize ferrous iron to ferric ion, maintaining the high redox potential required for the leaching process (Eq.1) [4].



In this context, the morphology and composition of the mineral surface can also significantly influence the efficiency of bioleaching. Understanding the morphological and elemental transformations that occur during bioleaching is crucial for optimizing metal recovery and minimizing environmental impact.

## 2 Material and methods

### 2.1 Sample preparation

The tetrahedrite ore sample was obtained from the Strieborná vein in the Rožňava ore field, eastern Slovakia. The sample was crushed and milled to a grain size of less than 100  $\mu\text{m}$ , followed by froth flotation to produce a tetrahedrite concentrate. This concentrate underwent further conditioning with diluted sulfuric

acid (pH 1) at 90 °C for 24 hours under a nitrogen atmosphere to remove residual siderite. The final siderite-free tetrahedrite concentrate was isolated by filtration, washing, and drying.

## 2.2 Bioleaching experiment

Tetrahedrite bioleaching was conducted using a chemolithotrophic iron-oxidizing bacterial strain *L. ferriphilum*. The bacteria were cultured in a liquid mineral medium (amounts per liter: 0.4 g  $MgSO_4 \cdot 7H_2O$ , 0.1 g  $(NH_4)_2SO_4$ , 0.04 g  $K_2HPO_4$  and 33.4 g  $FeSO_4 \cdot 7H_2O$ ) at 25 °C until the late exponential phase. The tetrahedrite concentrate was then introduced into sterile shaking flasks containing the bacterial cultures, achieving a pulp density of 2 %. The bioleaching experiments were carried out under aerobic conditions at pH 2, 25 °C, and 190 rpm.

## 2.3 Morphological and elemental analysis

Morphological and elemental analysis of the tetrahedrite concentrate before and after bioleaching were performed using a scanning electron microscope (SEM) MIRA 3 FE-SEM (TESCAN) equipped with an energy-dispersive X-ray (EDX) detector (Oxford Instruments). Surface morphology was observed, and elemental distribution was analyzed through EDX mapping.

## 3 Results and discussion

The individual tetrahedrite grains in the initial sample showed high copper (up to 40 wt%) and silver (up to 1 wt%) content, with substantial amounts of antimony (27 wt%) (Fig. 1a). The EDX mapping confirmed the presence of copper, antimony, and sulfur as major elements (Fig. 1b), along with traces of mercury, arsenic and zinc. The chemical composition suggested the presence of substitutional elements, indicative of the complex nature of tetrahedrite minerals.

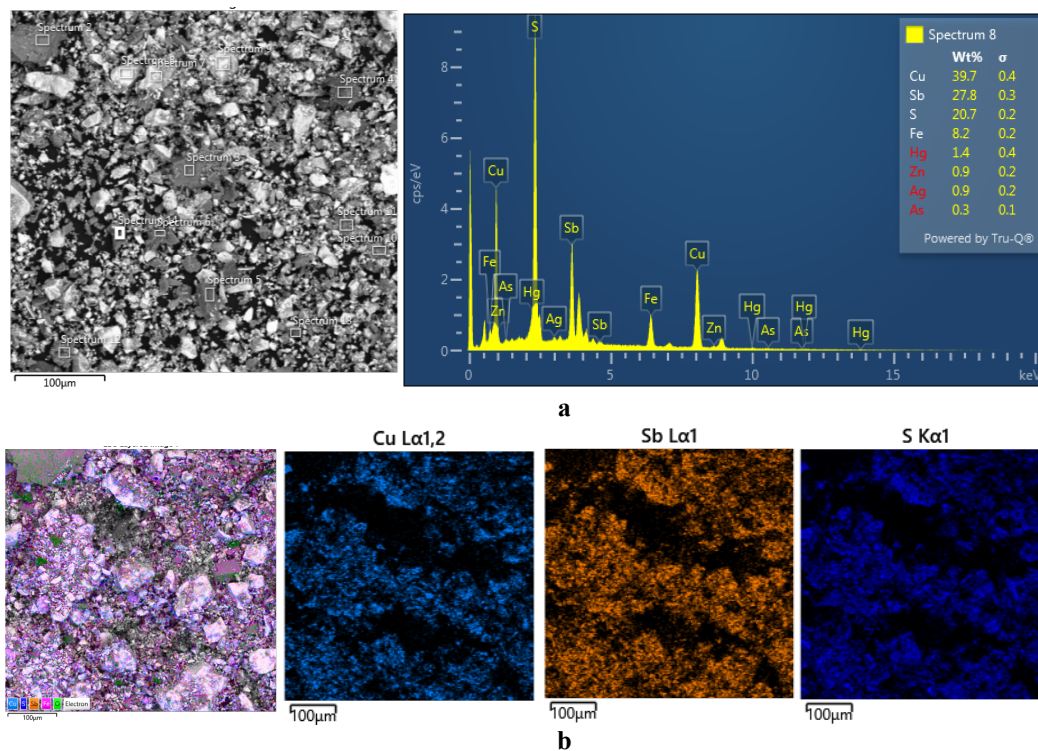


Fig. 1. Chemical composition (wt%) (a) and EDX mapping analysis (b) of the tetrahedrite concentrate

SEM-EDX analysis revealed significant changes in the surface morphology of tetrahedrite grains after bioleaching with *L. ferriphilum*. The initially smooth surface of the grains exhibited fracturing and the formation of alteration products post-bioleaching (Fig. 2, 3). The alteration crusts were heterogeneous and showed signs of hydration prior to SEM analysis, indicating substantial mineral dissolution during bioleaching. This alteration suggests a heterogeneous fluid-solid reaction coupled with bacterial oxidation.

The observed morphological changes can be attributed to the oxidative dissolution of the mineral matrix, where ferric iron acts as the primary oxidant. The presence of  $Fe^{3+}$  ions facilitates the breakdown of

the sulfide lattice, leading to the release of metal ions such as  $\text{Cu}^{2+}$  and  $\text{Sb}^{3+}$  into solution. Moreover, the fracturing and cracking of the mineral surface are indicative of a chemical attack by  $\text{Fe}^{3+}$ , coupled with the biological activity of *L. ferriphilum*. The combination of chemical and biological processes results in the enhanced dissolution of the mineral, as evidenced by the alteration products on the tetrahedrite surface.

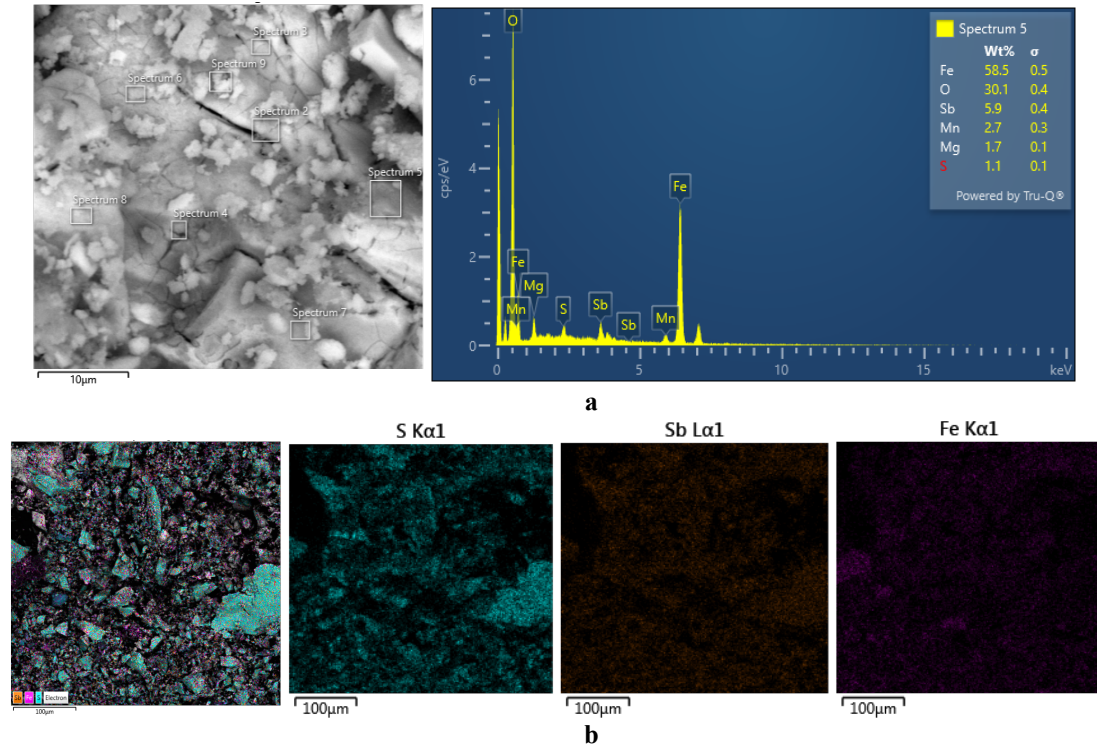


Fig. 2. Chemical composition of spectrum 5 (wt%) (a) and EDX mapping analysis (b) of the tetrahedrite concentrate surface after *L. ferriphilum* bioleaching

Post-bioleaching analysis indicated the extraction of Cu, Sb, S, As, Zn, and partial Ag into the leachate (data not shown). The iron-oxidizing activity of bacteria played a crucial role in maintaining high redox potential ( $\text{Fe}^{3+}/\text{Fe}^{2+}$  ratio) essential for the dissolution of sulfide minerals. The reaction of  $\text{Fe}^{3+}$  with the tetrahedrite surface emerged as the rate-determining step. Notably, antimony was partially immobilized as Sb(V) phases, as indicated by the probability of precipitation of secondary minerals such as tripuhyite ( $\text{FeSbO}_4$ ) and the formation of iron-antimony oxide (Eq. 2) [5, 6]:

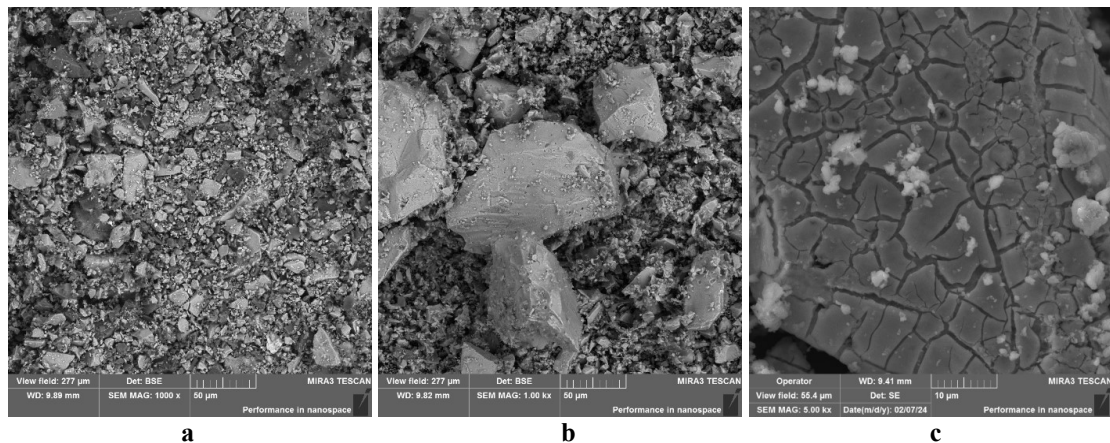
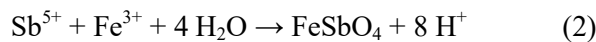


Fig. 3. Electron microscopy images (a) the tetrahedrite concentrate surface before bioleaching; (b, c) secondary electron images of the tetrahedrite concentrate surface after *L. ferriphilum* bioleaching

The observed effectiveness of *L. ferriphilum* in promoting tetrahedrite dissolution highlights the potential of bioleaching as a viable method for metal recovery from complex sulfide ores. This observation aligns with the findings of Kupka et al. (2023), where the kinetics of bacterial growth and iron oxidation were investigated, underscoring the role of temperature in bioleaching efficiency. The maintenance of high redox potential through bacterial oxidation ensures the continuous regeneration of  $\text{Fe}^{3+}$ , which is crucial for sustained mineral oxidation.

#### 4 Conclusions

Bioleaching of tetrahedrite using *L. ferriphilum* effectively alters the mineral's morphology, resulting in the selective extraction of valuable elements. The observed morphological changes, including surface fracturing and the formation of alteration crusts, indicate the dissolution of the mineral matrix. Elemental analysis revealed the mobilization of Cu, Sb, As, Zn, and Ag into the leachate, highlighting the potential of bioleaching as a tool for metal recovery.

#### Acknowledgements

Funded by the EU NextGenerationEU through the Recovery and Resilience Plan for Slovakia under the project No. 09I03-03-V04-00271.

#### References

- [1] Patrick, R.A.D., Hall, A.J. Silver substitution into synthetic zinc, cadmium, and iron tetrahedrites. *Mineralogical Magazine*, 47, 1983, p. 441-451.
- [2] Liu, H., Zeng, W., He, M., Lin, C., Ouyang, W., Liu, X. Occurrence, distribution, and migration of antimony in the Zijiang River around a superlarge antimony deposit zone. *Environmental Pollution*, 316, 2023, 120520.
- [3] Stančić, Z., Fiket, Ž., Vuger, A. Tin and Antimony as Soil Pollutants along Railway Lines & - A Case Study from North-Western Croatia. *Environments*, 9, 2022.
- [4] Kupka, D., Bártová, Z., Hagarová, L. Kinetics study comparing bacterial growth and iron oxidation kinetics over a range of temperatures 5-45 °C. *Hydrometallurgy*, 222, 2023, 106181.
- [5] Radková-Borčinová, A., Jamieson, H., Lalinská-Voleková, B., Majzlan, J., Števko, M., Chovan, M., Mineralogical controls on antimony and arsenic mobility during tetrahedrite-tennantite weathering at historic mine sites Špania Dolina-Piesky and Ľubietová-Svätodušná, Slovakia. *American Mineralogist*, 102, 2017, p. 1091-1100.
- [6] Rusínová, P., Kučerová, G., Voleková-Lalinská B., Mineralogical study of synthetic and natural tripuhite  $\text{FeSbO}_4$ . In International Symposium CEMC 2014, Masaryk University, Brno, p. 126-127.

## RESPONSE OF PATHOGENESIS RELATED PROTEINS TO COMBINED STRESS IN WHEAT

**Richard Hančinský<sup>a</sup>, Laura Žideková<sup>a</sup>, Monika Šutáková<sup>a</sup>, Pavol Hauptvogel<sup>b</sup>, Zuzana Gerši<sup>a</sup>,  
Ildikó Matušiková<sup>a</sup>**

<sup>a</sup> Faculty of Natural Sciences, University of St. Cyril and Methodius in Trnava,  
Námestie J. Herdu 2, 917 01 Trnava, Slovakia, richard.hancinsky@ucm.sk

<sup>b</sup> National Agricultural and Food Centre, Research Institute of Plant Production,  
Bratislavská cesta 122, 921 68 Piešťany, Slovakia

### Abstract

This study investigated the activity of pathogenesis-related (PR) proteins in wheat under cadmium-contaminated soil conditions for three different nitrogen regimes. The effects of cadmium and nitrogen supply treatment caused observable variation in both chitinase and  $\beta$ -1,3 glucanase protein activity. Results showed that wheat exhibited varying responses to cadmium stress depending on nitrogen availability. The findings suggest wheat growth-resistance trade-off strategies in presence of heavy metal stressor can be observed and further studied by focusing on selected PR proteins, and also that wheat's phytoremediation potential can be modulated by nitrogen management for remediating cadmium-contaminated sites.

**Keywords:** wheat, nitrogen, heavy metal, cadmium, PR-proteins, trade-off

### 1 Introduction

Pollution of the environment by anthropogenic activity is a worldwide problem that must be addressed not only through prevention but also by developing remediation strategies [1]. Soils polluted with heavy metals pose a health risk, as they can be absorbed by plants and thus enter the food chain, or they can be washed out of the soil and transferred to water sources [2]. As several approaches (physical, chemical, electrical, ex-situ) currently applied in remediation of metal polluted environment can themselves cause serious soil degradation [3], biological remediation methods (phytoremediation and bioremediation) are being increasingly preferred as a more sustainable alternative [4].

Phytoremediation removes toxic heavy metals from the soil by utilizing plants. It has several advantages over the classical methods: it is inexpensive, efficient, ecological, environmentally friendly, and suitable for use in large areas [5]. A number of hyperaccumulator plant species has been previously described [6] and are commonly recommended for phytoremediation programs, but some plants accumulating lower concentrations of heavy metal pollutants from soil are also getting some attention. Crop plants, as a consequence of long-term cultural use and selective breeding, have properties that are desired for in-situ application of phytoremediation programs, including low price, availability, consistent production of biomass, and an undemanding cultivation/harvesting process [7].

Wheat (*Triticum aestivum*) is one of principal grains together with maize and rice [8]. Even though global wheat production is not the largest among cereals, it is considered vitally important when it comes to use as human food source [9, 10]. Heavy metal uptake by wheat is mostly being explored in the scope of biofortification, aiming to improve nutritional values [11] focusing on beneficial effects of essential heavy metals. Focusing on non-essential highly toxic heavy metals in wheat is mainly important for prevention against contamination of an important food source [12, 13], but as mentioned before, could be also interesting for phytoremediation. It is known that crops are commonly subjected to agricultural practices which can reduce stress [14], including use of fertilizer, and thus influencing the growth-resistance trade-off balance by providing supplementary resources, which would also affect plant response other types of stress, including heavy metal stress and therefore affecting heavy metal uptake. Heavy metal resistance in plants is dependent on nutrients and energy utilization [15]. In case of combined stress, when nutrients are scarce, plant resistance can be dependent on resources necessary for plant growth, which means that soil nutrients can affect growth-resistance balance [16].

Previous studies found differences in Cd uptake, plant growth, and oxidative stress in wheat, depending on nitrogen supply [17]. In addition to parameters observed in this study, pathogenesis related proteins (PR proteins) were previously associated with heavy metal stress response by several crop



plants [18]. PR protein activity of chitinases and  $\beta$ -1,3 glucanases were also found to be responsive to nitrogen availability in wheat [19]. In this study we focused on PR protein activity in wheat under combined stress, caused by Nitrogen supply (deficiency and excess) and presence of  $\text{Cd}^{2+}$ .

## 2 Material and methods

### 2.1 Wheat plant cultivation

Wheat seeds (*Triticum aestivum* L.) were sterilized in 0.5 % sodium hypochlorite solution for 15 minutes and rinsed three times with distilled water. Seeds were then left to germinate for one week on moist sterile filter paper discs placed in petri dishes. Seven days old wheat seedlings were then transferred to hydroponic containers, each with 500 ml of modified Hoagland medium with different nitrogen supply conditions. Modified medium contained 0/7,5/35 mM  $\text{NH}_4\text{NO}_3$  (three different nitrogen conditions); 5 mM  $\text{K}_2\text{SO}_4$ ; 2 mM  $\text{CaCl}_2$ ; 2 mM  $\text{MgSO}_4$ ; 0.5 mM  $\text{Na}_2\text{SiO}_3$ ; 0.1 mM  $\text{KH}_2\text{PO}_4$ ; 50  $\mu\text{M}$   $\text{NaFe(III)EDTA}$ ; 50  $\mu\text{M}$   $\text{H}_3\text{BO}_3$ ; 5  $\mu\text{M}$   $\text{MnCl}_2$ ; 5  $\mu\text{M}$   $\text{ZnSO}_4$ ; 0.5  $\mu\text{M}$   $\text{CuSO}_4$ ; and 0.1  $\mu\text{M}$   $\text{Na}_2\text{MoO}_3$ .

After seven days of hydroponic cultivation, a subset of plants from each nitrogen condition group was subjected to the addition of 50  $\text{mg.l}^{-1}$   $\text{Cd}^{2+}$  in the form of  $\text{CdCl}_2$ . Plant samples for analysis were then collected two days after the addition of  $\text{CdCl}_2$  from both Cd treated and control plants grown in all three nitrogen supply conditions. Plants were grown in a cultivation chamber (KBWF 720, Binder) in controlled conditions throughout the experiment. Relative air humidity 60 %, temperature max. 24/18 °C, photoperiod 16/8 h, max. light intensity 11450 lx.

### 2.2 PR protein activity

Protein extract from plants was isolated according to Hurkman and Tanaku [20]. Each frozen plant tissue sample (~0.2 g) was homogenized and 320  $\mu\text{l}$  of solution buffer (0.1 M NaAc (pH 5.2) and 100 mM phenylmethylsulfonyl fluoride (PMSF)). After three centrifugation cycles (14000 g, 4 °C, 15 min), protein extracts were frozen using liquid nitrogen and stored at -80 °C until further processing. Concentrations of protein extracts was determined by measuring absorbance at 595 nm, using method by Bradford [21] using bovine serum albumin (Boehringer Mannheim – BSA) as a standard.

20  $\mu\text{g}$  of protein per sample was separated in polyacrylamide gels following the method of Laemmli et al. (1970). The 12.5 % (w/v) polyacrylamide gels contained 1 % (w/v) glycol chitin for chitinases and laminarin for  $\beta$ -1,3 glucanases. After electrophoresis, proteins were re-natured by washing the gels in 50 mM sodium acetate buffer (pH 5.2), 1 % Triton X-100 (v/v) for 24 h at room temperature in case of chitinases and in 0.5 M sodium acetate buffer (pH 5.2), 1 % Triton-X-100 (v/v) for 1 hour at 4 °C in case of glucanases. Gels were then washed in sterile water.

Chitinase activity gels were then incubated in for 2 hours at 37 °C, washed, and incubated in solution containing 10 mg Fluorescent Brightener 28 (Sigma); 50 ml 0.5 M Tris-HCl (pH 8.9) and 50 ml sterile water at room temperature for 15 minutes in dark. Chitinase activity was then detected under UV light.

Glucanase activity gels were incubated in 0.5 M sodium acetate (pH 5.2) for 1 hour at 37 °C and then placed in fixation solution (7 % (v/v) acetic acid and 20 % (v/v) methanol) for 5 minutes. After fixation, gel was washed and then boiled in 100 ml 1 M NaOH and 0.1 % tetrazolium chloride (TTC) until red bands indicating glucanase activity were visible (5-10 minutes). Gel was then placed in 7 % acetic acid solution to end the reaction. Glucanase activity was then detected by scanning the gel.

## 3 Results and discussion

Results of SDS-PAGE clearly revealed differences in PR protein activity for both  $\beta$ -1,3-glucanases and chitinases. Two clear protein fractions with chitinolytic activity were detected (Figure 1) with sizes of ~35 kDa and ~28 kDa. Both fractions showed sensitivity to nitrogen supply treatment and presence of Cd by exhibiting recognisable variation in activity. 35kDa fraction shows a clear observable variation between control and Cd treated plants, as well as between N treatments, while 28kDa fraction exhibited more subtle variation, which became apparent only after quantification (data not shown). Similar variable reactions were previously observed in wheat [19] for 35kDa chitinase fraction, but 28kDa fraction was not reported before in relation to heavy metal stress, but chitinases of similar size were documented in wheat as responsive to drought [22] and low temperatures [23].

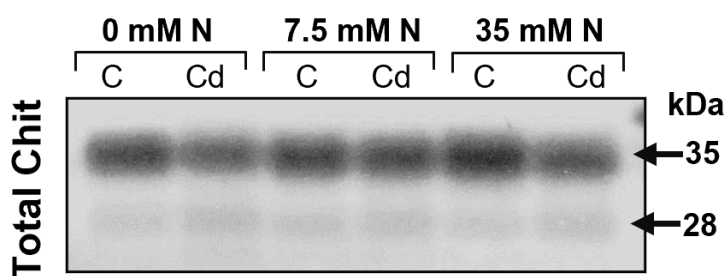


**Fig. 1. SDS PAGE chitinase activity photo**

0/7.5/35 mM Nitrogen supply groups are indicated above, each consisting of C (control) and Cd (50 mg l<sup>-1</sup> of Cd<sup>2+</sup> added in form of CdCl<sub>2</sub>); arrows indicate detected bands with respective size in kDa

Scan of SDS PAGE gel showing  $\beta$ -1,3 glucanase had two clear fractions with sizes of ~50kDa and ~30kDa (Figure 2). Both fractions showed variation between different nitrogen treatments as well as between control plants and plants grown in medium containing Cd. Variation of  $\beta$ -1,3 glucanase as a response to heavy metal stress was previously reported for other crop plants as well [24], supporting results obtained for wheat in this study.

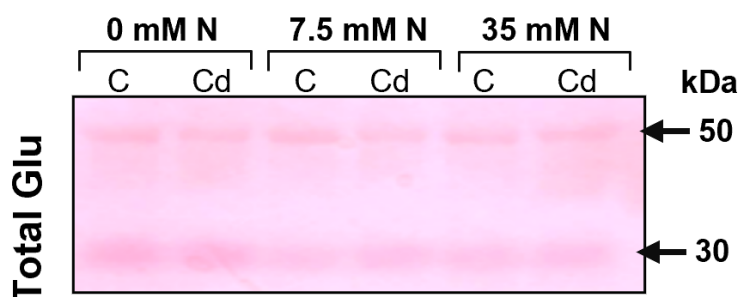


**Fig. 2. SDS PAGE  $\beta$ -1,3 glucanase activity scan**

0/7.5/35 mM Nitrogen supply groups are indicated above, each consisting of C (control) and Cd (50 mg l<sup>-1</sup> of Cd<sup>2+</sup> added in form of CdCl<sub>2</sub>); arrows indicate detected bands with respective size in kDa

Our results are in accordance with hypothesis by Zhang et al. [25] characterizing a signaling module which includes ethylene, jasmonate and low-affinity nitrate transporters (ET/JA/NRT). This module coordinates allocation of resources to address the trade-off between growth and adaptation to environmental stimuli. Given that ET/JA signaling also regulates many PR proteins [26], this model is likely responsible for the nitrate dependent activity of specific  $\beta$ -1,3 glucanases or chitinases on our experiment. We therefore conclude that selected PR-proteins can be used to further study growth resistance trade-off in wheat, as was previously suggested by Walters and Hiel [27].

#### 4 Conclusions

Quantification of individual isoforms of chitinases and  $\beta$ -1,3 glucanases based on obtained optical density of bands (OD data not shown) revealed considerable differences in their quantities between nitrogen supply treatment groups as well as between Cd treated plants and respective control groups. Changes in chitinase and  $\beta$ -1,3 glucanase activity between plants grown in optimal nitrogen supply conditions, and stressed plants in both nitrogen starvation and nitrogen excess conditions demonstrates the changes in energy consumption strategies dependent on availability of resources. Further there were also apparent changes in chitinase and  $\beta$ -1,3 glucanase activity in the presence of heavy metal stressor within all three nitrogen supply subsets of plants providing insight to wheat growth-resistance trade-off.

#### Acknowledgements

This work was supported by research grants APVV-15-0051 and APVV-21-0504. RH was supported by project from the Research Support Fund at the University of Ss. Cyril and Methodius in Trnava number FPPV-59-2024 (in frames of Early Stage Grant No. 09-i03-03-v05-00004, Recovery Plan scheme).

## References

- [1] RoyChowdhury, A., Datta, R., Sarkar, D. *Heavy Metal Pollution and Remediation*. In Green Chemistry: An Inclusive Approach. Elsevier, 2018, p. 359-373. ISBN 978-0-12-809270-5.
- [2] Ahmad, W., Alharthy, R.D., Zubair, M., Ahmed, M., Hameed, A., Sajjad, R. Toxic and heavy metals contamination assessment in soil and water to evaluate human health risk. *Scientific Reports*, 11, 2021, 17006.
- [3] Liu, L., Li, W., Song, W., Guo, M. Remediation techniques for heavy metal-contaminated soils: principles and applicability. *Science of The Total Environment*, 663, 2018, p.206-219.
- [4] Yan, A., Wang, Y., Tan, S.N., Mohd Yusof, M.L., Ghosh, S., Chen, Z. Phytoremediation: A Promising Approach for Revegetation of Heavy Metal-Polluted Land. *Frontiers in Plant Science*, 11, 2020, 359.
- [5] Thomas, G., Sheridan, C., Holm, P.E. A critical review of phytoremediation for acid mine drainage-impacted environments. *Science of The Total Environment*, 811, 2022, p. 1-13.
- [6] Reeves, R.D., Baker, A.J.M., Jaffré, T., Erskine, P.D., Echevarria, G., van der Ent, A. A global database for plants that hyperaccumulate metal and metalloid trace elements. *New Phytologist*, 218, 2018, p. 407-411.
- [7] De Bernardi, A., Casucci, C., Businelli, D., D'Amato, R., Beone, G.M., Fontanella, M.C., Vischetti, C. Phytoremediation Potential of Crop Plants in Countering Nickel Contamination in Carbonation Lime Coming from the Sugar Industry. *Plants*, 9 (5), 2020, 580.
- [8] Thudi, M., Palakurthi, R., Schnable, J.C., Chitikineni, A., Dreisigacker, S., Mace, E., Srivastava, R.K., Satyavathi, C.T., Odeny, D., Tiwari, V.K., Lam, H.M., Hong, Y.B., Singh, V.K., Li, G., Xu, Y., Chen, X., Kaila, S., Nguyen, H., Sicasankar, S., Jackson, S.A., Close, T.J., Shubo, W., Varshney, R.K. Genomic Resources in Plant Breeding for Sustainable Agriculture. *Journal of Plant Physiology*, 257 2021, 153351.
- [9] Langridge P. Wheat genomics and the ambitious targets for future wheat production. *Genome*, 56 (10), 2013, p. 545-547.
- [10] Igrejas, G., Branlard, G. *The Importance of Wheat*. In Wheat Quality for Improving Processing and Human Health. Springer International Publishing, 2020, p. 1-7. ISBN 978-3-030-34162-6.
- [11] Nie, Z., Zhao, P., Shi, H., Wang, Y., Qin, S., Liu, H. Nitrogen supply enhances zinc uptake and root-to-shoot translocation via up-regulating the expression of TaZIP3 and TaZIP7 in winter wheat (*Triticum aestivum*). *Plant and Soil*, 444, 2019, p.501-517.
- [12] Chaudri, A., McGrath, S., Gibbs, P., Chambers, B., Carlton-Smith, C., Godley, A., Bacon, J., Campbell, C., Aitken, M. Cadmium availability to wheat grain in soils treated with sewage sludge or metal salts. *Chemosphere*, 66, 2007, p. 1415-1423.
- [13] Gray, C.W., McLaren, R.G., Roberts, A.H.C. Cadmium concentrations in some New Zealand wheat grain. *New Zealand Journal of Crop and Horticultural Science*, 29 (2), 2001, p. 125-136.
- [14] Lemaire, G., Tang, L., Bélanger, G., Zhu, Y., Jeuffroy, M.H. Forward new paradigms for crop mineral nutrition and fertilization towards sustainable agriculture. *European Journal of Agronomy*, 125, 2021, 126248.
- [15] Portman, S.L., Kariyat, R.R., Johnston, M.A., Stephenson, A.G., Marden, J.H. Inbreeding compromises host plant defense gene expression and improves herbivore survival. *Plant signaling & behavior*, 10 (5), 2015, e998548.
- [16] Kruse, C., Jost, R., Lipschis, M., Kopp, B., Hartmann, M., Hell, R. Sulfur-enhanced defence: effects of sulfur metabolism, nitrogen supply, and pathogen lifestyle. *Plant biology*, 9 (5), 2007, p. 608-619.
- [17] Yotsova, E., Dobrikova, A., Stefanov, M., Misheva, S., Bardáčová, M., Matušíková, I., Žideková, L., Blehová, A., Apostolova, E. Effects of cadmium on two wheat cultivars depending on different nitrogen supply. *Plant Physiology and Biochemistry*, 155, 2020, p. 1428-1438.
- [18] Békésiová, B., Hraška, Š., Libantová, J., Moravčíková, J., Matušíková, I. Heavy-metal stress induced accumulation of chitinase isoforms in plants. *Molecular Biology Reports*, 35, 2008, p. 579-588.
- [19] Maglovski, M., Gregorová, Z., Rybanský, L., Mészáros, P., Moravčíková, J., Hauptvogel, P., Adamec, L., Matušíková, I. Nutrition supply affects the activity of pathogenesis-related  $\beta$ -1,3-glucanases and chitinases in wheat. *Plant Growth Regulation*, 81, 2017, p. 443-453.
- [20] Hurkman, W.J., Tanaka, C.K. Solubilization of plant membrane proteins for analysis by two-dimensional gel electrophoresis. *Plant physiology*, 81 (3), 1986, p. 802-806.



- [21] Bradford, M.M. A rapid and sensitive method for the quantitation of microgram quantities of protein utilizing the principle of protein-dye binding. *Analytical biochemistry*, 72, 1976, p. 248-254.
- [22] Gregorová, Z., Kováčik, J., Klejdus, B., Maglovski, M., Kuna, R., Hauptvogel, P., Matušíková, I. Drought-Induced Responses of Physiology, Metabolites, and PR Proteins in *Triticum aestivum*. *Journal of Agricultural and Food Chemistry*, 63 (37), 2015, p. 8125-8133.
- [23] Žur, I., Gołębiowska, G., Dubas, E., Golemić, E., Matušíková, I., Libantová, J., Moravčíková, J.  $\beta$ -1,3-glucanase and chitinase activities in winter triticales during cold hardening and subsequent infection by *Microdochium nivale*. *Biologia*, 68, 2013, p. 241-248.
- [24] Prišelová, B., Matušíková I. *Plant defense against heavy metals: the involvement of pathogenesis-related (PR) proteins*. In AWAAD, Amani S. - Kaushik, Geetanjali - Govil, J.N. Recent Progress in Medicinal Plant: mechanism and Action of Phytoconstituents. Studium Press LLC, 2011, p.179-205. ISBN 1-933699-21-3.
- [25] Zhang, G.B., Yi, H.Y., Gong, J.M. The Arabidopsis ethylene/jasmonic acid-NRT signaling module coordinates nitrate reallocation and the trade-off between growth and environmental adaptation. *Plant Cell*, 26 (10), 2014, p. 3984-3998.
- [26] Wu, H.J., Li, L., Zhang, F.X. The influence of interspecific interactions on Cd uptake by rice and wheat intercropping. *Review China Agricultural Science Technology*, 5, 2003, p. 43-47.
- [27] Walters, D., Heil, M. Costs and trade-offs associated with induced resistance. *Physiological and Molecular Plant Pathology*, 71 (1), 2007, p.3-17.



## POTENTIAL OF MYCORRHIZAL FUNGI IN THE EXTRACTION OF METALS FROM SOIL

**Pavol Hlubina<sup>a</sup>, Richard Hančinský<sup>a</sup>, Daniel Mihálik<sup>a,b</sup>, Pavol Hauptvogel<sup>b</sup>, René Hauptvogel<sup>b</sup>, Ildikó Matušiková<sup>a</sup>**

<sup>a</sup> Faculty of Natural Sciences, University of Ss. Cyril and Methodius in Trnava,  
Námestie J. Herdu 2, 917 01 Trnava, Slovakia,  
hlubinal@ucm.sk

<sup>b</sup> National Agricultural and Food Centre, Research Institute of Plant Production,  
Bratislavská cesta 122, 921 68 Piešťany, Slovakia,  
pavol.hauptvogel@nppc.sk

### Abstract

Within the four wheat varieties studied, we investigated the potential of using arbuscular mycorrhizal fungi as an aid to enhance the extraction of metals from the soil by agricultural crops. We focused on the interaction with Zn in the soil, as this element has a different spectrum of action ranging from essentiality to toxicity. Of the four varieties studied, PI264934 and Kirmizi Yazik best met the criteria for use in environmental biotechnology.

**Keywords:** arbuscular mycorrhizal fungi, remediation, zinc, soils

### 1 Introduction

Mycorrhizal fungi (AMF) represent an environmentally safe way to extract metals from polluted soil as part of environmental biotechnology. Their effect on enhancing remediation potential was investigated in the extraction of zinc (Zn) from soil. The model organisms were four wheat species.

There are now over 400 known plant species that can take up significantly higher concentrations of metals without showing signs of toxicity. We refer to such plants as hyperaccumulators. These include mainly species with low biomass, but more recently the focus has been on agricultural crops with high biomass and relatively high tolerance to metal toxicity. Indeed, heavy metals, organic contaminants, radionuclides, antibiotics and pesticides can be remediated using plants [1].

Microorganisms play an essential role in enhancing heavy metal phytoremediation [2, 3]. The scope for potential further research lies mainly in the determination of effective remediation resistance, as high concentrations of metals in soil can be toxic not only to plants but also to soil microorganisms, thereby interfering with their essential microbial activities, which also reduces soil fertility [4, 5].

In the context of soil-plant interaction, zinc is an exceptional micronutrient. Compared to other metals, it offers a spectrum of interactions and its impact ranges from essentiality to toxicity, depending on the amount and conditions [6-10].

In addition, the bioavailability of Zn is also significantly influenced by soil properties. Soils with low pH increase Zn solubility and uptake, while alkaline soils precipitate Zn, limiting its availability. Soil organic matter can bind Zn, reducing its immediate bioavailability, but slowly releases it over time [6, 11].

Arbuscular mycorrhizal fungi, primarily belonging to the phylum *Glomeromycota*, are mutualistic symbionts that form relationships with more than 70 % of plant species. They penetrate plant roots and form specialized structures called arbuscules in the cells of the root cortex [12]. AMFs increase the bioavailability of micronutrients such as Zn through several mechanisms. AMFs form an extensive hyphae network that increases the surface area for nutrient uptake outside the root zone. This network can make available nutrients that are otherwise unavailable to plant roots [13]. AMF absorb low-mobility mineral nutrients from the soil and transfer them to the plant with which they coexist in a symbiotic relationship. In return, the plant supplies the fungi with carbon compounds derived from photosynthesis [14]. AMF can also influence the expression of plant genes involved in nutrient transport. For example, genes responsible for Zn uptake are up-regulated in mycorrhizal roots, facilitating higher uptake of Zn from the soil and its subsequent translocation to different parts of the plant [15]. AMFs also improve soil structure by binding soil particles into aggregates, improving water retention and aeration, which in turn promotes better root growth and nutrient uptake [16].

## 2 Material and methods

### 2.1 Experimental material

As experimental material we used wheat varieties provided by the Gene Bank of Slovakia - *Triticum turgidum* subsp. Durum, varieties PI264934, PI264936 and Kirmizi Yazik. In pot experiments we used the soil additive SYMBIVIT® - MYcorrhizal Fungi, PRODUCT CODE: 99902241. Symbivit contains natural clay carriers, reproductive particles of 6 species of mycorrhizal fungi in the form of spores and parts of colonized plant roots, bioadditives supporting the development of mycorrhizal symbiosis (natural humates, seaweed extracts, ground rocks) powdered biodegradable polyacrylamide gel.

We planted 3 grains per variety in pots with 3 l of commercially purchased potting medium. For each variety, we planted 3 replicates of each of the following 4 variants: control (without any additive), 45 g SYMBIVIT® (variant with mycorrhizal fungi, AMH), 75 mg Zn<sup>2+</sup>/kg soil (variant with Zn in the form of sulfate), variant AMH+Zn.

Plants were cultivated in the culture room between April and May 2023. The set of plants of these varieties was cultivated for 120 days from planting to the ear maturity stage.

Leaf pigment content was determined using the procedure of Lichtenthaler and Wellburn (1983). The absorbance of the supernatant was measured at three different wavelengths of light (663 nm, 646 nm, 470 nm) on a Varian Cary 50 Conc UV-VIS spectrophotometer.

### 2.2 Zn content

Grain minerals as well as soil samples were analysed for Zn content in the accredited LABEKO Ecoanalytical Laboratory. For Zn content determination, we ground the grains of the experimental plants (TissueLyser LT) with a steel ball for 90 s and at maximum frequency (30 Hz). Subsequently, 200 mg of homogenized material was mineralized with concentrated HNO<sub>3</sub> by microwave digestion in closed cartridges in two steps. In the first step, mineralization was carried out at 180 °C for 30 min at a pressure of 20 bar 41, followed by 180 °C for 15 min. The mineralizate was quantitatively removed, acidified with HNO<sub>3</sub> solution and made up to 10 ml with deionized water.

### 2.3 Statistics and indices

Statistical analysis ANOVA and post-hoc Tukey's test and graph generation were performed in RStudio using the scientific libraries MultcompView, Agricolae and ggplot.

Finally, to compare a potential of four varieties of wheat for using in environmental biotechnology, we calculated four indices.

Zinc Resilience Index (ZRI) indicates how well a variety performs under zinc-deficient conditions compared to zinc-sufficient conditions, and is calculated as (Zn level in grain for control) / (Zn level in grain for Zinc treatment).

AMF Cooperation Index (ACI) was calculated to estimate how much a variety benefits from AMF in terms of zinc uptake as (Zn level in grain with AMF - Zn level in grain without AMF) / (Zn level in grain without AMF).

Biofortification Suitability Index (BSI) was calculated as (Zn level in grain for variety) / (Average Zn level in grain across all varieties) to measure how suitable a variety is for zinc biofortification, considering both yield and zinc content. Overall Performance Index (OPI) was expressed as a composite measure of the other indices to rank overall variety performance as average value of (ZRI + ACI + BSI).

## 3 Results and discussion

Wheat cultivars were tested for ability to accumulate Zn in grains. Addition of AMF to soil was expected to enhance plant growth and/or Zn transfer to grains. Plants of cultivar PI264934 had the tallest stature, while cultivars Kirmizi Yazik and IS Durablank had comparable stature. We did not observe a statistically significant change due to the effect of treatments, but AMF showed a tendency to promote growth in all cultivars, except for Kirmizi Yazik.

For selected cultivars, we determined the contents of photosynthetic pigments as indicators of tolerance to applied treatments. For the cultivars PI264936 and IS Durablank, we observed an increase in chlorophyll A, chlorophyll B and carotenoids when growing in the presence of AMH in the soil substrate, indicating mobilization of nutrients from the soil. As a result of zinc fertilizer top dressing in varieties PI264934 and PI264936, there was a decrease in photosynthetic pigments content, on the contrary, we observed a significant increase in varieties Kirmizi Yazik and IS Durablank as hormesis effect. The ratio of

chlorophylls A and B as an indicator of photosynthetic antennae maintenance [17] was significantly higher only in cultivar PI264934 after Zn application, unchanged in cultivar PI264936 and lower in cultivars Kirmizi Yazik and IS Durablank. From the results, we conclude that Kirmizi Yazik and IS Durablank cultivars are more tolerant to Zn than PI264934, PI264936.

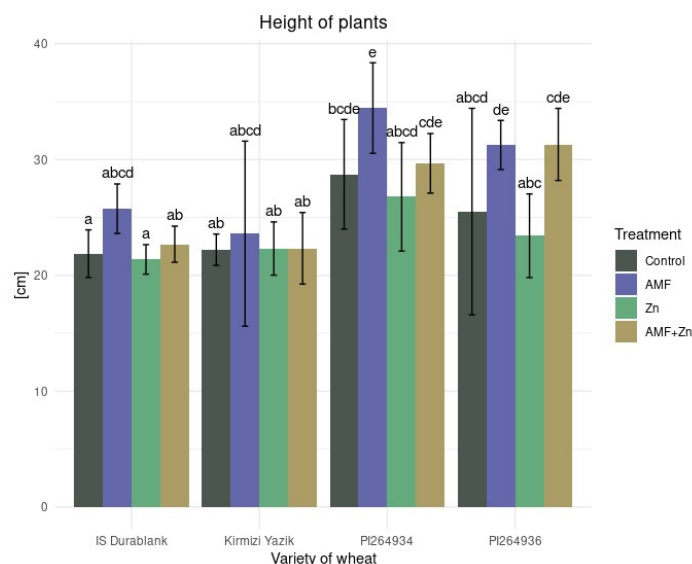


**Fig. 1. Height of experimental plants of four cultivars - cultivar PI264934, PI264936, Kirmizi Yazik and IS Durablank**  
Data represent mean values  $\pm$  SD (n=3)

For a given set of experimental plants, we also determined the corresponding Zn contents in grains (Table 1). The highest content in the control treatments was determined for the cultivar Kirmizi Yazik, the lowest for IS Durablank. The presence of AMH in the soil substrate after watering with Zn solution slightly contributed to Zn transport into the grains of cultivars PI264934 and PI264936, but not for the other two cultivars.

**Table 1. Grain Zn content for the experimental wheat varieties**

Wheat	Control	+AMF	+ Zn	+ AMF + Zn
<b>PI264934</b>	46.00	42.50	70.00	73.75
<b>PI264936</b>	61.25	48.75	82.5	83.75
<b>Kirmizi Yazik</b>	58.00	60.00	85.00	77.50
<b>IS Durablank</b>	50.00	42.50	75.00	60.00

The addition of AMF to the soil in combination with Zn top dressing had a synergistic effect and caused a significant increase in Zn content compared to the other experimental treatments in PI264934 or PI264936. Several studies have already shown that AMFs increase Zn concentration in soil and grains [13, 18], even protecting plants from excessive Zn accumulation at high Zn content in soil [19].

The Zn content in wheat grain is 31.84 mg/kg globally and varies among continents with an average of 25.10 mg/kg in Europe, 29.00 mg/kg in Africa, 33.63 mg/kg in Asia and 33.91 mg/kg in North America [20]. In our experiments, the addition of AMH and nutrient dressing resulted in Zn levels in wheat grains of approximately 50 mg/kg, with the Kirmizi Yazik variety accumulating the most Zn in the grains.

AMFs can modulate the ability of plants to grow in soils with higher metal content and at the same time take up Zn, making plants potential candidates for remediation and use in environmental biotechnology even in lower quality soils. Among the tested varieties, we evaluated the overall performance index, which yielded a ranking of the tested wheats for use in environmental biotechnology for metal (Zn) uptake from soil. The overall ranking shows that PI264934 and Kirmizi Yazik are the most suitable for use in environmental biotechnology among the varieties tested.

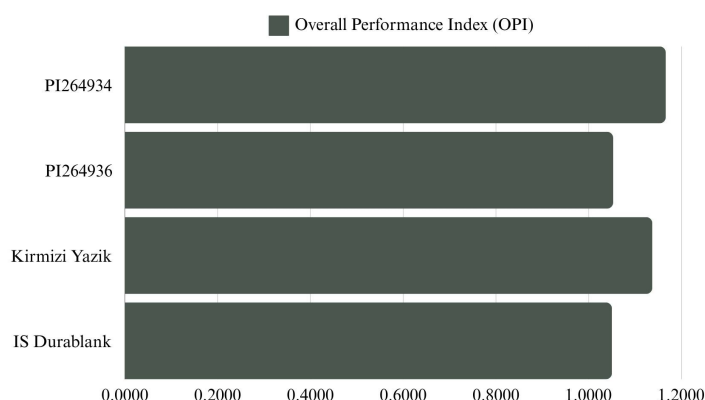


**Fig. 2. Comparison of indices for the potential use of the investigated varieties in environmental biotechnology for the extraction of metals from soil under the action of AMF**

#### 4 Conclusions

We studied the effect of AMF on Zn accumulation from soil on model organisms, four wheat varieties. Based on a comparison of the effects of different experimental treatments, PI264934 and Kirmizi Yazik showed the greatest potential for use in environmental biotechnology.

#### Acknowledgements

The work was carried out within the project APVV-21-0504.

#### References

- [1] Kafle, A., Timilsina, A., Gautam, A., Adhikari, K., Bhattarai, A., Aryal, N. Phytoremediation: Mechanisms, plant selection and enhancement by natural and synthetic agents. *Environmental Advances*, 8, 2022, p. 100203, doi: 10.1016/j.envadv.2022.100203.
- [2] Montreemuk, J., Stewart, T.N., Prapagdee, B. Bacterial-assisted phytoremediation of heavy metals: Concepts, current knowledge, and future directions. *Environmental Technology & Innovation*, 33, 2024, p. 103488, doi: 10.1016/j.eti.2023.103488.
- [3] van der Ent, A., Baker, A.J.M., Reeves, R.D., Pollard, A.J., Schat, H. Hyperaccumulators of metal and metalloids trace elements: Facts and fiction. *Plant and Soils*, 362 (1-2), 2013, p. 319-334, doi: 10.1007/s11104-012-1287-3.
- [4] Acar, Y.B., Alshawabkeh, A.N. Principles of electrokinetic remediation. *Environmental Science & Technology*, 27 (13), 1993, p. 2638-2647, doi: 10.1021/es00049a002.
- [5] Beesley, L., Moreno-Jiménez, E., Gomez-Eyles, J.E., Harris, E., Robinson, B., Sizmur, T. A review of biochars' potential role in the remediation, revegetation and restoration of contaminated soils. *Environmental Pollution*, 159 (12), 2011, p. 3269-3282, doi: 10.1016/j.envpol.2011.07.023.
- [6] Fageria, N.K., Baligar, V.C., Clark, R.B. Micronutrients in Crop Production. *Advances in Agronomy*, 77, 2002, p. 185-268, doi: 10.1016/S0065-2113(02)77015-6.
- [7] He, Z.L., Yang, X.E., Stoffella, P.J. Trace elements in agroecosystems and impacts on the environment. *Journal of Trace Elements in Medicine and Biology*, 19 (2-3), 2005, p. 125-140, doi: 10.1016/j.jtemb.2005.02.010.
- [8] Alloway, B.J. Soil factors associated with zinc deficiency in crops and humans. *Environmental Geochemistry and Health*, 31 (5), 2009, p. 537-548, doi: 10.1007/s10653-009-9255-4.
- [9] Hänsch, R., Mendel, R.R. Physiological functions of mineral micronutrients (Cu, Zn, Mn, Fe, Ni, Mo, B, Cl). *Current Opinion in Plant Biology*, 12 (3), 2009, p. 259-266, doi: 10.1016/j.pbi.2009.05.006.
- [10] White, P.J., Brown, P.H. Plant nutrition for sustainable development and global health. *Annals of Botany*, 105 (7), 2010, p. 1073-1080, doi: 10.1093/aob/mcq085.
- [11] Ma, X., Luo, W., Li, J., Wu, F. Arbuscular mycorrhizal fungi increase both concentrations and bioavailability of Zn in wheat (*Triticum aestivum* L) grain on Zn-spiked soils. *Applied Soil Ecology*, 135, 2019, p. 91-97, doi: 10.1016/j.apsoil.2018.11.007.

- [12] Tisserant, E., et al. Genome of an arbuscular mycorrhizal fungus provides insight into the oldest plant symbiosis. *Proceedings of the National Academy of Sciences of the U.S.A.*, 110 (50), 2013, p. 20117-20122, doi: 10.1073/pnas.1313452110.
- [13] Coccina, A., Cavagnaro, T.R., Pellegrino, E., Ercoli, L., McLaughlin, M.J. Watts-Williams, S.J. The mycorrhizal pathway of zinc uptake contributes to zinc accumulation in barley and wheat grain. *BMC Plant Biology*, 19 (1), 2019, p. 133, doi: 10.1186/s12870-019-1741-y.
- [14] Founoune-Mboupp, H., Diallo, B., Adigoun, R.F.R., Kane, A., Fall, A.F. Contribution of arbuscular mycorrhizal fungi to the bioavailability of micronutrients (iron and zinc) in millet accessions. *Frontiers in Plant Science*, 15, 2024, doi: 10.3389/fpls.2024.1364469.
- [15] Tamayo, E., Gómez-Gallego, T., Azcón-Aguilar, C., Ferrol, N. Genome-wide analysis of copper, iron and zinc transporters in the arbuscular mycorrhizal fungus *Rhizophagus irregularis*. *Frontiers in Plant Science*, 5, 2014, doi: 10.3389/fpls.2014.00547.
- [16] Rillig, M.C., Mummey, D.L. Mycorrhizas and soil structure. *New Phytologist*, 171 (1), 2006, p. 41-53, doi: 10.1111/j.1469-8137.2006.01750.x.
- [17] Lichtenthaler, H.K. Chlorophylls and Carotenoids: Pigments of Photosynthetic Biomembranes. *Methods in Enzymology*, 148, 1987, p. 350-382, doi: 10.1016/0076-6879(87)48036-1.
- [18] Li, J., Awasthi, M.K., Xing, W., Liu, R., Bao, H. Wang, X., Wang, J., Wu, F. Arbuscular mycorrhizal fungi increase the bioavailability and wheat (*Triticum aestivum* L.) uptake of selenium in soil. *Industrial Crops and Products*, 150, 2020, doi: 10.1016/j.indcrop.2020.112383.
- [19] Nguyen, T.D., Cavagnaro, T.R., Watts-Williams, S.J. The effects of soil phosphorus and zinc availability on plant responses to mycorrhizal fungi: a physiological and molecular assessment. *Scientific Reports*, 9 (1), 2019, p. 14880, doi: 10.1038/s41598-019-51369-5.
- [20] Wang, M., Kong, F., Liu, R., Fan, Q., Zhang, X. Zinc in Wheat Grain, Processing, and Food. *Frontiers in Nutrition*, 7, 2020, p. 124, doi: 10.3389/fnut.2020.00124.





## BIOLEACHING OF POTENTIALLY TOXIC ELEMENTS FROM CONTAMINATED GEOMATERIALS OF FORMER MINING SITE MEDZIBROD

Hana Horváthová<sup>a,b</sup>, Lubomír Jurkovič<sup>a</sup>, Tomáš Faragó<sup>a</sup>, Michaela Marníková<sup>a</sup>

<sup>a</sup> Comenius University, Faculty of Natural Sciences, Department of Geochemistry, Ilkovičova 6, 842 15 Bratislava, hana.horvathova@uniba.sk

<sup>b</sup> The Centre of Environmental Services, Ltd., Kuttlikova 17, 850 52 Bratislava

### Abstract

This study addresses the bioleaching of the potentially toxic elements (PTEs) arsenic (As) and antimony (Sb) from the former mining site Medzibrod (Slovakia) employing three combinations of supported bioremediation approaches – biostimulation of indigenous microflora of the mine soil with nutrients; and bioaugmentation of the mine soil with specialized bacteria *Cupriavidus oxalaticus*. The aim was to select the most suitable approach for PTE bioleaching based on its overall effectivity, and monitoring the process conditions to envisage the mechanism of releasing the PTEs from the solid material. The methods for bioleaching of PTEs from two mine soils consisted of adding nutrient-rich tryptic soy broth (TSB), and/or *C. oxalaticus* strain. Within the bioleaching process, pH, redox potential, concentration of microorganisms, and mine soil toxicity were measured. Experimental methods led to a significant reduction of As content in sludge material by 22.5 % to 30 % within 28 days, while a 6 % reduction in Sb content was achieved. Although seemingly modest, the removal of 1.3 g of antimony is a promising basis for future experiments, emphasizing the potential of bioremediation in addressing the PTE contamination. The results confirmed the potential of microorganisms in the treatment of highly contaminated mine soils, opening the possibility of the further recovery of PTEs.

**Keywords:** antimony, arsenic, bioleaching, *Cupriavidus oxalaticus*, mine soils

### 1 Introduction

Mining activities significantly impacted the economic and societal development in many countries. The territory of Slovakia is well known for its mineral wealth, which contributed to the development of several industrial areas. However, the consequences of its exploitation and processing on the environment are becoming more apparent, necessitating the implementation of solutions to eliminate these environmental burdens. Various PTEs are commonly found in the Earth's crust as natural geological formations. This geological background significantly affects the geochemical composition of the site, which is crucial for assessing threshold values for certain elements, such as PTEs [1]. However, elevated concentrations of these elements in the lithosphere are caused by anthropogenic activities, such as mining, which pose substantial risks to human populations and ecosystems already at low concentrations [2]. These elements fall under the purview of specific European Union regulations designed to mitigate risks associated with their usage [3, 4].

The significance of the PTEs lies in their versatile physical and chemical properties, which predetermine them for many industrial applications. They are irreplaceable e.g. in the electronic industry, metallurgy, digital technologies, robotics, and the defense industry. However, despite their unique properties, they are known also for their carcinogenicity, mutagenicity, and reproductive toxicity [2-4]. Since the occurrence of PTEs in various ecosystems is irreversible, it is necessary to focus either on the immobilization and preservation of the PTEs to avoid their release into the environment [5] respecting the physicochemical conditions of the given area or, on the contrary, focus on the enhanced mobilization of PTEs, resulting in the reduction of the contaminant load of the mine soil and obtaining of the raw material suitable for their recovery [4].

It is well known, that microorganisms use to inhabit each environment, not excluding the materials with a high load of contamination. Regardless of whether the contamination is organic or inorganic, the microorganisms, especially bacteria, can adapt and activate the „survival mechanisms“ which include the evolution of several metal resistance mechanisms, such as extra- and intracellular sequestration, exclusion by permeability barriers, enzymatic detoxification, reduction in sensitivity of cellular targets, and efflux pumps. These resistance mechanisms are the basis for the use of microorganisms in bioremediation approaches. Resistance systems are usually carried by plasmids or transposons and can be very effectively transferred to other community members [6]. The experimental approaches for bioleaching of PTEs presented in the paper are based on biostimulation of indigenous microflora by tryptic soy broth (TSB), bioaugmentation of the

mine soil by the bacteria *Cupriavidus oxalaticus*, and their combination. The solution of nutrient-rich TSB can re-activate the dormant-stage indigenous microorganisms and boost their metabolism so that they will activate their above-mentioned mechanisms for coping with the presence of PTEs. The *C. oxalaticus* strain is well known for its widespread use in bioleaching – it is resistant to PTEs and produces compounds effective in the mobilization of As and Sb. Moreover, it is a part of the indigenous microflora of mine soils [4]. Bioleaching belongs to economically advantageous green technologies which can become an add-on or complete alternative to the physicochemical methods for metal removal/recovery. This study aims to find a bioleaching approach with the highest performance and easiest possible implementation, with the potential to scale up to large volumes of substrates and with continuity with other industrial streams.

### 1.1 Deposit Medzibrod

The abandoned Sb-deposit Medzibrod is located in the north of central Slovakia, in Ďumbier Tatras - Močiar valley. Initially, it was a source of gold bound to pyrite-arsenopyrite ore, later antimonite. The production peak was achieved in the period from 1941 - 1945, when 9000 t of Sb ore was mined annually [7]. The entire site is composed of metamorphosed phyllites and green shales. Parent rock consists mainly of stibnite and pyrite. Mineralization occurs in lenses and veins. The deposit is associated with a complex of intensely metamorphosed rocks. Geochemically, elements are bound in mineralogical fractions of rocks, and under low pH values and reducing conditions, potential toxic pollutants are released in the form of cations. The ore formation exhibits a transitional type between Sb and Pb-Zn mineralization [8].

## 2 Material and methods

### 2.1 Sampling

The mine soil is a fine, clayey, waterlogged substance. Individual soil samples were collected using a soil auger from different soil horizons (M4A - pH 5.53, depth of sampling 42 cm, M4B - pH 6.2, depth of sampling 90 cm). The samples were air-dried and sieved to an analytical size (2 mm). Due to the testing of various experimental approaches, part of the mine soil samples was sterilized in an autoclave (120 kPa, 120 °C, 20 min) to prevent the influence of indigenous microflora. Further details of applied experimental approaches can be found in Table 1.

**Table 1. Summary of the experimental approaches**

Sample	Labeling	No. of replicates	Description	Purpose
<b>CONTROLS</b>				
Abiotic control	ABC	3	Sterilized mine soil + water	Assessment of the potential water leachability of PTEs.
Biotic control	BC	3	Non-sterilized mine soil + water	Monitoring of the impact of indigenous microflora from the substrate to PTE leaching.
<b>EXPERIMENTAL APPROACH (EA)</b>				
Biostimulation	EA1	3	Non-sterilized mine soil + TSB	Rehydration and nutrition of indigenous microflora of the substrate.
Biostimulation & bioaugmentation I.	EA2	3	Sterilized mine soil + TSB + <i>C. oxalaticus</i>	Introduction of specialized strain with bioleaching capability and its stimulation by the nutrient-rich medium.
Biostimulation & bioaugmentation II.	EA3	3	Non-sterilized mine soil + TSB + <i>C. oxalaticus</i>	Introduction of specialized strain with bioleaching capability and stimulation of both introduced strain and indigenous microflora of non-sterile sediment by nutrient-rich medium.

### 2.2 Preparation of the bacterial inocula

The bacterial strain *Cupriavidus oxalaticus* CCM 7669 was obtained from the Czech Collection of Microorganisms (CCM) in lyophilized form. The strain was revitalized according to the recommended protocol, in Tryptic Soy Broth (TSB). For obtaining the application inoculum, *C. oxalaticus* was aseptically subcultured to the pre-prepared sterile liquid TSB medium and cultivated on a rotary shaker (100 rpm) in  $t_{lab}$  and dark. For bioaugmentation, 10 ml of the inoculum was applied to the flasks.

### 2.3 Bioleaching experiments

The experiments were conducted in 250 ml Erlenmeyer flasks with 20 g of M4A or M4B mine soil. The mine soil was mixed with 100 ml of pre-sterilized medium (either distilled water or TSB, depending on the experimental approach described in Tab. 1). The leaching lasted for 28 days at  $t_{lab}$  with occasional shaking. At regular intervals, the physicochemical properties of the reaction mixture were measured (pH with Mettler Toledo SevenCompact™ S220; redox potential with Elmetron CPC-401 instrument). After 28 days, the leachate was separated from the solid fraction using centrifugation and filtration. Colony-forming unit (CFU) determination in the sample was performed aseptically in an inoculation box. A 100  $\mu$ l of sample was taken from the flask, suitably diluted tenfold in microcentrifuge tubes, and spread out to pre-prepared sterile solid TSB in Petri dishes. Analyses of the PTMs content were conducted at the accredited laboratory EL Ltd. (Spišská Nová Ves) using the AAS-F, AAS-HG, and AES-ICP methods. A seed germination test was performed on white mustard seeds *Sinapsis alba* to determine the toxic properties of contaminating substances on higher plant representatives. Fifteen seeds of *S. alba* were applied to the moisturized mine soil. After 72 h cultivation in  $t_{lab}$  and dark, the length of roots was measured and the root growth inhibition percentage was calculated according to Equation 1,

$$I_{\mu} = \frac{(L_c - L_s) \cdot 100 \%}{L_c} \quad (1)$$

where  $I_{\mu}$  represents the root growth inhibition,  $L_c$  arithmetic average of the root length in control (distilled water), and  $L_s$  arithmetic average of the root length in the sample.

### 3 Results and discussion

The experiments were focused on the bioleaching of PTEs, especially As and Sb from the mine soil sourced from the Medzibrod site with extensive mining history. According to previous investigations of the site, in Medzibrod mine soil, As and Sb occur in oxidized form, adsorbed (chemically bounded) onto secondary formed iron oxides and oxyhydroxides, which were formed in the tailing pond by crystallization from the pore waters [7]. Three bioleaching approaches based on biostimulation of the indigenous microflora by nutrients applied as TSB; and bioaugmentation of the mine soil by *C. oxalaticus* strain were employed. A detailed description of the experimental approaches can be found in Table 1. The initial analysis was the determination of the concentrations of PTEs in non-treated mine soils, which are considered input concentrations for assessing the performance of applied approaches. It can be observed that the elements As and Sb are the only ones exceeding the limit concentrations according to the Directive of the Ministry of Environment of the Slovak Republic No. 1/2015-7 [9]. The Directive defines indication criterion (ID), exceeding of which gives an obligation to monitor the contamination. If the concentration of a parameter is higher than the intervention criterion (IT), remediation is mandatory. Arsenic concentrations in the mine soil exceeded the IT criterion by 1.5 to 2.7 times, while Sb concentrations were up to 230 to 300 times higher (Table 2). In the further processing of the results, the focus was put on As and Sb.

**Table 2. Initial concentrations of selected elements in mine soils**

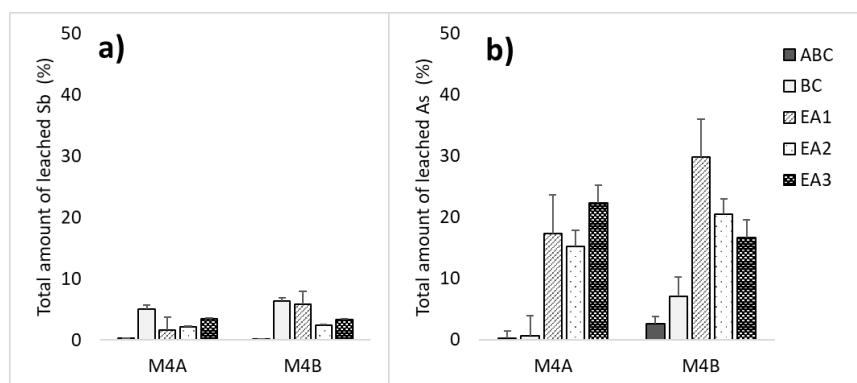
Parameter	Unit	M4A	M4B	Indication criterion (ID)	Intervention criterion (IT)
Cd	mg.kg <sup>-1</sup> dry matter	<0.2	<0.2	10	30
Ni		19.29	4.39	180	500
Pb		36.2	33.35	250	800
Sb		<b>18 649</b>	<b>24 151</b>	25	80
Zn		62	66	1 500	5 000
As		<b>212</b>	<b>373</b>	65	140

Table 3 summarizes the post-treatment concentrations of As and Sb in the mine soil. In each experimental approach, a decrease in the concentration of As and Sb was recorded, indicating the activity of indigenous microorganisms either individually or simultaneously with the introduced strain *C. oxalaticus*. The highest effectivity of Sb release – 6 % was achieved by the indigenous microflora, which was reactivated by water (BC) (Figure 1). Given the high initial concentration of Sb, 21 400 mg.kg<sup>-1</sup> (average of

M4A and M4B), this achievement is promising, as it implies the leaching of 1.3 g of Sb from 1 kg of dry mine soil. The results indicate that compared to Sb, As exhibited greater biological leachability in both mine soils. The same phenomenon was observed also in our previous study [4], as well as in Čerňanský et al. [10]. They obtained 29.2 % release of As and 13.6 % release of Sb from the impoundment material by *Aspergillus niger* when 1 g of sample was used. With the increasing amount of sample (10 g), the total concentration of released Sb remained the same, however, the concentration of leached As decreased to 6.7 % on average. It indicates that the weight of the substrate could influence the bioleaching effectivity. The most proven approach was EA1, the biostimulation of indigenous microflora with TSB. The bioleaching performance was 17 % in M4A and 30 % in M4B mine soil. As for arsenic, comparable bioleaching effectivity was achieved also by applying EA2 and EA3, combined approaches based on the introduction of *C. oxalaticus* strain. As confirmed previously, this strain was identified in the indigenous microflora of mine soil with a high load of As and Sb, therefore is adapted and equipped by mechanisms for the elimination of PTEs [4]. However, taking into account the follow-up applications, it is more advantageous to focus on approaches that do not require the production of bacterial inocula.

**Table 3. Post-treatment concentrations of As and Sb in mine soils**

	M4A		M4B	
	Sb	As	Sb	As
	mg.kg <sup>-1</sup> of dry matter		mg.kg <sup>-1</sup> of dry matter	
<b>Analytical control</b>	18 649	212	24 151	373
<b>ABC</b>	18 662	214	24 120	363
<b>BC</b>	17 590	211	22 625	347
<b>EA1</b>	18 157	173	22 740	262
<b>EA2</b>	18 059	177	23 565	297
<b>EA3</b>	17 799	162	23 343	311



**Fig. 1. Effectivity of Sb (a) and As (b) bioleaching**

In addition to determining the bioleaching capability, the focus was also put on outlining the potential mechanism of bioleaching. This was allowed by the measurement of pH, redox potential, course of the microbial concentration, and post-treatment toxicity. The pattern of PTE release from the substrate structure depends on the type of contamination, geochemical composition of the substrate, prevalent physicochemical conditions, composition of indigenous microflora, as well as on the activity of introduced microorganisms. The measurements shown in Table 4 were performed for M4A mine soil sample. Generally, the initial pH values were slightly acidic to neutral. For both abiotic and biotic controls, these values remained at a similar level throughout the 28-day-long bioleaching. A change occurred in all experimental approaches (EA1 – EA3), where the pH values slowly rose to slightly basic levels (approx. 8.7). Similar trend was observed in our previous study [4] where an increase of pH was also determined during the bioleaching of mine soil by activation of indigenous microflora by nutrient-rich medium SAB. Li et al. [5] observed the increase in pH while performing the bioprecipitation of Cd<sup>2+</sup> by the *Cupriavidus* sp. strain Cd02. It indicates, that indigenous strains, as well as *C. oxalaticus* could produce either substances, that increase the pH directly (e.g. lime) [5], or the pH increase can be the consequence of the dissolving of carbonates and sulphates, which can be found

in significant quantities in the mine soil. This dissolving might be a consequence of acid production (organic or sulphuric) by microorganisms, as the solid substrate does not produce active acidity. The acidity produced by the decomposition of sulphides (or microorganisms) is immediately neutralized by carbonates, which can result in a pH increase [7]. As stated by Li et al. [5], at higher pH, ligands (phosphate, carboxyl, amino group) are exposed on the bacterial cell surface, causing more negative charges, which support the electrostatically-driven biosorption of PTEs with a positive charge on their surface.

**Table 4. Initial and post-treatment physicochemical and biological properties of the reaction mixture**

M4A mine soil sample	pH		Redox potential (mV)		Concentration of microorganisms ( $\cdot 10^4$ CFU.ml <sup>-1</sup> )		I <sub>μ</sub> (%)
	Day 1	Day 28	Day 1	Day 28	Day 1	Day 28	Day 28
AC	6.51	5.75	214	142	1	15	-23.26
BC	6.28	6.30	223	21	10	120	-68.42
EA1	7.15	8.73	73	-298	100 000	12 435 000	100
EA2	7.11	8.79	12	-85	103 000 000	22 150	100
EA3	7.17	8.86	35	-126	734 724 675	378 000	100

The initial redox environment in both control samples was indifferent and remained similar within the bioleaching duration. Environments in all samples with applied experimental approaches were initially slightly reductive, ending as strong reductive, including many fluctuations within these two ranges. The drop in redox potential could be a consequence of hydrogen sulphide production [11], whereas the reaction mixture had an intensive H<sub>2</sub>S stench. Metal sulphides contained in the mine soil can be dissolved by the combined action of electron extraction by Fe<sup>3+</sup> ions and binding of protons by the sulphide moiety via valence band electrons. The chemical bond between metal and sulphur moiety can be broken by proton attack and, after binding two protons, hydrogen sulphide can be produced [11]. The concentration of microorganisms is expressed as the number of colony-forming units (CFU) per 1 ml of leachate. Microbial count in ABC remained relatively constant throughout the experiment, representing the background biomass concentration in all samples. In BC, a slight increase in CFU was observed. The moisturization of mine soil by distilled water or TSB led to microbial reactivation, which is interpreted as background concentration for experiments with non-sterile sediment. In EA1, non-sterile sediment was used along with the TSB medium. Consequently, the indigenous microflora was more effectively revived, resulting in significantly higher microorganism concentrations compared to both controls. In EA2 and EA3, a decreasing trend in CFU count was observed. The approaches differed only in mine soil sterility. In EA3, non-sterile sediment was used, leading to a higher CFU count in the Petri dish representing EA3 at the end of the experiment. Indigenous strains are used to the presence of PTEs and might possess tolerance and resistance mechanisms, so they can easily employ their mechanisms when their metabolism is activated. Unlike the collection strain *C. oxalaticus*, although versatile with confirmed mechanisms to deal with PTEs, it was not able to take hold in the environment with extreme concentrations of As and Sb. Determination of the toxicity by the *S. alba* seed germination test was the indirect confirmation of successful bioleaching. While soils from both controls had a stimulating effect (negative I<sub>μ</sub> values), all EAs were completely inhibiting. This implies that Sb and As were released from their bonds within the soil structure, causing toxicity to plant seeds. Although the bioleaching potential was indicated and the possible pattern of biologically-mediated release of PTEs was envisaged, further detailed geochemical, biochemical, and material research should be carried out to confirm these assumptions. An inseparable step, as the bioleaching sequel would be the recovery of PTEs, which can return these critical raw materials to usage.

#### 4 Conclusions

A series of bioleaching assays based on biostimulation, bioaugmentation, and their combination proved that this method can lead to the mobilization of PTEs arsenic and antimony. The approach based on the reactivation of indigenous microorganisms, as well as biostimulation with a nutrient-rich medium might be a sufficient basis for successful bioleaching. As for arsenic, biostimulation led to an average removal rate of 23.5 %. The releasing of 1.3 g of antimony from an initial concentration of 21 400 mg.kg<sup>-1</sup> was achieved only by the re-activation of indigenous microorganisms. Research of previous studies devoted to mine soil of Medzibrod, as well as monitoring of physicochemical and biological properties of bioleaching reaction mixtures suggest a potential mechanism of bioleaching, based on the interaction of carbonates and sulphides

from the mine soil with extracellular products of microbial metabolism, causing the change in pH and redox environment. That can lead to the release of the PTEs and their bioprecipitation on the microbial cell surface.

### Acknowledgements

The research was supported by the Slovak Research and Development Agency under the contract No. APVV-21-0212 “Selected environmental loads as a stress factor affecting biodiversity and health risks for exposed population groups”.

### References

- [1] Santos-Francés, F., Martínez-Graña, A., Rojo, P.A., Sánchez, A.G. Geochemical Background and Baseline Values Determination and Spatial Distribution of Heavy Metal Pollution in Soils of the Andes Mountain Range (Cajamarca-Huancavelica, Peru). *International Journal of Environmental Research and Public Health*, 14 (8), 2017, p. 859.
- [2] Hiller, E., Lalinská, B., Chovan, M., Jurkovič, L., Klimko, T., Jankulár, M., Hovorič, R., Šottník P., Fláková, R., Ženišová, Z., Ondrejková, I. Arsenic and antimony contamination of waters, stream sediments and soils in the vicinity of abandoned antimony mines in the Western Carpathians, Slovakia. *Applied Geochemistry*, 27, 2012, p. 598-614.
- [3] Carneiro, M.A., Pintor, A.M.A., Boaventura, R.A.R., Botelho, C.M.S. Arsenic and antimony desorption in water treatment processes: Scaling up challenges with emerging adsorbents. *Science of the Total Environment*, 929, 2024, p. 172602.
- [4] Horváthová, H., Schwarzkopfová, K., Vojtková, H., Jurkovič, L., Faragó, T., Boturová, K., Hiller, E., Urík, M., Vítková, M. Aerobic release of arsenic and antimony from mine soils by biostimulation of indigenous microbial activity and bioaugmentation with *Cupriavidus* genera of bacteria. *Plant and Soil*, 497, 2024, p. 175-197.
- [5] Li, F., Zheng, Y., Tian, J., Ge, F., Liu, X., Tang, Y., Feng, Ch. *Cupriavidus* sp. strain Cd02-mediated pH increase favoring bioprecipitation of Cd<sup>2+</sup> in medium and reduction of cadmium bioavailability in paddy soil. *Ecotoxicology and Environmental Safety*, 184, 2019, p. 109655.
- [6] Epelde, L., Lanzén, A., Blanco, F., Urich, T., Garbisu, C. Adaptation of soil microbial community structure and function to chronic metal contamination at an abandoned Pb-Zn mine. *FEMS Microbiology Ecology*, 91, 2015, p. 1-11.
- [7] Chovan, M., Lalinská, B., Šottník, P., Hovorič, R., Petrák, M., Klimko, T. Mineralogická a geochemická charakteristika zdrojov znečistenia na opustenom ložisku Sb-Au rúd Medzibrod. *Mineralia Slovaca*, 42, 2010, p. 95-108.
- [8] Mikuš, T., Bakos, F., Števko, M. New data on Au mineralization at the Medzibrod locality (Nízke Tatry Mts.), Slovak Republic. *Bulletin Mineralogie Petrologie*, 26 (2), 2018, p. 154-162.
- [9] Directive of Ministry of Environment of the Slovak Republic No. 1/2015-7 for the elaboration of risk assessment analysis of contaminated sites. [http://www.minzp.sk/files/sekcia-geologie-prirodných-zdrojov/ar\\_smernica\\_final.pdf](http://www.minzp.sk/files/sekcia-geologie-prirodných-zdrojov/ar_smernica_final.pdf). Accessed September 6, 2024 (In Slovak).
- [10] Čerňanský, S., Šimonovičová, A., Juhásová, J., Semerád, M. Bioleaching of arsenic and antimony from mining waste. *Acta Environmentalistica Universitatis Comenianae*, 24 (1), 2016, p. 5-9.
- [11] Rohwerder, T., Gherke, T., Kinzler, K., Sand, W. Bioleaching review part A: Progress in bioleaching: fundamentals and mechanisms of bacterial metal sulfide oxidation. *Applied Microbiology and Biotechnology*, 63, 2003, p. 239-248.

# CHALLENGES, FUTURE OUTLOOK AND ENVIRONMENTAL RISKS ASSOCIATED WITH THE USE OF PHOTOVOLTAIC TECHNOLOGY AS ALTERNATIVE ENERGY SOURCES IN THE CONTEXT OF SMART CITIES IN POLAND

Magdalena Jabłońska-Czapla<sup>a</sup>, George Yandem<sup>a</sup>, Joanna Willner<sup>b</sup>

<sup>a</sup> Institute of Environmental Engineering Polish Academy of Science, 41-819 Zabrze, Poland,  
magdalena.czapla@ipispan.edu.pl, george.yandem@ipispan.edu.pl

<sup>b</sup> Faculty of Materials Engineering, Silesian University of Technology, 40-019 Katowice, Poland,  
joanna.wilner@polsl.pl

## Abstract

The integration of photovoltaic panels in 21st-century urban landscapes has become widespread. Various types of renewable energy systems (RES), including different photovoltaic panel designs, are now commonly installed on rooftops, bus shelters, benches, city lampposts, and other urban infrastructure. The global push towards developing "smart cities" is aimed at maximizing the use of alternative energy sources with a positive environmental impact. However, alongside these advancements, new challenges are emerging due to the growing presence of electronic devices and their critical technological components. This article offers a critical analysis of smart city development worldwide, with a particular focus on Poland and the application of photovoltaics (PV). It examines the types of solar cells used in PV panels, weighing the benefits and risks of incorporating photovoltaics into smart cities, and considers the environmental implications and potential future issues related to the increasing presence of electronics, including PV panels, in urban environments.

**Keywords:** smart city, BIPV, photovoltaics, PV

## 1 Introduction

The global adoption of renewable energy sources (RES) is on the rise, driven in part by the increasing energy demand in previously less developed nations [1]. Solar energy, in particular, provides a cleaner alternative to traditional power sources and helps mitigate climate change. Around the world, a growing number of smart or green cities are being developed, equipped with advanced technology and supported by photovoltaic (PV) solutions. These cities feature innovations such as smart benches (solar-powered to offer charging ports and Wi-Fi), solar-powered lighting (reducing both energy usage and maintenance costs), solar-integrated bus stops (with lighting and digital displays powered by solar panels), and solar carports that generate electricity for electric vehicle (EV) chargers while providing shelter. In addition, building-integrated photovoltaics (BIPV) integrate PV panels into rooftops or facades, helping buildings meet their own energy needs and reducing grid reliance [2].

The smart city concept is gaining global momentum, with numerous examples showcasing the role of PV technology in promoting sustainability and improving urban living conditions. These cities utilize solar energy to meet growing energy demands while minimizing their environmental footprint. For instance, Barcelona has embraced solar energy on a large scale in both public and private sectors. New York features widespread rooftop solar installations across public buildings to encourage renewable energy use. Singapore, constrained by space, has adopted innovative urban planning and technology to maximize solar power. Cities like Helsinki and Oslo have prioritized sustainable energy solutions, including widespread PV panel installations. Amsterdam, a pioneer in smart city development, also incorporates solar energy in various urban projects [3].

## 2 Material and methods

### 2.1 PV panels applied in smart cities

Solar cells are generally categorized into three main types: crystalline silicon-based cells, thin-film cells, and hybrid cells. Crystalline silicon-based cells represent the first generation of solar technology and are made from semiconducting crystalline silicon, which can be either monocrystalline or polycrystalline. Monocrystalline silicon cells, known for their high efficiency and durability, are ideal for areas with limited space but high energy demands. On the other hand, polycrystalline cells are slightly less efficient but more

affordable, making them suitable for larger installations where space is not a constraint. Monocrystalline panels typically have an efficiency range of 18-22 %, while polycrystalline panels range from 16-18 %, both of which are commonly used in rooftop solar setups.

Crystalline silicon (both monocrystalline and polycrystalline) remains the leading photovoltaic technology today, along with second-generation thin-film solar cells. Thin-film cells, known for their lightweight and flexible nature, can be integrated into various surfaces such as building facades or structures with unconventional shapes [4]. They are gaining market share due to their lower material usage compared to traditional silicon-based cells, making them a more cost-effective option [5].

Photovoltaic (PV) modules consist of several materials, including glass, metals, semiconductors, and polymer layers, all tightly laminated together. Crystalline silicon (c-Si) cells, the most mature and widely used PV technology, currently dominate about 92 % of the global market. A typical PV cell consists of a p-doped wafer with a highly doped pn-junction. The surface is usually textured with pyramid (for monocrystalline) or random (for polycrystalline) structures and covered with an anti-reflective layer (ARL) to reduce light reflection. Silver and aluminium pastes are printed in a grid pattern on the front and back to create the electric field necessary for energy generation.

## **2.2 Benefits and risks of integrating solar panels in smart cities**

The adoption of smart solutions helps cities reduce energy consumption for lighting, leading to lower costs. This can be achieved through intelligent street lighting systems that adjust brightness based on factors like time of day, weather conditions, and traffic levels. Similarly, smart grids optimize electricity costs by better managing energy distribution [6]. These innovations also contribute to energy independence, as cities can generate their own power, decreasing their reliance on external sources and insulating them from price fluctuations and grid disruptions.

For instance, smart meters and remote reading systems—key components of smart grids—allow consumers to monitor their electricity use in real-time. This technology also enables remote control of energy consumption in homes, businesses, and offices, preventing grid overloads and conserving reserve power in power plants. By identifying network overloads and energy losses, distribution system operators can improve grid management, enhancing the quality, security, and efficiency of energy supplies.

On a larger scale, cities can save energy by aligning supply with actual demand, or by providing consumers with detailed information to make energy-efficient choices, considering both cost and environmental impact. Additionally, the growth of photovoltaic (PV) installations brings economic benefits, such as creating jobs in manufacturing, installation, and maintenance, which helps boost the local economy. Access to clean energy and smart infrastructure not only makes cities more sustainable but also significantly enhances their livability. A notable application of thin-film panels is in innovative photovoltaic systems integrated into smart city buildings, such as solar roof tiles, windows, and façades made from photovoltaic cells (known as Building Integrated Photovoltaics or BIPV). As the market for PV panels in renewable energy continues to grow, it is increasingly important to understand and mitigate the environmental risks associated with their use, ensuring safe operation and recycling practices. The scientific community should pay particular attention to all types of panels, including thin-film variants, especially those containing toxic elements like cadmium, tellurium, and TCE, to address potential environmental hazards.

## **2.3 Alternative energy sources based on solar energy in Poland**

The use of solar energy for electricity generation in Poland has been steadily increasing [7]. According to the Renewable Energy Institute, as of the third quarter of 2023, there were 6,929 photovoltaic projects with connection agreements in Poland, totalling over 18 GW of capacity. Over a six-month period, the capacity of grid-connected photovoltaic systems has nearly tripled [8]. Despite the varying weather conditions and seasonal changes, Poland has favourable conditions for photovoltaic (PV) systems. The Pomorskie, Zachodniopomorskie, and Kujawsko-Pomorskie Voivodeships lead in renewable energy production, driven by greater access to technology, funding programs, and a growing environmental awareness. Rising conventional energy costs have also spurred the installation of PV panels, particularly in large cities where both public buildings and private homes have adopted solar energy solutions [9]. A key feature of Poland's solar market is its decentralized nature, with widespread interest in small-scale energy generation among citizens. Solar-powered street lamps, municipal bike systems, and other installations are common in Polish cities, helping to reduce electricity costs. The government has also introduced various incentives, such as subsidies and tax benefits, to encourage both small-scale and larger PV installations. The



trend toward using alternative energy sources has become increasingly popular, further accelerating the sector's growth [10].

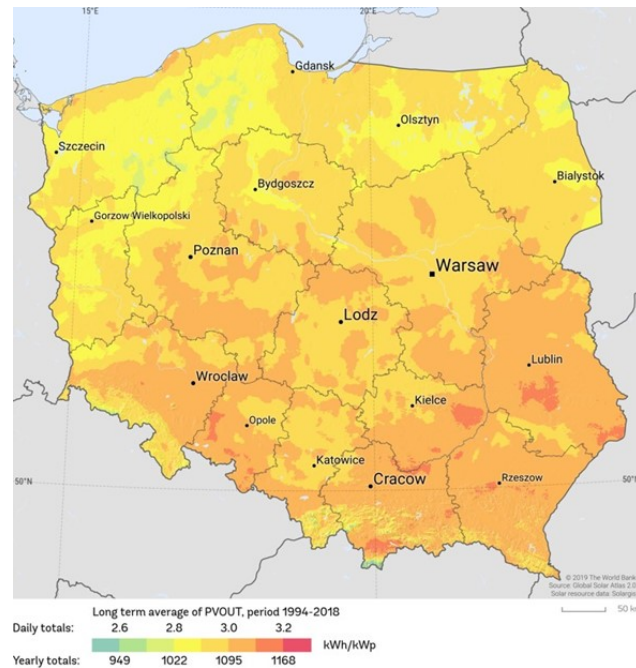


**Fig. 1. Photovoltaic electricity potential in Poland**

According to Solar Power Europe, Poland ranked fourth in the EU in 2023 for expanding installed PV capacity, following Germany, Spain, and Italy [11]. Figure 1 shows photovoltaic electricity potential in Poland. In 2023, Poland's solar market maintained a capacity of around 4.6 GW.

Poland is also embracing the smart city concept, incorporating advanced technologies and renewable energy to improve sustainability and urban living. Cities like Warsaw, Krakow, and Gdansk are at the forefront of this transformation. Warsaw, recognized as a smart city, has implemented initiatives such as smart street lighting, intelligent traffic management systems, and extensive sensor networks to monitor urban services. The city promotes the installation of PV panels on public buildings and homes, contributing to clean energy generation and carbon footprint reduction. Warsaw ranked 38<sup>th</sup> in the 2024 IMD Smart City Index [12].

Similarly, Krakow is investing in renewable energy, including solar farms and smaller PV projects. The city has introduced electric buses, smart parking systems powered by solar energy, and bike-sharing programs to improve mobility and reduce pollution. In the 2024 IMD ranking, Krakow holds the 78<sup>th</sup> position [12].

In Gdansk, located in the Pomerania region, smart waste management systems and the deployment of renewable energy technologies have helped optimize city operations. Further south, Wrocław integrates smart technologies into its urban planning, focusing on energy-efficient systems and digital services. Poznań, in central Poland, also emphasizes sustainability by using PV panels, green spaces, and smart public transport while leveraging data analytics and IoT (Internet of Things) to enhance governance and public services.

### 3 Conclusions

According to IRENA's 2019 report on the Future of Solar Photovoltaics [13], the widespread adoption of solar cells could contribute to 21 % of the total emission reduction potential within the energy sector when compared to other low-carbon technologies. As smart cities continue to develop, incorporating photovoltaic (PV) panels will remain a central priority. However, there is still a lack of comprehensive research on the long-term operation of PV systems, particularly concerning potential damage and the risk of toxic substances leaching into the environment over time. In conclusion, although photovoltaic panels are crucial for the sustainable growth of smart cities, it is important to take a balanced approach that considers both their advantages and potential drawbacks. Collaboration among policymakers, urban planners, and technology

developers is necessary to build resilient, environmentally friendly urban spaces that can adapt to future challenges. While PV panels help reduce carbon emissions, their lifecycle-spanning production, installation, and disposal-also poses environmental challenges. These include the extraction and processing of raw materials, the energy used in manufacturing, and the land required for large-scale solar farms. To minimize these impacts, effective recycling methods and material recovery strategies will be critical.

## Acknowledgements

The work was supported by statutory research no. 1a-149/24 Institute of Environmental Engineering Polish Academy of Science.

## References

- [1] Gnatowska, R., Moryń-Kucharczyk, E. The Place of Photovoltaics in Poland's Energy Mix. *Energies*, 14, 2021, 1471, <https://doi.org/10.3390/en14051471>.
- [2] Chattopadhyay, M., Rajavel, R. Solar PV Technology for Smart Cities of India. *International Journal of Recent Technology and Engineering*, 7, (5), 2019, p. 332-340.
- [3] 14 Top Smart Cities in the World. Caburntelecom, [https://caburntelecom.com/top-smart-cities/?gad\\_source=1&gclid=CjwKCAjw26KxBhBDEiwAu6KXtxnnMHoKRZexTIRBp0FjhuLcQm7bB2DytK5Xk9x53udCFZZIHGIc1xoCW7wQAvD\\_BwE](https://caburntelecom.com/top-smart-cities/?gad_source=1&gclid=CjwKCAjw26KxBhBDEiwAu6KXtxnnMHoKRZexTIRBp0FjhuLcQm7bB2DytK5Xk9x53udCFZZIHGIc1xoCW7wQAvD_BwE).
- [4] Chowdhury, M.S., Rahman, K.S., Chowdhury, T., Nuthammachot, N., Techato, K., Akhtaruzzaman, M., Tiong, S.K., Sophia, K., Amin, N. An overview of solar photovoltaic panels' end-of-life material recycling. *Energy Strategy Reviews*, 27, 2020, 100431, <https://doi.org/10.1016/j.esr.2019.100431>.
- [5] Zapf-Gottwick, R., Koch, M., Fischer, K., Schwerdt, F., Hamann, L., Kranert, M., Metzger, J., Werner, J. Leaching hazardous substances out of photovoltaic modules. *International Journal of Advanced Applied Physics Research*, 2 (2), 2015, p. 7-14, <https://doi.org/10.15379/2408-977X.2015.02.02.2>.
- [6] Cobelo-García, A., Filella, M., Croot, P., Frazzoli, C., Du Laing, G., Ospina-Alvarez, N., Zimmermann, S. COST action TD1407: network on technology-critical elements (NOTICE) - from environmental processes to human health threats. *Environmental Science and Pollution Research*, 22, 2015, p. 15188-15194, doi: 10.1007/s11356-015-5221-0
- [7] Igliński, B., Piechota, G., Kiełkowska, U., Kujawski, W., Pietrzak, M.B., Skrzatek, M. The assessment of solar photovoltaic in Poland: the photovoltaics potential, perspectives and development. *Clean Technologies and Environmental Policy*, 25, 2023, p. 281-298, <https://doi.org/10.1007/s10098-022-02403-0>.
- [8] IRE (Institute for Renewable Energy), Photovoltaic market in Poland 2023. Warszawa, 2023, <https://ieo.pl/en/pv-projects>.
- [9] Igliński, B., Piechota, G., Iglińska, A., Cichosz, M., Buczkowski, R. The study on the SWOT analysis of renewable energy sector on the example of the Pomorskie Voivodeship (Poland). *Clean Technologies and Environmental Policy*, 18, 2016, p. 45-61, <https://doi.org/10.1007/s10098-015-0989-7>.
- [10] Grębosz-Krawczyk, M., Zakrzewska-Bielawska, A., Glinka, B., Glińska-Neweś, A. Why do consumers choose photovoltaic panels? Identification of the factors influencing consumers' choice behavior regarding photovoltaic panel installations. *Energies*, 9 (14), 2021, 2674, <https://doi.org/10.3390/en14092674>.
- [11] SolarPower Europe (2023): EU Market Outlook for Solar Power 2023-2027.
- [12] <https://issuu.com/docs/e7a60c053affbf9e98fcba93afe857af?fr=sZjQ1ODcwMDMzODM>.
- [13] IRENA. Future of solar photovoltaic: deployment, investment, technology, grid integration and socio-economic aspects. A Global Energy Transformation, 2019.

## BIOLEACHING OF PLATINUM FROM TAILINGS IN THE KRUŠNÉ HORY MOUNTAINS

**Iva Janáková<sup>a</sup>, Vladimír Čablík<sup>a</sup>, Josef Škvarka<sup>a</sup>, Sarah Janštová<sup>a</sup>**

<sup>a</sup> Faculty of Mining and Geology, VSB - Technical University of Ostrava,  
17. Listopadu 2172/15, 708 00 Ostrava Poruba,  
iva.janakova@vsb.cz, vladimir.cablík@vsb.cz, josef.skvarka@vsb.cz, sarah.janstova@vsb.cz

### Abstract

This study explores the bioleaching of platinum group metals (PGMs) from polymetallic sulfide ores using the bacterium *Acidithiobacillus ferrooxidans*. Samples from two mining sites, Mikulov and Lehnschafter, were subjected to bioleaching experiments in the presence and absence of catalytic additives. Copper sulfate (CuSO<sub>4</sub>) and silver nitrate (AgNO<sub>3</sub>) were tested as catalysts to enhance platinum recovery. X-ray fluorescence spectroscopy (XRF) was employed to monitor the platinum content over a 28-day period. The results demonstrated that Cu<sup>2+</sup> ions significantly accelerated platinum dissolution, leading to a reduction in platinum concentration from 3549 mg/kg to zero in the Lehns sample. In contrast, the addition of Ag<sup>+</sup> ions showed no significant effect. This research underscores the potential of biotechnological methods, specifically bacterial leaching, as an eco-friendly and efficient approach for extracting platinum group metals from ore, especially with the aid of catalytic agents like copper.

**Keywords:** platinum, bioleaching, *Acidithiobacillus ferrooxidans*, arsenopyrite ore

### 1 Introduction

The six platinum-group metals (PGM), commonly referred to as the platinum metals, includes ruthenium, rhodium, palladium, osmium, iridium and platinum. These elements are widely dispersed and rare in the Earth's crust. Platinum occurrences are either pure or are the source of sulphide deposits of copper and nickel. Scales of polyxene are scattered among silicate grains in ultrabasic rocks [1-2].

Because platinum is excreted in metallic form, it was considered inert. However, recent studies [3-4] have shown a higher proportion of soluble platinum metal compounds. Platinum metals can transform into more soluble, bioavailable compounds once they enter the environment. This is due, for example, to siderophores - low molecular weight organic compounds produced by plants, fungi and bacteria to increase the availability of iron. These form soluble complexes with platinum and palladium, increasing their solubility and mobility. The potential to increase the bioavailability of platinum metals is also noted for other complexing agents such as ethylenediaminetetraacetic acid (EDTA) and humic substances, which increase the solubility of platinum and palladium in fats. This leads to their possible accumulation in aquatic organisms [5].

Despite extensive research focused on improving techniques for the bioleaching of various types of sulfide ores, such as pyrite, chalcopyrite, sphalerite, and galena [6-7], the leaching of arsenic ores with the addition of platinum is very rare. The low-cost requirements and environmental friendliness of biotechnology make this option attractive for the extraction of platinum and rare earth metals in general [8-9]. The aim of this article is to provide the necessary insights for the bioleaching of PGMs from primary sources. The following sections provide basic information on the mineralogy of the examined platinum-bearing ore, describe the bioleaching of the main mineral phases associated with PGMs, discuss the challenges and opportunities of PGM bioleaching, and propose a method for the bioleaching of PGM ores.

### 2 Material and methods

Samples were collected from two locations (Mikulov and Lehnschafter) following silver ore mining in the Mikulov ore district in the Ore Mountains. Both samples were crushed using a BB-200 jaw crusher (Retsch GmbH, Haan, DE) to a particle size of 10-30 mm, and the material was ground in a VMA-386 laboratory vibrating mill (VIPO, Czech Republic) to the desired particle size of 71-100 µm. This particle size was necessary to increase the likelihood of releasing Pt grains from arsenopyrite and chalcopyrite for subsequent bacterial leaching.

## 2.1 Location description

The Krušné Hory Mountains form a continuous mountain range stretching over 130 km in length and an average width of 40 km, formerly mined mainly for silver and to a lesser extent for lead and cobalt. The silver veins, characteristic of the Mikulov and Hrob ore district, consist mainly of quartz (SiO<sub>2</sub>) and minerals such as galena (PbS), sphalerite (ZnS), argentite (Ag<sub>2</sub>S), proustite (Ag<sub>3</sub>AsS<sub>3</sub>), pyrargyrite (Ag<sub>3</sub>SbS<sub>3</sub>) and tetrahedrite (Cu,Zn,Ag,Fe)<sub>3</sub>(Sb,As)S<sub>2-4</sub>). The most common ore mineral found almost everywhere in quartz veins in the Mikulov Valley is crystalline and granular arsenopyrite. Another abundant ore mineral interbedded in quartz is pyrite, which is accompanied in small amounts by sphalerite and chalcopyrite [10]. The most important minerals in the ore veins were galena with silver and noble silver ores (argentite, proustite, pyrargyrite, stephanite and polybasite are mentioned). At present, there are still many mining operations in Mikulov and its vicinity, as well as tailings, which represent waste material from the mining of silver-bearing ores. The Lehnshafter mine and its Mikulov tailings [11].

## 2.2 Mineralogical composition

The mineral composition of two samples was analyzed. The measurements were performed using a fully automated and modernized URD-6 diffractometer (Rich. Seifert-FPM, DE). The results of the mineralogical analysis showed that the ores exhibited very similar mineralogical compositions and consisted of more than 85 wt.% silicates, mainly quartz and muscovite, with smaller amounts of sulfides such as arsenopyrite, sphalerite, chalcopyrite, and galena. Arsenopyrite and chalcopyrite are the most represented sulfur compounds, occurring as disseminated and vein ores. The complete mineralogical analysis is presented in Table 1.

**Table 1. XRF X-ray diffraction**

Mineral	Mikulov	Lehnshafter
	Content (%)	
Quarz	72.09	75.03
Muscovite	16.35	10.92
Arsenopyrite	6.24	9.34
Chalcopyrite	2.07	0.57
Sphalerite	1.65	0.85
Fluorite	1.38	2.90
Galena	0.22	0.11

Due to the chalcophile nature of both samples, meaning they preferentially form bonds with sulfur rather than with oxygen, the occurrence of platinum is noted in the form of fine inclusions in chalcopyrite and arsenopyrite, as well as in sperrylite (PtAs<sub>2</sub>) and possibly also in daomanite (PtCuAsS<sub>2</sub>).

Platinum group elements (PGE) and concentrations of Cu, Fe, and As were analyzed using X-ray fluorescence spectroscopy (XRF) on a DELTA Premium instrument (OLYMPUS INNOV-X, s-Hertogenbosch, NL). The representation of the elements is shown in Table 2. The values of Pd, Os, Rh and were lower than the detection limits in samples.

**Table 2. Distribution of elements of interest in the samples**

	Pt	Fe	Cu	As
	(mg/kg)			
Mikulov	2640	37086	3023	7991
Lehnshafter	3679	3761	3761	12385

Pt tends to concentrate together with Cu, As, and Fe due to geological processes.

## 2.3 Bioleaching tests

Due to the high concentrations of relevant elements and the specific mineral composition, the *Acidithiobacillus ferrooxidans* bacterium was selected for the experiments. This bacterium, sourced from the Czech Collection of Microorganisms in Brno, can utilize sulfur or its reduced inorganic compounds as an

energy substrate. Unlike other species in the *Acidithiobacillus* genus, it is also capable of obtaining energy by oxidizing divalent iron to trivalent iron [12].

Tests were performed in 1000 ml Erlenmeyer flasks placed in an incubated Multitron II shaker (Infors AG, Bottmingen, CH). To compare the leaching efficiency of samples containing additives, leaching of samples without the addition of additives and without bacterial culture was also performed. For the cultivation of bacterial cells of *A. ferrooxidans*, Silverman's 9K medium was used, and approximately 6 liters of it were prepared for the experimental part of this work.

To two leached samples, additives in the amount of 10 ml were added to enhance metal extraction. In the leaching solution of sample no. 2, containing ore material from the Lehnschafter adit dump, a solution of copper(II) sulfate pentahydrate ( $\text{CuSO}_4 \cdot 5\text{H}_2\text{O}$ ) was added as a source of copper cations. To prepare the solution, 0.05 g of  $\text{CuSO}_4$  was weighed and subsequently dissolved in 1 l of distilled water. For comparison of the effect of  $\text{Cu}^{2+}$  cations during bioleaching of the ore, the sample was also leached without the addition of the additive and labeled as number 1. Sample no. 4, containing ore material from the Mikulov dump, was supplemented with a silver nitrate ( $\text{AgNO}_3$ ) solution. The additive, serving as a source of silver cations, was prepared by mixing 0.005 g of silver nitrate with 1 l of distilled water. The same sample was also leached without the addition of the  $\text{AgNO}_3$  solution and was labeled as number 3.

### 3 Results and discussion

Each trace element has chemical properties that are somewhat unique, and therefore unique geochemical information is contained in changes in the concentration of each element. Some, especially rare (noble) metals, are very unreactive and insoluble. Rare earths are interesting because they all have two electrons in the outer 6s orbital and differ only in the number of electrons in the 4f shell. Because they almost always have the same valence ( $3^+$ ), their bonding behavior is similar. They differ systematically in ionic radius, resulting in systematic differences in geochemical behavior. Their rarity is in part a consequence of their highly siderophilic character. The concentration of these elements in the silicate. Pt are all also chalcophile although to varying degrees [13].

The tailings were probably oxidized, which led to an increase in the concentration of Pt and other chalcophilic metals. The Pt ratio of the untreated ore samples varied from 2275 mg/kg to 3824 mg/kg (see Table 3 and 4).

**Table 3. Results of Pt bacterial leaching Dump Lehns**

	Pt (ATF)	Without ATF
(mg/kg)		
1. Dump Lehns		
Input	3824	3824
7 days	3603	3791
14 days	1879	3308
21 days	1791	3015
28 days	1271	2832
2. Dump Lehns + $\text{CuSO}_4$		
Input	3549	3549
7 days	3162	3407
14 days	2108	3136
21 days	933	2873
28 days	0	2691
3. Dump Lehns + $\text{AgNO}_3$		
Input	3606	3606
7 days	3600	3601
14 days	3583	3591
21 days	3535	3524
28 days	3527	3410

**Table 4. Results of Pt bacterial leaching Mikulov**

	Pt (ATF)	Without ATF
(mg/kg)		
1. Dump Mikulov		
Input	2375	2375
7 days	2106	2190
14 days	1835	2004
21 days	1724	1976
28 days	1607	1831
2. Dump Mikulov + CuSO <sub>4</sub>		
Input	2356	2356
7 days	2278	2237
14 days	2215	2224
21 days	2147	2190
28 days	2019	2133
3. Dump Mikulov + AgNO <sub>3</sub>		
Input	2740	2740
7 days	2549	2597
14 days	2356	2502
21 days	1802	2331
28 days	1656	2206

Figures 1 and 2 show that the platinum content decreases with increasing leaching time, indicating that platinum is dissolving into the solution.

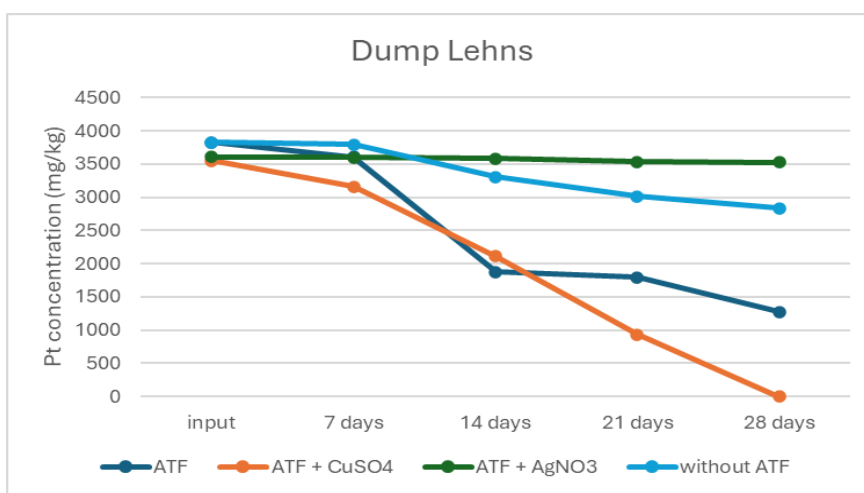


**Fig. 1. Pt bioleaching (Dump Lehns)**

The leached ore was found to contain significant concentrations of arsenic and copper. Consequently, CuSO<sub>4</sub> and AgNO<sub>3</sub> were selected as catalysts, with Cu<sup>2+</sup> and Ag<sup>+</sup> ions introduced into the leaching solution to enhance the process. Metal ions, particularly copper, are commonly employed as catalysts in biohydrometallurgy due to their ability to significantly accelerate bioleaching processes and improve metal recovery [14-15].

During the bioleaching experiments, X-ray fluorescence (XRF) spectrometry was used to monitor the depletion of platinum (Pt). The effects of bacterial leaching, both with and without the addition of catalysts, were investigated at the Lehns tailings site. The leaching progression is illustrated in Figure 1. In the presence of a catalyst, complete Pt removal was achieved within 28 days. In contrast, in the absence of a catalyst, Pt concentrations were reduced to 1271 mg/kg after the same period.

Leaching with the addition of Ag<sup>+</sup> ions showed no significant effect, as demonstrated in Figure 1.

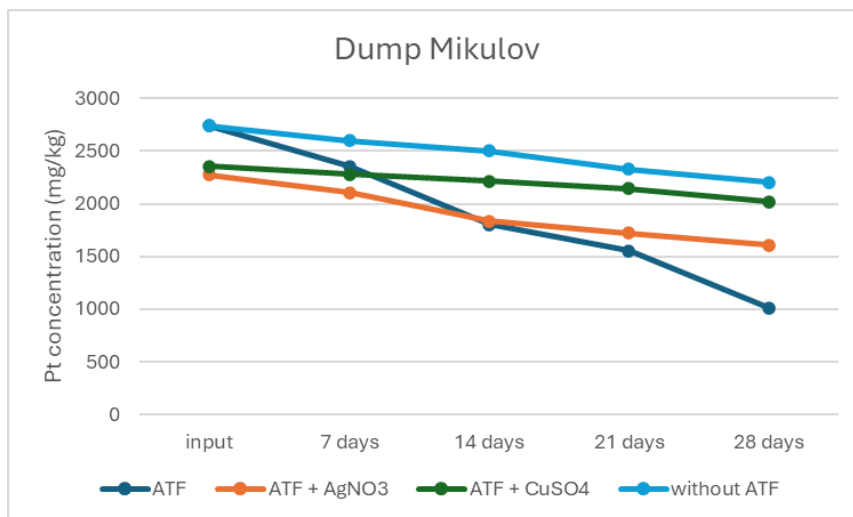


Fig. 2. Pt bioleaching (Dump Mikulov)

Both catalysts were used in the leaching of the Mikulov tailings as in the previous experiment. The sample with the addition of CuSO<sub>4</sub> as a catalyst had no effect. The second sample had a lower Pt content in the input (2275 mg/kg). It was confirmed that with the addition of catalyst, the Pt content decreased to 1010 mg/kg after 28 days of leaching.

The study confirms the role of bacteria *Acidithiobacillus ferrooxidans* in leaching iron polymetallic sulphidic ore and the usage of bioleached copper sulphate as catalyst in the oxidation of Pt.

#### 4 Conclusions

This study confirmed the effectiveness of bacterial leaching of platinum ores using the bacterium *Acidithiobacillus ferrooxidans* and highlighted the importance of adding Cu<sup>2+</sup> ions in the form of copper sulfate (CuSO<sub>4</sub>) as a catalyst to accelerate platinum leaching. The results showed that the presence of Cu<sup>2+</sup> ions significantly improved platinum solubility, with the platinum concentration in the Lehns sample decreasing from 3549 mg/kg to 0 mg/kg over 28 days. In contrast, the addition of Ag<sup>+</sup> ions in the form of silver nitrate (AgNO<sub>3</sub>) had no significant effect on platinum leaching. On the other side, bioleaching of the Mikulov sample with the addition of Ag<sup>+</sup> ions shows a significant decrease of 1084 mg/kg within 28 days. The research also confirmed that biological processes represent an environmentally friendly and efficient method for extracting precious metals, particularly due to their ability to increase the mobility of heavy metals in the processed ores.

#### Acknowledgements

The work was supported by Interreg Danube Region co-funded by the European Union, within project DRP0401069 - BioPrep, Biotechnological Innovations for Sustainable Flat Panel Displays Recycling.

This research was also funded by the Student Grant Competition financed by Faculty of Mining and Geology, VSB, Technical University of Ostrava, within project "Treatment options for gold-bearing polymetallic ore" (no. SP2024/106).

#### References

- [1] Hedrich, S., Kraemer, D., Junge, M., Marbler, H., Bau, M., Schippers, A. Bioprocessing of oxidized platinum group element (PGE) ores as pre-treatment for efficient chemical extraction of PGE. *Hydrometallurgy*, 196, 2020.
- [2] Dahlheimer, S.R., Neal, C.R., Fein B. Potential Mobilization of Platinum-Group Elements by Siderophores in Surface Environments. *Environmental Science*, 41 (3), 2007, p. 870-875.
- [3] Yopps, D.L., Baglin, E.G. *Bacterial preoxidation of stillwater complex, MT, platinum-group metal flotation concentrate and recovery of platinum-group metals by cyanidation and other leachants*. 1991.

- [4] Zhao, Y., Zhao, H., Shen, L., Qiu, G., Wang, Y. Study on the role of microbial metabolites in in-situ noncontact bioleaching of ion-adsorption rare earth ore. *Journal of Environmental Management*, 368, 2024, 122184, ISSN 03014797.
- [5] Liu, M., Zhu, J., Zhang, Ch., He, P., Chen, D. Effect of calcium lignosulfonate on surface modification and bioleaching of chalcopyrite. *Biochemical Engineering Journal*, 207, 2024, 109329, ISSN 1369703X.
- [6] Rouchalova, D., Rouchalova, K., Janakova, I., Cablik, V., Janstova, S. Bioleaching of Iron, Copper, Lead, and Zinc from the Sludge Mining Sediment at Different Particle Sizes, pH, and Pulp Density Using *Acidithiobacillus ferrooxidans*. *Minerals*, 10 (11), 2020, ISSN 2075-163X.
- [7] Kovaříková, H., Janáková, I., Čablik, V., Vrlíková, V. Bacterial Leaching of Polymetallic Ores from Zlatý Chlum Locality. Online. *Inženýria Mineralna*, 1(1), 2021, ISSN 1640-4920.
- [8] Chipise, L., Ndlovu, S., Shemi, A., Moodley, S.S., Kumar, A., Simate, G.S., Yah, C.S. Towards bioleaching of PGMS. *Minerals Engineering*, 202, 2023, 108291, ISSN 08926875.
- [9] Zimmermann, S., Menzel, C.M., Stüben, D., Taraschewski, H., Bernd, S. Lipid solubility of the platinum group metals Pt, Pd and Rh in dependence on the presence of complexing agents. *Environmental Pollution*, 124 (1), 2003, p. 1-5.
- [10] David, P., Soukup, V., David, P. *Krušné hory: s mapovým atlasem*. Průvodce po Čechách, Moravě a Slezsku. Praha: Soukup & David, 2002. ISBN 8086050238.
- [11] Urban, M. *Horní města Krušných hor: Ústecký kraj*. Sokolov: Fornica Publishing, 2015. ISBN 9788087194492.
- [12] Janakova, I., Fejfarova, B., Sigut, O., Cablik, V. Utilisation of *Acidithiobacillus ferrooxidans* Bacteria for Bioleaching of Waste Materials from Silver-Bearing Ore Mining. *Advances in Science and Technology*, 135, 2023, p. 3-11, ISSN 1662-0356.
- [13] White, W.M. *Geochemistry*. Hoboken, NJ: John Wiley, 2013. ISBN 978-0-470-65668-6.
- [14] Zhang, Y., Li, Q., Liu, X. Role of  $Ag^+$  in the Bioleaching of Arsenopyrite by *Acidithiobacillus ferrooxidans*. *Metals*, 10 (3), 2020.
- [15] Zhang, Y., Li, Q., Liu, X., Yin, H., Yang, Y., Xu, B., Jiang, T., He, Y. The catalytic effect of copper ion in the bioleaching of arsenopyrite by *Acidithiobacillus ferrooxidans* in 9K culture medium. *Journal of Cleaner Production*, 256, 2020, ISSN 09596526.



# DEVELOPMENT OF PASSIVE MINE WATER TREATMENT SCHEMES WITH THE APPLICATION OF MICROBIAL SULFATE REDUCTION IN A VERTICAL FLOW BIOREACTOR

Eberhard Janneck<sup>a</sup>, Mirko Martin<sup>a</sup>, Christine Stevens<sup>b</sup>, Sabrina Hedrich<sup>c</sup>

<sup>a</sup> GEOS Ingenieurgesellschaft mbH, Schwarze Kiefern 2, 09633Halsbrücke, Germany, m.martin@geosfreiberg.de

<sup>b</sup> Sächsisches Landesamt für Umwelt, Landwirtschaft und Geologie, Referat 44, Zur Wetterwarte 11, 01109 Dresden, Christine.Stevens@smekul.sachsen.de

<sup>c</sup> Technical University Bergakademie Freiberg, Institute of Biosciences, Research Group Microbiology and Biohydrometallurgy, Sabrina.Hedrich@bio.tu-freiberg.de

## Abstract

New studies on the development of passive water treatment schemes at three abandoned mining sites in Saxony, Germany, show the basic applicability of these methods at several locations in the Ore Mountains (Krušnohoří/Erzgebirge). All constructed pilot plants contain a vertical flow bioreactor (VFBR) for active microbial sulfate reduction in order to immobilize metals as poorly soluble metal sulfides in a specially developed substrate mixture for sulfate-reducing bacteria. The VFBR in combination with other passive treatment stages constitute one method, which can mitigate the pollution of rivers and streams with toxic elements from abandoned mines. The article discusses the advantages and disadvantages of the experimental setup used to obtain design criteria.

**Keywords:** polluted mine water, passive treatment, microbial sulfate reduction, vertical flow bioreactor

## 1 Introduction

In many regions of Central Europe (e.g. Krušnohoří, Thuringia, Moravia-Silesia, Male Karpaty, etc.) metal mining has been practiced for centuries. After 1990 many mines had to be closed and priority areas in the former mining regions have been rehabilitated. Nevertheless, there are many remaining effluents from abandoned mines without a legal successor, which exert a harmful impact on aquatic ecosystems today. As a result, large sections of river suffer from mine effluents containing toxic elements like As, Sb, Cd, Zn, Ni, Cu, U and others. Today more than 13,800 km of river in the Czech Republic, Slovakia, and Germany are polluted with these toxic elements.

In Saxony, Germany, water authorities are facing challenges with effluents from numerous abandoned metal and hard coal mines. Broadly 13 % of streams and rivers exceed their Environmental Quality Standards (EQS) for As, Cu, Zn, Cd or Ni due to mining. A recent extensive study [1] commissioned by the Saxon State Office for Environment, Agriculture and Geology examined the pollution of natural watercourses with metals from abandoned mines in the Ore Mountain region. Results allow a detailed breakdown of the overall pollution load to specific sub-sources including abandoned mines, spoil heaps and tailings. These smaller-scale sources are predestined for cost-effective and resource-saving passive treatment, which is considered to be the only economically viable method to achieve an improvement in the water quality of the affected rivers in the mining region of the Ore Mountains.

The metals Cd, Cu, Ni, Zn, which are often found in mining waters, form poorly soluble sulfides. They can be immobilized in bioreactors in which natural microbial sulfate reduction takes place. Based on the study [1], three model sites have been selected in Saxony where passive water treatment schemes were tested.

## 2 Material and methods

### 2.1 Water quality at the study sites

Table 1 shows the mining discharge and some chemical parameters of the selected study sites. The availability of data at the three locations varies. A variety of data is available at the tailings management facility (TMF) Hammerberg. Here the data given in Table 1 cover the last 10 years, while data from the other two locations are based on average values of the last 2 years. The elements Cd, Cu, Ni and Zn can be found at all three locations. They can be immobilised as sulfides in a strongly reducing environment.

**Table 1. Typical water quality at the selected study sites**

	Unit	St. Christoph adit, Breitenbrunn	Leachate from TMF Ehrenfriedersdorf	Leachate from TMF Hammerberg, Freiberg
Site no.		1	2	3 <sup>1)</sup>
Flow	l/s	4-6	4	4
pH	-	7.1	7.1	<b>5.5-6.5</b>
Sulfate	mg/	40	1050	1500
Aluminum	mg/l	0.066	0.2	<b>5-14</b>
Manganese	mg/l	0.013	7.5	17
Zinc	mg/l	<b>3-4</b>	<b>4.5</b>	<b>27-57</b>
Arsenic	µg/l	<b>41</b>	<b>1500</b>	5
Cadmium	µg/l	<b>16</b>	8.3	<b>100-520</b>
Copper	µg/l	6	2.6	<b>140-1020</b>
Iron	µg/l	<0.03	<b>9000</b>	15
Nickel	µg/l	3.1	<b>270</b>	<b>94-129</b>
Lead	µg/l	<0.5	<0.5	5-18

<sup>1)</sup> Where a range is given: the lower value represents the 25% percentile, the upper value the 75% percentile, otherwise it is the arithmetic average  
 Most relevant pollutants are marked with bold letters

## 2.2 Experimental setups

Initially, column experiments were conducted with mine water from Breitenbrunn to test suitable substrates and substrate mixtures for the sustained generation of reducing conditions. These are a prerequisite for the growth of sulfate-reducing bacteria. A mixture of travertine, wood chips (22 % by volume each), chopped straw (45 %) and commercial compost (11 %) (so-called biomix) proved to be very effective in this case. Fig. 1 shows the experimental setup for the column lab-tests. After the successful start of the column tests, a field test was carried out in an intermediate bulk container (IBC) directly at the mining site no. 1 (Fig. 2). The arrangement of the substrate layers was the same as in the laboratory test. Due to the larger volume of the IBC, a scale-up factor of 100 was achieved compared to the column tests.



**Fig. 1. Experimental setup for the column tests in the laboratory**

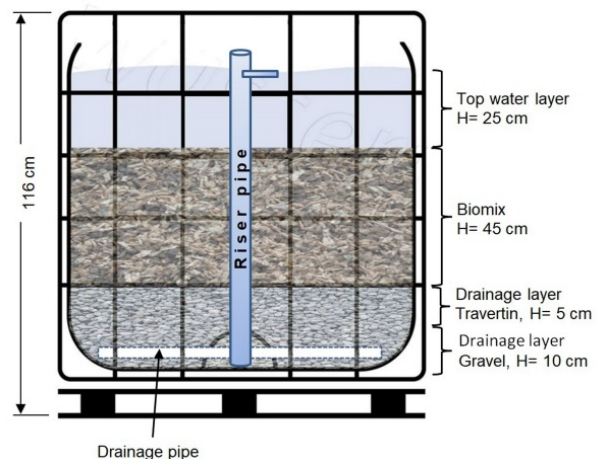


**Fig. 2. IBC used as vertical flow bioreactor for field tests with its different substrate layers**

Based on the experience with the IBC at Breitenbrunn, pilot scale experimental setups were designed for the other two mining sites. The experimental setups are somewhat more complex because iron (at site 2 Ehrenfriedersdorf) and aluminium (at site 3 Hammerberg) must be removed from the mine water in addition to the removal of Cd, Cu, Ni and Zn. In Fig. 3 and Fig. 4 drawings of the water treatment schemes at the study sites at Ehrenfriedersdorf and at Hammerberg are shown. Fig. 5 and Fig. 6 show photos of the installed equipment.

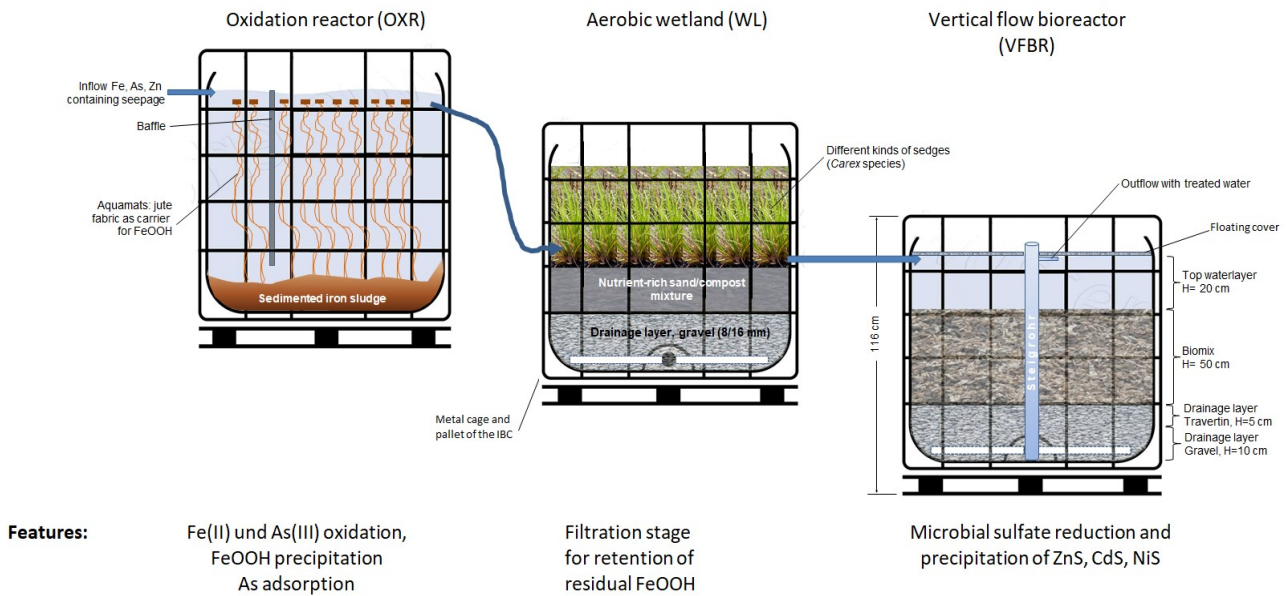


Fig. 3. Pilot scale setup for the treatment of spoil heap leachate at site no. 2 (Ehrenfriedersdorf)

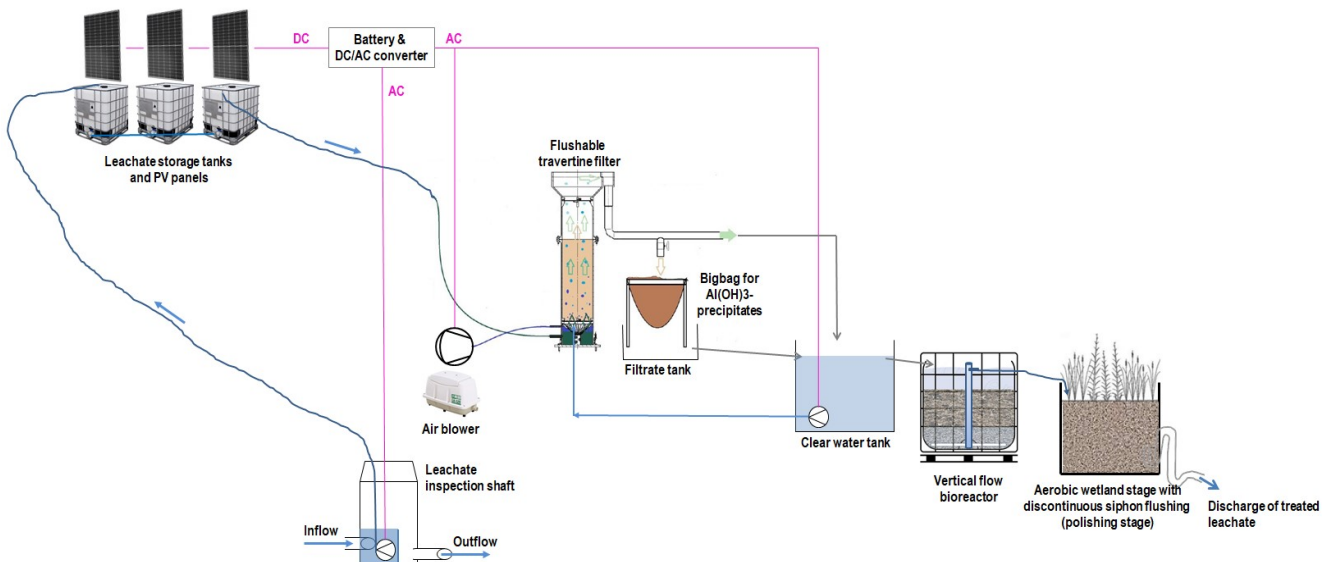


Fig. 4. Pilot scale setup for the treatment of TMF leachate at site no. 3 (Hammerberg near Freiberg)



Fig. 5. Equipment at Breitenbrunn (1) and Ehrenfriedersdorf (2)





Fig. 6. Equipment at the study site Hammerberg near Freiberg (site no. 3)

### 2.3 Microbial analyses

The microorganisms in the respective columns and pilot plants were monitored using light microscopy. Their activity was monitored by determining sulfate and sulfide concentrations. The microbial communities in the planktonic phase and the sediments were further analysed by next generation sequencing to determine the dominant taxa. Anaerobic enrichment cultures were set up using soluble substrates to cultivate sulfate-reducing microorganisms using water and sediment from the column experiments.

## 3 Results and discussion

It has to be mentioned that in all experiments (columns and VFBR-IBC) no specially cultivated SRB were added, but that the microbial sulfate reduction by the autochthonous sulfate reducers began 2-3 weeks after the start-up time.

As already reported in [3] the column experiments (Fig. 1) were conducted to test suitable substrates and substrate mixtures for the sustained generation of reducing conditions in a vertical flow reactor. A mixture of travertine, wood chips (22 % by volume each), chopped straw (45 %) and commercial compost (11 %) (so-called biomix) proved to be very effective in this case. Comparative studies with typical soluble substrates for sulfate reducers determined the advantage of the biomix and its better suitability in these processes. The microorganisms showed remarkable sulfate-reducing activity and cells were mostly attached to the solid substrate. The microbial communities in the columns were very diverse and were dominated by typical sulfate-reducing microorganisms, such as *Desulfovibrio* spp., *Methanosarcina* spp. and sulfite-reducing *Clostridium* spp.. Stable separation rates for zinc > 95 % were achieved over a period of approx. 2 years. In parallel, more systematic studies were carried out on the behavior of the metals Cd, Cu, Ni and Co as well as As. The experimental results showed high removal rates in the range of 95 – 98 % for all mentioned elements.

The results of the field test at the Breitenbrunn mine site are shown in Fig. 7. The biomix substrate in the aforementioned composition was quite effective in creating stable conditions for biochemical reduction. After an initial phase, the Zn separation was >90 %, sometimes >95 %. However, this dropped to 70 % after the start of the cold season (Oct./Nov.). The average separation performance over the entire testing period for zinc removal >95 % was determined to be 2.41 g/(m<sup>3</sup> × d) based on the volume of the biomix.

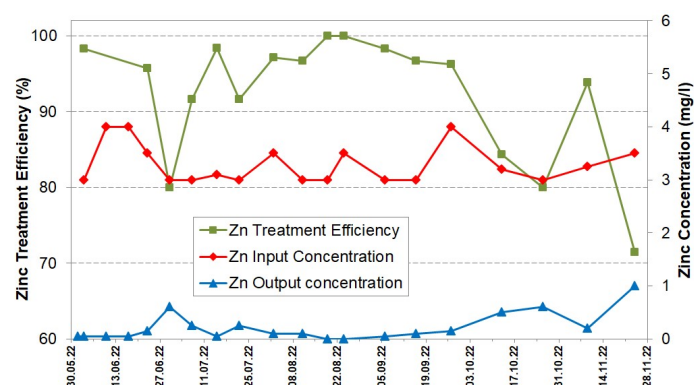
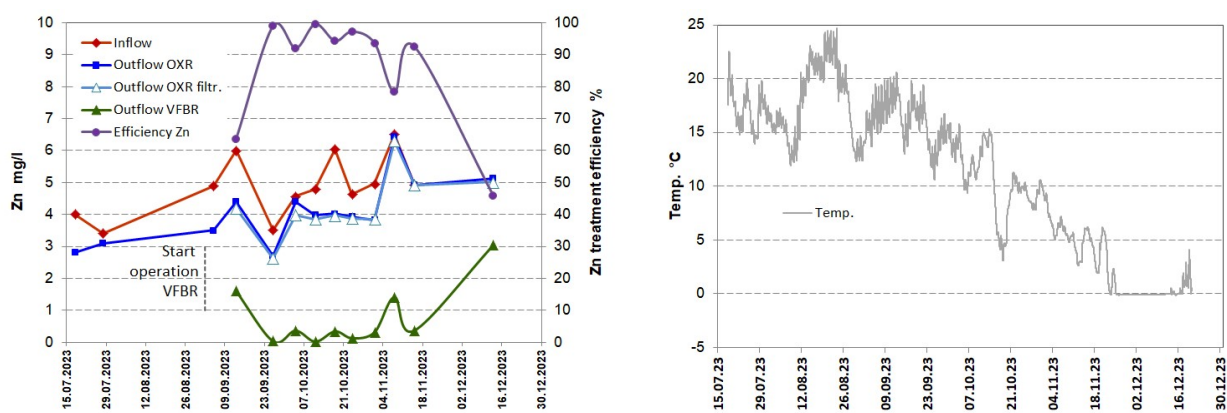


Fig. 7. Results at the mine site Breitenbrunn  
Inflow and outflow concentration of zinc during the pilot test and treatment efficiency

The results of the field test in Ehrenfriedersdorf were recently published in [2]. An almost complete oxidation of the Fe(II) and As(III) was achieved in the oxidation reactor (OXR). The retention of precipitated solids (FeOOH with adsorbed As) was not complete (70-90 %). However, the OXR outflow showed neither Fe nor As in dissolved form, but as particles. Fig. 8 shows the results for the Zn removal from the spoil heap leachate. As expected Zn passes through the OXR with low retention in the reactor which is probably caused by the partial adsorption on FeOOH. In the VFBR- after an initial delay a Zn retention of > 90 % was observed. For this site too, similar to Breitenbrunn, the treatment efficiency dropped sharply with the onset of the frost period. The same VFBR system as at site no. 1 (Breitenbrunn) was used. Following a start-up phase, the sulfate reduction started spontaneously solely due to the autochthonous SRB as before at site no. 1 (Breitenbrunn). Besides typical sulfate-reducing microorganisms, the community analysis also showed the presence of Cyanobacteria, diatoms and various common groundwater microorganisms. In order to prevent the entry of residual FeOOH into the VFBR, the system was supplemented by an intermediary IBC planted with sedges between the OXR and the VFBR. This IBC works as a filter for precipitates containing Fe and As. This new experimental setup is shown in Fig. 3 and has been in operation since July 2024.



**Fig. 8. Results for Zn removal from spoil heap leachate at the mine site Ehrenfriedersdorf (left) and temperature in the OXR (right)**

The pilot plant at Hammerberg recently started operating in July 2024. Here, too, sulfate reduction began spontaneously 3 weeks after commissioning. Results are still undergoing evaluation and are due to be published soon.

#### 4 Conclusions

Passive treatment is a suitable method for treating effluents ( $\leq 25$  l/s) from abandoned mine sites. In Saxony alone, the systematic investigations in [1] have shown a considerable number of metal-containing discharges from old adits, spoil heaps and tailing management facilities that could be treated in this way.

At the three test sites described, sulfate reduction started without inoculation with specially cultivated sulfate reducing bacteria and was maintained at a stable level. Only in the cold season, at temperatures  $< 4$  °C did the performance of the sulfate reduction and thus the metal separation drop sharply. This is a disadvantage of the experimental setup as used for cost reasons which is highly dependent on the ambient temperature.

In order to obtain more realistic design criteria in future investigations, it is planned to carry out field tests with earthworks of 1-1.7 m depth. There is a justified expectation that a satisfactory level of metal separation efficiency can also be achieved in the cold season, especially as the temperature of the mine effluents usually remains relatively constant at between 8 and 12 °C.

The same VFBR was used at the two mine sites no. 1 and no. 2 over a period of 3 years by moving it from one to the next mine site. A decrease in sulfate reduction was not observed. However, fresh substrate (biomix) can also be added if required.

Mine waters with different element combinations can be treated by a sequence of several treatment stages. In this way, clogging of the VFBR by iron and/or aluminum precipitates can be prevented.

## Acknowledgements

The research at Breitenbrunn site was financed by the Saxon State Office for Environment, Agriculture and Geology and the investigations at Ehrenfriedersdorf site are supported by the German Federal Ministry of Education and Research (BMBF) under contract no. FKZ 03WIR1906B (Project TERZinn). The pilot scale study at Hammerberg is also supported by the BMBF under contract no. FKZ 03WIR1920B within the rECOMine network [4].

## References

- [1] Martin, M., Dittrich, S., Eulenberger, S., Greif, A. Ermittlung der Belastungsquellen und Maßnahmen zur Verminderung der Bergbaubelastung im Rahmen der Umsetzung der EG Wasserrahmenrichtlinie-Zwickauer Mulde, Teilprojekte 1A-D. G.E.O.S. Ingenieurgesellschaft im Auftrag des Landesamtes für Umwelt, Landwirtschaft und Geologie des Freistaates Sachsen, Halsbrücke, 2024.
- [2] Janneck, E., Martin, M., Stevens, C., Hiller, A. Reducing water quality impacts from abandoned mines in Saxony - Challenges and benefits for passive treatment options. Proceedings of the International Mine Water Association Conference & West Virginia Mine Drainage Task Force Symposium, April 21–26, 2024, Morgantown, West Virginia, USA, p. 310-316. [online access 2024-08-31] WWW:[https://www.imwa.info/docs/imwa\\_2024/IMWA\\_2024\\_proceedings.pdf](https://www.imwa.info/docs/imwa_2024/IMWA_2024_proceedings.pdf)
- [3] Martin, M., Janneck, E., Stevens, C., Meyer, J., Hiller, A. Re-thinking passive treatment options as sustainable solution for reducing surface water quality impacts from abandoned mines in Saxony. In RE-THINKING MINING REMEDIATION - Innovative approaches towards sustainability. Extended Abstracts of the 5. International Mining Symposium WISSYM2023, p. 245-248. [online access 2024-08-31] WWW: <<https://www.wismut.de/de/wissym-2023-Kopie.php>>
- [4] rECOMine - rethinking resources [online access 2024-08-31] <<https://www.recomine.de/en/projects>>

## PROPOSAL OF THE LITHIUM-THIONYL CHLORIDE WASTE DETECTION FROM UNCONSUMED LIBS

**Natália Kabaňová<sup>a</sup>, Zita Tokárová<sup>a</sup>**

<sup>a</sup> Department of Chemistry, Institute of Chemistry and Environmental science, Faculty of Natural Sciences, University of Ss Cyril and Methodius in Trnava, Nám J. Hedru 2, 917 01 Trnava, Slovakia, kabanova1@ucm.sk

### Abstract

Lithium-ion batteries (LIBs Li/SOCl<sub>2</sub>) batteries are the most common power supplies for electric and electronic devices. Since only 5 % of used Li-ion batteries are recycled, the issue of easy detection of LIBs waste in combination with its removal became urgent. Although the lithium is not expected to bioaccumulate and its human and environmental toxicity is low the concentration of lithium/lithium ion in the surface and water possibly reaches higher amounts as is expected. Lithium is harmful for effects on embryo, glycogen synthesis, hematopoiesis and stimulate plant growth. However, the mechanism of lithium action is still unclear. We are presenting a novel manner for possible lithium-ion trapping. Using a double Schiff-base derived ligand/s, that is in fact a side product of the Ketcham reaction the nickel (II) and copper (II) complexes are formed. These are expected to exist in a form of metal-organic framework (MOF) with ability to adhere lithium/ lithium ions inside the cavity. In addition, the benzimidazole-based derivative acts as a detector and recapturing agent for thionyl chloride, as we have presented in our research quite recently.

**Keywords:** detector, double Schiff base, Lithium-ion battery, MOFs

## 1 Introduction

### 1.1 Lithium-thionyl chloride batteries (LIBs)

Composition of the LIBs consists of metallic lithium anode, a porous carbon cathode, and the non-aqueous SOCl<sub>2</sub>:LiAlCl<sub>4</sub> electrolyte. Thionyl chloride is effective as cathode and in the same time as electrolyte. The electron is released from the lithium atom according to electrochemical equations [1]:



Lithium thionyl chloride battery (SOCl<sub>2</sub>) is one of the most commonly used electric power sources effective due to the long shelf-life, stable discharge voltage, broad operation temperature range (from -50 °C to 80 °C), and high energy density [2]. Highest theoretical working voltage of LIBs is 3.6 V, excellent output specific energy (up to 590 Wh/kg) and large working temperature interval [3]. As the consequence of the self discharge of Li/SOCl<sub>2</sub> system LIBs has to be re-charged every 4-10 days [4]. Although the benefits, the basic drawback of LIBs is that almost 1/3 of stays unconsumed and goes to electric waste.

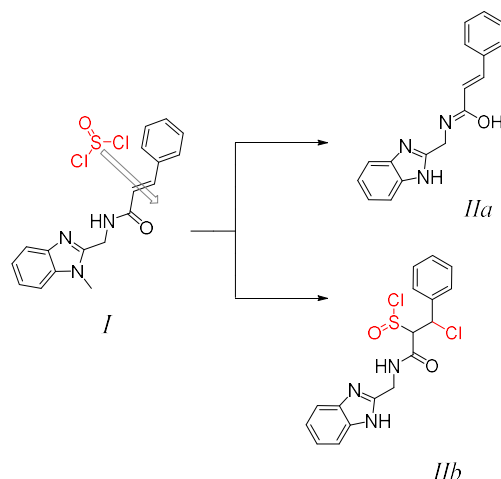
### 1.2 Detection of the thionyl chloride from LIBs batteries with tracing effect on Li<sup>+</sup>

A source of lithium posing impact to the environment is higher than expected. There are known cases when consumers routinely dispose the batteries along with other garbage in the municipal solid waste. The easy and rapid detection of SOCl<sub>2</sub> has a subsequent secondary impact on lithium's ion tracing from the noutilizable LIBs waste residuals. For this purpose we have designed and synthesized benzimidazole based detector with rapid response to the reaction with thionyl chloride. It is accompanied by an immediate color change detectable by eye (Scheme 1). These results were already prepared and accepted for publishing within IJEST [5].

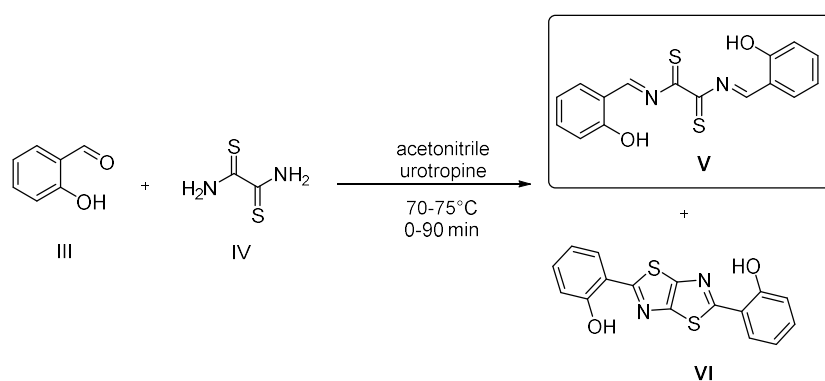
Another and more desirable detection of lithium ions could be provided by its bounding to coordination compounds able to create metal-organic frameworks (MOF).

Metal Organic Frameworks (MOFs) are crystalline porous solids composed of a three-dimensional (3D) network of metal ions held in place by multidentate organic molecules [6].

While studying the process of the Ketcham reaction we have detected a formation of by-product the double Schiff base (Scheme 2). Until now, a formation of the particular double Schiff base have been noticed only twice with no further relevance in synthesis [7, 8].



**Scheme 1. Structure of the benzimidazole based detector *N*-((1*H*-benzo[*d*]imidazol-2-yl)methyl)cinnamamide (**I**) and suggested products **IIa** and **IIb** after reaction of detector **I** with  $\text{SOCl}_2$**



**Scheme 2. Ketcham reaction (salicylaldehyde **III** with dithioamide **IV**) in acetonitrile with marked by-product - double Schiff base (**V**)**

We are now able to use possible ligand bounding with various metal ions. More specifically, coordination with  $\text{Ni}^{2+}$  and  $\text{Cu}^{2+}$  have been examined. In case of  $\text{Cu}^{2+}$  ions there are studies that suggested forming of MOFs with dithioamide as ligand. [9, 10] Together with the fact that the porous structure of MOFs could accommodate the deposited Li metal. The Co, Zn co-doping effectively improves the lithiophilicity of framework, which attracts  $\text{Li}^+$  [11]. This leads to assumption of the same detection mechanism with lithium ions. The suggestions are supported with results published by Biswal et al. in 2019 [12] showing the formation of the hexameric cluster composed of thiazolo[5,4-*d*]thiazole nickel complex building units (Figure 1). Cluster is effective as photoabsorber for solar hydrogen evolution.

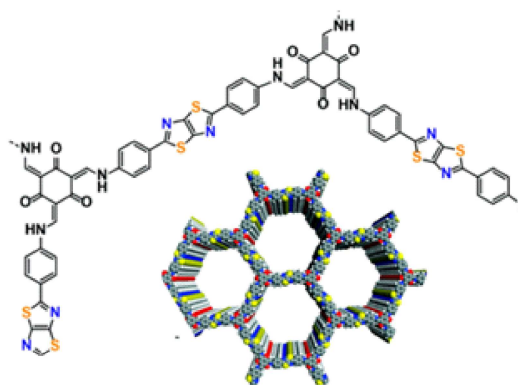


**Fig. 1. Thiazolo[5,4-*d*]thiazole-based  $\text{Ni}^{2+}$  coordination compound forming MOF-type scaffold for hydrogen absorption, according to Biswal et al. [12]**



## 2 Material and methods

### 2.1 General

All commercially available chemicals were used as received without further purification.

For synthesis of target derivate *I* have been used *o*-phenylenediamine (Thermoscientific, CAS no 95-54-5) and *N*-cinnamoylglycine 98 % (SIGMA-ALDRICH, CAS no 16534-24-0). For sensing have been used thionyl chloride (Merck, CAS no 7719-09-7).

For synthesis of target derivate *V* have been used salicylaldehyde (CAS No. 90-02-8), dithiooxamide (CAS No. 79-40-3), hexamethylenetetramine (urotropine) (CAS No. 100-97-0), acetonitrile (CAS No. 75-05-8)

For monitoring of the complex formation have been used nickel acetate and copper acetate solutions.

### 2.2 Synthesis method

Salicylaldehyde (3 mmol, 0.325 g) and dithiooxamide (3 mmol, 0.319 g) was dissolved into acetonitrile (5 ml) in the boiling flask. Subsequently, urotropin (0.3 mmol, 0.037 g) was added. The reaction mixture was heated to a temperature of 70-75 °C. From that moment, a fraction of the reaction mixture was taken regularly, every 2 minutes to 10 minutes from the start of heating. After 10 minutes (five fragments), fragments were taken every 5 minutes (four fragments) until 30 minutes of reaction time had elapsed. The next fragment was taken after 60 minutes and the last one at the end of the reaction time t. j. for 90 minutes. Fragments were taken with a volume of 0.4 ml.

### 2.3 Addition of nickel acetate - $\text{Ni}(\text{CH}_3\text{CO}_2)_2 \cdot 4 \text{H}_2\text{O}$

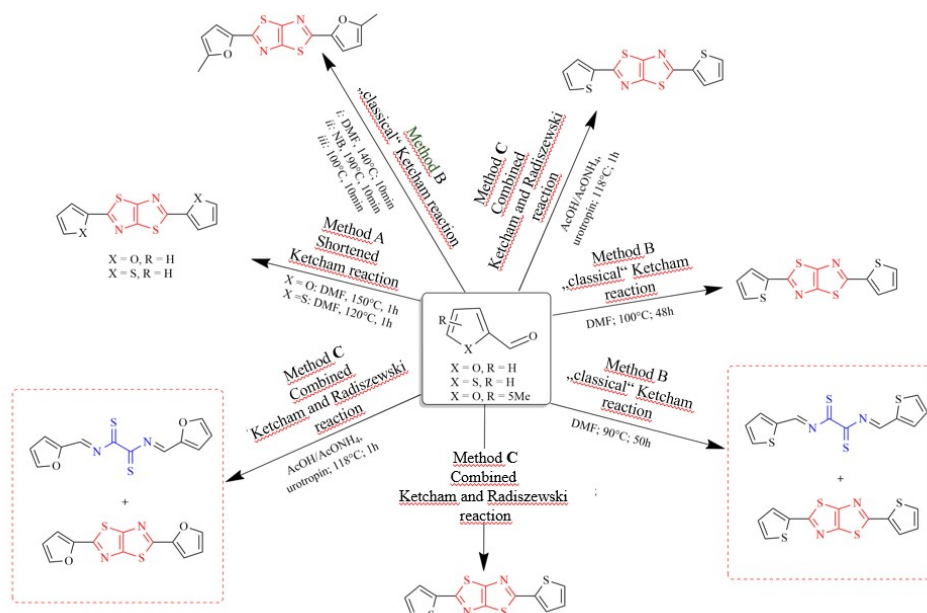
After removing and cooling fractions of the reaction mixture after 2, 4, 6, 8, 10, 15, 20, 25, 30, 60, 90 minutes, these fractions were diluted with acetonitrile to a volume of 2 ml, and the same amount of nickel acetate was added to each fraction - deep green aqueous solution. This was followed by monitoring the change in physical properties, especially the immediate color change of the solution from the original almost colorless or clear orange solutions to strongly dark blue to black solutions for all fractions taken. Another monitored phenomenon was the formation of a dark blue to black precipitated substance in the solution.

Reactions were monitored by thin layer chromatography (TLC) on plates pre-coated with silica gel (size of particles 200 - 400 mesh). <sup>1</sup>H NMR spectra were measured on a Bruker type instrument (400 MHz).

## 3 Results and discussion

The formation of possible by-product with the structure of double Schiff base ligand during the Ketcham reaction towards the thiazolo[5,4-*d*]thiazoles (Scheme 3) have prompted us to of the application potential to create the coordination compounds as scaffolds for lithium ion absorption. According to Scheme 3, it can be seen, that we have performed a series of reactions following the Ketcham reaction protocol. By varying reaction conditions not only the main products of the reaction - thiazolo[5,4-*d*]thiazoles were isolated, by under the specific conditions also the mixtures of the main product with by-product - the desired double Schiff base were identified. Reactions were performed using thiophene and furan-2-carbaldehydes.

Targeted Schiff-bases were isolated only in two-cases, both in the mixture with the main products of the Ketcham reaction, the thiazolo[5,4-*d*]thiazoles. Neverthelless, the geometry optimization by means theoretical calculations have showed that either in the case of furan-substituted double Schiff base or a ligand containing thiophene substitution are stable in a linear form (Figure 2). In fact, linear ligand are not ideal to afford coordination compounds with cross-linked scaffolds. Therefore, beyond varying the reaction conditions, the substrate - aldehyde have been switched from five-membered heterocycles to salicylaldehyde. Reaction of 1 equivalent of dithiooxamide with 1 equivalent of salicylaldehyde was conducted under the ambient reaction conditions, using acetonitrile as solvent and urotropine to maintain the pH of reaction slightly acidic (Scheme 2). Importantly, the geommetry optimization have revealed to stable bent-shaped structure of ligand *VI* as more stable over the linear (Figure 3). The bent-shaped ligand *VI* offers the coordination mode for metal ions inside the „cavity“.



Scheme 3. Synthetic efforts towards the double Schiff bases as by-products of the Ketcham reaction

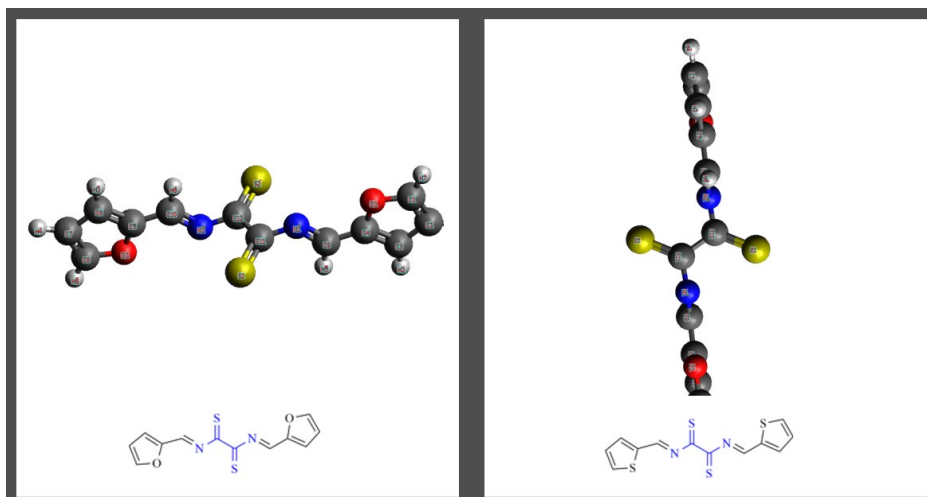


Fig. 2. Linear arrangement of furan-(left) and thiophene-substituted (right) double Schiff bases created during the Ketcham reaction towards the main products substituted thiazolo[5,4-*d*]thiazoles

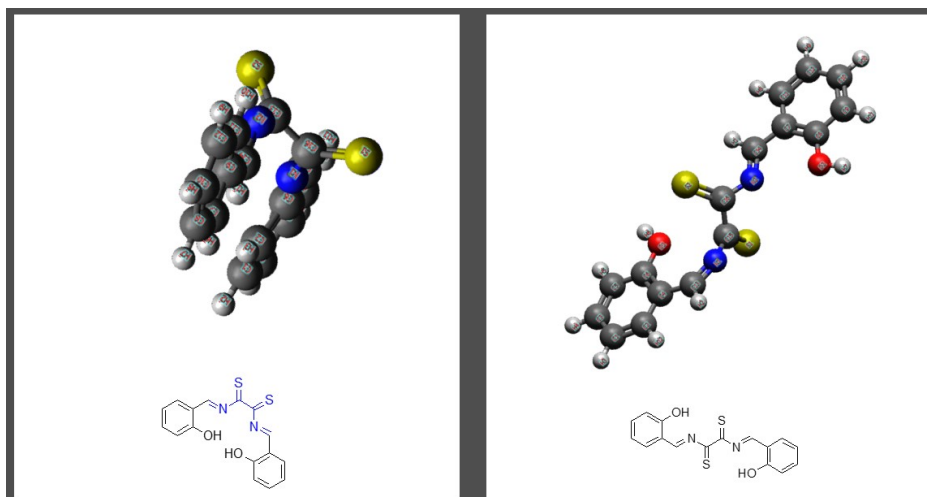
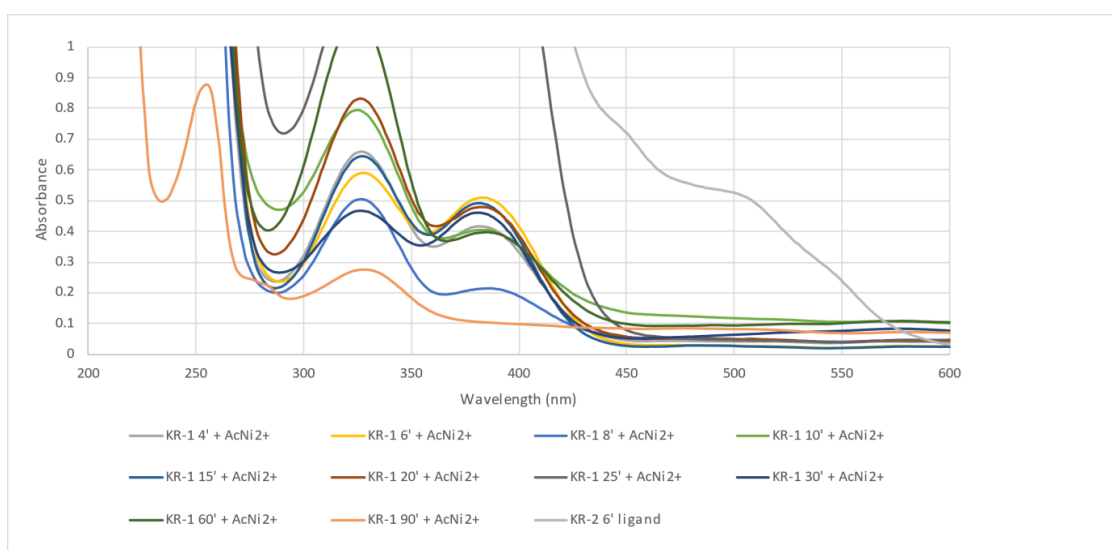


Fig. 3. Stable bent-shaped geometry of double Schiff base with the possible coordination mode inside the cavity (left) and unstable linear conformation (left)

Although the traces of double Schiff-base derived from salicylaldehyde *V* (Scheme 2) have been isolated as pure compound without the main thiazolo[5,4-*d*]thiazole *VI* (Scheme 2) and hence, proper structure have been identified, the isolation of higher amounts is challenging. As the consequence, we have performed the reaction in a manner in which the central atom in a form of nickel or copper acetate have been added to the mixture subsequently upon ligand formation. To prevent the formation of the main product, the amounts ranging from 1ml to 3 ml were removed from the reaction mixture during the processing in time intervals of minutes (4, 6, 8, 10, 15, 20, 25,30, 60 and 90 minutes). The formation of an appropriate complex was implied according to colour change as monitored by UV-Vis (Figure 4). From absorption maxima at  $\lambda_{\text{max}} = 505 \text{ nm}$  / grey line (Figure 4) it can be concluded, that double Schiff base *V* (Scheme 2) is released almost undetectably quickly, upon maximum of 4 minutes. It is evident, that after this reaction time absorption maxima falls below the visible region ( $< 400 \text{ nm}$ )  $\lambda_1 = 325 \text{ nm}$ ,  $\lambda_2 = 380 \text{ nm}$  corresponding most probably with the structure of thiazolo[5,4-*d*]thiazole *VI* (Scheme 2). Such result also confirms, that the coordination compounds derived from thiazolo[5,4-*d*]thiazole are rather rare or not possible to achieve.



**Fig. 4. Reaction monitoring of the Ketcham's reaction with the subsequent complexation with nickel acetate as the approach towards the formation of nickel complexes of double Schiff base ligand *VI***

Upon structure-identification process, what is currently quite challenging, since the isolation of stable double Schiff base *V* in higher amounts and quality are still under the progress, we will focus on a possibilities of lithium ions recapturing within the structure of isolated compounds. Herein, we are able theoretically predict the possible site of lithium ion capturing inside the coordination sphere of complex with double Schiff base as ligand and  $\text{Ni}^{2+}$  or  $\text{Cu}^{2+}$  as central atom (Figure 5). Appropriate complex should act as a building unit of crosslinked macrocycle of MOF-type. The work to that end requires further research.

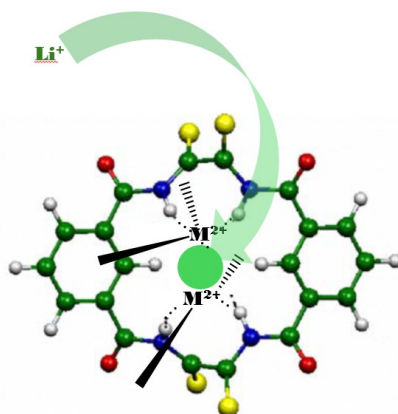


**Fig. 5. Theoretical proposal of the lithium recapturing mode inside the coordination sphere of  $\text{M}^{2+}$  complex ( $\text{M}^{2+} = \text{Ni}^{2+}, \text{Cu}^{2+}$ ) with double Schiff base *V* (Scheme 2)**

#### 4 Conclusions

To conclude, detection of the traces of thionyl chloride in environment could lead to detection of the  $\text{Li}^+$  ions from LIBs in landfills with waste from spent LIBs.

Detection of  $\text{Li}^+$  is quite desirable and we propose herein, that by the use coordination compound as a part of MOF- type cluster could be reached. Such type scaffold can act as lithium-ion absorber. Until now, by means of UV-Vis we were able to detect and distinguish between the formation of  $\text{Ni}^{2+}$  coordination compound with the double Schiff base *V* acting as ligand or pure thiazolo[5,4-*d*]thiazole created as the main product of the Ketcham reaction. Although, the structure investigation are under progress and we can currently end-up our research only with theoretical models and predictions of lithium recapturing mode, we have found, that the formation of the particular type of double Schiff base ligand is very fast process, in some cases undetectable. The Schiff base itself is suitable as ligand only if the bent-shaped geometry is preferred prior to the linear.

#### Acknowledgements

The work was supported by KEGA 009UCM-4/2004.

#### References

- [1] Katirci, G., Civan, F.E., Jung, S., Lee, C.B., Ülgüt, B. Electrochemical Impedance Spectroscopy (EIS) and non-linear harmonic analysis (NHA) of  $\text{Li-SOCl}_2/\text{SOCl}_2\text{Cl}_2$  batteries. *Electrochimica Acta*, 481, 2024, p. 143984, ISSN 0013-4686.
- [2] Martins, L.S., Guimarães, L.F., Botelho Junior, A.B., Tenório, J.A.S., Espinosa, D.C.R. Electric car battery: An overview on global demand, recycling and future approaches towards sustainability. *Journal of Environmental Management*, 295, 2021, p. 113091, ISSN 0301-4797.
- [3] Wei, J.H., Gao, X.T., Tan, S.P., Wang, F., Zhu, X.D., Yin, G.P. Acetylene Black Loaded on Graphene as a Cathode Material for Boosting the Discharging Performance of  $\text{Li/SOCl}_2$  Battery. *International Journal of Electrochemical Science*, 12 (2), 2017, p. 898-905, ISSN 1452-3981.
- [4] Sponitz, R.M., Yeduvaka, G.S., Nagasubramanian, G., Jungst, R. Modeling self-discharge of  $\text{Li/SOCl}_2$  cells. *Journal of Power Sources*, 163 (1), 2006, p. 578-583, ISSN 0378-7753.
- [5] Kabaňová, N., Tokárová, Z. Novel approach of thionyl's chloride detection and disposal using a benzimidazole-based derivative: perspectives and proposals. *International Journal of Environmental Sciences*, 2024, Accepted.
- [6] Gangu, K.K., Maddila, S., Mukkamala S.B., Jonnalagadda, S.B. A review on contemporary Metal-Organic Framework materials. *Inorganica Chimica Acta*, 446, 2016, p. 61-74, ISSN 00201693.
- [7] Bevk, D., Marin, L., Lutsen, L., Vanderzande, D., Maes, W. Thiazolo[5,4-*d*]thiazoles – promising building blocks in the synthesis of semiconductors for plastic electronics. *RSC Advances*, 3, 2013, p. 11418-11431.
- [8] Tokárová, Z., Eckstein-Andicsová, A., Balogh, R., Tokár, K. Survey of the Ketcham reaction for a series of furan-substituted thiazolo[5,4-*d*]thiazoles. *Tetrahedron*, 89, 2023, 132155.
- [9] Paul, A. Spectrophotometric Estimation of Copper(I) Using Rubeanic Acid. *Analytical Chemistry*, 35 (13), 1963, p. 2119-2121.
- [10] Gautam, R.K., Banerjee, S., Sanroman, M.A., Chattopadhyaya, M.C. Synthesis of copper coordinated dithiooxamide metal organic framework and its performance assessment in the adsorptive removal of tartrazine from water. *Journal of Environmental Chemical Engineering*, 5 (1), 2017, p. 328-340, ISSN 2213-3437.
- [11] Liu, X., Li, J., Xiao, Y., Dong, X., Tao, L., Liu, Z., Liu, Z., Zhang, J., Xu, S. The MOFs derived Co, Zn co-doping porous carbon framework as the collector for stable Li metal anodes. *Colloids and Surfaces A: Physicochemical and Engineering Aspects*, 702, 2024, 135112, ISSN 0927-7757.
- [12] Dessi, A., Calamante, M., Mordini, A., Zani, L., Taddei, M., Reginato, G. Microwave-activated synthesis of thiazolo[5,4-*d*]thiazoles by a condensation/oxidation sequence. *RSC Advances*, 4, 2014, 1322.

## NATURE-BASED RECOVERY OF METAL-POOR POST-PRODUCTION WASTES

**Waldemar Kepys<sup>a</sup>, Malgorzata Śliwka<sup>a</sup>, Malgorzata Pawul<sup>a</sup>**

<sup>a</sup>AGH University of Krakow, Faculty of Civil Engineering and Resource Management,  
Department of Environmental Engineering, 30-059 Krakow, Al. Mickiewicza 30, Poland, kepys@agh.edu.pl

### Abstract

Mining and metallurgical tailings represent a metal resource, but also a significant environmental problem. Depending on their properties, they can also be used in construction, road building, mining or land reclamation. The recovery of Zn and Pb from tailings dumped after ore processing is an example of the use of mineral wastes. This paper presents the results of a study on the possibilities of using post-flotation wastes deposited on old tailings disposal sites for land reclamation. The physical and chemical properties and ecotoxicity studies of the waste were carried out. The investigated waste is classified as silty sand, containing mainly carbonate and clay minerals and quartz. The chemical composition is mainly CaO, MgO, SiO<sub>2</sub>, Al<sub>2</sub>O<sub>3</sub>, SO<sub>3</sub> and ZnO. Despite the presence of heavy metals, their leachability does not pose a threat to the groundwater environment. Only the leachability of sulphates from the tested waste exceeds permissible quantities. The results of toxicity tests carried out on the tested waste: the *Lepidium sativum* germination test in an aqueous extract of the waste and the Phytotoxkit for the solid phase in relation to *Sorghum saccharatum*, *Lepidium sativum* and *Synapis alba* showed no phytotoxicity.

**Keywords:** post-flotation waste, waste utilization, reclamation, phytotoxicity

### 1 Introduction

The waste accumulated over many years at tailings disposal facilities, metallurgical waste dumps, metal ore tailings dumps or energy waste dumps can be anthropogenic deposits from which commercially usable raw materials can be obtained. Exploitation of such deposits contributes to the recovery of the waste stored therein, which is a substitute for natural resources, thus saving their resources and acquiring previously occupied land that can then be used in various ways. The recovery of raw materials from anthropogenic deposits, which has been ongoing for many years, nowadays fits into the model of a circular economy in force in the EU [1]. The type of potential raw materials collected in an anthropogenic deposit, as well as the profitability of their extraction, depends on a number of factors related to the source of the waste (type and quantity of waste deposited), the effectiveness of the former processing methods carried out (raw material content), the method of storage (selective, non-selective), the age of the deposit or the physical and chemical changes that have taken place within the deposit. The risks to the environment and human health from the operation of landfills are also important. All these aspects have impacted on the economic assessment of landfill mining processes [2, 3].

Non-ferrous and ferrous metals, plastics and combustible fractions (as fuels) are recovered from the landfills of municipal solid waste [4-6].

The extraction of metals from mineral landfills requires the use of technological operations known mainly from open-pit mining and processing operations used in the processing of metal ores. The result is metal concentrates and tailings that should be used as much as possible [7-9].

Base-metal tailings have been used as aggregates for mortars [10]. Reuse of these tailings produces mortars with good mechanical and durability performance, and the risk of metals release from tailings mortars is low. Thomas et al. [11] observed that copper tailing may be used as partial replacement of natural fine aggregates in cement concrete until 60 % replacement is achieved. According to [12], the best tailings reuse based on corrosion performance and cost efficiency analyses was utilisation of 5 % pre-wetted copper tailings either as a cement replacement or an additive material. Because of grain composition, post-flotation waste cannot be used in underground mines as hydraulic backfill. However, it can be used as a component of suspensions (with binding materials such as fly ash after coal combustion or cement) designed for sealing longwalls with cavings in underground mines [13].

In the case of reclamation works, the waste is used as a material or component of various blends in the technical phase to shape the relief and improve the physical and chemical properties of grounds, and in the biological phase, in the process of soil reconstruction [14, 15]. The application of waste in reclamation depends on fulfilling the requirements defined in legal acts, regarding the geo-mechanical effect of waste on

terrestrial and aquatic environment and vegetation. Thus, a certain scope of research must be conducted, including, first of all, an assessment of the amount of chemical pollutants from waste which can get into the environment, and the assessment of the impact of waste on living organisms, especially plants [16].

The article presents the results of studies on the possibility of use of post-processing waste in land reclamation. This waste was created in the process of re-flotation of old post-flotation waste after the processing of zinc and lead ores. The purpose of re-flotation was to recover metals from storage waste. Because the age of the landfill is several dozen years, the landfill was partly reclaimed, a comprehensive approach to its exploitation is important. Recovery of useful components from deposited waste, such as zinc and lead sulphides used for metal production is important, but the issue of residue management (waste) after the processing, especially after flotation, is important too. In order to avoid the build of a new repository, it is necessary to carry out a series of tests to determine the possibilities of their use. Due to environmental as well as social aspects (society's fear of exploitation of a disused landfill and construction of a new repository), it is necessary to develop methods for using this type of tailings. One of the considered possibilities of using this kind of waste is the use in engineering works. In order to determine the suitability of tested waste to the production of materials used for reclamation, tests of physical and chemical properties were carried out, as well as tests of their phytotoxic properties.

## 2 Materials and Methods

The subjects of studies were post-flotation waste, formed in the process of metal recovery from waste deposited in old repositories of a zinc and lead metallurgy plant. To define the possibilities of the utilisation of the examined waste, their physical, chemical and phytotoxic properties were determined.

Grain composition was marked with the laser diffraction method using the Analysette 22 by Fritsch. Phase composition was determined using the Philips APD PW 3020 X'Pert diffractometer. Chemical composition was determined by the Inductively Coupled Plasma Spectrometry/Atomic Emission Spectroscopy (ICP-AES) and by the Inductively Coupled Plasma Mass Spectrometry (ICP-MS) with the use of the Perkin Elmer Elan 6100 apparatus. Leachability tests were conducted according to the EN 12457-2 standard. The distilled water, with a liquid-to-solid ratio (L/S) of 10, was used as a leaching solution. The suspension was agitated in a plastic flask for 24 hours, then the mixture was filtered through a 0.45 µm membrane filter. The resulting leachate was analyzed for pH and trace elements using ICP-AES and ICP-MS methods. The amount of chlorides was analysed using the Volhard titration method.

Toxicity testing included a standard test of aqueous extract of waste in relation to the test plant (*Lepidium sativum*). The water extract was prepared from the waste (standard procedure), and then a range of solutions was prepared: 6.25 %, 12.5 %, 25 %, 50 %, and 100 %. 3 ml of the prepared solution was put to Petri dishes, lined with the filtration paper (three repetitions for each concentration); control dishes were also prepared. 10 seeds of *Lepidium sativum* were put to each dish and incubated for 72 hours. Then the length of roots was measured.

To assess the phytotoxicity of the waste, a Phytotoxkit test for the solid phase was also performed. The test is in accordance with ISO 18763. Waste and reference soil test objects (control objects) were prepared on Phytotoxkit test plates. The phytotoxicity of the waste was assessed in relation to *Lepidium sativum*, *Sorghum saccharatum* and *Sinapis alba*. Test plants were incubated in an incubator, at 25 °C in the dark. After three days, germination (germination inhibition) and early growth of test plants were assessed.

## 3 Results and discussion

The studied waste has very fine granulation (Fig. 1). It is typical of post-flotation waste and results from grinding the waste before it is flotated. Almost 50 % of grains are below 100 µm, and the maximum size of grains is 550 µm. The waste in its composition contains 68 % sand fraction and 32 % dust fraction and according to the soil classification guidelines in EN ISO 14688-2:2018 [17], the tested waste is classified as silty sand (siSa).

The dominant mineral phases are the common naturally occurring dolomite, calcite, quartz and kaolinite (Fig. 2).

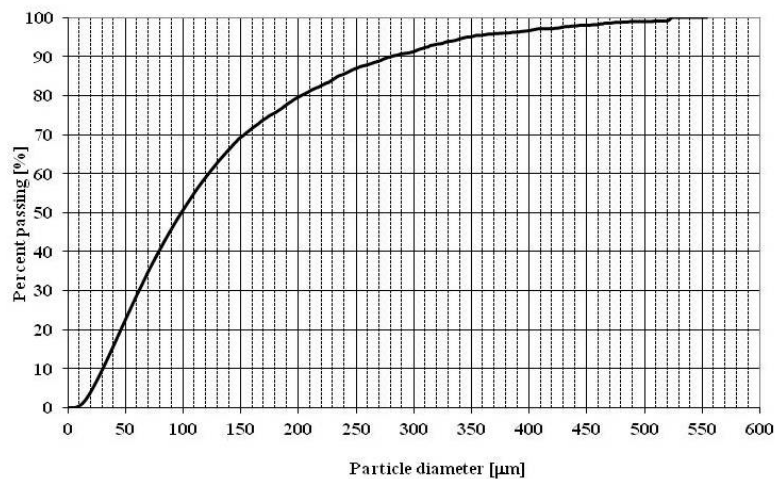


**Fig. 1. The grain size composition of the studied waste**

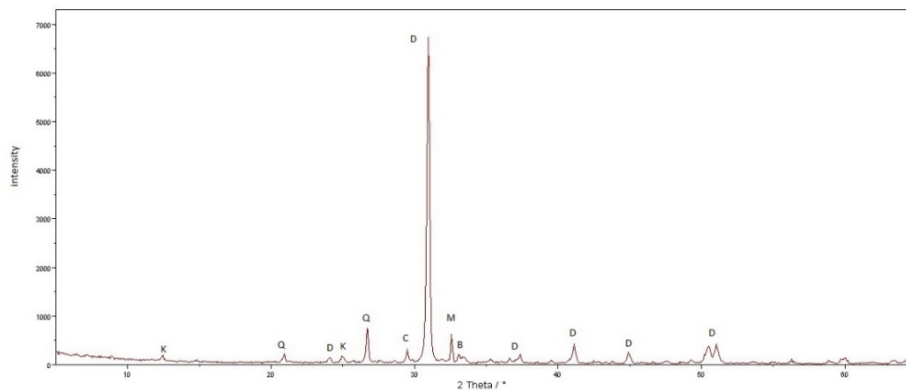


**Fig. 2. X-ray diffraction pattern of studied waste**  
(dolomite - D, quartz - Q, calcite - C, kaolinite - K, bassanite - B, merwinite - M)

Table 1 shows chemical composition of the studied post-flotation waste. The main elements are CaO, MgO, SiO<sub>2</sub>, Al<sub>2</sub>O<sub>3</sub>, which also occur in soils naturally. Note the content of ZnO and SO<sub>3</sub>, which is obvious, as the waste represents the residue from processed Zn and Pb ores.

Important problem that can arise when re-using waste for reclamation is its impact on the aquatic environment through the dissolution and leaching of substances contained in the waste. The results of the tests of leachability of the tested waste are presented in Table 2. The leachability results were compared with the upper limits of substances that are particularly harmful to the aquatic environment when introduced into soils and/or surface waters [18]. The pH value of the water extract complies with the limits. In the case of biological reclamation, the pH value has a significant impact on the growth, development and yield of plants. The most advantageous level is in the range from slightly acidic to neutral [19]. The pH values in the samples are close to neutral. Despite the presence of heavy metals in the studied waste, their leachability does not pose a threat to the aquatic environment. This is due to the occurrence of metals in bound forms, hardly soluble [20]. Only the value of sulphates exceeds the acceptable one (1354 mg SO<sub>4</sub><sup>2-</sup>/dm<sup>3</sup>, while the accepted value is 500 mg SO<sub>4</sub><sup>2-</sup>/dm<sup>3</sup>). The high leachability of sulphates, is a result of the weathering processes of sulphides present in the landfill waste, which can lead to acidification of the soil and water environment. Due to the concentration of sulphates, the direct addition of this waste to the ground is impossible. So this waste cannot be used as the final product in a reclamation process. Its application will depend on whether it can be blended with other materials to lower the leachability of pollutants, which is practiced in engineering works and usually means mixing waste in proper quantities with the subsoil and other ingredients. On the other hand, sulphur is a biogenic element, essential for plant life, which only takes it up from the soil solution in the form of sulphates. Therefore, the studied waste may have a positive effect on reducing the soil's sulphur deficit.

**Table 1. Chemical composition of post-flotation waste**

Major elements content [% dry mass]											
P <sub>2</sub> O <sub>5</sub>	Mn <sub>2</sub> O <sub>5</sub>	SiO <sub>2</sub>	Al <sub>2</sub> O <sub>3</sub>	Fe <sub>2</sub> O <sub>3</sub>	CaO	MgO	ZnO	PbO	K <sub>2</sub> O	Na <sub>2</sub> O	SO <sub>3</sub>
0.01	0.78	16.5	9.91	11.57	31.38	19.08	3.12	0.65	0.36	0.05	6.45
Trace element content [mg/kg]											
As	Cd	Cr	Cu	Co	Mo	Hg	Ni	Sn	Sr	Ti	
0.71	0.10	25.62	460.49	5.09	0.13	0.03	33.94	0.003	87.05	104.0	

**Table 2. Leachability of chemical pollutants from post-flotation waste**

Kind of pollution	Post-flotation waste [mg/dm <sup>3</sup> ]	Acceptable value according to [18] [mg/dm <sup>3</sup> ]	Kind of pollution	Post-flotation waste [mg/dm <sup>3</sup> ]	Acceptable value according to [18] [mg/dm <sup>3</sup> ]
pH	7.85	6.5-9	Mercury	0.0001	0.03
Sodium	1.48	800	Cadmium	0.0214	0.2
Potassium	2.75	80	Selenium	< 0.02	1
Calcium	499.9	no requirements	Antimony	0.00023	0.3
Magnesium	33.2	no requirements	Aluminium	0.002	3
Strontium	0.602	no requirements	Chromium	0.004	0.5
Manganese	2.039	no requirements	Molybdenum	0.015	1
Zinc	0.761	2	Titanium	< 0.002	1
Copper	0.0017	0.5	Arsenic	0.0012	0.1
Nickel	0.006	0.5	Chlorides	2.1	1000
Cobalt	0.0044	1	Sulphates	1354	500
Lead	0.0024	0.5			

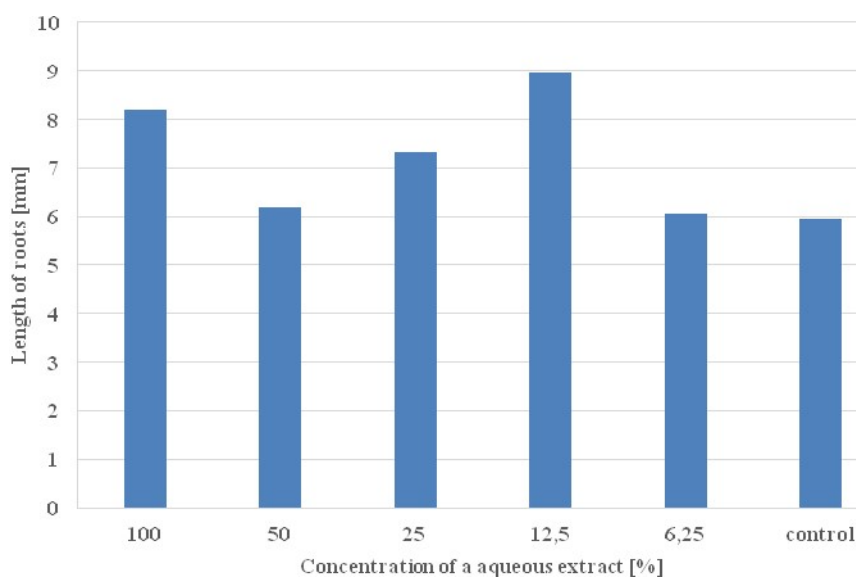


**Fig. 3. Average length of roots in water extracts**



The results of the phytotest relative to *Lepidium sativum*, carried out on waste water extracts, did not show any negative effect of the tested waste on the early growth of the test plants. In all the solutions tested, the average root lengths in the water extracts from the tested soils were longer than in the control sample (Fig. 3). This indicates that the tested wastes are not toxic to *Lepidium sativum*. The greater average root length in the test samples could indicate that the waste has stimulatory properties. To confirm or reject this thesis, Anova analysis and Tukey's post-hoc test were performed. This analysis did not show that the differences in root lengths between groups were significant. Figure 4 shows the range of root lengths in the aqueous extracts from the wastes tested.

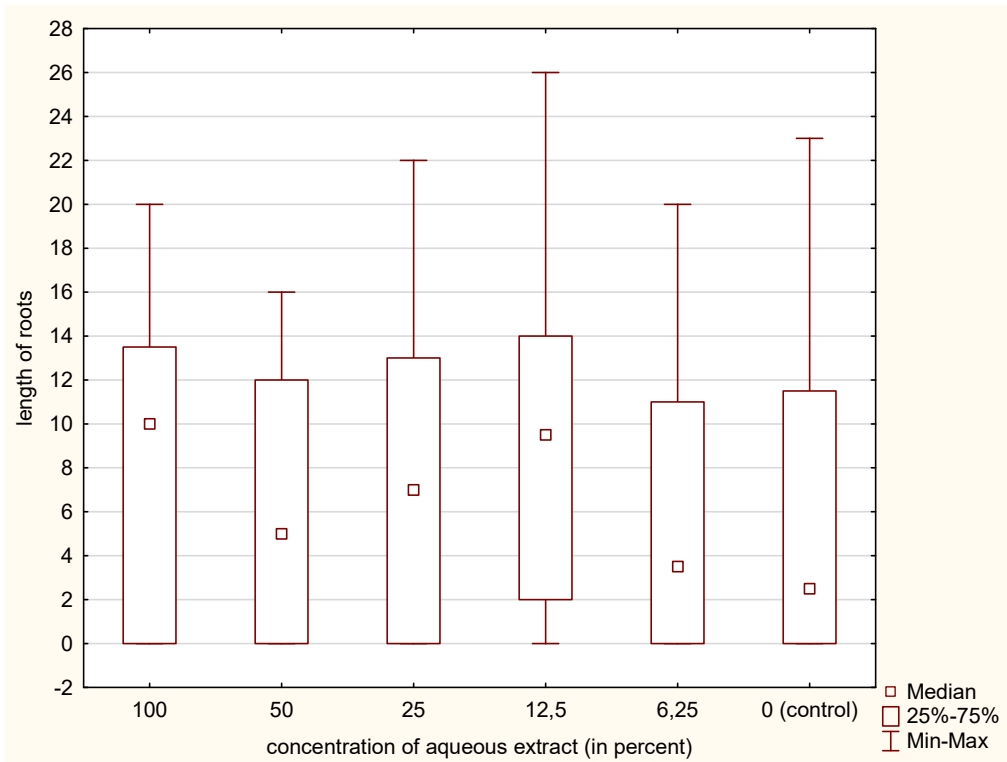


Fig. 4. Range of root lengths in water extracts from tested wastes

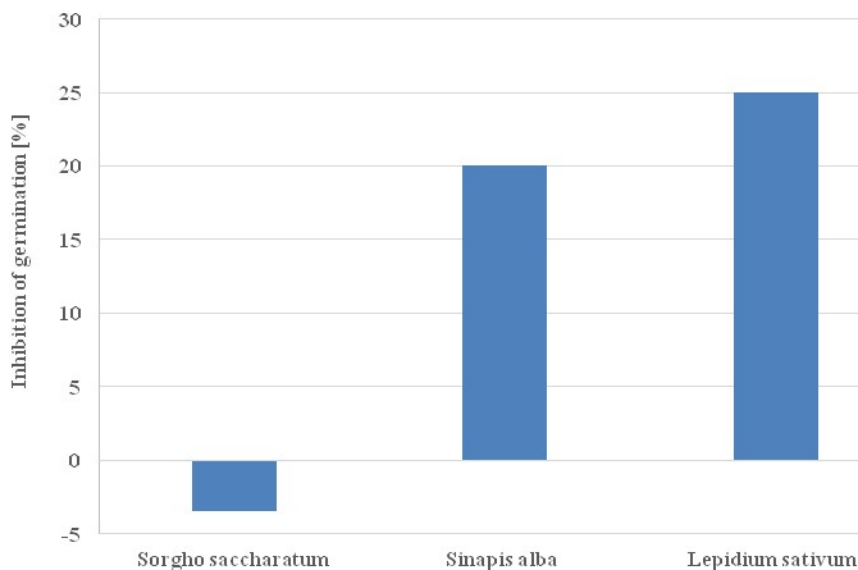


Fig. 5. Inhibition of germination in the Phytotoxkit test

On the basis of the analysis of the Phytotoxkit test results, the inhibition of plant germination in the experimental objects relative to the control objects was calculated (Fig. 5). A germination stimulation PE = -3.45 % (PE - phytotoxicity effect) was found for *Sorgho saccharatum*, no effect (PE up to 20 %) on the germination of *Sinapis alba* (PE = 20 %) and a low risk (20 % < PE ≤50 %) of *Lepidium sativum* (PE = 25 %). The different effects of the tested wastes on the germination and early growth of the test plants are related to the different environmental requirements of the species used in the Phytotoxkit test. However, no phytotoxicity of the tested wastes was found.

#### 4 Conclusions

The assessment of the properties of the examined post-flotation waste of lower content of metals was to identify the possibility of applying this waste for engineering purposes, including especially its ecological utilisation, e.g. in production a material (subsoil) for natural land reclamation.

The analysis of the granulometric composition showed that the examined material of granulation corresponds to silty sands. The main elements are CaO, MgO, SiO<sub>2</sub>, Al<sub>2</sub>O<sub>3</sub>, which also occur in soils naturally. Note the content of ZnO and SO<sub>3</sub>, which is obvious, as the waste represents the residue from processed Zn and Pb ores. When comparing waste leachability with legal requirements for wastewater released to the ground, the excess of the load of sulphate ions was found.

On the basis of the toxicity tests carried out, such as the germination test in the aqueous extract of the waste relative to *Lepidium sativum* and the standard Phytotoxkit microbiotest for the solid phase, no phytotoxicity of the mineral wastes tested was found.

The analysis of the physicochemical and ecotoxicological properties of the metal-poor post-production Zn and Pb wastes showed that the tested mineral wastes could be used as an additive to improve soil properties in the reclamation of degraded areas.

#### Acknowledgements

This work was conducted under scientific subsidy of Ministry of Education and Science (AGH No 16.16.100.215).

#### References

- [1] European Commission, Brussels, 26.1.2017, COM (2017) 33 final. Available online: [http://ec.europa.eu/environment/circular\\_economy/implementation\\_report.pdf](http://ec.europa.eu/environment/circular_economy/implementation_report.pdf).
- [2] Kieckhäfer, K., Breitenstein, A., Spengler, T.S. Material flow-based economic assessment of landfill mining processes. *Waste Management*, 60, 2017, p. 748-764, DOI: 10.1016/j.wasman.2016.06.012.
- [3] Quaghebeur, M., Laenen, B., Geysen, D., Nielsen, P., Pontikes, Y., Van Gerven, T., Spooren, J. Characterization of landfilled materials: screening of the enhanced landfill mining potential. *Journal of Cleaner Production*, 55, 2013, p. 72-83, DOI: 10.1016/j.jclepro.2012.06.012.
- [4] Rotheut, M., Quicker, P. Energetic utilisation of refuse derived fuels from landfill mining. *Waste Management*, 62, 2017, p. 101-117, DOI: 10.1016/j.wasman.2017.02.002.
- [5] Wagner, T.P., Raymond, T. Landfill mining: Case study of a successful metals recovery project. *Waste Management*, 45, 2015, p. 448-457, DOI: 10.1016/j.wasman.2015.06.034.
- [6] Masi, S., Caniani, D., Grieco, E., Lioi, D.S., Mancini, I.M. Assessment of the possible reuse of MSW coming from landfill mining of old open dumpsites. *Waste Management*, 34, 2014, p. 702-710.
- [7] Matusiak, P., Kowol, D. Application of the jug beneficiation operation for minerals recovery from mining waste deposits. *Mining Science – Mineral Aggregates*, 23, 2016, p. 115-125.
- [8] Kudełko, J., Nitek, D. Using waste from mining activity as a substitute for raw materials. *Cuprum*, 3, 2011, p. 61-63.
- [9] Zee van der, D.J., Achterkamp, M.C., de Visser B.J. Assessing the market opportunities of landfill mining. *Waste Management*, 24, 2004, p. 795-804, DOI: 10.1016/j.wasman.2004.05.004.
- [10] Argane, R., Benzaazoua, M., Hakkou, R., Bouamrane, A. Reuse of base-metal tailings as aggregates for rendering mortars: Assessment of immobilization performances and environmental behavior. *Construction and Building Materials*, 96, 2015, p. 296-306, DOI: 10.1016/j.conbuildmat.2015.08.029.
- [11] Thomas, B.S., Damare, A., Gupta, R.C. Strength and durability characteristics of copper tailing concrete. *Construction and Building Materials*, 48, 2013, p. 894-900.

- [12] Onuaguluchi, O., Eren, Ö. Reusing copper tailings in concrete: corrosion performance and socioeconomic implications for the Lefke-Xeros area of Cyprus. *Journal of Cleaner Production*, 112, 2016, p. 420-429, DOI: 10.1016/j.jclepro.2015.09.036.
- [13] Kępys, W. Residues from landfill mining as a component of waste-water suspensions. *Chemical Industry*, 96, 2017, p. 1680-1683, DOI: 10.15199/62.2017.8.10.
- [14] Śliwka, M., Pawul, M., Kępys, W., Pomykała, R. Waste management options for the combustion by-products in the context of the retardation of soil resources' depletion. *Journal of Ecological Engineering*, 18, 2017, p. 216-225, DOI: 10.12911/22998993/76213.
- [15] Śliwka, M., Uliasz-Bocheńczyk, A., Pawul, M. An appraisal of the properties of bottom waste obtained from bio-mass congestion to estimate the ways of its environmental use. *Polish Journal of Chemical Technology*, 19, 2017, p. 33-37, DOI: 10.1515/pjct-2017-0024.
- [16] Baran, A., Śliwka, M., Lis, M. Selected properties of flotation tailings wastes deposited in the Gilów and Żelazny Most waste reservoirs regarding their potential environmental management. *Archives of Mining Sciences*, 58, 2015, p. 969-978, DOI: 10.2478/amsc-2013-0068.
- [17] EN ISO 14688-2:2018. Geotechnical investigation and testing - Identification and classification of soil - Part 2: Principles for a classification.
- [18] Ordinance of the Minister of Environment of 1st September 2016 on the manner of conducting soil surface pollution assessments (Dz.U. 2016 poz. 1395) (in Polish).
- [19] Boroń, K., Klatka, S. Reaction and electrolytic conductivity of selected coal materials used in reclamation. *Ochrona Środowiska i Zasobów Naturalnych - Environmental Protection and Natural Resources*, 41, 2009, p. 385-390 (in Polish).
- [20] Baic, I. Analysis of the Chemical, Physical and Energetic Parameters of Coal Sludge Deposits Inventoried in the Silesian Province. *Rocznik Ochrona Środowiska - Annual Set The Environment Protection*, 15, 2013, p. 525-1548.



## DEVELOPMENT OF COPPER RECOVERY PROCESS FROM CALCOCITE-DOMINATED FLOTATION CONCENTRATE

Anna Khachatryan<sup>a</sup>, Narine Vardanyan<sup>a</sup>, Zaruhi Melkonyan<sup>a</sup>, Ruiyong Zhang<sup>b</sup>, Arevik Vardanyan<sup>a</sup>

<sup>a</sup>Department of Microbiology, SPC "Armbiotechnology" of the National Academy of Sciences of Armenia, 14 Gyurjyan Str., Yerevan 0056, Armenia, nvard@sci.am

<sup>b</sup>Key Laboratory of Marine Environmental Corrosion and Biofouling, Institute of Oceanology, Chinese Academy of Sciences, No. 7 Nanhai Road, Qingdao 266071, China

### Abstract

Chalcocite is the secondary sulfide mineral of copper with the highest copper concentration and is usually formed due to biooxidation reduction and migration of primary sulfide such as chalcopyrite. The understanding of copper recovery from chalcocite-dominant minerals and concentrates is critical for future applications. In this study, we evaluate the possibility of using biohydrometallurgical techniques to extract copper from chalcocite-rich copper flotation concentrate produced in Armenia. The concentrate was bioleached by mixed iron- and sulfur-oxidizing bacteria as well as indigenous strains Arm-12 and Kj, which were isolated from acid mine drainage (AMD) of polymetallic and copper mines (Armenia), respectively. In chalcocite bioleaching, the lack of iron metabolism is a key restricted factor. Therefore, the influence of exogenous ferrous and ferric iron on copper bioleaching from tested concentrate was studied. The effect of different functional parameters was also studied to optimize the process and enhance copper bioleaching efficiency.

**Keywords:** flotation concentrate, chalcocite, bioleaching of copper, sulfur-oxidizing bacteria

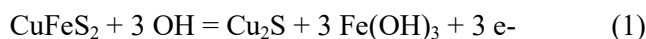
### 1 Introduction

Bioleaching is a cost-effective and environmentally friendly way to extract metals from low-grade and refractory ores. Moreover, bioleaching has gained increased attention in the last 10 years as a means of recovering copper from refractory ores and concentrates. The efficiency of copper extraction was shown to be depend of different parameters, including biological. Bioleaching of copper flotation concentrates with pure and mixed cultures of acidophilic mesophilic bacteria has been studied (Haghighi et al., 2013; Norris et al., 2010; Wang et al., 2022). Copper solubilization was highest in pure or mixed cultures including *A. ferrooxidans*. However, the use of indigenous bacterial strains and communities, adapted to the conditions of the ore, is considered to be more efficient than the application of exogenous strains (Cameron et al., 2010; Jia et al., 2016; Peng et al., 2019).

Among different parameters, mineral properties are of great importance affecting copper solubilization rates (Fu et al., 2016). Many studies have shown the feasibility of the microbial leaching of metal sulfide including secondary copper sulfides (Lee et al., 2011; Wang et al., 2020; Niu et al., 2015; Watling 2006; Zou et al., 2015; Amar et al., 2023). Investigations showed that bioleaching of copper sulfide minerals with adapted mesophilic bacterial cultures was technically feasible, and the preferential order of mineral bioleaching was chalcocite, bornite, cubanite, covellite, enargite, carrolite, chalcopyrite (Dew et al., 1999). It is well known that for copper sulphides, chalcocite and bornite are easily leached while covellite and chalcopyrite are more difficult to solubilize.

Investigations have revealed that properties of minerals, such as rest potential, lattice energy, and conductivity type are the key factors influencing the bioleaching of minerals. Among these parameters, rest potential and lattice energy can explain the difference in bioleaching of different copper sulfide minerals (Fu et al., 2016). Wu et al., 2019 investigated comparative bioleaching of secondary copper ores and pure minerals, and the mechanism of selective dissolution of chalcocite in bioleaching was explained. For pure minerals, the leaching efficiency of copper from chalcocite was higher than pyrite at the same leaching time. The authors concluded that controlling the solution potential at a lower level was beneficial to the selective leaching of chalcocite.

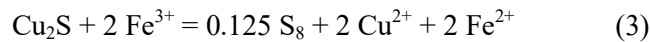
Chalcocite (Cu<sub>2</sub>S) is the main secondary copper sulfide with the highest copper content and is usually formed by oxidation of primary sulfides such as chalcopyrite (CuFeS<sub>2</sub>) (Wu et al., 2019) (Equation 1):



Chalcocite is soluble under acid and oxygenated conditions (Equation 2):



According to Equation 2, one mole of soluble copper is produced during the chemical oxidation of chalcocite. This reaction could explain the ~50 % solubilization detected in non-inoculated systems. Chalcocite can also be chemically leached by ferric iron according to Equation 3 (Schippers and Sand, 1999; Sand et al., 2001):



In chalcocite bioleaching, the lack of iron metabolism is a key restricting factor. Investigations have showed that the presence of ferrous ions (Fe (II)) or pyrite resulted in excellent copper extraction yields (Feng et al., 2021; Johnson et al., 2022). The bioleaching of chalcocite in industrial systems was improved by enhancing the iron-sulfur metabolism simultaneously using pyrite and sulfur oxidizers. In some studies, it is reported that iron and sulfur supplementation can greatly enhance bioleaching efficiency (Feng et al., 2019; Huang et al., 2019; Feng et al., 2021). Therefore, in this study, the promotion of iron and sulfur metabolism in the bioleaching of chalcocite in the presence of Fe (II) and sulfur oxidizers was explored.

However, despite a vast disparity in the composition of rocks, biohydrometallurgy proved to be an economically viable method compared to pyrometallurgical processing, allowing for robust extraction from low-grade and relatively complex copper ores and concentrates (Fu et al., 2014). Although copper recovery through bioleaching has increased worldwide (Roberto and Schippers, 2022), Armenia has no commercial experience in bioleaching operations.

This study aimed to investigate the effect of PD, pH, and particle size on the bioleaching of flotation copper concentrate using adapted indigenous bacterial strains.

The influence of exogenous  $\text{Fe}^{2+}$  and  $\text{Fe}^{3+}$  for the recovery of copper was studied as well. Indirect bioleaching of flotation copper concentrate using  $\text{Fe}^{3+}$  both biotic and abiotic origin was also studied. The surface area of the leaching solid phase can serve as an indicator of the bioleaching process. Therefore, in parallel mineralogical analyses of feed material and bioleaching residues were performed. These results may help us understand the bioleaching behaviour of secondary copper sulfide and improve the process operation.

## 2 Material and methods

### 2.1 Ore sample

A copper flotation concentrate from Syunik Province, Armenia was subjected to research. Using sieve set Analysette 3 Spartan Vibration-Siebmaschine (FRITSCHE GmbH) three fractions of copper concentrate which differed in particle size: <45  $\mu\text{m}$ ; 45-80  $\mu\text{m}$ ; 80-120  $\mu\text{m}$ ) were prepared and exposed to bioleaching tests. Copper in flotation concentrate was mainly represented by secondary sulfides (Table 1). 55-60 % of sulfide minerals consist of pyrite, 25-30 % secondary copper-rich sulfide minerals (bornite, chalcocite, covellite), 7-8 % chalcopyrite, as well as sphalerite, native copper, molybdenite, and possibly copper oxides associated with iron hydroxides. Other minerals were also present up to 7-8 %. Copper oxides do not exceed 1.5 wt.%. Sulfur was mostly presented in sulfide form.

**Table 1. Mineralogical analysis of the concentrate**

	Content, %									
	$\text{Cu}_{\text{total}}$	$\text{Cu}_{\text{oxide}}$	$\text{Cu}_{\text{secondary sulf.}}$	$\text{Cu}_{\text{primary sulf.}}$	$\text{S}_{\text{total}}$	$\text{S}_{\text{oxide}}$	$\text{S}_{\text{sulf.}}$	$\text{Fe}_{\text{total}}$	$\text{Fe}_{\text{oxide}}$	$\text{Fe}_{\text{sulf.}}$
Flotation concentrate	23.90	1.40	20.22	2.28	39.59	0.13	39.46	29.20	0.43	28.77

### 2.2 Leaching experiments

Bioleaching of copper flotation concentrate was performed using ArM1 native consortium as well as their association with *At. thiooxidans* SO-1 (KP455985) (Vardanyan and Vardanyan 2014). Bioleaching experiments were carried out in 250 mL Erlenmeyer flasks containing 100 mL of MAC (Mackintosh 1978) medium without iron ion at 30 °C, 180 rpm. The influence of PD (5; 10; and 15 %), pH (1.2; 1.5, and 1.8) as well as exogenous ferrous ion (Fe (II)) concentration (0.5 g/L; 1.0 g/L) were investigated. Bioleaching of

copper concentrate by an adapted consortium was also carried out. The amount of inoculum for used cultures was 10 %. All experiments were carried out in triplicate. For each bioleaching experiment chemical controls with the same conditions and without inoculum were included.

### 2.3 Physicochemical analyses

pH and redox potential were determined with a pH/mV Meter SevenExcellence (Mettler Toledo, Latvia) Copper and total iron were determined by a Microwave plasma atomic emission spectrometer (MP-AES, Agilent 4210). Concentrations of ferric (Fe(III)) and ferrous (Fe(II)) ions were determined by the complexometric method with EDTA (Lucchesi and Hirn, 1960).

## 3 Results and discussion

### 3.1 Effect of PD

To determine the optimal PD, experiments on bacterial leaching of copper flotation concentrate were carried out at 5, 10, and 15 % (Table 2). According to Table 4, the highest level of copper recovery (84 %) was observed at 5 % PD after 21 days of leaching. At a PD of 10 and 15 %, the extent of copper extraction decreased by approximately 1.5-2 times.

**Table 2. Influence of ferrous iron (Fe (II)) ions and sulfur-oxidizing bacteria *At. thiooxidans* SO-1 on bioleaching of copper by ArM1 ad consortium, (PD - 10 %; T=30 °C; 180 rpm)**

Sample	0		3		6	
	mg/L	%	mg/L	%	mg/L	%
ArM1 ad	4749	24.5	10468	54.1	14872	76.6
ArM1 ad + 0.5 g/L Fe (II)	4534	23.4	9399	48.4	15423	79.5
ArM1 ad +1.0 g/L Fe (II)	4534	23.4	11536	59.5	17625	90.8
ArM1 ad + <i>At.thiooxidans</i> SO-1	3890	20.1	8865	45.7	15280	78.7
ArM1 ad + <i>At.thiooxidans</i> SO-1+0.5 g/L Fe(II)	4581	23.0	9933	51.2	19170	98.8
Arm-12 ad + <i>At.thiooxidans</i> SO-1 +1.0 g/L Fe(II)	4581	23.0	10468	53.9	19715	101
<i>At. thiooxidans</i> SO-1	4749	24.5	11536	59.5	9918	51.1

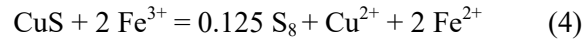
### 3.2 Effect of ferrous ions

In some studies, it is reported that iron and sulfur supplementation can greatly enhance copper bioleaching efficiency (Fu et al., 2016; Feng et al., 2019; 2021). Therefore, in this study, the promotion of iron and sulfur metabolism in the bioleaching of chalcocite in the presence of Fe (II) and sulfur oxidizers was explored. The influence of ferrous iron Fe (II) on the extraction of copper during bioleaching of copper concentrate with the ArM1 was studied. For this purpose, simultaneously with inoculation by ArM1, ferrous iron (Fe (II)) was added to the leaching medium at concentrations of 0.5 and 1.0 g/L (in the form of FeSO<sub>4</sub>·7H<sub>2</sub>O). According to Table 3, copper extraction by ArM1 was 76.6 % without the addition of iron ions for 6 days. Meanwhile, with the addition of Fe (II) ions in amounts of 0.5 and 1.0 g/L, the extraction of copper in the same period increased to 79.5 % and 90.8 %, respectively (Table 3). These results were in agreement with the research conducted by Haghghi et al., 2013, who reported that the addition of ferrous iron significantly increased the rate and extent of copper dissolution.

**Table 3. Influence of ferrous iron (Fe (II)) ions and sulfur-oxidizing bacteria *At. thiooxidans* SO-1 on bioleaching of copper by ArM1 ad consortium, (PD - 10%; T=30 °C; 180 rpm)**

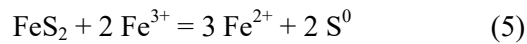
Sample	0		3 Days		6 Days	
	mg/L	%	mg/L	%	mg/L	%
ArM1 ad	4749	24.5	10468	54.1	14872	76.6
ArM1 ad + 0.5 g/L Fe(II)	4534	23.4	9399	48.4	15423	79.5
ArM1 ad +1.0 g/L Fe(II)	4534	23.4	11536	59.5	17625	90.8
ArM1 ad + <i>At.thiooxidans</i> SO-1	3890	20.1	8865	45.7	15280	78.7
ArM1 ad + <i>At.thiooxidans</i> SO-1+0.5 g/L Fe(II)	4581	23.0	9933	51.2	19170	98.8
Arm-12 ad + <i>At.thiooxidans</i> SO-1 +1.0 g/L Fe(II)	4581	23.0	10468	53,9	19715	101.0
<i>At. thiooxidans</i> SO-1	4749	24.5	11536	59.5	9918	51.1

As mentioned above, chalcocite is soluble in acid conditions in the presence of oxygen (Equation 2). However, chalcocite can also be oxidized by ferric iron (Equation 3) (Schippers and Sand, 1999; Sand et al., 2001). Moreover, ferric iron can “attack” covellite releasing another mole of copper, as presented in Equation 4 (Amar et al., 2023):



In the inoculated bioleaching systems in general and case of bioleaching of used flotation concentrate iron-oxidizing bacteria can oxidize the soluble ferrous iron supplying ferric iron to the solution and feeding Equations 3 and 4.

Besides the flotation concentrate used in this study is rich in pyrite. Consequently, during bioleaching of copper concentrate iron-oxidizing bacteria may contribute to not only chalcocite but also pyrite oxidation thus supplying ferric iron (Fe (III) to the leaching system (Equation 5):



The solubilized iron from the concentrate can stimulate both chalcocite and covellite dissolution. Fu et al., 2016 showed that the optimum concentration of ferrous ions was 1.5 g/L for bioleaching of djurleite and chalcopyrite (an inoculum of  $0.5 \times 10^8$  cells and the initial of L21). The initial ferrous ion concentrations optimal for bornite and covellite bioleaching were 4.5 g/ L (Fu et al., 2016).

Although the copper concentrate used in this study contains iron-bearing mineral pyrite that can provide the available iron sources for the growth of bacteria, the addition of ferrous iron to the culture medium significantly promotes copper extraction from the concentrate.

Wu et al., 2019 reported preferential bioleaching rates of copper minerals in copper ore with a high content of pyrite. It was shown that in the case of pure minerals, the leaching efficiency of chalcocite was higher than pyrite while bacteria increased the bioleaching efficiency of pyrite and chalcocite simultaneously by oxidizing  $\text{Fe}^{2+}$  to  $\text{Fe}^{3+}$  in the solution.

### 3.3 Influence of sulfur-oxidizing bacteria

*A. thiooxidans* is essential in bioleaching of metals from sulfide ores as reported by Feng et al., 2019. The effect of ferrous iron Fe (II) in combination with the sulfur-oxidizing bacterium *Acidithiobacillus thiooxidans* SO-1 on the decomposition of copper concentrate by ArM1 was studied. To do this, in addition to ArM1 consortium, Fe (II) ions in concentrations of 0.5 and 1.0 g/L, the sulfur-oxidizing bacterium *At. thiooxidans* SO-1 was added to the leaching medium. In this case, the concentrate was leached at 10 % PD, and ArM1 adapted (ad) consortium was used, which was previously adapted to 7 and 10 % PD (Table 3).

The data in Table 3 show that the use of the sulfur-oxidizing bacterium *At. thiooxidans* SO-1, leads to an increase in copper extraction compared to the ArM1 consortium. Besides, *At. thiooxidans* SO-1 and Fe (II) in a concentration of 0.5 g/L had the same effect on the bioleaching of copper concentrate. It should be noted that when *At. thiooxidans* SO-1 and Fe (II) were added to the leaching medium simultaneously with the inoculum (ArM1), copper extraction increased significantly reaching 99-101 %.

**Table 4. Influence of ferrous iron Fe (II) ions and *At. thiooxidans* SO-1 on leaching of copper, zinc, and ArM1 ad., (PD – 10 %; pH 1.8, T=30 °C; 180 rpm)**

Sample	%		
	Cu	Fe	Zn
Control	49.3	0.2	21.2
Control 1.0 g/L Fe(II)	54.5	5.99	24.8
ArM1 ad	79.5	5.6	58.9
ArM1 ad + 0.5 g/LFe(II)	90.6	13.2	86.2
ArM1 ad + 1.0 g/L Fe(II)	95.2	17.2	90.7
ArM1 ad + <i>At.thiooxidans</i> SO-1	77.8	10.0	72.4
ArM1 ad + <i>At.thiooxidans</i> SO-1+ 0.5 g/L Fe(II)	83.4	13.0	81.7
ArM1 ad + <i>At.thiooxidans</i> SO-1+1.0 g/L Fe(II)	83.16	15.2	81.0
<i>At.thiooxidans</i> SO-1	43.3	1.0	17.9



The use of *At. thiooxidans* SO-1 and Fe (II) also help to increase the extraction of zinc and iron by the adapted culture ArM1 consortium (Table 4). It should be noted that under the best conditions determined for copper extraction, maximum recovery was also observed for zinc and iron.

#### 4 Conclusions

This work was aimed at evaluation of a copper bio-recovery process from flotation concentrate via indigenous cultures. Compared to the abiotic control (chemical acid leaching), the extraction of copper from the concentrate increased approximately 2 times in the presence of ArM1 native consortium. The greatest amount of copper extraction by ArM1 consortium was observed at pH 1.8 and a PD of 5 %, particle sizes less than 45 microns, and between 45 to 80 microns. The use of an adapted consortium obtained by growing ArM1 with gradually increasing amounts of concentrate (PD 7 and 10 %), will significantly enhance the process rate and increase copper extraction about 1.3 times in comparison to the non-adapted consortium. The use of *At. thiooxidans* SO-1 and Fe (II) help to increase the extraction of copper as well as zinc and iron by the adapted consortium ArM1. It should be noted that under the best conditions determined for copper extraction, maximum recovery was also observed for zinc and iron.

#### Acknowledgements

This work was supported by the Higher Education and Science Committee of the Ministry of Science, Education, Culture, and Sports of the Republic of Armenia under Research project Grant number No. 22r1-031 and the Young Scientist Support Program Research project Grant number 23-YSIP-012.

#### References

- [1] Wang, L.M., Yin, S.H., Deng, B.N., Wu, A.X. Copper sulfides leaching assisted by acidic seawater-based media: ionic strength and mechanism. *Minerals Engineering*, 175, 2022, 107286.
- [2] Fang, X.D., Sun, S.Y., Liao, X.J., Li, S.P., Zhou, S.Y., Gan, Q.W., Zeng, L.T., Guan, Z.J. Effect of diurnal temperature range on bioleaching of sulfide ore by an artificial microbial consortium. *Science of The Total Environment*, 806, 2022, 150234.
- [3] Haghghi, H.K., Moradkhani, D., Sedaghat, B., Najafabadi, M.R., Behnamfard, A. Production of copper cathode from oxidized copper ores by acidic leaching and two-step precipitation followed by electrowinning. *Hydrometallurgy*, 133, 2013, p. 111-117.
- [4] Norris, P.R., Davis-Belmar, C.S., Nicolle, J.L.C., Calvo-Bado, L.A., Angelatou, V. Pyrite oxidation and copper sulfide ore leaching by halotolerant, thermotolerant bacteria. *Hydrometallurgy*, 104 (3-4), 2010, p. 432-436.
- [5] Peng, T., Chen, L., Wang, J., Miao, J., Shen, L., Yu, R., Gu, G., Qiu, G., Zeng, W.D. Dissolution and passivation of chalcopyrite during bioleaching by *Acidithiobacillus ferrivorans* at low temperature. *Minerals*, 9 (6), 2019, 332.
- [6] Cameron, R.A., Yeung, C.W., Greer, C.W., Gould, W.D., Mortazavi, S., Bédard, P.L., Morin, L., Lortie, L., Dinardo, O., Kennedy, K.J. The bacterial community structure during bioleaching of a low-grade nickel sulphide ore in stirred-tank reactors at different combinations of temperature and pH. *Hydrometallurgy*, 104 (2), 2010, p. 207-215.
- [7] Jia, Y., Sun, H., Chen, D., Gao, H., Ruan, R. Characterization of microbial community in industrial bioleaching heap of copper sulfide ore at Monywa mine, Myanmar. *Hydrometallurgy*, 164, 2016, p. 355-361.
- [8] Johnson, D.B., Bryan, C.G., Schlömann, M., Roberto, F.F. *Biomining Technologies: Extracting and Recovering Metals from Ores and Wastes*. Switzerland: Springer Nature, 2022.
- [9] Fu, K., Ning, Y., Chen, S., Wang, Z. Bioleaching of different copper sulphide minerals and their physicochemical properties dependence. *Mineral Processing and Extractive Metallurgy*, 125 (1), 2016, p. 1-4.
- [10] Wang, X., Ma, L., Wu, J., Xiao, Y., Tao, J., Liu, X. Effective bioleaching of low-grade copper ores: Insights from microbial cross experiments. *Bioresource Technology*, 308, 2020, 123273.
- [11] Lee, J., Acar, S., Doerr, D.L., Brierley, J.A. Comparative bioleaching and mineralogy of composited sulfide ores containing enargite, covellite and chalcocite by mesophilic and thermophilic microorganisms. *Hydrometallurgy*, 105(3-4), 2011, p. 213-221.

- [12] Niu, X., Ruan, R., Tan, Q., Jia, Y., Sun, H. Study on the second stage of chalcocite leaching in column with redox potential control and its implications. *Hydrometallurgy*, 155, 2015, p. 141-152.
- [13] Watling, H.R. The bioleaching of sulphide minerals with emphasis on copper sulphides - A review. *Hydrometallurgy*, 84 (1-2), 2006, p. 81-108.
- [14] Zou, G., Papirio, S., Lai, X., Wu, Z., Zou, L., Puhakka, J.A., Ruan, R. Column leaching of low-grade sulfide ore from Zijinshan copper mine. *International Journal of Mineral Processing*, 139, 2015, p. 11-16.
- [15] Amar, A., Massello, F.L., Costa, C.S., Castro, C., Donati, E.R. Bioleaching of a Chalcocite-Dominant Copper Ore from Salta, Argentina, by Mesophilic and Thermophilic Microorganisms. *Minerals*, 13 (1), 2023, 52.
- [16] Dew, D.W., Van, B.C., Mcewan, K., Bowker, C. Bioleaching of base metal sulphide concentrates: a comparison of mesophile and thermophile bacterial cultures. In Amils, R., Ballester, A., eds., *Biohydrometallurgy and environment towards the mining of 21st century*, parts A, Amsterdam, Netherlands, 1999, p. 229.
- [17] Wu, B., Yang, X., Wen, J., Wang, D. Semiconductor-Microbial Mechanism of Selective Dissolution of Chalcocite in Bioleaching. *ACS Omega*, 4 (19), 2019, p. 18279-18288.
- [18] Schippers, A., Sand, W. Bacterial leaching of metal sulfides proceeds by two indirect mechanisms via thiosulfate or via polysulfides and sulfur. *Applied and environmental microbiology*, 65 (1), 1999, p. 319-321.
- [19] Sand, W., Gehrke, T., Jozsa, P.G., Schippers, A. (Bio)chemistry of bacterial leaching-Direct vs. indirect bioleaching. *Hydrometallurgy*, 59 (2-3), 2001, p. 159-175.
- [20] Feng, S., Yin, Y., Yin, Z., Zhang, H., Zhu, D., Tong, Y., Yang, H. Simultaneously enhance iron/sulfur metabolism in column bioleaching of chalcocite by pyrite and sulfur oxidizers based on joint utilization of waste resource. *Environmental Research*, 194, 2021, 110702.
- [21] Feng, S.S., Li, K.J., Huang, Z.Z., Tong, Y.J., Yang, H.L. Specific mechanism of *Acidithiobacillus caldus* extracellular polymeric substances in the bioleaching of copper-bearing sulfide ore. *PloS One*, 14 (4), 2019, 18.
- [22] Huang, Z., Feng, S., Tong, Y., Yang, H. Enhanced 'contact mechanism' for interaction of extracellular polymeric substances with low-grade copper-bearing sulfide ore in bioleaching by moderately thermophilic *Acidithiobacillus caldus*. *Journal of Environmental Management*, 242, 2019, p. 11-21.
- [23] Fu, K.B., Lin, H., Luo, D.Q., Jiang, W.F., Zeng, P. Comparison of bioleaching of copper sulphides by *Acidithiobacillus ferrooxidans*. *African Journal of Biotechnology*, 13(5), 20014, p. 664-672.
- [24] Roberto, F.F., Schippers, A. Progress in bioleaching: Part B, applications of microbial processes by the minerals industries. *Applied Microbiology and Biotechnology*, 106, 2022, p. 5913-5928.
- [25] Vardanyan, N.S., Vardanyan, A.K. New Sulphur Oxidizing Bacteria Isolated from Bioleaching Pulp of Zinc and Copper Concentrates. *Universal Journal of Microbiology Research*, 2 (2), 2014, p. 27-31.
- [26] Mackintosh, M.E. Nitrogen Fixation by *Thiobacillus ferrooxidans*. *Journal of General Microbiology*, 105 (2), 1978, 215.

## INDIGENOUS ASSOCIATION PERSPECTIVE FOR COPPER BIOLEACHING

**Anna Khachatryan<sup>a</sup>, Narine Vardanyan<sup>a</sup>, Zaruhi Melkonyan<sup>a</sup>, Ruiyong Zhang<sup>b</sup>, Arevik Vardanyan<sup>a</sup>**

<sup>a</sup>Department of Microbiology, SPC “Armbiotechnology” of the National Academy of Sciences of Armenia, 14 Gyurjyan Str., Yerevan 0056, Armenia, [anna.khachatryan@asnet.am](mailto:anna.khachatryan@asnet.am)

<sup>b</sup>Key Laboratory of Marine Environmental Corrosion and Biofouling, Institute of Oceanology, Chinese Academy of Sciences, No. 7 Nanhai Road, Qingdao 266071, China

### Abstract

For biomining specialized microorganisms are used in order to recover valuable metals from ores via bioleaching. Important leaching bacteria are aerobic, acidophilic iron (II)- and/or sulfur compound-oxidizing species such as for example *Acidithiobacillus ferrooxidans*, mix cultures and indigenous consortium. Armanis is a Gold-Polymetallic Mine. Optimizing process parameters to guarantee the highest effective recovery of copper from the tested concentrate was the primary goal. Pure cultures of iron- and sulfur-oxidizing bacteria, as well as their association were used in the bioleaching of copper concentrate. Comparative studies on bioleaching of copper by the association of acidophilic iron and sulfur-oxidizing bacteria as well as native consortium Arm, isolated from acid mine drainage were carried out. At the beginning of the bioleaching process, the amounts of extracted copper by mixed culture and Arm consortium were equal, afterward the Arm indigenous consortium exhibited higher activity in terms of copper extraction. The application of molecular biological method (metagenomic) allowed more completely revealing the composition of bacterial communities in AMD of Armanis Gold-Polymetallic mine. By using metagenomics techniques, it was shown that water outflow samples contained the following genera: *Acidithiobacillus*, *Leptospirillum*, as well as *Acidiphilium* and other heterotrophic reducing bacteria.

**Keywords:** acid mine drainage, copper concentrate, biomining, bioleaching bacteria, indigenous consortium, metagenomics analysis

### 1 Introduction

Microorganism-based metal recovery from low-grade ores and mineral concentrates is an important and rapidly developing field of biotechnology. Using iron- and sulfur-oxidizing microorganisms to catalyze the dissolution of valuable metals from sulfide ores or concentrates is known as bioleaching (Méndez-García et al., 2015; Johnson and Quatrini, 2020). Acid mine drainage (AMD) is a very acidic effluent containing high levels of sulfates, metals, and sulfides. AMD management requires particular attention in order to avoid environmental adversity. AMDs are extremely acidic runoff formations that originate from the microbial oxidation of pyrite and other sulfide minerals, which results in the production of sulfuric acid and metal-rich solutions. AMD systems are common in our planet, although only a limited number of them have been microbiologically characterized (Méndez-García et al., 2015; Johnson and Quatrini, 2020). Major bacterial lineages detected in AMD systems include the phyla *Proteobacteria* (*Acidithiobacillus*, *Acidiphilium*, *Acidocella*, *Acidicaldus*, *Acidomonas*, *Acidisphaera*, “*Ferrofum*”, *Acidibacter*, and *Metallibacterium* spp.), *Nitrospirae* (*Leptospirillum* spp. such as *Leptospirillum ferrooxidans*, *Leptospirillum ferriphilum*, and *Leptospirillum ferrodiazotrophum*), *Actinobacteria*, *Firmicutes* (*Sulfobacillus* spp., and *Alicyclobacillus* spp.) and *Acidobacteria*. Archaea include the phyla *Euryarchaeota* (*Ferroplasma* spp. such as *Ferroplasma acidiphilum* and “*Ferroplasma acidarmanus*” *Acidiplasma cupricumulans*, and *Cuniculiplasma divulgatum* (Golyshina et al., 2000, 2009, 2016; Dopson et al., 2004; Baker et al., 2006, 2010; Golyshina, 2011; Chen et al., 2016, 2018; Gavrillov et al., 2019; Korzhenkov et al., 2019). These microorganisms are expected to be reservoirs of enzymes selected to resist acidic harsh conditions (at least regarding extracellular products) (Sharma et al., 2012), some of which might be of biotechnological relevance (Gomes et al., 2003; Adrio and Demain, 2014). Under the extremophilic AMD environment, acidophilic microbial communities belonging to Bacteria, Archaea, and Eukarya domains dominate, with members of phylum *Proteobacteria*, *Nitrospira*, *Actinobacteria*, *Firmicutes*, and *Acidobacteria* being the dominant bacterial taxa (Mesa et al., 2017; Lukhele et al., 2019; Distaso et al., 2020), as well as iron/sulfur-oxidizing microbes such *Leptospirillum Ferrofum*, *Acidothiobacillus* occurring in an environmentally dependent biogeographic pattern (Kuang et al., 2013, 2016; Wang et al., 2019b).

## 2 Material and methods

### 2.1 Bioleaching assays

The samples were taken into sterile 50 ml Falcon tube. In-situ parameters such as pH, redox potential, electrical conductivity and total dissolved solids were measured directly using multiparameter YSI 556 MPS (Aqua TROLL 500 Multiparameter Sonde). The samples were stored at  $4 \pm 0.1$  °C in refrigerator. For the bioleaching of Armanis concentrate was preliminary milled to a size of <45 mkm. The Machintosh medium without ferrous iron (Fe (II)) (pH 1.0) was used as a solvent medium. The pH and ORP in the media were measured using a Thermo Scientific Orion 3Star portable meter (Orion 3Star Portable, Thermo Scientific, Beverly, MA, USA). The leaching intensity of concentrate samples was estimated by the amount of Fe (III), Fe (II), as well as Cu (II) ions released to the medium. The content of Fe<sup>2+</sup> and Fe<sup>3+</sup> was determined by the complexometric method with EDTA. Cu ion concentration was tested by lab2-Atomic Absorption Spectrophotometer (AAS) (ID 1.6). Experiments were performed in triplicate. The data were analyzed statistically by Excel using student t-test and the presented data in the text are the average values from repeated experiments with  $\pm 2$  % variation (in standard deviation).

### 2.2 Chemical composition of samples

The samples were analyzed for chemicals elements (Fe, Cu, Pb, Zn, As, Sn, Ni and Al) using the AAS (Atomic Absorption Spectrophotometer, SP-IAA1800H). Standard solutions were used to make (to construct) the appropriate calibration curves. Then the absorbance of the sample solutions was measured to determine the concentration of metal ions (Fe, Cu, Pb, Zn, As, Sn, Ni and Al). Each sample was analyzed in triplicate and mean value of absorbance was used to calculate the heavy metals concentrations (Table 1).

**Table 1. Main element contents in the concentrates**

Chemical analysis (%)											
Sample	Cu	Fe	Si	Al	Mg	Ca	Mn	Ni	Co	Mo	Zn
	12	28.5	0.5	0.4	0.002	1.0	0.07	0.001	0.02	0.1	4.3

This produces a mine water discharge characterized by elevated acidity, high concentration of sulfates and metals such as Fe, Cu, Pb, Zn, As, Sn, Ni and Al elements. However, at lower pH the competition between metal and hydrogen ions increases. In general, the concentration of Fe and Cu, in sample was higher.

### 2.3 DNA extraction for metagenomic sequencing

DNA extraction for metagenomic studies was performed according to the Fast DNA TMSpin Kit for Soil protocol. DNA purity and concentration were checked using a Thermo Scientific™, NanoDrop™ One Microvolume ND-1000 UV-Vis spectrophotometer (NanoDrop Technologies, Wilmington, DE, United States, respectively). Sequencing libraries were constructed using NEBNext Ultra™ DNA library prep kit for Illumina (NEB, United States) following the manufacturer's instructions. The size distribution and concentration of purified products in libraries were determined. After the index coded samples were clustered according to the manufacturer's recommendations. The libraries were sequenced on the Illumina HiSeq 2500 platform.

## 3 Results and discussion

### 3.1 Bioleaching of copper concentrate from Armanis Gold-Polymetallic Mine

The aim of this work is to study bioleaching of Armanis Gold-Polymetallic Mine by pure and mixed culture and indigenous consortia in the process of bioleaching. A comparative study was carried out. The experiments were carried out at 2.0 % density of the pulp. Comparative study was performed by pure mixed cultures of sulfur oxidizing *Acidithiobacillus caldus*, iron oxidizing *Leptospirillum feriphillum* CC and Arm indigenous consortium were studied.

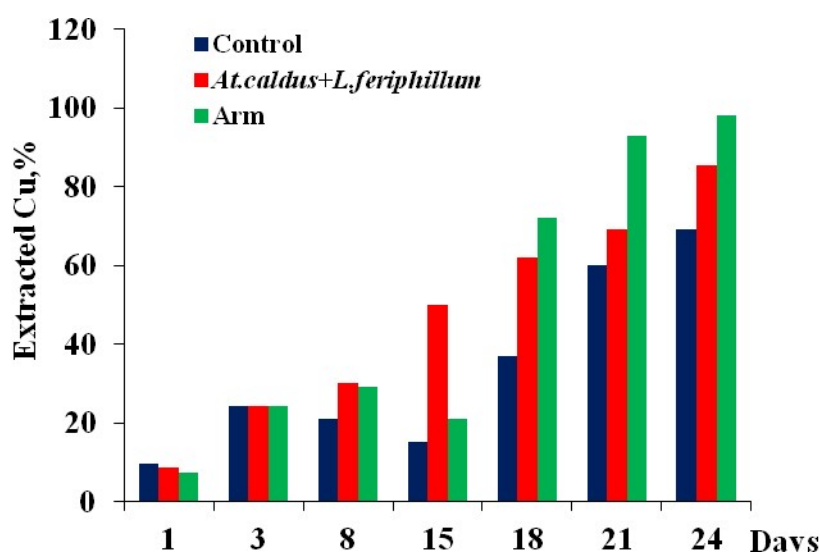


Fig. 1. Extraction of copper from Armanis Copper concentrate (Armenia) by *L.ferriphilum* CC, *At.caldus*, and their mixed culture and Armanis culture community (pH 1.8, PD - 2.0 %, t - 37 °C, 170 rpm)

It was revealed that the use of Arm indigenous consortium in copper concentrate allowed increasing the extent of copper. Extraction of copper from Armanis concentrate by mixed cultures enhances by 1.32 and 1.26 times in the presence of *L.ferriphilum* CC and *A.caldus* respectively (Fig. 1). Comparative studies have been shown of the activities of bacterial consortia Arm indigenous consortium with addition of  $Fe^{2+}$  as a source of energy and without  $Fe^{2+}$ . The results show the addition of  $Fe^{2+}$  has a significant effect on consortia bacterial growth and bioleaching. However when used mixed culture and indigenous consortium increases the copper extraction.

### 3.2 Metagenomic analysis

Microbial genomes were constructed from the metagenomic sequencing data obtained from the 3 samples described above. Metagenomics analysis revealed the identification of Kingdom. The microbial composition of the Arm indigenous consortium showed that the native samples were dominated by genera of Bacteria, Eukaryota and Archaea. The proportion of Bacteria (approximately 98-100 %) in the Arm was much higher than Eukaryota (10 %) (Figure 2). The most abundant Proteobacteria and Bacteroidetes were assigned to 11 and 1 genera, respectively, which includes classified, as well as non-classified bacterial groups. The most abundant genera are presented in Figure 3. At the class level, the prevalent reads are distributed across Flavobacteria, Betaproteobacteria, Gammaproteobacteria, and Sphingobacteria, which belong to phyla Proteobacteria and Bacteroidetes (Fig. 2).

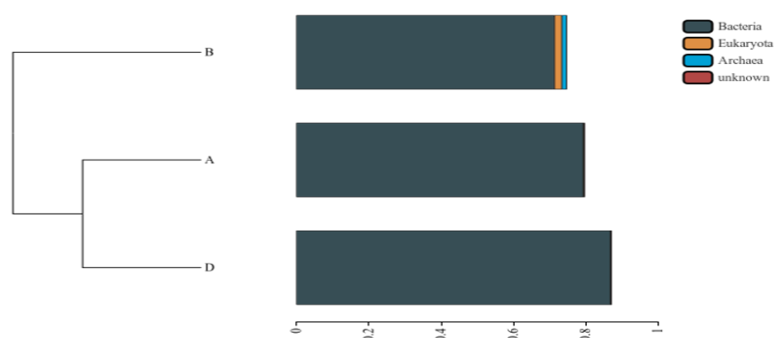
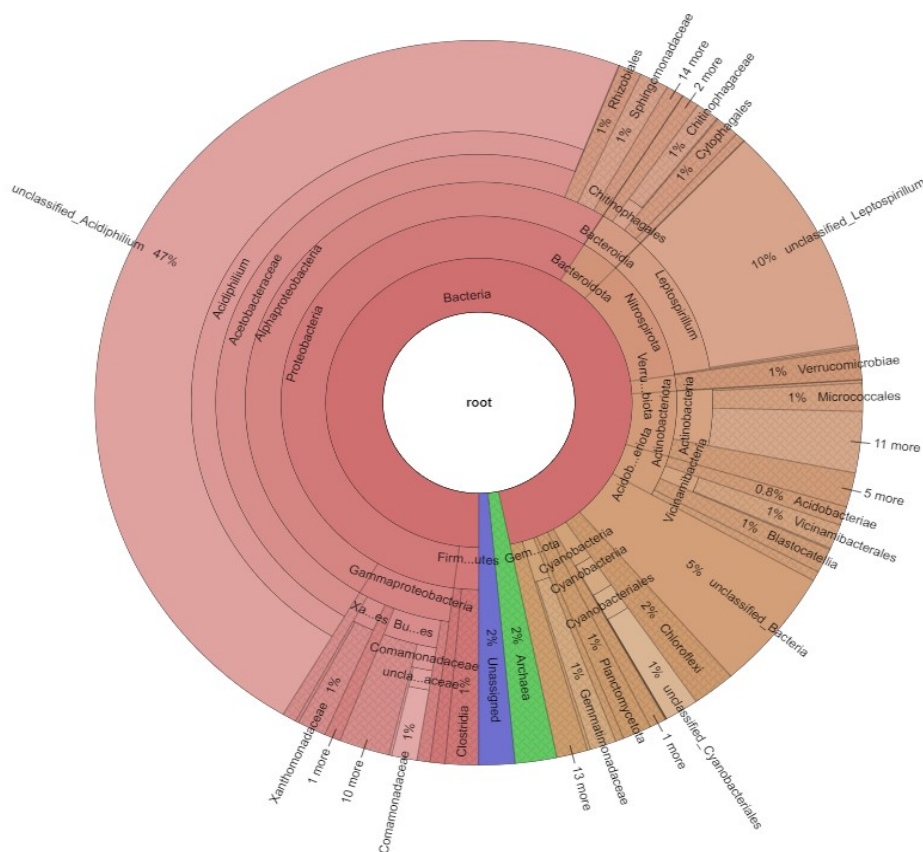


Fig. 2. Relative abundances of phylogenetic groups in the Armanis Copper concentrate

As has been shown Figure 3 Krona graphs have been used to show the entire taxonomy, from kingdom up to species level. The microbiome of Baner showed phylum-wise dominance of *Acidiphillum* (47 %), followed by *Leptospirillum* (10 %), *Actinobacteria* (0.8 %), *Verrucomicrobia* (1 %), Rhizobiales (1 %), Archaea (2 %), and *Firmicutes* (1 %), which is the same pattern, phylum level analysis revealed a dominance of *Proteobacteria* (94 %), *Actinobacteria* (2 %), *Verrucomicrobia* (1 %), and *Bacteroidetes* (1 %).



**Fig. 3. Krona map representing the taxonomic composition of the entire bacterial community revealed by metagenome sequencing**

The color of each slice is based on sequence abundance, not on phylogenetic relatedness. This information is based on the Silva database used by Mothur to generate the Krona chart. Slices with no taxonomic affiliation also include several taxonomic groups with a low number of sequences.

#### 4 Conclusions

It was revealed that the use of Arm indigenous consortium in copper concentrate allowed increasing the extent of copper. Extraction of copper from Armanis concentrate by mixed cultures enhances by 1.32 and 1.26 times in the presence of *L. ferriphillum* CC and *A.caldus* respectively (Fig. 1). Comparative study was performed by pure mixed cultures of sulfur oxidizing *Acidithiobacillus caldus*, iron oxidizing *Leptospirillum ferriphillum* CC and Arm indigenous consortium were studied. However, studies have shown that the indigenous consortium of Arm is more active than the mixed cultures above demonstrated that the indigenous strains had a stronger colonization ability and were more suitable for leaching high-oxidative oxide-sulfide copper minerals. The microbial composition of the Arm indigenous consortium showed that the native samples were dominated by genera of Bacteria, Eukariota and Archaea. The microbiome of Baner showed phylum-wise dominance of *Acidiphillum* (47 %), followed by *Leptospirillum* (10 %), *Actinobacteria* (0.8 %), *Verrucomicrobia* (1 %), Rhizobiales (1 %), Archaea (2 %), and *Firmicutes* (1 %), which is the same pattern, phylum level analysis revealed a dominance of *Proteobacteria* (94 %), *Actinobacteria* (2 %), *Verrucomicrobia* (1 %), and *Bacteroidetes* (1 %).

## Acknowledgements

This work was supported by the Higher Education and Science Committee of the Ministry of Science, Education, Culture, and Sports of the Republic of Armenia under Research project Grant number No. 22rl-031; and the Young Scientist Support Program Research project Grant number 23-YSIP-012.

## References

- [1] Méndez-García, C., Mesa, V., Sprenger, R.R., Richter, M., Diez, M.S., Solano, J. Microbial stratification in low pH oxic and suboxic macroscopic growths along an acid mine drainage. *ISME Journal*, 8, 2014, p. 1259-1274.
- [2] Johnson, D.B., Quatrini, R. Acidophile microbiology in space and time. *Current Issues in Molecular Biology*, 39, 2020, p. 63-76.
- [3] Golyshina, O.V., Pivovarova, T.A., Karavaiko, G.I., Kondratéva, T.F., Moore, E.R., Abraham, W.R., Lünsdorf, H., Timmis, K.N., Yakimov, M.M., Golyshin, P.N. *Ferroplasma acidiphilum* gen. nov., sp. nov., an acidophilic, autotrophic, ferrous-iron-oxidizing, cell-wall-lacking, mesophilic member of the Ferroplasmaceae fam. nov., comprising a distinct lineage of the Archaea. *International Journal of Systematic and Evolutionary Microbiology*, 3, 2000, p. 997-1006.
- [4] Golyshina, O.V., Yakimov, M.M., Lünsdorf, H., Ferrer, M., Nimtz, M., Timmis, K. N., Wray, V., Tindall, B.J., Golyshin, P.N. *Acidiplasma aeolicum* gen. nov., sp. nov., a euryarchaeon of the family Ferroplasmaceae isolated from a hydrothermal pool, and transfer of *Ferroplasma cupricumulans* to *Acidiplasma cupricumulans* comb. nov. *International Journal of Systematic and Evolutionary Microbiology*, 59, 2009, p. 2815-2823.
- [5] Dopson, M., Baker-Austin, C., Hind, A., Bowman, J. P., Bond, P.L. Characterization of *Ferroplasma* isolates and *Ferroplasma acidarmanus* sp. nov., extreme acidophiles from acid mine drainage and industrial bioleaching environments. *Applied and Environmental Microbiology*, 70, 2004, p. 2079-2088, doi 10.1128/AEM.70.4.2079-2088.2004.
- [6] Baker, B.J., Tyson, G.W., Webb, R.I., Flanagan, J., Hugenholtz, P., Allen, E.E., Banfield, J.F. Lineages of acidophilic archaea revealed by community genomic analysis. *Science*, 314, 2006, p. 1933-1935, doi 10.1126/science.1132690.
- [7] Korzhnikov, A.A., Toshchakov, S.V., Bargiela, R., Gibbard, H., Ferrer, M., Teplyuk, A.V., Jones, D.L., Kublanov, I.V., Golyshin, P.N., Golyshina, O.V. Archaea dominate the microbial community in an ecosystem with low-to-moderate temperature and extreme acidity. *Microbiome*, 7 (11), 2019.
- [8] Sharma, A., Kawarabayasi, Y., Satyanarayana, T. Acidophilic bacteria and archaea: acid stable biocatalysts and their potential applications. *Extremophiles*, 16, 2012, p. 1-19.
- [9] Gomes, I., Gomes, J., Steiner, W. Highly thermostable amylase and pullulanase of the extreme thermophilic eubacterium *Rhodothermus marinus*: production and partial characterization. *Bioresource Technology*, 90, 2003, p. 207-214
- [10] Chen, L., Hu, M., Huang, L., Hua, Z., Kuang, J., Li, S., Shu, W.S. Comparative metagenomic and metatranscriptomic analyses of microbial communities in acid mine drainage. *ISME Journal*, 9, 2015, p. 1579-1592.
- [11] Mesa, V., Gallego, J. L., González-Gil, R., Lauga, B., Sánchez, J., Méndez-García, C., Peláez, A.I. Bacterial, archaeal, and eukaryotic diversity across distinct microhabitats in an acid mine drainage. *Frontiers in Microbiology*, 8, 2017, 1756.
- [12] Bomberg, M., Mäkinen, J., Salo, M., Kinnunen, P. High diversity in iron cycling microbial communities in acidic, iron-rich water of the Pyhäsalmi mine, Finland. *Geofluids*, 2019, 7401304.





## INFLUENCE OF FACTORS ON ZINC INTAKE IN SELECTED VARIETIES OF *TRITICUM DURUM* FOR IMPROVING NUTRITION IN POPULATIONS

**Alexandra Kinder<sup>a</sup>, Pavol Hlubina<sup>a</sup>, René Hauptvogel<sup>b</sup>, Pavol Hauptvogel<sup>b</sup>, Ildikó Matusšíková<sup>a</sup>**

<sup>a</sup> Faculty of Natural Sciences, University of St. Cyril and Methodius in Trnava,  
Námestie J. Herdu 2, 917 01 Trnava, Slovakia, kinder3@ucm.sk

<sup>b</sup> National Agricultural and Food Centre, Research Institute of Plant Production,  
Bratislavská cesta 122, 921 68 Piešťany, Slovakia

### Abstract

Malnutrition due to lack of zinc intake is a worldwide problem. It is most pronounced especially in developing countries, but it is also relevant for developed countries. Thus, not only is there a need to increase global food production but also the production of food with greater nutritional quality. The inclusion of nutritional traits (Zn and Fe, and their bioavailability) is, therefore, an important consideration for breeding programs. Plants also need zinc in the right amount, because it is involved in various physiological functions and enzyme activities, including the production of proteins and auxins, glucose metabolism, building the immune system and the proper function of cell membranes. A possible solution with demonstrably positive results is the agronomic biofortification of wheat. We analyze a set of 13 varieties of durum wheat (*Triticum durum*) for Zn tolerance and Zn accumulation in grains. By conventional laboratory procedures of molecular biology, phenotyping and analytical chemistry, we select varieties suitable for biofortification programs. We will compare the mechanisms that could be responsible for the observed differences, such as the accumulation of metabolites or the activity of genes for the production of phytochelatin. The goal of the research is also to evaluate the effect of arbuscular mycorrhizal fungi (AMF) on the uptake and accumulation of Zn in the grains of the tested varieties. We are currently analyzing the data from the phenotyping of the experimental material, while evaluating the effect of AMF, soil application of Zn and their combination on the growth, development and photosynthetic parameters of plants. Preliminary results confirm intraspecific variability in Zn tolerance and the effect of mycorrhizal fungi.

**Keywords:** durum wheat, zinc, biofortification, phenotyping

### 1 Introduction

Durum wheat is one of the main sources of calories and protein in many developing countries. Due to the limited supply of zinc to the above-ground parts of the plant due to antinutrients and insufficient biofortification, the population faces a lack of micronutrients such as zinc and subsequent health problems. Biofortification of crops, i.e. enhancing micronutrient concentration in the edible part of the crops by plant breeding, has been proposed as one of the most cost effective and environmentally safe approaches to alleviate malnutrition [1]. Agronomic biofortification of Zn is considered the method of choice to increase Zn content in wheat grain because it can improve Zn content as well as crop yield in the short term. Agronomic biofortification includes the application of fertilizers to the soil and to the leaves [2]. The Zn content in wheat grains is influenced by the application technique and time concerning crop developmental stages. Unlike agronomic biofortification, advances in genomics, especially the availability of high-throughput genotyping assays such as whole genome resequencing, GBS, SNP arrays, etc., have facilitated trait mapping in plant species such as wheat with large and complex genomes [3]. Plant phenotyping is the assessment of complex plant properties such as growth, development, tolerance, resistance, architecture, physiology, ecology, yield and basic measurement of individual quantitative parameters that form the basis for the assessment of complex properties that are necessary for a better understanding of intake, allocations and translocations of zinc in durum wheat [4]. Plant phenotyping has proven to be a very promising method for assessing the condition of plants due to biotic and abiotic stress [5].

### 2 Material and methods

In our experiment we selected 13 durum wheat genotypes: 1296, 1352, 1N1, IS Durablank, IWA8611094, Kirmizi Yazlik, Nursith, PI 264932, PI 264933, PI 264934, PI 264936, PI 264989 and PI 278269. We performed 4 treatment methods in four repetitions where we had a total of 208 flower pots. Our variants treatments were:

A (Control, C) - Klasmann substrate,

- B (Mycorrhiza, M) - Klasmann substrate and mycorrhiza fungi,
- C (Zinc application, Zn) - Klasmann substrate and addition of fertilizer with zinc,
- D (M and Zn) - Klasmann substrate and addition of mycorrhizal fungi and fertilizer with zinc.

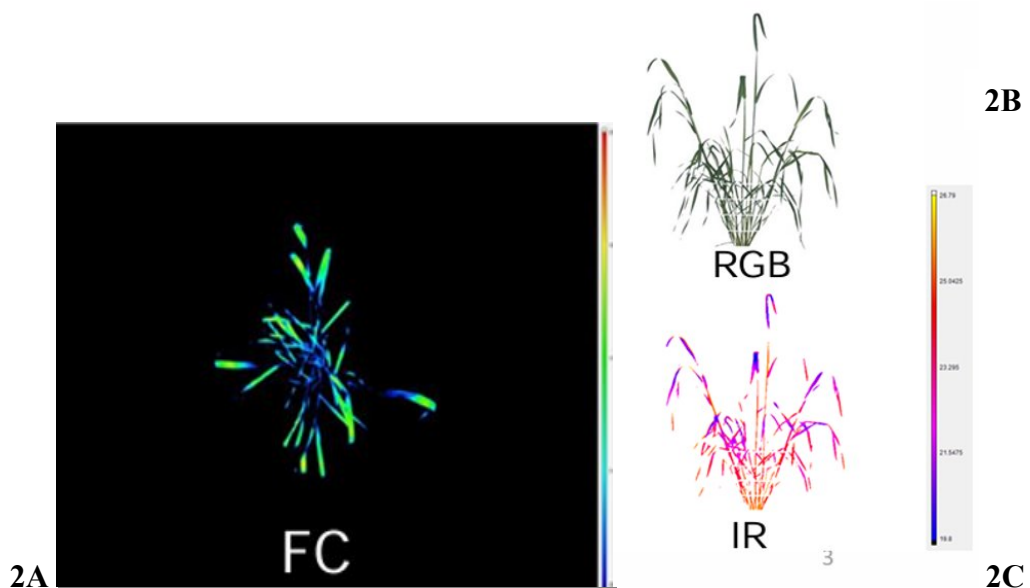
Plants were phenotyped over 7 weeks (Fig. 1). We measure plant growth dynamics (RGB imaging), leaf temperature (IR imaging) and photosystem II. Parameters (FC chlorophyll fluorescence) (Fig. 2 A-D) on the phenotyping line (Fig. 1). Our grain samples were weighed to 200 mg and concentrated nitric acid HNO<sub>3</sub> was added to them in the amount of 8 ml. Subsequently, the samples were mineralized (Anton Paar Microwave digestion system) and diluted in test tubes with ultra-pure water to a volume of 25 ml.

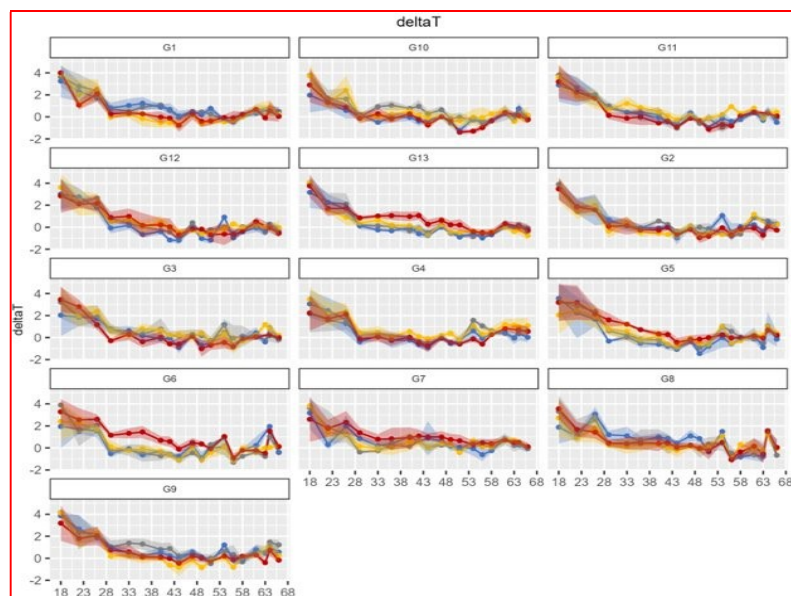


Fig. 1. The figure shows a phenotyping line showing pots of wheat plant

### 3 Results and discussion

Similar researches were conducted in the biofortification and enrichment of wheat grain with Zn [6, 7]. Parameters evaluated during phenotyping indicate plant fitness under given growth conditions. Leaf temperature changes are shown when Zn, mycorrhizal fungi or their combination was applied into soil (Fig. 2 2D). These data are currently being evaluated. Zinc content is being analyzed in soil as well as wheat grains. We also plan to compare the mechanisms that could be responsible for the observed differences, such as the accumulation of metabolites or the activity of genes for production of phytochelatin. In frames of this, we measure plant growth dynamics (RGB imaging) (Fig. 2 2B), leaf temperature (IR imaging) (Fig. 2 2C) and photosystem II. Parameters (FC chlorophyll fluorescence) (Fig 2 2A).





2D

**Fig. 2. (A-D) Representative pictures of the recorded images of the analyzed plants (panels A-C) and a preview of the results of changes in leaf temperature under the given experimental conditions (D)**

#### 4 Conclusions

As part of the phenotyping, you detected changes in the spectra, which clearly indicate the effect of individual factors of zinc addition, but also of mycorrhizae on leaf temperature or photosynthetic parameters. It is not yet clear how these changes are consistent with the Zn content in the grains. The results could be useful for breeders to create varieties with significant phytic acid and micronutrient content, which may lead to the development of varieties rich in the required micronutrients to overcome hidden hunger in the population. At the same time, from the results of our project, we will ecologically evaluate the possibilities of modulation of Zn intake and accumulation in grains, which will help biofortification programs.

#### Acknowledgements

The work is supported by the Slovak Research and Development Agency under grant no. APVV-21-0504.

#### References

- [1] Magallanes-López, A.M., Hernandez-Espinosa, N., Velu, G., Posadas-Romano, G., Ordoñez-Villegas, V.M.G., Crossa, J., Ammar, K., Guzmán, C. Variability in iron, zinc and phytic acid content in a worldwide collection of commercial durum wheat cultivars and the effect of reduced irrigation on these traits. *Food Chemistry*, 237, 2017, p. 499-505.
- [2] Singh, S., Kaur, J., Ram, H., Singh, J., Kaur, S. Agronomic bio-fortification of wheat (*Triticum aestivum* L.) to alleviate zinc deficiency in human being. *Reviews in Environmental Science and Biotechnology*, 22 (2), 2023, p. 505-526, doi: 10.1007/s11157-023-09653-4.
- [3] Gupta, O.P., Singh, A.K., Singh, A., Singh, G.P., Bansal, K.C., Datta, S.K. Wheat Biofortification: Utilizing Natural Genetic Diversity, Genome-Wide Association Mapping, Genomic Selection, and Genome Editing Technologies. *Frontiers in Nutrition*, 9, 2022, 826131, doi: 10.3389/fnut.2022.826131.
- [4] Watt, M., Fiorani, F., Usadel, B., Rascher, U., Muller, O., Schurr, U. Phenotyping: New Windows into the Plant for Breeders. *Annual review of plant biology*, 71, 2020, p. 689-712, doi: 10.1146/annurev-arplant-042916-041124.
- [5] Costa, C., Schurr, U., Loreto, F., Menesatti, P., Carpentier, S. Plant Phenotyping Research Trends, a Science Mapping Approach. *Frontiers in Plant Science*, 9, 2019, 1933, doi: 10.3389/fpls.2018.01933.
- [6] Luís, I.C., Lidon, F.C., Pessoa, C.C., Marques, A.C., Coelho, A.R.F., Simões, M., Patanita, M., Dôres, J., Ramalho, J.C., Silva, M.M., Almeida, A.S., Pais, I.P., Pessoa, M.F., Reboredo, F.H., Legoinha, P., Guerra, M., Leitão, R.G., Campos, P.S. Zinc Enrichment in Two Contrasting Genotypes of *Triticum*

*aestivum* L. Grains: Interactions between Edaphic Conditions and Foliar Fertilizers, *Plants*, 10 (2), 2021, 204, doi: 10.3390/plants10020204.

- [7] Watts-Williams, S.J., Jewell, N., Brien, C., Berger, B., Garnett, T., Cavagnaro, T.R. Using High-Throughput Phenotyping to Explore Growth Responses to Mycorrhizal Fungi and Zinc in Three Plant Species. *Plant Phenomics*, 2019, 5893953, doi:10.34133/2019/5893953.

## GROWTH YIELD OF AUTOTROPHIC Fe-OXIDIZERS ON FERROUS IRON AND TETRAHEDRITE

**Daniel Kupka<sup>a</sup>, Lenka Hagarová<sup>a</sup>, Zuzana Bártová<sup>a</sup>, Lucia Ivaničová<sup>a</sup>**

<sup>a</sup> Institute of Geotechnics of the Slovak Academy of Sciences,  
Watsonova 45, 040 01 Košice, Slovakia, dankup@saske.sk

### Abstract

This study describes the bioleaching of tetrahedrite concentrate by acidophilic chemolithotrophic iron- and sulfur-oxidizing bacteria under aerobic conditions, using stirred slurry technique. On-line gas analyses showed, that the efficiency of bacterial CO<sub>2</sub> fixation, i.e., the ratio of CO<sub>2</sub> fixed to oxygen consumed, changed during the course of tetrahedrite bioleaching. In the initial stage, the exponentially grown culture oxidized abundant dissolved ferrous iron that served as an electron donor. The rates of CO<sub>2</sub> and O<sub>2</sub> consumption increased exponentially, and growth yield coefficient ( $Y_{OX}$ ) approached 0.06 (C-mole/O-mole), which is typical value for cultures grown on ferrous sulfate. Iron acts as an important intermediary electron carrier in the tetrahedrite oxidation reactions. Bacterial Fe<sup>2+</sup> oxidation rate highly outcompeted the concurrent Fe<sup>3+</sup> reduction rate at the tetrahedrite surface, which caused the exhaustion of Fe<sup>2+</sup> and limitation of bacterial growth and oxidation rates by the availability of the energetic substrate. In the next stage of bioleaching, the ratio of CO<sub>2</sub> fixed to oxygen consumed has increased, approaching almost twice the yield value that would be predicted from exclusive growth on ferrous iron, most likely due to co-utilization of sulfur intermediates or any other type of electron donor. Our observations are consistent with previously published findings that the efficiency of CO<sub>2</sub> fixation is much greater when sulfur rather than ferrous ion is being oxidized, showing that the transport of electrons derived from RISC yielded more energy than the transport of electrons from Fe<sup>2+</sup>.

**Keywords:** *Acidithiobacillus*, *Leptospirillum*, tetrahedrite, bioleaching, iron, growth yield

### 1 Introduction

Tetrahedrite is a copper antimony sulfosalt that can be described by the simplified chemical formula Cu<sub>12</sub>Sb<sub>4</sub>S<sub>13</sub>. There is a complete solid solution between the antimony end-member tetrahedrite, and the arsenic end-member tennantite (Cu<sub>12</sub>As<sub>4</sub>S<sub>13</sub>). In nature, the minerals of the tetrahedrite group constitute a complex isotypic series with multiple iso- and heterovalent substitutions [1-5]. The general structural formula of tetrahedrite-tennantite series is: (Cu,Ag)<sub>6</sub>[Cu<sub>4</sub>(Fe,Zn,Hg,Cd)<sub>2</sub>](Sb,As,Bi)<sub>4</sub>S<sub>13</sub> based on  $\Sigma_{apfu} = 29$  [1].

Tetrahedrite and tennantite are significant copper and precious-metals resources. However, their separation from primary copper sulphides (chalcocite Cu<sub>2</sub>S, covellite CuS, chalcopyrite CuFeS<sub>2</sub>) is difficult. Both tetrahedrite and tennantite are remarkable for the number of minor elements (Hg, Zn, Bi, Se) they can incorporate, and these two minerals are frequently the major sources of such often unwelcome minor elements in flotation Cu-concentrates. They are equally a major contributors of undesirable pollutants (As, Hg, Sb) to the processing streams [6]. Consequently, only tetrahedrite deposits rich in gold and silver have been exploited in the past.

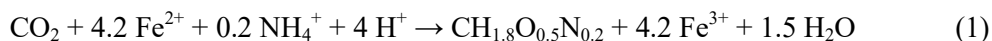
Nowadays, the exploitation of tetrahedrite-tennantite deposits is being revisited, justified mostly by the high precious-metals content of those deposits. Furthermore, given the continued strategic importance of raw materials for the EU manufacturing industry, antimony (Sb) as well as arsenic (As), amongst another 34 mineral raw materials, were added to the list of Critical Raw Materials (CRM) for Europe published by the European Commission (COM/2023/160 final).

Tetrahedrite is generally known as a refractory mineral characterized by its recalcitrance to acid chemical leaching. Natural and synthetic tetrahedrite dissolve very slowly in acidic aqueous solutions that contain ferric iron at the temperature range between 65 and 95 °C. The rates are almost immeasurably slow below 60 °C [7-9]. Higher metal extraction rates can be achieved by mechanical pre-treatment of tetrahedrite by high-energy milling [10-12]. In the current investigation the oxidation of tetrahedrite was mediated by iron-oxidizing bacteria in acid sulfate media at ambient temperature (25 °C). Iron acts as an important intermediary electron carrier in the tetrahedrite oxidation reactions. Ferric iron is chemical oxidant for dissolution of sulphide minerals under acidic conditions. The role of acidophilic prokaryotes in this process is to oxidize ferrous iron to ferric iron and help to maintain high redox potential, defined by the Fe<sup>3+</sup>/Fe<sup>2+</sup>

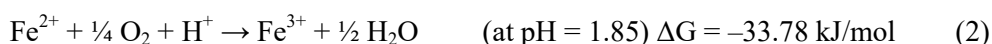
ratio. Acidophilic iron-oxidizing bacteria, particularly members of the genera *Acidithiobacillus* and *Leptospirillum*, have shown high efficiency in oxidizing iron, thereby enhancing the dissolution of sulphide minerals. These bacteria survive and benefits at low pH and generally exhibit a remarkable tolerance to dissolved metal ions. The efficiency of these bacteria in wide temperature range has been studied, demonstrating that their growth and iron oxidation kinetics can vary significantly with temperature changes [13].

### 1.1 Energy coupling during inorganic substrate oxidation in relation to growth rate and yield

The synthesis of biomass requires a carbon source and an N-source. In addition, there is a need for an electron donor (D). Autotrophically growth bacteria use CO<sub>2</sub> as C-source, consequently there is a need for an electron donor to reduce CO<sub>2</sub> to biomass. Reducing equivalents stored in the form of soluble ferrous iron or Fe<sup>2+</sup>-bearing solid phases, including iron sulfide minerals and reduced inorganic sulfur compounds (RISC) may serve as significant source of energy for lithotrophic microbial oxidation coupled to aerobic respiration. When bacteria use CO<sub>2</sub> as a C-source for autotrophic growth, NH<sub>4</sub><sup>+</sup> as nitrogen source and Fe<sup>2+</sup> as the electron donor, assuming that the biomass composition is represented by C<sub>1</sub>H<sub>1.8</sub>O<sub>0.5</sub>N<sub>0.2</sub> the anabolic reaction for synthesis of biomass can be derived using elemental and charge balances [14-16],



where 4.2 moles of Fe<sup>2+</sup> are needed for the synthesis of one mole of biomass by reducing CO<sub>2</sub>. The production of biomass from the inorganic building compounds requires input of Gibbs energy which is delivered by catabolic redox reaction of ferrous iron oxidation with oxygen as electron acceptor:



This energy is coupled to anabolism to drive the anabolic reactions. The total need for Fe<sup>2+</sup> (electron donor) per C-mole of biomass is composed of the anabolic need (Reaction 1) and the catabolic need (Reaction 2).

In 1949, Monod [17] proposed the concept of the yield of biomass on substrate. This yield was originally considered to be a characteristic constant of a microorganism for a specific substrate. Later, Pirt [18] showed that the biomass yield was only constant at high growth rates, and that the yield dropped at low growth rates because of maintenance and/or endogenous processes. Following these initial studies, maximum biomass yields have been determined experimentally for many microorganisms growing on a wide variety of substrates.

## 2 Material and methods

### 2.1 Sample preparation

The tetrahedrite sample was obtained from the Strieborná vein in the Rožňava ore field, eastern Slovakia. The raw ore was crushed and milled to a grain size < 100 μm, followed by the froth flotation to collect a high grade tetrahedrite concentrate. The flotation concentrate was further conditioned with diluted sulphuric acid (pH 1) at 90 °C under N<sub>2</sub> atmosphere to remove residual siderite.

### 2.2 Bacterial strains and incubation conditions on ferrous iron

Three strains of chemolithotrophic, acidophilic, iron-oxidizing bacteria were used in the experiments: *Acidithiobacillus ferrivorans* SS3 (DSM 17398), *Acidithiobacillus ferrooxidans* (DSM 14882) and *Leptospirillum ferriphilum* (DSM 14647). The bacteria were incubated in mineral salt medium that contained: 1.6 mM MgSO<sub>4</sub>·7H<sub>2</sub>O, 0.76 mM (NH<sub>4</sub>)<sub>2</sub>SO<sub>4</sub>, 0.23 mM K<sub>2</sub>HPO<sub>4</sub> and 120 mM FeSO<sub>4</sub>·7H<sub>2</sub>O in 30 mM H<sub>2</sub>SO<sub>4</sub>. The initial pH of the medium was ~ 1.6. The cultures grew in magnetically stirred and properly aerated baffled reaction vessels with the working volume 0.5 L. The incubation was carried out in a batch mode, yet the O<sub>2</sub> and CO<sub>2</sub> for the bacterial growth was continuously supplied by air passing through the headspace of the reactor above the liquid.

### 2.3 Bioleaching of tetrahedrite

Tetrahedrite bioleaching was carried out at similar conditions, using above mentioned bacterial strains and liquid medium. The tetrahedrite concentrate was introduced to bacterial cultures grown on ferrous iron,

achieving a pulp density of 2 %. The bioleaching experiments were carried out under aerobic conditions at 25 °C, in magnetically stirred reactors at 250 rpm and in baffled shaking flasks at 200 rpm.

## 2.4 The bacterial cells and biomass quantification

Direct microscopic counting of the bacterial cells was carried out using a Neubauer chamber with a special depth of 0.01 mm. In this work, instead of the number of bacterial cells, the biomass concentration (X) is expressed in the moles of organic carbon per liter, consequently, yield of biomass on ferrous iron  $Y_{SX}$  is defined as the C-mole of biomass produced per mole of ferrous iron (i.e. electron donor) utilized.

## 2.5 Gas analysis

The on-line measurement of the oxygen and carbon dioxide consumption from the reactors headspace was used to accurately measure the bacterial growth and bio-oxidation kinetics of ferrous iron and tetrahedrite. Paramagnetic oxygen analyzer and infrared carbon dioxide analyzer (Sable Systems) were used for O<sub>2</sub> and CO<sub>2</sub> analyses in inlet and outlet air respectively.

## 2.6 pH/ORP and chemical analyses

Combined glass pH electrodes (Radiometer Analytical) and combined Pt-Ag/AgCl redox electrodes (InLab Mettler Toledo) were used for pH and oxidation-reduction potential (ORP) measurement respectively. Ferric iron was determined by UV-spectrophotometric method at 300 nm [19, 20]. Ferrous iron concentrations were determined by modified *o*-phenantroline spectrophotometric method, insensitive to Fe<sup>3+</sup> interference [21]. The samples of tetrahedrite leachate were analysed using AAS Varian AA240Z, AA240FS and ICP-MS 7700 Agilent. Sulphate concentration was determined by ion chromatography Dionex ICS 5000.

## 3 Results and discussion

### 3.1 Energy coupling during ferrous iron oxidation in relation to growth rate and yield

Iron oxidation, carbon dioxide and oxygen consumption reflect the anabolic and catabolic reactions of bacterial cells population growing on Fe<sup>2+</sup>. In the experiments it need to be provided, that other relevant sub-processes like O<sub>2</sub> and CO<sub>2</sub> mass transfer are sufficiently fast and do not determine the rate of bacterial growth and oxidation. The rate of bacterial growth (the rate of biomass production)  $r_X$ , is equal to the rate of carbon dioxide utilization  $-r_{CO_2}$ . Fig. 1 depicts the total rates  $r_{O_2}$ ;  $r_{CO_2}$  (in mmol L<sup>-1</sup> h<sup>-1</sup>) and the corresponding net cumulative amounts of O<sub>2</sub> consumed and CO<sub>2</sub> fixed (in mmol L<sup>-1</sup>) by bacterial culture growing on ferrous iron.

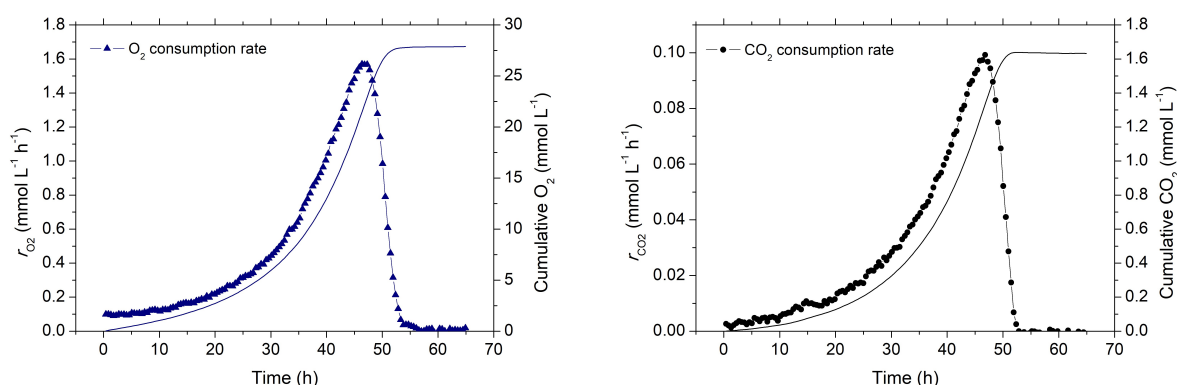


**Fig. 1.** Total rate of O<sub>2</sub> and CO<sub>2</sub> consumption and net cumulative amounts of O<sub>2</sub> and CO<sub>2</sub> utilization by bacterial culture *At. ferrivorans* during batch incubation on ferrous iron at 25 °C

In this article biomass concentration (X) is expressed in the moles of carbon (CO<sub>2</sub> fixed) per liter, consequently, yield of biomass on ferrous iron  $Y_{SX}$  is defined as the C-mole of biomass produced per mole of ferrous iron (i.e. electron donor) utilized. Accordingly,  $1/Y_{SX}$  equals the total ferrous iron, both anabolic and catabolic, needed to synthesize one C-mole of biomass.



$$r_X = -r_{\text{Fe}^{2+}} \cdot Y_{\text{SX}} \quad \frac{1}{Y_{\text{SX}}} = \frac{-r_{\text{Fe}^{2+}}}{r_X} \quad (3)$$

Similarly, the production rate of biomass is equal to the oxygen consumption rate multiplied by the yield of biomass on oxygen (equation 4).

$$r_X = -r_{\text{O}_2} \cdot Y_{\text{OX}} \quad \frac{1}{Y_{\text{OX}}} = \frac{-r_{\text{O}_2}}{r_X} \quad (4)$$

The stoichiometric parameter  $1/Y_{\text{ox}}$  is expressed as follows:

$$\frac{1}{Y_{\text{OX}}} = \frac{1 - 4.2Y_{\text{SX}}}{4Y_{\text{SX}}} \quad (5)$$

Because the biomass production rate,  $r_X$ , is equal to the carbon dioxide consumption rate  $-r_{\text{CO}_2}$ , substituting  $1/Y_{\text{SX}}$  and  $1/Y_{\text{ox}}$  over equations 3 - 5, the relation between the oxidation rate of ferrous iron and the oxygen and carbon dioxide consumption rates follows from the stoichiometry of equation 6 [22].

$$-r_{\text{Fe}^{2+}} = -4r_{\text{O}_2} - 4.2r_{\text{CO}_2} \quad (6)$$

The net amount of oxidized iron can be calculated from the net amount of  $\text{O}_2$  and  $\text{CO}_2$  consumed. Fig. 2 shows decrease of ferrous iron concentration calculated by the integration of  $\text{Fe}^{2+}$  oxidation rate (Eqn. 6) over the time of incubation and residual  $\text{Fe}^{2+}$  concentration determined by chemical analyses of the culture medium. This plot shows that the measured and calculated ferrous iron concentrations are in a good correlation. Starting with a known initial biomass concentration  $C_{X(0)}$ , the biomass concentration  $C_{X(t)}$  at any particular time of the experiment is known from the integration of  $\text{CO}_2$  fixation rate profile. The oxygen consumption rate,  $-r_{\text{O}_2}$  and carbon dioxide consumption rate,  $-r_{\text{CO}_2} = r_X = (dC_X/dt)$ , are known on-line, accordingly the specific rates defined per unit of biomass can be calculated. Specific oxygen consumption rate,  $q_{\text{O}_2}$ , is defined as the oxygen consumption rate per unit of biomass  $q_{\text{O}_2} = r_{\text{O}_2}/C_X$ . Specific growth rate,  $\mu$ , is defined by:  $\mu = r_X/C_X$ .

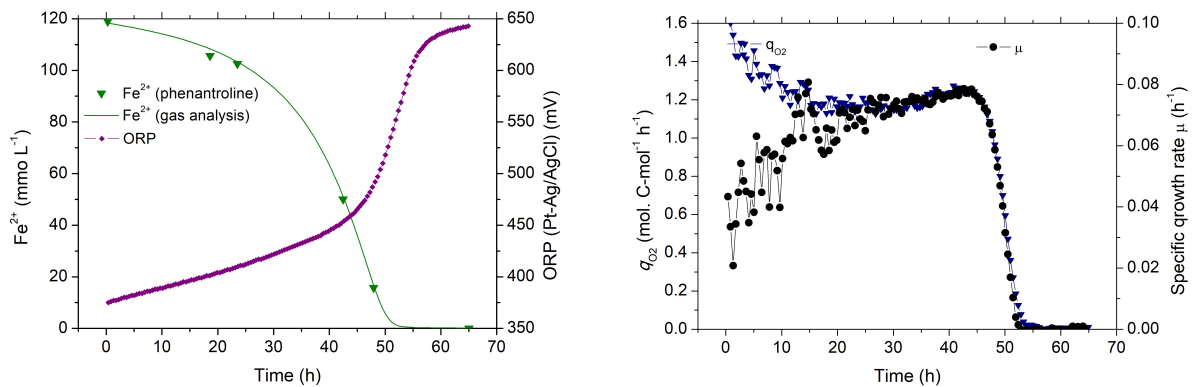


**Fig. 2. (A) The decrease of  $\text{Fe}^{2+}$  concentration measured and calculated from the gas analysis and the increase of redox potential of the medium**

**Fig. 2. (B) The biomass specific oxygen consumption rate  $q_{\text{O}_2}$  (in mol  $\text{C}$ -mol biomass/time) and specific growth rate  $\mu$  ( $\text{h}^{-1}$ ) during batch incubation of *At. ferrivorans* on ferrous iron at 25 °C**

Biomass yield on oxygen is denoted by the symbol  $Y_{\text{OX}}$  and has the dimension C-molX produced/mol oxygen consumed. In the course of batch incubation, the  $Y_{\text{OX}}$ , i.e., the  $r_{\text{CO}_2}/r_{\text{O}_2}$  molar ratio gradually increased and approached the value of 0.06 (60  $\mu\text{moles CO}_2$  fixed per millimole  $\text{O}_2$  consumed). The efficiency of carbon dioxide fixation is directly related to the cell yield. Strong correlation was observed between ferrous iron oxidation and carbon dioxide fixation in the exponentially growing cultures with the yield coefficient ( $Y_{\text{SX}}$ ) approaching 14  $\mu\text{mol CO}_2$  fixed per mole  $\text{Fe}^{2+}$  oxidized. This value corresponds well to *A. ferrooxidans* yield values on ferrous iron reported in previous works [22-25].



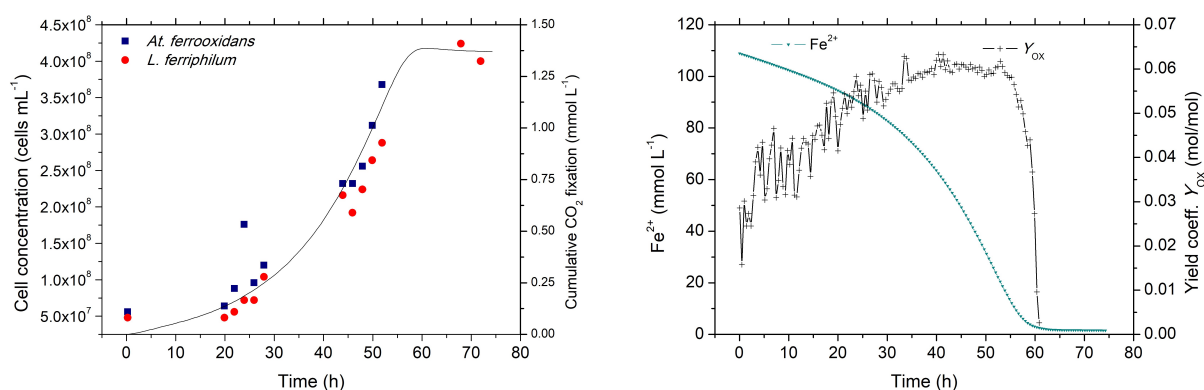


**Fig. 3. (A) Bacterial cell counts and net biomass C-concentration calculated from the gas analysis**  
**Fig. 3. (B) Fe<sup>2+</sup> profile and yield coefficient Y<sub>OX</sub> (in mol/mol) during the incubation**  
**of *At. ferrooxidans* on ferrous iron at 20 °C**

Direct microscopic counting of the bacterial cells using Neubauer chamber with a special depth of 0.01 mm revealed exponential increase of the cell number with time (Fig. 3A). The specific growth rate calculated from the cell concentration profile at *At. ferrooxidans* was  $\mu = 0.050 \pm 0.004 \text{ h}^{-1}$  and  $\mu = 0.054 \pm 0.0025 \text{ h}^{-1}$  at *L. ferriphilum*. The specific biomass growth rate calculated from the CO<sub>2</sub> fixation rate profile using on-line gas analysis was  $\mu = 0.056 \pm 0.00055 \text{ h}^{-1}$  and  $\mu = 0.051 \pm 0.00086 \text{ h}^{-1}$  at *At. ferrooxidans* and *L. ferriphilum* respectively. The value of the yield coefficient, obtained from direct counting of the cells was  $6.35 \cdot 10^{10}$  cells per g Fe<sup>2+</sup> oxidized, which is significantly higher, than the yields referred in previous works.

Unreasonably broad range of values are reported for the numbers of cells of *At. ferrooxidans* produced per unit of ferrous iron oxidized when using direct microscopic counting. The reported yield values range from approximately  $1.7 \pm 0.4 \cdot 10^{10}$  to  $5 \cdot 10^{10}$  cells/g Fe<sup>2+</sup> oxidized:  $1.7 \pm 0.4 \cdot 10^{10}$  cells/g Fe<sup>2+</sup> [26];  $2.23 \cdot 10^{10}$  cells/g Fe<sup>2+</sup> [27];  $2.3 \cdot 10^{10}$  cells/g Fe<sup>2+</sup> [28];  $1.79 \cdot 10^{10}$  -  $3.58 \cdot 10^{10}$  cells/g Fe<sup>2+</sup> (Bryan et al 2012);  $3.8 \cdot 10^{10}$  cells/g Fe<sup>2+</sup> [29];  $3.9 \cdot 10^{10}$  cells/g Fe<sup>2+</sup> [30];  $4.7 \cdot 10^{10}$  cells/g Fe<sup>2+</sup> in continuous culture [31];  $5 \cdot 10^{10}$  colonies/g Fe<sup>2+</sup> obtained by a MPN dilution method [23].

Our direct microscopic counting using a Neubauer chamber showed even higher values (up to  $6 \cdot 10^{10}$ ) of cells produced per gram of Fe<sup>2+</sup> oxidized. However, it is important to note that these values are approximate and can vary significantly based on the specific experimental conditions and can be affected by several factors, including subjective judgment, sampling variability and sample heterogeneity, leading to a broad range of reported values. Variability can arise from differences in counting techniques. Clumping or aggregation of cells can occur, making it difficult to obtain a representative sample for counting. Uneven distribution can lead to variations in the number of cells observed and contribute to the broad range of reported values. Direct microscopic counting typically does not distinguish between viable and non-viable cells or account for variations in cell morphology. It may include cells that are not actively metabolizing or are damaged, leading to inconsistent results. Additionally, *Acidithiobacilli* can exhibit morphological variations depending on growth conditions, and different morphotypes may be counted differently. Direct microscopic counting often involves counting cells in a small sample volume, which may not represent the entire culture or system. Variations within the culture or sampling bias can influence the reported cell counts, contributing to the broad range of values.

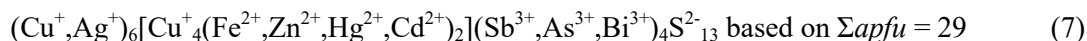
It is essential to consider the specific experimental conditions and methodologies employed when interpreting and comparing these values. To obtain more accurate and consistent measurements, carefully controlled experiments using standardized methods to quantify cell numbers, staining techniques to differentiate viable and non-viable cells and combining direct microscopic counting with other quantitative techniques like flow cytometry must be performed.

Therefore, in the current article, instead of the number of cells, we used the amount of fixed carbon to express biomass concentration and yield coefficients, which are in good agreement with many published scientific works.

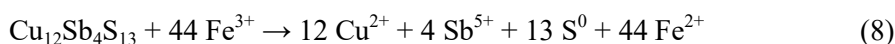
### 3.2 Energy coupling during bioleaching of tetrahedrite in relation to growth rate and yield

The crystal chemistry of natural tetrahedrite samples examined by microprobe analyses revealed that the sum of monovalent metals (Cu<sup>+</sup> + Ag<sup>+</sup>) is usually 10 *apfu* with six of them hosted at the M(1) site and

four at M(2). The total numbers of anions is usually 13 ( $S^{2-} + Se^{2-}$ ) *apfu*, yielding 26 negative charges. As the sum of 10 monovalent cations ( $Cu^+ + Ag^+$ ) and 4 trivalent cations ( $Sb^{3+} + As^{3+} + Bi^{3+}$ ) gives + 22 charges, the excess of -4 charges is balanced by the accommodation of 2  $Me^{2+}$  cations distributed over the M(1) site (C constituent). The latter acts as a “charge compensating cations” that fixes the B:C constituent atomic ratio to 4:2 in the general formula [1].



The reaction of tetrahedrite during chemical leaching with ferric iron yielded mostly elemental sulfur and pentavalent antimony [8] according to Equation (8). The oxidation of 1 mole of tetrahedrite (nominally  $Cu_{10}^+Cu_2^{2+}Sb_4^{3+}S_{13}^{2-}$ )<sup>1</sup> involves the transfer of 44 moles of electrons.



The reaction products are  $Cu^{2+}$  and  $S^0$  together with  $Sb^{5+}$ , the latter precipitates in the presence of ferric iron. Elemental sulfur is the principal S-containing reaction product of chemical oxidation when tetrahedrite dissolves in media with ferric iron at temperatures <100 °C.

In the bioleaching tests, the oxidation of tetrahedrite was mediated by iron-oxidizing bacteria in acid sulfate media at ambient temperature (25 °C). The tetrahedrite concentrate was introduced to bacterial cultures of *At. ferrooxidans*, *At. ferrivorans* and *L. ferriphilum* grown on ferrous iron. The experiments were carried out in magnetically stirred reactors and in shaking flasks.

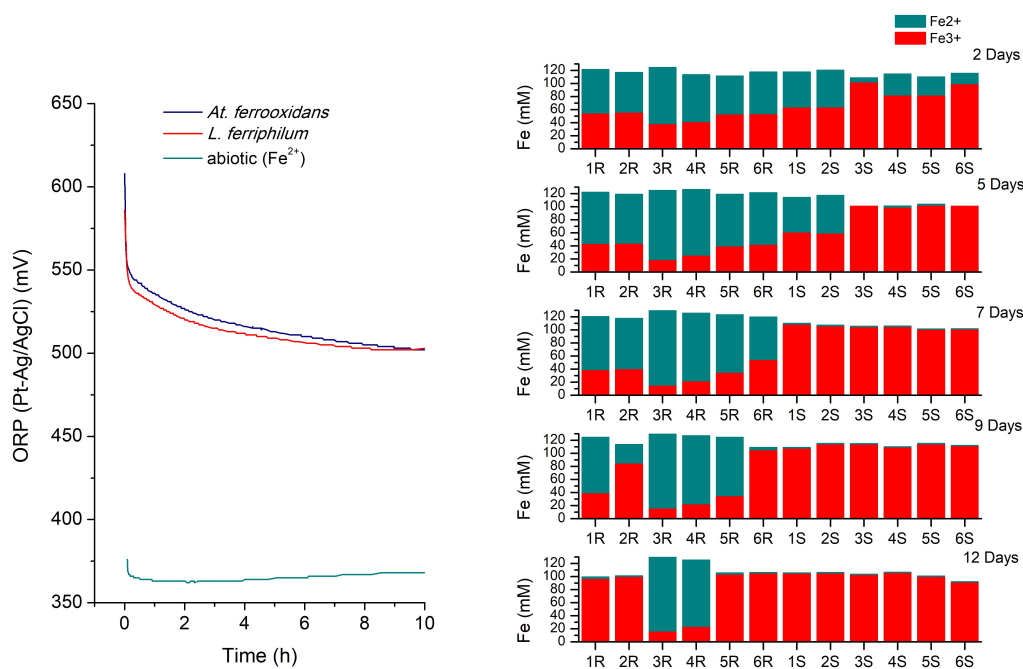


**Fig. 4. (A) Sharp drop of the redox potential at the start of tetrahedrite bioleaching**

**Fig. 4. (B) Iron speciation during the initial 12 days of tetrahedrite bioleaching**

Series “R” = stirred reactors, series “S” = shaking flasks

Culture *At. ferrooxidans* (1-2), *At. ferrivorans* (3-4) and *L. ferriphilum* (5-6)

Fig. 4A shows the sharp drop of the redox potential at the start of bioleaching which is related to a rapid change in the  $Fe^{3+}/Fe^{2+}$  ratio due to reduction of ferric iron with tetrahedrite (Eq. 8). In the initial stage (lag phase) of bioleaching, the bacterial growth and iron oxidation activity ceased and ferrous iron accumulates in the leach liquors (Fig. 5C). The lag period varied between individual strains and was shortest

<sup>1</sup> The nominal tetrahedrite formula ( $Cu_{10}^+Cu_2^{2+}Sb_4^{3+}S_{13}^{2-}$ ) was adopted for simplicity of the next discussion.

at *L. ferriphilum* and longest at *At. ferrivorans*. The iron oxidation accelerated earlier at cultures incubated in shaking flasks (series “S” in Fig. 4B) compared to the cultures in stirred reactors (series “R” in Fig. 4B).

During the exponential phase, the growing cultures oxidized abundant dissolved ferrous iron that served as an electron donor. The rates of CO<sub>2</sub> and O<sub>2</sub> consumption increased exponentially, (time period 4 - 7.5 days in the graphs in Fig. 5) and growth yield coefficient ( $Y_{OX}$ ) approached 0.06 (C-mole/O-mole), which is typical value for cultures grown on ferrous sulfate (see Fig. 3B). Iron acts as an important intermediary electron carrier in the tetrahedrite oxidation reactions. Bacterial Fe<sup>2+</sup> oxidation rate highly outcompeted the concurrent Fe<sup>3+</sup> reduction rate at the tetrahedrite surface. The exhaustion of Fe<sup>2+</sup> caused limitation of bacterial growth and oxidation rates by the energetic substrate. In the next stage of bioleaching, (time period from 7.5 days onwards in Fig. 5) the ratio of CO<sub>2</sub> fixed to oxygen consumed has increased, approaching almost twice the yield value that would be predicted from exclusive growth on ferrous iron. The higher yield is most likely due to co-utilization of sulfur intermediates or any other type of electron donor. Our observations are consistent with previously published findings that the efficiency of CO<sub>2</sub> fixation is much greater when sulfur rather than ferrous ion is being oxidized, showing that the transport of electrons derived from RISC yielded more energy than the transport of electrons from Fe<sup>2+</sup>.

An important parameter in biotechnological processes is the yield ( $Y_{DX}$ ) of biomass (X) on the available substrate electron donor (D).  $Y_{DX}$  is defined as C-mol of biomass produced per amount of electron donor consumed (in C-mol for organic or in moles for inorganic donors). Roels [16] showed that biomass yields for aerobic growth appear to depend on the degree of reduction of the carbon and energy substrate. Reducing equivalents stored in the form of soluble Fe<sup>2+</sup> or solid ferrous iron in sulfide minerals and reduced inorganic sulfur compounds (RISC) may serve as significant source of energy for lithotrophic microbial oxidation coupled to aerobic respiration. Beck and Shafia [32] showed that the efficiency of CO<sub>2</sub> fixation, i.e., the ratio of CO<sub>2</sub> fixed to oxygen consumed, is much greater when sulfur rather than ferrous ion is being oxidized, confirming, that the transport of electrons derived from RISC yielded more energy than the transport of electrons from Fe<sup>2+</sup>. However, we also observed an increase in growth yield at *Leptospirillum*-like bacteria that do not oxidize RISC. Nevertheless, in the case of an indirect mechanism, tetrahedrite is completely chemically oxidized by Fe<sup>3+</sup> and the role of acidophilic prokaryotes in this process is to oxidize ferrous iron to ferric iron. Therefore, the reason for the higher growth yield is not clear. Most probably the microorganisms utilize reducing equivalents stored in the form of Cu<sup>+</sup> and Sb<sup>3+</sup> in the reversal electron flow. The amount of Gibbs energy for biomass synthesis for autotrophic growth only depends on the C-source and electron donor for reversed electron transport. It does not depend on the nature of the catabolic reaction and the electron acceptor used. The anabolic reaction (Eq. 1) does not involve the electron acceptor. The electron acceptor is only relevant for the amount of catabolic energy which can be obtained from the electron donor.

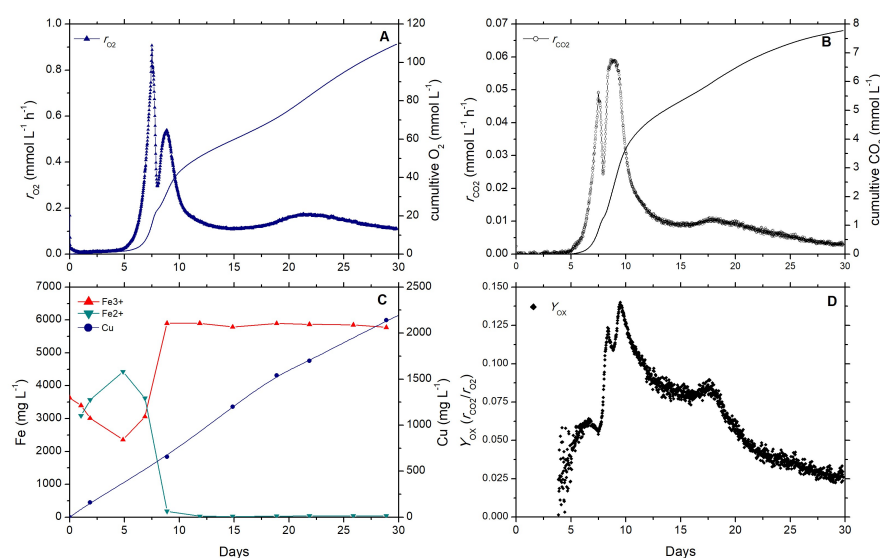


**Fig. 5. Bioleaching of tetrahedrite by *L. ferriphilum* at 25 °C**

- (A) Oxygen consumption rate and cumulative O<sub>2</sub> consumption. (B) CO<sub>2</sub> fixation rate and cumulative CO<sub>2</sub> fixed, (C) Fe speciation and Cu extraction during bioleaching of tetrahedrite, (D) Changes of the  $r_{CO_2}/r_{O_2}$  i.e. the yield coefficient  $Y_{OX}$  in the course of tetrahedrite oxidation**

#### 4 Conclusions

Exponentially grown cultures of *At. ferrooxidans*, *At. ferrivorans* and *L. ferriphilum* on ferrous iron, have shown nearly constant specific growth rates and specific oxidation rates in a relatively large pH range 1.6 to 2.1. On-line measurements of the oxygen and carbon dioxide consumption rates revealed, that the  $r_{\text{CO}_2}/r_{\text{O}_2}$  molar ratio at cultures growing on ferrous iron approaches the value of 0.06. In this study the biomass yield was not corrected for maintenance energy (or endogenous metabolism). Those parameters could be observed in continuous incubation mode. Nevertheless, even in the batch incubation it is possible to observe the increase of the biomass yield during the acceleration phase. In the exponential phase, the yield coefficient  $Y_{\text{OX}}$  approached 60 mmoles of  $\text{CO}_2$  fixed per mole of  $\text{O}_2$  consumed and does not change during the period of unlimited growth. The yield coefficient corresponds to 14 mmoles of  $\text{CO}_2$  fixed per mole of  $\text{Fe}^{2+}$  oxidized.

The efficiency of bacterial  $\text{CO}_2$  fixation, i.e. the biomass yield coefficient  $Y_{\text{OX}}$  during the course of tetrahedrite bioleaching has increased, approaching almost twice the yield value that would be predicted from exclusive growth on ferrous iron. The higher yield is most likely due to co-utilization of sulfur intermediates or any other type of electron donor.

Considering the unreasonably broad range of reported values of yield coefficient when using direct microscopic counting of bacterial cells, we rather prefer the parameter total (organic) carbon to express the amount of biomass and yield coefficients, which are in good agreement with many published scientific works.

The observed effectiveness of acidophilic Fe- and S- oxidizing bacteria in promoting tetrahedrite dissolution highlights the potential of bioleaching as a viable method for metal recovery from complex sulphide ores. This observation aligns with the findings of Kupka et al. (2023), where the kinetics of bacterial growth and iron oxidation were investigated, underscoring the role of temperature in bioleaching efficiency. The maintenance of high redox potential through bacterial oxidation ensures the continuous regeneration of  $\text{Fe}^{3+}$ , which is crucial for sustained mineral oxidation.

#### Acknowledgements

Funded by the EU NextGenerationEU through the Recovery and Resilience Plan for Slovakia under the project No. 09I03-03-V04-00271. The work has been supported by Slovak Research and Development Agency within the projects APVV-20-0108-0140 and the project VEGA 2/108/23.

#### References

- [1] Biagioni, C., Sejkora, J., Musetti, S., Velebil, D., Pasero, M. Tetrahedrite-(Hg), a new ‘old’ member of the tetrahedrite group. *Mineralogical Magazine*, 84 (4), 2020, p. 584-592.
- [2] Patrick, R.A.D., Hall, A.J. Silver substitution into synthetic zinc, cadmium, and iron tetrahedrites. *Mineralogical Magazine*, 47 (345), 2018, p. 441-451.
- [3] King, R.J. The tetrahedrite group. *Geology Today*, 17 (2), 2001, p. 77-80.
- [4] Repstock, A., Voudouris, P., Zeug, M., Melfos, V., Zhai, M., Li, H., Kartal, T., Matuszczak, J. Chemical composition and varieties of fahlore-group minerals from Oligocene mineralization in the Rhodope area, Southern Bulgaria and Northern Greece. *Mineralogy and Petrology*, 110 (1), 2016, p. 103-123.
- [5] Moëlo, Y., Makovicky, E., Mozgova, N.N., Jambor, J.L., Cook, N., Pring, A., Paar, W., Nickel, E.H., Graeser, S., Karup-Møller, S., Balic-Žunic, T., Mumme, W.G., Vurro, F., Topa, D., Bindi, L., Bente, K., Shimizu, M. Sulfosalt systematics: a review. Report of the sulfosalt sub-committee of the IMA Commission on Ore Mineralogy. *European Journal of Mineralogy*, 20 (1), 2008, p. 7-46.
- [6] Filippou, D., St-Germain, P., Grammatikopoulos, T. Recovery of metal values from copper - Arsenic minerals and other related resources. *Mineral Processing and Extractive Metallurgy Review*, 28 (4), 2007, p. 247-298.
- [7] Dutrizac, J.E., Morrison, R.M. *The Leaching of Some Arsenide and Antimonide Minerals in Ferric Chloride Media*. In *Hydrometallurgical Process Fundamentals*, R.G. Bautista, Editor. Springer US: Boston, MA, 1984, p. 77-112.
- [8] Riveros, P.A., Dutrizac, J.E. The leaching of tennantite, tetrahedrite and enargite in acidic sulphate and chloride media. *Canadian Metallurgical Quarterly*, 47 (3), 2008, p. 235-244.
- [9] Correia, M., Carvalho, J., Monhemius, J. The leaching of tetrahedrite in ferric chloride solutions. *Hydrometallurgy*, 57, 2000, p. 167-179.

- [10] Baláž, P., Kammel, R., Kušnierová, M., Achimovičová, M. Mechano-chemical treatment of tetrahedrite as a new non-polluting method of metals recovery. In Hydrometallurgy '94, international symposium organized by the Institution of Mining and Metallurgy and the Society of Chemical Industry, and held in Cambridge, England, from 11 to 15 July, 1994. Springer Netherlands: Dordrecht, 1994, p. 209-218.
- [11] Baláž, P. *Influence of mechanical activation on bacterial leaching of minerals*. In Process Metallurgy, P. Baláž, Editor. Elsevier, 2000, p. 195-212.
- [12] Balaz, P., Kammel, R., Sekula, F. and Jakabský, Š. Mechano-chemical leaching: the possibility to influence the rate of metals extraction from refractory ores. Proceedings of the XX International Mineral Processing Congress: 21-26 September 1997, Aachen, Germany, 1997, p. 149-159.
- [13] Kupka, D., Bártová, Z., Hagarová, L. Kinetics study comparing bacterial growth and iron oxidation kinetics over a range of temperatures 5-45 °C. *Hydrometallurgy*, 222, 2023, 106181.
- [14] Heijnen, J.J. *A Thermodynamic Description of Microbial Growth and Product Formation*. In The Metabolic Pathway Engineering Handbook. CRC Press, 2009, p. 11-32.
- [15] Roels, J.A. Application of Macroscopic Principles to Microbial Metabolism (Reprinted from Biotechnology and Bioengineering, vol. 22, 1980, p. 2457-2514). *Biotechnology and Bioengineering*, 103 (1), 2009, p. 2-59.
- [16] Roels, J.A. *Energetics and kinetics in biotechnology*. Elsevier Biomedical Press, 1983.
- [17] Monod, J. The growth of bacterial cultures. *Annual Review of Microbiology*, 3, 1949, p. 371-394.
- [18] Pirt, S.J. The maintenance energy of bacteria in growing cultures. *Proceedings of the Royal Society of London. Series B, Biological sciences*, 163 (991), 1965, p. 224-231.
- [19] Basaran, A.H., Tuovinen, O.H. An ultraviolet spectrophotometric method for the determination of pyrite and ferrous ion oxidation by *Thiobacillus ferrooxidans*. *Applied Microbiology and Biotechnology*, 24 (4), 1986, p. 338-341.
- [20] Mandl, M., Nováková, O. An ultraviolet spectrophotometric method for the determination of oxidation of iron sulphide minerals by bacteria. *Biotechnology Techniques*, 7 (8), 1993, p. 573-574.
- [21] Herrera, L., Ruiz, P., Aguillon, J.C., Fehrmann, A. A new spectrophotometric method for the determination of ferrous iron in the presence of ferric iron. *Journal of Chemical Technology and Biotechnology*, 44 (3), 1989, p. 171-181.
- [22] Boon, M., Luyben, K., Heijnen, J.J. The use of on-line off-gas analyses and stoichiometry in the bio-oxidation kinetics of sulphide minerals. *Hydrometallurgy*, 48 (1), 1998, p. 1-26.
- [23] Tuovinen, O.H., Kelly, D.P. Studies on the growth of *Thiobacillus ferrooxidans*. *Archiv für Mikrobiologie*, 88 (4), 1973, p. 285-298.
- [24] Boon, M., Ras, C., Heijnen, J.J. The ferrous iron oxidation kinetics of *Thiobacillus ferrooxidans* in batch cultures. *Applied Microbiology and Biotechnology*, 51 (6), 1999, p. 813-819.
- [25] Boon, M., Heijnen, J.J., Hansford, G.S. Recent developments in modelling bio-oxidation kinetics .1. Measurement methods. Minerals Bioprocessing II, ed. D.S. Holmes and R.W. Smith, 1995, p. 41-61.
- [26] Mesa, M.M., Macías, M., Cantero, D. Mathematical model of the oxidation of ferrous iron by a biofilm of *Thiobacillus ferrooxidans*. *Biotechnology Progress*, 18 (4), 2002, p. 679-685.
- [27] Braddock, J.F., Luong, H.V., Brown, E.J. Growth Kinetics of *Thiobacillus ferrooxidans* Isolated from Arsenic Mine Drainage. *Applied and Environmental Microbiology*, 48 (1), 1984, p. 48-55.
- [28] Molchanov, S., Gendel, Y., Ioslavich, I., Lahav, O. Improved Experimental and Computational Methodology for Determining the Kinetic Equation and the Extant Kinetic Constants of Fe(II) Oxidation by *Acidithiobacillus ferrooxidans*. *Applied and Environmental Microbiology*, 73 (6), 2007, p. 1742-1752.
- [29] Beck, J.V., Shafia, F.M. Effect of phosphate ion and 2,4-dinitrophenol on the activity of intact cells of *Thiobacillus ferrooxidans*. *Journal of Bacteriology*, 88 (4), 1964 p. 850-857.
- [30] Tuovinen, O.H., Kelly, D.P. Biology of *Thiobacillus ferrooxidans* in relation to the microbiological leaching of sulphide ores. *Zeitschrift für allgemeine Mikrobiologie*, 12 (4), 1972, p. 311-346.
- [31] MacDonald, D.G., Clark, R.H. The oxidation of aqueous ferrous sulphate by *Thiobacillus ferrooxidans*. *The Canadian Journal of Chemical Engineering*, 48 (6), 1970, p. 669-676.
- [32] Beck, J.V., Brown, D.G. Direct sulfide oxidation in the solubilization of sulfide ores by *Thiobacillus ferrooxidans*. *Journal of Bacteriology*, 96 (4), 1968, p. 1433-1434.



## BIOLEACHING OF MINE WASTES FROM THE ABANDONED MINING DEPOSITS IN SLOVAKIA

Alena Luptáková<sup>a</sup>, Magdaléna Bálintová<sup>b</sup>, Oľga Šestinová<sup>a</sup>, Daniela Guglietta<sup>c</sup>,  
Stefano Ubaldini<sup>c</sup>, Miloslav Lupták<sup>d</sup>

<sup>a</sup> Institute of Geotechnics of Slovak Academy of Sciences, Department of Mineral Biotechnology,  
Watsonova 45, Kosice, SK-040 01, Slovak Republic, [luptakal@saske.sk](mailto:luptakal@saske.sk)

<sup>b</sup> Department of Environmental Engineering, Civil Engineering Faculty, Technical University in Kosice,  
Vysokoskolska 4, Kosice, SK-042 00, Slovak Republic, [magdalena.balintova@tuke.sk](mailto:magdalena.balintova@tuke.sk)

<sup>c</sup> Institute of Environmental Geology and Geoengineering, CNR, Area della Ricerca di Roma RM 1 - Montelibretti,  
Via Salaria Km 29,300 - 00015 Monterotondo Stazione, ROMA, Italy,  
[stefano.ubaldini@igag.cnr.it](mailto:stefano.ubaldini@igag.cnr.it), [daniela.guglietta@igag.cnr.it](mailto:daniela.guglietta@igag.cnr.it)

<sup>d</sup> Institute of Materials and Quality Engineering, Faculty of Materials, Metallurgy and Recycling,  
Technical University in Kosice, Letna 9, Kosice, SK-042 00, Slovak Republic, [miloslav.luptak@tuke.sk](mailto:miloslav.luptak@tuke.sk)

### Abstract

Sulphidic mining wastes in the form of heaps, dumps and tailings are negative residuals of mining and mineral processing. They are a long-term source of contamination because they are subject to intensive mechanical, chemical and biological transformation processes that result in the leaching of various toxic elements into the environment. However, these mining wastes have a positive side as well. Although they contain low concentrations of toxic elements, they are potentially utilizable as the alternative raw resource of metals include critical metals. There are several technologies for processing mining dumps and heaps. These include the bioleaching with sulphur- and iron-oxidizing bacteria of the genus *Acidithiobacillus*.

The focus of this work was to study the bioleaching of solid mine wastes taken from the mine heap of an abandoned mining area - Zlatá baňa. *Acidithiobacillus ferrooxidans* bacteria were used in the experiments. The tests were carried out in laboratory conditions.

**Keywords:** sulphidic mining wastes, bioleaching, metals, *Acidithiobacillus ferrooxidans*

### 1 Introduction

Wastes coming from ore mining and mineral processing, such as heaps, dumps, mine water outflows from shafts and tunnels, drainage water from heaps, dumps and tailings can be an interesting secondary raw material source of metals [1-2]. These wastes are negative residuals of mining and mineral processing. They present sources of contamination for the environment in the surrounding of the old, closed or abandoned mining areas, and therefore many of these sites in Slovakia are classified as environmental burdens, marked in literature as “old mining burdens” [3-4]. Environmental burdens in terms of legislation are integrated in several strategic documents of the Government of the Slovak Republic [5].

Low-grade sulphidic mining wastes in the form of heaps, dumps and tailings are integral part of the active but mainly finished mining activity on ore deposits. They contain toxic elements, mainly metals and metalloids. They consist of heterogeneous materials deposited here over many years of intensive mining activity and mineral processing. They are a long-term source of contamination because they are subject to intensive mechanical, chemical and biological transformation processes that result in the leaching of various toxic elements into the environment. The main risk is the bioavailability of metals and the entrance into the food chain. Environmental contamination is indicated by the occurrence of secondary minerals, which are present in a metastable form in the surface areas of the ore bodies and in the heaps of wastes after mining. Secondary minerals precipitate at the places where drainage waters flow out from heaps [6]. Metals that come into surface waters by groundwater, mine water, and flow water have different mobility [7]. Besides the traditional methods aimed at assessing the content of toxic elements in the natural environment, the “biomonitoring methods”, based on the ability of living organisms to respond to environmental stress, are getting to the forefront [8].

There are several technologies for processing mining dumps and heaps. These include leaching in connection with subsequent extraction of metals from leach solutions [9]. During leaching of solid wastes, metals are leached into the solution. Their subsequent removal from the leach solution e.g. by selective precipitation it makes it possible to obtain metals in suitable forms for further use. Leaching of mining waste

can take place under the influence of chemical as well as chemical-biological processes, i.e. bioleaching processes with the participation of a biological component - microorganisms [10]. Although bioleaching as a progressive technology of mining, processing of minerals and environmental protection has been applied in practice only since the mid-50s of the twentieth century, the first mentions of some of its "forms" are known 1000 years BC [11]. In connection with landfills of mining wastes containing sulphide minerals, bioleaching with sulphur- and iron-oxidizing bacteria of the genus *Acidithiobacillus* (SFeOB) is the most studied, which due to their metabolism cause oxidation of metal sulphides, thus dissolving sulphides and thus leaching metals into leach solution [12]. The activity of SFeOB based on the biogeochemical sulphur cycle in nature is associated with the activities of sulphate-reducing bacteria (SRB) of the genus *Desulfovibrio*. SRBs are able to reduce sulphate sulphur to sulphide sulphur in the form of hydrogen sulphide. Subsequently, hydrogen sulphide precipitates metals to form metal sulphides [10]. The bioreductive properties of SRB can thus be used in the recovery of metals from mining effluents in the form of metal sulphides. The study of these processes provides the possibility of recovering mining waste as a source of utility metals including critical metals.

Typical examples of old mining loads in Slovakia are mainly abandoned deposits Smolník, Pezinok, Ľubietová, waste deposit in Šobov and others. The main sources of environmental risks of these deposits are heaps, outflows of mine waters from mining areas, drainage water from heaps, dumps and tailings with over-limit concentrations of metals, metalloids and sulphates, in comparison to Government Regulation No. 269/2010 Coll. [3].

Mining localities with the little attention so far to the environmental contamination are the abandoned deposits - Dubnické opalove bane and Zlatá Baňa [8]. These deposits have long been used intensively for the extraction of Au, Sb, Hg and also opal, whose deposits have been unique till the 19th century. Opal mining was significant in the second half until the end of the 18th century [13]. Continuation of mining activity was mining of antimony. At the beginning of the 20th century, after the end of the mining activities, the area was devastated by numerous remains of mining activities. There are a huge number of extensive heaps, open mine tunnels and several shafts. In spite of the serious environmental situation and the persisting environmental problems, no attention has been paid to this area in terms of scientific research. It is necessary to focus on obtaining a comprehensive set of knowledge regarding the environmental status of this former mining area, which has not yet been evaluated for this purpose. The self-improvement of the situation in the abandoned mining sites mentioned above is not possible, but it is possible to focus on methods of its remediation or valorisation as secondary sources of raw materials - Cu, Fe, Zn, Hg, Pb etc., as well as of critical raw materials such - Co, Ni, Mg, Sb, Sr, Ti etc.

This article focused on the preliminary study of bioleaching of solid mining wastes taken from the heap of abandoned mining area Zlatá Baňa. The sulphur and iron oxidizing bacteria *Acidithiobacillus ferrooxidans* (AF) were used in the experiments. Experimental works were focused on the leaching of selected metals (Fe, Zn, Pb, As and Sb) under the influence of AF bacteria at the laboratory conditions.

## 2 Material and methods

### 2.1 Microorganisms

The sulphur and iron-oxidizing bacteria *Acidithiobacillus ferrooxidans* (AF) used in the experiment was isolated from two different localities of Eastern Slovakia. Bacteria were isolated from the acid mine drainage effluent from the Pech shaft, the Smolník deposit (AF-S) and from the seepage water flowing out of the heap Zlatá Baňa (AF-ZB). A selective nutrient medium 9K [14] was applied for the isolation, cultivation and preparation of the active bacterial culture of AF.

### 2.2 Samples of solid mine wastes

The four soil samples were collected from abandoned mining area Zlatá Baňa. Sampling was performed from 30 cm depth of the mine waste heap and the samples were saved into plastic bags. All collected material was dried at laboratory temperature, quartered, grounded and sieved under 63 µm. The chemical composition of solid mine wastes was analysed by X-ray fluorescence analysis (XRF) using a SPECTRO iQ II (Ametek, Germany). The mineralogical composition was analyzed by X-ray qualitative diffraction analysis using X-ray diffractometer D8 Advance (Bruker, Germany).



### 2.3 Bioleaching experiments

Based on the results of XRF analysis, one representative sample of the mine waste (ZB) was tested in the bioleaching experiments. Sample was ground to a particle size  $\leq 63 \mu\text{m}$ . Bioleaching of the ZB sample was performed using bacterial culture of AF-S and AF-ZB. Bioleaching experiments were carried out under aerobic conditions at 30 °C in 250 ml Erlenmeyer flasks containing 100 ml of acid sulphate media 9K without iron (with a composition for 1 liter of medium -  $\text{MgSO}_4 \cdot 7\text{H}_2\text{O}$  (0.4 g),  $(\text{NH}_4)_2\text{SO}_4$  (0.1 g),  $\text{K}_2\text{HPO}_4$  (0.04 g), 5 ml 5 M  $\text{H}_2\text{SO}_4$ ). Pulp density was 3 % and pH 1.5. The inoculum of used cultures was 5 % and all experiments were carried out in duplicate. The samples were mixed at 150 revolutions/min. For each bioleaching experiment chemical controls with the same conditions and without inoculum were included. Concentrations of Fe, Zn, Pb, As and Sb in leachates were analysed at chosen intervals. pH was measured by pH meter PHM210 (MeterLab, France) experiments. Concentration of metals in leachates were determined by atomic absorption spectrometry (AAS) using a Varian 240FS/240 Z spectrometer (Varian, Australia).

### 3 Results and discussion

Chemical composition of the studied mine waste sample ZB is presented in Table 1.

**Table 1. The chemical analysis of Zlatá Baňa sample tested in the bioleaching experiments**  
(values of selected majority elements, XRF analysis)

Sample	Fe	Zn	Pb	As	Sb
	(mg/kg)				
ZB	46020.0	310.8	1518.0	291.9	402.5

Figure 1 shows the trend of the bioleaching of Fe from the studied solid sample ZB throughout the duration of the experiment. Biotic samples (ZB-AF-S) and (ZB-AF-ZB) have been observed to contain higher concentrations of Fe in the leachates than in the abiotic samples (ZB-K). Maybe the reason for the difference in the leached concentration of Fe has to do with the activity of bacterial culture (AF). A difference in the use of autochthonous (ZB-AF-ZB) and non-autochthonous bacterial culture ZB-AF-S) was not observed, because in both conditions, the concentration of leached Fe was approximately the same.

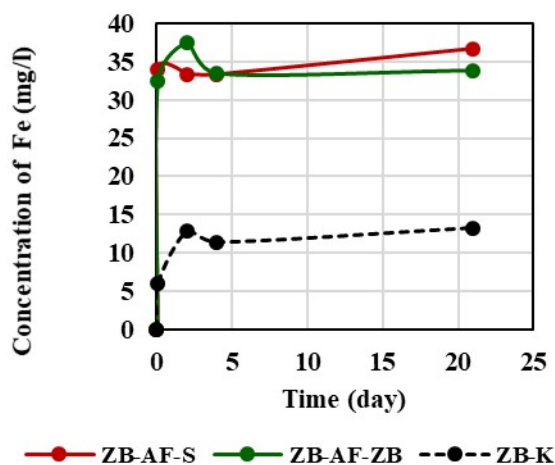


**Fig. 1 .The changes of Fe concentration at bioleaching tests**

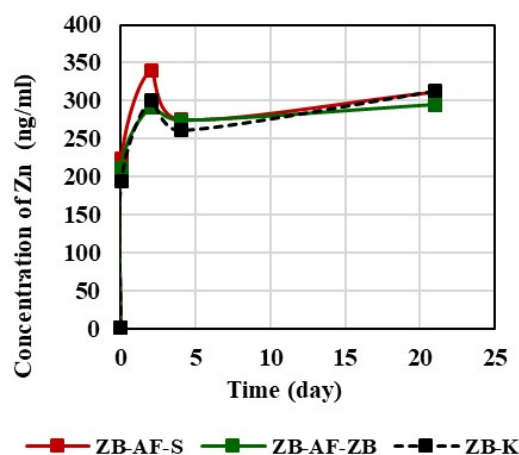


**Fig. 2. The changes of Zn concentration at bioleaching tests**

Figures 2 - 5 show the course of leaching of zinc, lead, arsenic and antimony. Similar to the leaching of Fe, a difference in the use of autochthonous (ZB-AF-ZB) and non-autochthonous bacterial culture (ZB-AF-S) was not detected. In addition to that, biotic and abiotic samples were observed to contain approximately the same concentrations of investigated elements in the leachates. Probably the leaching of elements was caused by the applied nutrient medium and not under the influence of bacteria. The highest increase of the Zn concentration in the liquid phase for biotic, as well as abiotic samples was observed after two days. Subsequently the concentration of Zn decreased, later gradually slightly increased, and finally reached the value 300 - 310 ng/ml at the end of the experiment. The highest increase of the Pb concentration

in the leachates was observed after two days (in ng/ml): 210, 240 and 244 in samples ZB-AF-S, ZB-K and ZB-AF-ZB, respectively. Next the concentration of Pb very much slightly decreased and this trend was observed until the end. The final concentrations of Pb reached the following values (in ng/ml): 200, 220 and 240 in samples ZB-AF-ZB, ZB-AF-S and ZB-K, respectively. The highest increase of the As and Sb concentration in the all leachates was observed after two hours, so it can be said that it happened immediately after the addition of acid sulphate media 9K medium without iron (As - 49.0 ng/ml; Sb - 6.3 ng/ml). Subsequently the concentration of As decreased, after four days was almost stabilized until the end of the experiment, when the concentration of As achieved values of 16-18 ng/ml. In all leachates the concentration of Sb gradually decreased after four days, and finally reached the value 3.5 ng/ml.

Figure 6 shows the pH changes in the liquid phase at the start and the end of bioleaching tests. There were no significant changes in the pH values of the liquid phases. Bacteria AF had an appropriate pH for their growth.

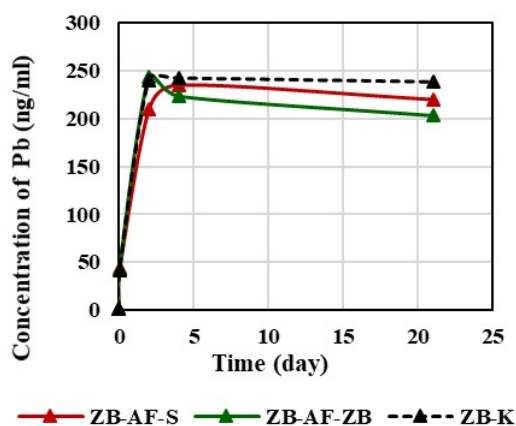


Fig. 3. The changes of Pb concentration at bioleaching tests

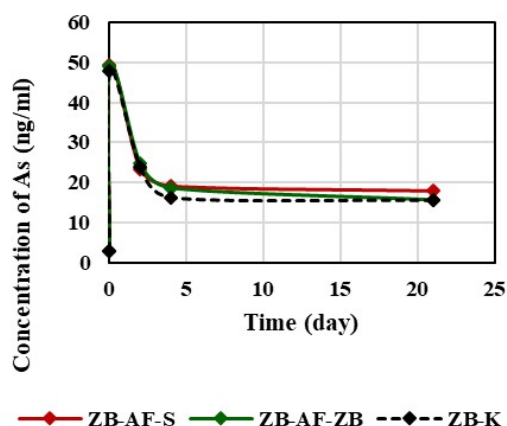


Fig. 4. The changes of As concentration at bioleaching tests

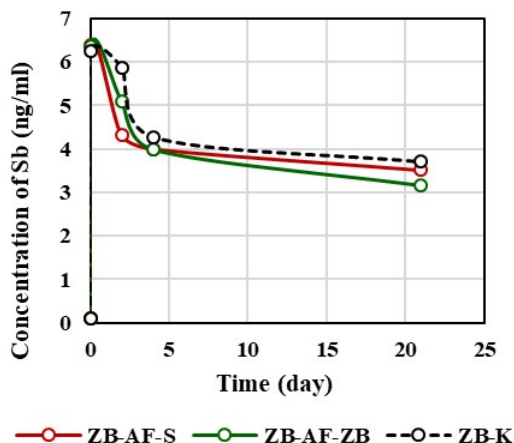


Fig. 5. The changes of Sb concentration at bioleaching tests

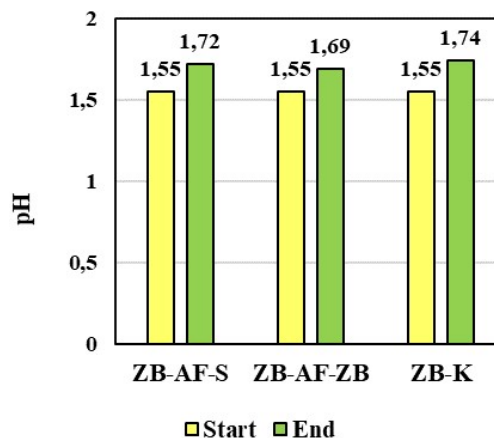


Fig. 6. The changes of pH at bioleaching tests

#### 4 Conclusions

The achieved results of the preliminary bioleaching tests of the soil samples collected from abandoned mining area Zlatá Baňa documented that: only in biotic samples (ZB-AF-S) and (ZB-AF-ZB) have been observed to contain higher concentrations of iron in the leachates than in the abiotic samples (ZB-K); the difference in the use of autochthonous (ZB-AF-ZB) and non-autochthonous bacterial culture (ZB-AF-S) was not observed; during of the leaching of zinc, lead, arsenic and antimony, the biotic also abiotic samples were observed to contain approximately the same concentrations of investigated elements in the leachates. Probably the leaching of elements was caused by the applied nutrient medium and not under the influence of bacteria.

There were no significant changes in the pH values of the liquid phase, the bacteria had an appropriate pH for their growth. Control samples (ZB-K) were not contaminated with AF bacteria. The activity of AF bacteria may have been affected by the increased concentration of As and Pb in the leachates [15]. Perhaps the adaptation of bacteria to the given conditions is a partial solution.

Now we cannot explain the leaching of selected metals trends. They are preliminary tests. More research is needed. Research using living organisms such as bacteria is unpredictable and fraught with many questions.

### Acknowledgements

The work was supported by the Slovak Grant Agency for Science Grant No. 2/0108/23, Grant No. 1/0213/22 and Slovak Research and Development Agency under the contract APVV-20-0140.

### References

- [1] Lottermoser, B.G. *Mine Wastes: Characterization, Treatment, and Environmental Impacts*. Third Edition. Springer, Berlin, Heidelberg, 2010, 400 p. ISBN 978-3-642-12418-1.
- [2] Mehta, N., Dino, G.A., Passarella, I., Ajmone-Marsan, F., Rossetti, P., De Luca, D.A. Assessment of the possible reuse of extractive waste coming from abandoned mine sites: case study in Gorno, Italy. *Sustainability*, 12 (6), 2020, p. 2471-2493.
- [3] Šottník, P., Jurkovič, L., Hiller, E., Kordík, J., Slaninka, I. *Environmental burdens*. Banská Bystrica: Slovenská agentúra životného prostredia, 2015, 303 p. ISBN 978-80-89503-42-1.
- [4] Andráš, P., Križáni, I. Influence of the Exploitation of Raw Materials on the Environment. *Životné Prostredie*, 44 (1), 2010, p. 20-23.
- [5] RIS3 SK. [on-line]: <https://www.minedu.sk/data/att/15670.pdf>.
- [6] Lintnerová, O., Šoltés, S., Šottník, P. *Environmental risks of acid mining in the abandoned Smolník deposit*. Bratislava: PF UK, 2009. 229 p. ISBN 978-80-223-2764-0.
- [7] Rieuwerts, J.S., Thornton, I., Farago, M.E., Ashmore, M.R. Factors influencing metal bioavailability in soils: preliminary investigations for the development of a critical loads approach for metals. *Chemical Speciation & Bioavailability*, 10 (2), 1998, p. 61-75.
- [8] Demková, L., Árvay, J., Bobuľská, L., Hauptvogel, M., Hrstková, M. Open mining pits and heaps of waste material as the source of undesirable substances: biomonitoring of air and soil pollution in former mining area (Dubník, Slovakia). *Environmental Science and Pollution Research*, 26 (34), 2019, p. 35227-35239, doi: 10.1007/s11356-019-06582-0.
- [9] Hennebel, T., Boon, N., Maes, S., Lenz, M. Biotechnologies for critical raw material recovery from primary and secondary sources: R&D priorities and future perspectives. *New Biotechnology*, 32 (1), 2015, p. 121-1277, doi: 10.1016/j.nbt.2013.08.004.
- [10] Johnson, D.B. Biomining-biotechnologies for extracting and recovering metals from ores and waste materials. *Current Opinion in Biotechnology*, 30 (24-31), 2014, doi: 10.1016/j.copbio.2014.04.008.
- [11] Ehrlich, H.L. Past, present and future of biohydrometallurgy. *Hydrometallurgy*, 59 (2), 2001, p. 127-134.
- [12] Donati, E.R., Sand, W. *Microbial processing of Metal Sulfides*. Dordrecht: Springer, 2007. ISBN 987-1-4020-5589-8.
- [13] Caucia, F., Ghisoli, C., Marinoni, L., Bordoni, V. Opal, a beautiful gem between myth and reality. *Neues Jahrbuch für Mineralogie-Abhandlungen: Journal of Mineralogy and Geochemistry*, 190 (1), 2013, p. 1-9.
- [14] Karavajko, G.I., Rossi, G., Agate, A.D., Groudev, S.N., Avakyan, Z.A. *Biogeotechnology of metals*. Centre of projects GKNT, Moscow, 1988, 350 p.
- [15] Gu, T., Rastegar, S.O., Mousavi, S.M., Li, M., Zhou, M. Advances in bioleaching for recovery of metals and bioremediation of fuel ash and sewage sludge. *Bioresource Technology*, 261, 2018, p. 428-440.



## BIOLEACHING OF TETRAHEDRITE FROM THE STRIEBORNÁ VEIN OF THE ROŽŇAVA ORE FIELD

**Eva Mačingová<sup>a</sup>, Daniel Kupka<sup>a</sup>, Alena Luptáková<sup>a</sup>, Dávid Jáger<sup>a</sup>**

<sup>a</sup> *Institute of Geotechnics of SAS, Watsonova 45, Košice, Slovakia,  
macingova@saske.sk, dankup@saske.sk, luptakal@saske.sk, jager@saske.sk*

### Abstract

Complex sulfide minerals of the tetrahedrite group, that is notable for the different elements stable in its structure, are a significant copper, precious/noble-metals and other valuable metals resources. Particular component of these minerals are difficult to separate and treat. The antimony and arsenic content causes technological problems during copper metallurgy along with ecological problems related to the hazardous emissions. Moreover, tetrahedrite is interest of the potential Sb recovery. Alkaline leaching in a medium containing sodium sulfide offers a hydrometallurgical approach to provides selective dissolution of different components from the minerals into the leach solution. The goal of the present work was to evaluate the possibility of antimony separation from a tetrahedrite rich flotation concentrate by bioleaching at a higher pH as an analogy to the caustic hydrometallurgical treatment. The bioleaching was performed at anaerobic condition using sulfate reducing bacteria, which produce significant amounts of dihydrogen sulfide in the process of dissimilatory anaerobic respiration. The tetrahedrite sample used in these investigations originated from the Strieborná vein of the Rožňava mine situated on eastern Slovakia.

**Keywords:** tetrahedrite-tennantite concentrate, alkaline leaching, bioleaching, sulfate reducing bacteria

### 1 Introduction

Antimony is a shiny grey metalloid known since ancient times when it was used in medicine and cosmetics. It is an element present in relatively small concentrations in the earth's crust, rarely found in pure metallic form. Antimony compounds are found in several types of ore to form over 100 different minerals. Although not used in large quantities, antimony is used extensively for many purposes. Its biggest application today is as a flame retardant, which accounted for around half of global usage in 2023. Antimony is used as decoloring agents in optical glass (binoculars, phone screens, photovoltaic glass), in lead-acid batteries, in military equipments. It is also used as a metals strengthener for babbitt bearings in wind and hydro turbines. Antimony now plays an essential role in large-scale renewable energy storage batteries, which is critical to the clean energy movement [1]. Antimony due to its growing economic significance and supply risk is repeatedly included in the List of critical raw materials of the EU. EU 100 % import reliance increase the importance of local sources [2].

Global growth for base metals demand results to the attention to the low grade and complex sulfide ore processing. Based on above mentioned, Slovak deposits of critical and other significant minerals/metals were reevaluated as it is reported in [3]. Currently nine no exploited antimony deposits are registered with reserves of 55 358 t of Sb. In Little Carpathians at Pezinok four deposits with average grades of 3.22 % antimony is situated. Five Dúbrava deposits with average grades of 1.86 % antimony in Low Tatras is located [4]. The potential in Sb production has the Strieborná deposit placed in eastern Slovakia near the town of Rožňava. [5]. Major vein minerals are siderite and quartz-sulfide minerals. The most abundant sulphide minerals are tetrahedrite, chalcopyrite, pyrite and arsenopyrite. A more brittle tetrahedrite variety with steel blue colour and high metallic lustre is usually enriched by Cu, Ag, Bi, Sb and Hg. A darker low lustre variety contains more Zn and Fe. The high content of silver in tetrahedrite was the reason for the name of the Strieborná vein [6]. According to a National Instrument (NI) 43-101 technical report estimate from the year 2015, the Strieborná deposit contained resources of 2.3 million metric tons with average grades of 0.85 % antimony, 1.2 % copper, and 267 grams per metric ton silver [7].

The majority of antimony extractive processes involve pyrometallurgical methods. These methods continue to dominate today [8]. However, complex sulfide minerals are difficult to separate by selective flotation and the associated elements as antimony and arsenic have adverse effect to their pyrometallurgical processing as significantly affect the quality of the copper product. Besides, the emission of toxic antimony and arsenic compounds during the conventional treatment process cause serious environmental problems [9-

11]. Hydrometallurgical treatment offers a cost effective and environmentally friendly process for the selective dissolution of the different elements from the complex sulfide minerals. Hydrometallurgical processing of tetrahedrite is possible by way of acidic oxidative leaching or alkaline leaching. In acidic oxidation media, dissolution of copper and iron occurs and, depending on the leaching conditions, also antimony. Alkaline leaching in a sodium sulfide environment selectively dissolves antimony, while copper and iron remain in the solid residue. Alkaline sodium sulfide solution acts as a universal solvent for most antimony compounds. Conversely, most metals are highly insoluble in this solution. Exceptions would include arsenic, tin and mercury. After liquid/solid separation, the deposition of antimony metal from the alkaline sulfide solution via electrowinning can be carried out. This process also regenerates sulfide in the solution, allowing effective recycle of the lixiviant back to the leach stage [8]. The feasibility of antimony solubilization in both, acidic and basic media results from its amphoteric nature [10, 11].

In this work the bioleaching of tetrahedrite flotation concentrate as an alternative of chemical alkaline leaching was studied with aim to antimony selective recovering. The test was performed at higher pH in the presence of sulfate reducing bacteria consortium, of which metabolic product is dihydrogen sulfide.

## 2 Materials and methods

### 2.1 Materials

The tetrahedrite used in this investigation originated from the Strieborná deposit situated within the Rožňava ore field. The ore sample were crushed approx. to 100 µm and processed by froth flotation. The upgraded concentrate sample contained about 73 % of tetrahedrite and about 21 % of siderite [5]. Concentrations of analysed elements are shown in the Table 1

**Table 1. Chemical composition of the tetrahedrite concentrate**

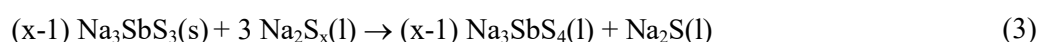
Cu	Sb	Fe	As	Zn	Ag	Mn
(wt%)						
30.31	22.21	9.03	2.03	0.75	0.55	0.11

### 2.2 Methodology

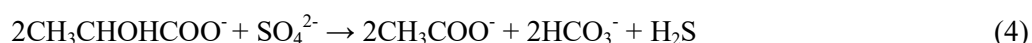
Our shared efforts were focused on the development of low-cost, effective, environmental friendly biotechnologies enabling extraction and recovery of metallic raw materials. The aim of our work was the treatment a tetrahedrite rich flotation concentrate by selective dissolution of elements. The first concept had target the bioleaching of the concentrate in acidic and aerobic condition at ambient temperature by three strains of iron-oxidizing bacteria as equivalence of chemical acidic oxidative leaching. The role of bacteria in the process was the Fe<sup>3+</sup> oxidizing agent regeneration and high redox potential maintenance. The positive biocatalyzing effect led to the selective extraction of Cu, Zn, Ag, Pb, Sb and As into the solution [12, 13].

The present work is aimed to the second option of the leaching in the presence of a sulfate reducing bacteria at a higher pH as an analogy to the hydrometallurgical treatment of tetrahedrite by alkaline leaching in a sodium sulfide environment. By commercial caustic leaching of tetrahedrite selective and effective dissolution of antimony and arsenic in the form of tri- to pentavalent soluble complex (thioanions) is achieved and copper in the form of insoluble sulfides is obtained. The extraction rate is significantly enhancing with ascending leaching time and reaction temperature and by increased concentration of sodium sulfide and sodium hydroxide in the lixiviant. NaOH avoid hydrolysis of sulfide to hydrogen sulfide and dihydrogen sulfide, which reduce the efficiency of the leaching. The degree of antimony and arsenic dissolution is intensified with mineral particle size decrease [11, 14].

The chemistry of tetrahedrite leaching in alkaline sulfide solution can be expressed by equations [10, 11, 14]:



In the bioleaching experiment sulfate reducing bacteria (SRB) was used. SRBs are defined as a diverse group of heterotrophic, strictly anaerobic bacteria. Their basic metabolic process is dissimilatory anaerobic respiration, in which the bacteria oxidize the organic substrate or molecular hydrogen and reduce sulfate, occasionally sulfites and thiosulfates. SRBs produce significant amounts of sulfane in this process. For their growth, the optimal values are pH 6.5 - 7.5 and redox potential in the range of -100 mV to -300 mV [15, 16]. The SRBs used in the bioleaching experiment were isolated from the source of geothermal well of natural mineral water near Košice (Slovakia). Isolation and subsequent cultivation were performed under anaerobic conditions at 30 °C and pH 7.5, using a selective nutrient medium DSM-63 according to J. Postgate [15]. The chemical composition of medium promotes the preferential growth of SRB from the genera *Desulfovibrio* and *Desulfotomaculum*. The source of the organic substrate in this nutrient medium is sodium lactate and sulfate serves as the sole electron acceptor. The metabolic process of incomplete heterotrophic oxidation of lactate associated with sulfate reduction is described by the equation:



Although the optimal pH value for growth for SRB is about 7.5, in the literature is reported that SRBs can thrive at pH 8.5 and are able to tolerate pH 10 [17]. Considering the conditions of the alkaline leaching process of tetrahydrite in a sodium sulfide environment, we focused on the adaptation of SRB to higher pH values. The adaptation proceeded in several steps. The medium pH was stepwise increased during the cultivation of SRB from an optimal value of 7.5 to 8.0, followed by 8.5 to 9.0. The metabolic activity of SRB was still noticed at the pH values of 8.0 and 8.5. Inhibition occurred at pH 9.0, even after repeated attempts of incubation. Consequently, in bioleaching experiments, the bacterial cultures grown at pH 8.5 was used. Study with the cultures grown at pH 7.5 was also realised to observe the differences in the bioleaching performance at different pH values.

### 2.3 Experimental set up

Sample of tetrahydrite concentrate obtained by froth flotation was used for the experiments. The mineral sample was sterilized at 105 °C for one hour. Bioleaching experiments were performed in batch mode in media with pH 8.5 and pH 7.5 with slurry density of 20 g tetrahydrite sample per liter of liquid nutrient medium. 20 % (vol) of bacterial SRB cultures grown anaerobically were inoculated in the biotic samples (BS). Abiotic controls (AC) contained only the tetrahydrite in sterile liquid medium. The experiments were performed in parallels. The cultures were incubated statically at 30 °C under anaerobic conditions in 500 ml culture flask. The metabolic activity of SRBs during the bioleaching experiments was evaluated based on the loss of sulfates and the production of sulfane in the liquid medium. The sulfate concentration was determined by ion chromatography (Dionex ICS 5000, Thermo Scientific, USA) and the positivity of the sulfane was confirmed by spectrophotometric method (VIS spectrophotometer HACH DR 1900). The concentration of selected metals Sb, As, Fe, Cu, Zn, Mn, Ag in the leachate was determined by AAS (Varian AA240FS, Australia) and ICP-MS (Agilent 7700, Agilent Technologies, Inc. Wilmington, USA) analysis respectively. The elemental composition of metal sulfides was evaluated by energy dispersive X-ray spectroscopy (EDX) (Oxford Instrument, Oxford, UK). Bioleaching experiments were performed for six weeks. The liquid samples for the analyses were withdrawn at weekly intervals.

## 3 Results and discussion

In the experiments performed in media with a pH value of 7.5, in spite of retry no SRB metabolic activity was recorded in biotic samples. No decrease of sulfate concentration occurred and the presence of sulfane in growth media was not confirmed. As it is shown in the Figures 1 and 2, the course of metal leaching in BS and in AC was very similar, whereas dissolution of individual metals occurred wholly by growth media. The noticeable leaching occurred in the case antimony, the concentration of which achieved a value of 1970 µg/l in BS and in AC a value of 1960 µg/l. Arsenic reached concentration of 456 µg/l in BS and of 521 µg/l in AC. The concentration of Cu in BS was 7.8 µg/l and in AC 6.1 µg/l. During the experiment (> 14 days), pH decrease was noticed to 6.92 and 6.55 in the BS and AC, respectively.

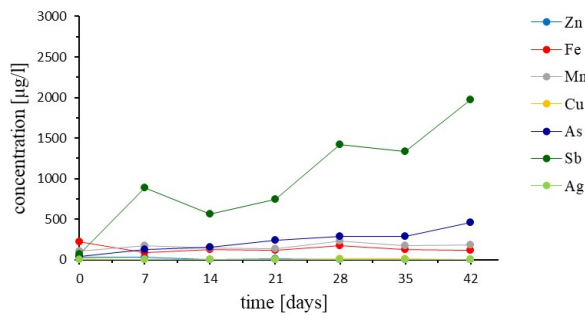


**Fig. 1. Dissolution of metals from tetrahedrite concentrate in the presence of SRBs at the pH of 7.5**

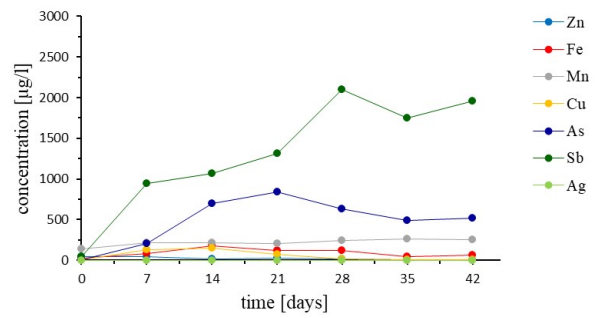


**Fig. 2. Dissolution of metals from tetrahedrite concentrate in abiotic series at pH of 7.5**

The evidence of SRB metabolic activity in experiment conducted at pH 8.5 was a significant difference compared to the previous procedure. In growth media the formation of sulfane was confirmed with concurrent decrease in the concentration of sulfates. Over the 14 days, the values of pH declined to 7.20 and 7.24 in the BS and AC, respectively. The graphs (Figures 3 and 4) indicate quantities of metals and metalloids extracted from the tetrahedrite concentrate to the aqueous medium during leaching period.

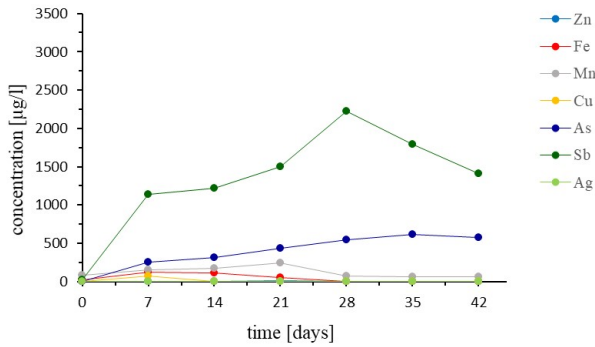


**Fig. 3. Dissolution of metals from tetrahedrite concentrate in the presence of SRBs at the pH of 8.5**

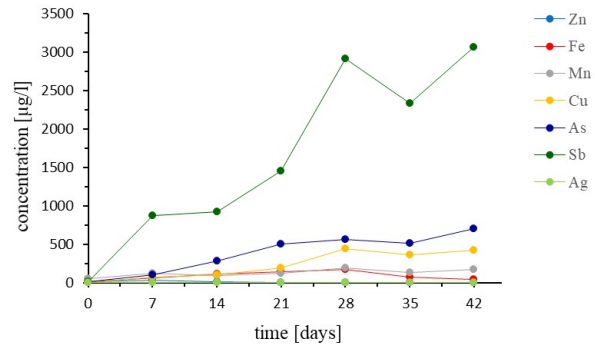


**Fig. 4. Dissolution of metals from tetrahedrite concentrate in abiotic series at pH of 8.5**

In the early of experiment there was no significant difference of the amounts of leached metals in the presence or absence of SRBs. The decrease of metal concentration with advanced time of bioleaching (> 28 days) in the biotic series was probably due to the production of sulfane and subsequent creation of tri- and pentavalent soluble thioanions of antimony and arsenic, following by formation of colloidal sulfides at near-neutral pH [18]. This presumption was affirmed by colouring of liquid media and presence of colloidal clusters (Figure 5). Precipitation of sulfides of respective metals after acidification of the sample was confirmed by EDX analysis (Figure 6). The final concentration of antimony reached the value of 1410 µg/l in BS, and 3060 µg/l in AC. Concentration of arsenic achieved a value of 576.4 µg/l in BS and 702 µg/l in AC.

Concentration of copper in aqueous medium was 424 µg/l in AC and markedly lower 0.3 µg/l in BS, presumably due to its expected precipitation in the form of sulfides.

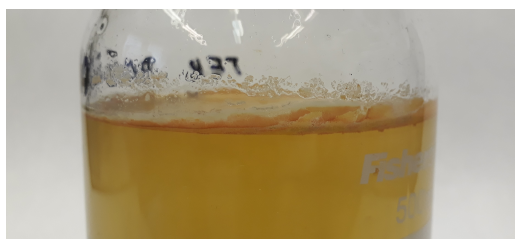


**Fig. 5. Leaching experiment BS at pH 8.5**

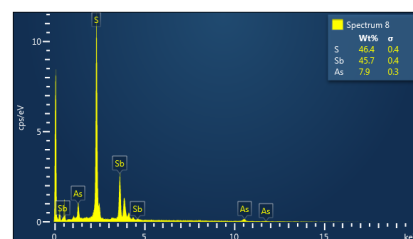


**Fig. 6. EDX analysis of As-Sb precipitates**



The possible reason for different bacterial activity of SRBs in biotic samples at pH values of 7.5 and 8.5 is the presence of toxic metals. Different pH in growth media after addition of tetrahedrite can affect the speciation of present elements, what determines their bioavailability and toxicity. Diverse chemical forms of particular metals can contribute to inhibition of SRBs growth in the intricate multicomponent system of nutrient medium, tetrahedrite sample and organic residues from the flotation process.

#### 4 Conclusions

It can be concluded that during bioleaching experiments using SRBs, it is not possible to meet the efficiency defined for the hydrometallurgical processing of tetrahedrite by alkaline leaching in a sodium sulfide environment. The obtained results evidenced, that during the experiments, particular metals were leached only by the nutrient medium. Higher concentrations of metals were recorded in lixiviant with higher value of pH. The metabolic activity of SRB associated with the production of sulfane was manifested by a decrease in the concentration of metals by precipitation of the corresponding sulfides.

#### Acknowledgements

The work has been supported by Slovak Research and Development Agency within the project APVV-20-0140 and by the Scientific Grant Agency under the contract 2/0108/23.

#### References

- [1] Perpetua Resources, Antimony: A Mineral with a Critical Role in the Green Future (Accessed August 26, 2024 at <https://www.visualcapitalist.com/sp/why-antimony-is-critical-to-the-green-future/>)
- [2] Grohol, M., Veeh, C. European Commission, Study on the Critical Raw Materials for the EU 2023 - Final Report, 158 p. Publication Office of the European Union, 2023, Luxembourg.
- [3] Šoltés, S., Kúšik, D., Mižák, J., Kubač, A. *Raw materials of the Slovak Republic*, Slovak Minerals Yearbook, 2020, p. 48-49. State Geological Institute of Dionyz Stur, Bratislava, 2021. ISBN 978-80-8174-060-2. (In Slovak)
- [4] Government of the Slovak Republic, Final report on prospecting and exploration of mineral resources, 2010 (Accessed August 29, 2024 at [https://www.google.com/search?q=About+https://lrv.rokovania.sk/data/att/114716\\_subor.doc&tbm=ilp&sa=X&ved=2ahUKEwiOiL\\_Vr6mIAxWY7wIHHTCYFvkQv5AHegQIABAC](https://www.google.com/search?q=About+https://lrv.rokovania.sk/data/att/114716_subor.doc&tbm=ilp&sa=X&ved=2ahUKEwiOiL_Vr6mIAxWY7wIHHTCYFvkQv5AHegQIABAC)) (In Slovak)
- [5] Hredzák, S., Matik, M., Šestinová, O., Kupka, D., Hančulák, J., Zubrik, A., Znamenáčková, I., Dolinská, S., Sisol, M., Marcin, M. Characterization of polymetallic ore and flotation concentrate from the Mária Mine (Rožňava, Spiš-Gemer Ore Mts., Eastern Slovakia). In IOP Conf. Series: Earth and Environmental Science 906, 2021, 012137, doi:10.1088/1755-1315/906/1/012137.
- [6] Mikuš, T., Kondela, J., Lacko, S., Milovská, S. Garavellite and associated sulphosalts from the Strieborná vein in the Rožňava ore field (Western Carpathians). *Geologica Carpathica*, 69 (3), 2018, p. 221-236, doi: 10.1515/geoca-2018-0013.
- [7] Matzko, J.R. 2015 U.S. Geological Survey Minerals Yearbook- 2015, Slovakia (Advance Release), p. 40.1-40.6.
- [8] Anderson, C.G., Krys, L.E. Leaching of Antimony from a Refractory Precious Metals Concentrate In: Proceedings of the Fourth International Symposium on Hydrometallurgy, 1993, Salt Lake City, Utah, p. 341-363.
- [9] Baláž, P., Achimovičová, M. Selective leaching of antimony and arsenic from mechanically activated tetrahedrite, jamesonite and enargite. *International Journal of Mineral Processing*, 81, 2006, p. 44-50, <https://doi.org/10.1016/j.minpro.2006.06.004>.
- [10] Sekula, F., Baláž, P., Jusko, F., Molnár, F., Jakabský, Š. Hydrometallurgical technology of tetrahedrite concentrate processing from the Mária mine locality in Rožňava. *Acta Montanistica Slovaca*, 3 (1), 1998, p. 149-156. (In Slovak)
- [11] Awe, S.A., Sandström, Å. Selective leaching of arsenic and antimony from tetrahedrite rich complex sulphide concentrate using alkaline sulphide solution. *Minerals Engineering*, 23, 2010, p. 1227-1236, doi:10.1016/j.mineng.2010.08.018.
- [12] Hagarová, L., Kupka, D., Bártová, Z., Hredzák, S. Bacterial leaching of tetrahedrite from the Silver vein in the Rožňava ore field. In Proceedings of the Conference GEOCHÉMIA 2020, State Geological Institute of Dionyz Štúr, Bratislava, 2020, p. 39-45. ISBN 978-80-8174-054-1. (In Slovak)

- [13] Hagarová, L., Bártová, Z., Jurkovič, E., Kupka, D., Čičáková, C. Recovery of antimony by bioleaching of tetrahedrite. In Proceedings of the Conference GEOCHÉMIA 2024, State Geological Institute of Dionýz Štúr, Bratislava, 2024, p. 56-59. ISBN 978-80-8174-075-6. (In Slovak)
- [14] Awe, S.A., Samuelson, C., Sandström, Å. Dissolution kinetics of tetrahedrite mineral in alkaline sulphide media. *Hydrometallurgy*, 103, 2010, p.167-172, doi:10.1016/j.hydromet.2010.03.014.
- [15] Postgate, J.R. *The Sulfate-Reducing Bacteria*. 2nd edition, Cambridge University Press, Cambridge, United Kingdom, 1984, 224 p. ISBN-10 052125791.
- [16] Ya-Nan, X., Yinguang, C. Advances in heavy metal removal by sulfate-reducing bacteria. *Water Science & Technology*, 81 (9), 2020, p. 1797-1827, doi: 10.2166/wst.2020.227.
- [17] Tang, K., Baskaran, V., Nemati, M. Bacteria of the sulphur cycle: An overview of microbiology, biokinetics and their role in petroleum and mining industries. *Biochemical Engineering Journal*, 44, 2009, p. 73-94, doi:10.1016/j.bej.2008.12.011.
- [18] Stankoviansky, S. Qualitative analytical chemistry. Slovenské vydavateľstvo technickej literatúry, Bratislava, 1965, 494 p. (In Slovak)

## APPLICATION OF HAMILTON INCYTE SENSOR FOR THE MICROBIAL INHIBITION ANALYSIS OF *ACIDITHIOBACILLUS FERRIDURANS* BACTERIA

**Valéria Má dai-Üveges<sup>a</sup>, Lisani Nimira Budagodge<sup>a</sup>, Ljudmilla Bokányi<sup>a</sup>**

<sup>a</sup> University of Miskolc, Miskolc, Hungary, [valeria.uveges@uni-miskolc.hu](mailto:valeria.uveges@uni-miskolc.hu), [lisaninadeeshani@gmail.com](mailto:lisaninadeeshani@gmail.com), [ljudmilla.bokanyi@uni-miskolc.hu](mailto:ljudmilla.bokanyi@uni-miskolc.hu)

### Abstract

In bioleaching applications, inhibition effect of certain metals, solubilised from the solid feed plays a significant role in the assessment of economic feasibility. Especially, in case of secondary raw materials, such as waste lithium-ion batteries from electric cars, the bioleaching can be an eco-friendly alternative for the chemical leaching, but still has the disadvantages such as low pulp density and elongated residence time due to toxic effect of diffused ions in the suspension, among other factors. The aim of our research is to monitor the inhibition effect of different lithium compounds, now battery black mass material and later pure lithium salts, by Hamilton online cell monitoring system. It was revealed, that the application of its Incyte sensor, which enables real time measurement of permittivity values, corresponds to the living cell density in the suspension even in case of *Acidithiobacillus* bacteria. Inhibition experiments were carried out in the Bioprocessing Laboratory, University of Miskolc with *Acidithiobacillus ferridurans* bacteria, cultivated in 9K nutrition solution. LiFePO<sub>4</sub> battery black mass was added at late log phase of bacterial growth, up to 5 g/L of black mass, the growth curves of these runs are compared to the undisturbed one, without adding any alien materials.

**Keywords:** bacterial growth, inhibition, Hamilton, Incyte sensor

### 1 Introduction

Hungary aims to become the world's largest battery manufacturer and subsequently the leading producer of electric vehicles [1]. Additionally, the European Union plans to ban conventional vehicles by 2035, and globally, every new car sold is expected to be electric by 2040. This transition will pose significant challenges in managing lithium-ion batteries in the future, but since the global market for lithium-ion batteries (LiBs) has experienced already relentless growth over the past decade, particularly in the last five years, therefore the task has been given to researchers to find an economical feasible way to recycle batteries, in the concept of environment sustainability.

Spent LiBs contain toxic metals such as copper, nickel, and organic chemicals such as toxic and flammable electrolytes creating risk when disposed directly into the environment [2]. Globally, less than 5 % of lithium-ion batteries (LiBs) are recycled at the end of their lifecycle, resulting in the majority being disposed of in landfills [3]. Consequently, valuable metals are removed from the material flow, necessitating extensive mining and processing operations to obtain new raw materials for battery production. This situation is not only economically burdensome due to the high costs associated with mining but also environmentally detrimental, as it depletes the Earth's finite resources [4].

Different recycling techniques, such as mechanical, thermal, hydrometallurgical, and mechano-chemical methods, or combinations of these, can be used for the sake of recycling.

Microbial metal extraction, known as bioleaching, presents an effective solution for recycling lithium-ion batteries (LiBs) by utilizing naturally occurring microorganisms to dissolve metals from mineral sources [5]. This eco-friendly process requires minimal energy and avoids the production of sulfur dioxide and other toxic gases [6], enabling a closed-loop system for recycling waste batteries into new ones [7]. The most active bacteria in bioleaching, *Acidithiobacillus thiooxidans* (*At. thiooxidans*) and *Acidithiobacillus ferrooxidans* (*At. ferrooxidans*), operate effectively in acidic environments with a pH range of 1.5 to 3. These acidophilic bacteria have particular importance in bioleaching since they are iron- and sulfur-oxidizing, chemoautotrophic, gram-negative, aerobic, non-spore forming, and can be cultivated at ambient temperature [8].

A culture medium containing essential elements is vital for bacterial growth. Among various nutrient media, the '9K' medium is the most used due to its significantly higher metal extraction capability [9]. Sub-culturing bacteria in their own medium by maintaining a 1:9 ratio between the bacterial inoculum and the growth medium accelerates their activity faster [10].

In bioleaching, both particle size and pulp density of the concentrate or ore determine the available surface area for the process. Although operating at high solids concentrations is economically beneficial, practical limitations restrict the achievable pulp density [9]. A study on LiCoO<sub>2</sub>-based black mass was reported that the maximum pulp density tolerated by *At. ferrooxidans* is 20 g/L, as metal toxicity, particularly from cobalt, causes inhibitory effects at higher pulp densities [11]. While acidophilic bacteria exhibit higher tolerance to heavy metals including copper, nickel, zinc, and cobalt; various strains display different levels of metal sensitivity [12]. Tuovinen et al. [13] reported that cobalt exerts the highest toxic effect compared to other heavy metals.

*At. ferrooxidans* is capable of oxidizing ferrous iron in the presence of relatively high concentrations (10 g/L) of Zn, Ni, Cu, Co, Mn, and Al. Meanwhile, its iron-oxidizing activity is inhibited by Ag, Te, As, and Se at much lower concentrations (5-10 g/L). Therefore, it is crucial to gradually adapt bacteria to the specific environment to mitigate the inhibitory effects of toxic metals and allow for increased metal concentrations [13]. In an adaptation study [14] on waste LiBs using *At. ferrooxidans*, the adaptation process was started at 2.5 g/L and was gradually increased to 10 g/L, which was identified as the maximum pulp density limit. Heydarian et al. [15] studied the bioleaching of spent laptop lithium-ion batteries using a consortium of adapted acidophilic bacteria including *At. ferrooxidans* and *At. thiooxidans*. The adaptation process was conducted with pulp densities ranging from 2.5 g/L to 40 g/L, since 40 g/L identified as the bacterial tolerance threshold.

*Acidithiobacillus ferridurans*, a close relative of *Acidithiobacillus ferrooxidans*, capable of oxidizing sulfur, and hydrogen besides iron. The facultative anaerobe bacteria show some unique adaptations, such as tolerance to extreme acidity and metals, and it has similar iron oxidation rates to *Acidithiobacillus ferrooxidans*, with some variations in pH tolerance [16]. It has been used for bioleaching uranium, demonstrating significant recovery rates under specific conditions, indicating the potential of related strains in bioleaching applications [17].

In two step bioleaching, the "black mass," referring to the solids from spent LiBs, should be introduced once the bacteria reach the late logarithmic phase [6, 7].

Indirect leaching has been explored in several studies as a method to overcome bacterial inhibition by metals. In this approach, bacteria act as catalysts without directly contacting the surface of waste LiBs. They oxidize elemental sulfur to sulfate, producing biogenic sulfuric acid (H<sub>2</sub>SO<sub>4</sub>), and convert Fe<sup>2+</sup> to Fe<sup>3+</sup>. This biogenic sulfuric acid then leaches metals from the waste LiBs [12]. The indirect, non-contact bioleaching method for metal recovery from LiB waste, using both biogenic acid and biogenic iron in sequential batch leaching, has demonstrated promising efficiency, particularly for cobalt recovery [18].

Temperature pretreatment of black mass has been employed in the literature to significantly mitigate the inhibitory effects of binders and electrolytes, though it does not address jarosite formation, which can reduce leaching efficiency [7]. Roy et al. [11] has reduced the amount of potassium and ammonia salts in the 9K medium to prevent jarosite formation and Zhao et al. [19] demonstrated that ferrous ions oxidize most effectively in acidic conditions, within a pH range of 1.8 to 2.8, resulting in fewer jarosite deposits during the leaching process.

In order, to predict, whether two step bioleaching, when black mass introduced once the bacteria reach the late logarithmic phase (direct) or cell free bioleaching (indirect) will be the most effective option to be applied, inhibition analysis have to be done prior to expensive bioleaching experiments. Although there are not many data about *At. ferridurans*, protein profiles analysis could even differentiate *At. ferrooxidans* strains, that considerably differ in the tolerance to metal sulfates. The difference can be 30-70 % as revealed by Random Amplified Polymorphic DNA (RAPD) data, reported by Novo et al. [20]. This fact also highlights the importance of inhibition analysis, even in case of a better-known strain.

Growth monitoring in the presence of toxic components can be difficult and often provides uncertain results by finite dilution process or direct cell count under microscope, especially for *Acidithiobacillus* bacteria, where jarosite formation occurs during growth. These methods require sampling, which usually hold the highest error risk. The simplest and user-friendly method is provided by Hamilton online cell monitoring system, using Incyte sensor to measure permittivity during the cultivation process realtime, directly in the reactor.

## 2 Material and methods

### 2.1 Hamilton online cell monitoring device

Inhibition measurements were carried out by Hamilton Bonaduz on-line cell monitoring system at Institute of Raw Materials Preparation and Environmental Technology, University of Miskolc. The system consists of four measuring rods and an Arc View controller display. Besides the pH and dissolved oxygen meters, the so called Incyte and Dencytee sensors are for cell density measurements. Dencytee is an innovative optical sensor for total cell density measurement, which works with adjustable light source, while Incyte's mission is to measure living cells in suspension via dielectric spectroscopy. Online monitoring of permittivity using Incyte enables early detection of process deviations without sampling and supports process adjustments. Viable cell permittivity is measured at the frequency specific to the cell type: typically, 1 MHz for mammalian cells and bacteria (or 2 MHz for yeast). This is continuously and automatically updated with the value of the permittivity measured in the background at high frequency [21].

This system was designed to mammalian cells, yeast and high-density bacterial fermentation; however our attempt is to use this device for *Acidithiobacillus ferridurans* is the first one in the history of Hamilton. Hamilton sensors during work in Bioprocessing laboratory at University of Miskolc are shown in Fig. 1.

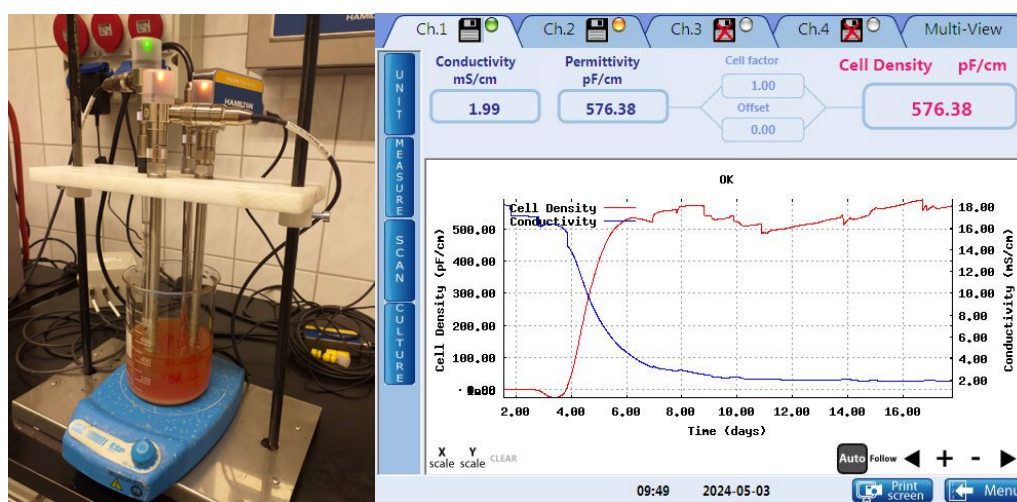


Fig. 1. Hamilton online cell monitoring system and a printscreen of the display (experiment: 5g/l LFP inhibition)

### 2.2 Cultivation of bacteria

During the experiments *Acidithiobacillus ferridurans* ATCC 33020 bacteria were used. The strain was isolated from acid mine drainage in Slovakia and kindly provided by the Institute of Geotechnics of the Slovak Academy of Sciences. The composition of the nutrient solution used for cultivation per 1 litre total volume is as follows. Solution 'A' consists of 3 g  $(\text{NH}_4)_2\text{SO}_4$ , 0.1 g KCl, 0.5 g  $\text{K}_2\text{HPO}_4$ , 0.5 g  $\text{MgSO}_4 \cdot 7\text{H}_2\text{O}$ , 0.0144 g  $\text{Ca}(\text{NO}_3)_2 \cdot 4\text{H}_2\text{O}$  and 700 ml deionized water. The iron (II) sulphate solution 'B' (consists of 44.24 g  $\text{FeSO}_4 \cdot 7\text{H}_2\text{O}$ , 10 ml 1N  $\text{H}_2\text{SO}_4$  and 300 ml deionized water) is not autoclavable, because the  $\text{Fe}^{2+}$  ion would be oxidised, so this solution was filter-sterilised before being mixed with the autoclaved sterilised and cooled solution 'A'. The pH of the solution was adjusted to 2.3-2.5 by further addition of sulphuric acid. Inoculation was done using 1:9 ratio with filtrated old culture and fresh 9K. Bacteria of uniform age were obtained by inoculating twice, with a one-week interval between inoculations prior to each experiment.

### 2.3 Inhibitors

$\text{LiFePO}_4$  (LFP) type automotive battery was collected and discharged to remove any residual electric charge. In order to the separation of black mass a series of unit operations were carried out. Initially, a two-stage shredding by rotary shear shredder and hammer crusher was done followed by thermal treatment at 60 °C to remove most of the electrolyte solvent and finally size separation by hand sieving was carried out. Black mass was separated at 1 mm, water washed and dried before analysis and experiments. Fe, P, Cu contents were measured using ED-XRF (energy dispersive X-Ray Fluorescence Spectroscopy), and samples were dissolved in strong hydrochloric acid to determine the exact soluble lithium content by atomic absorption spectroscopy (AAS, PerkinElmer Analyst 400). The main detected elements distribution in LFP

black mass was 65 % Fe, 22 % P and 9 % Cu, and Al 2 %. The concentration of lithium was measured as 2.89 % (m/m) [22].

Inhibition analysis for LFP battery black mass was carried out with *At. ferridurans* at 0.5, 1 and 2 g/L, and 5 g/L concentration, the waste powder ( $x < 1\text{mm}$ ) was added at late log phase and suspension was agitated 8 hours/day.

### 3 Results and discussion

The working principle of Dencytee sensor predicted, that this sensor is not capable to perform reliable results in our system. Even without bacteria, in the sterile 9K nutrition solution the lack of agitation resulted in significant changes in the values. In case of bacteria cultivation, the values are much higher, but this case, it can be caused by the fine precipitate, which formed and settled onto the measuring window of the sensor. When LFP black mass was added, after 150 hours of working, the mean value jumped from 250 to 2700 unit. This clearly shows, that for inhibition or bioleaching monitoring, this sensor is not suitable.

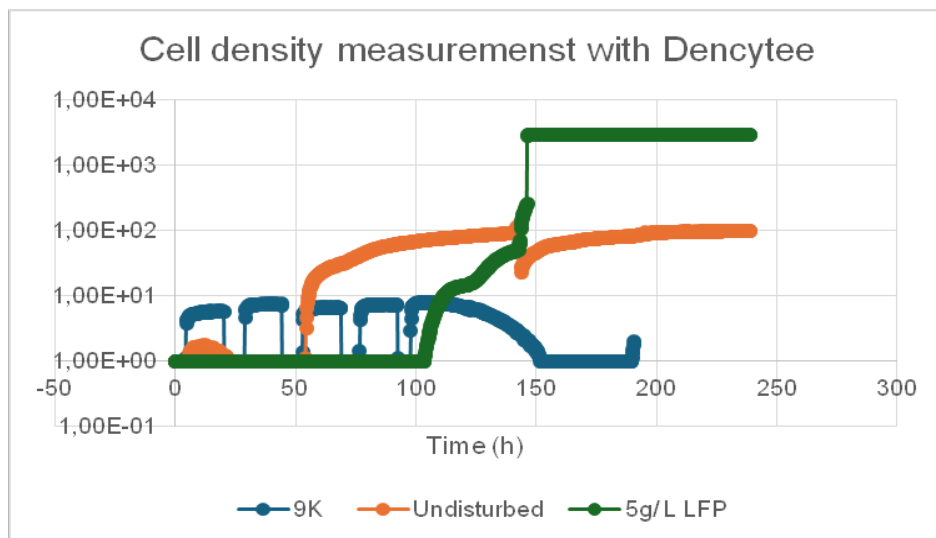


Fig. 2. Cell density in function of time, measured by Dencytee sensor in sterile 9K solution, *At. Ferridurans* under “ideal” cultivation and when 5 g/l LFP black mass powder is added at late log phase (corrigated values)

Considering the graphs related to the conductivity data on Fig. 3, served by Hamilton device, it can be seen, that for growth monitoring, conductivity measurements can be used as an indicator, especially for the logarithmic phase, but when  $\text{Fe}^{2+}$  oxidation finished, the curves are not very informative.

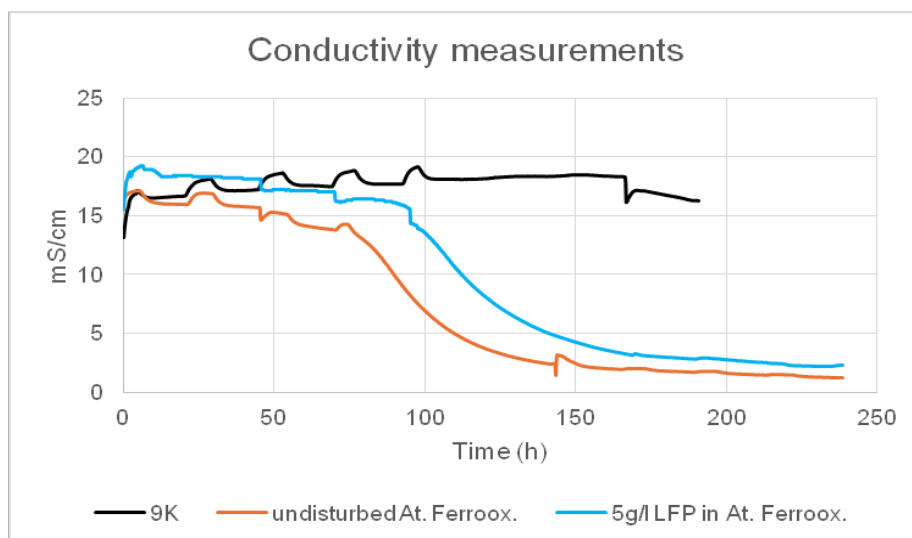
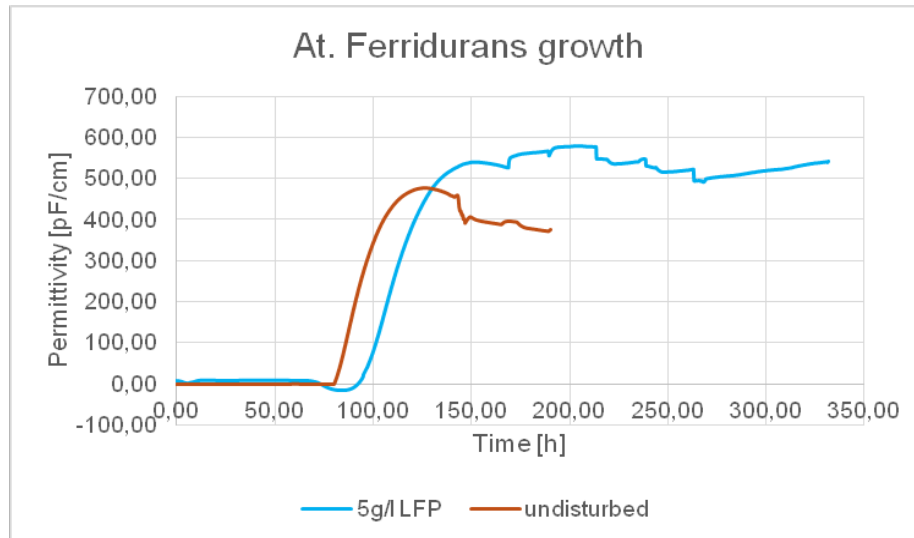


Fig. 3. Conductivity values in function of time in sterile 9K solution, *At. Ferridurans* at undisturbed cultivation and when 5 g/L LFP black mass powder is added at late log phase

Incyte sensor measurements results can be seen in Fig. 4-5. To have better visibility, in Fig. 4, the basic growth curve of *At. ferridurans* in 9K solution is to be compared to the case, when 5 g/L LFP black mass powder was added to the system after 150 h operation time. The curve has a higher maximum compared to the base curve, the log phase is more protracted and the decay phase occurs later.



**Fig. 4. Growth curves of *At. Ferridurans* by Hamilton Incyte sensor alone and with additional 5 g/L LFP black mass powder**

From the diagrams of Fig. 5, it was found, that compared to the others, it seems that the concentration of 0.5 g/L shows the highest growth peak, but to reach the maximum, elongated time was demanded. Bacterial density was overall positively influenced by the added LFP, but 0.5 g/L black mass concentration is too low from a technological point of view. When the concentration was increased to 1 g/L, a prolonged lag phase can be seen after the addition of LFP, and then, almost without plateau, the number of living cells starts to decrease. This latter phenomenon is more pronounced at 2 g/L. If the concentration is increased further, the inhibitory effect predominates over the assumed nutrient role of iron and phosphorus, so that the maximum of the curve is lower than before, but still exceeds the base curve (see Fig. 4), and the system has a prolonged plateau, which may be technologically advantageous.

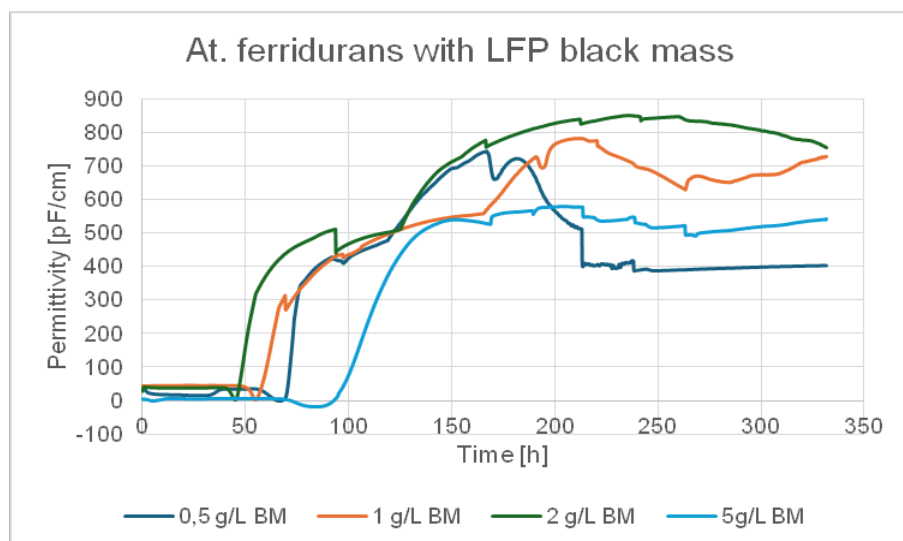


**Fig. 5. Growth curves of *At. Ferridurans* by Hamilton when LFP black mass powder was added at late log phase**

Based on the results of our bioleaching experiments with this LFP black mass and *At.ferridurans*, it was proved, that when the pulp density raised from 2 g/l to 5 g/L, and especially to 10 g/L, the Li recovery in solution significantly improved [23].

#### 4 Conclusions

Based on the results, a concentration of 5 g/L seems to be optimal for bioleaching experiments and further increase in pulp density is possible.

Experiments are underway to investigate the effect of different pure lithium salts on bacterial growth and to confirm the hypothesis that some of the battery constituents act as inhibitors and others as a useful nutrient.

Bioleaching represents a key innovation in e-waste recycling, offering a greener, more cost-effective, and scalable solution for metal recovery. As research progresses, it holds the potential to revolutionize the recycling industry by minimizing environmental impact while efficiently recovering valuable resources. Inhibition analysis by online cell monitoring system can serve as a useful background for bioleaching process development.

#### References

- [1] Bloomberg, The Mission to Create Europe's Battery Hub, Whatever the Cost, 2024, <https://www.bloomberg.com/news/features/2023-09-19/orban-wants-to-make-hungary-europe-s-ev-battery-hub>, accessed date 2024.06.22.
- [2] Lisboa, D., Snee, T. A review of hazards associated with primary lithium and lithium-ion batteries. *Process safety and environmental protection*, 89 (6), 2011, p. 434-442.
- [3] Grist, Most of the lithium batteries end up in a landfill. A new bill aims to change that, 2024, <https://grist.org/politics/most-lithium-batteries-end-up-in-a-landfill-a-new-bill-aims-to-change-that>, accessed date 2024.06.22.
- [4] Zeng, X., Li, J., Liu, L. Solving spent lithium-ion battery problems in China: Opportunities and challenges. *Renewable and Sustainable Energy Reviews*, 52, 2015, p. 1759-1767.
- [5] Marcincakova, R., Kadukova, J., Mrazikova, A., Velgosova, O., Luptakova, A., Ubaldini, S. Metal bioleaching from spent lithium-ion batteries using acidophilic bacterial strains. *Inzynieria Mineralna*, 17 (1), 2016, p. 117-120.
- [6] Mishra, D., Kim, D.J., Ahn, J.G., Rhee, Y.H. Bioleaching: a microbial process of metal recovery; a review. *Metals and Materials International*, 11, 2005, p. 249-256.
- [7] Malavasi, P., Aatach, M., Gaydardzhiev, S. Bioleaching of black mass of spent LiBs—process parameters and material characterization. In The 11th International Symposium on Biomining (Biomining'23, MEI Conferences), 2023.
- [8] Bosecker, K. Bioleaching: metal solubilization by microorganisms. *FEMS Microbiology reviews*, 20 (3-4), 1997, p. 591-604.
- [9] Deveci, H., Akcil, A., Alp, I. Parameters for control and optimization of bioleaching of sulfide minerals. In Materials Science and Technology Symposium: Process Control and Optimization in Ferrous and Non-Ferrous Industry, 2003, p. 9.
- [10] Wang, J., Bai, J., Xu, J., Liang, B. Bioleaching of metals from printed wire boards by *Acidithiobacillus ferrooxidans* and *Acidithiobacillus thiooxidans* and their mixture. *Journal of Hazardous Materials*, 172 (2-3), 2009, p. 1100-1105.
- [11] Roy, J.J., Madhavi, S., Cao, B. Metal extraction from spent lithium-ion batteries (LIBs) at high pulp density by environmentally friendly bioleaching process. *Journal of Cleaner Production*, 280, 2021, p. 124242.
- [12] Roy, J.J., Cao, B., Madhavi, S. A review on the recycling of spent lithium-ion batteries (LIBs) by the bioleaching approach. *Chemosphere*, 282, 2021, p. 130944.
- [13] Tuovinen, O.H., Niemelä, S.I., Gyllenberg, H.G. Tolerance of *Thiobacillus ferrooxidans* to some metals. *Antonie van Leeuwenhoek*, 37 (1), 1971, p. 489-496.
- [14] Mishra, D., Kim, D.J., Ralph, D.E., Ahn, J.G., Rhee, Y.H. Bioleaching of metals from spent lithium-ion secondary batteries using *Acidithiobacillus ferrooxidans*. *Waste management*, 28 (2), 2008, p. 333-338.



- [15] Heydarian, A., Mousavi, S.M., Vakilchap, F., Baniasadi, M. Application of a mixed culture of adapted acidophilic bacteria in two-step bioleaching of spent lithium-ion laptop batteries. *Journal of Power Sources*, 378, 2018, p. 19-30.
- [16] Hedrich, S., Johnson, D. *Acidithiobacillus ferridurans* sp. nov., an acidophilic iron-, sulfur- and hydrogen-metabolizing chemolithotrophic gammaproteobacterium. *International Journal of Systematic and Evolutionary Microbiology*, 63 (11), 2013, p. 4018-4025.
- [17] Jalali, F., Fakhar, J., Zolfaghari, A. On using a new strain of *Acidithiobacillus ferridurans* for bioleaching of low-grade uranium. *Separation Science and Technology*, 55, 2020, p. 994-1004.
- [18] Boxall, N.J., Cheng, K.Y., Bruckard, W., Kaksonen, A.H. Application of indirect non-contact bioleaching for extracting metals from waste lithium-ion batteries. *Journal of Hazardous Materials*, 360, 2018, p. 504-511.
- [19] Zhao, K., Gu, G., Wang, X., Yan, W., Qiu, G. Study on the jarosite mediated by bioleaching of pyrrhotite using *Acidithiobacillus ferrooxidans*. *Bioscience Journal*, 33 (3), 2017, p. 721-729.
- [20] Novo, M.T., Garcia, O., Ottoboni, L.M. Protein Profile of *Acidithiobacillus ferrooxidans* Strains Exhibiting Different Levels of Tolerance to Metal Sulfates. *Current Microbiology*, 47, 2003, p. 492-496.
- [21] AG Hamilton Bonaduz, Online cell monitoring system, Instruction Manual, 2017.
- [22] Spekker, D. Az LFP típusú Li-ion akkumulátorok bioeljárás-technikai reciklálsági lehetőségeinek kísérleti vizsgálata. BSc Thesis, University of Miskolc, 2024.
- [23] Mádainé-Úveges, V., Butylina, S., Sethurajan, M., Nouaili, A., Spekker, D., Bokányi, L. Bioleaching of valuable metals from black mass originated from LFP and NMC Li-ion batteries. In 18th European Symposium on Comminution & Classification (ESCC 2024), 24-26 June 2024, Miskolc - Hungary, p. 4.



## SUBSTRATE LIMITATION IN BIOLEACHING CULTURES OF SULFUR-OXIDIZING BACTERIA

**Martin Mandl<sup>a</sup>, Jiří Kučera<sup>a</sup>, Jitka Vechetová<sup>a</sup>**

<sup>a</sup> Department of Biochemistry, Faculty of Science, Masaryk University, CZ-61137 Brno, mandl@chemi.muni.cz, jiri.kucera@sci.muni.cz, vechetova.jitka@seznam.cz

### Abstract

Substrate limitation plays a negative role in all bioprocesses, so it is crucial to know whether its impact can be reduced or eliminated. Regarding acid bioleaching, the limitation by elemental sulfur, CO<sub>2</sub> and O<sub>2</sub> was investigated. *Acidithiobacillus ferrooxidans* was used as a model organism. Linear growth and sulfuric acid formation during the active growth phase were detected. Based on the kinetics of cell growth and substrate oxidation, linear kinetics in sulfur-oxidizing cultures indicated limitation by elemental sulfur. This hypothesis could be supported by the low bioavailability of the pure sulfur substrate, as most sulfur was present as insoluble reservoir. Using mass spectrometry to check for sufficient dissolved CO<sub>2</sub> and O<sub>2</sub> in the cultures, a direct relationship between linear kinetics and sulfur limitation was confirmed. CO<sub>2</sub> limitation seems more dangerous than O<sub>2</sub> limitation, but unlike sulfur limitation, it is potentially controllable. Aeration parameters were specified to eliminate CO<sub>2</sub> limitation without adding CO<sub>2</sub> to the air.

**Keywords:** *Acidithiobacillus*, aeration, bioleaching, substrate limitation, sulfur oxidation

### 1 Introduction

Sulfuric acid forms an essential environment for acid bioleaching of metals from low-grade ores, wastes, or concentrates to ensure conditions for metal extraction and their solubility in the leaching solution [1]. *Acidithiobacillus ferrooxidans* is a usual model organism [2, 3] although mixed cultures are more common in nature. In the case of sulfide minerals containing iron, sulfuric acid keeps acid conditions for the oxidation activity of ferric iron. If no iron is present, it represents the only extraction medium. As elemental sulfur may be either the substrate that has been directly added to form sulfuric acid for metal extraction [3] or can be an intermediate in metal sulfide oxidation [4], its bacterial oxidation to sulfuric acid represents a fundamental role in the mechanism of acid bioleaching.

Because CO<sub>2</sub> is a source of cell carbon and O<sub>2</sub> is required for energy formation under aerobic conditions, these gases are other essential substrates. Substrate limitation is a negative process for both biochemical (biotechnological) and economic reasons. Since the basic parameters of oxygen limitation have already been described [5], this study aimed to investigate substrate limitation, emphasizing elemental sulfur and CO<sub>2</sub>.

### 2 Material and methods

#### 2.1 Bacteria, culture conditions and analytical procedures

*Acidithiobacillus ferrooxidans* (CCM 4253) was grown on elemental sulfur under conditions described earlier [6]. Large-scale growth experiments were conducted using a 10-l bioreactor (Infors HT, Techfors-S). Dissolved CO<sub>2</sub> and O<sub>2</sub> concentrations in the sulfur-oxidizing cultures at 30 °C were detected using a compact membrane inlet mass spectrometer (MIMS, HPR-40 DSA, Hiden Analytical, UK) in a reaction vessel of 130 mL. Parameters characterizing CO<sub>2</sub> and O<sub>2</sub> limitations were evaluated as previously described [5].

### 3 Results and discussion

In our bioleaching studies, *A. ferrooxidans* produced sulfuric acid from elemental sulfur [3] and was therefore used as a model organism. Although the fact that bacteria oxidize elemental sulfur to sulfuric has been known for a very long time, the nature of the sulfur substrate and the oxidation mechanism are still unclear. Older designs have been previously summarized [6]. A specific type of colloidal sulfur has been suggested to be a bioavailable substrate for bacteria [7, 8], and the metabolic bottleneck is the slow formation of a colloidal sulfur substrate from excess insoluble sulfur in the culture. In a more active culture, sulfur limitation can quickly occur, similar to O<sub>2</sub> or CO<sub>2</sub> limitation. This was demonstrated by linear kinetics of growth and sulfur oxidation consistent with the Monod equation and the kinetics of fixed volume fed-batch culture, indicating limitation by the above 3 substrates, because this kinetic approach has the same

interpretation of substrate limitation by both elemental sulfur and gaseous substrates. Based on changes in aeration intensity [6], we ruled out limitation by gaseous substrate and suggested limitation by elemental sulfur. This hypothesis was now directly confirmed by the fact that the sulfur-oxidizing culture was maintained in both CO<sub>2</sub> and O<sub>2</sub> excess monitored by MIMS and the observed linearity and rate of the bioprocess did not change. Thus, the primary source of limitation was the sulfur substrate, which could not be easily influenced. However, even at high aeration rates, linear kinetics always resulted from sulfur limitation. The limitation by sulfur substrate can be the main factor influencing the overall kinetics of bioleaching processes.

Another source of limitation was CO<sub>2</sub>, rather than O<sub>2</sub>, when aeration intensity was insufficient. The critical CO<sub>2</sub> and O<sub>2</sub> concentrations, representing the lowest CO<sub>2</sub> and O<sub>2</sub> concentrations that do not limit the rate of CO<sub>2</sub> assimilation or cell respiration during sulfur oxidation ( $5 \times K_m$ ), were  $0.65 \pm 0.21$  and  $2.5 \pm 1.4$   $\mu\text{M}$  for CO<sub>2</sub> and O<sub>2</sub>, respectively.

#### 4 Conclusions

Linear cell growth in sulfur-oxidizing cultured was related to elemental sulfur limitation even under sufficient aeration conditions (no CO<sub>2</sub> or O<sub>2</sub> limitation). The conversion of elemental sulfur to a more bioavailable sulfur substrate creates a rate-limiting bottleneck for bacterial sulfur oxidation. Critical CO<sub>2</sub> and O<sub>2</sub> concentrations were determined to avoid limitation by the gaseous substrates.

#### Acknowledgements

The work was supported by the program Interreg V-A Austria-Czech Republic, projects ATCZ291 (OPTIMO) and ATCZ00043 (PHOS4PLANT), and by the Masaryk University Program MUNI/A/1582/2023.

#### References

- [1] López-Martínez, A., Martínez-Prado, M.A., Núñez-Ramírez, D.M., Anguiano-Vega, G.A., Soto-Cruz, N.O. Acidophilic bacteria for metal extraction: biotechnological characteristics and applications. *Brazilian Journal of Chemical Engineering*, 2024, <https://doi.org/10.1007/s43153-024-00434-2>.
- [2] Li, Z., Sun, M.Y., Xia, Q.L., Yu, Z.Q., Zhao, M., Li, W.H., Zhang, D.N., Fan, Y.Q., Xu, D.K., Wang, F.H. Accelerated microbial corrosion of 316 L SS in extreme acidic environment by a typical bioleaching strain *Acidithiobacillus ferrooxidans*. *Corrosion Science*, 238, 2024, 112353.
- [3] Kremser, K., Thallner, S., Strbik, D., Spiess, S., Kucera, J., Vaculovic, T., Vsiansky, D., Haberbauer, M., Mandl, M., Guebitz, G.M. Leachability of metals from waste incineration residues by iron- and sulfur-oxidizing bacteria. *Journal of Environmental Management*, 280, 2021, 111734.
- [4] Borilova, S., Mandl, M., Zeman, J., Kucera, J., Pakostova, E., Janiczek O., Tuovinen, O.H. Can sulfate be the first dominant aqueous sulfur species formed in the oxidation of pyrite by *Acidithiobacillus ferrooxidans*? *Frontiers in Microbiology*, 9, 2018, 3134.
- [5] Mandl, M., Pakostova, E., Poskerova, L. Critical values of the volumetric oxygen transfer coefficient and oxygen concentration that prevent oxygen limitation in ferrous iron and elemental sulfur oxidation by *Acidithiobacillus ferrooxidans*. *Hydrometallurgy*, 150, 2014, p. 276-280.
- [6] Ceskova, P., Mandl, M., Helanova, S., Kasparovska, J. Kinetic studies on elemental sulfur oxidation by *Acidithiobacillus ferrooxidans*: Sulfur limitation and activity of free and adsorbed bacteria. *Biotechnology and Bioengineering*, 78, 2002, p. 24-30.
- [7] Mandl, M., Pokorna, B., Gavlasová, P. Bacterial oxidation of elemental sulfur: Changes in oxidation kinetics *Advanced Materials Research*, 20, 2007, p. 477-480.
- [8] Pokorna, B., Mandl, M., Borilova, S., Ceskova, P., Markova, R., Janiczek, O. Kinetic constant variability in bacterial oxidation of elemental sulfur. *Applied and Environmental Microbiology*, 73, 2007, p. 3752-3754.

## CHITINASES ARE ACTIVE IN FLAX IN PRESENCE OF TOXIC METALS AND MIGHT INDICATE PHYTOREMEDIATION POTENTIAL

Mária Pavlovičová<sup>a,b</sup>, Simona Ilavská<sup>a</sup>, Richard Hančinský<sup>a</sup>, Pavol Hauptvogel<sup>b</sup>, Ildikó Matusíková<sup>a</sup>

<sup>a</sup> Faculty of Natural Sciences, University of Ss. Cyril and Methodius in Trnava, Námestie J. Herdu 2, 917 01 Trnava, Slovakia, ildiko.matusikova@ucm.sk

<sup>b</sup> National Agricultural and Food Centre, Research Institute of Plant Production, Bratislavská cesta 122, 921 68 Piešťany, Slovakia, pavol.hauptvogel@nppc.sk

### Abstract

Cadmium (Cd) sensitivity in plants varies both within and among species, influenced by genetic background, environmental conditions, and cultivation practices. Flax (*Linum usitatissimum* L.) shows significant variability in its response to Cd<sup>2+</sup>, affecting shoot growth and photosynthetic efficiency across different varieties. Chlorophyll and carotenoid content varied notably among the 13 tested flax varieties, indicating differential tolerance mechanisms. Chitinases, enzymes involved in plant defense, are believed to play a key role in mediating cadmium tolerance. A genome-wide analysis of flax identified 69 chitinase genes with 32 encoding GH 18 family domain proteins and 37 encoding GH 19 family domain proteins. This gene family expansion, likely due to whole genome duplication, may contribute to enhanced stress tolerance. Sequence analysis classified the chitinases into various classes, with classes I and II, often linked to stress response, showing highest abundance. Variable chitinase expression among flax varieties plays possible role in cadmium tolerance during early development stages. These findings highlight the importance of chitinases in enhancing flax's resilience to cadmium toxicity and underscore the potential of selective breeding for improved tolerance and phytoremediation applications.

**Keywords:** genome, glucanhydrolase, *Linum usitatissimum*, metal tolerance

### 1 Introduction

Since the mid-1990s, the use of fiber crops like flax has been considered in relation to their ability to tolerate and absorb heavy metals from the soil. Several studies have described certain flax varieties' high tolerance to cadmium ions and their ability to accumulate cadmium from the soil [1, 2]. Research has shown that flax is relatively tolerant and can act as an accumulator of cadmium (Cd), copper (Cu), lead (Pb), and zinc (Zn) [1, 3, 4]. For example, Angelova et al. [3] found that mature flax (variety Kaliakra) grown in an industrially polluted area with Cd concentrations of 12 mg/kg of soil accumulated cadmium in the roots (8.7 mg/kg dry weight) and stems (7.3 mg/kg dry weight) in comparable amounts, much higher than in the leaves, capsules, and seeds ( $\leq 2$  mg/kg dry weight).

Flax's sensitivity to cadmium, however, is quite variable. For instance, Pavlovičová et al. [5] compared six varieties and linked their tolerance to chitinase enzyme activity. Chitinases are glucan hydrolases that play an indirect role in plants' responses to various environmental stresses, including heavy metals. Metwally et al. [6] and Mészáros et al. [7, 8] also demonstrated a direct relationship between chitinase activity and the degree of tolerance to these stresses. The chitinase gene family in flax has been only partially studied [5], and despite the knowledge of the flax genome, this enzyme family has not been thoroughly characterized. This study presents the foundations for further research aimed at selecting cadmium-tolerant flax varieties, correlating this trait with the activity of chitinase family members.

### 2 Material and methods

#### 2.1 Plant material and testing for metal tolerance

A set of flax (*Linum usitatissimum* L.) varieties, Belinka, Escalina, Laura, Jitka, Ilona, Flanders, Marina, Szeged 30, Azur, Modran, Texa, Rekord, Wiera, Verum, Liral Sussex, Krasnoder, Jugoslavik viner, Ilgermila II, Hohenheim, Gisa, Lilas, Dearo, Rastatter Weiss, Mume, Solido, Diana, Pastel, Stamkanovits, Shakhimskaja, Rembrandt and Purple. After surface sterilization using 5 % (v/v) sodium hypochlorite for 10 min and careful washing with sterile deionised water, 6 seeds per variety/variant were germinated and cultivated in presence/absence of CdCl<sub>2</sub> solution (0 and 20 mg.L<sup>-1</sup>) in Petri dishes with Hoagland nutrient solution (400 mg.L<sup>-1</sup> KNO<sub>3</sub>, 350 mg.L<sup>-1</sup> MgSO<sub>4</sub>.7H<sub>2</sub>O, 300 mg.L<sup>-1</sup>, NaH<sub>2</sub>PO<sub>4</sub>.2H<sub>2</sub>O, 400 mg.L<sup>-1</sup> CaCl<sub>2</sub>, 350 mg.L<sup>-1</sup> NaNO<sub>3</sub>) with/without the addition of a 20 mg.L<sup>-1</sup> CdCl<sub>2</sub>. Cultivation occurred at room at a photoperiod of 16 hours light/ 8 hours dark with maximum intensity 11 450 lx; temperature max. 28 °C

(light)/ min. 18 °C (dark) for 8 days. Growth parameters (weight and length) were measured for experimental plants and tolerance indexes were expressed as ratio of values for metal-exposed plants to corresponding controls (in %).

## 2.2 Determination of photosynthetic pigments

Photosynthetic pigment concentrations (sum of chlorophylls *a* and *b* (Chl(*a*+*b*)), content of total carotenoids (Car)) was carried out according to Lichtenthaler [10] in 50 mg (fresh weight) of plant tissue. Ratios of Cd-treated plant/ values for control were calculated to allow comparison among varieties [4].

## 2.3 Identifying chitinases in flax genome

Keyword “chitinase” was used to search the Phytozome v.12 database (<https://phytozome.jgi.doe.gov/pz/portal.html>). The obtained sequences were filtered for the presence of Pfam domains PF00182 or PF00704, typical for GH19 and GH18 family (respectively). Corresponding cDNAs were analyzed to estimate molecular weight and isoelectric point pI values using bioinformatic tool Compute pI/Mw on the ExPasy server ([https://web.expasy.org/compute\\_pi/](https://web.expasy.org/compute_pi/)). Sequences were aligned using Clustal Omega program (EMBL-EBI, <https://www.ebi.ac.uk/>) and phylogenetic tree was visualized using TreeView program (TreeView™ ©Genealogy Supplies, Jersey).

## 3 Results and discussion

Metal sensitivity to plants varies among as well as within species. This diversity can be attributed to genetic background, external conditions but also cultivation practices and has been often described [11]. Differences in seed yield, straw weight, and growth rates among different flax varieties gain complexity in presence of toxic elements in soils such as cadmium [1, 3, 5]. Germinating and growth of flax in presence of Cd<sup>2+</sup> affected shoot growth and considerable differences were observed among flax varieties tested (Fig. 1), as has been observed by others [1, 3, 5].

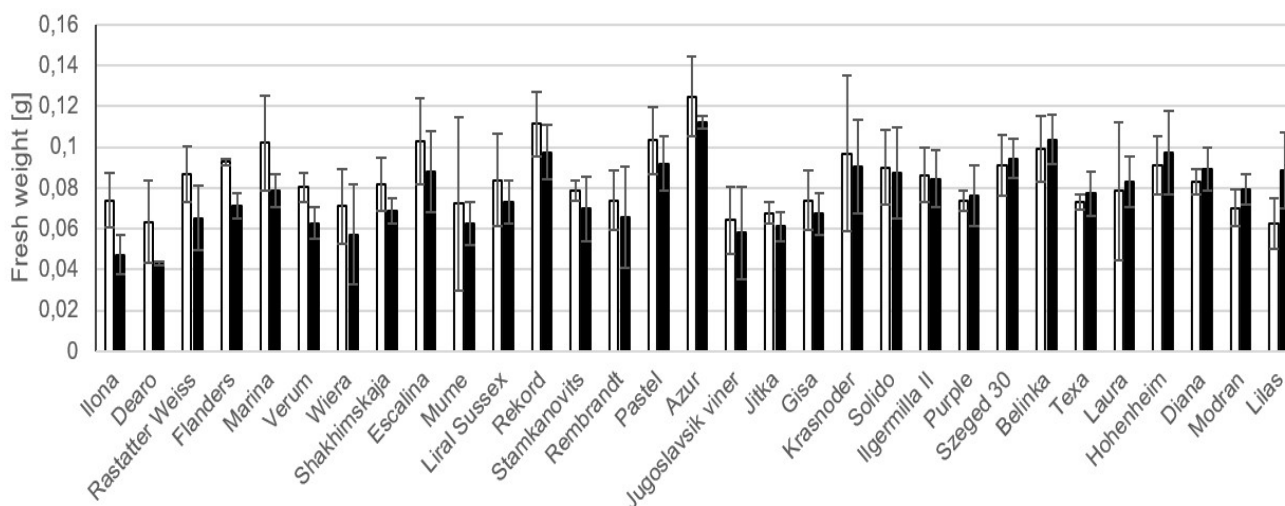


**Fig. 1. Fresh weight of flax varieties in absence (white columns) and presence (black columns) of cadmium**  
Data represent average values ± SD (n=6)

Efficient defense needs energy resources. The functionality of photosynthetic apparatus is routinely evaluated not only as an indicator of metal damage [7, 12, 5], but also as prerequisite to gain further resources for active defense [13, 14]. Negative impact of heavy metals including cadmium has often been described [5, 7, 8], though hermetic effects at lower metal concentrations have also been reported [15]. The sensitivity of flax varieties, especially during germination, therefore, might be crucial for plant performance and subsequent remediation potential. The flax varieties indeed exerted considerable variance in total chlorophyll as well as carotenoid contents (Fig. 2).

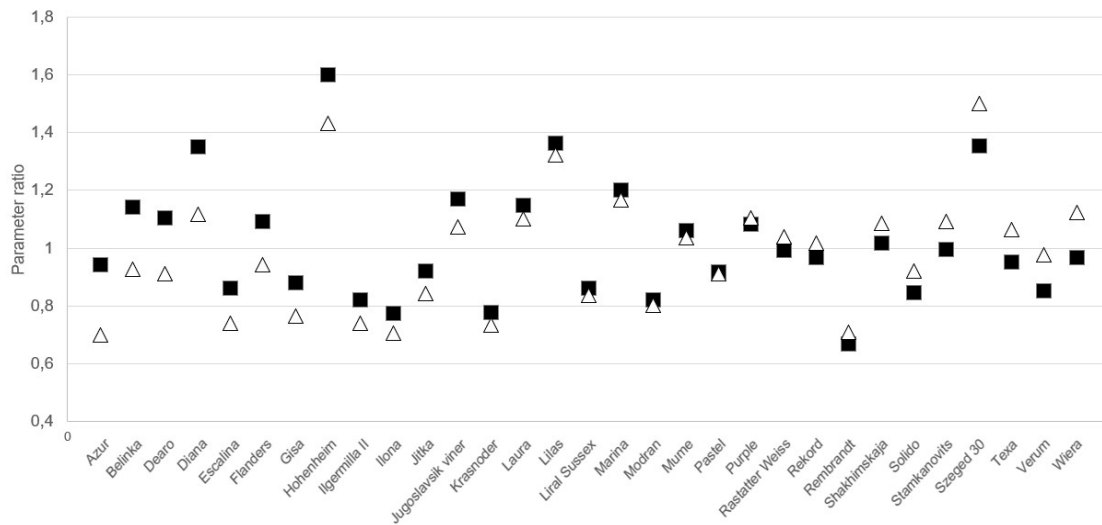


**Fig. 2. Tolerance indexes to cadmium calculated for sum content of chlorophyll *a* and *b* (triangles), as well as carotenoid content (squares) of flax varieties**  
Average values (n=6); SD for clarity not shown

Tolerance mechanisms against cadmium are quite well described, especially for some model or crop species. Of these, chitinases have been studied in more detail in soybean or some other species [7, 8, 16]. Though chitinase activation in presence of Cd<sup>2+</sup> has been reported [5], the chitinase gene family in flax has been described only partially [9]. As flax genome is available, we screened it using a keyword to identify gene family members. We identified 69 chitinase genes, of which 32 encoded proteins with a GH 18 family domain; these genes have not been extensively described in the literature. A total of 37 genes encoded proteins with a GH 19 family domain, corresponding to chitinases previously identified and described by [9]. Apparently, the size of this gene family is larger than that of Arabidopsis (23 genes) [17], while whole genome duplication event is likely responsible for the gene family enlargement. *In silico* analyses revealed variable molecular weights ranging from 8.1 to 50.3 kDa, with a comparable distribution of acidic and basic isoforms (28 and 32, respectively), while the remaining isoforms had a neutral pI. The family members we grouped into different classes using Clustal Omega programme (Fig. 3). Contribution into certain chitinase class indicates possible function; the class I and II chitinases (family GH19) have been mostly reported as enzymes responding to stress conditions.

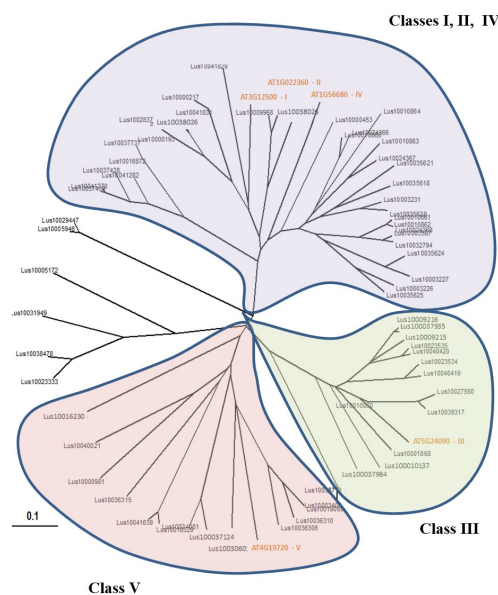


**Fig. 3. Cladogram of 69 chitinase sequences from flax and 5 chitinase sequences from Arabidopsis (with red letters) generated by "default" conditions of Clustal Omega**

The classification of chitinases from flax is consistent with previous findings of high sequence relatedness of class I and II and IV chitinases, respectively. Duplication of the genes may have allowed adaptive changes in function. Previously, the evolutionary divergence of specific classes of chitinases was attributed to coevolution with pathogenic fungi [18]. In addition, tandem duplication of chitinases, as it were, could also occur together with other defense-related proteins as a mechanism leading to evolutionary novelty [19]. Chitinase expression in flax has been studied in few varieties and showed variation in certain isoforms [5]. Whether these isoforms are indeed important for flax tolerance to metal toxicity at early stage of development remains to be elucidated. Considering that metal toxicity causes dehydration, oxidative stress and membrane damage, involvement of chitinases (albeit indirectly) in seedling tolerance likely contributes to plant ability to withstand soil pollution.

#### 4 Conclusions

Flax exhibits significant variability in its morpho-physiological parameters related to cadmium tolerance, with chitinases likely playing a key role in this process. The chitinase gene family in flax is notably larger compared to other species, suggesting that this expansion may be linked to its adaptive response to environmental stress, including heavy metal exposure. Chitinases, which are involved in plant defense mechanisms, seem to contribute to the enhanced tolerance observed in some flax varieties, making them a focal point for future research aimed at improving cadmium tolerance through selective breeding, but also flax use in soil remediation programmes.

#### Acknowledgements

This work was supported by research grants APVV-15-0051 and APVV-21-0504. RH was supported by project from the Research Support Fund at the University of Ss. Cyril and Methodius in Trnava number FPPV-59-2024 (in frames of Early-Stage Grant No. 09-i03-03-v05-00004, Recovery Plan scheme).

#### References

- [1] Bjelková, M., Genčurová, V., Griga, M. Accumulation of cadmium by flax and linseed cultivars in field-simulated conditions: A potential for phytoremediation of Cd-contaminated soils. *Industrial Crops and Products*, 33, 2011, p. 761-774.
- [2] Praczyk, M., Heller, K., Silska, G., Braniecki, P. (*Linum usitatissimum* L.) genotypes cultivated for medicinal purposes. *Herba Polonica*, 61 (1), 2015, p. 19-30, doi:10.1515/hepo-2015-0007.
- [3] Angelova, V., Ivanova, R., Delibaltova, V., Ivanov, K. Bio-accumulation and distribution of heavy metals in fibre crops (flax, cotton, hemp). *Industrial Crops and Products*, 19, 2004, p. 197-200.
- [4] Douchiche, O., Chaïbi, W., Morvan, C. Cadmium tolerance and accumulation characteristics of mature flax, cv. Hermes: Contribution of the basal stem compared to the root. *Journal of Hazardous Materials*, 235-236, 2012, p. 101-107, <https://doi.org/10.1016/j.jhazmat.2012.07.027>.
- [5] Pavlovičová, M., Gerši, Z., Bardáčová, M., Ranušová, P., Horník, M., Matušiková, I. Variable accumulation of cadmium in flax (*Linum usitatissimum* L.). *Nova Biotechnologica et Chimica*, 19 (1), 2020, p. 70-79.
- [6] Metwally, A., Finkemeier, I., Georgi, M., Dietz, K.J. Genotypic variation of the response to cadmium toxicity in *Pisum sativum* L. *Journal of Experimental Botany*, 56 (409), 2005, p. 167-178, ISSN 1460-2431.
- [7] Mészáros, P., Mojžiš, J., Lacko-Bartošová, M. Cultivar-specific kinetics of chitinase induction in soybean roots during exposure to arsenic. *Molecular Biology Reports*, 40 (3), 2013, p. 2127-2138, ISSN 1573-4978.
- [8] Mészáros, P., Jareková, L., Lacko-Bartošová, M. Plant chitinase responses to different metal-type stresses reveal specificity. *Plant Cell Reports*, 33 (22), 2015, p. 1789-1799, ISSN 1432-203X.
- [9] Mokshina, N., Gorshkova, T., Deyholos, M.K. Chitinase-like (CTL) and cellulose synthase (CESA) gene expression in gelatinous-type cellulosic walls of flax (*Linum usitatissimum* L.) bast fibers. *Plos One*, 9 (6), 2014, p. 1-11, ISSN 1932-6203.
- [10] Lichtenthaler, H.K. Chlorophylls and carotenoids: Pigments of photosynthetic biomembranes. *Methods in Enzymology*, 148, 1987, p. 350-382, [https://doi.org/10.1016/0076-6879\(87\)48036-1](https://doi.org/10.1016/0076-6879(87)48036-1).
- [11] You, F.M., Jia, G., Xiao, J., Duguid, S.D., Rashid, K.Y., Booker, H.M., Cloutier, S. Genetic variability of 27 traits in a core collection of flax (*Linum usitatissimum* L.). *Frontiers in Plant Sciences*, 8, 2017, p. 1636, doi:10.3389/fpls.2017.01636.



- [12] Živčák, M., Olšovská, K., Slamka, P., Galambošová, J., Rataj, V., Shao, H.B., Brestič, M. Application of chlorophyll fluorescence performance indices to assess the wheat photosynthetic functions influenced by nitrogen deficiency. *Plant Soil and Environment*, 60 (5), 2014, p. 210-215, doi:10.17221/73/2014-PSE.
- [13] George, S., Aswathi, K.P.R., Puthur, J.T. Photosynthetic functions in plants subjected to stresses are positively influenced by priming. *Plant Stress*, 4, 2022, p. 100079, <https://doi.org/10.1016/j.stress.2022.100079>.
- [14] Zhang, F., Wan, X., Zhong, Y. Nitrogen as an important detoxification factor to cadmium stress in poplar plants. *Journal of Plant Interactions*, 9 (1), 2014, p. 249.
- [15] Nascarella, M.A., Stoffolano, J.G. Jr., Stanek, E.J. III, Kostecki, P.T., Calabrese, E.J. Hormesis and stage specific toxicity induced by cadmium in an insect model, the queen blowfly, *Phormia regina* Meig. *Environmental Pollution*, 124 (2), 2003, p. 257-262, doi:10.1016/s0269-7491(02)00479-7.
- [16] Békésiová, B., Hraska, S., Libantová, J., Moravčíková, J., Matušíková, I. Heavy-metal stress induced accumulation of chitinase isoforms in plants. *Molecular Biology Reports*, 35 (4), 2008, p. 579-588, doi:10.1007/s11033-007-9127-x.
- [17] Passarinho, P.A., de Vries, S.C. Arabidopsis chitinases: A genomic survey. *Arabidopsis Book*, 1, 2002, e0023, doi:10.1199/tab.0023.
- [18] Tiffin, P. Comparative evolutionary histories of chitinase genes in the genus *Zea* and family Poaceae. *Genetics*, 167, 2004, p. 1331-1340.
- [19] Bishop, J.G., Dean, A.M., Mitchell-Olds, T. Rapid evolution in plant chitinases: Molecular targets of selection in plant-pathogen coevolution. *Proceedings of the National Academy of Sciences of the United States of America*, 97 (9), 2000, p. 5322-5327.



## BIOLOGICAL METHODS OF METAL RECOVERY FROM MINERAL WASTE AND METAL-POOR ORES

**Małgorzata Pawul<sup>a</sup>, Waldemar Kępys<sup>a</sup>, Małgorzata Śliwka<sup>a</sup>**

<sup>a</sup> AGH University of Krakow, Faculty of Civil Engineering and Resource Management, pawul@agh.edu.pl

### Abstract

Treatment of the environment with the participation of microorganisms, especially autochthonous ones, is a method that allows use of natural processes occurring in the environment. Bioremediation allows the removal of various pollutants, including metals, using the specific abilities of microorganisms. In the environment, this process often involves specific plant species (phytoremediation). Biological methods (bioremediation, phytoremediation) also allow the recovery of metals from ores or waste by bioleaching or phytoextraction (hyperaccumulator). Biological methods of metal recovery with the participation of microorganisms and plants, including phytomining, which fits perfectly into the extremely current concept of the circular economy, will be discussed in the article.

**Keywords:** phytomining, bioleaching, phytoextraction, metal recovery

### 1 Introduction

With intensive economic development, the demand for metals, especially those used in modern technologies, is increasing. Over time, metal ore deposits will become depleted and it will be necessary to exploit poorer ores or look for new solutions to obtain the necessary raw materials. At the same time, huge amounts of processing waste from metal ore mining, containing metals in low concentrations, are accumulated in landfills. At present, these waste can be regarded as potential deposits, because technologies to recover the metals they contain exist. For example, waste from the mining of zinc and lead ores is already being reprocessed. Technology for reprocessing and reuse of post mining waste accumulated in settlers and heaps continues to develop, enabling old landfills to be exploited in an economically viable manner. One of the developing directions for extracting metals from mineral (post processing) waste or poor ores is biomining, including phytomining. The use of biological methods allows metals to be extracted from waste or ores containing very low concentrations of these metals. The use of microorganisms to extract metals in practice has been known since the eighteenth century, when copper was extracted in this way from rocks in Rio Tinto, Spain [6, 14].

The uptake of metals from a polluted environment by bacteria or plants is bioextraction. It is one of the bioremediation processes. In the literature, you can also find the terms phytoextraction and phytoremediation. These are narrower concepts and concern the use of various plant species to extract pollutants from the environment (phytoextraction) or reduce toxic effects in another way [3].

Biomining (including phytomining) is a kind of extension of bioextraction (phytoextraction). Since plants take metals from the environment and accumulate them in their bodies, it was assumed that these metals could then be obtained from plants. This is not yet a widely used solution, but there are a number of studies confirming that it is possible. Plants that grow well on a substrate rich in metals are called metalophytes, if they take large amounts of metals from the substrate and accumulate them in their bodies, they are called hyperaccumulators. Plants with such abilities are used in phytomining to obtain metals, e.g. nickel, zinc, lead, cobalt, copper, selenium, silver and gold [5] and rare earth metals [8].

Phytomining can be used in cases where traditional processing methods, despite technological progress, still cannot be used because the concentration of metals in the deposit is too low. In this case, post-industrial waste, including processing waste and metal-contaminated soils [5], can be treated as the deposit. Metals can also be recovered from other waste, such as used batteries, accumulators, electronic equipment, sewage sludge and many others.

Considering the environmental aspect, this form of obtaining metals allows for their removal from land and waste, and thus purifying the environment from toxic substances. It should also be remembered that sowing the ground with plants protects the ground from water and wind erosion. Therefore, it is possible to combine the reclamation of contaminated land with the extraction of metals [5].

The final stage of obtaining metals in phytomining is their separation from plant biomass. For this purpose, biomass is burned and metals are recovered in metallurgical processes. In addition to

hydrometallurgy or pyrometallurgy, biometallurgical processes (bioleaching) are also used here. In biometallurgy, mainly bacteria and fungi from the chemolithotroph group are used [4].

This process can also be used on its own, without prior phytoextraction and combustion of biomass, to extract metals from sewage sludge, industrial waste, waste concentrates, and poor ores.

Bioleaching is also used in bioremediation to remove toxic contaminants (including heavy metals) from the environment. The process itself is the same, but its purpose is different.

## 2 Characteristic of hyperaccumulating plants

Hyperaccumulators are plants that have the ability to take up substances from the substrate in much larger quantities than other plants and to accumulate these substances in plant tissues. In the case of metallophytes, they take up and accumulate metals. It is important that the elements taken up from the substrate should be accumulated in the above-ground parts of plants, because the above-ground parts are collected and subsequently metals are recovered from them. The concentrations of the elements taken up and accumulated in the tissues of hyperaccumulating plants are from 100 to 1000 times higher than in the tissues of other plants [7, 11, 12, 15]. There are about 500 species of hyperaccumulators [whisker], most of them have the ability to take up and accumulate nickel [5].

When describing the accumulation capacity of plants, several parameters are given. The first is the content of a given element in mg/kg of dry plant mass. For each element that is taken up, threshold values of its concentration in tissues are established, above which the plant can be considered as hyperaccumulator (Table 1). The remaining parameters are bioaccumulation factor (BAF) and translocation factor (TF). BAF determines the efficiency of taking up and accumulating a given element and is calculated as the ratio of its concentration in the above-ground parts of plants to its concentration in the substrate. TF is the ratio of the concentration of a given element in the above-ground parts of the plant to its concentration in the roots. The higher the TF, the better the metal taken up is transported from the roots to the plant shoots and accumulated there. In order for a plant to be considered as hyperaccumulator, both TF and BAF should have values above 1. There are documented cases when BAF ranges from a few to dozens [5].

Table 1 lists examples of hyperaccumulators for various metals. These include annual herbaceous plants, perennials, shrubs and trees, including ornamental plants such as many species of alyssum [2, 5, 8, 15]. Some of the hyperaccumulators have the ability to accumulate more than one metal. Examples include *Bereya codii* or *Allyssum murale* (Fig. 1) which accumulate both nickel and cobalt [1].

**Table 1. Selected examples of hyperaccumulator plants**

Metal	Hyperaccumulation Threshold (mg/kg)*	Plant species	Metal concentration (mg/kg)*
Ni	1000	<i>Alyssum baldaccii</i>	1430-17670
		<i>Berkeya coddii</i>	40-5800
		<i>Rinorea bengalensis</i>	20,000-25100
Cd	100	<i>Impatiens walleriana</i>	1168
		<i>Pteris vittata</i>	6434
		<i>Thlaspi caerulescens</i>	380-7400
Co	300	<i>Berkeya coddii</i>	40-2116
		<i>Allyssum murale</i>	2070
		<i>Buchnera henriquesii</i>	404-930
Zn	3000	<i>Brassica juncea</i>	11700
		<i>Potentilla griffithii</i>	11400
		<i>Thlaspi caerulescens</i>	10000

\*in the dry mass of the plant



**Fig. 1. *Alyssum murale***

(photograph by Opiola J., Wikimedia Commons, licence: GNU Free Documentation License)

Plants used in phytomining should also have several other features:

- rapid growth and a large amount of biomass (the larger the amount of biomass is the greater the amount of recovered element),
- high tolerance to the element taken up and other environmental pollutants,
- easy adaptation to new habitats (then the plant can be used, for example, in different climate zones),
- resistance to pathogens and pests,
- mechanisms that repel herbivores to prevent the introduction of toxic metals into the food chain [8, 9].

Since it is difficult to find plants that have all of these features, those that will work best in the given conditions are used.

### **3 Stages of metal extraction in phytomining**

The first step to obtaining metals in phytomining is to conduct soil tests for the concentration of the desired metal and its bioavailability. Metals can be obtained from post-industrial waste, including processing waste containing the desired metal. They can also be obtained from soils and land contaminated with a given metal.

The next step is the selection and cultivation of appropriate plants (hyperaccumulators). If necessary, appropriate agrotechnical procedures can be applied to increase of yields or increase of the bioavailability of metals. Yield increases can be achieved by using appropriate fertilizers. Increased bioavailability of metals can be achieved by regulating soil pH (acidification) or adding chelating compounds such as citric acid or EDTA [5, 8, 9, 13]. Both the addition of acidifying substances (e.g. sulphates) and chelating compounds can increase the BAF bioaccumulation factor [5] even several times.

The ability of plants to accumulate pollutants does not always go hand in hand with rapid biomass growth. It is important to mention that there is research in genetic engineering to breed a plant that will have both of these characteristics [8].

The collected plants (their above-ground parts) are burned. The concentration of metals in the ash increases significantly. Ash rich in metals constitutes bio-ore. Metals are recovered from it using pyrometallurgical, hydrometallurgical or biometallurgical methods. Pyrometallurgical methods refer to traditional smelting of metals at high temperature. Hydrometallurgical methods consist in leaching of metals from ash using leaching agents and then separating them from the solution. For this purpose, methods such as ion capture, liquid separation, ion exchange, and electrochemical reduction can be used. Biometallurgical methods have been developing in recent years and consist in the use of bacteria, fungi or algae to bioleach metals from ash after burning the biomass of hyperaccumulating plants [4, 16].

The bioleaching process involves the oxidation of hydrogen sulphide, sulphur or sulphur compounds by microorganisms. As a result of this process, sulphuric acid is formed, the pH decreases and metals are solubilized. From the oxidation process, microorganisms draw energy needed to synthesize sugars from carbon dioxide and water (chemosynthesis). Another group of microorganisms can oxidize iron Fe<sup>+2</sup> to Fe<sup>+3</sup>, also obtaining energy from this process. Both groups of microorganisms are classified as chemolithotrophs. This natural process is used in biometallurgy. Bacteria that can be used include *Acidithiobacillus thiooxidans* (oxidize sulphur compounds), *Acidithiobacillus ferrooxidans* (oxidize iron). Other species of the *Acidithiobacillus* family as well as bacteria from the *Leptospirillum*, *Sulfobacillus*, *Picrophilus* families and fungi such as *Penicillium*, *Aspergillus* and *Alternaria* are also used in the bioleaching process [10, 14, 16].

From the resulting solution, metals can be recovered by chemical reaction, e.g. electrolysis. In the bioleaching process, metals such as Al, Zn, Cu, Cd, Mn, Ni, Sn, Co, Li, V, Mo, Au, Ag and Pt can be recovered [4]. Bioleaching can be carried out in heaps or dumps, but then the substrate must be sealed and the leachate collection system must be ensured. This process can also be carried out in bioreactors.

The bioleaching process can be used not only for the recovery of metals from ash in phytomining but also as a stand-alone process for the recovery of metals from other wastes (e.g. flotation waste, used batteries, electronic equipment, sewage sludge and slag from metallurgy). It is also used in the bioremediation of contaminated soils [16].

Bioleaching is a low-polluting process, but it is not easy. To achieve high efficiency in bioleaching metals, it is necessary to ensure appropriate process conditions, such as pH, temperature, redox potential, presence of nutrients, substrate particle size and the ratio of the mass of solids to the volume of liquid (pulp density) [16].

After harvesting hyperaccumulating plants, the soil should be re-tested for metal content to see if there are enough to repeat the process. If so, the plants can be re-sown and another batch of metals can be recovered from them.

#### 4 Conclusions

Growing demand for certain metals and, at the same time, depletion of existing resources leads to increased need for effective methods of metal extraction from poor ores, waste or contaminated soil. A promising method that allows this is phytomining. So far, several hundred species of plants that are very good at accumulating various metals from the substrate containing them have been identified. It is worth to note that phytomining method may be used to extract elements from substrate with low concentration of metals where other methods cannot be used.

In addition to plants, phytomining can use bacteria or fungi to extract metals from the resulting bio-ore by bioleaching. This process can also be used on its own to leach metals from waste or soil containing them.

Biomining is a process considered environmentally friendly. The greatest advantage of this method is the possibility of obtaining metals from a poor substrate, as already mentioned. It should also be remembered that the use of biological methods instead of traditional mining and metallurgy allows for the avoidance of a number of adverse effects on the environment. Additionally, it allows toxic metals removal from the environment (usually from waste and soil). An additional benefit in phytomining is the thermal energy released during the combustion of biomass.

During the extraction of metals by biological methods, pollutants are also produced, but in much smaller quantities than in the case of traditional methods. During the combustion of biomass, pollutants such as nitrogen oxides and sulfur oxides are released into the atmosphere. Carbon dioxide is also produced, but it has been previously bound by these plants and does not constitute an additional load introduced into the atmosphere. During the leaching of bio-ore, sewage and waste will be produced, and their type depends on the method used. Biometallurgy is less burdensome to the environment than hydrometallurgy, but its disadvantage is the long time needed for metal leaching. Despite this, the prevailing belief is that bioleaching will be an alternative to chemical leaching [16].

#### References

- [1] Bani, A., Echevarria, G., Sulce, S., Morel, J.L. Improving the agronomy of *Alyssum murale* for extensive phytomining: A five-year field study. *International Journal of Phytoremediation*, 17, 2015, p. 117-127.

- [2] Galardi, F., Corrales, I., Mengoni, A., Pucci, S., Barletti, L., Barzanti, R., Gonnelli, C. Intra-specific differences in nickel tolerance and accumulation in the Ni-hyperaccumulator *Alyssum bertolonii*. *Environmental and Experimental Botany*, 60, 2007, p. 377-384.
- [3] Gawroński, St. Perspektywy i ograniczenia fitoremediacji 1999, VI Sympozjum: Biotechnologia Środowiskowa, Wrocław.
- [4] Kasina, M., Jarosz, K., Salamon, K., Wierzbicki, A., Mikoda, B., Michalik, M. Bioleaching using *Acidithiobacillus Thiooxidans* - an option for elemental recovery from highly alkaline waste incineration ash? *Gospodarka Surowcami Mineralnymi - Mineral Resources Management*, 38 (3), 2022, p. 105-120.
- [5] Kikis, C., Thalassinos, G., Antoniadis, V. Soil Phytomining: Recent Developments - A Review. *Soil Systems*, 8 (1), 2024.
- [6] Klimiuk, E., Łebkowska, M. *Biotechnologia w ochronie środowiska*. Warszawa: PWN, 2003.
- [7] Kramer, U. Metal hyperaccumulation in plants. *Annual Review of Plant Biology*, 61, 2010, p. 517-534.
- [8] Krzciuk, K. Fitogórnictwo pierwiastków ziem rzadkich jako metoda zrównoważonego gospodarowania nieodnawialnymi zasobami Ziemi. *Kosmos - Problemy Nauk Biologicznych*, 68, 3, 2019.
- [9] Kumari, P., Kumar, P., Kumar T. An overview of phytomining: a metal ext process from plant species. *Journal of Emerging Technologies and Innovative Research*, 6, 2019.
- [10] Macaskie, L.E., Dean, A.C.R. Microbial metabolism, desolubilisation and deposition of wastes. Biological Waste Treatment. *Advances Biotechnological Processes*, 12, 1989, p. 159-201.
- [11] Reeves, R.D. Metal-Accumulating Plants. *Phytoremediat. Of Toxic Metals: Using Plants to Clean Up the Environment*. Ensley, B.D., Ed.; John Wiley & Son: London, UK, 2000, p. 193-229.
- [12] Reeves, R.D. Hyperaccumulation of trace elements by plants. *Phytoremediat. Of Metal-Contaminated Soils*. Morel, J.L., Echevarria, G., Goncharova, N., Eds.; Springer: New York, NY, USA, 2006, p. 1-25.
- [13] Sheoran, V., Sheoran, A., Poonia, P. Phytomining: a review. *Minerals Engineering*, 22, 2009, p. 1007-1019.
- [14] Waraczewska, Z., Niewiadomska, A., Grzyb, A. Wybrane metody bioremediacji in situ z wykorzystaniem mikroorganizmów. *Woda-Środowisko-Obszary Wiejskie*, 18 (63), 2018.
- [15] Van der Ent, A., Baker, A.J.M., Reeves, R.D., Pollard, A.J., Schat, H. Hyperaccumulators of metal and metalloid trace elements: Facts and fiction. *Plant and Soil*, 362, 2013, p. 319-334.
- [16] Worwag, M. Use of *Acidithiobacillus thiooxidans* and *Acidithiobacillus ferrooxidans* in the Recovery of Heavy Metals from Landfill Leachates. *Energies*, 14, 2021, 3336.





## POSSIBILITY OF RECOVERING METALS FROM USED ELECTRONIC EQUIPMENT

**Mariola Saternus<sup>a</sup>, Magdalena Lisińska<sup>b</sup>**

<sup>a</sup> Silesian University of Technology, ul. Krasińskiego 8, 40-019 Katowice, Poland, mariola.saternus@polsl.pl

<sup>b</sup> Zakłady Mechaniczne „WIROMET” S.A., ul. Wyzwolenia 27, 43-190 Mikołów, Poland, magdalena.lisinska04@gmail.com

### **Abstract**

Currently, we are observing rapid development of technology in the world, which results in an increase in production and, at the same time, sales, among others, electrical and electronic devices. Emerging new technologies and the globalization of the electrical and electronic equipment market result in a continuous increase in the amount of electrical and electronic waste. The lifespan of electronic components, which at the end of the 20th century ranged from 4 to 6 years, was shortened to 2 years in the first decade of the 21st century. This waste is also an extremely valuable source of many metals, such as copper, iron, zinc, tin, nickel, aluminum, gold, silver and palladium. An example is mobile phones containing printed circuit boards (PCB) - carriers of many metals. The metals contained in PCBs can be present in much higher concentrations than in conventional ore deposits, which makes waste printed circuit boards a particularly interesting material for recycling. The process of recovering metals from these wastes is a combination of physical, chemical, thermal and metallurgical processes. The main methods of recovering metals from PCBs are the pyrometallurgical method and the hydrometallurgical method. However, no single approach is sufficient to successfully recover metals, so it is better to perform the process using a combination of different extraction methods. The article will discuss the main trends in the possibilities of recovering metals from PCBs from mobile phones.

**Keywords:** electronic waste, PCB, metal recovery, recycling

### **1 Introduction**

Waste of electrical and electronic equipment (WEEE) such as computers, TV-sets, fridges and cell phones is a complex mixture of materials, which can cause major environmental and health problems due to their hazardous contents or not proper disposal. Total amount of produced WEEE reached 44 million tonnes in 2017 and is assumed to increase about 4-5 % every year; in 2050 it is expected to produce about 3.4 billion tonnes of waste per year. The service life of electronic components, which at the end of the 20th century was 4 to 6 years, was shortened to 2 years in the first decade of the 21st century [1]. The properties of electronic waste, as well as its diverse composition, have caused it to constitute a significant part of the stream of hazardous waste, which can pose a serious threat to human health and life, but also to the environment. They contain toxic components, such as heavy metals (lead, mercury, cadmium and chromium), polymers, organic materials, such as flame retardants, which contain bromine, chlorine, fluorine. This waste is also an extremely valuable source of numerous metals, such as copper, iron, zinc, tin, nickel, aluminum, gold, silver, palladium. Examples are mobile phones containing printed circuit boards - carriers of many metals.

Nowadays, most electrical and electronic devices contain printed circuit boards. The metals contained in PCBs can occur in much higher concentrations than in conventional ore deposits, which makes waste printed circuit boards a particularly interesting material for recycling. Table 1 compares the concentrations of selected metals (Cu, Sn, Zn, Pb, Fe, Ni, Au, Ag, Pd) found in printed circuit boards with the content of these metals in ores [2-4].

The recycling of printed circuit boards involves many steps. Figure 1 shows a general flowchart of the metal recovery process from these wastes using a combination of physical, chemical, thermal, and metallurgical processes. No single approach is sufficient by itself for efficient metal recovery, therefore it is beneficial to perform this process using a combination of different extraction methods.

The main methods of metal recovery from PCBs are: pyrometallurgical method [5] and hydrometallurgical method [6]. Pyrometallurgy is a commonly used method of metal recovery, including incineration, smelting in a plasma furnace or blast furnace, sintering, high-temperature melting of waste materials. More than 70 % of PCB waste is processed in smelters without mechanical treatment. Hydrometallurgical techniques largely include acid leaching, which is currently the most popular leaching method and has many advantages, including high leaching rate and fast kinetics, but is quite corrosive. After

leaching, various routes are used to separate metals from solutions - these include cementation, solvent extraction, and electrolysis.

**Table 1. Metal content in ores and PCBs**

	Metal content, %	
	Ores	PCB
Cu	0.5 - 3.0	12.0 - 29.0
Sn	0.2 - 0.8	1.1 - 4.8
Fe	30.0 - 60.0	0.1 - 11.4
Pb	0.3 - 7.5	1.3 - 3.1
Zn	1.7 - 6.4	0.1 - 2.7
Ni	0.7 - 2.0	0.3 - 1.6

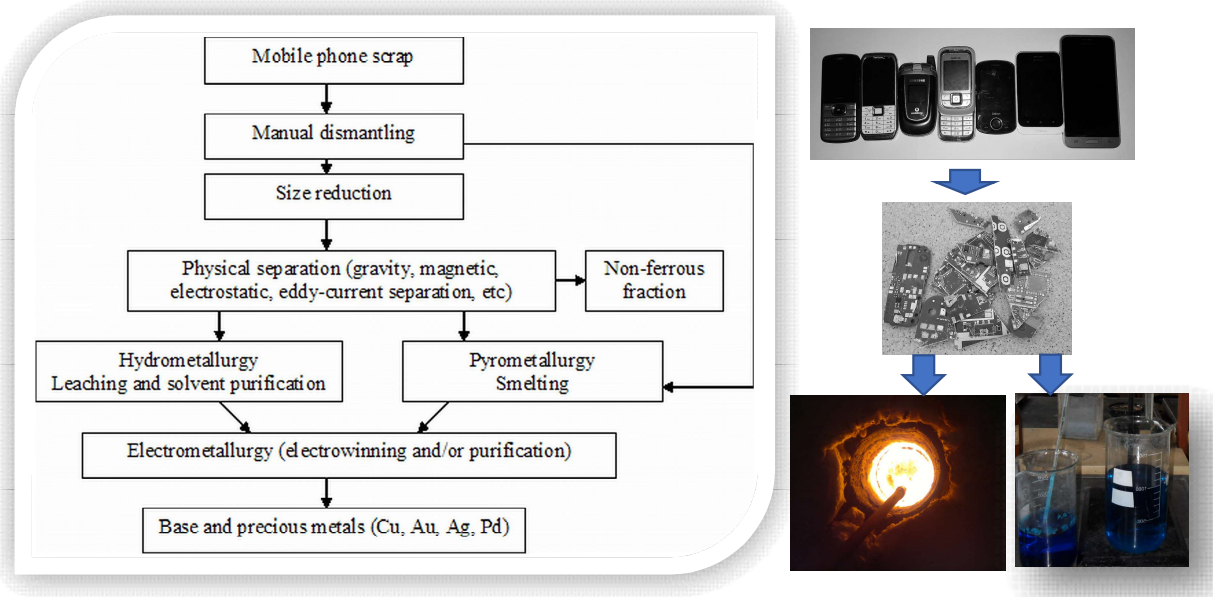


**Fig. 1. Schematic presentation of the main methods of recovering metals from PCBs**

## 2 Material and methods

Used mobile phones from various manufacturers, obtained from the domestic market, were used as research material. After their disassembly and PCB fragmentation, the chemical composition was determined using ASA. The chemical composition is presented in Table 2.

**Table 2. The chemical composition of the studied PCB**

Metal, wt.%					
Cu	Fe	Sn	Zn	Ni	Pb
31.97	2.90	2.47	0.31	0.91	0.34

Based on the results of previous own studies [7, 8], the following were selected for the metal recovery studies from the crushed PCB:

- sulfuric acid (VI) as a medium for effective leaching of Fe and Sn,
- nitric acid (V) and oxidants (H<sub>2</sub>O<sub>2</sub>, O<sub>3</sub>) for the extraction of Cu, and other metals from PCB (Zn, Ni, Pb),
- process temperature 298-353 K.

The subsequent stages of the studies were presented in the form of a block diagram - Fig. 2.

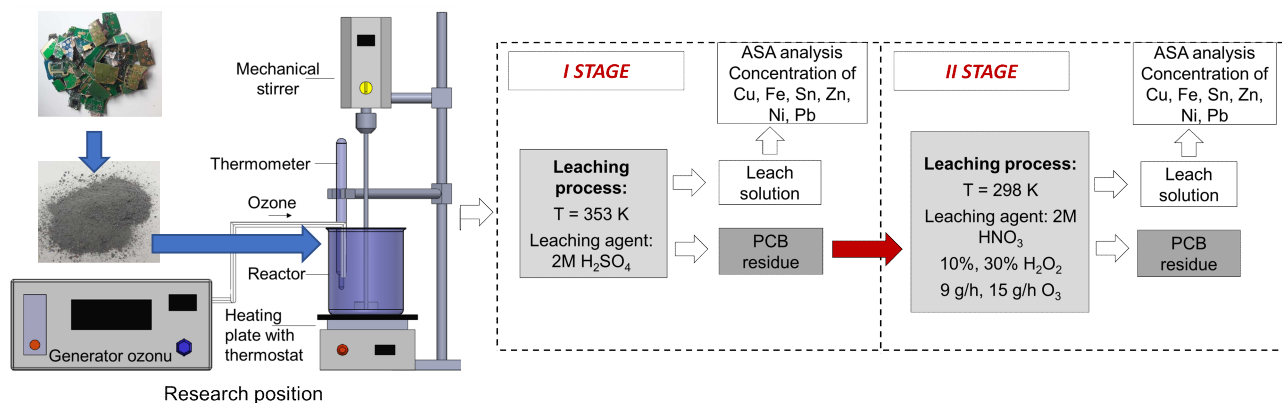


Fig. 2. Scheme of the conducted research

### 3 Results and discussion

Figure 3 shows the results of two-stage leaching of Cu, Fe, Sn, Zn, Ni and Pb from PCBs. In the first stage, 100 % of tin and practically 89 % of iron were leached. In the second stage, practically 100 % of the remaining metals were leached, except for lead. The efficiency of the metal leaching process is significantly influenced by the addition of an oxidizing agent. When using  $\text{H}_2\text{O}_2$  and  $\text{O}_3$ , a common trend of intensive increase in the concentration of Cu and Pb in the solution during the tests is visible. However, a clear intensification of the leaching process of these metals occurs when using ozone. The use of two stages and the indicated leaching agents and other parameters such as temperature 298-353 K, S/L=1/10, 400 rpm, allows for over 90-100 % recovery of all metals from this waste.

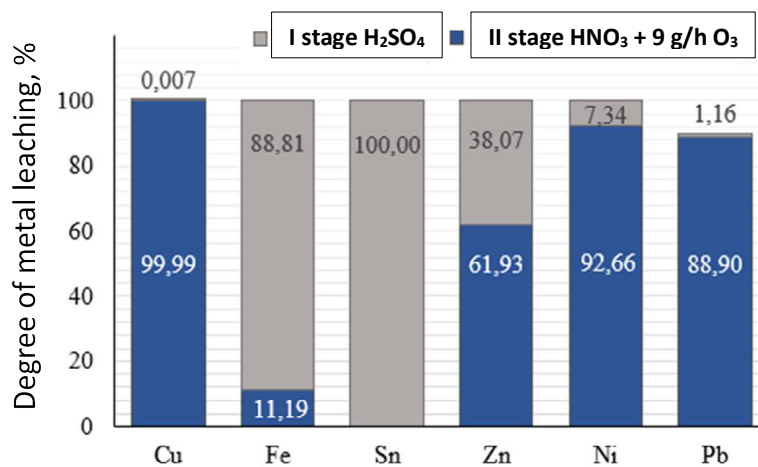


Fig. 3. Results of two-stage leaching of Cu, Fe, Sn, Zn, Ni and Pb from PCBs

### 4 Conclusions

Laboratory tests in the field of hydrometallurgical processing of printed circuit boards have a wide spectrum of activity. Various leaching methods can be found in scientific publications, such as acid, alkaline, pressure and oxidative leaching. Individual metals cannot be obtained in one step, hence the authors of various works use multi-stage processing of these wastes, using a mixture of various acids and oxidant additives. In the first stages, it is possible to leach metals that do not require the use of aggressive reagents, e.g. zinc and tin. In the next stages, it will be mainly copper leaching with the addition of oxidants, and in the last stage it will be mainly precious metals.

Generally, the process of recovering metals from PCBs is a complex and complicated process, mainly due to the heterogeneity of the material and the possibility of individual elements influencing the chemical reactions between metals and acids, sometimes a given reaction is inhibited by the occurrence of coexisting reactions blocking, for example, further leaching of a given metal.

## Acknowledgements

The work was supported by Grants 11/020/BK\_24/0129 (Silesian University of Technology).

## References

- [1] Szwech, M., Kotarba, M., Jakubowska, M. Recycling of electronic waste - new approach. *Elektronika: konstrukcje, technologie, zastosowania*, 55 (1), 2014, p. 37-38.
- [2] Kaya, M. *Printed Circuit Boards (PCBs)*, Chapter 2. Electronic Waste and Printed Circuit Board Recycling Technologies: The Minerals, Metals & Materials Series, Springer, Cham, 2019.
- [3] Witkowska-Kita, B., Biel, K., Orlicka, A. Metale krytyczne, strategiczne i deficytowe w odpadach zużytego sprzętu elektrycznego i elektronicznego. *Przegląd Górniczy*, 74 (12), 2018, p. 9-14.
- [4] Bizzo, W.A., Figueiredo, R.A., de Andrade, V.F. Characterization of Printed Circuit Boards for Metal and Energy Recovery after Milling and Mechanical Separation. *Materials*, 7, 2014, p. 4555-4566.
- [5] Kucharski, M. *Recykling metali nieżelaznych*. Wydaw. Akademii Górniczo-Hutniczej: Kraków, 2010.
- [6] Cui, J., Roven, H.J. *Electronic waste. Waste: A handbook for Management*. Elsevier, 2011, p. 281-296.
- [7] Lisińska, M., Saturnus, M., Willner, J., Fornalczyk, A. The role of oxidizing agents in the leaching process electronic waste. *Archives of Metallurgy and Materials*, 63 (2), 2018, p. 963-968.
- [8] Lisińska, M., Saturnus, M., Willner, J. Research of leaching of the printed circuit boards coming from waste mobile phones. *Archives of Metallurgy and Materials*, 63 (1), 2018, p. 143-147.

## STABILITY OF BIOLOGICALLY PRODUCED SILVER NANOPARTICLES IN VARIOUS ENVIRONMENTS

**Jana Sedlakova-Kadukova<sup>a,b</sup>, Veronika Demcakova<sup>c</sup>**

<sup>a</sup> Institute of Chemistry and Environmental Sciences, Faculty of Natural Sciences, Ss. Cyril and Methodius University in Trnava, Nám. J. Herdu 2, Trnava, 917 01, Slovakia; jana.sedlakova.fpv@ucm.sk

<sup>b</sup> ALGAJAS s.r.o., Pražská 16, 040 11, Košice, jana.sedlakova@algajas.com

<sup>c</sup> Faculty of Natural Science, Pavol Jozef Safarik University in Kosice, Srobarova 2, 041 54, Kosice, Slovakia; veronika.demcakova1@student.upjs.sk

### Abstract

Due to growing application of silver nanoparticles in various fields in the recent years, we face increased contamination of all ecosystems. However, we do not understand the real effect and risks of nanoparticles for human body as well as environment, yet. In the article we have studied stability of biologically produced nanoparticles in the presence of higher NaCl concentrations and under temperature in range of -20 – 37 °C. The most significant effect resulting in high instability of nanoparticles and extensive aggregation followed by sedimentation was observed for very low temperature of -20 °C and elevated concentration of NaCl. From our results it is visible that to understand fate of silver nanoparticles in the various environmental compartments, it is important to know their behaviour under various environmental contamination.

**Keywords:** silver nanoparticles, biological production, stability, green algae

### 1 Introduction

Based on their unique physical, chemical and biological characteristics are silver nanoparticles (AgNPs) very often used in various fields, such as medicine, drug delivery, material disinfection, electronics, catalysis, agriculture etc.[1, 2]. However, their application results in the increase of silver concentrations in all environmental components with serious impact on ecosystems [3]. To understand behavior of silver nanoparticles in various environments, it is very important to predict their fate, including toxicity, in ecosystems and consider risk their application can present.

Nanoparticles have high surface/volume ratio leading to very high surface energy leaving the colloid solution in metastable state. To get to lower surface energy state (aggregation) energetic barrier must be overcome. To stabilize colloid solution, sufficient energetic barrier that would prevent aggregation has to be present [4]. Other way, how to stabilize colloid solution is sterical stabilization using various lyophilic layers that would sterically stop the aggregation [5].

The aim of the article was to simulate effect of basic environmental conditions on stability of biologically prepared silver nanoparticles. The first of studied conditions was temperature related to seasonal temperature changes, increase of temperature in surface waters as well as stability of nanoparticles at human body temperature. The second one was salinity as silver is known to precipitate easily with Cl<sup>-</sup> ions. The human body as well as sea water environments were simulated.

### 2 Material and methods

#### 2.1 Biological production of silver nanoparticles

Silver nanoparticles were prepared using the alga *Parachlorella kessleri*. Following a modified procedure, an extract was prepared from the algae, after which an AgNO<sub>3</sub> solution was added to the extract to achieve a final silver concentration of 100 mg/l [6].

#### 2.2 Temperature effect study

5 ml of solution containing biologically produced silver nanoparticles was pipetted into tubes and placed into environment with -20 °C (freeze), 4 °C (refrigerator), 18 °C (laboratory cabinet), and 37 °C (incubator) for 24 hours. Sample placed at 4 °C was used as control. UV-vis spectrum was measured at the beginning of the experiment and at the end.

### 2.3 Salinity effect study

10 ml of biologically produced silver nanoparticles was pipetted into plastic tubes. Experiments were carried out as triplicates. First set as a control without addition of NaCl, into second and third sets of tubes 0.09 g and 0.3 g of NaCl was added, respectively, and mixed. Resulting NaCl concentrations were as follows:

- Set 1 – 0 % (control)
- Set 2 – 0.9 %
- Set 3 – 3 %

Samples were stored at 4 °C for 24 hours. UV-vis spectrum was measured at the beginning of the experiment and after 24 hours of experiments.

## 3 Results and discussion

### 3.1 Effect of temperature

Temperature is the most common factor affecting nanoparticles in the environment having significant effects on their stability. Temperature in range of 4 – 37 °C has no effect on AgNPs stability leaving the UV-vis spectrum without changes after 24 hours. However, very low temperature of -20 °C resulted in significant changes in AgNPs solutions. Silver aggregates were visible in the bottom of the tubes, as well (Fig. 1). Significant decrease of absorbance intensity and peak shift to higher wavelengths confirm nanoparticle aggregation. MacCuspie [7] after freezing citrate stabilized silver nanoparticles observed their irreversible aggregation. Similarly, Forbes et al. [8] studied effect of temperature on various nanoparticles stability. They found that the most stable were nanoparticles at 4 °C, however, in temperature range of 4 – 37 °C for 14 days significant changes were not observed.

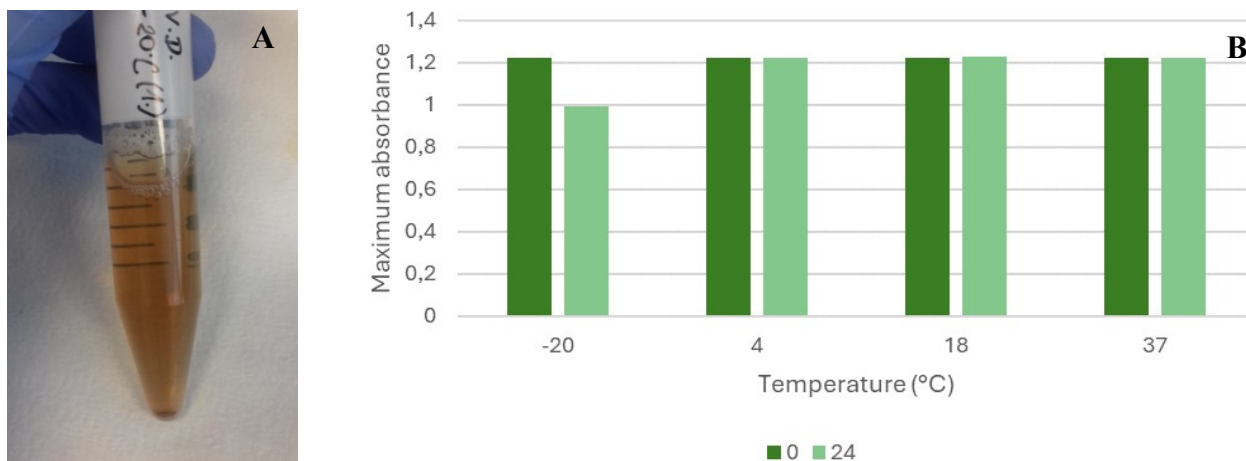


**Fig. 1. Sedimentation of silver after 24 hours at -20 °C (A), differences in maximum absorbance of silver nanoparticles solution after 24 hours at various temperatures (B)**

### 3.2 Effect of salinity

Based on chemical characteristics of silver, stability of nanoparticles in NaCl solutions was also studied. The environment like human body was simulated by salinity 0.9 % equal to physiological solution. Sea water environment was simulated by 3 % salinity. Significant changes of UV-vis spectrum were observed immediately after addition of NaCl crystals into solutions (Fig. 2).

In solution with 0.9 % NaCl peak shift to lower wavelengths was observed suggesting reduction of silver nanoparticles size or aggregation and sedimentation of larger nanoparticles and only small nanoparticles stayed in the solution. After 24 hours reduction of absorbance intensity and sedimentation on the tube bottom were observed, as well.

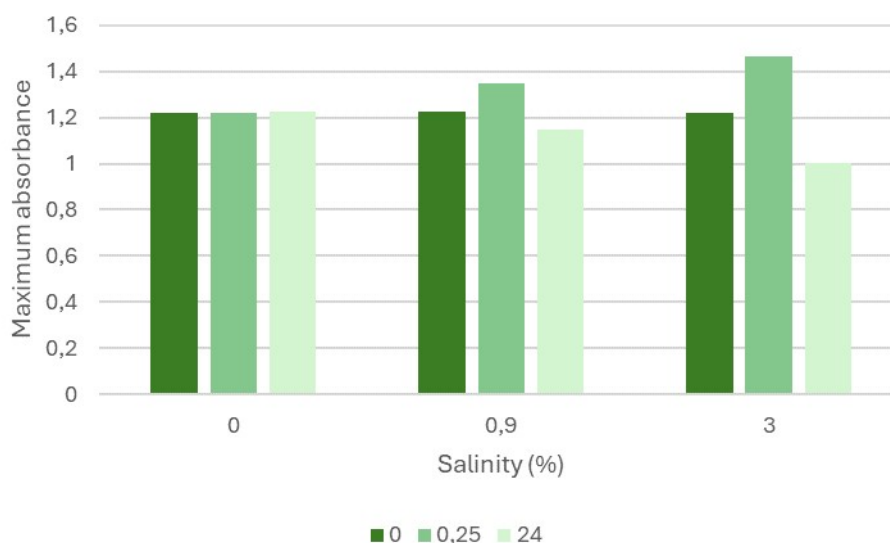


**Fig. 2. Differences in maximum absorbance of silver nanoparticles solution after 15 minutes and 24 hours at various salinities**

In 3 % NaCl solution, absorbance reduction was more significant with fast sedimentation of nanoparticles on the tube bottom. Changes of color in AgNPs solution were visible macroscopically from yellow brown to light yellow. The higher NaCl concentration, the faster sedimentation was observed (Fig. 3). Similarly, Levard et al. [9] found that Cl<sup>-</sup> ions react with surface atoms of AgNPs resulting in solid AgCl precipitation. Reaction rate depends on NaCl concentration. The higher the Cl/Ag ratio, the higher the reaction rate. Chinnapongose et al. [10] found that concentration of NaCl higher than 0.1 % leads to AgNPs instability. They suggested AgNPs agglomeration followed by sedimentation as the main mechanism responsible for their instability in the presence of NaCl. On the other hand, Mokhtari et al. [11] observed that living microorganisms were able to turn forming precipitates of AgCl back into AgNPs. Thus, the study in real environments is necessary to understand the real fate of silver nanoparticles in sea water environment.

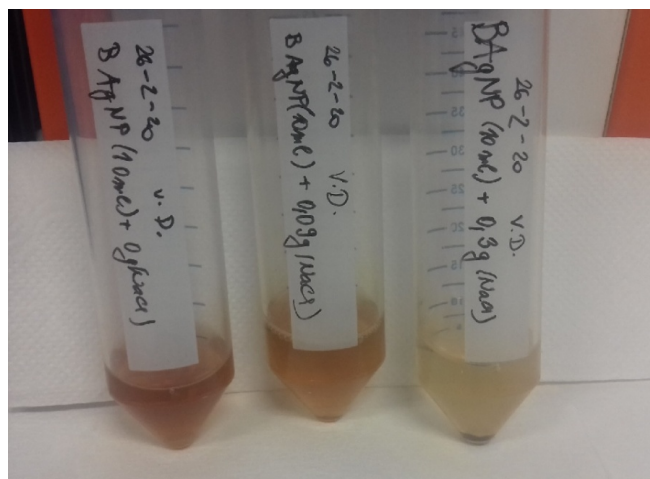


**Fig. 3. Sedimentation and color changes of silver nanoparticles solution after addition of NaCl. from left – control, 0.9 % and 3 % NaCl**

#### 4 Conclusions

Studying the effect of the environment on nanoparticle stability we found that temperature in range of 4 – 37 °C does not significantly affected their stability, although the best temperature for long term storage is temperature about 4 °C thus keeping nanoparticles in refrigerator is the most suitable way of storage. However, at -20 °C strong aggregation was observed with very low nanoparticles stability.

The presence of NaCl decreased stability of AgNPs. With increasing NaCl concentration, AgNPs stability decreased, and fast aggregation was observed.

## Acknowledgements

The work was supported by project VEGA 1/0018/22.

## References

- [1] León-Silva, S., Fernández-Luqueño, F., López-Valdez, F. Silver Nanoparticles (AgNP) in the Environment: A Review of Potential Risks on Human and Environmental Health. *Water, Air, & Soil Pollution*, 227, 2016, p. 1-20.
- [2] Anand, R., Bhagat, M. Silver Nanoparticles (AgNPs): as Nanopesticides and Nanofertilizers. *MOJ Biology and Medicine*, 4 (1), 2019, p. 19-20.
- [3] Kah, M.A., Kookana, R.S., Gogos, A., Bucheli, T.D. Critical Evaluation of Nanopesticides and Nanofertilizers against their Conventional Analogues. *Nature Nanotechnology*, 13 (8), 2018, p. 677-684.
- [4] Phan, H.T., Haes, A.J. What Does Nanoparticle Stability Mean? *The Journal of Physical Chemistry C*, 123 (27), 2019, p. 16495-16507.
- [5] Novák, J. a kol. *Fyzikální chemie - bakalářský a magisterský kurz*. Praha: VŠCHT. 2008, 506 p.
- [6] Kadukova, J. Surface Sorption and Nanoparticle Production as a Silver Detoxification Mechanism of the Freshwater Alga *Parachlorella kessleri*. *Bioresource Technology*, 216, 2016, p. 406-413.
- [7] MacCuspie, R.I. Characterization of Nanomaterials for NanoEHS Studies. In: Hull, M. S. – Bowman, D. M. *Nanotechnology Environmental Health and Safety: Risks, Regulation, And Management*. 3. Ed. Oxford: Elsevier. 2018, p. 59-82.
- [8] Forbes, N.A., Yuan, T.T., Desilva, M.N. *Silver Nanoparticle Storage Stability in Aqueous and Biological Media*. San Antonio: Naval Medical Research, 2015, 21 p.
- [9] Levard, C. Effect of Chloride on the Dissolution Rate of Silver Nanoparticles and Toxicity to *E. Coli*. *Environmental Science & Technology*, 47 (11), 2013, p. 5738-5745.
- [10] Chinnapongse, S.L., MacCuspie, R.I., Hackley, V.A. Persistence of Singly Dispersed Silver Nanoparticles in Natural Freshwaters, Synthetic Seawater, and Simulated Estuarine Waters. *Science of the Total Environment*, 409, 2011, p. 2443-2450.
- [11] Mokhtari, N. Biological Synthesis of Very Small Silver Nanoparticles by Culture Supernatant of *Klebsiella Pneumonia*: The Effects of Visible-Light Irradiation and the Liquid Mixing Process. *Materials Research Bulletin*, 44 (6), 2009, p. 1415-1421.



# IDENTIFICATION OF HIGHLY SPECIFIC METAL-BINDING PEPTIDES FOR THE SELECTIVE RECOVERY OF METALS FROM WASTE STREAMS

**Anna Sieber<sup>a</sup>, Nora Schönberger<sup>b</sup>, Franziska Lederer<sup>b</sup>, Doris Ribitsch<sup>c,d</sup>, Georg M. Guebitz<sup>a,b</sup>**

<sup>a</sup> KI-MET GmbH, Stahlstraße 14, 4020 Linz, [anna.sieber@ki-met.com](mailto:anna.sieber@ki-met.com)

<sup>b</sup> Department of Biotechnology, Helmholtz Institute Freiberg for Resource Technology, Helmholtz Center Dresden-Rossendorf, Bautzner Landstraße 400, 01328 Dresden

<sup>c</sup> Department of Agrobiotechnology, IFA-Tulln, Institute of Environmental Biotechnology, BOKU University of Natural Resources and Life Sciences Vienna, Konrad-Lorenz-Straße 20, 3430 Tulln an der Donau

<sup>d</sup> Austrian Centre of Industrial Biotechnology, Konrad-Lorenz-Straße 20, 3430 Tulln an der Donau

## Abstract

Commercial recycling of lithium-ion batteries (LIBs) often ends with the so-called black mass. This fine-grained powder contains critical raw materials and economically important metals. Bioleaching can be performed to solubilize most of the metals but the selective recovery of these metals still remains a challenge. In this study, phage surface display (PSD) was used for the identification of promising metal-binding peptide candidates. In initial PSD experiments, a plethora of peptides were screened, and promising peptides have been identified binding to nickel-, cobalt- and manganese-ions. The peptides were analyzed according to their binding affinity to the corresponding metal ions. First results indicate that these peptides can be used to selectively separate metal ions in aqueous solutions. Attaching these newly identified peptides to a suitable carrier material will make it possible to extract the specific metals from complex solutions like the spent lithium-ion batteries.

**Keywords:** selective metal recovery, metal-binding peptides, phage surface display, polymetallic waste streams

## 1 Introduction

The amount of electronic waste worldwide keeps on growing rapidly with a growth rate of 3-5 % each year and is predicted to increase to 75 million tons by the year 2030. Electronic waste presents an attractive secondary resource of many economically important and critical metals, but the recycling of this heterogeneous waste is notoriously difficult [1]. Especially spent lithium-ion batteries (LIBs) often end up in landfills whilst containing substantial amounts of critical metals such as Co, Ni, Mn or Li [2]. The recently adapted EU Battery Regulation states that 65 and 70 % of Li-based batteries need to be recycled by 2025 and 2030, respectively. Additionally, 90 and 95 % of Co, Ni and Cu should be recycled by 2025 and 2030, respectively [3].

Lithium-ion battery recycling results in a fine-grained active material which contains critical raw materials such as lithium, phosphorous, cobalt, silicon, and graphite as well as nickel, copper, and manganese. By applying bioleaching, these metals can be solubilized leading to the formation of acidic polymetallic solutions (pH <3). However, the selective recovery of these metals remains a challenge due to the high risk of co-precipitation of Ni<sup>2+</sup>, Co<sup>2+</sup>, Mn<sup>2+</sup>, and Cu<sup>2+</sup> because of the similar solubility of their hydroxides [4]. Peptides are highly sensitive and selective towards their target and recently, there is an increasing interest in exploiting peptide-metal interactions for resource recovery processes. Metal-binding peptides can be identified by using phage display technology. Within this method a random peptide library is created and displayed on the surface of bacteriophages. This library can then be screened against a variety of different targets, enabling the enrichment of peptides with a high affinity for the target [5].

In this study, metal ions were immobilized onto agarose beads and used as a target. To identify peptides that bind strongly to the immobilized metal ions, several screening rounds were performed to enrich for strong binders. Promising peptide candidates could be enriched for nickel-, cobalt-, and manganese-ions. These peptides are further evaluated according to their selective binding properties. Preliminary results show that these peptides can be used to selectively recover the metal ions from aqueous solutions.

## 2 Material and methods

### 2.1 Target preparation

For nickel and cobalt screenings, commercial agarose beads preloaded with the respective metal were used. However, for manganese none such beads were available. Hence the loading of agarose beads with manganese was performed according to the provider's protocol. 6 ml of Purecube NTA Agarose suspension

was washed 3 times with MQ-H<sub>2</sub>O followed by 3 washing steps with sodium acetate buffer (50 mM, pH 6.0). Afterwards, the washed beads were incubated with 6 ml of manganese solution (2.5 % w/v) at 22 °C for 2 hours at 950 rpm. After several washing steps with MQ-H<sub>2</sub>O and Tris-HCl buffer (20 mM, pH 7.5), the metal loaded beads were resuspended in agarose storage buffer (pH 6.5) to yield a 50 % suspension and stored at 4 °C.

The metal concentration on the beads was determined by ICP-OES. Briefly, 100 µl of beads were incubated with 1 M HNO<sub>3</sub> at 70 °C for 1 hour. After centrifugation, an aliquot of the supernatant was sent to a scientific partner for ICP-OES measurements.

## 2.2 Determination of phage concentration

For the determination of the phage concentration, titration experiments were performed. The standard protocol was adapted to 24 well plates. Well plates with LB agar containing IPTG (50 µg/ml), Xgal (40 µg/ml) and tetracycline (20 µg/ml) were prepared. LB media was inoculated with one colony of an *E. coli* ER2738 plate and incubated at 37 °C, 200 rpm until an optical density (OD<sub>600</sub>) of 0.5 was reached. Appropriate dilutions of the phage solutions were prepared in LB media to ensure the possibility of counting single plaque forming units. From each dilution step, 10 µl of phage solution were used to infect 200 µl of *E. coli* culture. After 5 minutes, 10 µl of the infected *E. coli* solution was pipetted onto a well of the 24-well agar plate and coated with 200 µl of pre-warmed soft agar. The plates were incubated at 37 °C overnight. The next day, blue plaques were counted and the phage concentration was calculated.

## 2.3 Biopanning

Metal-loaded beads were washed with TBS-T buffer (pH 7.5), followed by incubation with the phage library for 1 hour at 22 °C and 950 rpm. After that, the beads were washed again 10x with TBS-T buffer to remove unbound phage. Different elution methods were performed to elute the phages from the beads. 10 µl of each step (input phage and eluted phage) were kept for phage titration. The rest of the eluted phage was used to infect an *E. coli* ER2738 culture (at an OD<sub>600</sub> between 0.05 and 0.1) and the infected culture was incubated at 37 °C for 4.5 hours. After that, the culture was centrifuged and amplified phages were precipitated and purified from the culture supernatant.

After 3 rounds of biopanning, the eluted fraction was titrated onto a LB/IPTG/Xgal plate and incubated overnight at 37 °C. 20 clones were randomly picked from this plate, phage DNA was extracted and send for sequencing.

## 3 Results and discussion

The amount of metal that was loaded onto the NTA-Beads was determined via ICP-OES (Table 1). The amount of metal on the different beads is comparable and in range with values that other researcher have reported after loading agarose beads with metals e.g. Matys et al. report 10.4 µg/mg bound nickel and 9 µg/mg bound cobalt [6].

**Table 1. Metal ion concentration on the NTA-beads after loading**

(Concentrations were determined via ICP-OES)

Metal ion	µg metal / mg beads
Ni	8.72 ± 1.53
Co	7.24 ± 0.02
Mn	5.20 ± 0.09

The titration results of the biopanning for manganese are presented in Figure 1. In this biopanning two different elution methods were tested. First, phages were eluted with a low pH glycine-HCl buffer, followed by direct incubation of the beads with an *E. coli* culture (biological elution). Both eluates were subsequently amplified. The phage titer after amplification is similar for both different elution methods. This shows that after the glycine elution there were still some phages attached to the beads that could be eluted with the biological elution. The sequencing of selected phage clones showed different amino acid sequences of the peptides.

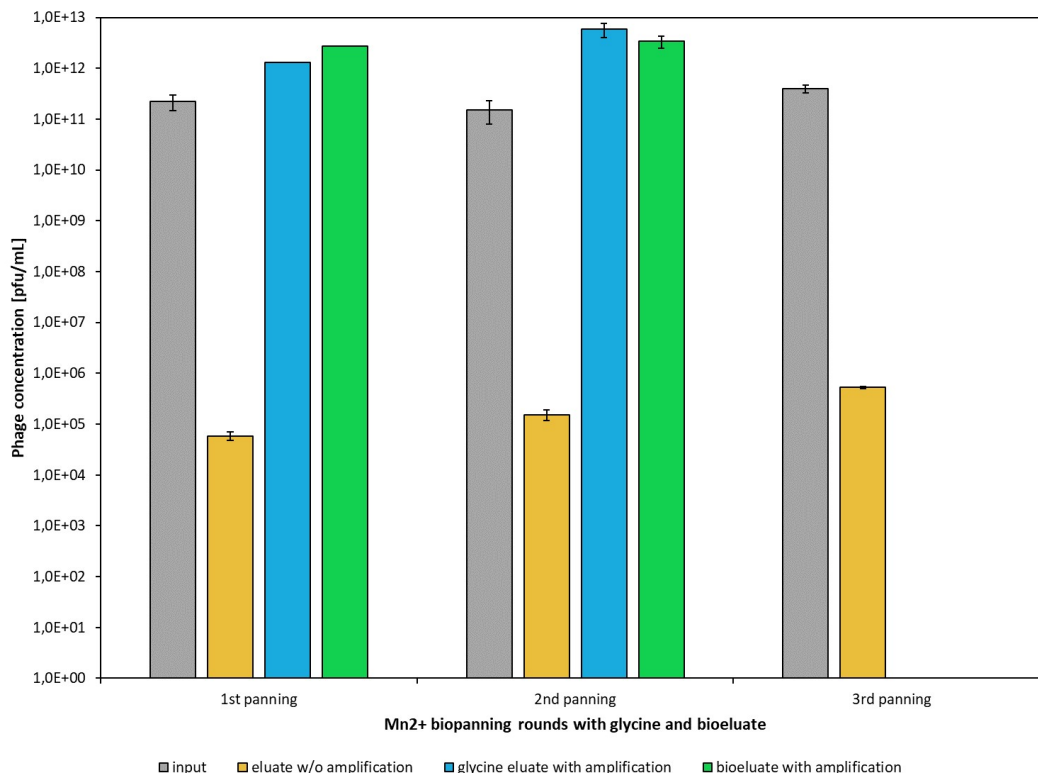


**Fig. 1. Phage concentrations [pfu/ml] after each of the 3 biopanning steps**

Depicted is the input phage fraction (grey), the eluate before amplification (yellow), the glycine eluate after amplification (blue) and the biological elution after amplification (green)

#### 4 Conclusions

The here presented study aims to identify and characterize short peptides that bind selectively and with high affinity to nickel-, cobalt-, and manganese-ions. To identify these peptides, an appropriate screening method was set up using metal-loaded agarose beads. Biopanning rounds could successfully be performed and different elution methods were tested. The identified peptides will further on be tested in batch studies to preselect the most promising binders. The metal-binding capacity of these peptides will then further be characterized by isothermal titration calorimetry.

#### Acknowledgements

The authors gratefully acknowledge the funding support of K1-MET GmbH, the metallurgical competence center. The Module FuLIBatteR is supported by COMET (Competence Center for Excellent Technologies), the Austrian program for competence centers. COMET is funded by the Federal Ministry for Climate Action, Environment, Energy, Mobility, Innovation and Technology, the Federal Ministry for Labour and Economy, the Federal States of Upper Austria and Styria as well as the Styrian Business Promotion Agency (SFG). Furthermore, Upper Austrian Research GmbH continuously supports the module. Besides the public funding from COMET, this research project is partially financed by the company partners Audi, BRAIN Biotech, Ebner Industrieofenbau, RHI Magnesita, Saubermacher, TÜV SÜD Landesgesellschaft Österreich, voestalpine High-Performance Metals, and VTU Engineering and the scientific partners acib, Coventry University, Montanuniversitaet Leoben, University of Natural Resources and Life Sciences, and UVR-FIA.

#### References

- [1] Chakankar, M., Lederer, F., Jain, R., Matys, S., Kutschke, S., Pollmann, K. State-of-the-Art Biotechnological Recycling Processes. *Management of Electronic Waste*, 2024, p. 375-405, <https://doi.org/10.1002/9781119894360.ch15>.

- [2] Lalropuia, L., Kucera, J., Rassy, W.Y., Pakostova, E., Schild, D., Mandl, M., Kremser, K. Guebitz, G.M. Metal recovery from spent lithium-ion batteries via two-step bioleaching using adapted chemolithotrophs from an acidic mine pit lake. *Frontiers in Microbiology*, 15, 2024, 1347072, doi: 10.3389/fmicb.2024.1347072.
- [3] Regulation (EU) 2023/1542 of the European Parliament and of the Council of 12 July 2023 concerning batteries and waste batteries, amending Directive 2008/98/EC and Regulation (EU) 2019/1020 and repealing Directive 2006/66/EC. (2023). Available at: <https://eur-lex.europa.eu/legal-content/EN/TXT/?uri=OJ:L:2023:191:TOC>.
- [4] Or, T., Gourley, S.W.D., Kaliyappan, K., Yu, A., Chen, Z. Recycling of mixed cathode lithium-ion batteries for electric vehicles: Current status and future outlook. *Carbon Energy*, 2 (1), 2020, p. 6-43, <https://doi.org/10.1002/cey2.29>.
- [5] Braun, R., Bachmann, S., Schönberger, N., Matys, S., Lederer, F., Pollmann, K. Peptides as biosorbents - Promising tools for resource recovery. *Research in Microbiology*, 169 (10), 2018, p. 649-658, <https://doi.org/10.1016/j.resmic.2018.06.001>.
- [6] Matys, S., Schönberger, N., Lederer, F.L., Pollmann, K. Characterization of specifically metal-binding phage clones for selective recovery of cobalt and nickel. *Journal of Environmental Chemical Engineering*, 8, 2020, 103606, doi: 10.1016/j.jece.2019.103606.

## INVESTIGATING MITOCHONDRIAL CONTRIBUTIONS TO MAGNETORECEPTION IN *SACCHAROMYCES CEREVISIAE* AND THEIR POTENTIAL BIOTECHNOLOGICAL APPLICATIONS UNDER VARIED MAGNETIC FIELDS

**Miroslava Sincak<sup>a</sup>, Jozef Nosek<sup>b</sup>, Alena Luptakova<sup>c</sup>, Petr Jandacka<sup>d</sup>, Miloslav Luptak<sup>e</sup>,  
Jana Sedlakova-Kadukova<sup>a,f</sup>**

<sup>a</sup> Faculty of Natural Science, University of Cyril and Methodius in Trnava, Nam. J. Herdu 2, 917 01 Trnava

<sup>b</sup> Department of Biochemistry, Faculty of Natural Sciences, Comenius University in Bratislava,  
Safarikovo namestie 6, 814 99 Bratislava

<sup>c</sup> Institute of Geotechnics, Slovak Academy of Sciences, Watsonova 45, 040 01 Kosice

<sup>d</sup> Czech University of Life Sciences Prague, Faculty of Forestry and Wood Sciences,  
Kamycka 129, 165 00 Praha 6 - Suchbátka, Czech Republic

<sup>e</sup> Technical University of Kosice, Faculty of Materials, Metallurgy and Recycling, Letna 9, 042 00 Kosice

<sup>f</sup> ALGAJAS s.r.o., Pražská 16, 04 011 Kosice

### Abstract

The phenomenon of non-specific magnetoreception, or the perception of magnetic fields different from Earth's geomagnetic field, remains largely unexplored with various theoretical mechanisms proposed. One of the most debated potential mechanisms involves the impact of magnetic fields on mitochondrial metabolism. In this study, we investigated this hypothesis using *Saccharomyces cerevisiae* yeast strains with ( $\rho^+$ ) and without functional mitochondria ( $\rho^0$ ). These strains were exposed to a moderately strong magnetic field (2.5 mT) for 24 hours.

Our experiments revealed that yeast with functional mitochondria exhibited a 30 % increase in growth under the 2.5 mT magnetic field, whereas the  $\rho^0$  yeast showed only an 18 % increase. The statistically significant differences between the control and experimental groups highlight the critical role of mitochondria in magnetoreception. These findings indicate that while mitochondria are crucial for detecting stronger magnetic fields, they may not be as important for magnetic field detection. This underscores the complexity of non-specific magnetoreception.

**Keywords:** biotechnology, mitochondria, yeast, magnetoreception

### 1 Introduction

Nonspecific magnetoreception, the ability to perceive magnetic fields, leads to various biological effects across all organisms. Exposure to magnetic fields can accelerate cell metabolism, alter reactive oxygen species (ROS) levels, influence calcium concentration, and affect mitochondrial membranes and enzymes. These fields are used in medicine for cancer treatment and have potential in biotechnology for applications like stabilizing bacterial communities in wastewater treatment plants. However, the overall impact of magnetic fields on biological systems remains underexplored.

Mitochondria are particularly susceptible to magnetic fields due to their large size, electron-transparent matrix, and lower membrane potential [1]. ROS generation within a cell depends on factors like cellular O<sub>2</sub> availability, redox state, respiratory rate, electron carrier concentration, mitochondrial inner membrane potential, and post-translational modifications of respiratory chain proteins [2]. Magnetic field exposure has been linked to changes in calcium uptake [3], ATP production [4], enzymatic activity [5], mitochondrial respiration decline [6], and elevated ROS production [7]. Sun et al. [3] suggested that extensive electron leakage from the mitochondrial electron transport chain could be a primary cause of electromagnetic field-induced damage.

Four main effects of magnetic fields related to mitochondrial function include impacts on ion transport, radical pairs and ROS, ATP production, and membranes. These effects may stem from fundamental magnetic responses, potentially involving DNA damage and mitochondrial membrane perturbation. Lednev et al. [8] proposed that weak microtesla and nanotesla alternating magnetic fields might influence the spins of electrons or hydrogen nuclei in biological molecules. Changes in mitochondrial function may account for many observed biological effects in earlier experiments [9].

Mitochondria exhibit rhythmic processes at radio wave frequencies [10]. These processes involve reactions producing harmful superoxide anions, countered by enzymes like superoxide dismutase [11]. Magnetic fields might disrupt these processes, affecting energy flow and function [9]. Radical-pair processes

in mitochondria might explain observed effects of low-frequency or static magnetic fields, suggesting a mechanism for various biological phenomena. Static magnetic fields can also alter the oscillation of electromagnetic fields, a phenomenon known as magnetic field modulation or coupling [12]. This effect depends on factors like the static magnetic field strength, oscillating field frequency, and material characteristics [13].

This study investigates the effects of intermediate static magnetic fields (2.5 mT) on yeast strains with ( $\rho^+$ ) and without ( $\rho^0$ ) functional mitochondria. The aim is to explore the role of functional mitochondria in magnetoreception and its impact on yeast growth and survival.

## 2 Material and methods

### 2.1 Cultivation

Two yeast strains of *Saccharomyces cerevisiae* were obtained from Comenius University in Bratislava, Slovakia:  $\rho^+$  (CML282, genotype: MATa, ura3-1, ade2-1, leu2-3,112, his3-11,15, trp1- $\Delta$ 2, can1-100, CMVp (tetR-SSN6)::LEU2) and  $\rho^0$  (CML282 without mtDNA). The yeast were cultured in liquid YPD medium for 18 hours. Subsequently, 10 ml of the culture was transferred to 20 ml tubes and exposed to a magnetic field generated by a coil (sample) or placed next to the coil in the geomagnetic field (control). After 24 hours of exposure, the samples were moved to the geomagnetic field for an additional 24 hours, along with the control. All experiments were performed in triplicate in the dark at room temperature.

### 2.2 Magnetic field

The magnetic field was generated by passing an electrical current through a custom-made copper coil (5 cm long, 1 cm wide) immersed in the cultivation media for 48 hours. The field's flux density (B) was measured at the coil's center using a VEMA 04 fluxgate magnetometer with 2 nT/LSB sensitivity and a 1000 Hz sampling rate. The magnetometer was calibrated with a neural network-based method.

### 2.3 Analyses

Growth changes were assessed by counting cells in a Bürker chamber at specific time intervals: 0, 2, 5, 24, 26, 32, and 48 hours. Growth curves were constructed based on cell counts every two hours, except during the night. pH and redox potential were measured using a multimeter (WTW™ inoLab™ 9630) at three points: after culturing the initial culture, after 24 hours, and after 48 hours in the magnetic field.

## 3 Results and discussion

The yeast culture, with or without mitochondria, exposed to a magnetic field of 2.5 mT, exhibited significantly greater growth stimulation compared to the control (Fig. 1).

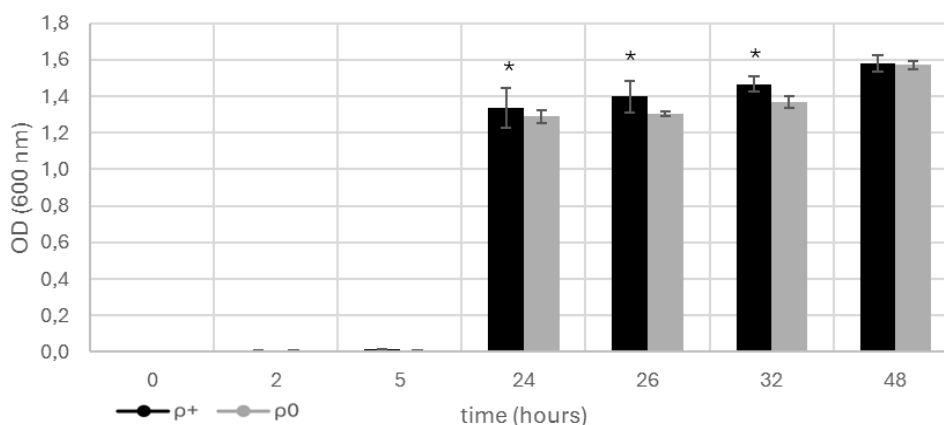


**Fig. 1. The effect of a 2.5 mT magnetic field on the growth  $\rho^0$  and  $\rho^+$  yeast compared to the corresponding control (\*Difference is significant at  $p < 0.05$ )**

We observed that the magnetic field had a more pronounced effect on yeast with functional mitochondria ( $\rho^+$ ) compared to those without ( $\rho^0$ ). Specifically,  $\rho^+$  yeast showed a growth increase of 6-31 %, whereas  $\rho^0$  yeast exhibited a 4-18 % increase. The cell density difference between  $\rho^+$  and  $\rho^0$  yeast was up to

10 %. Control cultures, regardless of mitochondrial presence, did not show significant differences in cell density under laboratory conditions. These findings suggest that mitochondria enhance the ability of yeast to detect and respond to moderately strong magnetic fields, affecting cellular metabolism.

**Table 1. The effect of a 2.5 mT magnetic field on the growth properties of  $\rho^+$  and  $\rho^0$  yeast compared to the corresponding control (shaded cell indicate significant difference according to double-tailed t-test)**

Time (hours)	Difference between $\rho^0$ and control	p-value	Difference between $\rho^+$ and control	p-value
0	0		0	
2	0		0	
5	-1.7	0.1261	6.6	0.0331
24	16.7	0.0229	31.3	0.0036
26	18.1	0.0034	26.6	0.0125
32	16.2	0.0044	27.1	0.0058
48	4.4	0.0142	14.1	0.0004

This finding is novel, as only a few studies have focused on moderately strong static magnetic fields (in the millitesla range) and there is a lack of data on how the absence of mitochondria affects yeast survival and growth under static magnetic fields.

Previous research primarily examined alternating magnetic fields, revealing mostly negative impacts on mitochondrial metabolism. Effects included extensive electron leakage from the mitochondrial electron transport chain [14], increased intracellular ROS levels [15, 16], decreased mitochondrial respiration and balance [5], and damage to mitochondrial DNA and calcium uptake [3]. These studies spanned a range of electromagnetic fields, from weak low-frequency to radio-frequency.

Conversely, Luukkonen et al. [17] and Yamashita et al. [18] reported increased mitochondrial activity following exposure to an alternating magnetic field (50 Hz, 100 mT). This increase was attributed to extensive lipid peroxidation in SH-SY5Y cell lines and enhanced mitochondrial respiration. Binhi's biophysical model [19] explains this effect by suggesting that microtesla and nanotesla alternating magnetic fields influence the spins of electrons or hydrogen nuclei in biological molecules. These models suggest that the effective amplitude of the magnetic field influences radical-pair reactions, which may affect calcium transport and ATP generation in mitochondria [9].

#### 4 Conclusions

Our study sheds light on the role of mitochondria in the magnetoreception of *Saccharomyces cerevisiae* under different magnetic field conditions. The data indicate that mitochondria are important for the magnetoreception of moderately strong static magnetic fields (2.5 mT), as shown by the different growth responses in yeast strains with functional mitochondria ( $\rho^+$ ) versus those without ( $\rho^0$ ). Specifically,  $\rho^+$  yeast exhibited greater sensitivity to the magnetic field, with growth stimulation ranging from 6 % to 31 %, compared to 4 % to 18 % in  $\rho^0$  yeast.

These findings highlight the complexity of magnetoreception, and the intricate role mitochondria play in these processes. The mechanisms by which mitochondria and other cellular components detect and respond to magnetic fields are not yet fully understood. This study emphasizes the need for further research to clarify these mechanisms, especially the varied responses to different magnetic field strengths and conditions. Gaining a deeper understanding of these processes is essential for advancing our knowledge of cellular magnetoreception and its broader implications in biology and medicine.

#### Acknowledgements

The work was supported by financial by projects VEGA 1/0018/22 and 2/0108/23, APVV-21-0504 and FPPV-03-2024.

#### References

- [1] Fu, J.P., Mo, W.C., Liu, Y., He, R.Q. Decline of cell viability and mitochondrial activity in mouse skeletal muscle cell in a hypomagnetic field. *Bioelectromagnetics*, 37 (4), 2016, p. 212-222.

- [2] Zhang, B., Tian, L. Reactive oxygen species: Potential regulatory molecules in response to hypomagnetic field exposure. *Bioelectromagnetics*, 41 (8), 2020, p. 573-580.
- [3] Sun, C., Zhu, L., Qin, H., Su, H., Zhang, J., Wang, S., Xu, X., Zhao, Z., Mao, G., Chen, J. Inhibition of mitochondrial calcium uptake by Ru360 enhances the effect of 1800 MHz radio-frequency electromagnetic fields on DNA damage. *Ecotoxicology and Environmental Safety*, 264, 2023, p. 115472.
- [4] Sharpe, M.A., Baskin, D.S., Pichumani, K., Ijare, O.B., Helekar, S.A. Rotating magnetic fields inhibit mitochondrial respiration, promote oxidative stress and produce loss of mitochondrial integrity in cancer cells. *Frontiers in Oncology*, 11, 2021, p. 768758
- [5] Falone, S., Santini Jr, S., Cordone, V., Cesare, P., Bonfigli, A., Grannonico, M., Di Emidio, G., Tatone, C., Cacchio, M., Amicarelli, F. Power frequency magnetic field promotes a more malignant phenotype in neuroblastoma cells via redox-related mechanisms. *Scientific reports*, 7 (1), 2017, p. 11470.
- [6] Osera, C., Amadio, M., Falone, S., Fassina, L., Magenes, G., Amicarelli, F., Ricevuti, G., Govoni, S., Pascale, A. Pre-exposure of neuroblastoma cell line to pulsed electromagnetic field prevents H<sub>2</sub>O<sub>2</sub>-induced ROS production by increasing MnSOD activity. *Bioelectromagnetics*, 36 (3), 2015, p. 219-232.
- [7] Xu, S., Zhou, Z., Zhang, L., Yu, Z., Zhang, W., Wang, Y., Wang, X., Li, M., Chen, Y., Chen, C., He, M. Exposure to 1800 MHz radiofrequency radiation induces oxidative damage to mitochondrial DNA in primary cultured neurons. *Brain research*, 1311, 2010, p. 189-196.
- [8] Lednev, V.V. Biological effects of the extremely weak alternating magnetic fields: the identification of primary targets. *Modelling of Geophysical Processes*, 2003, p. 130-136.
- [9] Krylov, V.V., Osipova, E.A. Molecular biological effects of weak low-frequency magnetic fields: Frequency-amplitude efficiency windows and possible mechanisms. *International Journal of Molecular Sciences*, 24 (13), 2023, p. 10989.
- [10] Canseven, A.G., Coskun, S., Seyhan, N. Effects of various extremely low frequency magnetic fields on the free radical processes, natural antioxidant system and respiratory burst system activities in the heart and liver tissues. *Indian Journal of Biochemistry & Biophysisc*, 45 (5), 2008, p. 326-331.
- [11] Blackman, C.F., Benane, S.G., House, D.E. Frequency-dependent interference by magnetic fields of nerve growth factor-induced neurite outgrowth in PC-12 cells. *Bioelectromagnetics*, 16 (6), 1995, p. 387-395.
- [12] Saito, H., Ito, R., Egawa, G., Li, Z., Yoshimura, S. Direction detectable static magnetic field imaging by frequency-modulated magnetic force microscopy with an AC magnetic field driven soft magnetic tip. *Journal of Applied Physics*, 109 (7), 2011.
- [13] Patruno, A., Tabrez, S., Pesce, M., Shakil, S., Kamal, M.A., Reale, M. Effects of extremely low frequency electromagnetic field (ELF-EMF) on catalase, cytochrome P450 and nitric oxide synthase in erythro-leukemic cells. *Life sciences*, 121, 2015, p. 117-123.
- [14] Santini, S.J., Cordone, V., Falone, S., Mijit, M., Tatone, C., Amicarelli, F., Di Emidio, G. Role of mitochondria in the oxidative stress induced by electromagnetic fields: focus on reproductive systems. *Oxidative Medicine and Cellular Longevity*, 2018, p. 5076271.
- [15] Gurhan, H., Bruzon, R., Kandala, S., Greenebaum, B., Barnes, F. Effects induced by a weak static magnetic field of different intensities on HT-1080 fibrosarcoma cells. *Bioelectromagnetics*, 42 (3), 2021. p. 212-223.
- [16] Calcabrini, C., Mancini, U., De Bellis, R., Diaz, A.R., Martinelli, M., Cucchiaroni, L., Sestili, P., Stocchi, V., Potenza, L. Effect of extremely low-frequency electromagnetic fields on antioxidant activity in the human keratinocyte cell line NCTC 2544. *Biotechnology and applied biochemistry*, 64 (3), 2017, p. 415-422.
- [17] Luukkonen, J., Liimatainen, A., Juutilainen, J., Naarala, J. Induction of genomic instability, oxidative processes, and mitochondrial activity by 50 Hz magnetic fields in human SH-SY5Y neuroblastoma cells. *Mutation Research/Fundamental and Molecular Mechanisms of Mutagenesis*, 760, 2014, p. 33-41.
- [18] Yamashita, K., Saito, M. Effects of middle-level static magnetic field on metabolic activity of mitochondria. *Electrical Engineering in Japan*, 137 (1), 2001, p.36-41.
- [19] Binhi, V.N. Primary physical mechanism of the biological effects of weak magnetic fields. *Biophysics*, 61 (1), 2016, p. 170-176.



## INDUSTRIAL EMISSION IMPACT ON METAL ACCUMULATION IN PARK-SOILS USING EKOTOXICITY TESTS ASSOCIATED WITH THE SOIL ORGANIC MATTER ASSESSMENT

Oľga Šestinová<sup>a</sup>, Lenka Findoráková<sup>a</sup>, Jozef Hančulák<sup>a</sup>

<sup>a</sup> Institute of Geotechnics, Slovak Academy of Sciences, Watsonova 45, 040 01 Košice, Slovakia, sestinova@saske.sk

### Abstract

The purpose of this study was to investigate the potentially toxic effect related of elements in city park soils from Košice, using biological tests (Phytotoxicity on *Sinapis alba*, acute and avoidance tests with the *Dendrobaena veneta*). The three city parks were selected, namely soils from the city park Jazero, park Anička and park in Barca. Košice, the city in eastern Slovakia, is exposed to urban contamination sources such as municipal sphere, road traffic, and various industrial sources (TEKO, U.S.Steel). Median concentrations Fe, Mn, Cu, Zn, As, Cr, Co, Ni and Pb, physicochemical properties, granulometric distribution, bioaccumulation factor (BF) and correlation matrix of data were assessed in the park soils. Exceeded toxic element concentration limits according to law No. 220/2004 coll. were in order of As> Cu> Zn>Cr in park soils of the lake marked as 1La and 1Lb. The highest median concentrations were in the case As approximately 3.5 times; for Cu of 2.7 times; and for Zn of 1.3 times; for Cr of 1.1 more than limit value. Similarly, exceed median values of elements in park soils of the Anička 2Aa and 2Ab, were in the order of Cr > Cu > Zn. The BF was in the range 0.02-0.80 ( $p < 0.05$ ), indicating the easy translocation of Fe, Mn, Cu, Zn, As, Cr, Co, Ni, Pb into earthworms tissues from the park soils. This study also described the changes of SOM, SOC in different soil depth also before and after earthworm experiments. It was found that the soil organic matter (SOM) and soil organic carbon (SOC) stocks decreased with increasing soil depth. SOM and SOC contents were significantly higher in topsoil according than in subsoil. Using earthworm the SOM contents has doubled in some samples.

**Keywords:** park-soil, bioassay, toxic effect, potential toxic elements, organic matter

### 1 Introduction

With the rapid industrialization and urbanization during the last decades, urban environments have been experiencing serious deterioration; especially industrial emissions have significantly polluted the natural environments all the city parks. Consequently, health and wellbeing of urban residents are affected by this deteriorated environment. As a neutral attribute of urban activities, urban surface soil is the primary sink of all pollutants, including potential toxic elements (PTEs). Both natural processes, such as the weathering of rocks, and human activity, such as industrial emissions, mining, and inappropriate waste management, can release these toxic elements into the environment [1-3]. The main objective of this work was support the interpretation of the eco-toxicological data and to enhance our understanding of potential ecological risk for urban soil such as city parks in Košice. The impact of PTEs (Fe, Mn, Cu, Zn, As, Cr, Co, Ni and Pb) on human health varies depending on the particular element, its concentration, the length of exposure, and each person's vulnerability. These elements can be easily transported from site to site by several atmospheric activities, e.g., wind and runoff water. Consequently, they can accumulate on the topsoil by atmospheric deposition, according to Hančulák et al. [4]. Elements can diffuse to urbanized environments from vehicle emissions, traffic activities, industrial activities, and any other anthropogenic activities [5-6]. In recent decades, with the emergence of various chemical pollutants and their entry into the food chain, concerns about the increase in disease have increased; together with other variables has increased risk of cancers [7-8]. The soils with lower (sub-lethal) pollutant concentrations require more sensitive test methods such as behavioral tests (Avoidance behavior response) in their risk assessment. An earthworm avoidance test has potential advantages for study of evaluation of hazardous soils sites and proved as a quick approach to determining the presence of contaminants. The earthworm (*Dendrobaena veneta*) takes up and retains metals from soil containing of potential toxic elements. Earthworms are widely recognized for their ability to enhance the decomposition of organic matter and play a critical role in nutrient turnover. Earthworm species interact with each other in soils, but these interactions are poorly understood. Moreover, these key soil organisms are influenced by abiotic soil components such as organic matter [9-11]. Phytotoxkit is an alternative test procedure that enables determination of the biological effects of chemical compounds on plants. Assessment of soil phytotoxicity is based on germination and seedling growth of the terrestrial plant (mustard *Sinapis alba*) [12- 15]. The evaluation of urban soil organic matter and soil organic carbon storage

is important due to assess the urbanization impact on global carbon cycle [16-17]. Currently, the study of SOC stocks in urban soils receives little attention, yet the urban environment has a unique set of specific properties and processes (e.g. soil sealing, functional zoning, settlement history) that affect SOC stocks and their spatial variability. From this point of view it is necessary to monitor SOM and SOC content. When studying SOM and SOC in urban soils, it is essential to take into account that urban soils are created by anthropogenic activities (e.g. physical disturbance, land-use and relevant management practices), causing that the amount of SOC be substantially different from natural soils [18-20].

## 2 Material and methods

### 2.1 Soils and methods used

Samples of topsoil (0-10 cm) marked as (a), and subsoil (10-30 cm) marked as (b) were taken from 3 Košice city locations, in year 2023 (Table 1). The three city parks were selected, namely soils from the city park Jazero, park Anička and park in Barca. The samples were from the localities: 1L a, b / park soil Košice-Lake, west (heating plant TEKO), 2A – a, b / park soil Košice Anička, north (recreation area, near the former SMZ plant), 3B – a, b / park soil Košice – Barca, south (the park is a protected zone with rare trees and lake with aquatic flora and living faun; such as swans, ducks). A mixed (composite) sample of urban soils was taken from 3 sampling areas within one location from the Košice park. Mixed park soil samples were air-dried, sieved to less than 2 mm. In all samples pH was measured with a potentiometric glass electrode in H<sub>2</sub>O and KCl solution (ISO/DIS10390). For soil analyses were used control reference soil (CS-MicroBioTests, Belgium). Granulometric analysis was performed using the instrument Mastersizer 2000E laser diffraction particle size analyzer and sampling using Scirocco 2000 M dry feeder with automatic detection, measuring range -0.02-2000 µm. Total concentrations of potential toxic elements (Fe, Mn, Cu, Zn, As, Cr, Co, Ni and Pb) were determined by the X-ray fluorescence spectrometry method (SPECRO XEPO 3, range of elements Na (11)-U (92), scattering targets: Mo, Co, Al<sub>2</sub>O<sub>3</sub>, Pd, HOPG-crystal, X-ray lamp (type VF50): Pd with Be window, resolution: 15 keV on line K<sub>α</sub> Mn). For the XRF analysis the 5g of homogenized sample with 1 g of Clarinet micro powder C (CEREOX BM-0002-1) were used and then pressed under 15 t to a pellet with a 32 mm diameter. The concentrations of elements in the *D. veneta* tissue were determined after mineralization with a mixture of acids HNO<sub>3</sub>/HF/H<sub>3</sub>BO<sub>3</sub> (5:2:20) in the system (MWS33, Germany) by the atomic absorption spectrometry (AAS-Varian, Australia). C, H, N, S content was identified by an elementary analyzer Vario MACRO cube (Elementary Analyses system GmbH, Germany) using a thermal conductivity detector. A combustion tube was set up at 1150 °C and the reduction tube at 850 °C. Sulfanilamide (C=41.81 %, N=16.26 %, H=4.56 %, S=18/0.62 %) was used as the C, H, N, S standard. For estimating SOM the loss-on-ignition (LOI) method was used. For this purpose we used programmable muffle furnace (LAC, s.r.o.). The results were based on soil dry weight. The certified-reference soil Eutric Cambisols S-VM was used to validation of data. The concentration values of potential toxic elements in park soils were compared according to limit values of Slovak soils No.220/2004 coll. [21].

### 2.2 Experimental set up - phytotoxicity test

The phytotoxkit measures the decrease (or the absence) of the seed germination and growth of the roots after 3 days (at 25 °C) of seeds exposure of higher plants to contaminated matrix in comparison to the control soil. Ten seeds of each plant were positioned at the test plate on a filter paper placed on top of the soil. The analyses and the length measurements were performed using the Image Tool 3.0 for Windows. The bioassays were performed in six replicates. The percent inhibition of seed germination (ISG) and of root growth (IRG) was calculated with the equation 1,

$$\text{ISG/IRG} = (A-B/A) \times 100 \quad (1)$$

where A is the mean seed germination or root length in the control soil; and B is the mean seed germination or root length in the test soil (mm).

### 2.3 Avoidance responses test

Earthworms are regarded as “soil ecosystem engineers” and play keystone roles in soil formation and the decomposition of organic matter. As such, earthworms are widely recommended as model organisms for monitoring soil quality and assessing the ecotoxicity of pollutants because they are sensitive to soil contaminants [22]. Earthworm (*D. veneta*) avoidance tests were based on ISO 17512-1/2008 [23]. The test containers were incubated at 20±2 °C and a 16:8 h light: dark photoperiod for 48 h. The tests were run in

5 replicates. At the end of the test period the earthworms were counted in each side of the replicates. The amount of earthworms counted was converted to a percentage of avoidance based on equation 2,

$$R (\%) = ((C - T) / N) \times 100 \quad (2)$$

where R = avoidance; C = number of worms in control soil (CS); T = number of worms in each soil; N = total number of worms. Thus, positive values account for avoidance of earthworms in test soil, while neutral or negative responses represent indifference or preference of the test substance. The avoidance test with *D. veneta* has numerous advantages (short test period, comparatively lower work expense, sensitivity at least equal to that of the reproduction test) [24-25].

## 2.4 Statistical analysis

All data were analyzed using StatSoft, v.12.0 statistical software [26]. Data from 7 days acute tests and avoidance behavior response tests were analyzed using the Pearson's matrix correlation. Bioaccumulation factor (BF) were calculated according to (OECD, 2010), based on equation 3,

$$BF = ((M_{WT}) / (M_S)) \quad (3)$$

where  $M_{WT}$  = metal concentration in worm tissues;  $M_S$  = metal concentration in soil. The combination of chemical measurements with the calculation of (BF) and r-Person matrix correlations can be a useful tool in risk assessment.

## 3 Results and discussion

### 3.1 Potential toxic elements contamination and acid-base indicators

In study area according to the Reference Base for Soil Resources [27] and the Slovakia soil types [28] the soil types were established as *Anthrosols*. The values of the park soils reaction measured on the Košice city area are listed in Table 1. The research showed that the investigated soils are neutral to slightly alkaline (pH 6.9 to 8.2) – Barca, Lake and strongly alkaline (pH 7.7 to 8.9) - Anička. The park soils Košice - Anička were obtain of the near former magnesite plant (Slovak Magnesite Plant), therefore a soil reaction can move above pH 8. The obtained pH data shows that with the depth of soil sampling the soil alkalinity is increased. In the Table 1, there are the results of the median contaminant levels of used soils. Exceeded concentration limits according to law No. 220/2004 coll. of toxic elements in park soils of the Lake (1La and 1Lb) were in the following order: As>Cu>Zn>Cr. The highest median concentrations were in the case of As approximately 3.5 times; for Cu of 2.7 times; and for Zn of 1.3 times; for Cr of 1.1 more than limit value. Metal particles released during fuel combustion (heating plant TEKO) and other chemical compounds present in exhaust gases can be deposited on the soil along roads, leading to the gradual accumulation of PTE in these areas. Similarly, exceed median values of elements in park soils Anička (2Aa and 2Ab) were in the order: Cr>Cu>Zn in the case Cr of 2.0 times higher, Cu of 1.9 times, and Zn of 1.1times. The obtained data shows the wide toxic element concentration ranges with the depth of soil sampling. Road transport can significantly affect the accumulation of potential toxic elements in soil and plants, such as city parks. Traffic seems to be one of the sources of these metals also, but the influence of other factors cannot be excluded. The results of the median concentrations in the Barca park soils (3Ba, respectively 3Bb) were within the limit values, even though according to Hančulák et al. [4], the main sources of pollution in 2021 were iron and steel plants - U.S.Steel, Košice for the Barca urban district.

Table 1. Selected properties and median contaminant levels of the soils

pH/Elements Units	Limit	1L		2A		3B		CS	SS
		a	b	a	b	a	b		
pH/KCl	-	7.8	7.9	7.7	8.4	6.9	7.2	6.6	5.2
pH/H <sub>2</sub> O	-	8.1	8.2	8.3	8.9	7.7	7.9	6.5	5.7
Fe (%)	-	4.2	4.5	3.2	2.9	3.4	3.1	0.2	0.8
Mn (%)	0.3	0.2	0.2	0.1	0.1	0.1	0.1	-	-
Cu (mg/kg)	70.0	192.6	186.5	137.3	130.6	39.7	33.3	6.3	36.6
Zn (mg/kg)	140.0	179.1	165.0	158.4	138.1	141.6	110.3	7.9	102.9
As (mg/kg)	33.0	117.0	112.5	20.7	21.4	10.4	11.3	-	5.2
Cr (mg/kg)	90.0	99.8	87.9	181.5	108.0	79.3	68.8	5.3	48.3
Co (mg/kg)	20.0	15.9	13.2	15.6	21.2	22.0	17.6	-	-
Ni (mg/kg)	60.0	59.8	53.9	53.9	53.1	57.8	53.5	19.5	26.2
Pb (mg/kg)	115.0	51.2	48.9	45.3	44.5	52.4	39.0	23.0	18.6

Limit of elements - law SR 220/2004, CS-Control soil, SS-Shop soil

### 3.2 Phytotoxicity tests

The obtained results of the contact arrangement phytotoxicity (Fig. 1-2) showed that the city park soil from Anička (2Aa -52 % and 2Ab - 55 %) had more than 50 % inhibition of the seed germination and root growth in the mustard *S. alba* compared to the control soil. Soil samples in the city parks Košice Lake and Barca (1La, 1Lb and 3Ba, 3Bb) showed growth inhibition percentage and of germination inhibition less over than park soils from Anička (2Aa and 2Ab), in the range of 25 % to 38 %. The transfer of potential toxic elements within the soil-plant chain is a part of the biochemical cycling of chemical elements-it is an element flow from nonliving to the living compartments of the biosphere. There are many factors that might have an impact on this plant response. Since elements with similar physico-chemical properties may replace one another in enzymatic pathways and receptor proteins, they compete for absorption, transport, and accumulation. According to the author Fu et. al., knowledge of the ability of native wild plants to take up and transfer metals is useful in screening for potential phytoremediation [29-31].

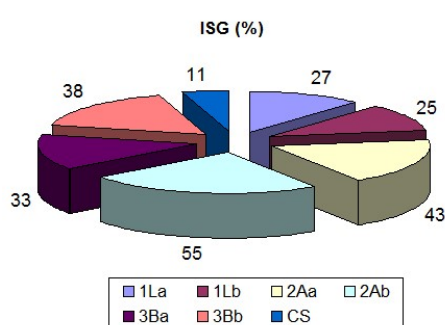


Fig. 1. Average germination indexes ISG values in city park soils, Košice

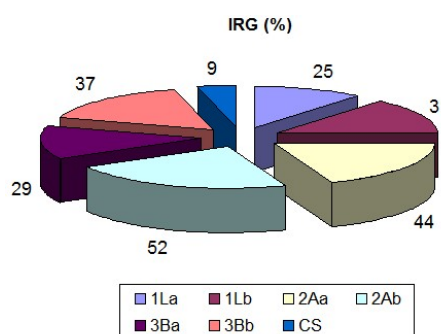


Fig. 2. Average germination indexes IRG values in city park soils, Košice

### 3.3 Acute and avoidance responses tests

Table 2 shows the potential effect of toxic elements on earthworm's mortality and correlation matrix between toxic elements and acute mortality in the 7 days tests of (*D. veneta*). Low mortality effects were recorded in the acute tests with *D. veneta*. The highest correlation coefficients among concentration of the elements and mortality after 7 days bioassays, which ranged between -0.11 and 0.55, decreased in the order As>Pb>Cu>Zn>Mn>Cr>Ni>Co>Fe for the soils - Lake (1La,b), (Table 2). In addition, Cu was significantly positive correlated between acute mortality *D. veneta* and copper concentration and ( $r=0.48$ ,  $p=0.05$ ) for the park subsoils Anička (2Ab). The above results reflect that not only earthworms may be able to detect metals, but in fact they may also change their behavioral response over time.

Table 2. Correlation matrix of the city parks soil among 7 days acute mortality tests (*D. veneta*) and toxic element concentrations

(N=25)	1La	1Lb	2Aa	2Ab	3Ba	3Bb
M/7 day	1	2	1	2	2	2
Fe	-0.21	0.20	0.45*	-0.22	-0.27	0.25
Mn	-0.29	-0.15	0.08	-0.18	0.10	0.26
Cu	0.19	0.36	0.23	0.48*	0.40	-0.46*
Zn	0.24	0.31	0.05	-0.13	0.32	0.26
As	0.55*	-0.28	0.12	0.34	0.19	0.25
Cr	-0.17	-0.26	-0.44*	0.15	0.38	-0.25
Co	-0.24	-0.22	0.16	0.11	-0.18	-0.22
Ni	0.14	0.24	0.20	0.12	0.27	-0.33
Pb	0.38	0.11	0.16	-0.09	-0.17	0.14

(M) - absolute number of dead earthworms; acute tests of mortality after 7 days bioassays

\*Correlations are significant at over 0.5 and - 0.5 levels

Bioaccumulation factor (BF) was calculated to determine the bioavailability of Fe, Mn, Cu, Zn, As, Cr, Co, Ni, Pb in earthworms tissue for city park soils after 7 days bioassays (Table 3), based on equation 3. The BF was in the range of 0.01-0.80 ( $p<0.05$ ), indicating the easy translocation of these elements into

earthworms from the park soils. Results were with statistical significance, within the treatments at  $p < 0.05$  level. The results of the Avoidance tests (A-test) and concentration of toxic elements in earthworm tissues from the park topsoils and subsoils Lake (1La,b) are in the same decreasing order  $As > Zn > Co > Cu > Ni > Pb > Cr > Fe > Mn$ . The obtained results indicate that the most accumulated elements were As, Zn, Co and Cu, which may be a consequence of the heating plant TEKO. The results for the Anička (2Aa) topsoil are  $As > Pb > Cu > Ni > Zn > Co > Cr > Fe > Mn$ , and for the Anička (2Ab) subsoils are  $As > Pb > Cu > Ni > Zn > Cr > Fe > Co > Mn$ , it means that the topsoils and subsoils from the Anička were preferred most accumulated of elements As, Pb, Cu and Ni.

Values for the Barca (3Ba) topsoil are  $Cu > As > Fe > Zn > Pb > Co > Cr > Ni > Mn$  and for the Barca (3Bb) subsoil are  $Cu > As > Zn > Fe > Pb > Co > Cr > Ni > Mn$ . The results from the Barca were observed the most bound elements Cu, As, Fe, Zn of the topsoils and subsoils, which speaks of emissions influence coming from the U.S.Steel plant, Košice (Table 3). Several factors control the processes of mobility and availability of elements; in general, they are of geochemical, climatic, biological, as well as of anthropogenic origin.

**Table 3. Bioaccumulation factors for toxic elements in earthworm tissues and park soils after 7 days bioassays**

(N=30)	1La	1Lb	2Aa	2Ab	3Ba	3Bb
Fe	0.02	0.02	0.05	0.06	0.18	0.19
Mn	0.01	0.01	0.05	0.05	0.04	0.04
Cu	0.05	0.05	0.12	0.12	0.68	0.80
Zn	0.10	0.11	0.08	0.09	0.16	0.20
As	0.25	0.26	0.32	0.31	0.29	0.27
Cr	0.02	0.02	0.05	0.08	0.04	0.05
Co	0.05	0.08	0.07	0.05	0.05	0.06
Ni	0.03	0.03	0.12	0.12	0.04	0.05
Pb	0.02	0.02	0.17	0.17	0.05	0.07

Figure 3 shows avoidance responses of *D. veneta* in city park soils, Košice. Zero mortality effects were recorded in the tests of avoidance with *D. veneta*. The percentage of avoidance response of the earthworms found in the double control was within the range -20 % to 70 % for all areas of the city park soils Košice, for after 48 h, based on equation 2. The significant ( $P < 0.05$ ) avoidance by *D. veneta* were 70 % in soils La: depth 0-10cm, and 1Lb: depth 10-30cm were 40 %, Košice-Lake, west (in near heating plant TEKO). The highest concentrations of potential toxic elements such, as Cu, Zn, As, Cr (Table 1), were recorded in these soil samples, also. The park soils in Košice showed slightly cooperatively accumulation Cr, As, Cu and Zn in avoidance behavior response, which speaks of the avoidance of the worms in studied soil for the samples 1La, b; 2Ab and 3Bb. Only topsoils are 2Aa and 3Ba have  $R = -20$  %, which means indifference or soil preference.

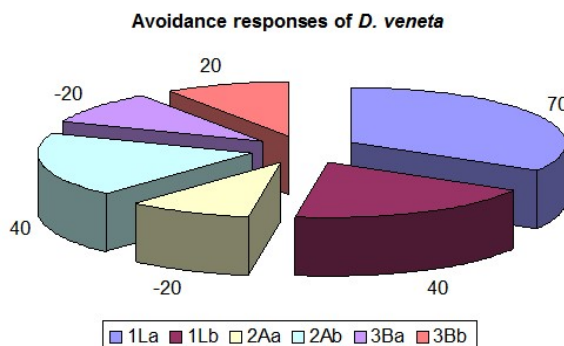


**Fig. 3. Avoidance responses of *D. veneta* in city park soils, Košice**

Metal particles released during fuel combustion (heating plant TEKO) and other chemical compounds present in exhaust gases can be deposited on the soil along roads, leading to the gradual accumulation of PTE in these areas. Several factors can influence potential toxicity PTE distribution, including natural processes,

anthropogenic activities, and soil characteristics of the local urban park. Road transport can significantly affect the accumulation of potential toxic elements in soil and plants, such as city parks. In the context of metal pollution, the resistance of vulnerable individuals and their population maintenance plays important roles in ecosystem stability, and related studies are necessary. Environmental monitoring and pollution assessment on the whole city scale are highly important to figure out the contamination level and spatial distribution of pollution. This information will be offer useful information to promote pollution control.

### 3.4 Granulometry, SOM and SOC characterization before and after earthworm experiments

Granulometric analysis performed on samples (200 μm) confirmed the following three fractions classified according to the ČSN ON 736518: sand (100-2000 μm) which represents 17.54-38.78 %, the second silt (10-100 μm), which represents 54.23-69.31 % and the third fraction clay (<2μm) which represents 4.80-13.14 %. From obtained granulometric results it is evident that the main fraction in all monitored soils is silt. Silt fraction is the same or decreases slightly with decreasing depth.

For estimating SOM the loss-on-ignition (LOI) method was used because by this method it is possible to measure organic matter and whereas usually organic carbon can be calculated using the SOM value [32]. For this purpose we used programmable muffle furnace (LE laboratory chamber furnace up to 1100 °C). Before it the 5 g of samples were heated at 105 °C for 12 h to remove soil moisture, after that they were combusted at 375 °C for 17 h. From these measurements we calculated SOM based on equation 4,

$$SOM_{LOI} = ((W_{105^{\circ}C} - W_{375^{\circ}C}) / W_{105^{\circ}C}) \times 1000 \quad (4)$$

where  $W_{105^{\circ}C}$  and  $W_{375^{\circ}C}$  are the soil weights after combustion at 105°C and 375°C, respectively.

Many works described for this purpose LOI at 550 °C [33-34], but we used LOI at 375 °C, because the ignition temperature 375 °C is ideal considering minimizing the weight loss of the structural water of clay minerals in the samples [32], and Pribyl [33] suggests that use of too low or too high temperature for LOI can be impact the results of organic carbon estimation. Also, soil organic matter should be calculated based on equation 5, created by Van Bemmelen (1890) [35]:

$$SOM (\%) = SOC (\%) \times 1.724 \quad (5)$$

According to Heaton [35], the conversion factor 1.724 usually underestimates the SOC. Conversion factor may vary based of another factors of soils, from this point of view was conversion factor change to 2 according Pribyl [33] research of soils, so the new equation 6:

$$SOM (\%) = SOC (\%) \times 2 \quad (6)$$

When the SOM is established experimentally (in our case by LOI method), so after that the SOC is possible to calculate from the following equation 7:

$$SOC (\%) = SOM (\%) / 2 \quad (7)$$

**Table 4. Elemental CHNS; SOM and SOC in (wt. %) before and after earthworm experiments**

Soil	Depth	C <sub>t</sub> *	H <sub>t</sub> *	N <sub>t</sub> *	S <sub>t</sub> *	SOM <sub>LOI</sub>	SOC <sub>calc.</sub>	SOM <sub>LOI(AE)</sub>	SOC <sub>calc.(AE)</sub>
1L <sub>a</sub>	0-10	3.34	0.56	0.33	0.04	4.07	2.04	5.22	2.61
1L <sub>b</sub>	10-30	2.80	0.55	0.30	0.03	3.45	1.73	4.13	2.07
2A <sub>a</sub>	0-10	2.68	0.66	0.32	0.04	3.33	1.67	3.69	1.85
2A <sub>b</sub>	10-30	2.14	0.68	0.33	0.05	2.31	1.16	4.93	2.47
3B <sub>a</sub>	0-10	2.86	0.89	0.34	0.03	3.54	1.77	6.03	3.02
3B <sub>b</sub>	10-30	2.00	0.75	0.29	0.03	2.83	1.42	5.27	2.64

\*t-total; exp- experimental; LOI- loss-on-ignition, calc-calculated from equation 3, 4, AE-after earthworms experiments

Differences in SOM content between studied localities are associated with pH, soil depth, vegetative cover and topographic position. SOM content before earthworms experiment were lower than SOM after earthworms experiments. These points to the fact that the presence of earthworms not only reduced the concentration of some toxic elements, but also increased the SOM content, thereby the quality of the soils was increased.

## 4 Conclusions

The identification of pollution status is an essential step for assessing the potential impact of park soil toxic elements pollution. Selecting a suitable method should be one of the most important aspects of toxic

elements evaluation. The obtained results show that the samples from Lake (1La,b) were the most contaminated, which is related to the fact that these samples were taken from the area closest to the source of contamination (TEKO heating plants). The highest contamination was indicated by the results of XRF analyses as well as ecotoxicity tests (Phytotoxicity, Acute and Avoidance responses tests with *Dendrobena veneta*), which showed a positive correlation between the studied toxic elements and earthworm mortality. *Dendrobena veneta* decrease the contamination in some samples and also increase their quality due to the increased content of SOM after *Dendrobena veneta* experiments. All techniques and methods were used mainly for park soil rapid screening. Obtained results can be used for further relevant research such as for potential phytoremediation.

### Acknowledgements

This research has been financially supported by the Slovak Grant Agency for the VEGA Project No. 2/0136/23, then by the Slovak Research and Development Agency No. 20/0140/21.

### References

- [1] Dat, N.D., Nguyen, V.T., Vo, T.D.H., Bui, X.T., Bui, M.H., Nguyen, L.S.P., Nguyen, X.C., Tran, A.T.K., Nguyen, T.T.A., Ju, Y.R., Huynh, T.M.T., Nguyen, D.H., Bui, H.N., Lin, C. Contamination, source attribution, and potential health risks of heavy metals in street dust of a metropolitan area in Southern Vietnam. *Environmental Science and Pollution Research*, 28, 2021, p. 50405-50419.
- [2] Alsbou, E.M.E., Al-Khashman, O.A. Heavy metal concentrations in roadside soil and street dust from Petra region, Jordan. *Environmental Monitoring and Assessment*, 190 (48), 2018, <https://doi.org/10.1007/s10661-017-6409-1>.
- [3] Zhou, H., Ouyang, T., Guo, Y., Peng, S., He, C., Zhu, Z. Assessment of soil heavy metal pollution and its ecological risk for city parks, vicinity of a landfill, and an industrial area within Guangzhou, South China. *Applied Sciences*, 12 (18), 2022, 9345, <https://doi.org/10.3390/app12189345>.
- [4] Hančulák, J., Šestinová, O., Findoráková, L. Characteristics and Seasonal Variations of Atmospheric Deposition of Selected Elements in the Urban and Industrial Environment of Košice (Slovakia). In IOP Conference Series: Earth and Environmental Science, 2021, vol. 906, iss. 1, art. no. 012100. ISSN 1755-1307.
- [5] Burt, R., Hernandez, L., Shaw, R., Tunstead, R., Ferguson, R., Peaslee, S. Trace element concentration and speciation in selected urban soils in New York City. *Environmental Monitoring and Assessment*, 186 (1), 2013, p. 195-215, <https://doi.org/10.1007/s10661-013-3366-1>.
- [6] Madrid, L., Díaz-Barrientos, E., Madrid, F. Distribution of Heavy Metal Contents of Urban Soils in Parks of Seville. *Chemosphere*, 49, 2021, p. 301-1308.
- [7] Li, J., Wang, G., Liu, F., Cui, L., Jiao, Y. Source apportionment and ecological-health risks assessment of heavy metals in Topsoil near a factory, central China. *Expo Health*, 13, 2021, p. 79-92, <https://doi.org/10.1007/s12403-020-00363-8>.
- [8] Radomirović, M., Čirović, Ž., Maksin, D., Bakić, T., Lukić, J., Stanović, S., Onjia, A. Ecological risk assessment of heavy metals in the soil at a former painting industry facility. *Frontiers in Environmental Science*, 8, 2020, 560415, <https://doi.org/10.3389/fenvs.2020.560415>.
- [9] Šestinová, O., Hančulák, J., Findoráková, L. Environmental risk assessment of metal-contaminated areas using different bioassays. In *Nova Biotechnologica et Chimica*, 19 (2), 2020, p. 183-191.
- [10] Petit-dit-Grézériat, L., Vallayer, M., Rault, M., Pelosi, C. *Aporrectodea caliginosa* life history traits are improved by positive earthworm interaction and organic matter addition. *European Journal of Soil Biology*, 122, 2024, 103654.
- [11] Latha, V., Basha, P.M. Avoidance response in three ecologically different earthworm species exposed to heavy metal spiked soils of Cr and Zn: A comparative study. *International Journal of Scientific & Engineering Research*, 10 (6), 2019, p. 532-538.
- [12] Zhang, W.T., You, M., Hu, Y.H. The distribution and accumulation characteristics of heavy metals in soil and plant from Huainan coalfield, China. *Environmental Progress & Sustainable Energy*, 35 (4), 2016, p. 1098–1104, doi:10.1002/ep.12336.
- [13] Phytotoxkit Seed germination and early growth microbiotest with higher plants. Standard operational procedure, Nazareth: Micro BioTests Inc. Belgium, 2004.

- [14] Šestinová, O., Findoráková, L., Hančulák, J., Szabová, Z. Ecotoxicological Tests of Metal-Contaminated soils. In IOP Conference Series: Earth and Environmental Science, 2021, vol. 906, iss. 1, art. no. 0121099. ISSN 1755-1307, <https://doi.org/10.1088/1755-1315/906/1/012099>.
- [15] Bottinelli, N., Kaupenjohann, M., Märten, M., Jouquet, P., Soucémarianadin, L., Baudin, F., Tran, T.M., Rumpel, C. Age matters: fate of soil organic matter during ageing of earthworm casts produced by the anecic earthworm *Amyntas khami*. *Soil Biology and Biochemistry*, 148, 2020, Article 107906.
- [16] Pataki, D.E., Alig, R.J., Fung, A.S., Golubiewski, N.E., Lankao, P.R. Urban ecosystems and the north American carbon cycle. *Global Change Biology*, 12 (11), 2006, p. 2092-2102, <https://doi.org/10.1111/j.1365-2486.2006.01242.x>.
- [17] Yan, Y., Kuang, W., Zhang, C., Chen, C. Impacts of impervious surface expansion on soil organic carbon a spatially explicit study. *Scientific Reports* 5 (1) 2015, 17905, <https://doi.org/10.1038/srep17905>.
- [18] Sarzhanov, D.A., Vasenev, V.I., Vasenev, I.I., Sotnikova, Y.L., Ryzhkov, O.V., Morin, T. Carbon stocks and CO<sub>2</sub> emissions of urban and natural soils in Central Chernozemic region of Russia. *Catena*, 158, 2017, p. 131-140, <https://doi.org/10.1016/j.catena.2017.06.021>.
- [19] Zhang, M., Weng, S., Gao, H., Liu, L., Li, J., Zhou, X. Urbanization degree rather than methanotrophic abundance decreases soil CH<sub>4</sub> uptake. *Geoderma*, 404, 2021a, 115368, <https://doi.org/10.1016/j.geoderma.2021.115368>.
- [20] Zhang, P., Wang, Y., Sun, H., Qi, L., Liu, H., Wang, Z. Spatial variation and distribution of soil organic carbon in an urban ecosystem from high-density sampling. *Catena*, 2021b, 204:105364. <https://doi.org/10.1016/j.catena.2021.105364>.
- [21] Law No.220/2004, Supp. 2, on the Protection and Use of Agricultural Land and on the Amendment to Act no. 245/2003 Coll. on Integrated Prevention and Control of Environmental Pollution, Slovak Republic, 2004.
- [22] Huang, C., Wang, W., Yue, S., Adeel, M., Qiao, Y. Role of biochar and *Eisenia fetida* on metal bioavailability and biochar effects on earthworm fitness. *Environmental Pollution*, 263, 2020, Article 114586.
- [23] ISO (2008) Soil quality—Avoidance test for testing the quality of soils and the toxicity of chemicals—test with earthworms (*Eisenia fetida*). ISO 17512-1, International Organization for Standardization, Geneva.
- [24] Santisteban, J. I., Mediavilla, R., López-Pamo, E., Dabrio, C. J., Zapata, M. B. R., García, Martínez-Alfraro, P. E. Loss on ignition: A qualitative or quantitative method for organic matter and carbonate mineral content in sediments? *Journal of Paleolimnology*, 32, 2004, p. 287-299, doi:10.1023/B:JOPL.0000042999.30131.5b.
- [25] Hund-Rinke, K., Achazi, R., Römbke, J., Warnecke, D. Avoidance test with *Eisenia fetida* as indicator for the habitat function of soils: Results of a laboratory comparison test. *Journal Soils and Sediments*, 3 (1), 2003, p. 7-12.
- [26] StatSoft, Inc STATISTICA, “data analysis software system”, version 12, 2013.
- [27] IUSS Working Group WRB (2015) World Reference Base for Soil Resources 2014, update 2015 International soil classification system for naming soils and creating legends for soil maps. World Soil Resources Reports No. 106. FAO, Roma IT EU, 192.
- [28] VÚPOP (2019) Pôdny portál SR. [www.podne.mapy.sk](http://www.podne.mapy.sk).
- [29] Fu, S., Wei, Ch., Xiao, Y., Li, L., Wu, D. Heavy metals uptake and transport by native wild plants: implications for phytoremediation and restoration. *Environmental Earth Science*, 78, 2019, 103.
- [30] Šestinová, O., Findoráková, L. Assessment of Eastern Slovakia sediments genotoxicity and phytotoxicity using screening tests: Chromotests and Phytotoxkit. *Fresenius Environment Bulletin*, 26, (3), 2017, p. 2454-2462.
- [31] Valerio, M.E., Garcia, J.F., Peinado, F.M. Determination of phytotoxicity of soluble elements in soils, based on a bioassay with lettuce (*Lactuca sativa L.*). *The Science of the Total Environment*, 378, 2007, p. 63-66.
- [32] Ball, D.F. Loss-on-ignition as an estimate of organic matter and organic carbon in non-calcareous soils. *Journal of Soil Science*, 15, 1964, p. 84-92.
- [33] Pribyl, D.W. A critical review of the conventional SOC to SOM conversion factor. *Geoderma*, 156, 2010, p. 75-83, doi:10.1016/j.geoderma.2010.02.003.



- [34] Heiri, O., Lotter, A. F., Lemcke, G. Loss on ignition as a method for estimating organic and carbonate content in sediments: reproducibility and comparability of results. *Journal of Paleolimnology* 25, 2001, p. 101-110.
- [35] Heaton, L., Fullen, M.A., Bhattacharyya, R. Critical analysis of the van Bemmelen conversion factor used to convert soil organic matter data to soil organic carbon data: Comparative analyses in a UK loamy sand soil. *Espaço Aberto, PPGG UFRJ*, 6 (1), 2016, p. 35-44, doi:10.36403/espacoaberto.2016.5244.



## RECOVERY OF METALS FROM MINERAL WASTE USING PHYTOREMEDIATION SUPPORTED BY COHERENT LIGHT STIMULATION

Małgorzata Śliwka<sup>a</sup>, Małgorzata Pawul<sup>a</sup>, Waldemar Kępcys<sup>a</sup>

<sup>a</sup> AGH University of Krakow, Faculty of Civil Engineering and Resource Management, [sliwka@agh.edu.pl](mailto:sliwka@agh.edu.pl)

### Abstract

The ability of plants to remediate environmental pollutants such as nutrients, organic compounds, including petroleum substances, NaCl and heavy metals, has been used in practice for the treatment of sewage, soil and chemically degraded land, and in the biological reclamation of degraded areas. Phytoextraction also enables the recovery of metals from poor ores and mineral waste (including post-flotation). The efficiency of metal recovery based on the phytoremediation process can be additionally increased by using laser stimulation of plants (coherent light stimulation) to accelerate these plants growth and increase the amount of biomass. This results in greater process efficiency. Preliminary research related to the use of laser stimulation of plants (hyperaccumulators), in terms of increasing the efficiency of the metal recovery process from mineral waste, poor ores and polluted areas (phytoremediation) will be discussed in the speech.

**Keywords:** laser stimulation, phytomining, phytoremediation, metals, mineral waste

### 1 Introduction

The ability of plants to remove pollutants from the environment is the response of these organisms to stress factors, in this case pollutants present in the environment. The process of phytoremediation can proceed by phytoextraction, phytodegradation, phytostabilization, phytovolatilization and even by phytostimulation with the participation of soil microorganisms (plants stimulate the development of microorganisms). From the point of view of the possibility of recovering metals from poor ores or mineral wastes, the phytoextraction process is the most relevant. Phytoextraction involves the accumulation of metals in plant tissues, and species with outstanding accumulation abilities are called hyperaccumulators. Hyperaccumulators accumulate metals in amounts greater than 1 % (for Mn), for elements such as Co, Cu, Pb, Ni, Zn in amounts greater than 0.1 %, and for Cd in amounts greater than 0.01 % of leaf dry weight. The group of hyperaccumulators includes about 400 plant species. Their feature is the bioconcentration factor, which should be greater than 1.

Methods to increase the accumulation capacity of plants are mainly related to genetic engineering, carrying out agrotechnical treatments (irrigation, fertilization) and using non-toxic chelating agents. It is also possible to use coherent light stimulation of plants to increase the growth of their biomass and more efficient uptake of metals from the environment.

Coherent light in the visible radiation range, emitted by low-power lasers, has a significant effect on bioenergetic processes in living organisms. The stimulation effect depends on the amount of energy delivered, the time and method of irradiation (continuous or fractionated exposure) and the type of biological material. The biostimulation effect is related to the absorption of low-energy-density coherent light by specific biologically active compounds or cellular organelles, and the result can be a change in cell metabolism [1-3]. Biostimulative effects are considered to be those in which the observed changes at the cellular level are not a response to stress, since the absorbed radiation should initiate certain processes, but must not cause tissue destruction. The characteristics of light emitted by lasers, such as its coherence and polarization, allow better penetration into the tissues. The wavelength (color of the light), which depends on the energy charge carried, is also of great importance in achieving the effect of laser biostimulation. It has been shown, among other things, that helium-neon laser light He-Ne ( $\lambda=632$  nm), with a pink color, affects cytochrome oxidase [4]. On the other hand, celadon-colored light ( $\lambda=514$  nm) emitted by the argon laser influences the synthesis of nucleic acids (DNA), and thus stimulates plant cell division processes [5]. The effect of biostimulation depends on the parameters of irradiation and the physicochemical state of the cell. Light, depending on the length of the equivalent wavelength, is absorbed by a specific photoreceptor. The choice of energy dose should depend on the type of tissue (thickness of layers and sensitivity), and the duration of irradiation and type of exposure (continuous or intermittent) should be selected so that the minimum dose initiating energy processes can be delivered. Also important are the cell's oxidation-reduction

potential, ATP/ADP and ATP/NADP ratios, and physicochemical parameters such as pH, temperature and external substrate supply [6].

The first work related to the practical application of laser biostimulation in agriculture was conducted by Injuszin in the 1960s. Research conducted by his team in Kazakhstan showed the possibility of increasing the yield of some cereal and vegetable species as a result of their pre-sowing irradiation with a helium-neon laser. Stimulation also had the effect of accelerating germination and increasing the plants' resistance to unfavorable environmental factors, making it possible in practice to move the crop border and increase crop yields by about 20 % compared to unexposed plants [1, 7]. Further studies have shown that the effect of biostimulation is greater in vegetable plants than in cereal plants. Experiments related to the agricultural application of laser biostimulation are being carried out in many research centers, especially with a view to increasing the germination and emergence of plants.

The ecological application of laser biotechnology, to optimize the natural processes that occur in the environment was proposed by Dobrowolski [8, 9]. An experiment conducted on crops grown in industrially polluted areas, found an increase in yields of potatoes (more than doubled) and flax. There was also a several-fold increase in the iron content of irradiated potato tubers and a reduction in the content of lead (0.95 mg/kg in the control group; 0.50 mg/kg in the experimental group) and copper (4.05 mg/kg in the control group; 3.65 mg/kg in the experimental group) [10]. In contrast, flax seed showed an increase in zinc content in plants exposed with the control group (469.2 mg/kg : 97.0 mg/kg). In experiments conducted on the grounds of ZGH Boleslaw in Bukowno and Chelm Cement Plant, the effect of laser stimulation on changes in the content of various elements in *Salix viminalis*, *Salix acutifolia* and *Salix* cv. Rapp was shown to depend on the parameters of irradiation of the cuttings [5]. Further experiments conducted on willow cuttings (different varieties) showed acceleration of rhizogenesis, shoot growth, resistance to unfavorable environmental factors, including chemical pollution of soils [11]. Experiments conducted on various plant species that can be used to form green belts along traffic routes showed the possibility of accelerating plant growth, increasing the assimilative area of plants, increasing their resistance to pollution, and differences in the accumulation of elements in plants with different stimulation parameters. The willow plant *Salix viminalis*, after exposure of cuttings to argon laser (514 nm), showed a tendency to significantly increase bioaccumulation of some elements. The accumulation of Cu, Cr, Mn and Fe in the biomass of the plants increased by an average of twofold, while Zn and Pb increased by about 50 % compared to unexposed plants [12]. Promising results were obtained after irradiation of different plant species used in phytoremediation treatments. Coherent light exposure of plants such as *Salix viminalis* [13] and *Phragmites australis* and *Lemna minor* resulted in stronger stimulation of their growth, biomass increase and, consequently, uptake of biogenes and other elements [14-16].

## 2 Material and methods

In the preliminary experiment, two species of hydrophytes were used as metal-accumulating plants - Duckweed (*Lemna minor*) and Yellow Iris (*Iris pseudoacorus*). Selected species of plants are used in hydrophytic wastewater treatment plants for removal of nutrients (N, P). The main objective of the experiments was to evaluate the possibility of increasing the uptake of nutrients from wastewater by plants exposed to laser stimulation. In addition, the plant material was analyzed for the content of selected metals in the biomass.

Plants were planted under field conditions in identical ponds prepared for this purpose for three growing seasons. The ponds were filled with an equal volume of municipal wastewater after mechanical and biological treatment (from the Kraków Płaszów treatment plant).

A laser diode emitting light with a wavelength corresponding to pink color ( $\lambda=660\text{nm}$ ) with a power of 21.9 mW, (energy density  $2\text{W}/\text{m}^2$ ) (DLS) and an Ar argon laser type ILA -120 made by Carl Zeiss Jena, emitting light with a wavelength corresponding to celadon color ( $\lambda=514\text{nm}$ ) with a power of 21mW, (energy density  $4\text{W}/\text{m}^2$ ) (Ar) were used as coherent light sources.

Plants were irradiated from a distance of 20 cm, with the radiation beam incident perpendicularly on the material. The optimal irradiation parameters were selected individually for each species (preliminary experiments). Plants were irradiated as follows:

- Duckweed (*Lemna minor*), whole plants: DLS 3x3 s.,  $\lambda=660\text{ nm}$ ; laser Ar 3x3 s.,  $\lambda=514\text{ nm}$
- Yellow iris (*Iris pseudoacorus*), rhizomes: DLS 3x30 s.,  $\lambda=660\text{ nm}$ ; Ar laser 3x30 s.,  $\lambda=514\text{ nm}$

Chemical analysis of the plant material, in terms of changes in the degree of accumulation of elements in the control and experimental groups, was carried out by ICP-MS mass spectrometry and ASA atomic absorption spectrometry.

At the end of each of the three growing seasons, the content of heavy metals zinc (Zn), nickel (Ni), cadmium (Cd), lead (Pb) and the biogenic elements nitrogen (N) and phosphorus (P) in plant biomass was measured.

A kit consisting of a Nikon Eclipse e6000 microscope with a module for visualization and processing of microscope images, a Nikon DXM 1200 digital camera, a Nikon Coolpix 995 digital camera and Aphelion image analysis software, version 3.0, was used to measure biomass growth.

### 3 Results and discussion

During the experiment, in the case of *Lemna minor*, significant differences were observed in the condition of plants exposed to coherent light and in the control object (Fig.1).

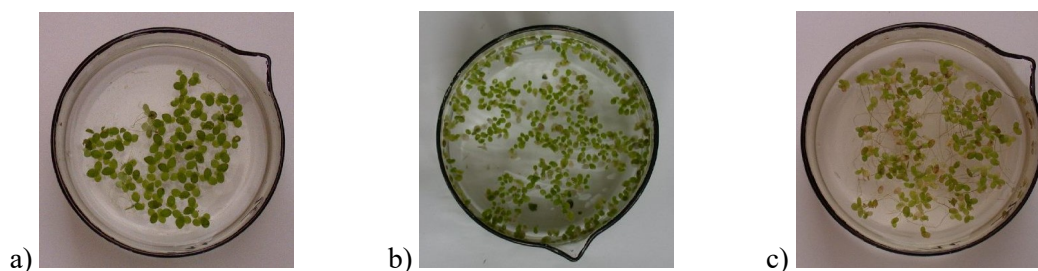


**Fig. 1. Comparison of *Lemna minor* condition from different experimental groups**

a) Plants irradiated with argon laser (514 nm), b) Plants irradiated with laser diode (670 nm), c) Plants from control group (Photo: M. Śliwka)

Plants irradiated with the argon laser had a larger leaf area, and no discoloration was observed on the leaf surface. The largest biomass increase was observed for plants irradiated with a 660 nm laser diode (Fig. 2).

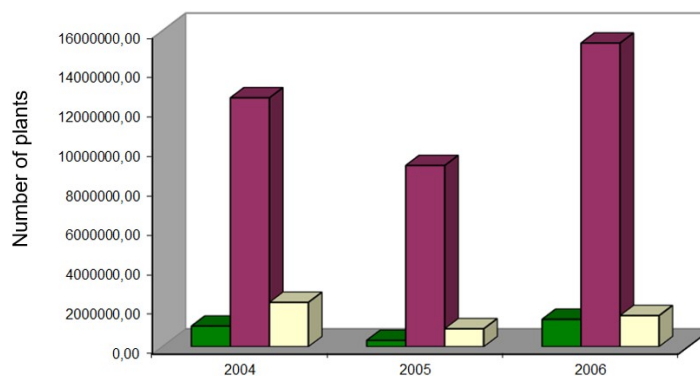


**Fig. 2. Increase in biomass of duckweed in ponds in successive years of the experiment (2004-2006)**

(green - argon laser, pink - laser diode, yellow - control group) [11, 15]

Based on the chemical analysis of the plant material, there was a twice-increased content of nitrogen and phosphorus in the biomass of duckweed after it was irradiated with an argon laser compared to the control group. The group irradiated with a laser diode ( $\lambda=660\text{nm}$ ), also showed a higher content of these elements in the biomass, compared to the unexposed group of plants. In the case of yellow iris, no such differences in nutrient element content were found in the biomass of the leaves.

Differences in the ability to take up nutrients from wastewater, may be due to the peculiarities of the two species of selected hydrophytes. Duckweed is characterized by an increased ability to accumulate nutrients compared to other hydrophytes, per unit of dry mass (luxury consumption).

Due to the content of metals such as lead, nickel, cadmium and zinc in domestic wastewater, as well as their adverse effects on living organisms and ecosystems, the content of these elements in the biomass of experimental plants was determined. The highest contents of Zn, Cd and Ni, in successive vegetation seasons, were found in the duckweed control group and in the biomass of yellow iris, also from the unexposed group. Elevated Pb content was obtained in the biomass of the duckweed in the argon laser-stimulated plant group and in the yellow iris biomass from control group (Fig. 3, Fig. 4).

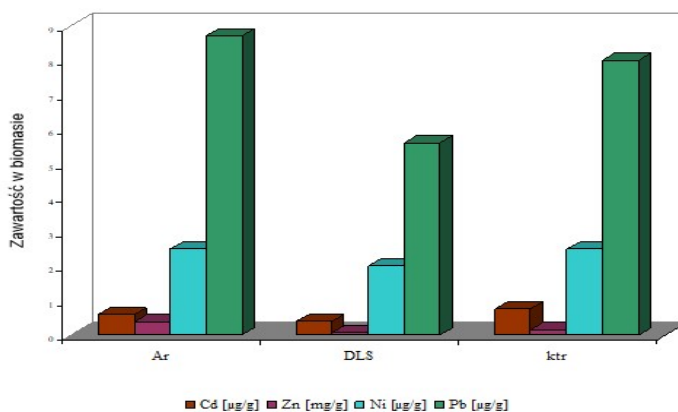


**Fig. 3. Comparison of Zn, Ni, Cd and Pb content in biomass of *Lemna minor* in different experimental groups at the end of the third growing season**

(ktr - control group, Ar - argon laser irradiated group  $\lambda=514$  nm, DLS laser diode irradiated group  $\lambda=660$  nm) [15, 16]

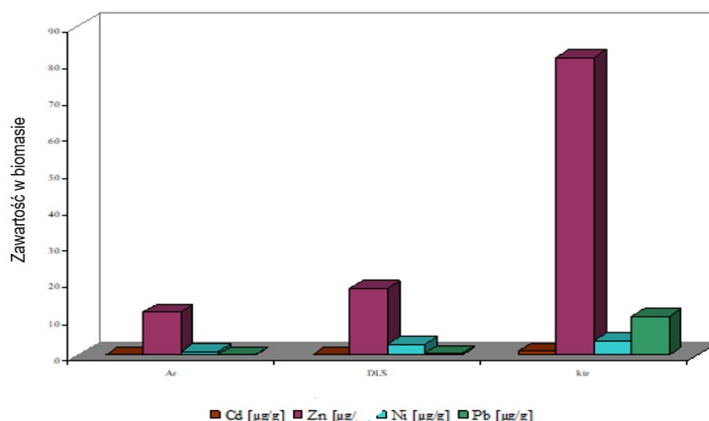


**Fig. 4. Comparison of the metal content in the biomass of *Iris pseudoacorus* in different experimental groups during the last growing season**

(ktr - control group, Ar - argon laser irradiated group  $\lambda=514$  nm, DLS laser diode irradiated group  $\lambda=660$  nm) [15, 16]

Because hydrobotanical treatment plants are mainly used to treat domestic wastewater, it is advisable to select the parameters of laser stimulation in such a way as to reduce the accumulation of metals in the biomass of plants, thereby reducing the possibility of phytotoxic effects. The decrease in the ability to phytoremediate metals may be particularly applicable to crops in highly contaminated areas.

The parameters of laser stimulation of the experimented plants were optimized to increase their biomass growth, which also redirects to the uptake of nutrients. Analysis of metal content in the biomass was an additional observation. The observed effect of laser stimulation on the degree of heavy metal accumulation in the biomass of plants therefore provides a basis for the development of its optimal parameters, in terms of increasing phytoaccumulation.

#### 4 Conclusions

The results obtained allow us to formulate the conclusion that it is possible to experimentally optimize the parameters of laser stimulation of hydrophytes, in order to increase their bioremediation capacity.

Studies on the effect of coherent light on different plant species, show that laser biostimulation is non-specific, stimulation parameters should be selected individually for each plant species. Appropriate selection of such parameters as wavelength (radiation energy), energy density, as well as the time and method of exposure (type of exposure), can contribute to increased germination strength, faster growth and increased yield of stoned plants, as well as increased resistance to stress factors, such as environmental pollution and low temperature.

An additional effect is also the effect of stimulation on the bioaccumulation of elements in plant tissues, this is particularly promising for the possibility of increasing the effectiveness of environmental cleanup treatments based on the phenomenon of phytoremediation, or in the biological reclamation of degraded areas.

## References

- [1] Injuszyn, V.T. *Laser technology in the service of agriculture*. New Agriculture. Warsaw, 1977. p. 21-26.
- [2] Bryszewska, M., Leyko, W. *Biophysics for biologists*. PWN Scientific Publishers, Warsaw, 1997.
- [3] Dobrowolski, J.W., Rózanowski, B., Zielińska-Loek, A. *Application of laser biostimulation in environmental biotechnology*. Biotechnologia Środowiskowa. Wrocław, 1999, p. 313-320.
- [4] Injuszyn, W.T., Rapen, A.C., Kremer, Ł. *Problemy bioenergetyki organizmu i stymulacja lazernym izlucieniem*. Alma-Ata, 1976.
- [5] Dobrowolski, J.W., Rózanowski, B. Influence of low-energy laser irradiation on rabbit and human lymphocytes in vitro, biological effects of low-energy laser irradiation. Biomedical Optics Conference. San Jose. USA, 1995.
- [6] Warnke, U. *Influence of light on cell respiration*. Electromagnetic Bioinformation. Urban und Schwarzenberg. Munchen, 1989.
- [7] Injuszyn, W.T., Iliasow, T.U., Fiedorowa, N.N. *Łuć laziera i urażaj*. Alma-Ata, 1981.
- [8] Dobrowolski, J.W. Pro-ecological biotechnology as a key to environmental upgrading. *Environmental Engineering*, 6, Krakow, 2001.
- [9] Dobrowolski, J.W. *Application of laser biostimulation in eco-engineering and eco-development, Engineering for eco-development. Ecological Engineering*, 6, Warsaw, 2002, p. 194-196.
- [10] Dobrowolski, J. W., Wąchalewski, T., Smyk, B., Rózycki, E., Barabasz, W. Experiments on the influence of laser light on some biological elements of natural environment. *Environmental Management and Health*, 8 (4), 1996, p. 136-141.
- [11] Jakubiak, M., Śliwka, M. The Application of Laser Biostimulation for more Efficient Phytoremediation of Soil and Waste Water. *Polish Journal of Environmental Studies*, 15 (5c), 2006, p. 176-178.
- [12] Dobrowolski, J.W., Zielinska-Loek, A. *The laser photostimulation of willow cuttings planted alongside main roads and change of concentration of elements in the willow's organs*. Mengen und Spurenelemente. Friedrich-Schiller-Universitat, Leipzig, 21, 2002, p. 334-340.
- [13] Dobrowolski, J.W., Rożanowski, B. *The influence of laser light on accumulation of selected macro-trace and ultra elements by some plants*. Menege und Spurenelemente. Friedrich-Schiller-Universitat, Jena, 1998, p.147-156.
- [14] Dobrowolski, J.W., Rożanowski, B., Zielinska-Loek, A., Śliwka, M., et al. Perspectives of application of laser biostimulation for more bioremediation of soil and wastewater. Int. Conference on Bioremediation of Soil and Groundwater. Politechnika Slaska, Krakow, 2004, p. 133-148.
- [15] Śliwka, M. The application of laser biostimulation of duckweed (*Lemna minor*) for the purification of sewage treatment process. *Polish Journal of Environmental Studies*, 13, 2004, p. 55-59.
- [16] Jakubiak, M., Śliwka, M. Innovative methods of wastewater management and reclamation of degraded lands. *Polish Journal of Environmental Studies*, 17, (3A), 2008, p. 245-248.





## GEOCHEMICAL FRACTIONATION OF ARSENIC AND ANTIMONY IN CO-CONTAMINATED SOILS IN A FORMER MINING AREA IN PEZINOK, SLOVAKIA

Veronika Špirová<sup>a</sup>, Tomáš Faragó<sup>a</sup>, Peter Hlaváč<sup>a</sup>, Martina Vítková<sup>b</sup>, Szimona Zarzsevszkij<sup>b</sup>,  
Eubomír Jurkovič<sup>a</sup>

<sup>a</sup> Comenius University in Bratislava, Faculty of Natural Sciences, Department of Geochemistry,  
Ilkovičova 6, 842 15 Bratislava, Slovak Republic, veronika.spirova@uniba.sk

<sup>b</sup> Czech University of Life Sciences Prague, Faculty of Environmental Sciences, Department of Environmental  
Geosciences, Kamýcká 129, 165 00 Praha - Suchbátka, Czech Republic

### Abstract

Arsenic (As) and antimony (Sb) are commonly occurring metalloids in the soils of mining sites and industrial areas all around the world. Metalloids bind to mineral and organic fractions present in soils through various mechanisms that influence their geochemical lability. The knowledge about geochemical fractionation of As and Sb is therefore crucial in the process of environmental and health risks assessment. In this study, a sequential extraction procedure tailored specifically for metalloids was used to identify individual fractions of As and Sb in soils. The results of the extraction experiments showed that the average proportion of As bound to individual fractions decreased in the order: fraction bound to amorphous Fe and Al oxyhydroxides (AFO) > specifically bound fraction > residual fraction > fraction bound to crystallized Fe and Al oxyhydroxides (CFO) > non-specifically bound fraction. Relatively different behavior was observed in the case of Sb, where the average proportion of Sb bound to individual fractions decreased in the order: residual fraction > AFO ≈ CFO >> non-specifically bound fraction ≈ specifically bound fraction. The results showed a rather small amount of the non-specifically bound and thus the most mobile and bioaccessible fraction of As (on average 0.9 % of the total content (7.45 mg.kg<sup>-1</sup>)) and Sb (on average 0.8 % of the total content (5.43 mg.kg<sup>-1</sup>)) in soils. However, changes in environmental and geochemical conditions, as well as the influence of anthropogenic activities in the future, may lead to the release of even more stable forms of As and Sb into the environment.

**Keywords:** metalloids, sequential extraction, mobility, bioaccessibility

### 1 Introduction

Trace elements, including metalloids As and Sb, are the key pollutants of environmental compartments in areas with active or former mining activities. The main sources of contamination are mining and smelting waste deposits and mine drainage. Deposited waste material is subjected to erosion and weathering processes, which release these pollutants into the surrounding area. Composition of soils, sediments and tailings, meteorological and climate conditions, natural processes and anthropogenic activities as well as metalloids properties have a significant influence on their behavior in environment [1, 2]. Effective immobilization of both metalloids was noticed in solid matrices naturally rich in soil organic matter, organo-mineral complexes and iron oxyhydroxides, such as goethite, hematite, ferrihydrite, tripuhyite or magnetite [3-8]. Trace elements are bound to or released from soils by the means of various mechanisms, such as adsorption/desorption, precipitation/dissolution, complexation or redox reactions that have a significant impact on their geochemical stability and thus mobility and bioaccessibility [4]. In co-contaminated soils, Sb is usually less mobile than As due to the stronger binding of Sb to solid particles and a tendency of As to be effectively replaced by phosphate in the soil sorption complex [4, 9]. However, opposite behaviour of Sb was reported by Almås et al. [10] who noticed effective but only temporary bonding of Sb to iron-based particles due to the high geochemical lability of Sb. Moreover, Hockmann et al. [11] consider Sb prone to mobilization in redox-variable environments and Dousova et al. [5] noticed higher mobility of Sb as a result of more selective adsorption and slower reaction rate with lower binding energy of Sb when compared to As. Depending on the oxidation-reduction conditions, As and Sb occur in the solutions most often in the form of oxyanions with an oxidation state of 3+ (antimonite, arsenite) or 5+ (antimonate, arsenate) [5, 12]. The sorption behavior of oxyanionic metalloids is different from the behavior of cationic metals [4, 13]. Determination of total concentration of metal(loid)s in solid matrices does not provide information about their mobility. Several single and sequential extraction procedures (SEPs) were developed in order to evaluate the geochemical fractionation and lability of metal(loid)s in soils. Conventional extraction procedures according to Tessier et al. [14], European Community Bureau of Reference (BCR)

three-step sequential extraction procedure, toxicity characteristic leaching procedure (TCLP) [15] and their various modifications are primarily suitable for cationic metals. However, these SEPs were also applied to oxyanionic metalloids As and Sb [1, 16]. Wenzel et al. [17] do not recommend using SEPs designed for cationic metals for anionic pollutants but developed SEP tailored specifically for oxyanionic metalloids instead. Sequential extraction procedure according to Wenzel et al. [17] distinguishes 5 geochemical fractions of oxyanionic metalloids: (1) non-specifically bound fraction, (2) specifically bound fraction, (3) fraction bound to amorphous and poorly-crystallized iron (Fe) and aluminum (Al) hydrous oxides, (4) fraction bound to well-crystallized Fe and Al hydrous oxides and (5) residual fraction. Although, SEP according to Wenzel et al. [17] was primarily developed for As, the applicability of the procedure to Sb has been tested and verified by several authors [1, 2, 18, 19]. The first fraction represents relatively easily exchangeable and the most mobile and bioaccessible phase of metalloids, while the highest geochemical stability is assigned to the residual fraction.

In this study, geochemical fractionation of As and Sb in highly co-contaminated soils and tailing material was investigated applying the first four steps of the SEP [17] in order to assess the potential of metalloids to migrate from soils into other environmental compartments.

## 2 Material and methods

### 2.1 Site description

The investigated area is an abandoned mining site located in the south-west of Slovakia in the Malé Karpaty Mts. near the town of Pezinok. The environment at the site and surrounding areas is polluted with As and Sb due to the pyrite-pyrrhotite and Sb ores exploitation and processing which took place from 1790s until 1991. Tailings as the solid residue of ore processing and mine drainage flowing out from adits are the two main and continuous sources of pollution at the site. The area has not been remediated yet but vegetation was able to grow over the slopes of the tailings and on the surrounding soil.

### 2.2 Soil and tailing sampling and processing

Three composite samples from the depth 0-30 cm were collected. Two samples were forest soils (PK-1 and PK-3) and one sample was sampled from the slope of the tailing deposit (PK-2). Soil sample PK-1 was collected approximately 20 m from the foot of the tailing deposit, being influenced by the mine water drainage from Budúcnosť adit and partially by the run-off from the tailings. Sample PK-2 was collected from the slope of the tailing deposit and was highly oxidized and weathered. Soil sample PK-3 was collected from the area right under the tailing and therefore highly influenced by the run-off from the deposit. Samples were air-dried, homogenized and sieved ( $\varnothing$  2 mm). Basic soil and tailing properties were determined as follows: total organic carbon content (TOC) was determined according to the Ľurin in Nikitin modification; pH and electrical conductivity (EC) were measured in 1:2.5 soil-to-solution (demineralized water or  $0.01 \text{ mol.L}^{-1} \text{ CaCl}_2$ ) ratio; water holding capacity (WHC) was determined according to Dugan et al. [20] and soil texture was determined by the hydrometer method. Bulk chemical concentrations of metal(loid)s and major elements in solid matrices were determined in a mixture of concentrated  $\text{HNO}_3$ ,  $\text{HCl}$  and  $\text{HF}$  assisted by microwave total digestion [21]. Inductively coupled plasma optical emission spectrometer (ICP OES; Thermo Scientific iCAP 7000) or inductively coupled plasma mass spectrometer (ICP MS; Thermo Scientific iCAP Q) were used to measure dissolved concentrations of metal(loid)s and major elements in all solutions.

### 2.3 Sequential extraction procedure

The first four extraction steps according to Wenzel et al. [17] were carried out as follows: samples in triplicates (1 g) were weighed in 50 ml PP centrifugation tubes and 25 ml of extraction reagents were added sequentially (Table 1). After each extraction step the liquid phase was separated from the solid phase by centrifugation for 15 min at  $1700 \times g$  and decanted. In order to prevent re-sorption/precipitation of metalloids and carry over in the next extraction steps, the solution entrapped in the remaining sample was collected in subsequent wash steps and combined with the corresponding extract. Solutions were filtered through 0.45 mm PES syringe filter into PP tubes and stored in a freezer ( $-20 \text{ }^\circ\text{C}$ ) until analyzed by ICP-OES/MS. The residue after the 4<sup>th</sup> extraction step was not extracted as described by the SEP. The residual fractions of As and Sb were calculated from the total dissolved concentrations of metalloids in soils.

**Table 1. Individual steps of the SEP**

Step	Extraction reagent	Extraction conditions	Wash step
1	(NH <sub>4</sub> ) <sub>2</sub> SO <sub>4</sub> (0.05 mol.L <sup>-1</sup> )	25 ml; 4 hours shaking (20 °C)	None
2	(NH <sub>4</sub> )H <sub>2</sub> PO <sub>4</sub> (0.05 mol.L <sup>-1</sup> )	25 ml; 16 hours shaking (20 °C)	None
3	NH <sub>4</sub> -oxalate buffer + oxalic acid (pH 3.25) (= 0.2 mol.L <sup>-1</sup> Di-ammonium oxalate-monohydrate + oxalic acid dihydrate addition to adjust pH)	25 ml; 4 hours shaking in the dark (20 °C)	12.5 ml of NH <sub>4</sub> -oxalate buffer + oxalic acid (pH 3.25); 10 minutes shaking in the dark, 20 °C
4	NH <sub>4</sub> -oxalate buffer + ascorbic acid (pH 3.25) (= 0.2 mol.L <sup>-1</sup> Di-ammonium oxalate-monohydrate + ascorbic acid addition to adjust pH)	25 ml; 30 minutes shaking in a water bath at 96 ± 3 °C in the light	12.5 ml of NH <sub>4</sub> -oxalate buffer + oxalic acid (pH 3.25); 10 minutes shaking in the dark, 20 °C

### 3 Results and discussion

#### 3.1 Characteristics of bulk soils and tailing material

Basic soil properties and total dissolved concentrations of As, Fe, S and Sb are listed in Table 2. Forest soils PK-1 and PK-3 have slightly acidic pH, while much lower soil reaction of tailings PK-2 is probably caused by the production of H<sub>2</sub>SO<sub>4</sub> solution due to the oxidation and weathering of sulfidic minerals occurring in the material [22]. The tailing material PK-2 was characterized by sandy texture, relatively low TOC content and thus the lowest WHC. On the other hand, very high WHC of the forest soil PK-3 could be attributed to the high content of decomposing organic matter, such as fragments of leaves and branches. The forest soil PK-1 has been constantly influenced by mine water drainage as well as by high groundwater level that resulted in the formation of a gleyic fluvisol with higher content of clays. The total concentration of investigated elements was extremely high in all three samples. The highest contents of As, Fe, S and Sb were found in the tailing material PK-2 and were associated with primary minerals (pyrite, pyrrhotite, arsenopyrite, berthierite, gudmundite), secondary and tertiary minerals (goethite, tripuhyite and ferrihydrite) [6, 7, 23].

**Table 2. Basic soil and tailing properties and bulk concentrations of selected elements**

Sample	PK-1 forest soil	PK-2 tailing material	PK-3 forests soil
pH (H <sub>2</sub> O)	6.7	3.41	6.54
pH (CaCl <sub>2</sub> )	5.93	3.3	6.01
EC (H <sub>2</sub> O) (μS.cm <sup>-1</sup> )	161	2,360	265
EC(CaCl <sub>2</sub> ) (μS.cm <sup>-1</sup> )	1,963	3,710	2,070
TOC (%)	5.7	1.29	5.27
Sand (%)	47	76	69
Silt (%)	38	16	23
Clay (%)	15	8	9
WHC (%)	86	49	136
As (mg.kg <sup>-1</sup> )	1,328	14,397	1,558
Fe (mg.kg <sup>-1</sup> )	27,091	91,363	27,045
S (mg.kg <sup>-1</sup> )	841	16,084	926
Sb (mg.kg <sup>-1</sup> )	1,140	15,066	1,328

#### 3.2 Geochemical fractionation of As and Sb in soils and tailing material

The average extracted amounts of As and Sb in % and in mg.kg<sup>-1</sup> in individual extraction steps are shown in Figure 1. Based on the results, the sorption behavior of As and Sb in the studied soils and tailing material varied significantly. Differences in sorption behavior of metalloids could be explained mostly by pH and redox dependent sorption and different structural ordering of As and Sb oxyanions and thus differences in affinity for sorption sites [5].

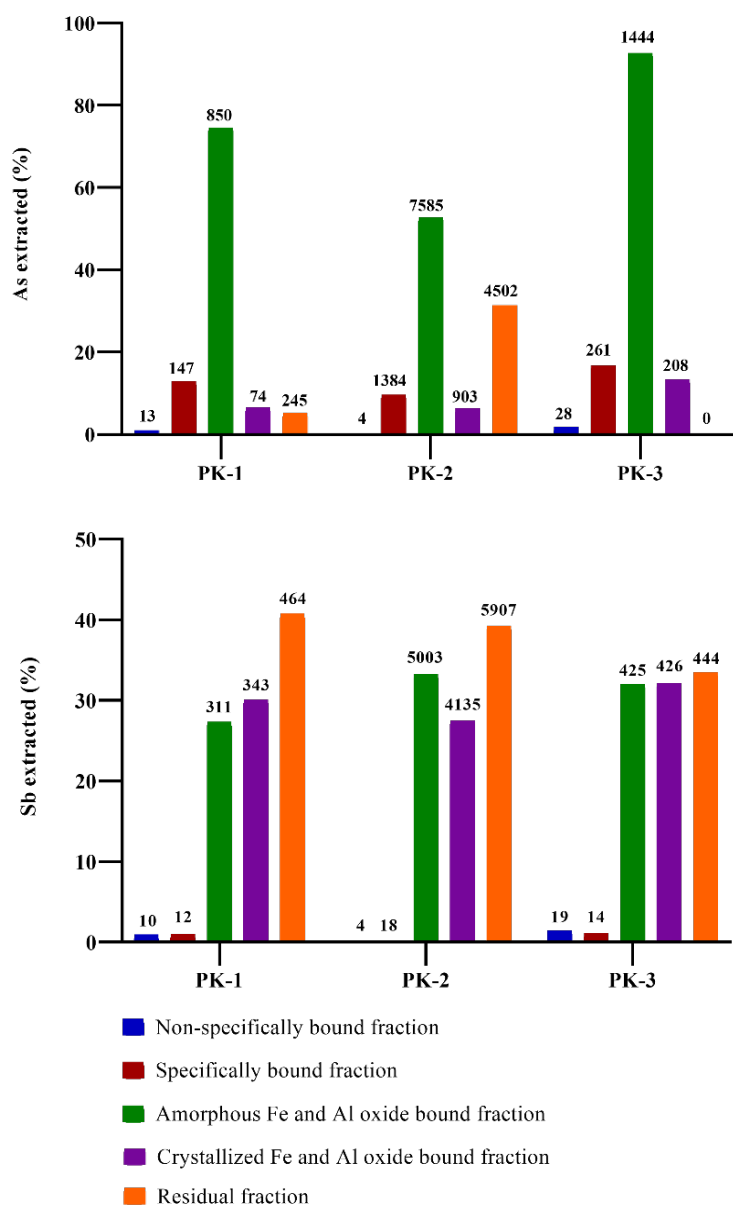


**Fig. 1. Average extracted fractions of metalloids from the total concentrations in soils and tailing material**  
 Values above the columns represent the average concentration of As and Sb in extracts in  $\text{mg.kg}^{-1}$

### 3.2.1 Non-specifically bound fraction

The results (Figure 1) showed very low concentrations of both metalloids in the non-specifically bound fraction that represents the most mobile and easily exchangeable forms of As and Sb. The non-specifically sorbed As and Sb constituted of 0.03-1.8 % and 0.02-1.4 % of the total concentrations, respectively. Non-specific sorption is reversible and is characterized by weak physical bonding such as electrostatic coulombic interactions and formation of outer-sphere complexes [13, 17]. Sulphate anions tend to sorb onto the surfaces of variable charge minerals, forming primarily outer-sphere complexes and thus displace As and Sb anions from their sorption sites [1, 4]. Low extracted concentrations of As and Sb in forest soils PK-1 and PK-3 could be attributed to the decreased ability of sulphate to compete for sorption sites with arsenate and antimonate as the soil pH increases [9]. Jain and Loeppert [24] noticed strong inhibition of arsenite sorption on ferrihydrite at acidic pH by sulphate. The tailing material PK-2 has acidic pH and is rich in iron oxides including ferrihydrite, but concentrations of extracted As and Sb by the sulphate solution were negligible indicating that both metalloids are retained by soil components mostly in a different manner. Low concentrations of As and Sb in non-specifically bound fractions were reported also in other works [1, 2, 3, 18].

### 3.2.2 Specifically bound fraction

Specific sorption is characterized by the formation of stronger chemical bonds with a covalent character and inner-sphere complexes. It is more selective and less reversible than non-specific sorption [4]. The solution of  $(\text{NH}_4)\text{H}_2\text{PO}_4$  was able to extract slightly higher concentrations of As than the solution of  $(\text{NH}_4)_2\text{SO}_4$  in the previous extraction step. This might be explained by the similar tetrahedral structure of arsenate and phosphate and their competitive behavior for the same sorption sites on mineral surfaces as explained by Violante [9]. Wenzel et al. [17] suggested that phosphate was effectively extracting varied proportions of the inner-sphere surface complexes of As. Violante et al. [25] found that arsenate was effectively desorbed by phosphate from ferrihydrite that is a common mineral phase occurring also in soils and tailings at Pezinok site [6]. The proportion of specifically bound As (10-17 %) was higher than the proportion of Sb (0.12-1%), which is consistent with other studies [1, 18]. Antimonate has different molecular structure and smaller charge density than arsenate and phosphate and was therefore attracted by different sorption sites [5].

### 3.2.3 Fraction bound to AFO

The largest fraction of As (52-92 %) was associated with AFO while significantly lower concentrations were noticed for Sb (27-33 %). Amorphous and poorly crystallized Fe oxides (ochres) in form of rims and grains on primary minerals are considered very effective sorbents of both metalloids. The enrichment of ochres by As and Sb varies with the type of mineral phase occurring in the environment. Majzlan et al. [6, 7] previously reported that in Pezinok, ferrihydrite is the main constituent of ochres and an effective scavenger of As, while Sb dominates in poorly-crystallized tripuyite. High quantity of ferrihydrite at the investigated site and rare occurrence of tripuyite could explain different amounts of As and Sb in oxalate extracts. Several authors reported that As, in general, has a greater tendency to bind to metal oxides in comparison to Sb [5, 18]. Garau et al. [26] observed lower Sb affinity towards ferrihydrite at pH 6 and 7, while sorption of As was less pH dependent.

### 3.2.4 Fraction bound to CFO

Well-crystallized Fe/Al oxides such as goethite or hematite retained significantly lower amounts of As (6-13 %) when compared with As associated with the AFO fraction (52-92 %). The proportion of Sb sorbed by CFO ranged from 27 to 32 % and was similar to the proportion of Sb retained by the AFO phase. Most of the crystallized Fe oxides are formed during the transformation or ageing of amorphous ferrihydrite [27]. As a result of such transformation process, As can be desorbed from the sorption sites and thus mobilized [7]. On the other hand, during the transformation process, Sb can be incorporated into the structure of certain CFOs [27]. Since the fraction of As bound to CFO was relatively low, it can be expected that minerals such as goethite or hematite are not dominant phases in the studied soils and tailing material.

### 3.2.5 Residual fraction

Amounts of As and Sb associated with the residual fraction were in the ranges of 0-31 % and 33-40 %, respectively. The highest content of Sb in residual fraction might be explained by the affinity of Sb towards soil organic matter and sulfides [18]. The fraction of As and Sb associated with soil organic matter and sulfides was not targeted by the used SEP. High content of TOC in forest soils (PK-1 and PK-3) and very high content of S in the tailing material (PK-2) could explain the highest concentrations of Sb associated with residual fraction. Significant association of Sb with soil organic matter and sulfur was reported by several authors [5, 18, 28].

## 4 Conclusions

Based on the results of the SEP used in this study, it can be concluded that the geochemical behavior of As and Sb was different. Arsenic was more mobile than Sb in the studied soils and tailing material. The largest fractions of both metalloids were associated with more stable mineral phases. More concretely, As was associated mostly with AFO (e.g. ferrihydrite), while the highest portion of Sb was associated with the residual fraction (e.g. soil organic matter, sulfides or silicates). Despite low mobility and bioavailability of both metalloids, changes in pH, redox potential and alteration of other environmental and geochemical conditions might cause the release of even more stable forms of As and Sb and thus increase environmental and health risks.

## Acknowledgements

This research was supported by the Slovak Research and Development Agency (project no. APVV-21-0212) and by the European Union under the Horizon Europe project (RIA), project number 101112723 - Achieving remediation and governing restoration of contaminated soils now (ARAGORN). The expressed opinions and views are those of the authors and do not necessarily reflect the requirements of the European Union. The European Union is not responsible for them.

## References

- [1] Tan, D., Long, J., Li, B., Ding, D., Du, H., Lei, M. Fraction and mobility of antimony and arsenic in three polluted soils: A comparison of single extraction and sequential extraction. *Chemosphere*, 213, 2018, p. 533-540.
- [2] Okkenhaug, G., Zhu, Y.G., Luo, L., Lei, M., Li, X., Mulder, J. Distribution, speciation and availability of antimony (Sb) in soils and terrestrial plants from an active Sb mining area. *Environmental Pollution*, 159, 2011, p. 2427-2434.
- [3] Ye, T., Liu, T., Yi, H., Du, J., Wang, Y., Xiao, T., Cui, J. In situ arsenic immobilization by natural iron (oxyhydr)oxide precipitates in As-contaminated groundwater irrigation canals. *Journal of Environmental Sciences*, In press, 2024.
- [4] Caporale, A.G., Violante, A. Chemical processes affecting the mobility of heavy metals and metalloids in soil environments. *Current Pollution Reports*, 2, 2016, p. 15-27.
- [5] Dousova, B., Buzek, F., Herzogova, L., Machovic, V., Lhotka, M. Effect of organic matter on arsenic(V) and antimony(V) adsorption in soils. *European Journal of Soil Science*, 66, 2015, p. 74-82.
- [6] Majzlan, J., Lalinská, B., Chovan, M., Bläß, U., Brecht, B., Göttlicher, J., Steininger, R., Hug, K., Ziegler, S., Gescher, J. A mineralogical, geochemical, and microbiological assessment of the antimony- and arsenic-rich neutral mine drainage tailings near Pezinok, Slovakia. *American Mineralogist*, 96, 2011, p. 1-13.
- [7] Majzlan, J., Lalinská, B., Chovan, M., Jurkovič, E., Milovská S., Göttlicher, J. The formation, structure, and ageing of As-rich hydrous ferric oxide at the abandoned Sb deposit Pezinok (Slovakia), *Geochimica et Cosmochimica Acta*, 71, 2007, p. 4206-4220.
- [8] Hiller, E., Jurkovič, L., Faragó, T., Vítková, M., Tóth, R., Komárek, M. Contaminated soils of different natural pH and industrial origin: The role of (nano) iron- and manganese-based amendments in As, Sb, Pb, and Zn leachability. *Environmental Pollution*, 285, 2021, 117268.
- [9] Violante, A. Chapter Three - Elucidating Mechanisms of Competitive Sorption at the Mineral/Water Interface. *Advances in Agronomy*, 118, 2013, p. 111-176.
- [10] Almás, Á.R., Pironin, P., Okkenhaug, G. The partitioning of Sb in contaminated soils after being immobilization by Fe-based amendments is more dynamic compared to Pb. *Applied Geochemistry*, 108, 2019, 104378.
- [11] Hockmann, K., Lenz, M., Tandy, S., Nachtegaal, M., Janousch, M., Schulin, R. Release of antimony from contaminated soil induced by redox changes. *Journal of Hazardous Materials*, 275, 2014, p. 215-221.
- [12] Lee, J.C., Kim, E.J., Kim, H.W., Baek, K. Oxalate-based remediation of arsenic bound to amorphous Fe and Al hydrous oxides in soil. *Geoderma*, 270, 2016, p. 76-82.
- [13] Violante, A., Pigna, M. Sorption-desorption processes of metals and metalloids in soil environments. *Journal of Soil Science and Plant Nutrition*, 8, 2008, p. 95-101.
- [14] Tessier, A., Campbell, P.G.C., Bisson, M. Sequential extraction procedure for the speciation of particulate trace metals. *Analytical Chemistry*, 51 (7), 1979, p. 844-851.
- [15] US EPA Method 1311 Toxicity characteristic leaching procedure. 1992, p. 1-35.
- [16] Gil-Díaz, M., Rodríguez-Valdés, E., Alonso, J., Baragaño, D., Gallego, J.R., Lobo, M.C. Nanoremediation and long-term monitoring of brownfield soil highly polluted with As and Hg. *Science of the Total Environment*, 675, 2019, p. 165-175.
- [17] Wenzel, W.W., Kirchbaumer, N., Prohaska, T., Stingeder, G., Lombi, E., Adriano, D.C. Arsenic fractionation in soils using an improved sequential extraction procedure. *Analytica Chimica Acta*, 436, 2001, p. 309-323.
- [18] Ngo, L.K., Price, H.L., Bennett, W.W., Teasdale, P.R., Jolley, D.F. DGT and selective extractions reveal differences in arsenic and antimony uptake by the white icicle radish (*Raphanus sativus*). *Environmental Pollution*, 259, 2020, 113815.

- [19] Zarzsevszkij, S., Vítková, M., Zelená Pospíšková, K., Kolařík, J., Böserle Hudcová, B., Jurkovič, E. Management of a contaminated mine soil: Effect of soil water content on antimony and arsenic immobilisation by iron-based amendments and biochar composites. *Soil Use and Management*, 40, 2024, e12968.
- [20] Dugan, E., Verhoef, A., Robinson, S., Sohi, S. Bio-char from sawdust, maize stover and charcoal: Impact on water holding capacities (WHC) of three soils from Ghana. In Proceedings of the 19th World Congress of Soil Science, Soil Solutions for A Changing World. 1-6 August 2010, Brisbane, Australia, Published on DVD.
- [21] US EPA Method 3051a, Microwave Assisted Acid Digestion of Sludges, Sediments, Soils, and Oils. 2007, p. 1-30.
- [22] Chovan, M., Háber, M., Jeleň, S., Rojkovič, I. (eds.) *Ore textures in the Western Carpathians*. Slovak Academic Press, Bratislava, 1994, 219 p. ISBN 80-85665-24-7.
- [23] Chovan, M., Rojkovič, I., Andráš, P., Hanas, P. Ore mineralization of the Malé Karpaty Mts. *Geologica Carpathica*, 43, 1992, p. 275-286.
- [24] Jain, A., Loeppert, R.H. Effect of competing anions on the adsorption of arsenate and arsenite by ferrihydrite. *Journal of Environmental Quality*, 29, 2000, p. 1422-1430.
- [25] Violante, A., Del Gaudio, S., Pigna, M., Ricciardella, M., Banerjee, D. Coprecipitation of arsenate with metal oxides. 2. Nature, mineralogy, and reactivity of iron(III) precipitates. *Environmental Science and Technology*, 41 (24), 2007, p. 8275-8280.
- [26] Garau, G., Lauro, G.P., Diquattro, S., Garau, M., Castaldi, P. Sb (V) adsorption and desorption onto ferrihydrite: influence of pH and competing organic and inorganic anions. *Environmental Science and Pollution Research*, 26, 2019, p. 27268-27280.
- [27] Bolanz, R.M., Bläss, U., Ackermann, S., Ciobota, V., Rösch, P., Tarcea, N., Popp, J., Majzlan, J. The effect of antimonate, arsenate, and phosphate on the transformation of ferrihydrite to goethite, hematite, ferrioxyhyte, and tripuhyite. *Clays and Clay Minerals*, 61 (1), 2013, p. 11-25.
- [28] Bagherifam, S., Brown, T.C., Bagherifam, S., Baglieri, A. Sequential extraction of labile and recalcitrant fractions of soil organic matter: A case study focusing on antimony (Sb) in humic acids, fulvic acids and humin fractions of long-term aged contaminated soils. *Environmental Pollution*, 327, 2023, 121610.





## APPLICATION OF GAS NANOBUBBLES IN WASTEWATER TREATMENT AND METHANE DIGESTION: ADVANTAGES AND CHALLENGES

**Lesław Świerczek<sup>a</sup>, Jan Cebula<sup>a</sup>, Adam Cenian<sup>a</sup>**

<sup>a</sup> *Institute of Fluid-Flow Machinery, Polish Academy of Sciences,  
Fiszera 14 st., Gdańsk 80-231, Poland,  
leslaw.swierczek@imp.gda.pl, j.cebula@jcm.paf.edu.pl, cenian@imp.gda.pl*

### **Abstract**

This study investigates the application of nanobubble (NB) technology in enhancing anaerobic digestion and wastewater treatment processes. Nanobubbles, gas-filled cavities with diameters around 100 nm, possess unique properties such as high surface area-to-volume ratios, negative zeta potential ( $\zeta$ -potential), and prolonged stability in liquids, making them highly effective in improving gas transfer, microbial activity, and pollutant removal. In a methane digestion plant, oxygen nanobubbles significantly reduced hydrogen sulfide ( $H_2S$ ) concentrations by over 90 % while slightly increasing methane yields. In a wastewater treatment plant, nanobubble aeration increased dissolved oxygen levels by 35 % and enhanced organic matter breakdown while reducing energy consumption compared to conventional aeration systems. Despite these advantages, challenges such as sludge floating and the need for improved oxygen delivery systems were observed. This research highlights the potential of nanobubbles in optimizing biogas production and wastewater treatment efficiency, while also addressing some operational challenges that require further investigation.

**Keywords:** nanobubbles, anaerobic digestion, wastewater treatment, oxygen transfer efficiency, hydrogen sulfide reduction, microbial activity enhancement

### **1 Introduction**

Water deficiency and pollution are pressing global issues, intensified by rapid industrialization and urbanization, which have overwhelmed conventional water treatment processes. In response, NB's have emerged as a promising technology for enhancing water treatment and methane digestion. Defined as gas-filled cavities with diameters around 100 nm, NBs possess unique characteristics such as high surface area-to-volume ratios, negative zeta potential, and long stability in liquids, making them highly effective in applications like wastewater treatment and methane production [1]. Unlike conventional macro- and microbubbles, which quickly collapse, NBs persist in water, facilitating more efficient processes such as flotation, aeration, and chemical-free oxidation [2, 3]. Their ability to enhance the removal of organic pollutants, heavy metals, and improve aerobic and anaerobic digestion holds significant promise [4, 5].

However, there are notable challenges associated with NB technology. One key issue is the lack of understanding regarding how NBs behave in complex water matrices, which can affect their efficiency [6]. Additionally, inconsistencies in the literature regarding the precise mechanisms of NBs, especially concerning their stability and effectiveness, pose challenges to their widespread adoption [7]. Economic viability and large-scale environmental impacts also remain underexplored, raising concerns about their practical application beyond the laboratory setting [8].

This paper describes the unusual properties of nanobubbles in water, selected methods for their production, and initial observations and conclusions drawn from the author's own research utilizing the mentioned technology. The obtained results and observations address both the advantages and challenges of applying nanobubble technology in wastewater treatment and methane digestion, providing insights into future developments and potential solutions.

#### **1.1 Key properties of nanobubbles**

Nanobubbles exhibit unique physiochemical properties that distinguish them from larger microbubbles, making them particularly interesting for a wide range of applications. Bulk nanobubbles, are dispersed throughout solutions and are less likely to adhere to surfaces. They are characterized by their high internal pressure, which is inversely proportional to their diameter. This results in a high internal pressure that prevents the gas inside the nanobubbles from reaching equilibrium with its surroundings, leading to their persistence despite expectations of rapid dissolution [9].

One of the most remarkable characteristics of NBs is their extraordinary stability in liquids, which defies classical thermodynamic principles. Conventional bubbles collapse within seconds or minutes due to high internal pressure and gas dissolution into the liquid. However, NBs, due to their nanoscale size, remain stable in solution for extended periods-ranging from days to months. Nirmalkar et al. [10] observed that NBs retained their size for over 170 days, with no significant change in diameter. This stability is partly due to the high zeta potential of NBs, which contributes to their ability to remain dispersed without merging [11]. Nanobubbles also serve as effective nucleation sites for crystal growth and can be loaded with surfactants to modify their interfaces [12, 13]. Despite their small size, NBs exhibit high surface energy, which can lead to significant changes in response to fluctuations in concentration or temperature [14].

Due to small size and large surface area-to-volume ratio NBs are able to dissolve gases more effectively into liquid media. For instance, Xiao and Xu [15] found that oxygen nanobubbles had 1.5 times the mass transfer efficiency of larger bubbles, while Fan et al. [16] reported that ozone nanobubbles were 4.7 times more efficient. This property makes NBs highly beneficial for applications like water treatment, where efficient aeration is crucial.

It's worth mentioning that NBs possess the ability to generate hydroxyl radicals ( $\bullet\text{OH}$ ), superoxide anion radicals ( $\text{O}_2^{\bullet-}$ ), and singlet oxygen ( $^1\text{O}_2$ ). Mentioned reactive oxygen species are highly reactive and can degrade pollutants or natural complex polymers (e.g. lignin), which makes NBs useful for advanced oxidation processes. However, the exact mechanisms behind radical generation remain under investigation [17].

## 1.2 Nanobubbles generation methods

The generation of NBs involves several methods, each affecting their properties and effectiveness for various applications. Traditional methods for creating microbubbles have been adapted to produce nanobubbles, aiming for cost-effectiveness, simplicity, and scalability in industrial settings.

One common approach is cavitation, which induces rapid pressure changes in a liquid to form vapor-filled cavities. Hydrodynamic cavitation uses pressure drops and surface roughness to produce nanobubbles, while acoustic cavitation relies on ultrasonic energy to create and collapse microscopic bubbles. The size and concentration of nanobubbles produced by these methods depend on factors such as the dissolved gas concentration and acoustic parameters [10, 18].

Venturi-type generators and ejector-type generators are specific implementations of cavitation techniques. Venturi-type generators accelerate a two-phase flow through a venturi tube, causing macrobubbles to shrink into microbubbles due to rapid pressure changes. This method is noted for its low energy consumption and compact design, yielding a high density of microbubbles [19]. Ejector-type generators use stepwise shrinking and enlarging liquid flow channels to induce cavitation, leading to microbubble formation through self-suction of gas.

Other cavitation-based methods include gas-water circulation, where gas introduced into a vortex is converted into microbubbles by disrupting the vortex, and pressurization followed by decompression, which generates microbubbles from a supersaturated solution as gas escapes [20, 21].

Membrane-based methods involve injecting gas through porous materials to create nanobubbles. By forcing gas through membranes with specific pore sizes, such as ceramic membranes with pores between 50 and 150 nm or porous-glass membranes, a range of bubble sizes can be produced. For instance, Shirasuporous-glass membranes have been used to create monodispersed nanobubbles with diameters ranging from 360 to 720 nm, demonstrating how pore size can influence bubble size [22, 23].

Electrolysis is another technique used to generate nanobubbles through electrochemical reactions at electrodes. For example, alternating polarity electrolysis of water, using a  $\text{Na}_2\text{SO}_4$  solution and specific electrode configurations, has been effective in producing bulk nanobubbles with controlled sizes. Voltage pulses create nanobubbles with initial sizes of 60 to 80 nm, which may increase to around 250 nm after the electrical pulses are stopped [24].

In conclusion, NBs hold considerable promise for advancing water treatment and methane digestion due to their unique properties. In this context, mechanical cavitation methods and membrane-based techniques offer the most promising advantages due to their effectiveness and scalability. Therefore, these methods have been chosen for introduction to full-scale research.

## 2 Material and methods

### 2.1 Methane digestion plant research

The aim of this study was to evaluate the impact of introducing oxygen NB's into the fermentation liquid on the concentration of H<sub>2</sub>S in the produced biogas. To address the high and fluctuating levels of H<sub>2</sub>S caused by substrate variability, a micro-/nano-oxygenation method was applied in the biogas reactor using membrane technology.

The research was conducted at an agricultural biogas plant with a capacity of 0.99 MW, located in southeastern Poland. The biogas plant primarily processes natural waste, including agricultural residues, garden waste, waste produced by the food sector, and animal manure.

An injector with a specially designed ceramic sintered membrane was directly introduced into the fermentation mass mixing system. The membrane had a pore size of 200-500 nm. Oxygen was supplied to the membrane at a rate of 2-4 m<sup>3</sup>/h. Biogas composition, including H<sub>2</sub>S content, was monitored for one year.

### 2.2 Wastewater treatment plant research

The aim of the study was to determine the impact of NB oxygenation on key wastewater treatment parameters. Due to significant seasonal fluctuations in wastewater volume and a decline in treatment efficiency, a NB oxygenation system was introduced. The research was conducted at a small municipal wastewater treatment plant located in northern Poland. The plant is designed to treat domestic wastewater generated by a nearby resort. Initially, the plant was equipped to handle a wastewater load expressed in terms of equivalent population (EP) not exceeding 75, with a maximum wastewater flow (Q<sub>max</sub>) designed at 1.5 m<sup>3</sup>/h. A 2m<sup>3</sup> Micro-Nano Bubble Generator (Qingdao Aozengnier Purification Equipment Co., Ltd), capable of producing oxygen nanobubbles smaller than 100 nm, was implemented. The schematic of the nanobubble aeration system is shown in Figure 1.

In presented studies, the performance of the original aeration system was compared with the new nano-aeration system. Monitoring was conducted for parameters such as pH, Dissolved Oxygen (DO), and RedOx potential at the wastewater inlet to the reactor and the RedOx potential of the effluent leaving the aeration chamber. Each aeration system was monitored for two days using the CX-804 controller (Elmetron, Poland) during the tourist peak season.

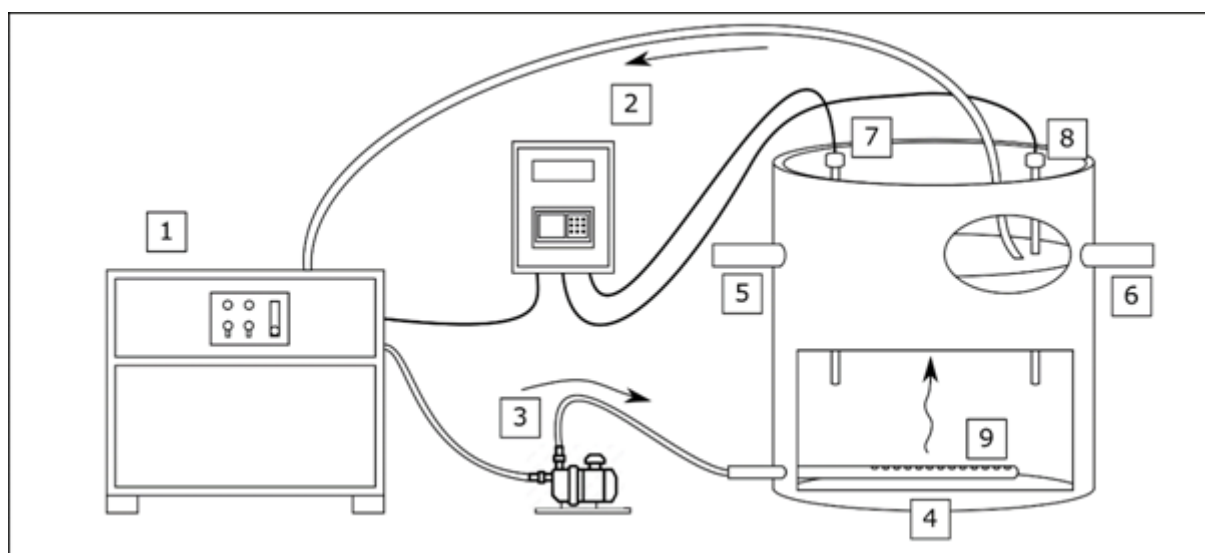


**Fig. 1. Nanoaeration system implementet in existing WWTP located in Bure Misie Foundation**

- (1) - nanobubble generator, (2) - monitoring and control device, (3) - recirculation pump, (4) - bioreactor, (5) - wastewater inlet, (6) - wastewater outlet, (7) - pH, Red-Ox potential and dissolved oxygen probe, (8) - Red-Ox potential probe, (9) - aeration pipes

## 3 Results and discussion

### 3.1 Anaerobic digestion

While methane (CH<sub>4</sub>) can be a valuable fuel when captured, its production through anaerobic digestion often leads to H<sub>2</sub>S formation, which inhibits CH<sub>4</sub> production and requires removal for biogas applications, such as electricity generation or natural gas replacement. Traditional post-treatment methods for H<sub>2</sub>S

removal, such as biotrickling filtration and chemical scrubbing, are effective but costly and generate waste. Emerging strategies like substrate pretreatment and in-situ process regulation (e.g. microaeration) are more cost-effective, reducing H<sub>2</sub>S formation and enhancing CH<sub>4</sub> production during anaerobic digestion [25].

As mentioned earlier, NBs play a significant role in enhancing anaerobic digestion by increasing water molecule mobility. Their small size and high zeta potential facilitate nutrient delivery to biofilms and boost microbial and enzyme activity [26]. NBs also generate radicals that improve the oxidative decomposition of substrates by microorganisms [27].

In the present study, it was found that after one year of introducing oxygen in the form of micro-/nano-bubbles, the H<sub>2</sub>S concentration in biogas was significantly reduced. The H<sub>2</sub>S concentration data is presented in Figure 2. Regardless of seasonal substrate variations, H<sub>2</sub>S levels dropped from an average of 4000 ppmv to approximately 100 ppmv. This reduction significantly improved biogas quality, which can extend the lifespan of gas engines used for electricity generation in biogas plants [28].

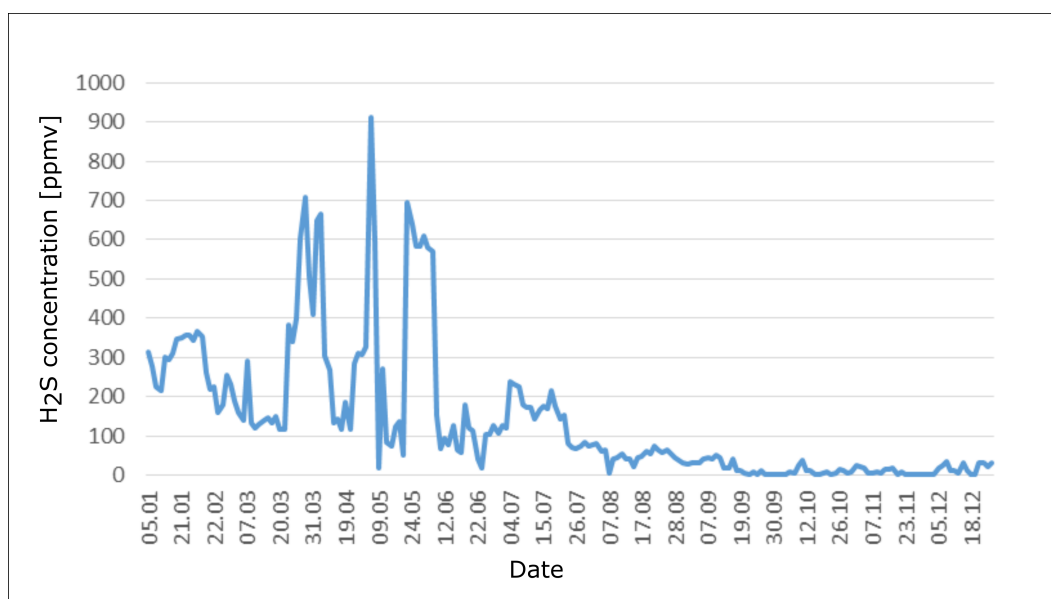


**Fig. 2. H<sub>2</sub>S concentration fluctuations during one year of membrane aeration**

Regarding biogas composition, it was noted that the CH<sub>4</sub> content in the biogas slightly increased, from an average of 55 % during the initial days of the experiment to 62 %. As mentioned, the improvement in biogas production efficiency and CH<sub>4</sub> content is likely due to the partial degradation of organic matter, which facilitates biological breakdown.

Literature studies have demonstrated that NB's can enhance the anaerobic digestibility of various substrates. For instance, CH<sub>4</sub> productivity improvements ranging from 3 % to 40 % have been observed with different gas types compared to controls. Air-NB creates a microaerobic environment that promotes the growth of lignocellulose-degrading microbes and improves cellulose reduction more effectively than CO<sub>2</sub>-NB [29]. O<sub>2</sub>-NB has also been shown to significantly increase CH<sub>4</sub> yields and reduce cellulose crystallinity [30]. Moreover, NB's improve enzyme activities involved in substrate degradation, such as alkaline phosphatase and protease, which accelerates the conversion of macromolecules into volatile fatty acids (VFAs) [31, 29]. Increased relative abundances of microbial communities such as *Chloroflexi* and *Bacteroidetes* have been observed with air-NBs, which may enhance cellulose degradation. The presence of *Methanosaeta* and *Methanobacterium* in NB reactors further supports enhanced methane production and interspecies hydrogen transfer [29].

However, introducing NB technology in anaerobic digestion presents several challenges. While NBs improve mass transfer, enhance microbial activity, and increase CH<sub>4</sub> production, their integration into anaerobic systems requires careful balancing. One challenge is the potential for oxygen leakage into the system, which could disrupt the strictly anaerobic conditions required for methane production. Additionally, NBs can increase biofilm thickness, leading to operational issues such as clogging and reduced efficiency. Managing these effects requires optimizing bubble size, injection rates, and reactor design to fully harness the benefits without compromising the anaerobic digestion process.

### 3.2 Wastewater treatment

Aeration is crucial for delivering oxygen in wastewater treatment processes, though it accounts for 70-80 % of the total energy consumption [32]. The efficiency of aeration depends heavily on dissolved oxygen (DO) levels, which influence biological activity. Traditional aeration methods include shearing the liquid surface with mixers or turbines and releasing air through various materials. Fine bubbles are more efficient in oxygen transfer compared to coarse bubbles, owing to their lower interfacial velocity gradients [33].

Nanobubbles present a promising alternative due to their superior mass transfer efficiency and stability compared to conventional coarse bubbles. They can improve aeration efficiency and reduce energy costs in aerobic biological systems, such as biofilm and activated sludge reactors. Research by Xiao and Xu (2020) demonstrated that air NBs have approximately 1.5 times higher oxygen diffusion coefficients than coarse bubbles, enhancing microbial community dynamics and enzyme activity [15]. In comparison to conventional fine bubble aeration, NBs result in higher oxygen concentrations, lower sludge production, and improved organic matter decomposition [34]. Fine bubbles, combined with deep subsurface infiltration systems, improve nitrogen and phosphorus removal, while NBs show superior performance in removing suspended solids and nitrogen compared to bottom aeration [35, 36].

In the current study, a traditional aeration system generating coarse bubbles in the aeration chamber was compared with a NB oxygenation system. Figure 3 illustrates changes in DO, pH, and RedOx potential at the inflow and outflow of the aeration chamber over time when using the original blower installed at the treatment plant. Figure 4 presents changes in these parameters with nanobubble aeration.

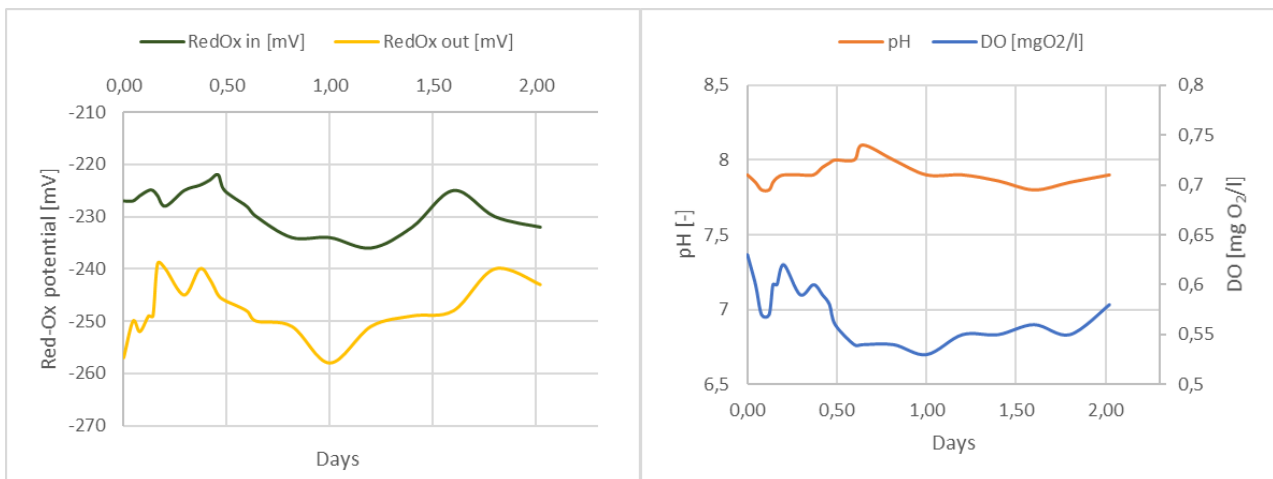


**Fig. 3. Changes in RedOx potential, pH, and DO during a 2-day experiment with traditional coarse bubble aeration**

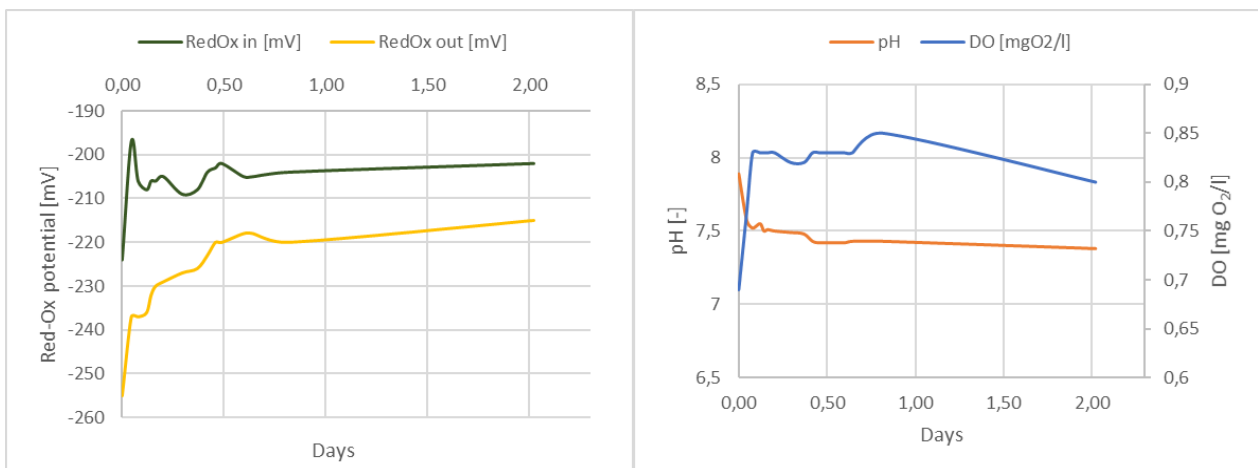


**Fig. 4. Changes in RedOx potential, pH, and DO during a 2-day experiment with nanobubble aeration**

It was observed that the reactor was heavily loaded with organic matter, as indicated by the low RedOx potential at the outflow and low DO levels. After introducing the nanobubble system, both RedOx potential and DO levels increased almost immediately. However, after two days, the aeration chamber remained overloaded. Notably, the NB system increased DO by an average of 35 %.

The original blower consumed about 60 m<sup>3</sup>/h of air, while the NB generator required only 0.3 m<sup>3</sup>/h, with comparable energy consumption. This confirms that mass transfer efficiency with NB's is significantly higher. However, to meet oxygen demand in this treatment plant, a more powerful NB generator would be necessary.

Literature studies have shown that air micro-nano bubbles are effective in treating wastewater from various sources. For example, in sugar industry wastewater, air NBs reduced chemical OD by 85 %, total suspended solids by 79 %, and removed 66.21 % of total coliforms [37, 38]. Xiao et al. (2021) found that NBs increased the size and thickness of activated sludge and biofilm by 23.35 % and 86.67 %, respectively, improving total nitrogen removal by 10.58 % [39].

Despite these benefits, there were some issues. Irreversible sludge floating and cloudier effluent due to the proliferation of filamentous bacteria were observed, as noted by Yaparathne et al. [40]. Additionally, NBs alone cannot provide the necessary shear stress to manage biofilm thickness. This suggests that combining NB aeration with mechanical bubbling or optimizing reflux ratios is essential for achieving optimal performance.

#### 4 Conclusions

Nanobubble technology presents significant advantages in both anaerobic digestion and wastewater treatment, primarily through enhanced gas transfer, improved microbial activity, and greater pollutant removal efficiency. The introduction of micro-/nanobubbles in anaerobic digestion effectively reduced H<sub>2</sub>S levels and can increase CH<sub>4</sub> production, offering a promising alternative to traditional H<sub>2</sub>S removal methods. In wastewater treatment, NB aeration demonstrated superior oxygen transfer efficiency, reducing energy consumption while improving water quality parameters. However, challenges such as maintaining the anaerobic environment in methane digesters and managing biofilm growth in wastewater treatment systems were observed. Addressing these challenges requires optimizing NB generator designs and aeration methods to fully realize the benefits of this technology in large-scale applications. Further research is needed to explore the long-term economic viability and scalability of NB's for widespread industrial use.

#### Acknowledgements

This study was carried out within the NURSECOAST-II project entitled: "Model Nutrients Reduction Solutions In Near-Coast Touristic Areas" co-financed by the Interreg Baltic Sea Region Programme.

#### References

- [1] Alheshibri, M., Qian, J., Jehannin, M., Craig, V.S.J. A History of Nanobubbles. *Langmuir*, 32 (43), 2016, p. 11086-11100.
- [2] Demangeat, J.L. Gas nanobubbles and aqueous nanostructures: the crucial role of dynamization. *Homeopathy*, 104 (2), 2015, p. 101-115.
- [3] Takahashi, M., Shirai, Y., Sugawa, S. Free-Radical Generation from Bulk Nanobubbles in Aqueous Electrolyte Solutions: ESR Spin-Trap Observation of Microbubble-Treated Water. *Langmuir*, 37 (16), 2021, p. 5005-5011.
- [4] Bui, T.T., Han, M. Decolorization of dark green Rit dye using positively charged nanobubbles technologies. *Separation and Purification Technology*, 233, 2020, p. 116034.
- [5] Chuenchart, W., Karki, R., Shitanaka, T., Marcelino, K.R., Lu, H., Khanal, S.K. Nanobubble technology in anaerobic digestion: A review. *Bioresource Technology*, 329, 2021, p. 124916.
- [6] Kyzas, G.Z., Bomis, G., Kosheleva, R.I., Efthimiadou, E.K., Favvas, E.P., Kostoglou, M., Mitropoulos, A.C. Nanobubbles effect on heavy metal ions adsorption by activated carbon. *Chemical Engineering Journal*, 356, 2019, p. 91-97.
- [7] Pal, P., Joshi, A., Anantharaman, H. Nanobubble ozonation for waterbody rejuvenation at different locations in India: A holistic and sustainable approach. *Results in Engineering*, 16, 2022, p. 100725.
- [8] Haris, S., Qiu, X., Klammler, H., Mohamed, M.M.A. The use of micro-nano bubbles in groundwater remediation: A comprehensive review. *Groundwater for Sustainable Development*, 11, 2020, p. 100463.

- [9] Duval, E., Adichtchev, S., Sirotkin, S., Mermet, A. Long-lived submicrometric bubbles in very diluted alkali halide water solutions. *Physical Chemistry Chemical Physics*, 14 (12), 2012, p. 4125-4132.
- [10] Nirmalkar, N., Pacek, A.W., Barigou, M. On the Existence and Stability of Bulk Nanobubbles. *Langmuir*, 34 (37), 2018, p. 10964-10973.
- [11] Ahmed, A.K.A., Sun, C., Hua, L., Zhang, Z., Zhang, Y., Zhang, W., Marhaba, T. Generation of nanobubbles by ceramic membrane filters: The dependence of bubble size and zeta potential on surface coating, pore size and injected gas pressure. *Chemosphere*, 203, 2018, p. 327-335.
- [12] Michalopoulou, A., Michailidi, E., Favvas, E., Maravelaki, N.P., Kilikoglou, V., Karatasios, I. Comparative Evaluation of the Morphological Characteristics of Nanolime Dispersions for the Consolidation of Architectural Monuments. *International Journal of Architectural Heritage*, 14 (7), 2020, p. 994-1007.
- [13] Ahmed, A.K.A., Sun, C., Hua, L., Zhang, Z., Zhang, Y., Marhaba, T., Zhang, W. Colloidal Properties of Air, Oxygen, and Nitrogen Nanobubbles in Water: Effects of Ionic Strength, Natural Organic Matters, and Surfactants. *Environmental Engineering Science*, 35(7), 2018, p. 720-727.
- [14] Guo, Z., Zhang, X. Enhanced fluctuation for pinned surface nanobubbles. *Physical Review E*, 100 (5), 2019.
- [15] Xiao, W., Xu, G. Mass transfer of nanobubble aeration and its effect on biofilm growth: Microbial activity and structural properties. *Science of The Total Environment*, 703, 2020, p. 134976.
- [16] Fan, M., Tao, D., Honaker, R., Luo, Z. Nanobubble generation and its applications in froth flotation (part II): fundamental study and theoretical analysis. *Mining Science and Technology (China)*, 20 (2), 2010, p. 159-177.
- [17] Sakr, M., Mohamed, M.M., Maraqa, M.A., Hamouda, M.A., Hassan, A.A., Ali, J., Jung, J. A critical review of the recent developments in micro-nano bubbles applications for domestic and industrial wastewater treatment. *Alexandria Engineering Journal*, 61 (8), 2022, p. 6591-6612.
- [18] Lee, J.I., Yim, B.S., Kim, J.M. Effect of dissolved-gas concentration on bulk nanobubbles generation using ultrasonication. *Scientific Reports*, 10 (1), 2020.
- [19] Yoshida, A., Takahashi, O., Ishii, Y., Sekimoto, Y., Kurata, Y. Water purification using the adsorption characteristics of microbubbles. *Japanese Journal of Applied Physics, Part 1: Regular Papers and Short Notes and Review Papers*, 47, 2008, p. 6574-6577.
- [20] Khuntia, S., Majumder, S.K., Ghosh, P. Microbubble-aided water and wastewater purification: A review. *Reviews in Chemical Engineering*, 28 (4-6), 2012, p. 191-221.
- [21] Takahashi, H. 1. Evaluation of Drug Safety from Clinical Trial to Postmarketing Study. *Rinsho yakuri/Japanese Journal of Clinical Pharmacology and Therapeutics*, 40 (1), 2009, p. 2-6.
- [22] Kukizaki, M., Goto, M. Size control of nanobubbles generated from Shirasu-porous-glass (SPG) membranes. *Journal of Membrane Science*, 281 (1), 2006, p. 386-396.
- [23] Bari, S.D., Robinson, A.J. Experimental study of gas injected bubble growth from submerged orifices. *Experimental Thermal and Fluid Science*, 44, 2013, p. 124-137.
- [24] Postnikov, A.V., Uvarov, I.V., Penkov, N.V., Svetovoy, V.B. Collective behavior of bulk nanobubbles produced by alternating polarity electrolysis. *Nanoscale*, 10 (1), 2018, p. 428-435.
- [25] Vu, H.P., Nguyen, L.N., Wang, Q., Ngo, H.H., Liu, Q., Zhang, X., Nghiem, L.D. Hydrogen sulphide management in anaerobic digestion: A critical review on input control, process regulation, and post-treatment. *Bioresour. Technol.*, 346, 2022, p. 126634.
- [26] Wang, X., Yuan, T., Guo, Z., Han, H., Lei, Z., Shimizu, K., Zhang, Z., Lee, D.J. Enhanced hydrolysis and acidification of cellulose at high loading for methane production via anaerobic digestion supplemented with high mobility nanobubble water. *Bioresour. Technol.*, 297, 2020, p. 122499.
- [27] Yang, X., Nie, J., Wei, Y., Zhao, Z., Shimizu, K., Lei, Z., Zhang, Z. Simultaneous enhancement on lignin degradation and methane production from anaerobic co-digestion of waste activated sludge and alkaline lignin supplemented with N<sub>2</sub>-nanobubble water. *Bioresour. Technol. Reports*, 11, 2020, p. 100470.
- [28] Stanuch, I., Sozańska, M., Biegańska, J., Cebula, J., Nowak, J. Fluctuations of the elemental composition in the layers of mineral deposits formed on the elements of biogas engines. *Scientific Reports*, 10 (1), 2020, p. 1-12.
- [29] Wang, X., Yuan, T., Lei, Z., Kobayashi, M., Adachi, Y., Shimizu, K., Lee, D.J., Zhang, Z. Supplementation of O<sub>2</sub>-containing gas nanobubble water to enhance methane production from anaerobic digestion of cellulose. *Chemical Engineering Journal*, 398, 2020, p. 125652.

- [30] Wang, X., Lei, Z., Shimizu, K., Zhang, Z., Lee, D.J. Improved methane production from corn straw using anaerobically digested sludge pre-augmented by nanobubble water. *Bioresource Technology*, 311, 2020, p. 123479.
- [31] Hou, T., Zhao, J., Lei, Z., Shimizu, K., Zhang, Z. Enhanced energy recovery via separate hydrogen and methane production from two-stage anaerobic digestion of food waste with nanobubble water supplementation. *Science of The Total Environment*, 761, 2021, p. 143234.
- [32] Sun, J., Liang, P., Yan, X., Zuo, K., Xiao, K., Xia, J., Qiu, Y., Wu, Q., Wu, S., Huang, X., Qi, M., Wen, X. Reducing aeration energy consumption in a large-scale membrane bioreactor: Process simulation and engineering application. *Water Research*, 93, 2016, p. 205-213.
- [33] Puig, S., Corominas, L., Traore, A., Colomer, J., Balaguer, M.D., Colprim, J. An on-line optimisation of a SBR cycle for carbon and nitrogen removal based on on-line pH and OUR: the role of dissolved oxygen control. *Water Science and Technology*, 53 (4–5), 2006, p. 171-178.
- [34] Ahmadi, M., Nabi Bidhendi, G., Torabian, A., Mehrdadi, N. Effects of nanobubble aeration in oxygen transfer efficiency and sludge production in wastewater biological treatment. *Journal of Advances in Environmental Health Research*, 6 (4), 2018, p. 225-233.
- [35] Zhou, L.V, Shan-chang, C., Ting, C., Jian, W.G. Applied research of micro-nano-bubble aeration technology on treatment of domestic sewage. *Guangzhou Chem. Ind*, 42, 2014, p. 122-124.
- [36] Wang, H., Zhang, L. Research on the nitrogen removal efficiency and mechanism of deep subsurface wastewater infiltration systems by fine bubble aeration. *Ecological Engineering*, 107, 2017, p. 33-40.
- [37] Leyva, M., Flores, J.V. Reduction of COD and TSS of waste effluents from a sugar industry through the use of air micro-nanobubbles. *Journal of Nanotechnology*, 2 (1), 2018, p. 7-12.
- [38] Reyes, R., Flores, J.V. Efficiency of micro-nanobubbles for wastewater treatment in puerto bermúdez, oxapampa, pasco. *Journal of Nanotechnology*, 1 (1), 2017, p. 18-24.
- [39] Xiao, W., Xu, G., Li, G. Effect of nanobubble application on performance and structural characteristics of microbial aggregates. *Science of The Total Environment*, 765, 2021, p. 142725.
- [40] Yapararne, S., Doherty, Z.E., Magdaleno, A.L., Matula, E.E., MacRae, J.D., Garcia-Segura, S., Apul, O.G. Effect of air nanobubbles on oxygen transfer, oxygen uptake, and diversity of aerobic microbial consortium in activated sludge reactors. *Bioresource Technology*, 351, 2022, p. 127090.



## IRON BIONANOPARTICLES (Fe-BNPs) DERIVED FROM GRAPE POMACE

**Marcela Tlčíková<sup>a</sup>, Hana Horváthová<sup>a,b</sup>, Viktorie Víchová<sup>c</sup>, Eubomír Jurkovič<sup>a</sup>**

<sup>a</sup> Comenius University in Bratislava, Faculty of Natural Science, Department of Geochemistry, Ilkovičova 6, 842 15 Bratislava, Slovakia; tlcikova2@uniba.sk, lubomir.jurkovic@uniba.sk

<sup>b</sup> The Centre of Environmental Services, Ltd., Kutlíkova 17, 852 50, Bratislava, horvathova@cenvis.sk

<sup>c</sup> Czech Advanced Technology and Research Institute, Regional Centre of Advanced Technologies and Materials, Palacký University Olomouc, Šlechtitelu 27, 783 71 Olomouc, Czech Republic; viktorie.vichova@upol.cz

### Abstract

This study is focused on green synthesis of iron bionanoparticles (Fe-BNPs) derived from grape pomace and grape berries, and their subsequent application to remove the polychlorinated biphenyls (PCBs). Characterization of biomaterial was performed solely with Fe-BNPs derived from grape pomace. Transmission electron microscopy (TEM) and scanning electron microscopy (SEM) determined that the synthesized structure is in nanoscale (mostly up to 100 nm). The valence state of chelated iron in Fe-BNPs was monitored using Mössbauer spectroscopy. The formation of a doublet defined the majority representation of Fe (III) over Fe (II). Determination of the specific surface area with nitrogen proved that Fe-BNPs from the grape pomace are a potentially effective sorbent with a specific surface area of 382 m.g<sup>-1</sup> and containing mesopores. To verify the interaction of iron with polyphenols, the grape pomace extract itself and then the extract after the addition of iron salt were measured using Fourier-transform infrared spectroscopy (FTIR). A FTIR spectrometer recorded wavenumbers at approx. 2800 cm<sup>-1</sup> (aldehydes) and 1750 cm<sup>-1</sup> (carboxylic acids). Application of Fe-BNPs from pomace achieved the highest degradation of the sum of 7 PCB congeners in 14 days (62 %). The degradation results indicate a similar percentage decrease of PCBs ( $\Sigma$  7 congeners of PCBs) when applying Fe-BNPs from pomace and Fe-BNPs from grapes, thus this work is also based on the topic of food waste recovery and circular economy.

**Keywords:** iron bionanoparticles, green synthesis, polychlorinated biphenyls, degradation, grape pomace, circular economy

## 1 Introduction

Iron-based nanoparticles (Fe-BNPs) have gained significant attention in recent years due to their potential for green synthesis and versatile applications, particularly in environmental and biomedical fields. The natural abundance, biocompatibility, and advantageous redox properties of iron make it an attractive material for nanoparticle synthesis, aligning with the principles of green chemistry that emphasize sustainability and environmental impact reduction. Unlike more expensive and less sustainable metals, iron is widely available and cost-effective, enabling large-scale production of nanoparticles suitable for diverse applications, including pollution remediation and medical therapies.

### 1.1 Green synthesis

Green synthesis approaches utilize natural matrices such as plants, bacteria, fungi, and agricultural by-products like grape pomace. Key parameters for the plant-based synthesis of bionanoparticles include the choice of raw materials, reaction conditions, incubation time, and the resulting particle size and morphology, which collectively determine their potential applications. In the preparation of plant extracts, specific plant parts such as leaves, stems, flowers, and roots may be used individually, or the entire plant matrix containing bioactive compounds can be employed [1]. The matrices involved in the synthesis should contain a certain percentage of polyphenols, which are frequently highlighted in the literature as key components in nanoparticle synthesis. However, lipids, proteins, vitamins, and various other organic molecules that contain hydroxyl groups (OH-) also participate in the reaction [2]. Extract from these matrices interact with metal salts to produce nanoparticles, with polyphenols and other bioactive compounds playing a major role in reducing and stabilizing the metal ions.

When ferrous salts interact with polyphenols, they form networked complexes, as illustrated in Fig. 1. Metal ions typically prefer octahedral geometry; hence, Fe<sup>2+</sup>/Fe<sup>3+</sup> ions can associate with three catecholate or gallate molecules, simultaneously reducing Fe<sup>3+</sup> to Fe<sup>2+</sup> ions. During metal reduction, polyphenols are oxidized to semiquinone, which is protonated at low pH, leading to neutralization. Once the semiquinone form of polyphenols is generated, it can further reduce additional Fe<sup>3+</sup> ions while oxidizing the semiquinone to quinone. However, these reactions have been observed primarily at very low pH levels. At higher pH

levels, around 7, these  $\text{Fe}^{3+}$  reduction processes are inhibited due to the formation of bis- and tris-polyphenol complexes with iron. Both of these reduction mechanisms contribute to the antioxidant and prooxidant activities of polyphenol molecules [3, 4]. These processes are pH-sensitive and contribute to catalytic activities such as Fenton reactions, which generate reactive oxygen species (ROS) for pollutant degradation [5]. This biocompatibility ensures the safe integration of Fe-BNPs into biological and environmental systems, making them ideal for applications such as targeted drug delivery, catalysis, and the degradation of environmental pollutants.

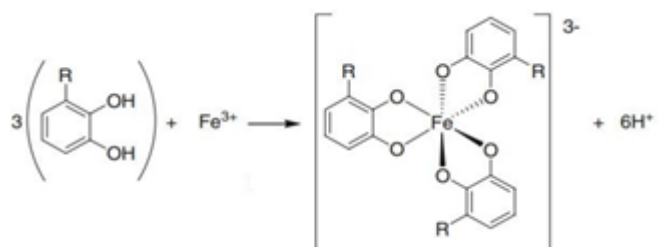


**Fig. 1. Illustration of the reaction mechanism of Gallates (R=OH) or Catechols (R=H) with Ferric Iron, leading to the formation of an Octahedral Network Structure (Perron et al., 2009)**

## 1.2 Characterisation of iron bionanoparticles

Characterization of synthesized bionanoparticles is essential for understanding their physicochemical properties, such as size, shape, stability, polydispersity, and surface area. A visible colour change upon the addition of metal salts to aqueous extracts often indicates nanoparticle formation, while the Tyndall effect in colloidal solutions can confirm their presence [6]. Post-synthesis, nanoparticles are typically separated by high-speed centrifugation and analysed using various advanced techniques. Key characterization methods include both microscopic and spectroscopic techniques. Microscopic methods like atomic force microscopy (AFM), scanning electron microscopy (SEM), and transmission electron microscopy (TEM) provide direct imaging of the nanoparticles, revealing detailed morphological data. Spectroscopic methods, including UV-VIS spectroscopy, dynamic light scattering (DLS), X-ray diffraction (XRD), energy-dispersive spectroscopy (EDS), Fourier-transform infrared spectroscopy (FT-IR), and Raman spectroscopy, offer indirect insights into nanoparticle composition, structure, and surface properties. UV-VIS spectroscopy detects optical properties, while DLS measures particle size and surface charge. EDS maps elemental composition, and XRD identifies structural characteristics, such as crystalline phases [7]. FT-IR and Raman spectroscopy are used to analyse functional groups and surface interactions. This combined approach is crucial for accurately defining the nanoparticles' physical and chemical attributes, enabling their effective application in various fields.

## 1.3 Application of iron bionanoparticles

Recent studies have demonstrated the efficacy of Fe-BNPs derived from grape pomace in degrading polychlorinated biphenyls (PCBs), achieving significant reductions in PCB concentrations. This application highlights the dual benefits of utilizing waste-derived materials: promoting circular economy principles by repurposing agricultural by-products and contributing to environmental remediation efforts [8]. The integration of green synthesis methods for nanoparticle production supports the broader goal of sustainable development, offering a pathway to more eco-friendly and cost-effective technologies for pollutant removal [4]. Further research is needed to optimize these synthesis processes and expand the applications of Fe-BNPs across various environmental and industrial challenges.

## 2 Material and methods

### 2.1 Green synthesis of iron bionanoparticles

Frozen crushed grape berries (5 g) were placed into a boiling flask, followed by the addition of 500 mL of distilled water. The extraction process was conducted in a water bath at a constant temperature (80 °C) for 2 hours, using a magnetic stirrer with a heating plate. The extract was cooled to room temperature, and the remaining solid residues were removed through filtration using gauze and filter paper. Iron precursor  $\text{FeSO}_4 \cdot 7\text{H}_2\text{O}$  was added to the extract [9] and the pH of the solution was adjusted to a range of 7-8 using 0.3 M NaOH. Green synthesis was performed on a reciprocal shaker (100 rpm), in the dark, at

room temperature for a duration of 48 hours. The resulting nanoparticles were then centrifuged (Hettich, Universal 320-R) in 50 mL conical centrifuge tubes at 9500 rpm for 15 minutes. The majority of the supernatant was decanted, while the sedimented bionanoparticles were resuspended in the remaining 3 mL of supernatant and immediately used in degradation experiments and for characterization of the iron bionanoparticles.

## 2.2 Characterization of iron bionanoparticles

The surface of nanoparticles and their size and shape were studied with electron microscopes. The transmission electron microscope (TEM) JEM-2100 (JEOL Ltd., Japan) was used for the nZVI particles images obtained at an electron acceleration voltage of 200 kV.

The morphology of the samples was examined by SEM using a JSM-7900F Jeol scanning electron microscope with an accelerating voltage of 5.0 kV. Energy Dispersive Spectrometry (EDS) was performed to verify the composition of the samples using Jeol JED-2300 SDD detector, with acquisition time of 60 second and under an accelerating voltage of 15.0 kV.

The specific surface area (SSA) of the sample could significantly affect the reactivity of the material. SSA was determined via gas sorption analysis performed by means of N<sub>2</sub> adsorption/desorption measurements at 77 K on a volumetric gas adsorption analyzer (Autosorb iQ XR, Anton-Paar Quanta Tec, USA) up to 0.965 p/p<sub>0</sub>.

X-ray powder diffraction (XRD) measurement was used to distinguish the crystalline phase in the samples. The measurements were performed with the Aeris diffractometer (Malvern PANalytical, Ltd, USA) operating in Bragg-Brentano geometry.

The <sup>57</sup>Fe zero-field Mössbauer spectra were recorded at room temperature employing a Mössbauer spectrometer (MS2007) operating in a constant acceleration mode and equipped with a 50 mCi <sup>57</sup>Co(Rh) source. The values of the isomer shift are referred to  $\alpha$ -Fe foil sample at room temperature.

Fourier transform infrared (FT-IR) absorption spectra were measured on an FT-IR spectrometer Nicolet iS5 (Thermo electron, USA) employing attenuated total reflection (ATR) on a ZnSe crystal, using 64 scans with resolution of 2 cm<sup>-1</sup>. The IR absorption spectra were recalculated from ATR to absorbance and baseline correction.

## 2.3 Degradation experiments of PCBs

Under defined laboratory conditions, 100 mL of minimal mineral medium, 185  $\mu$ L of Delor 103 solution, and 3 mL of freshly synthesized Fe-BNPs derived from grape berries and pomace were added to reagent bottles. The pH of the solution was adjusted to a range of 6 to 7 with 3M NaOH. Experimental conditions were 120 rpm, 25 °C, in the dark for 7 and 14 days. The reagent bottles were sealed with stoppers to prevent oxygen interference, as the presence of oxygen inhibits the reductive activity of the nanoparticles. Remaining non-degraded PCB congeners were extracted by two-step extraction using n-Hexane and extracted organic phase of the samples was analysed on GC-ECD (HP 5890, Agilent, USA). Based on the calibration of a standard mixture of seven monitored indicator PCB congeners (PCB 8; PCB 28; PCB 52; PCB 101; PCB 118; PCB 138; PCB 153), the percentage reduction of individual chlorinated biphenyls in the samples was evaluated using the peak areas and calculated with following equation (1):

$$P = \left( \frac{\text{control} - \text{sample}}{\text{control}} \right) * 100 \% \quad (1)$$

## 3 Results and discussion

### 3.1 Characterisation of iron bionanoparticles

The primary characterization of the biomaterial was performed using Fe-BNPs derived from grape pomace. TEM and SEM analyses revealed that the synthesized Fe-BNPs are predominantly nanoscale, with particle sizes mostly under 100 nm, confirming their classification as nanoparticles in Fig. 2. EDS analysis indicated that the material is homogeneous, with distinct clusters exhibiting a porous structure, which enhances their potential as sorbents. The elemental analysis of the sample revealed that carbon and iron were the predominant elements, highlighting the primary constituents of the synthesized bionanoparticles. The presence of iron is particularly significant, as it plays a crucial role in the material's functionality, especially in environmental and catalytic applications. Iron's abundance not only confirms successful synthesis but also

underscores the material's potential efficacy in redox reactions, such as those involved in the degradation of contaminants. The presence of other elements such as magnesium, phosphorus, potassium, calcium, and silicon were also detected, aligning with expectations given the complex nature of the natural matrix used for synthesis. These elements are commonly found in biological materials and can contribute to the overall stability and functionality of the nanoparticles. For instance, magnesium and calcium often play supportive roles in enhancing the structural integrity of the nanoparticles, while phosphorus can participate in surface interactions that influence the nanoparticles' reactivity [10].

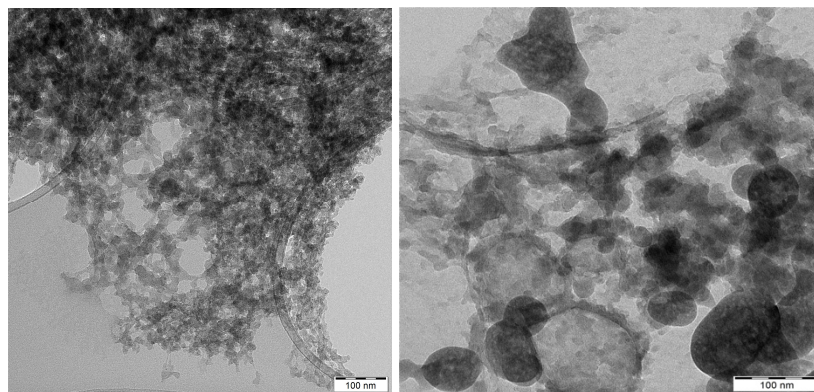


**Fig. 2. Transmission electron microscopy of Fe-BNPs derived from grape pomace (100 nm)**

X-ray diffraction (XRD) analysis revealed that the Fe-BNPs are amorphous, lacking detectable crystalline phases, which indicates a disordered atomic structure. The amorphous nature enhances surface reactivity and catalytic performance due to the high density of reactive sites and flexibility in structure. This structural disorder is advantageous for environmental remediation applications, as it supports enhanced pollutant degradation capabilities. The absence of long-range order also facilitates surface modifications, highlighting the potential of amorphous Fe-BNPs as efficient materials in functional applications [11].

Mössbauer spectroscopy revealed that the iron in the Fe-BNPs predominantly exists in the Fe(III) valence state, with a smaller proportion of Fe(II), suggesting that the oxidation of iron may be accelerated by changes in pH from acidic to neutral conditions or after exposure in the air. Further characterization of the Fe-BNPs from grape pomace was conducted using nitrogen adsorption-desorption techniques to determine the specific surface area and pore characteristics. The results indicated a specific surface area of 382 m<sup>2</sup>/g, with the presence of mesopores, highlighting that Fe-BNPs are outstanding sorbents with a high capacity for adsorbing contaminants. Their porous nature, combined with a large surface area, underscores their effectiveness in capturing pollutants, making them suitable for environmental applications. To assess the interaction between iron and polyphenols present in the grape pomace, FTIR spectroscopy was employed. The FTIR spectra of the Fe-BNPs showed absorption bands at approximately 2800 cm<sup>-1</sup> (aldehyde groups) and 1750 cm<sup>-1</sup> (carboxylic acid groups), which are characteristic of polyphenolic compounds. These findings suggest that polyphenols are involved in the chelation and stabilization of iron within the nanoparticles. The presence of these functional groups partially confirms the interaction between polyphenols and iron, indicating that these organic molecules play a significant role in the formation and stability of the Fe-BNPs, enhancing their structural and functional properties.

### 3.2 Degradation experiments of PCBs

The Fe-BNPs synthesized from grape pomace and grape berries exhibited significant efficacy in degrading polychlorinated biphenyls (PCBs), achieving a degradation of 62 % and 60 % of the sum of monitored PCB congeners over a 14-day period, respectively (Fig. 3). The similar degradation efficiencies observed for both sources indicate the potential of Fe-BNPs in environmental remediation. Longer exposure times are expected to further enhance PCB degradation, as results showed greater efficacy over 14 days compared to 7 days. However, the experiments were conducted under optimal anaerobic conditions, which favoured the activity of the bionanoparticles; such conditions may not be easily replicated *in situ* due to the susceptibility of Fe-BNPs to oxidation. Further research is necessary to address these oxidation challenges and to optimize conditions for *in situ* applications. Increasing the concentration of Fe-BNPs or adjusting the dosing frequency could potentially improve degradation rates and extend their effectiveness over time. These findings highlight the feasibility of using Fe-BNPs derived from agricultural waste, supporting the broader

goals of food waste valorization and the circular economy by converting waste materials into functional nanomaterials for pollutant removal.

The commercial mixture Delor 103 used in the experiment contains the highest concentrations of lower chlorinated PCBs, such as PCB 8 (6 %), PCB 28 (22 %), and PCB 52 (2 %). The remaining PCBs were present in trace amounts, which likely facilitated their faster degradation during the experiment. The subsequent removal of lower chlorinated PCBs was observed. Notably, the degradation effects of Fe-BNPs derived from grapes and grape pomace were similar, with a significant difference observed only for PCB 118. Less chlorinated PCBs undergo slower dechlorination compared to highly chlorinated PCBs due to the increase in the energy of the lowest unoccupied molecular orbital (LUMO) as chlorine atoms are progressively removed from the PCB molecule. Chlorine atoms in *para*- or *meta*- positions are dehalogenated more rapidly than those in *ortho*- positions. An increased number of chlorine atoms in ortho-positions can hinder the dechlorination process by increasing the torsional angle between the benzene rings, which may obstruct the sorption process [12].

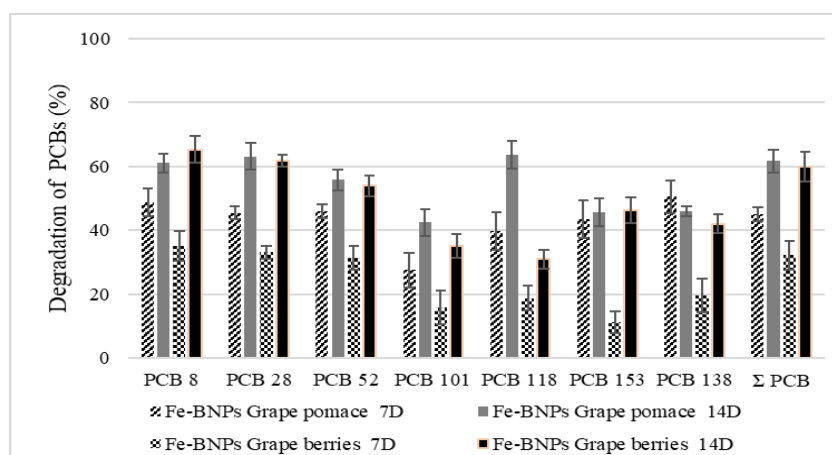


**Fig. 3. Degradation of PCBs (artificially contaminated water medium) by Fe-BNPs derived from grape pomace and grape berries**  
Experimental conditions: 100 rpm, 25 °C, 7 and 14 days

#### 4 Conclusions

This study underscores the significance of green synthesis techniques in producing effective iron-based nanoparticles for environmental applications. The Fe-BNPs synthesized from grape pomace exhibit excellent sorbent properties. These findings suggest that Fe-BNPs derived from grape pomace, a common agricultural waste product, offer an eco-friendly and sustainable approach to nanoparticle production, providing a promising material for environmental remediation technologies.

The implications of this work extend to the fields of nanotechnology, environmental science, and waste management, highlighting the dual benefits of pollutant removal and resource recovery. By integrating waste-derived materials into remediation processes, this study aligns with the principles of circular economy, supporting sustainable development and environmental protection. Future research should focus on optimizing the synthesis conditions to further enhance the reactivity and stability of Fe-BNPs and explore their application across a broader range of environmental contaminants.

#### Acknowledgements

The work was supported by excellent student grant UK/3039/2024. Funded by the EU NextGenerationEU through the Recovery and Resilience Plan of the Slovak Republic within the framework project no. 09I03-03-V05-00012. Thanks to Czech Advanced Technology and Research Institute - CATRIN in Olomouc (CZ) for enabling measurements and characterization of bionanoparticles.

## References

- [1] Ingale, A.G., Chaudhari, A.N. Biogenic synthesis of nanoparticles and potential applications: An eco-friendly approach. *Nanomedicine & Nanotechnology*, 4 (2), 2013.
- [2] Pal, G., Rai, P., Pandey, A. Green synthesis of nanoparticles: A greener approach for a cleaner future. *Micro and Nano Technologies*, 2019, p. 1-26.
- [3] Perron, N.R., Brumaghim, J.L. A Review of the antioxidant mechanisms of polyphenol compounds related to iron binding. *Cell Biochemistry Biophysic*, 53, 2009, p. 75-100.
- [4] Horváthová, H., Dercová, K., Tlčíková, M., Hurbanová, M. Biologická syntéza nanočastíc: Rastlinné bionanočastice železa pre remediáciu kontaminovaného životného prostredia. *Chemické listy*, 116, 2022, p. 405-415.
- [5] Dikshit, P.K., Kumar, J., Das, A.K., Sadhu, S., Sharma, S., Singh, S., Gupta, P.K., Kim, B.S. Green synthesis of metallic nanoparticles: Applications and Limitations. *Catalysts*, 11 (8), 2021, p. 902.
- [6] Poinern, G.E.J. A Laboratory Course in Nanoscience and Nanotechnology: Murdoch University Perth, Western Australia, CRC Press, 2014. ISBN 978-1-4822-3104-5.
- [7] Markova, Z., Novak, P., Kaslik, J., Plachtova, P., Brazdova, M., Jancula, D., Siskova, K.M., Machala, L., Marsalek, B., Zboril, R., Varma, R. Iron (II,III)- polyphenol complex nanoparticles derived from green tea with remarkable ecotoxicological impact. *Chemistry Engineering*, 2 (7), 2014, p. 1674-1680.
- [8] Tlčíková, M., Horváthová, H., Dercová, K., Majčinová, M., Hurbanová, M., Turanská, K., Jurkovič, E. Plant-Based Substrates for the Production of Iron Bionanoparticles (Fe-BNPs) and Application in PCB Degradation with Bacterial Strains. *Processes*, 12, 2024, p. 1695.
- [9] Solmošiová, M., Hrdlička, L., Prousek, J. *Aplikované prírodné vedy*. Celoslovenská študentská vedecká konferencia. Bratislava, 9.11.2016, p. 47.
- [10] Wieszczycka, K., Staszak, K., Woźniak-Budych, M.J., Litowczenko, J., Maciejewska, B.M., Jurga, S. Surface functionalization - The way for advanced applications of smart materials. *Coordination Chemistry Reviews*, 436 (1), 2021, 213846.
- [11] Guo, Z., Liu, Z., Tang R. Applications of amorphous inorganics as novel functional materials. *Materials Chemistry Frontiers*, 8, 2024, p. 1703-1730.
- [12] Lowry, G.V., Johnson, K.M. Congener-specific dechlorination of dissolved PCBs by microscale and nanoscale zerovalent iron in a water/methanol solution. *Environmental Science Technology*, 38 (19), 2004, p. 5208-5216.



## TWO-STAGE ECO-FRIENDLY APPROACH FOR RECOVERY OF COPPER FROM PRINTED CIRCUIT BOARDS (PCBs)

**Arevik Vardanyan<sup>a</sup>, Narine Vardanyan<sup>a</sup>, Anna Khachatryan<sup>a</sup>, Nelli Abrahamyan<sup>a</sup>, Zaruhi Melkonyan<sup>a</sup>**

<sup>a</sup> "SPC" Armbiotechnology" of NAS of Armenia, 14 Gyurjyan str., 0056, Yerevan, Armenia, arevik.vardanyan@asnet.am, nvard@sci.am, anna.khachatryan@asnet.am, nelly-abrahamyan95@mail.ru, zaruhi.melkonyan@gmail.com

### Abstract

Pyrometallurgy is the primary method used to extract precious metals from PCBs. Nevertheless, pyrometallurgy is an extremely energy-intensive process that releases hazardous substances because of PCBs content. Nowadays, bioleaching is thought to be a cutting-edge method for removing metal from a variety of secondary source materials and wastes. Thus, it is especially crucial to create novel, economical, and energy-efficient methods for effectively recovering metal from PCBs while also being ecologically benign. In light of this, bioleaching appears to be a viable method. Bioleaching experiments were performed two using biogenic ferric iron as an oxidizing agent obtained from iron-oxidizing bacteria *Leptospirillum ferriphilum* CC (OM272948). The 48-hour experiment was carried out at 10 % pulp density (PD), pH 1, and 20 g/L Fe<sup>3+</sup>, 40 °C and 400 rpm, with each stage lasting 24 hours. The results show that leaching non-ferrous metals from PCBs may be accomplished with two steps of bioleaching.

**Keywords:** printed circuit boards (PCBs), acidophilic microorganisms, biogenic ferric iron, two-stage bioleaching

### 1 Introduction

According to Kaya (2016) [1], waste electronic and electrical equipment (WEEE) makes about 8 % of all municipal waste and is growing by 4-5 % year. WEEE is primarily produced by four sources: office machines, industrial equipment/machines, hospital medical equipment, and small and big residential appliances. 3-5 % of the total volume of WEEE is made up of PCBs, which are the primary component of WEEE [2, 3]. PCBs are made up of 20 % Cu, 5 % Al, 1 % Ni, 1.5 % Pb, 2 % Zn, and 3 % Sn (w/w) with 250 ppm Au, 1000 ppm Ag, and 110 ppm Pd respectively [1, 2, 4].

PCB recycling is important for the environment and the economy. PCB disposal may release potentially hazardous substances into soil and water, increasing the risk of toxicity to food chains [5]. However, PCBs may also be a secondary source of important metals like Cu, Zn, Al, Ni, and Au.

Pyrometallurgy is the primary method used to treat PCBs to recover valuable metals; however, during this process, part of the metals, including aluminum, iron, and precious metals, are lost in the slag [6]. In addition, pyrometallurgy is an energy-intensive process. Moreover, harmful dioxins and other chemicals are released when plastics are present in PCBs. Thus, it is especially crucial to develop novel, energy- and cost-efficient methods for the effective recovery of metal from PCBs.

Biohydrometallurgy is a very promising technique from this perspective. Brierley and Brierley (2001) [7] describe bioleaching as a well-known commercial use of biohydrometallurgy to treat mineral ores. This biological technique is easier, more economical, and less harmful to the environment than traditional pyrometallurgy. The foundation of bioleaching is the capacity of bacteria, fungus, or other microorganisms to generate leaching agents. Specifically, ferrous iron to ferric iron, a potent oxidative agent, and elemental sulfur to sulfuric acid, so generating leaching agents, can be oxidized by acidophilic autotrophic bacteria (direct mechanism) [8, 9]. Thus, in contrast to chemical treatment, bioleaching involves the biological production of the reagents required for metal recovery, which has clear benefits for process economics and environmental effect in terms of carbon emissions.

Actually, bioleaching is now thought of as a cutting-edge method for removing metal from a variety of secondary source materials and wastes. Some research in the literature [10-12] discusses the use of bioleaching for the treatment of wasted PCBs by acidophilic microorganisms. The purpose of this work is to compare the copper recovery effectiveness of one- and two-stage PCB treatment techniques, which correspond to direct and indirect bioleaching mechanisms.

## 2 Material and methods

### 2.1 Preparation of PCBs

Multi-layer printed circuit boards, mostly from abandoned computers, were used in this project. The PCB samples were utilized in the tests after being cut into  $1.5 \times 1$  cm pieces with scissors. Before bioleaching, the broken PCBs were boiled in 10 % NaOH for fifteen minutes to remove the passive layer (green solder mask) that was present. Following a thorough washing with distilled water, the samples were dried and kept ready for bioleaching.

### 2.2 Culture growth and preparation of lixiviant

Cultivated in MAC medium containing 44.2 g/L  $\text{FeSO}_4 \cdot 7\text{H}_2\text{O}$  at 40 °C for 4-5 days. The obtained culture liquid (lixiviant) was used for bioleaching applications. The cell number was determined by direct counting under a microscope (Optica B-810, Italy) using a Thoma Chamber. The initial cell number for *L. ferriphilum* CC was  $2.5 \times 10^7$  cells/mL.

The biolixiviant used for leaching was obtained based on an iron-oxidizing culture *Leptosprillum ferriphilum* CC (OM272948) [13]. *L. ferriphilum* CC was grown in modified 9K medium (0.5 g/L  $(\text{NH}_4)_2\text{SO}_4$ , 0.5 g/L  $\text{MgSO}_4 \cdot 7\text{H}_2\text{O}$ , 0.5 g/L  $\text{K}_2\text{HPO}_4$ , 0.05 g/L KCl, 0.01 g/L  $\text{Ca}(\text{NO}_3)_2$ ) containing 25 g.L<sup>-1</sup> ferrous iron (supplemented as  $\text{FeSO}_4 \cdot 7\text{H}_2\text{O}$ ). The growth of bacteria as described previously was carried out inside a bio-fermenter (Bionet Baby 0) coupled to the control unit, to follow gas supply, stirring rate, pH, Eh, and temperature. The fermenter filled in with 2 L medium was inoculated at 10 % (v/v) of bacterial culture ( $2.6 \times 10^8$  cells/mL) and pH adjusted to 1.8-1.9 using 10N  $\text{H}_2\text{SO}_4$ . The fermenter was operated at a temperature of 30 °C, stirring speed of 80 rpm, and 1 lpm air-flow. After 5-7 days of cultivation, a reddish coloration of the culture medium was observed due to the oxidation of  $\text{Fe}^{2+}$  to  $\text{Fe}^{3+}$ . The redox potential of the lixiviant was around 700 mV (Ag/AgCl ref.). The quantitative determination of bacterial cells during bioleaching experiments was carried out by a serial end-point dilution technique known as the “most probable number” (MPN) method [14].

### 2.3 Bioleaching

Two-stage bioleaching of ground  $\leq 2$  cm size fraction of PCBs was performed inside a 2 L jacketed reactor coupled to a circulating bath maintaining a constant operating temperature of 40 °C required to sustain eventual bacterial growth. The reactor was connected to a condenser to prevent excessive evaporation and a tunable compressor to supply air [15]. Leaching experiments were performed under starting pH of 1 (10N  $\text{H}_2\text{SO}_4$  was used for pH adjustment) and 20 g/L concentration of  $\text{Fe}^{3+}$  as an oxidizing agent. The duration of the bioleaching experiment was 48 h, with each stage being fixed to 24 h. To realize this, after elapsing the first 24 h of leaching, the pregnant solution (PLS) was decanted and fresh lixiviant was added to the reactor. Solution sampling was performed at the start of the experiment, 1 h, 2 h, 3 h, 4 h, 5 h, 6 h, 7 h, and 24 h of each stage. After bioleaching, the residue was recovered as two different granulometric fractions: “coarse” (1-2 mm) and “fine” (below 1 mm). The “coarse” fraction was obtained after sieving, while the “fine” fraction was the one remaining after vacuum filtration of the PLS. Following separation, “coarse” and “fine” fractions were dried and used for microscopic inspection.

### 2.4 Scanning electron microscopy (SEM) and energy dispersive X-ray spectroscopy (EDS)

PCBs were observed concerning morphology and phase liberation by a SEM-based automated mineralogy system-Zeiss sigma 300 FEG “Mineralogic”-coupled to two Bruker EDS x Flash 6|30 X-ray energy dispersion spectrometers (silicon drift detector). The SEM-EDS analyses were carried out using a probe current of 2.3 nA with an accelerating voltage of 20 kV at a working distance of 8.5 mm. A mapping mode was performed using a 3 to 5  $\mu\text{m}$  step size and a dwell time of 55 ms. Analytical conditions such as contrast and brightness were set up manually to provide best possible contrast between the observed phases (plastics, composites, metals). System magnification was set to 6000 X and voltage tension to 20 kV.

### 2.5 Analytical determinations

Metals in the pregnant leach solution (PLS) were analyzed by inductively coupled plasma optical emission spectroscopy (ICP-OES). The solid residue after leaching was dried, oven-treated at 900 °C for 240 min, ground in an agate mortar or a ring mill, and digested in aqua regia before being analyzed, similar



to the liquid samples. Ferrous and ferric iron concentration was determined by an Ethylenediaminetetraacetic acid (EDTA) based complexometric titration [16].

### 3 Results and discussion

In our previous experiments, we studied the effect of different oxidizing agent ( $\text{Fe}^{3+}$ ) concentrations, varying pH, and pulp density (PD) on metal extraction efficiency [15]. In this study to characterize feed and residue material after bioleaching, PCBs were subjected to two-stage subsequent bioleaching via biologically obtained  $\text{Fe}^{3+}$  by *L. ferriphilum* CC. To mimic closely industrially relevant applications 10 % of PD was chosen. During the entire two-stage bioleaching (24 h + 24 h) at 10 % PD, pH 1, and 20 g.L<sup>-1</sup> ferric iron the overall metal yield was 95 % for Cu and 87 % for Ni with almost complete recovery of Zn (Figure 1).

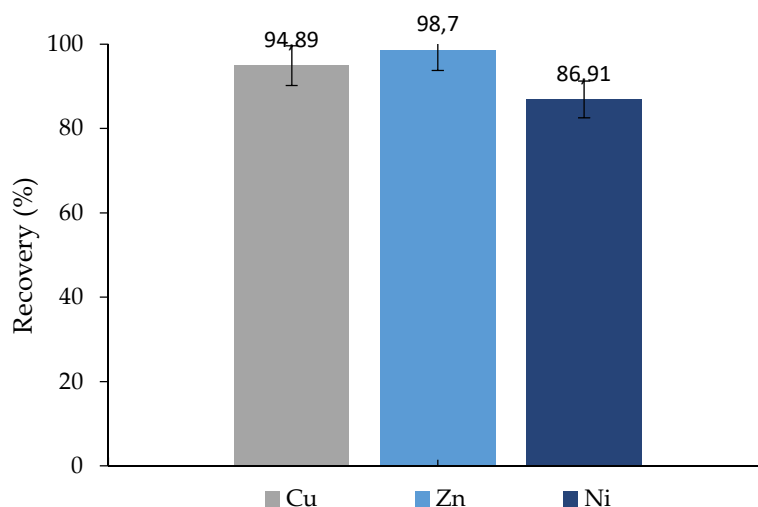


**Fig. 1. Recovery of metals from PCBs at two-stage leaching**  
(Conditions: PD 10 %; pH 1;  $\text{Fe}^{3+}$  concentration 20 g/L; 40 °C, 1 standard liter per minute (slpm); 600 rmp, duration 24 h + 24 h)

The recovery of Al was about 3 % (data not shown) which corresponds to our previous results [15]. This low recovery level is most likely due to the intrinsic refractoriness of the aluminum met in PCBs (e.g. as an alloy), and the presence of surface coatings or encapsulation within the PCB matrix.

pH and the oxidation-reduction potential (ORP) is also an important parameter that reflects the oxidation and reduction reactions taking place during the leaching process. pH increases during the bioleaching process from 1 to 1.93 and 1.21 in the first and the second stages respectively. This could be attributed to the alkaline compounds found in PCBs, which consume the acid reflecting in increase in pH of the lixiviant. Besides, the pH increase could have resulted from bacterial oxidation of  $\text{Fe}^{2+}$  to  $\text{Fe}^{3+}$  known as an acid (proton) consumption process. It is assumed that the maximum recovery of metals takes place mainly during the first stage, which was reported in our previous experiments [15]. This explains the non-substantial changes in pH observed in the second stage of leaching.

In the first stage ORP of the bacterial solution dropped sharply from 608 mV to 346 mV (Ag/AgCl), for 1 h of leaching due to the reduction of  $\text{Fe}^{3+}$  ions to  $\text{Fe}^{2+}$  (redoxolysis). During the second stage, ORP declined at a slower pace from 593 to 460 mV (Ag/AgCl), which proves the assumption that leaching takes place mainly in the first stage with the elevated ORP values indicating the prevalence of  $\text{Fe}^{3+}$  over  $\text{Fe}^{2+}$  in the lixiviant.

As shown in Table 1 after 3 h of leaching there was a distinct drop in bacterial population in the PLS - from 108 to 102 cells/mL. After 3 h of leaching no growth of bacteria was observed due to the inhibitory effect of PCBs on bacterial activity given their heterogenous composition carrying a variety of hazardous compounds and because of the initial low pH.

**Table 1. Bacteria enumeration during the bioleaching**  
(PD 10 %, initial pH 1, Fe<sup>3+</sup> 20g/L, 40 °C, air 1 slpm, 600 rpm, duration 24 h)

Duration (h)	Number of cells (cells/mL)
0	2.6x10 <sup>8</sup>
1	1.1x10 <sup>7</sup>
3	3.0x10 <sup>2</sup>
5	N/D*
24	N/D

\*N/D - not detected

It was important to assess and track visually the evolution of PCBs fragments and their morphology before and after leaching. Due to the disparities in their chemical composition, plastics (dark) and metallic (bright) may be distinguished in the backscattered electrons (BSE) images, which present signals from a polished section in greyscale. Commonly energy dispersive spectroscopy (EDS) is used to obtain added information to differentiate the composition of the detected metallic particles. It is worth noting that PCBs have a multi-element base composition [16], so a large number of elements are expected to be found. The primary metals that comprise PCBs, according to an EDS mapping, are Cu, Zn, Sn, Ti, Ba, Pb, Fe, and Au. However, these metals are usually met as alloys between each other.

#### 4 Conclusions

Conditions that have previously [15] been found to be optimal (pH 1, 10 % PD, and 20 g/L Fe<sup>3+</sup>) were used for a two-stage bioleaching of PCBs which allowed reaching up to 95 % extraction of copper. The results obtained indicate that Cu as well as other metals in PCBs may be efficiently leached by a two-stage process involving bio-oxidation coupled to subsequent redoxolysis.

#### Acknowledgements

The work was supported by the Science Committee of the Republic of Armenia, in the frames of the research project no 21T-1F124.

#### References

- [1] Kaya, M. Electronic Waste and Printed Circuit Board Recycling Technologies, 2019.
- [2] Faraji, F., Golmohammadzadeh, R., Rashchi, F. Fungal bioleaching of WPCBs using *Aspergillus niger*: Observation, optimization, and kinetics. *Journal of Environmental Management*, 217, 2018, p. 775-787.
- [3] Vermeşan, H., Tiuc, A.E., Purcar, M. Advanced recovery techniques for waste materials from IT and telecommunication equipment printed circuit boards. *Sustainability*, 12, 2020, p. 1-23.
- [4] Birloaga, I., Vegliò, F. Study of multi-step hydrometallurgical methods to extract the valuable content of gold, silver and copper from waste printed circuit boards. *Journal of Environmental and Chemical Engineering*, 4, 2016, p. 20-29.
- [5] Wang, L., He, J., Xia, A., Cheng, M., Yang, Q., Du, C., Wei, H., Huang, X., Zhou, Q. Toxic effects of environmental rare earth elements on delayed outward potassium channels and their mechanisms from a microscopic perspective. *Chemosphere*, 181, 2017, p. 690-698.
- [6] Cui, J., Zhang, L. Metallurgical recovery of metals from electronic waste: a review. *Journal of Hazardous Materials*, 158, 2008, p. 228-256.
- [7] Brierley, J.A., Brierley, C.L. Present and future commercial applications of biohydrometallurgy. *Hydrometallurgy*, 59, 2001, p. 233-239.
- [8] Gadd, G.M. Microbial influence on metal mobility and application for bioremediation. *Geoderma*, 122, 2004, p. 109-119.
- [9] Sand, W., Gehrke, T., Jozsa, P.G., Schippers, A. (Bio) chemistry of bacterial leaching - Direct vs. indirect bioleaching. *Hydrometallurgy*, 59, 2001, p. 159-175.

- [10] Brandl, H., Bosshard, R., Wegmann, M. Computer-munching microbes: Metal leaching from electronic scrap by bacteria and fungi. *Hydrometallurgy*, 59 (2-3), 2001, p. 319-326.
- [11] Ilyas, S., Ruan, C., Bhatti, H.N., Ghauri, M.A., Anwar, M.A. Column bioleaching of metals from electronic scrap. *Hydrometallurgy*, 101, 2010, p. 135-140.
- [12] Ilyas, S., Lee, J.C., Chi, R.A. Bioleaching of metals from electronic scrap and its potential for commercial exploitation. *Hydrometallurgy*, 131-132, 2013, p. 138-143.
- [13] Vardanyan, A., Khachatryan, A., Castro, L., Willscher, S., Gaydardzhiev, S., Zhang, R., Vardanyan, N. Bioleaching of Sulfide Minerals by *Leptospirillum ferriphilum* CC from Polymetallic Mine (Armenia). *Minerals*, 13, 2023, p. 243.
- [14] Erkmen, O. Practice 4 - Most probable number technique. In *Microbiological Analysis of Foods and Food Processing Environments*; Elsevier: Amsterdam, The Netherlands, 2022, p. 31-37.
- [15] Vardanyan, A., Vardanyan, N., Aâatch, M., Malavasi, P., Gaydardzhiev, S. Bio-Assisted Leaching of Non-Ferrous Metals from Waste Printed Circuit Boards - Importance of Process Parameters. *Metals*, 12, 2022, <https://doi.org/10.3390/met12122092>.
- [16] Lucchesi, C.A., Hirn, C.F. EDTA Titration of total Iron in Iron(II) and Iron(III) mixtures. Application to Iron driers. *Analytical Chemistry*, 32, 1960, p. 1191.
- [17] Korf, N., Løvik, A.N., Figi, R., Schreiner, C., Kuntz, C., Mähltitz, P.M., Rösslein, M., Wäger, P., Rotter, V.S. Multi-element chemical analysis of printed circuit boards - challenges and pitfalls. *Waste Management*, 92, 2019, p. 124-136.



## PRELIMINARY STUDY ON COPPER ADSORPTION FROM AQUEOUS SOLUTIONS USING WASTE CORDIERITE

**Joanna Willner<sup>a</sup>, Agnieszka Fornalczyk<sup>a</sup>, Rafał Zawisz<sup>b</sup>**

<sup>a</sup> Faculty of Materials Engineering, Silesian University of Technology, Krasińskiego 8, 40-019 Katowice, Poland,  
joanna.willner@polsl.pl, agnieszka.fornalczyk@polsl.pl

<sup>b</sup> Ad Moto Rafał Zawisz, Srokwiecka 5, 41-106 Siemianowice Śląskie, Poland, rafal@filtracjaoleju.pl

### Abstract

Waste cordierite, typically regarded as a waste residue after hydrometallurgical recovery of valuable metals (Pt, Pd, Rh) from automotive catalytic converters, could hold significant potential as a sustainable adsorbent for environmental applications. The paper presents preliminary research results on the Cu adsorption from aqueous solution on waste cordierite as an adsorbent. The results demonstrate that the choice of acid in chemical activation significantly influences the sorption capacity of the cordierite material. The highest copper adsorption rate, reaching 97.6 %, was observed when the cordierite was activated with oxalic acid, indicating that this acid (next to citric acid and hydrochloric acid) provides the most effective surface modification for enhancing copper ion binding. Further research to verify and optimize the sorption conditions for Cu and for a broader range of pollutants will be continued.

**Keywords:** cordierite, spent auto catalyst converters, copper, adsorption, adsorbent

## 1 Introduction

Sorption processes are widely used to purify industrial wastewater from organic and inorganic pollutants, arousing great interest among researchers. Although sorption technologies have been known for many years, the search for inexpensive sorbents with high efficiency in removing pollutants is still an important area of research. Local raw materials, such as natural materials and agricultural and industrial wastes, can be successfully used as economical adsorbents. Various bio-waste sources are gaining importance, originating from agricultural production, the food industry, wood processing, fishing, and the municipal economy [1, 2]. However, more and more often is also talk about the possibility of using industrial wastes originating from the metallurgical industry, e.g. blast furnace slag, red mud, and copper slag, to develop effective adsorbents for purifying pollutants in water [3]. In addition to waste slags from pyrometallurgical processes, some mineral materials remaining after hydrometallurgical metal recovery processes may also have sorption potential for metal ions. An example is the ceramic material of a car catalytic converter, which is made mainly of silicon, aluminum, and magnesium oxides in the form of cordierite  $2\text{MgO} \cdot 2\text{Al}_2\text{O}_3 \cdot 5\text{SiO}_2$ . It is common knowledge that used car catalytic converters after their operation are a valuable source of platinum group metals PGM (Pt, Pd, Rh), the recovery of which is the main goal of recycling used catalysts. On the other hand, the residue from the hydrometallurgical metal recovery process - the ceramic carrier - is treated as waste. The composition of the ceramic monolith of used catalytic converters, which is 48-52 % silicon oxide ( $\text{SiO}_2$ ), 32-36 % aluminum oxide ( $\text{Al}_2\text{O}_3$ ), and 8-14 % magnesium oxide (MgO) [4, 5], indicates the possibility of testing this raw material for its sorption potential. The study aimed to determine the preliminary sorption capabilities of waste cordierite, as a potential adsorbent of copper from aqueous solutions.

## 2 Material and methods

### 2.1 Characteristics of material

The study was conducted on waste cordierite, a residual material left after the leaching of PGM - specifically platinum (Pt), palladium (Pd), and rhodium (Rh) - from automotive catalytic converters (Fig. 1). The leaching process was carried out using a hydrochloric acid (HCl) and hydrogen peroxide ( $\text{H}_2\text{O}_2$ ) solution, heated to 60 °C over 5 hours. Following the recovery of PGM, the residual cordierite material was dried, and then ground to achieve a uniform particle size. This treatment prepared the material for further modification and testing.

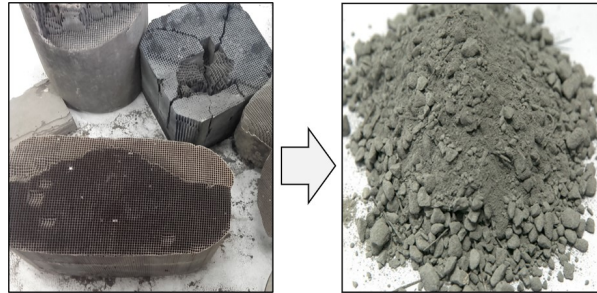


**Fig. 1. Cordierite - the tested sorption material before and after grinding**

## 2.2 Experimental methods

The adsorption experiments were performed in Erlenmeyer flasks with continuous agitation provided by a magnetic stirrer set at 295 rpm for 2 hours. The conditions of the experiments were carefully controlled to ensure consistency, with a solid-to-liquid ratio (S/L) of 1:40 and a temperature of 23 °C. The copper solution used in the study had an initial concentration of 5 mg/l. Following the adsorption process, the concentration of copper remaining in the solution was measured using an inductively coupled plasma spectrometer ICP-OES (ICP\_PRO X Duo, Thermo Scientific).

## 3 Results and discussion

Figure 2 illustrates the degree of copper (Cu) removal from the solution, highlighting the impact of the activation method (i.e. type of acid used) on the efficiency of the adsorption process. The results demonstrate that the choice of acid significantly influences the sorption capacity of the cordierite material. The highest copper adsorption rate, reaching 97.6 %, was observed when the cordierite was activated with oxalic acid, indicating that this acid provides the most effective surface modification for enhancing copper ion binding. In comparison, citric acid activation resulted in a lower but still notable adsorption efficiency of 73.3 %. The lowest degree of copper removal, 51.4 %, was achieved with hydrochloric acid (HCl).

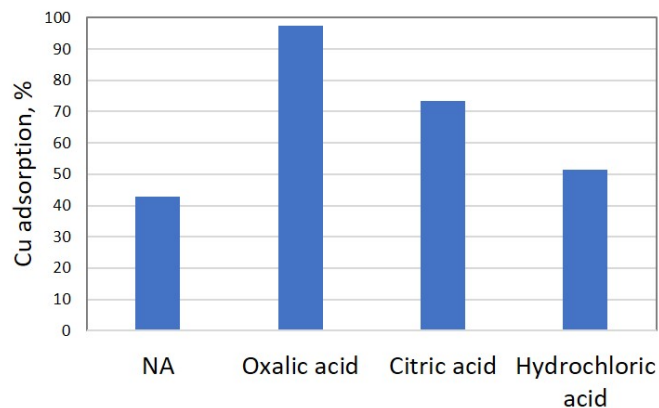


**Fig. 2. Copper adsorption on waste cordierite depending on the type of activation (NA - not-activated)**

## 4 Conclusions

Preliminary research results indicate that waste cordierite demonstrates significant promise as an adsorbent for copper ions. The material's composition, primarily consisting of silicon oxide, aluminum oxide, and magnesium oxide, contributes to its effectiveness in removing copper from aqueous solutions, and chemical activation with oxalic acid improved the adsorption properties of waste cordierite. These findings suggest that cordierite, often considered waste after the recovery of precious metals from catalytic converters, can be repurposed as a valuable and cost-effective adsorbent in wastewater treatment applications. Given these promising results, further detailed studies are planned to explore the sorption capabilities of waste cordierite for Cu and other metal ions, such as lead, and nickel.

## Acknowledgements

The work was supported by project 11/020/SDU/10-21-01 of the Silesian University of Technology in the "Excellence Initiative - Research University" program - priority research area POB6.3 Circular economy.

## References

- [1] Singh, S., Kumar, V., Datta, S., Dhanjal, D.S., Sharma, K., Samuel, J., Singh, J. Current advancement and future prospect of biosorbents for bioremediation. *Science of the Total Environment*, 709, 2020, 135895, p. 1-24.
- [2] Madeła, M. *Bioodpady jako biosorbenty w ujęciu gospodarki cyrkulacyjnej* in *Inżynieria środowiska i biotechnologia - wyzwania i nowe technologie*. Wydawnictwo Politechniki Częstochowskiej, 2022. ISBN 978-83-7193-900-6.
- [3] Rangappa, H.S., Herath, I., Lin, C, Subrahmanyam, Ch. Industrial waste-based adsorbents as a new trend for removal of water-borne emerging contaminants. *Environmental Pollution*, 343, 2024, 123140, p. 1-18.
- [4] Tomašić, V., Jović, F. State-of-the-art in the monolithic catalysts/reactors. *Applied Catalysis A: General*, 311 (1-2), 2006, p. 112-121.
- [5] Govender, S., Friedrich, H.B. Monoliths: a review of the basics, preparation methods and their relevance to oxidation. *Catalysts*, 7 (2), 2017.







Slovak Academy of Sciences  
Institute of Geotechnics



### Scientific focus

The Institute of Geotechnics SAS, established in 1954, has a dominant position in Slovak Republic within the basic and applied research in the area of rock cutting, mineral processing, mechanochemistry, mineral biotechnologies and environmental protection.

Subjects of activity:

- basic research of processes in the field of rock cutting, rock mechanics and underground constructions, the transport of energy and mass in the rock disintegration processes; basic research of solid dispersions origin patterns and their properties modifications by physical, mechanical, chemical and biotechnological processes; qualitative and quantitative evaluation of phase interactions at the disperse systems formation and at their spreading in working and living environment,
- application of theoretical knowledge from presented areas for detailing the top technologies principles in the following fields: rock cutting, mineral processing, monitoring of selected components of working and living environment, monitoring of environmental, chemical and geological changes in the waste repositories with the aim of ecological remediation,
- advisory and expertise services related to main activities,
- scientific education (PhD.) in terms of generally valid legislation,
- publication of the scientific-research activities.

Current research activities of IGT SAS issue from the Institute's tradition related to the mining activities in Slovakia strongly connected to mineral exploitation, mineral processing and beneficiation of raw materials.

After the regression in mining industry in 1990s, the IGT SAS has begun the transition to the new research activities:

- rock cutting and drilling, vibrations in rock drilling, TBM tunnelling,
- mineral processing by physical, chemical and biotechnological methods,
- mechanosynthesis and mechanochemical activation of minerals and materials,
- (nano)materials development for environmental applications,
- mineral and environmental bio- and nano-technologies,
- remediation and recovery of mining and industrial areas,
- removal of toxic substances from waters and soils, treatment of acid mine drainage, biodegradation of organic pollutants in soils,
- industrial waste treatment.

### Scientific departments

The Institute of Geotechnics SAS is divided into 5 research departments, a central analytical laboratory and a service department supporting the research. The scientific departments cover the main scope of the institute, i.e. experimental research, scientific projects and publishing of results. Senior scientists, research fellows, PhD .students and technicians are all involved in the implementation of the scientific project tasks, and contribute to acquisition of additional financial support by applying for project proposals at international and national project agencies (EU H2020/FP7, ERDF, APVV, VEGA, etc.). For project implementation, the research teams are formed across the departments, providing strong interdisciplinary knowledge and experience.

#### Department of Destructional and Constructional Geotechnics

#### Department of Environment and Hygiene in Mining

#### Department of Mechanochemistry

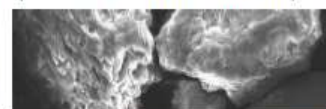
#### Department of Mineral Biotechnologies

#### Department of Physical and Physico-Chemical Mineral Processing Methods

Department of Mineral Biotechnologies focuses on environmental, biogenic and bio-transformation processes in relation to minerals, raw materials, industrial wastes in new environmentally acceptable processing technologies.

#### Bioremediation of mining and industrial waste effluents

- biodegradation, biosorption, bioprecipitation, biovolatilization,
- bacterial dissimilatory reduction of iron, sulphate, nitrate, (per)chlorate,
- ion exchange,
- advanced oxidation processes (AOPs),
- toxicity and biodegradability assessment (respirometric methods).



#### Degradation of organic pollutants in waters and soils

- biodegradation of organic pollutants in groundwaters, waste waters and soils,
- contaminant-specific monitoring of the degradation based on the extraction of the analyte from the matrix before analysis,
- contaminant-non-specific monitoring of organic matter mineralization based on oxygen and carbon dioxide gas analysis (respirometric methods).



#### Biocorrosion & biodeterioration of synthetic and industrial materials

- bio corrosion of building composite materials,
- bio-deterioration of underground storage structures.

#### Bioleaching & metal mobilization

- dissolution of minerals by bacterial oxidation of iron and/or reduced inorganic sulfur compounds,
- bacterial reductive dissolution of iron oxides,
- liberation of iron impurities from nonmetallic by bacterial by-products.



The **Faculty of Natural Sciences** has become an important part of the University of St. Cyril and Methodius. The mission of the Faculty is to create a modern educational environment that reflects current trends and demands in the field of natural sciences. Our long-term goal is to educate and train students in accredited bachelor's, master's, and doctoral degree programs, with an emphasis on their practical application in the future.

**Študy programmes:**

- Applied analytical chemistry
- Applied biology
- Applied informatics
- Chemistry
- Protection and restoration of the environment



UNIVERSITY OF SS. CYRIL  
AND METHODIUS IN  
TRNAVA



ÜCM  
FACULTY  
OF NATURAL  
SCIENCES





# ROOTED IN NATURE, ADVANCING THROUGH BIOTECHNOLOGY

## AIMS

Inspired directly by nature we develop biotechnologies with the elegance that nature itself would design. With huge enthusiasm, we dedicate ourselves to exploring natural principles, particularly in the field of metal-microbe interactions, regardless of whether these metals are found in ores or waste. We seek ways to utilize this knowledge for the benefit of people, but with respect for other organisms. And we love to teach about it.

## ACTIVITIES

Environmental School  
Environmental Biotechnology Centre  
Nanoparticle Production  
Training

## PROJECTS

Microbes and Metals Teaching Green  
Technology (224 100 38)  
funded by International Visegrad Fund

BioPrep - Biotechnological Innovations  
for Sustainable Flat Panel Displays  
Recycling (DRP0401069)  
funded by Interreg Danube Region  
Programme

## SPONSORS

---



**AMEDIS spol. s r.o.**  
Mlynská 10, 921 01 Piešťany  
tel.: 00421-33-774 4230, 774 4231  
e-mail: [amedis.pn@amedis.sk](mailto:amedis.pn@amedis.sk)

The company AMEDIS spol. s r.o. was founded in Slovakia in 1991.

The subject of the activity is 30 years of business and educational activities related to the sale and service of laboratory and medical equipment. We represent top manufacturers of a wide range of laboratory instruments and analyzers as well as medical radiotherapy irradiation, imaging, planning and dosimetric systems.

The company AMEDIS spol. s r.o. also ensures highly professional installation and service support of the sold devices. Our experienced service engineers have over 30 years of experience in service and application support. The younger members of the team have been with our customers for more than 15 years. They completed a number of professional trainings and coped with dozens of seemingly intractable challenges.

Many of our customers have become our friends, which we greatly appreciate.

In 2006, we introduced a quality management system according to the ISO 9001 standard, its successful implementation is regularly checked by external audits. Since 2015, we have adopted environmental protection measures, namely the ISO 14001 standard and the OHSAS 18001 occupational health and safety standard. Our philosophy is not only sales, but also high-quality and qualified support for sold devices.

In the field of laboratory accessories, the company has exclusive representation of the following brands:



And many more...

SPONSORS



## Avantor Supports Customers from Discovery to Delivery

Avantor®, is a leading life science tools company and global provider of mission-critical products and services to customers in the life sciences and advanced technology industries. From discovery to delivery, we work side-by-side with scientists around the world to enable breakthroughs in medicine, healthcare, and technology at scale.

Our portfolio is used in virtually every stage of the most important research, development and production activities at more than 300,000 customer locations in 180 countries. For more information, visit [avantorsciences.com](http://avantorsciences.com) and find us on LinkedIn, X (Twitter) and Facebook.



**We set science in motion to create a better world**

**CONTACT:**

VWR International s. r. o.  
Pražská 442, 281 67 Stříbrná Skalice  
Tel.: +421 2 321 010 33, E-mail: [info.sk@vwr.com](mailto:info.sk@vwr.com)



Biotechnology&Metals 2018



Proceedings: Proceedings of the 6<sup>th</sup> International Scientific Conference on Biotechnology and Metals

Editors: Jana Hroncová, Eva Mačingová, Alena Luptáková, Jana Sedláková-Kaduková

Publishers: Institute of Geotechnics, Slovak Academy of Sciences, Košice & Slovak Mining Society  
at the Institute of Geotechnics SAS

Reviewers: All conference papers went through the anonymous review process

Year: 2024

Pages: 273

ISBN: 978-80-89883-15-8

**ISBN: 978-80-89883-15-8**